FTF CLOSURE CAP CONCEPT AND INFILTRATION ESTIMATES

M. A. Phifer
W. E. Jones
E. A. Nelson
M. E. Denham
M. R. Lewis
E. P. Shine

OCTOBER 2007

Savannah River National Laboratory
Washington Savannah River Company
Savannah River Site
Aiken, SC 29808

SRNL

DISCLAIMER

Printed in the United States of America

Prepared For
U.S. Department of Energy

FTF CLOSURE CAP CONCEPT AND INFILTRATION ESTIMATES

M. A. Phifer
W. E. Jones
E. A. Nelson
M. E. Denham
M. R. Lewis
E. P. Shine

OCTOBER 2007
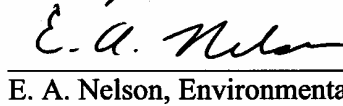
REVIEWS AND APPROVALS

Authors
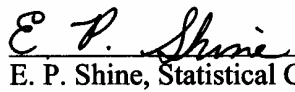
_____   10/11/07

M. A. Phifer, Environmental Restoration Technology Section   Date

_____   10/11/07

W. E. Jones, Environmental Restoration Technology Section   Date
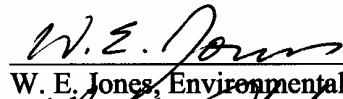
_____   10/11/07

E. A. Nelson, Environmental Analysis Section   Date
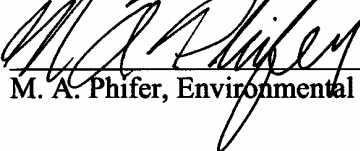
_____   10/11/2007

M. E. Denham, Environmental Restoration Technology Section   Date

_____   10/15/07

M. R. Lewis, Geotechnical Engineering Section, SRS Site Engineering   Date

_____   10/11/07

E. P. Shine, Statistical Consulting Section   Date
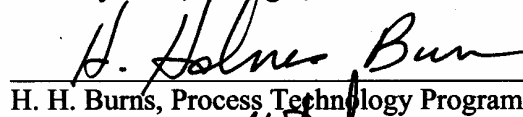
Design Check

_____   10/11/07

W. E. Jones, Environmental Restoration Technology Section   Date

_____   10/11/07

M. A. Phifer, Environmental Restoration Technology Section   Date

Approvals

_____   10/11/07

R. S. Aylward, Manager, Environmental Restoration Technology Section   Date

_____   10/16/07

H. H. Burns, Process Technology Programs   Date

_____   10/11/07

T. W. Coffield, SRIP – Regulatory Documentation   Date

LIST OF MAJOR REVISIONS

Notes to the list of major revisions:
1. Revision bars are not utilized within the text for revisions that consist of the addition of an entire section, appendix, etc., or the essential complete rewrite of an entire section, appendix, etc. Such revisions are shaded in <mark>yellow</mark> in this table.
2. Revision bars are utilized within the text for revisions within an existing section, appendix, etc. Such revisions may or may not be noted in this table.
3. Only major revisions are noted; minor revisions (e.g., changes in Section, Table, and Figure numbers; typographical error corrections; spelling corrections; minor word changes for clarification) are denoted with revision bars within the text only.

Revision Number	Date	Sections	Comment
0	4/16/07	All	Initial Issue
1	6/4/07	1.0	Added configuration #1a and the closure cap degradation mechanism evaluation
		4.3	Added clarification concerning the design of the erosion barrier as a barrier to burrowing animals
		4.4.9	Added information on stone QA/QC, the use of weathering analogs, and the future evaluation to determine the material that will be used to infill the stone voids
		5.0	Added configuration #1a
		5.3.3	Added HELP model input for erosion barrier with sandy soil infill (configuration #1a)
		5.3.4	Added table containing literature values of the saturated hydraulic conductivity of sand
		5.5	Added HELP model results for the initial conditions of configuration #1a
		6.0	Added configuration #1a
		7.0	Inserted entirely new section to address potential FTF Closure Cap degradation mechanisms
		8.0	1) Reference section became Section 8.0 rather than Section 7.0 as in revision 0 of the document; 2) Added additional references
		Appendix F	Inserted entirely new appendix to provide calculations for the HELP model input for an erosion barrier with sandy soil infill (configuration #1a)
		Appendix G	Inserted entirely new appendix to provide HELP model input for an erosion barrier with sandy soil infill (configuration #1a)
		Appendix H	Inserted entirely new appendix to provide HELP model annual water balance data for an erosion barrier with sandy soil infill (configuration #1a)

Revision Number	Date	Sections	Comment
2	10/12/07	1.0	Updated Executive Summary with additional information provided in revision 2
		3.0	Divided the background section into the following two subsections: 3.1 FTF Background; and 3.2 Background Water Balance and Infiltration Studies
		3.2	Inserted entirely new section to address background water balance and infiltration studies
		4.3	1) Divided the foundation layer into an upper and lower layer; 2) Eliminated the elevation difference between the top rip rap and the vegetative soil cover in Figure 12
		4.4	Added an additional FTF Closure Cap plot plan and cross-sections
		4.4.1	Divided the foundation layer into an upper and lower layer
		4.4.3	Added wrinkle control to the HDPE geomembrane QA/QC requirements
		4.4.9	1) Added additional stone QA/QC; 2) Divided analogs to be considered into above and below grade analogs; 3) Added additional analogs for consideration
		4.4.13	Added additional stone QA/QC
		4.4.14	Added additional stone QA/QC
		5.0	Descriptions of the seven configurations evaluated were revised for clarity
		5.1	Added new Section 5.1 which provides the following: 1) Additional description of the HELP model and its use; 2) Detail concerning the appropriateness of its use; 3) A commitment to evaluate other models as a replacement to the HELP model
		5.2	Section 5.2 was previously Section 5.1. Added information on 1) Evaporative zone depth; 2) Maximum leaf index; 3) Methodology used by the HELP model to estimate evapotranspiration; 4) Precipitation data set statistical detail
		5.3	Section 5.3 was previously Section 5.2.
		5.4	Section 5.4 and all its subsections were previously Section 5.3.

Revision Number	Date	Sections	Comment
2 (cont.)		5.4.5	1) Added wrinkle control to the HDPE geomembrane QA/QC requirements; 2) Revised HELP model geomembrane placement quality designation to be consistent with HELP model guidance provided by Schroeder et al. 1994a and 1994b
		5.4.7	Divided the foundation layer into an upper and lower layer
		5.4.8	Divided the foundation layer into an upper and lower layer
		5.5	Section 5.5 was previously Section 5.4.
		5.6	Section 5.6 was previously Section 5.5. This section was essentially entirely rewritten as follows: 1) Added additional detail concerning the initial water balance for all seven configurations considered; 2) Divided the foundation layer into an upper and lower layer; 3) Revised HELP model geomembrane placement quality designation to be consistent with HELP model guidance provided by Schroeder et al. 1994a and 1994b; 4) Provided a comparison of the configuration #6 HELP model water balance to the water balance from background studies
		7.0	Added information addressing the potential for mineral precipitation and microbial growth in the lateral drainage layer
		7.2	1) Reworded sentence on death of pine trees for clarity; 2) Provided additional detail on pine tree succession assumptions
		7.4.1	Added additional detail concerning granite weathering for both above and below grade stone
		7.4.2	Added information concerning uprooted wind-thrown trees as a potential erosion barrier degradation mechanism
		7.5.1	Added information concerning the potential for clogging of the filter fabric overlying the lateral drainage layer as a degradation mechanism
		7.8	Added the following open design issues: 1) sufficiency of 50-foot extension of the closure cap beyond the sides of the tanks; 2) Interface of the Lateral drainage layer with the side-slope rip rap; 3) Practicality and benefit of conducting an electrical leak detection survey of the HDPE geomembrane

Revision Number	Date	Sections	Comment
2 (cont.)		8.0	Inserted entirely new section to address FTF Closure Cap degradation and infiltration modeling over 10,000 years
		9.0	1) Reference section became Section 9.0 rather than Section 8.0 as in revision 1 of the document; 2) Added additional references
		Appendix G	All the tables in Appendix G were revised as follows: 1) Divided the foundation layer into an upper and lower layer; 2) Revised HELP model geomembrane placement quality designation to be consistent with HELP model guidance provided by Schroeder et al. 1994a and 1994b; 3) Descriptions of the seven configurations evaluated were revised for clarity
		Appendix H	The tables in Appendix H were essentially entirely rewritten as follows: 1) Divided the foundation layer into an upper and lower layer; 2) Revised HELP model geomembrane placement quality designation to be consistent with HELP model guidance provided by Schroeder et al. 1994a and 1994b; 3) Descriptions of the seven configurations evaluated were revised for clarity; 4) Added detailed water balance data tables for all seven configurations considered
		Appendix I	Inserted entirely new appendix to provide FTF Closure Cap degraded property value calculations
		Appendix J	Inserted entirely new appendix to provide HELP model input for FTF Closure Cap configuration #1a over 10,000 years
		Appendix K	Inserted entirely new appendix to provide the configuration #1a detailed HELP model annual water balance data over time
		Appendix L	Inserted entirely new appendix to provide a detailed probability based root penetration model

TABLE OF CONTENTS

LIST OF FIGURES

LIST OF TABLES

LIST OF ACRONYMS

#	number
%	percent
°C	degrees Celsius
°F	degrees Fahrenheit
η	porosity
θ_v	volumetric moisture content
ψ	suction head
ρ_b	dry bulk density
ρ_p	particle density
A	drainage area in acres
A	constant (in OIT depletion rate equation)
C	runoff coefficient (unitless)
CF	velocity correction factor
cfs	cubic feet per second
cm-H_2O	centimeters of water
cm/s	centimeters per second
D_{50}	median stone diameter
D_{100}	maximum stone diameter
E_a	activation energy of the antioxidant depletion reaction (kJ/mol);
F	flow concentration factor (unitless)
ft	feet
g/m^2-day	grams per square meter per day
g/cm^3	grams per cubic centimeter
H	elevation difference in feet
hr	hour
I	precipitation in inches/hour
in	inches
kPa	kiloPascals
K_{sat}	Saturated Hydraulic Conductivity
L	drainage length in miles
lbs/ft^2	pounds per square foot
mg/L	milligrams/liter
mil	thousandth of an inch
min	minute
mm	millimeter
MPV	maximum permissible velocity
Mrad	megarad (1,000,000 rads)
msl	mean sea level
na	not applicable
No.	number

precip	precipitation
psf	pounds per square foot
psi	pounds per square inch
Q_{cal}	calculated flow
R	hydraulic radius
P	initial geomembrane OIT value
R	universal gas constant (8.31 j/mol)
RH	polymer chain
$R^\bullet$	free radical
$ROO^\bullet$	peroxide free radical
ROOH	hydroperoxides (i.e., oxidized polymer chains)
s	saturation
S	OIT depletion rate
t	time
t_c	time of concentration
T	test temperature in absolute Kelvin (K)
UV	ultraviolet
V	velocity
vol	volume
wt%	weight percent
y	depth in feet
yr	year

AASHTO   American Association of State Highway and Transportation Officials
ASTM   ASTM International (formerly American Society of Testing and Materials)
ATG   Atmospheric Technologies Group
CCL   compacted clay liners
CD   compact disc
CL   sandy clays with low plasticity
CLM   Central Climatology Site
CLSM   Controlled Low Strength Material
CN   runoff curve number
CPT   Cone Penetrometer
CREAMS   Chemicals, Runoff, and Erosion from Agricultural Management Systems
D&D   Decontamination and Demolition
DRI   Desert Research Institute
FTF   F-Area Tank Farm
GDOT   Georgia Department of Transportation
GCL   Geosynthetic Clay Liner
GRI   Geosynthetic Research Institute
GSA   General Separations Area
HDPE   High Density Polyethylene
HELP   Hydrologic Evaluation of Landfill Performance
HMR   Hydrometeorological Report
HP-OIT   high pressure-oxidative induction time
Instal.   Installation
K_{sat} Saturated Hydraulic Conductivity
LLRW   Low-Level Radioactive Waste
LVZ   Lower Vadose Zone
LS   loamy sand
NCSU   North Carolina State University
NIST   National Institutes of Standards and Technology
NRC   Nuclear Regulatory Commission
NWS   National Weather Service
OIT   oxidative induction time
ORWBG   Old Radioactive Waste Burial Ground
PA   Performance Assessments
PGA   peak ground acceleration
PMP   probable maximum precipitation
PVC   polyvinyl chloride
Recirc.   recirculation
Sat. Hyd.   saturated hydraulic
SC   clayey sands
SCL   sandy clay loam
SCS   Soil Conservation Service
SDF   Saltstone Disposal Facility
SL   sandy loams
SM   silty sand

SRL	Savannah River Laboratory
SRNL	Savannah River National Laboratory
SRP	Savannah River Plant
SRS	Savannah River Site
TFBUT	Test Facility – Bentonite Umbrella Test
TIN	Triangulated Irregular Network
USACE	United States Army Corps of Engineers
USCS	Unified Soil Classification System
USDA	United States Department of Agriculture
USEPA	United States Environmental Protection Agency
USGS	United States Geological Survey
WES	Waterways Experiment Station
WSSC	Weathering System Science Consortium
WVT	water vapor transmission
XRD	x-ray diffraction

This page intentionally left blank.

1.0 EXECUTIVE SUMMARY

The F-Area Tank Farm (FTF) closure cap is primarily intended to provide physical stabilization of the site, minimize infiltration, and provide an intruder deterrent. It is anticipated that the closure cap will be installed over all twenty-two waste tanks and associated ancillary equipment at the end of the operational period. Conceptualization of the FTF Closure Cap, initial infiltration estimates through seven different closure cap configurations, and infiltration estimates over 10,000 years through the preferred configuration are provided herein.

Four FTF Closure Cap layouts were evaluated within Section 4.1. The layout selected for further consideration consists of a single FTF Closure Cap over all tank groupings with decontamination and demolition (D&D) of the 242-16F Evaporator Building to an elevation of 298 ft-msl (i.e., to the elevation of the top of the Type IIIA tank condenser housings). Such a layout results in a maximum closure cap slope length of approximately 585 ft. This slope length was utilized as the basis for scoping level calculations conducted to determine closure cap physical stability requirements relative to erosion. The closure cap physical stability requirements (Section 4.2) were determined consistent with Nuclear Regulatory Commission (NRC) requirements relative to erosion potential resulting from a Savannah River Site (SRS) specific probable maximum precipitation (PMP) event (Abt and Johnson 1991 and Johnson 2002). These calculations resulted in a vegetative soil cover with a maximum 2 percent slope over a 585 ft slope length and specified stone sizes and thicknesses for an erosion barrier, side slopes, and toe of the side slopes. Based upon the selected closure cap layout and the requirements for closure cap physical stability, scoping level closure cap conceptual design and constructability are provided in Sections 4.3 and 4.4.

Based upon this scoping level conceptual design, the Hydrologic Evaluation of Landfill Performance (HELP) Model has been utilized to produce 100 annual simulations of the initial infiltration through seven different FTF Closure Cap configurations for annual precipitations ranging from approximately 30 to 60 inches/year (Section 5.0). The summary initial infiltration results for each of the seven configurations are shown in Table 1.

It is recommended that either closure cap configuration #1 or #1a, both of which consist of a composite hydraulic barrier with an overlaying lateral drainage layer and an erosion barrier be utilized as the FTF Closure Cap (Section 6.0). This recommendation is being made for the following reasons:
- It results in the least infiltration to the tanks.
- The use of a composite hydraulic barrier (i.e., high density polyethylene (HDPE) geomembrane underlain by a geosynthetic clay liner (GCL)) provides defense-in-depth by the providing a HDPE geomembrane with a significantly lower saturated hydraulic conductivity underlain by the GCL to plug any holes that may develop in the HDPE geomembrane.
- The use of a lateral drainage layer prevents the buildup of significant hydraulic head over the composite hydraulic barrier, which could lead to significantly more infiltration as the composite hydraulic barrier degrades over time.

- The use of an erosion barrier provides long-term physical stability for the closure cap.
- The only difference between configurations #1 and #1a is the material used to infill the erosion barrier stone. The material to be used to fill the voids between barrier stones has yet to be selected.

Table 1. Summary Initial Infiltration Results

Configuration Number and Description	Average Annual Initial Infiltration (inches/year)	Initial Annual Infiltration Range (inches/year)
#1 Composite barrier, lateral drainage layer, and erosion barrier with controlled low-strength material (CLSM) infill	0.00016	0.00006 to 0.0002
#1a Composite barrier, lateral drainage layer, and erosion barrier with sandy soil infill	0.00088	0.00009 to 0.0049
#2 HDPE geomembrane as sole hydraulic barrier, lateral drainage layer, and erosion barrier with CLSM infill	0.012	0.005 to 0.014
#3 GCL as sole hydraulic barrier, lateral drainage layer and erosion barrier with CLSM infill	0.74	0.32 to 0.89
#4 Composite barrier and erosion barrier with CLSM infill (no lateral drainage layer)	0.019	0.005 to 0.022
#5 Composite barrier and lateral drainage layer (no erosion barrier)	0.00086	0.00008 to 0.0049
#6 Soils only closure cap (no composite barrier, lateral drainage layer, or erosion barrier)	16.45	0.02 to 30.8

An evaluation of potential FTF Closure Cap degradation mechanisms (Section 7.0) has resulted in the identification of the following mechanisms that cannot be appropriately addressed by design and are considered applicable and significant:
- Vegetative cover succession
- Erosion of upper soil layers
- Silting-in of the lateral drainage layer
- Antioxidant depletion, thermal oxidation, and tensile stress cracking of the HDPE geomembrane
- Divalent cation exchange with the sodium bentonite GCL

The impact of these degradation mechanisms on the FTF Closure Cap configuration #1a (composite barrier, lateral drainage layer, and erosion barrier with sandy soil infill) layers have been estimated in terms of material property changes over time. These estimated degraded material properties over time have been inputted to the HELP model (Section 8.0) in order to produce an estimate of the infiltration through the closure cap over time as an input to the FTF PORFLOW vadose zone modeling. The results of this infiltration modeling are provided graphically in Figure 1.
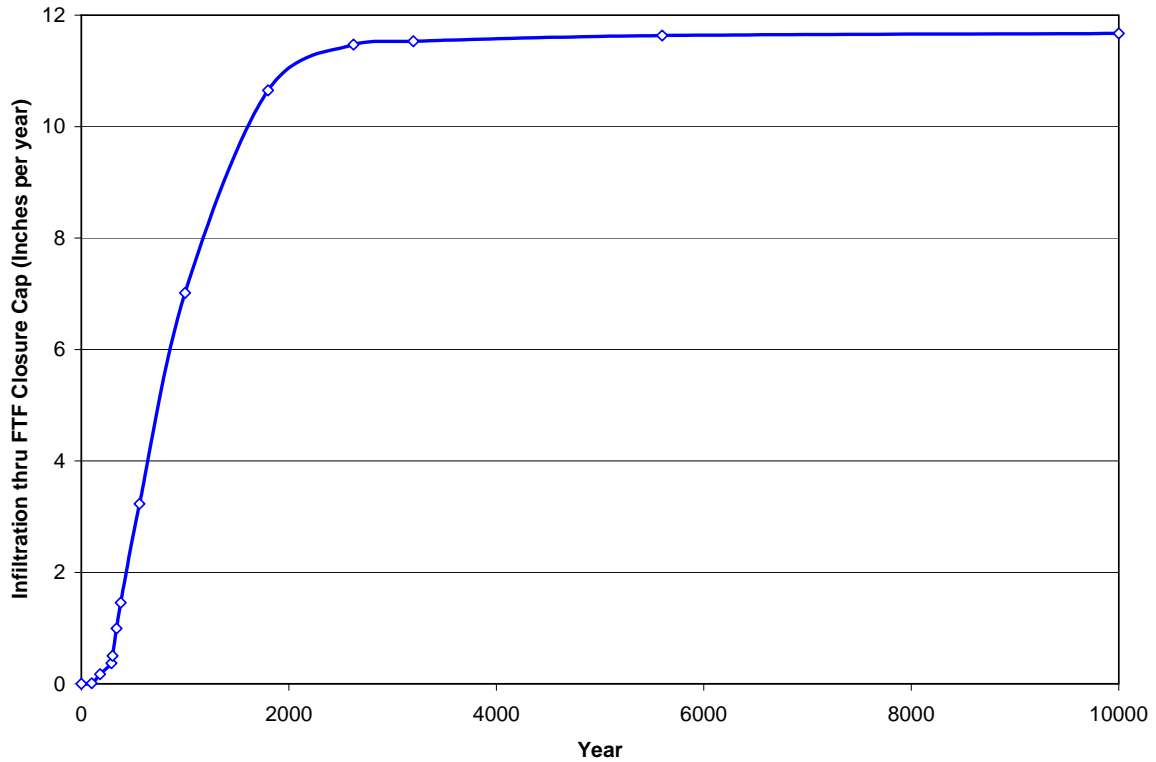
Figure 1. Results of Infiltration Modeling

The closure cap design and infiltration information provided herein is preliminary and conceptual in nature, being consistent with a scoping level concept. Final design and a re-evaluation of infiltration will be performed near the end of the operational period. Technological advances, increased knowledge, and improved modeling capabilities are all likely and will result in improvements in both the closure cap design and infiltration estimates.

This page intentionally left blank.

2.0 INTRODUCTION

The F-Area Tank Farm (FTF) closure cap is primarily intended to provide physical stabilization of the site, minimize infiltration, and provide an intruder deterrent. It is anticipated that the closure cap will be installed over all twenty-two waste tanks and associated ancillary equipment at the end of the operational period. The operational period is that period of time during which waste will be removed from the tanks and the tanks will be grouted up. During the operational period it is assumed that active FTF facility maintenance will be conducted sufficient to prevent infiltration of rainwater into the tanks and subsurface discharge out of the tanks. After installation of the closure cap, it is assumed that a 100-year institutional control period will begin, during which active FTF facility maintenance will be conducted sufficient to prevent pine forest succession and to repair any significant erosion. After the institutional control period, it is assumed that a 10,000-year post-closure compliance period will begin, during which no active FTF facility maintenance will be conducted. A potential exception to the cessation of all active maintenance during the post-closure compliance period involves the use of bamboo as a final vegetative cover. If it is determined that bamboo is a climax species that prevents or greatly slows the intrusion of pine trees, it is assumed that bamboo will be planted as the final vegetative cover at the end of the 100-year institutional control period. If bamboo is planted, maintenance, which may extend into the post-closure compliance period, will be required to establish a dense bamboo ground cover over the entire area. After such a dense bamboo ground cover has been established, all active FTF facility maintenance will cease. Degradation of the closure cap will accelerate once active FTF facility maintenance has ceased.

Conceptualization of the FTF closure cap, initial infiltration estimates through seven different closure cap configurations, and infiltration estimates over 10,000 years through the preferred configuration are provided herein. The closure cap design and infiltration information provided herein is preliminary and conceptual in nature, being consistent with a coping level concept. In other words, it provides sufficient information for planning purposes, to evaluate the closure cap configuration relative to its constructability and functionality, and to estimate infiltration over time through modeling. It is not intended to constitute final design. Final design and a re-evaluation of infiltration will be performed near the end of the operational period. Technological advances, increased knowledge, and improved modeling capabilities are all likely and will result in improvements in both the closure cap design and infiltration estimates.

This page intentionally left blank.

3.0 BACKGROUND

3.1 FTF BACKGROUND

The General Separations Area (GSA) of the Savannah River Site (SRS) is located atop a ridge running southwest-northeast that forms the drainage divide between Upper Three Runs to the north and Fourmile Branch to the south as shown in Figure 2. The GSA contains the F and H-Area Separations Facilities, the S-Area Defense Waste Processing Facility, the Z-Area Saltstone Facility, and the E-Area Low-Level Waste Disposal Facilities. The F-Area Tank Farm (FTF) is located within F-Area in the GSA, as seen in Figure 2. Also as seen in Figure 2, natural surface drainage from the FTF is toward Fourmile Branch. The FTF is a nearly rectangular shaped area comprises approximately 20 acres, which is bounded by SRS coordinates N 76,604.5 to N 77,560.0 and E 52,435.0 to E 53,369.0.

The FTF includes twenty-two waste tanks, which were emplaced between 1951 and 1976. Figure 3 provides an aerial view of the FTF looking southwest toward the 281-8F and 241-97F basins. Figure 4 provides a layout of the FTF tank groups along with the numerical designation of each tank. Figure 5 provides the topography of the FTF and surrounding area. Figure 6 provides a layout of the significant ancillary equipment in relation to the tanks.

In general the construction of each tank group consisted of digging an excavation and stockpiling the excavated soil, emplacing a concrete work slab on the floor of the excavation to provide a stable work platform for tank construction activities, constructing the tanks, and backfilling around the tanks utilizing the previously stockpiled soil. The tanks were installed during four separate construction episodes, with a different tank design for each episode, leading to the designation of the following four different tank groups:

- The first group of eight tanks (tanks 1 through 8), designated Type I Waste Tanks, was constructed in 1951. The backfill around this group of tanks extends approximately 9 ft above the flat topped tanks to a finished grade ranging from 274 to 282 ft-msl.
- The second group of four tanks (tanks 17-20), designated Type IV Waste Tanks, was constructed in 1956. Approximately 2-ft 8-in of backfill was placed over the domed tank tops to a finished grade ranging from 268 to 277. Additionally the concrete 242-F evaporator building, the top of which is at an elevation of 293.5 ft-msl, was built in the center of this grouping of four tanks.
- The third grouping of two tanks (tanks 33 and 34), designated Type III Waste Tanks, was constructed in 1969. The backfill around this group of tanks extends to the top of the tank perimeter walls but does not cover the sloping tank top itself. The finished grade, including the tank tops, of this grouping ranges from 283 to 285 ft-msl.
- The fourth and final group of eight tanks (tanks 25-28 and 44-47), designated Type IIIA Waste Tanks, was constructed in two phases in 1975 and 1976, respectively. The backfill around this group of tanks also extends to the top of the tank perimeter walls but does not cover the sloping tank top itself. The finished grade, including the tank tops, of this grouping ranges from 285 to 288 ft-msl. Additionally the concrete 242-16F evaporator building, the top of which is at an elevation of 325.67 ft-msl, was built in the middle of this grouping of eight tanks.

Within the FTF a maximum elevation difference of 20 ft exists in the finished grade between tank groupings. An elevation difference of 57.67 ft exists between the top of the 242-16F evaporator building and the lowest finished grade elevation in the FTF (i.e., tank group 2 (tanks 17-20)). The following types of ancillary equipment are associated with the FTF in addition to the evaporator buildings previously mentioned: the catch tank, pump pits, and diversion boxes. Table 2, Table 3, and Table 4 provide pertinent information regarding the location and elevation of the tanks, concrete housings on top of the tanks, and significant ancillary equipment, respectively. Significant ancillary equipment are those that have been designated as requiring intruder protection in association with the closure cap due to the anticipated left-in-place radionuclide inventory. Significant ancillary equipment include the evaporator buildings, catch tank, and pump pits. The diversion boxes are not considered significant ancillary equipment requiring intruder protection. Additionally waste transfer lines will also require intruder protection. Most existing waste transfer lines are located below current grade; however a few above grade waste transfer lines, such as that associated with Tank 7, exist which will require consideration to ensure that they receive the proper intruder protection.
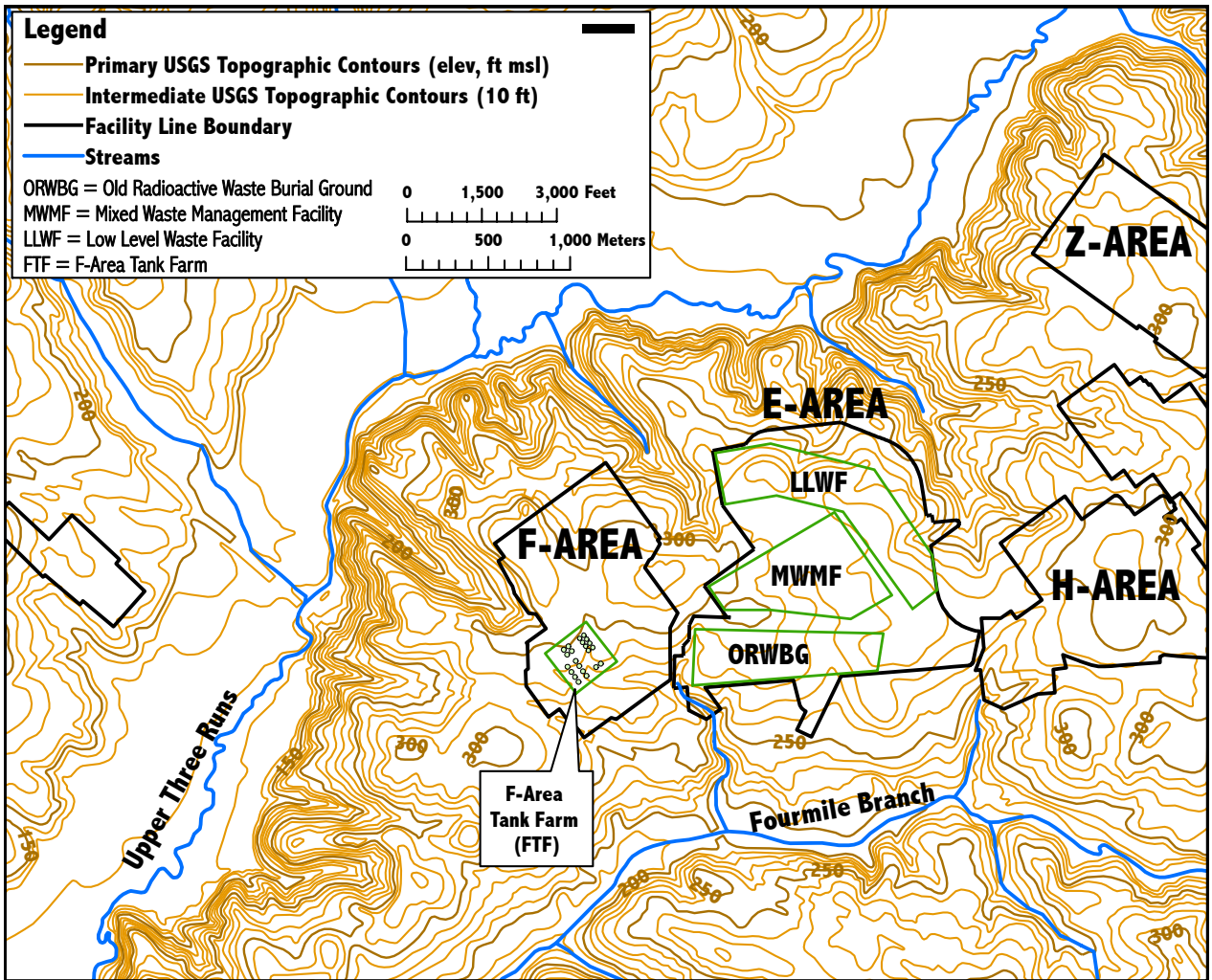
Figure 2. General Separations Area (GSA) Topography and FTF Location

Figure 3.   FTF Aerial View
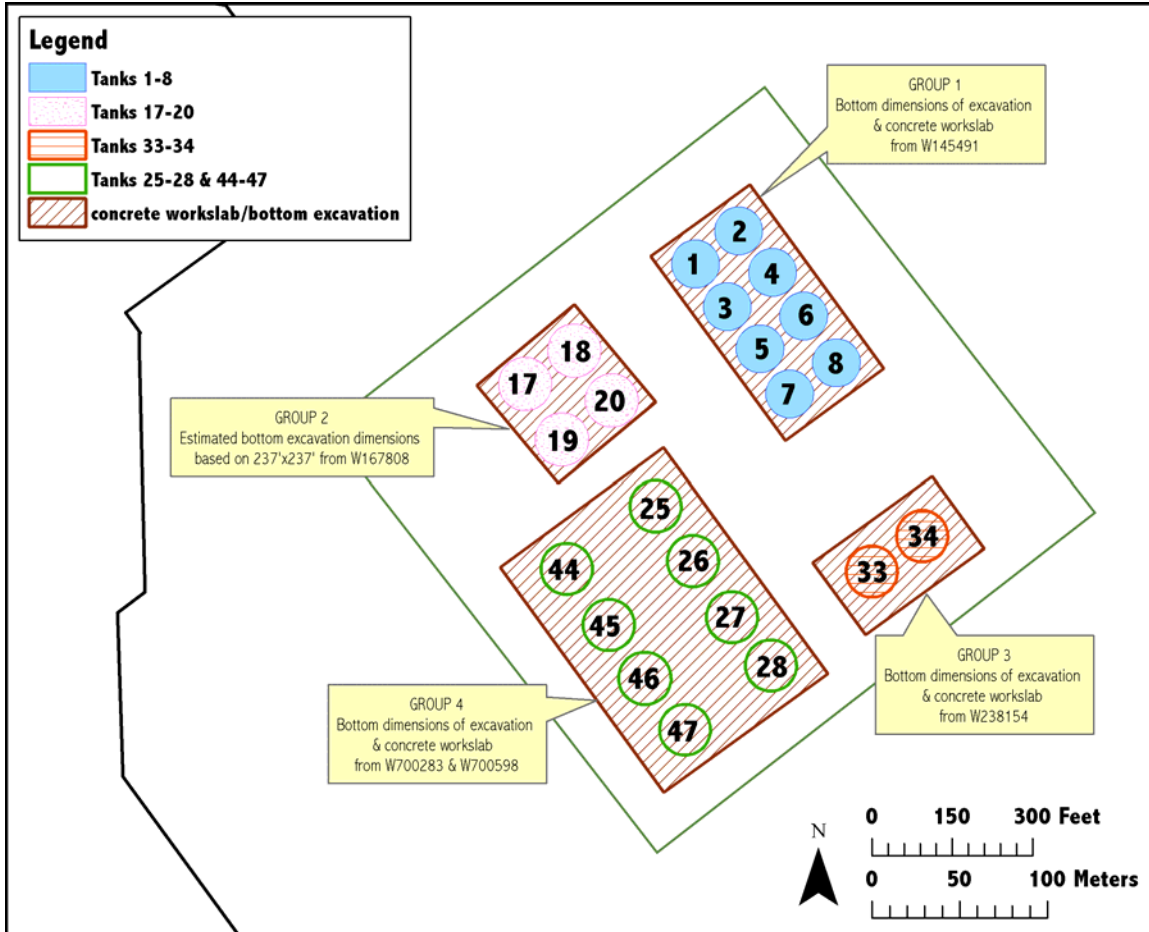
Figure 4. FTF Tank Layout

Figure 5.   FTF Topography
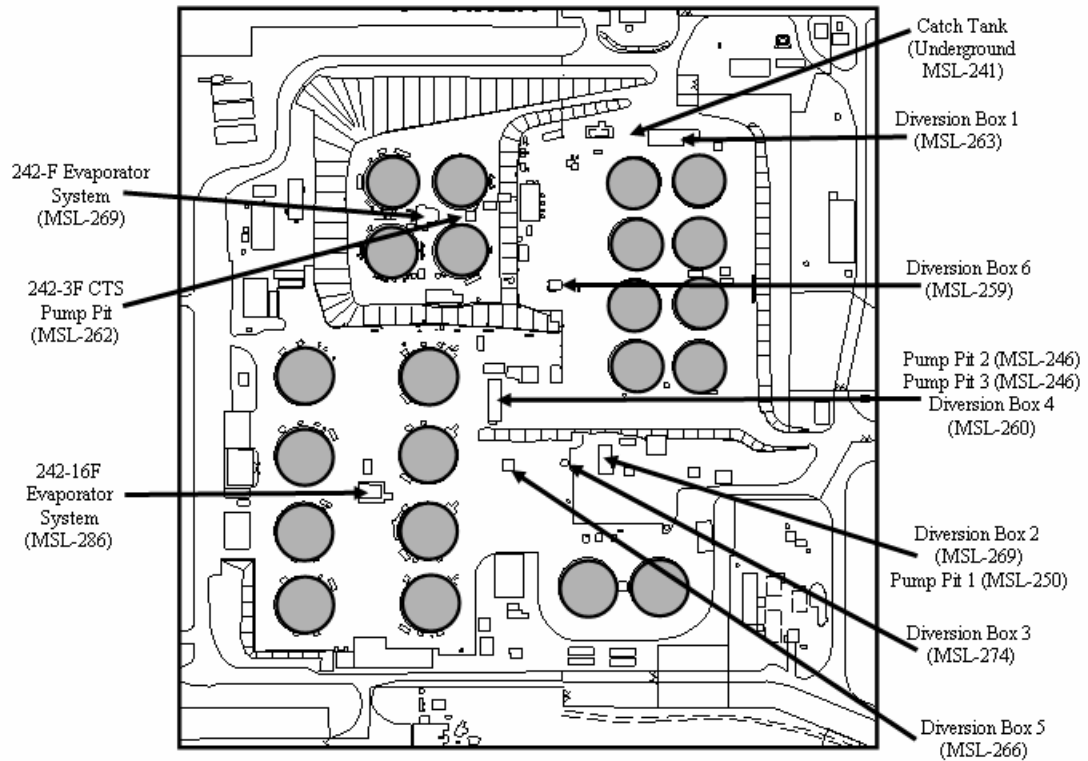
Figure 6. FTF Significant Ancillary Equipment Layout

All elevations shown on Figure 6 are bottom elevations of the ancillary equipment in feet above mean sea level.

Table 2. FTF Tank Locations and Elevations

FTF Tank	Tank Outside Radius	Reference Drawings	Tank Center SRS North (ft)	Tank Center SRS East (ft)	Top of Tank Center Elevation (ft-msl)	Top of Tank Perimeter Elevation (ft-msl)	Elevation of Finished Grade at Tank Center (ft-msl)	Elevation of Finished Grade at Tank Perimeter (ft-msl)	Range of Tank Grouping Finished Grade Elevation (ft-msl)	Reference Drawings
1	41.92	W145225	77385.0	53116.0	271.2	271.2	280	variable	274 to 282	W715441
2	41.92	W145225	77385.0	53220.0	271.2	271.2	280	variable	274 to 282	W715441
3	41.92	W145225	77285.0	53116.0	269.8	269.8	278.5	variable	274 to 282	W715441
4	41.92	W145225	77285.0	53220.0	269.8	269.8	278.5	variable	274 to 282	W715441
5	41.92	W145225	77185.0	53116.0	268.4	268.4	277	variable	274 to 282	W715441
6	41.92	W145225	77185.0	53220.0	268.4	268.4	277	variable	274 to 282	W715441
7	41.92	W145225	77085.0	53116.0	268 [1]	268 [1]	275.5	variable	274 to 282	W715441
8	41.92	W145225	77085.0	53220.0	268 [1]	268 [1]	275.5	variable	274 to 282	W715441
17	44.53	W167477	77385.0	52723.0	277.83 [2]	265.12 [3]	277.08	269.5	268 to 277	W166430, W167477
18	44.53	W167477	77385.0	52835.0	277.83 [2]	265.12 [3]	277.08	269.5	268 to 277	W166430, W167477
19	44.53	W167477	77273.0	52723.0	276.91 [2]	264.2 [3]	276.16	268.5	268 to 277	W166430, W167477
20	44.53	W167477	77273.0	52835.0	276.91 [2]	264.2 [3]	276.16	268.5	268 to 277	W166430, W167477
33	47.5	W238163	76723.3	53040.5	285.2	284.2	285.2	284.2	283 to 285	W238155, W238875
34	47.5	W238163	76723.3	53155.5	285.2	284.2	285.2	284.2	283 to 285	W238155, W238875
25	47.5	W700813	77070.0	52785.0	286.65	285.65	286.65	285.65	285 to 288	W700159, W701330, W703129
26	47.5	W700813	76940.0	52785.0	288	287	288	287	285 to 288	W700159, W701330, W703129
27	47.5	W700813	76815.0	52785.0	288	287	288	287	285 to 288	W700159, W701330, W703129
28	47.5	W700813	76695.0	52785.0	286.65	285.65	286.65	285.65	285 to 288	W700159, W701330, W703129
44	47.5	W706442	77070.0	52585.0	286.33	285.33	286.33	285.33	285 to 288	W700159, W701330, W703129
45	47.5	W706442	76940.0	52585.0	287.76	286.76	287.76	286.76	285 to 288	W700159, W701330, W703129
46	47.5	W706442	76815.0	52585.0	287.76	286.76	287.76	286.76	285 to 288	W700159, W701330, W703129
47	47.5	W706442	76695.0	52585.0	286.33	285.33	286.33	285.33	285 to 288	W700159, W701330, W703129

[1] Might be 267 ft-msl rather than 268 ft-msl (ft-msl = feet mean sea level)
[2] Elevation of tank center riser
[3] Elevation of top of dome ring

Table 3. Concrete Housings on Top of the Tanks

FTF Tank	Description of Primary High Point Concrete Housing on Tank	Primary High Point Elevation (ft-msl)	Description of Secondary High Point Concrete Housing on Tank	Secondary High Point Elevation (ft-msl)
1	2'-6" risers (W149522)	282.1	2' and 3'-6" risers (W149522)	< 282.1
2	2'-6" risers (W149522)	282.1	2' and 3'-6" risers (W149522)	< 282.1
3	2'-6" risers (W149522)	280.7	2' and 3'-6" risers (W149522)	< 280.7
4	2'-6" risers (W149522)	280.7	2' and 3'-6" risers (W149522)	< 280.7
5	2'-6" risers (W149522)	279.3	2' and 3'-6" risers (W149522)	< 279.3
6	2'-6" risers (W149522)	279.3	2' and 3'-6" risers (W149522)	< 279.3
7	2'-6" risers (W149522)	278.9	2' and 3'-6" risers (W149522)	< 278.9
8	2'-6" risers (W149522)	278.9	2' and 3'-6" risers (W149522)	< 278.9
17	center riser (W167477)	277.83	na	na
18	center riser (W167477)	277.83	na	na
19	center riser (W167477)	276.91	na	na
20	center riser (W167477)	276.91	na	na
33	duct and riser (W238157)	294.2	condenser concrete shielding (W237814)	291.2
34	duct and riser (W238157)	294.2	condenser concrete shielding (W237814)	291.2
25	condenser housing (W700813)	296.65	duct and riser (W701310)	295.07
26	condenser housing (W700813)	298	duct and riser (W701310)	296.42
27	condenser housing (W700813)	298	duct and riser (W701310)	296.42
28	condenser housing (W700813)	296.65	duct and riser (W701310)	295.07
44	condenser housing (W706442)	296.33	duct and riser (W706441)	294.75
45	condenser housing (W706442)	297.76	duct and riser (W706441)	296.18
46	condenser housing (W706442)	297.76	duct and riser (W706441)	296.18
47	condenser housing (W706442)	296.33	duct and riser (W706441)	294.75

Notes:

The reference drawing is provided in parenthesis

na = not applicable

Table 4. FTF Significant Ancillary Equipment Locations and Elevations

Ancillary Equipment Bldg # & Name	SRS North (ft)	SRS East (ft)	Description of Location	Elevations (ft-msl)	Description of Elevation
Catch Tank	77476.0	53081.0	northeast corner (W715441)	258.29	top of concrete roof (W146075, W146600)
	77457.0	53037.0	southwest corner (W146600)		
242-F Evaporator Building and Pot	77329.0	52779.0	Building center-line (W236139, W166430)	294.5	top of removable concrete roof slabs (W230284)
	77329.0	52784.0	Evaporator pot center-line (W236139)	293.5	top of concrete walls (W230284)
242-3F CTS Pump Pit	77329.0	52851.7	Building center-line (W236128, W236135))	268.83	top concrete slab (W236128
Pump Pit #1 and Diversion Box #2	76954.3	53078.0	northeast corner (W235643)	279.5	top of concrete roof (W235643. W235647)
241-21F Pump Pits #2 and #3 and Diversion Box #4	77062.0	52901.0	northeast corner (W701347)	277.58	top of concrete wall (W701670)
	77062.0	52881.0	northwest corner (W701347)		
	76995.0	52881.0	southwest corner (W701347)		
	76995.0	52901.0	southeast corner (W701347)		
242-16F Evaporator Building and Pot	76877.6	52697.6	Evaporator pot center-line (W700159)	325.67	top of concrete walls and removable roof slabs (W703022, W704039)
				310.17	top of upper floor concrete slab (W703022, W704039)
				287.67	top of ground floor concrete slab (W703022, W704039)

Note: The diversion boxes are not considered significant ancillary equipment since they have not been designated as requiring intruder protection. Therefore diversion boxes 1, 3, 5, and 6, which are not associated with a significant ancillary equipment item, are not included in the table.

3.2 BACKGROUND WATER BALANCE AND INFILTRATION STUDIES

Numerous water balance and infiltration studies have been conducted in and around the Savannah River Site (SRS) by various organizations including the Savannah River Laboratory (SRL), the United States Geological Survey (USGS), the State University of New York at Brockport, the Pennsylvania State University, the University of Arizona, and the Desert Research Institute (DRI). Finding from eight such studies are reported in Section 3.2.1 and summarized in Section 3.2.2.

3.2.1 Background Water Balance and Infiltration Studies Findings

Cahill 1982
The USGS (Cahill 1982) conducted a study at the Barnwell Low-Level Radioactive Waste (LLRW) Disposal Facility "to determine the geologic and hydrologic conditions near the burial site and to measure migration of leachates from buried waste into the surrounding unconsolidated sediments." The Barnwell LLRW Disposal Facility is located immediately to the east of the Savannah River Site (SRS). As part of this study hydrologic budget estimates were made. Precipitation estimates for the Barnwell facility were based upon the National Weather Service (NWS) station near Blackville, South Carolina. The mean annual precipitation reported from this station for the years 1951 to 1980 was 46.62 inches. Aquifer recharge (i.e., infiltration) estimates were made based upon measurements of discharge to local streams (i.e., stream flow measurements over defined steam reaches). It was assumed that on average aquifer recharge (i.e. infiltration) was equal to discharge from the aquifers to local streams.

Cahill (1982) made three infiltration estimates based upon stream flow measurements over defined steam reaches of Marys Branch Creek, Lower Three Runs, and the Duncannon Creek. Table 5 provides the results of the infiltration estimates made by Cahill (1982). Cahill (1982) concluded that infiltration "appears to range from about 14 to 17 inches/year." Based upon these infiltration estimates Cahill (1982) selected an infiltration rate of 15 inches/year to utilize within a 3-dimensional finite-difference groundwater flow model of the Barnwell facility. For the Barnwell facility Cahill (1982) stated, "Overland flow" (i.e., runoff) "is rare, occurring only during intense rainfall where forest litter has been removed, as in cultivated fields and along roadways." Therefore, Cahill (1982) assumed essentially no runoff from the Barnwell facility. Although evaporation measurements using 4-foot diameter pans were made at the NWS station and at the Barnwell facility, this data was not utilized by Cahill (1982) to make an estimate of evapotranspiration. The evapotranspiration estimate was made simply by subtracting the infiltration and runoff estimates from the average annual precipitation. In summary Cahill (1982) reported that of the mean annual precipitation of 46.62 inches (1951 to 1980) at the Barnwell facility about 60 to 70 percent of it returned to the atmosphere by evapotranspiration (i.e., 28 to 32.6 inches), 30 to 40 percent became infiltration (i.e,. 14 to 19 inches), and essentially 0 percent became runoff.

Table 5.   Barnwell LLRW Disposal Facility Infiltration Estimates by Cahill (1982)

Stream	Infiltration Estimate (inches/year)	Cahill (1982) Comment
Marys Branch Creek	14.5	This estimate may be low since some underflow may not be accounted for
Lower Three Runs	17.6	This estimate may be high due to the effect of leakage from Par Pond
Duncannon Creek	14	This estimate may be low since some underflow may not be accounted for

Hubbard and Emslie 1984
The State University of New York at Brockport in conjunction with the Savannah River Laboratory (SRL) (Hubbard and Emslie 1984) conducted a water budget evaluation for the Savannah River Plant (SRP) Old Radioactive Waste Burial Ground (ORWBG). Precipitation was measured at F-Area from 1963 to 1973 and at the ORWBG from 1974 to 1982. An average annual precipitation of 47.32 inches/year was measured during this time period (1963 to 1982). Evapotranspiration was evaluated by four different methods as outlined in Table 6. Although the average evapotranspiration for the four methods of estimation was 32.57 inches/year, Hubbard and Emslie (1984) took an evapotranspiration of 30 inches/year for determination of an estimated infiltration. Runoff was estimated at 2 inches/year based upon stream flow records, a soil survey inspection, and visual observations of runoff at the ORWBG. Infiltration was estimated by subtracting evapotranspiration and runoff from the average annual precipitation, resulting in an estimated value of 15 inches/year. Based upon these estimates Hubbard and Emslie (1984) produced the following annual water balance for the ORWBG:

- Precipitation = 47 inches/year
- Evapotranspiration = 30 inches/year
- Runoff = 2 inches/year
- Infiltration = 15 inches/year

Table 6. Evapotranspiration Estimates by Hubbard and Emslie (1984)

Method of Estimation	Evapotranspiration (inches/year)
Stream basin water balance method: The streamflow of three nearby streams (South Fork of the Edisto River, Upper Three Runs Creek, and Marys Branch) expressed as water yield in inches was subtracted from the average annual precipitation	31.17
Thornthwaite Method based upon the average monthly temperature and precipitation	36.13
1974 through 1978 monthly evaporation pan data from Blacksville, South Carolina multiplied by monthly pan coefficients developed at the USDA research watersheds at Tifton, Georgia	33.27
SRP ORWBG lysimeter water balance data	29.7
Average	**32.57**

Hubbard 1986

The State University of New York at Brockport in conjunction with the Savannah River Laboratory (SRL) (Hubbard 1986) provided an updated ORWBG water balance based upon an evaluation of five years worth of data from the Defense Waste Lysimeter study modified with data from evaporation pan climatic data and other watershed, lysimeter, and runoff studies. The Defense Waste Lysimeters were six or ten foot in diameter, were filled with soil from the ORWBG, and did not allow runoff because the lysimeters extended above the ground surface. The vegetative cover of most lysimeters consisted of a sparse coverage of bahia grass and herbaceous plants, however some of the ten-foot diameter lysimeters contained 10 to 14 foot high pine trees. Analysis of five and a half years worth of data resulted in the following average annual water balance for the Defense Waste Lysimeters from 1980 through 1985:

- Rainfall = 47.0 inches/year
- Infiltration and runoff = 19.6 inches/year
- Evapotranspiration = 27.4 inches/year

Hubbard (1986) considered the following data in arriving at an estimated ORWBG water balance:

- Runoff estimates from other sources ranging from1 to 3 inches/year
- Other evapotranspiration estimates ranging from 30 to 34 inches/year

Based upon this data Hubbard (1986) produced the following estimated annual water balance for the ORWBG:

- Precipitation = 48 inches/year
- Evapotranspiration = 30 inches/year
- Runoff = 2 inches/year
- Infiltration = 16 inches/year

Hubbard (1986) also made the following observations regarding the water balance data produced from the Defense Waste Lysimeters:

"Lysimeter studies indicate that about 12 inches more water is lost annually to the atmosphere by evapotranspiration with deep-rooted pine trees present than in areas where bare soil or shallow-rooted grass cover occur. … "In forested areas near the burial ground, evapotranspiration is estimated to be about 40 inches annually, and therefore recharge to the water table is about 6 inches."

Parizek and Root 1986
The Pennsylvania State University (Parizek and Root 1986) conducted a hydrologic water budget study of the McQueen Branch watershed, located in the central portion of the SRS as part of the development of a groundwater model. The McQueen Branch watershed consisted of approximately 67% pine trees, 18% hardwood, 15% grass and unvegetated of which approximately 2% are impervious surfaces such as pavement. The field study was conducted from November 1, 1982 to May 18, 1984. In order to arrive at the hydrologic water budget Parizek and Root (1986) measured precipitation within the watershed; took stream flow measurements in order to determine the stream baseflow and runoff; calculated runoff from impervious areas; took water level measurements within water table wells in order to determine changes in groundwater storage; took soil-moisture measurements in order to determine changes in vadose zone water storage; estimated evapotranspiration using the Penman-Monteith evaporation method based upon watershed weather and vegetation data; estimated underflow through the McBean beneath the stream gauge; and estimated leakage through the Green Clay aquitard. Table 7 provides the three hydrologic water budgets that Parizek and Root (1986) produced from their study: annual water budget based upon >18 months of data; annual water budget based upon 13 months of data; and assumed average annual water budget.

Table 7. Parizek and Root (1986) McQueen Branch Watershed Water Budget Summary

Water Budget Parameter	>18 Month Annual Water Budget (inches/year)	13 Month Annual Water Budget (inches/year)	Assumed Average Annual Water Budget (inches/year)
Precipitation	52.40	48.44	47.78
Runoff	3.41	3.32	2
Evapotranspiration	34.07	30.95	30.78
Infiltration	15.26	14.17	15

Hubbard and Englehardt 1987

The State University of New York at Brockport in conjunction with the University of Arizona (Hubbard and Englehardt 1987) utilized the Chemicals, Runoff, and Erosion from Agricultural Management Systems (CREAMS) model to produce estimated annual water balances for the SRP Burial Ground utilizing site specific weather data from 1961 to 1986. "The CREAMS model was developed by the US Department of Agriculture Research Service for the Environmental Protection Agency under the Clean Water Act, to give "reasonable estimates" of the water balance used to calculate diffuse pollution transported with surface runoff in small, cropped agricultural areas." Additionally the infiltration, percolation, and evapotranspiration routines of the HELP model (Schroeder et al. 1994b) are almost identical to those used in the CREAMS model. Table 8 provides the CREAMS water balance produced for the minimum, average, and maximum site-specific precipitation recorded from 1961 to 1986.

Table 8. SRP Burial Ground Estimated Water Balance from 1961 to 1986

Parameter	Precipitation (inches/year)	Runoff (inches/year)	Evapotranspiration (inches/year)	Infiltration (inches/year)
Minimum	34.67	0.13	29.06	4.97
Average	48.51	1.21	32.60	14.70
Maximum	71.88	4.12	35.92	32.14
Standard Deviation	8.73	0.90	2.64	6.04

Dennehy and McMahon 1989

The United States Geological Survey (USGS) (Dennehy and McMahon 1989) conducted a study at the Barnwell Low-Level Radioactive Waste (LLRW) Disposal Facility "of water movement in and adjacent to trenches excavated in the unsaturated zone and assesses the principal factors affecting this movement." The Barnwell LLRW Disposal Facility is located immediately to the east of the Savannah River Site (SRS). As part of this study hydrologic budget estimates were made for an undisturbed portion of the site. The mean annual precipitation reported from the NWS station near Blackville, South Carolina station for the years 1883 to 1983 was 47.8 inches (121.5 cm). However precipitation at the Barnwell facility was also measured with an onsite meteorologic station. Precipitation for the study period from July 1983 through June 1984 was measured at 56.7 inches (144 cm) with the on-site station. The actual evapotranspiration was estimated using the Bowen ratio/energy budget method with necessary input variables measured with the on-site meteorologic station. Evapotranspiration for the study period from July 1983 through June 1984 was estimated at 39.8 inches (101 cm) using this methodology.

"Zero runoff was assumed to have occurred during this period." "The net change in the unsaturated zone was negligible", based upon tensiometer measurements. "The hydrologic budget is given by the equation $R = P - ET - RO \pm dS/dt$ where R = recharge to the saturated zone; P = precipitation ET = evapotranspiration; RO = runoff; and dS/dt = storage changes in the unsaturated zone. Based upon this equation, the recharge (i.e. infiltration) for the study period from July 1983 through June 1984 was estimated at 16.9 inches (43 cm). Based upon a mean annual precipitation of 47.8 inches, the results of this study, and an assumption of a linear relationship between precipitation, and evapotranspiration and infiltration, a mean annual evapotranspiration and infiltration of 33.5 and 14.3, respectively, result. Where land surface conditions are different such that measurable runoff is possible, Dennehy and McMahon (1989) assume that infiltration would probably be less.

Young and Pohlmann 2001
The Desert Research Institute (DRI) (Young and Pohlmann 2001) conducted both deterministic and probabilistic (100 Monte Carlo runs) modeling utilizing the computer code HYDRUS 2-D (finite difference model solving Richard's equation) to estimate infiltration at the Savannah River Site (SRS) E-Area. Estimates of evapotranspiration were made using the model of Feddes et al. (1978). The following types of data were utilized as input to the modeling effort:
- E-Area stratigraphic layering based upon cone penetrometer (CPT) data
- E-Area soil texture, saturated hydraulic conductivity, and water retention properties determined from the laboratory testing of undisturbed soil samples taken with depth
- E-Area soil water content with depth from water content reflectometer and neutron probe measurements
- E-Area soil water potential (matrix potential) with depth from tensiometers
- Meteorological data from weather stations at SRS and Augusta, Georgia

Based upon this methodology Young and Pohlmann 2001 produced the following estimated E-Area infiltration:
- The deterministic modeling resulted in an infiltration estimate of 9.5 inches/year.
- The probabilistic (100 Monte Carlo runs) modeling resulted in a median infiltration estimate of 9.1 inches/year with a 90% confidence interval of 8.1 to 9.8 inches/year.

While the modeling effort by Young and Pohlmann (2001) produced evapotranspiration estimates in the process of estimating infiltration, they did not report their evapotranspiration estimates within the document. However based upon their infiltration estimates, the associated evapotranspiration estimates would have had to be relatively high (at least in the 30s of inches/year range).

Young and Pohlmann 2003

The Desert Research Institute (Young and Pohlmann 2003) refined the modeling that they performed in 2001 (Young and Pohlmann 2001) by the following:

- Incorporating addition E-Area soil texture, saturated hydraulic conductivity, and water retention data determined from the laboratory testing of undisturbed soil samples taken with depth
- By apportioning potential evaporation between soil evaporation and plant transpiration
- Considering plant cover at 0, 50, and 100 percent

They conducted probabilistic (100 Monte Carlo runs) modeling utilizing the computer code HYDRUS 2-D (finite difference model solving Richard's equation) to estimate infiltration at the Savannah River Site (SRS) E-Area under conditions of 0, 50, and 100 percent plant cover. Estimates of evapotranspiration were made using the model of Feddes et al. (1978).

Based upon this methodology Young and Pohlmann 2003 produced E-Area infiltration estimates of 11.7, 7.1, and 5.0 inches/years for plant cover of 0, 50, and 100 percent, respectively.

While the modeling effort by Young and Pohlmann (2003) produced evapotranspiration estimates in the process of estimating infiltration, they did not report their evapotranspiration estimates within the document. However based upon their infiltration estimates, the associated evapotranspiration estimates would have had to be relatively high (at least in the 30s of inches/year range).

3.2.2 Background Water Balance and Infiltration Studies Summary

Eight water balance and infiltration studies were evaluated. They included both field and modeling studies and ranged in scale from 55-gallon drum lysimeters to entire watersheds. Table 9 provides the nominal water balance and infiltration estimate produced from each of the eight studies along with the median of the nominal water balance values of the eight Studies. Table 10 provides the range of values reported by Hubbard and Englehardt (1987) for precipitation ranging from 34.7 to 71.9 inches/year. As seen in Table 9 and Table 10, precipitation is distributed, in decreasing order, into evapotranspiration, infiltration, and runoff. Precipitation is seen to range from 35 to 72 inches/year with a median of the eight studies nominal values of 47.8 inches/year. Evapotranspiration is seen to range from 29 to 36 inches/year with a median of the eight studies nominal values of 31.2 inches/year. Infiltration is seen to range from 5 to 32 inches/year with a median of the eight studies nominal values of 14.8 inches/year. Runoff constitutes very little of the water balance; it is seen to range from 0.1 to 4 inches/year with a median of the Eight studies nominal values of 1.6 inches/year. Clearly evapotranspiration dominates the water balance distribution of precipitation at the SRS.

Table 9. Nominal Water Balance and Infiltration Estimate Produced from each of Eight Studies [1]

Source	Nominal Annual Precipitation (inches/year)	Nominal Annual Runoff (inches/year)	Nominal Annual Evapotranspiration (inches/year)	Nominal Annual Infiltration (inches/year)
Cahill (1982)	46.62	0	31.62	15
Hubbard and Emslie (1984)	47	2	30	15
Hubbard (1986)	48	2	30	16
Parizek and Root (1986)	47.78	2	30.78	15
Hubbard and Englehardt (1987)	48.51	1.21	32.60	14.70
Dennehy and McMahon (1989)	47.8	0	33.5	14.3
Young and Pohlmann (2001)	10-year Augusta, GA data from 1977 to 1987	Assumed to be 0	Determined but not reported within the document [2]	9.1
Young and Pohlmann (2003)	10-year Augusta, GA data from 1977 to 1987	Assumed to be 0	Determined but not reported within the document [2]	11.7
Median of the eight Studies Nominal Values [3]	47.79	1.6	31.2	14.85

[1] All of these studies assumed that the change in water storage was a minor water budget component

[2] Based upon the infiltration estimates, the associated evapotranspiration estimates would have had to be relatively high (at least in the 30s of inches/year range).

[3] The median of the eight studies nominal values does not include precipitation, runoff, and evapotranspiration from Young and Pohlmann (2001 and 2003)

Table 10. Hubbard and Englehardt (1987) Water Balance Range

Parameter	Precipitation (inches/year)	Runoff (inches/year)	Evapotranspiration (inches/year)	Infiltration (inches/year)
Range	34.7 to 71.9	0.1 to 4.1	29.1 to 35.9	5.0 to 32.1

4.0 FTF CLOSURE CAP SCOPING LEVEL CONCEPT

The FTF closure cap is primarily intended to provide physical stabilization of the site, to minimize infiltration, and to provide an intruder deterrent. It is anticipated that the closure cap will be installed over all twenty-two waste tanks and associated ancillary equipment at the end of the operational period. Final closure will consist of site preparation and construction of an integrated closure system composed of one or more closure caps installed over all the waste tanks and significant ancillary equipment and a drainage system. The closure cap design and installation will take into account the waste tank and ancillary equipment characteristics and location, disposition of non-disposal structures and utilities, site topography and hydrogeology, potential exposure scenarios, and lessons learned implementing other closure systems, including other Savannah River Site (SRS) facilities and Uranium Mill Tailings sites.

The FTF is currently in the operational period, during which waste will be removed from the tanks and the tanks will be grouted. It is currently anticipated that the operational period will last to some time between 2020 and 2030. The closure cap information provided herein is consistent with the level of detail associated with a scoping level concept. That is this report provides sufficient information for planning purposes and to evaluate the closure cap configuration relative to its constructability and functionality, but it is not intended to constitute final design. Final design will not be performed until near the end of the operational period prior to actual installation of the closure cap. Technological advances in materials and closure cap design may necessitate that changes to the FTF closure cap concept discussed herein be made at the time of final design. Additionally as more material property data becomes available, the material property data utilized for modeling will be updated to be consistent with the advances in knowledge. Any such changes will be considered acceptable so long as the overall closure cap performance is equivalent to or better than that discussed herein in terms of site physical stabilization, infiltration minimization, and the provision of an intruder deterrent. An independent Professional Engineer will be retained by SRS to certify that the FTF closure system has been constructed in accordance with the approved closure plan and the final drawings, plans, and specifications at the time of closure.

4.1 FTF CLOSURE CAP SCOPING LEVEL LAYOUT

A scoping level evaluation of the FTF closure cap layout was conducted in order to determine the following:

- Whether or not the tank groupings could be covered with individual closure caps over each grouping.
- The maximum slope length that should be considered for the closure cap physical stability conceptualization and for determination of the infiltration through the closure cap.

Four potential closure cap layouts were evaluated based upon the following three assumptions:

- D&D of significant concrete structures on the waste tanks (Table 3), of the 242-F and 242-16F concrete evaporator buildings (Table 4), and of other significant ancillary equipment (Table 4) should be minimized to the extent practicable.
- Intruder protection provided by the closure cap will be required over the tanks (Table 2 and Table 3), the evaporator buildings, the catch tank, and pump pits (Table 4). Intruder protection provision by the closure cap is taken to mean that a minimum of 10 ft of clean material must overlie the item being protected.
- The closure cap is assumed to have the following characteristics:
  - Maximum top surface slopes of 1.5%
  - Maximum side slopes of 33.3%
  - Extend a minimum of 50 ft out from the outside wall of all tanks
  - Minimum thickness of 13 ft over items requiring intruder protection (10 ft between the top of the item and the top of an erosion barrier for intruder protection plus 3 ft of soil above the erosion barrier for water storage for the promotion of evapotranspiration)

4.1.1 Closure Cap Layout Scenario #1:

The first potential closure cap layout evaluated was that of a separate closure cap over each of the four tank grouping (i.e., 1-8, 17-20, 33-34, and 25-28/44-47) with minimal D&D of the 242-16F Evaporator Building and drainage in between the separate closure caps. For this scenario the top of the 242-16F Evaporator Building was assumed to be removed down to an elevation of 310.17 ft-msl (i.e., down to the top of the upper floor concrete slab (Table 4)). Figure 7 presents the results of this layout evaluation. Due to the significant elevation differences between the high points associated with each tank grouping, it is virtually impossible to have appropriate side slopes (i.e. maximum 33.3%) and drainage between any of the tank groupings. Additionally excavation would likely be required in the areas between tank groupings to achieve proper drainage. Finally such closure caps would not cover diversion boxes 3, 5, and 6 nor any waste transfer lines between tank groupings.

4.1.2 Closure Cap Layout Scenario #2:

The second layout evaluated was also that of a separate closure cap over each of the four tank grouping (i.e. 1-8, 17-20, 33-34, and 25-28/44-47) with D&D of the 242-16F Evaporator Building and drainage in between the separate closure caps. For this scenario the top of the 242-16F Evaporator Building was assumed to be removed down to an elevation of 298 ft-msl (i.e., down to the top of the Type IIIA tank (i.e. tanks 25-28/44-47) condenser housings (Table 3)). Figure 8 presents the results of this layout evaluation.

Due to the significant elevation differences between the high points associated with each tank grouping, it is virtually impossible to have appropriate side slopes and drainage between tank groupings 17-20 and 25-28/44-47 and between tank groupings 1-8 and 33-34. Additionally excavation would likely be required in the areas between tank groupings to achieve proper drainage. Finally such closure caps would not cover diversion boxes 3, 5, and 6 nor any waste transfer lines between tank groupings.

4.1.3 Closure Cap Layout Scenario #3:

The third layout evaluated was that of a single FTF closure cap over all tank groupings (i.e., 1-8, 17-20, 33-34, and 25-28/44-47) with D&D of the 242-16F Evaporator Building, removal of all above tank components from tanks 33 and 34 (Table 3), and minimization of fill. For this scenario the top of the 242-16F Evaporator Building was assumed to be removed down to an elevation of 298 ft-msl (i.e. down to the top of the Type IIIA tank (i.e., tanks 25-28/44-47) condenser housings (Table 3)). Figure 9 presents the results of this layout evaluation. Such a layout results in the peak of the closure cap being located between tanks 26 and 27 and a maximum slope length of approximately 740 ft.

4.1.4 Closure Cap Layout Scenario #4:

The fourth and final layout evaluated was that of a single FTF closure cap over all tank groupings (i.e., 1-8, 17-20, 33-34, and 25-28/44-47) with D&D of the 242-16F Evaporator Building and without minimization of fill. For this scenario the top of the 242-16F Evaporator Building was assumed to be removed down to an elevation of 298 ft-msl (i.e., down to the top of the Type IIIA tank (i.e. tanks 25-28/44-47) condenser housings (Table 3)). Figure 10 presents the results of this layout evaluation. Such a layout results in the peak of the closure cap being located over the 241-21F pump pits #2 and #3 and diversion box #4 and a maximum slope length of approximately 585 ft.

4.1.5 Closure Cap Layout Summary

Closure cap layout scenarios #1 and #2 (Figure 7 and Figure 8) were discounted from further consideration, since it is virtually impossible to have appropriate side slopes and drainage between tank groupings, excavation would likely be required in the areas between tank groupings, and diversion boxes 3, 5, and 6 nor any high level transfer lines between tank groupings would be covered by the closure cap. Closure cap layout scenarios #3 (Figure 9) was discounted in favor of closure cap layout scenarios #4 (Figure 10), since it required removal of all above tank components from tanks 33 and 34 and resulted in a maximum slope length greater than that of layout scenarios #4. Greater slope lengths result in shallower surface slopes, larger size stones in the erosion barrier and side slopes, and increased infiltration. The closure cap layout scenarios #4 (Figure 10) maximum slope length encompasses that of the layout scenarios #1 and #2 (Figure 7 and Figure 8) but not that of layout scenarios #3 (Figure 9).

Based upon the above scoping level evaluation of the FTF closure cap layout, it has been decided that the scoping level closure cap physical stability calculations (i.e., closure cap surface slope and stone size for the erosion barrier, side slopes, and toe) would be based upon the maximum slope length of the closure cap layout scenarios #4 (Figure 10; i.e., 585 ft).
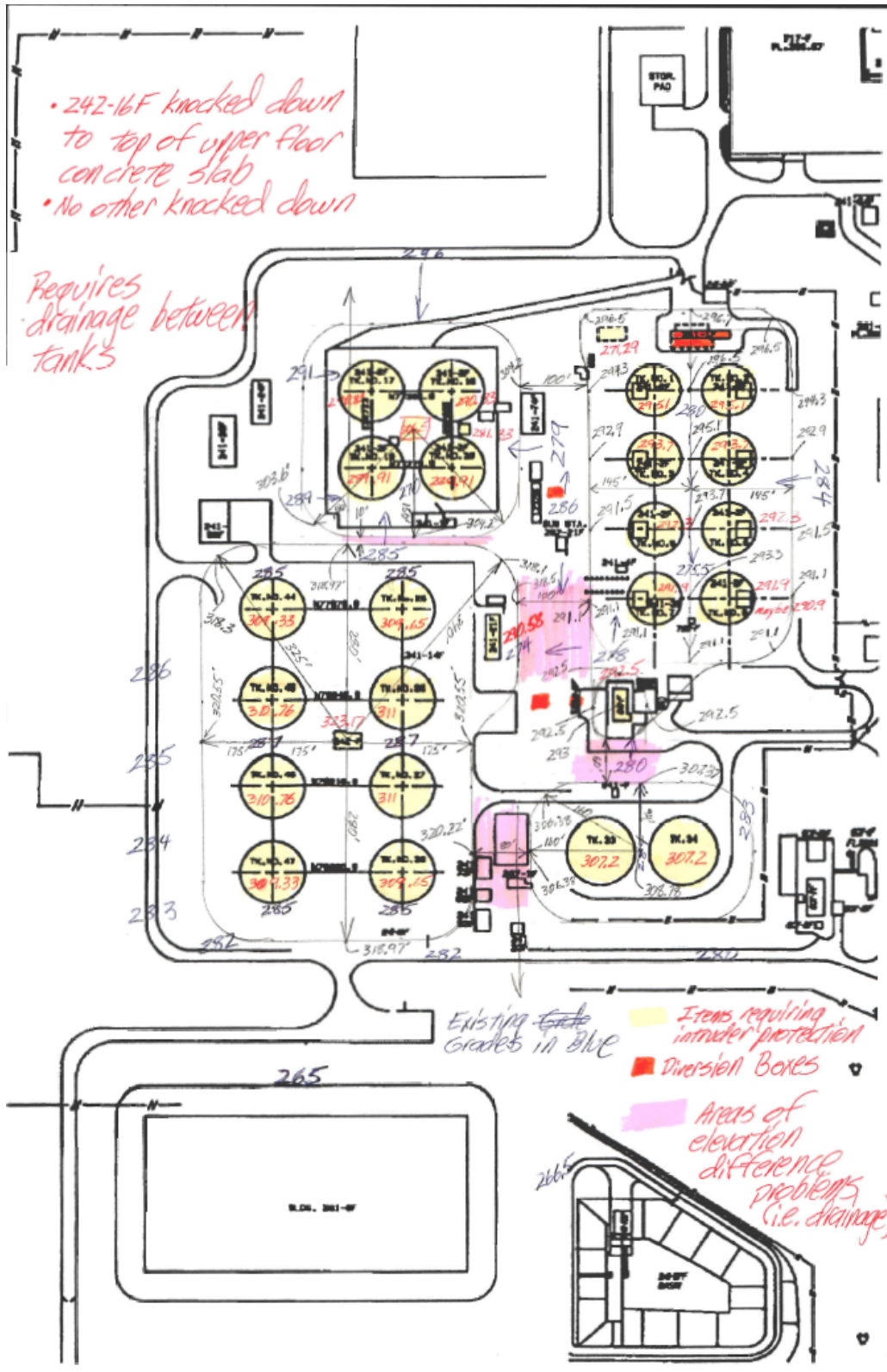
Figure 7.   Closure Cap Layout Scenario #1
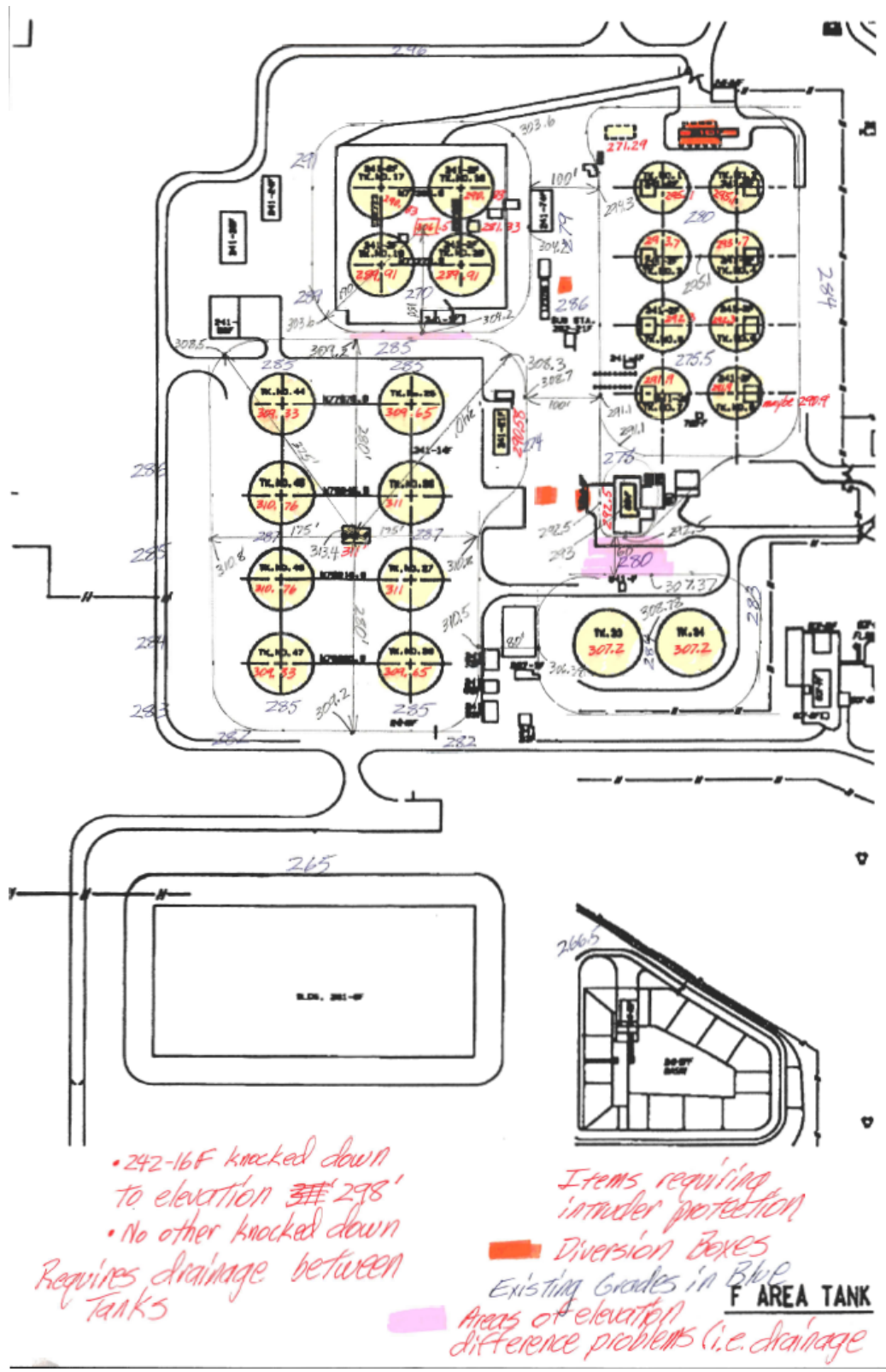
Figure 8.   Closure Cap Layout Scenario #2
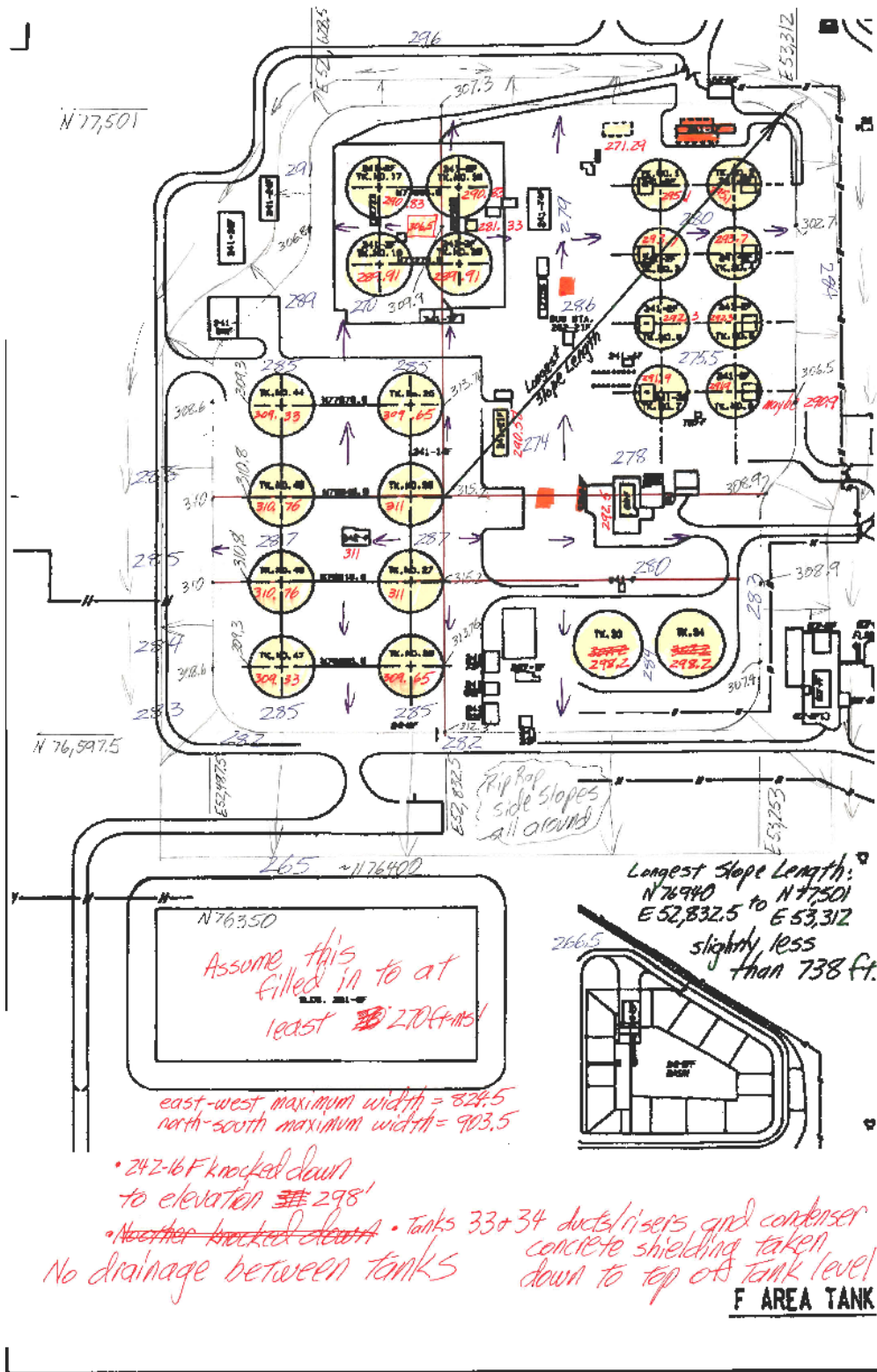
Figure 9.   Closure Cap Scenario Layout #3
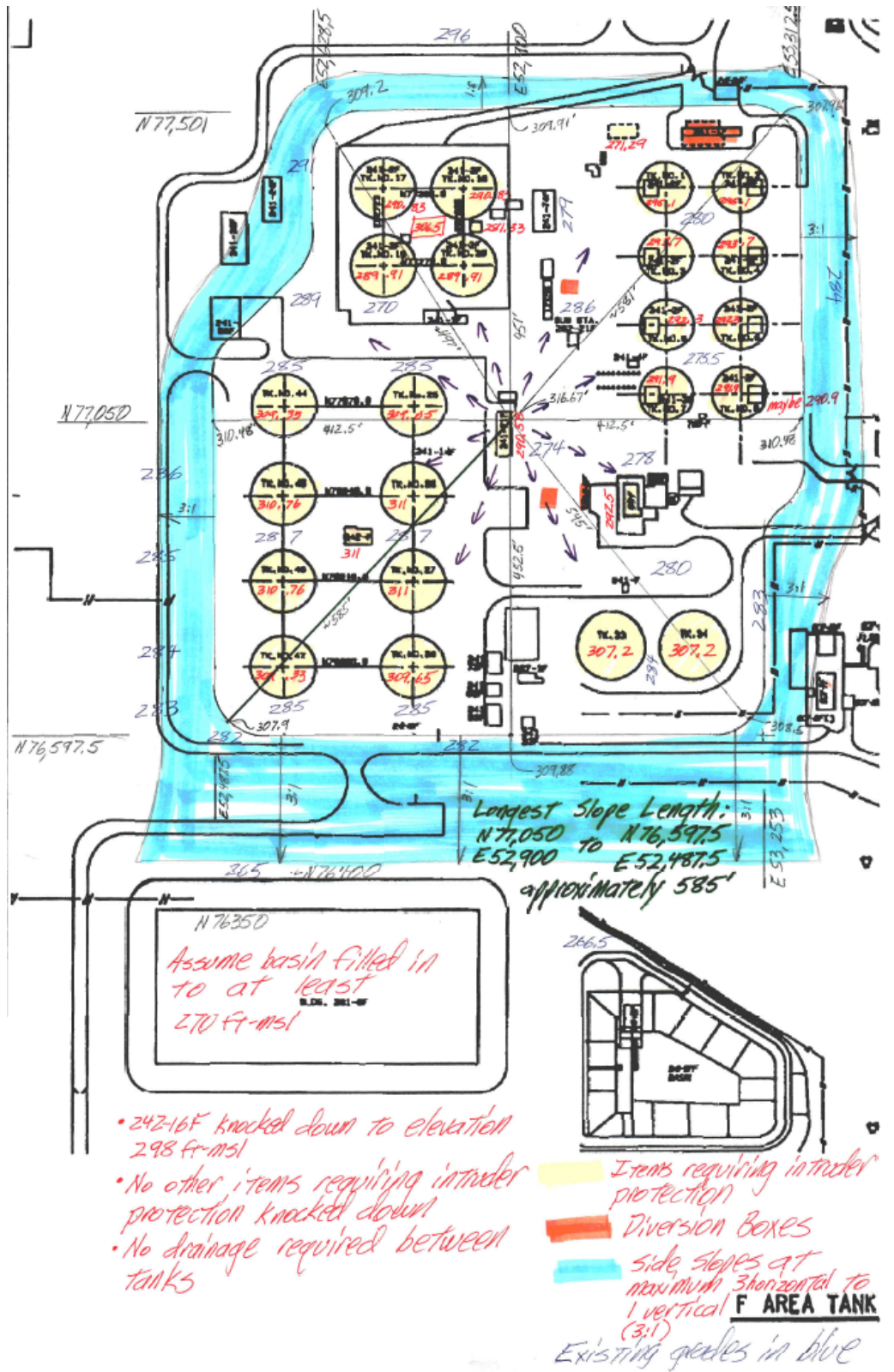
Figure 10.   Closure Cap Scenario Layout #4

4.2 FTF CLOSURE CAP SCOPING LEVEL PHYSICAL STABILITY REQUIREMENTS

Scoping level calculations have been made in order to determine closure cap requirements for physical stability. The calculations have been made consistent with Abt and Johnson 1991 and Johnson 2002 to assess physical stability requirements relative to erosion potential resulting from a SRS-specific probable maximum precipitation (PMP) event over a maximum 585-ft slope length (see Section 4.1). A PMP is defined as the theoretically greatest depth of precipitation for a given duration that is physically possible over a given storm size area at a particular geographic location. Stability calculations for the following key components of the closure cap are provided in detail in Appendix A:

- Vegetative soil cover
- Erosion barrier
- Side slope
- Toe of the side slope

As discussed in detail in Appendix A these calculations resulted in the following conclusions:

- A 2 percent slope over a 585-ft slope length for the vegetative soil cover is considered physically stable (i.e. prevents the initiation of gullying during a PMP event). Maximum acceptable slopes for portions of the closure cap with slope lengths less than 585 ft may be greater than 2 percent, if it is determined that they are physically stable during the actual closure cap design process.
- An erosion barrier consisting of 12-in thick riprap with a D_{50} (median size) of 2.5 in on a 585-ft long, 2 percent slope is considered physically stable (i.e. prevents any riprap movement during a PMP event). Based upon the D_{50} of 2.5 in, rock consistent with Type B riprap from Table F-3 of Johnson 2002 or Size R-20 riprap from Table 1 of ASTM 1997 is suitable for use in the erosion barrier.
- Side slope riprap that is 24 in thick with a D_{50} (median size) of 9.1 in on a 120-ft long, 33.3 percent slope receiving drainage from a 585-ft long, 2 percent slope is considered physically stable (i.e. prevents any riprap movement during a PMP event). Based upon the D_{50} of 9.1 in, rock consistent with Type D riprap from Table F-3 of Johnson 2002 or Size R-150 riprap from Table 1 of ASTM 1997 is suitable for use on the side slopes.
- Toe of the side slope riprap that is 42 in thick, extends out 20 ft from the side slope, and has a D_{50} (median size) of 11.6 in is considered physically stable (i.e., prevents any riprap movement due to receiving runoff from the 2 percent, 585-ft top slope and 33.3 percent, 120-ft side slope during a PMP event). Based upon the D_{50} of 11.6 in, rock consistent with Type D riprap from Table F-3 of Johnson 2002 or Size R-300 riprap from Table 1 of ASTM 1997 is suitable for use on the toe.

Erosion barrier, side slope, and toe riprap size may be smaller for portions of the closure cap with shorter slope lengths than those used to determine the requirements outlined above, if it is determined that the smaller sized riprap is stable versus a PMP event during the actual closure cap design process.

4.3 FTF CLOSURE CAP SCOPING LEVEL LAYERS AND FUNCTIONALITY

It is anticipated that the FTF closure cap will consist of the layers outlined in Table 11 from top to bottom (also see Figure 11). Table 12 provides an overview of the function of each of these layers. Figure 12 provides scoping concepts for the side slopes and toes of the closure cap based upon Section 4.2.

Table 11. Generic FTF Closure Cap Layers

Layer [1]	Layer Thickness (in)
Vegetative Cover	Not applicable
Topsoil	6
Upper Backfill	30
Erosion Barrier	12
Geotextile Fabric	-
Middle Backfill	12
Geotextile Filter Fabric	-
Lateral Drainage Layer	12
Geotextile Fabric	-
High Density Polyethylene (HDPE) Geomembrane	0.06 (60 mil)
Geosynthetic Clay Liner (GCL)	0.2
Upper Foundation Layer	12
Lower Foundation Layer	72 (minimum)

Based upon Phifer and Nelson 2003 Table 4.7-1 with the addition of the HDPE geomembrane
[1] The layers are arranged in the table to reflect their order from top to bottom in the FTF Closure Cap. Detailed explanations of the layers are provided in the text.

Table 12.   Function of the FTF Closure Cap Layers

Layer	Function
Vegetative Cover	The vegetative cover will be established to promote runoff, minimize erosion, and promote evapotranspiration. The initial vegetative cover will be a persistent grass such as Bahia. If it is determined that bamboo is a climax species that prevents or greatly slows the intrusion of pine trees, bamboo will be planted as the final vegetative cover at the end of the 100-year institutional control period.
Topsoil	The topsoil will be designed to support a vegetative cover, promote runoff, prevent the initiation of gullying, and provide water storage for the promotion of evapotranspiration.
Upper Backfill	The upper backfill will be designed to increase the elevation of the closure cap to that necessary for placement of the topsoil and to provide water storage for the promotion of evapotranspiration.
Erosion Barrier	The erosion barrier will be designed to prevent riprap movement during a PMP event and therefore form a barrier to further erosion and gully formation (i.e. provide closure cap physical stability). It will be used to maintain a minimum 10 ft of clean material above the tanks and significant ancillary equipment to act as an intruder deterrent. It will also act to preclude burrowing animals from access to underlying closure cap layers. It also provides minimal water storage for the promotion of evapotranspiration.
Geotextile Fabric	This geotextile fabric will be designed to prevent the penetration of erosion barrier stone into the underlying middle backfill and to prevent piping of the middle backfill through the erosion barrier voids.
Middle Backfill	The middle backfill will provide water storage for the promotion of evapotranspiration in the event that the topsoil and upper backfill are eroded away since the overlying erosion barrier provides only minimal such water storage.
Geotextile Filter Fabric	This geotextile fabric will be designed to provide filtration between the overlying middle backfill layer and the underlying lateral drainage layer. This filtration will allow water to freely flow from the middle backfill to the lateral drainage layer while preventing the migration of soil from the middle backfill to the lateral drainage layer.
Lateral Drainage Layer	The lateral drainage layer will be a coarse sand layer designed to: • Divert infiltrating water away from the underlying tanks and ancillary equipment and transport the water to the perimeter drainage system, in conjunction with the underlying composite hydraulic barrier (i.e., HDPE geomembrane and GCL), and • Provide the necessary confining pressures to allow the underlying GCL to hydrate properly.

Table 12. Function of the FTF Closure Cap Layers - continued

Layer	Function
Geotextile Fabric	This geotextile fabric will be a nonwoven geotextile fabric designed to protect the underlying HDPE geomembrane from puncture or tear during placement of the overlying lateral drainage layer.
HDPE Geomembrane	The high density polyethylene (HDPE) geomembrane will form a composite hydraulic barrier in conjunction with the GCL. The composite hydraulic barrier will be designed to promote lateral drainage through the overlying lateral drainage layer and minimize infiltration to the tanks and ancillary equipment.
GCL	The Geosynthetic Clay Liner (GCL) will form a composite hydraulic barrier described above in conjunction with the HDPE geomembrane. As part of the composite hydraulic barrier the GCL is designed to hydraulically plug any holes that may develop in the HDPE geomembrane.
Foundation Layer: • Upper Foundation Layer • Lower Foundation Layer	The foundation layer will be designed to: • Provide structural support for the rest of the overlying closure cap, • Produce the required contours and produce a slope of 2 percent for the overlying layers, • Produce the maximum 3:1 side slopes of the closure cap, • Provide a suitable surface for installation of the GCL (i.e. a soil with a moderately low permeability and a smooth surface free from deleterious materials), • Promote drainage of infiltrating water away from and around the tanks and ancillary equipment, and • Contain utilities, equipment, facilities, etc. that are not removed from above current grade prior to installation of the closure cap.
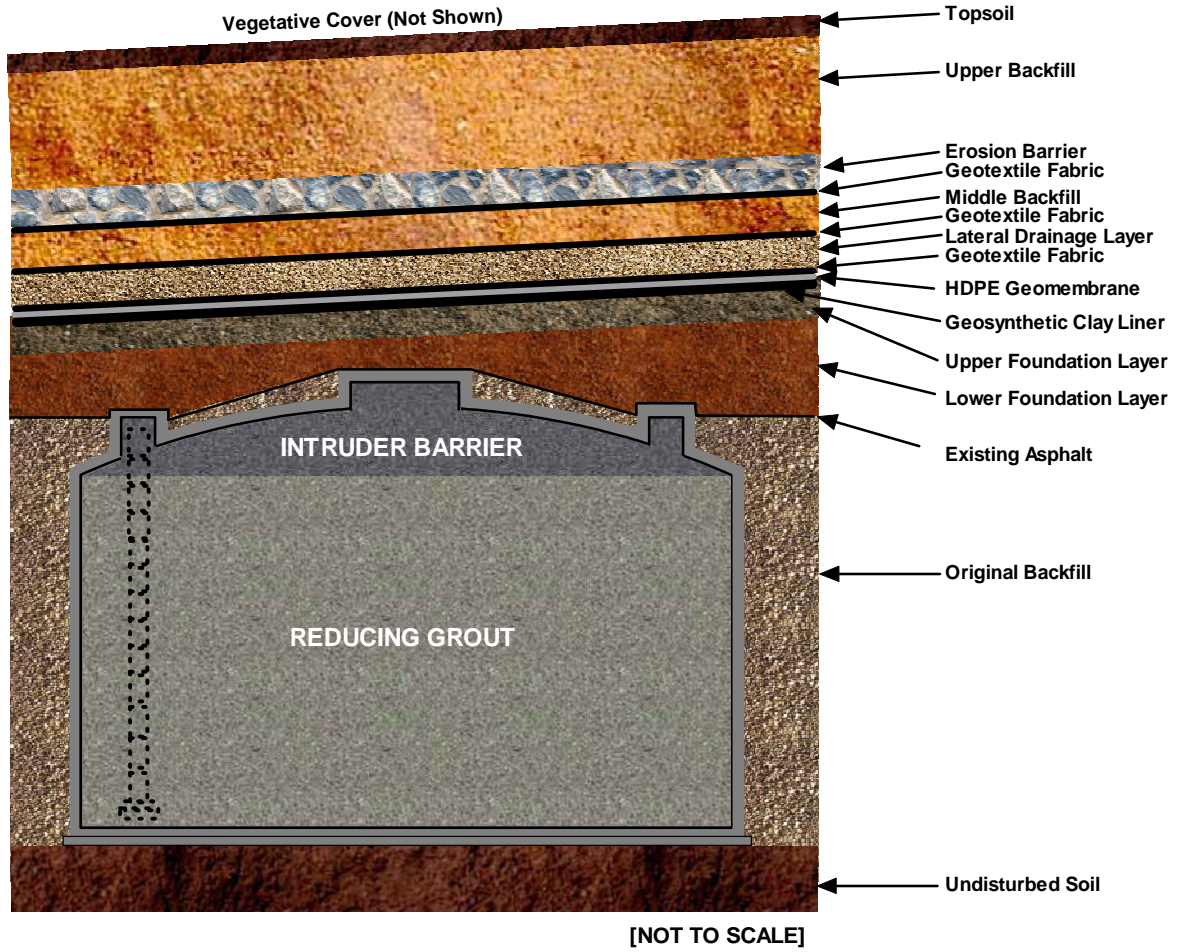
Figure 11. Generic FTF Closure Cap
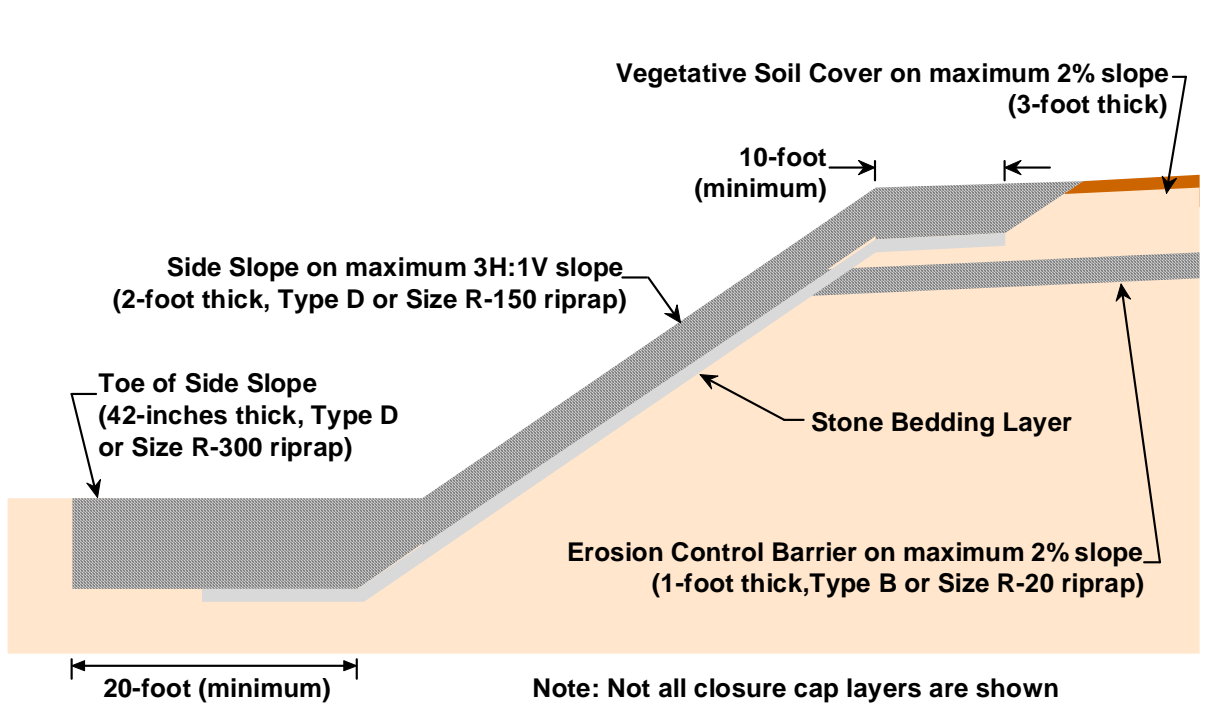
Figure 12. Generic Closure Cap Side Slope and Toe Configuration

4.4 FTF CLOSURE CAP SCOPING LEVEL DESIGN AND CONSTRUCTABILITY

Scoping level design and construction information associated with each of the Table 11 closure cap layers and for the side slopes and toes are provided in the following discussion. A scoping level aerial plot plan of the FTF Closure Cap is provided in Figure 13, and a scoping level footprint of the FTF Closure Cap with the location of cross-sections through the cap denoted is provided in Figure 14. Scoping level cross-sections A-A, B-B, and C-C are provided in Figure 15, and scoping level cross-sections D-D and E-E are provided in Figure 16.

Site preparation will be required to prepare the FTF area for installation of the closure cap. The exact nature of such site preparation has not yet been determined; however it will need to address the following:

- Subsidence potential associated with subsurface items that contain significant void space,
- Above grade structures, utilities, equipment, etc. that could interfere with closure cap construction, and
- Existing surfaces (i.e. soils, asphalt, riprap, concrete tank tops, significant ancillary equipment, etc.) over which the closure cap will be constructed.

It is anticipated that subsurface items containing significant void space, such as piping, tanks, pump pits, diversion boxes etc., above a to-be-determined size will be grouted to eliminate subsidence potential. It is also anticipated that above grade structures, utilities, equipment, etc. (other than substantial above grade concrete associated with the tanks and significant ancillary equipment) that could interfere with closure cap construction will be removed from the FTF area prior to installation of the closure cap.

The existing surfaces (i.e., soils, asphalt, riprap, concrete tank tops, and significant ancillary equipment) over which the closure cap will be constructed must be prepared prior to closure cap construction. It is anticipated that existing soil surfaces will have 3 to 6 in of soil removed to eliminate any topsoil and vegetation present, will be rough graded to establish a base elevation, and will be compacted with a vibratory roller. Existing asphalt surfaces directly over tanks and significant ancillary equipment will probably be left in place; however such surfaces between tanks and significant ancillary equipment may need to be broken up or removed in order to prevent the asphalt from acting as a perched water zone within the closure cap and to promote downward infiltration around the tanks and significant ancillary equipment. It is anticipated that existing riprap will be removed or that the voids within the existing riprap surfaces will be filled to eliminate subsidence potential. It is anticipated that no preparatory actions will be required for the tank tops themselves other than that necessary to provide appropriate protection during closure cap construction. It is anticipated that the significant ancillary equipment will require grouting in order to eliminate subsidence potential.

The following pages provide detailed information regarding the purpose, design, and constructability of each of the FTF Closure Cap layers. Layers are discussed in order of their placement (i.e., from bottom to top of the closure cap) beginning with the foundation layer and ending with the vegetative cover.
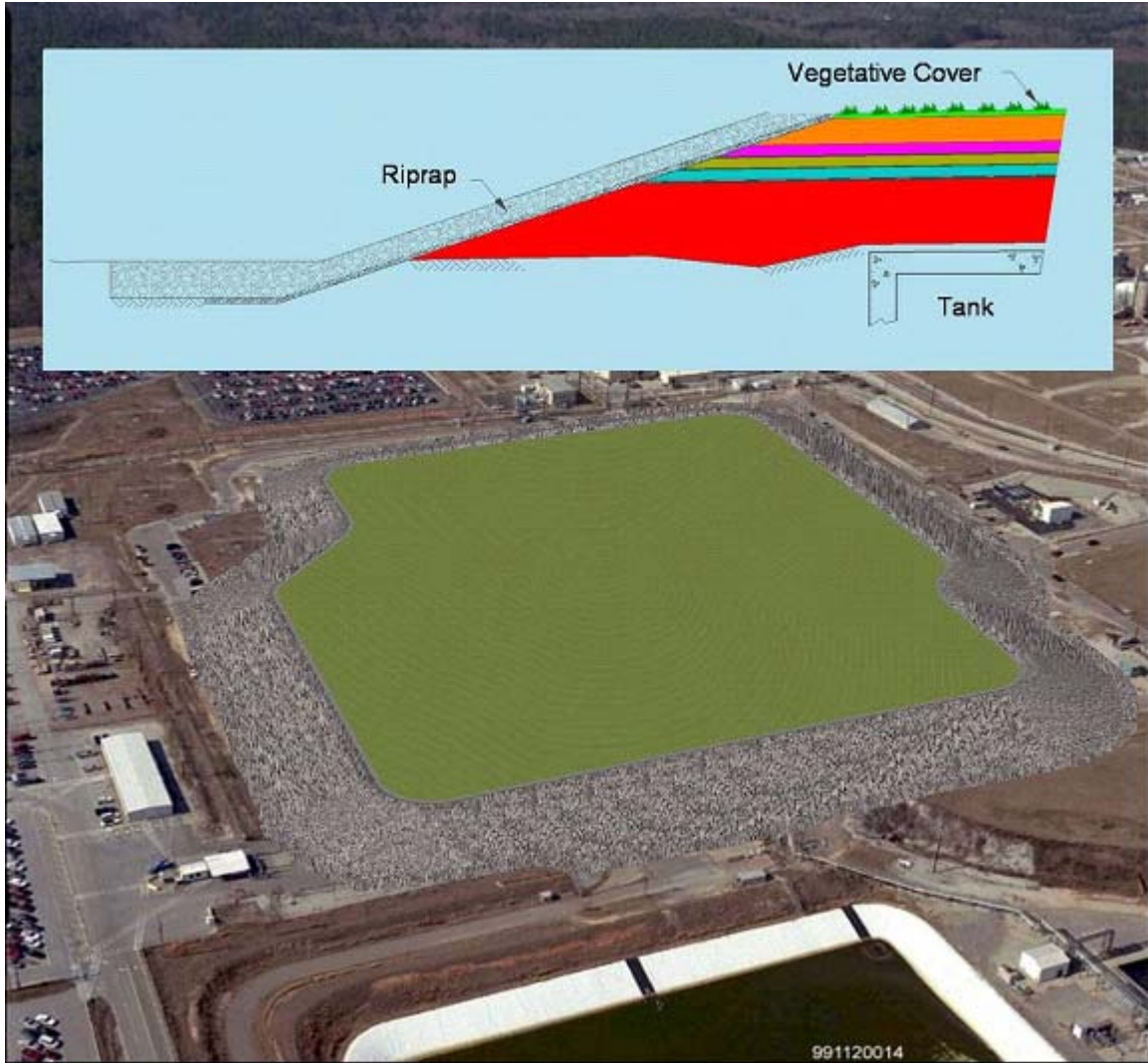
Figure 13.   FTF Closure Cap Scoping Level Aerial Plot Plan

Figure 14.   FTF Closure Cap Scoping Level Footprint with Cross-Section Locations
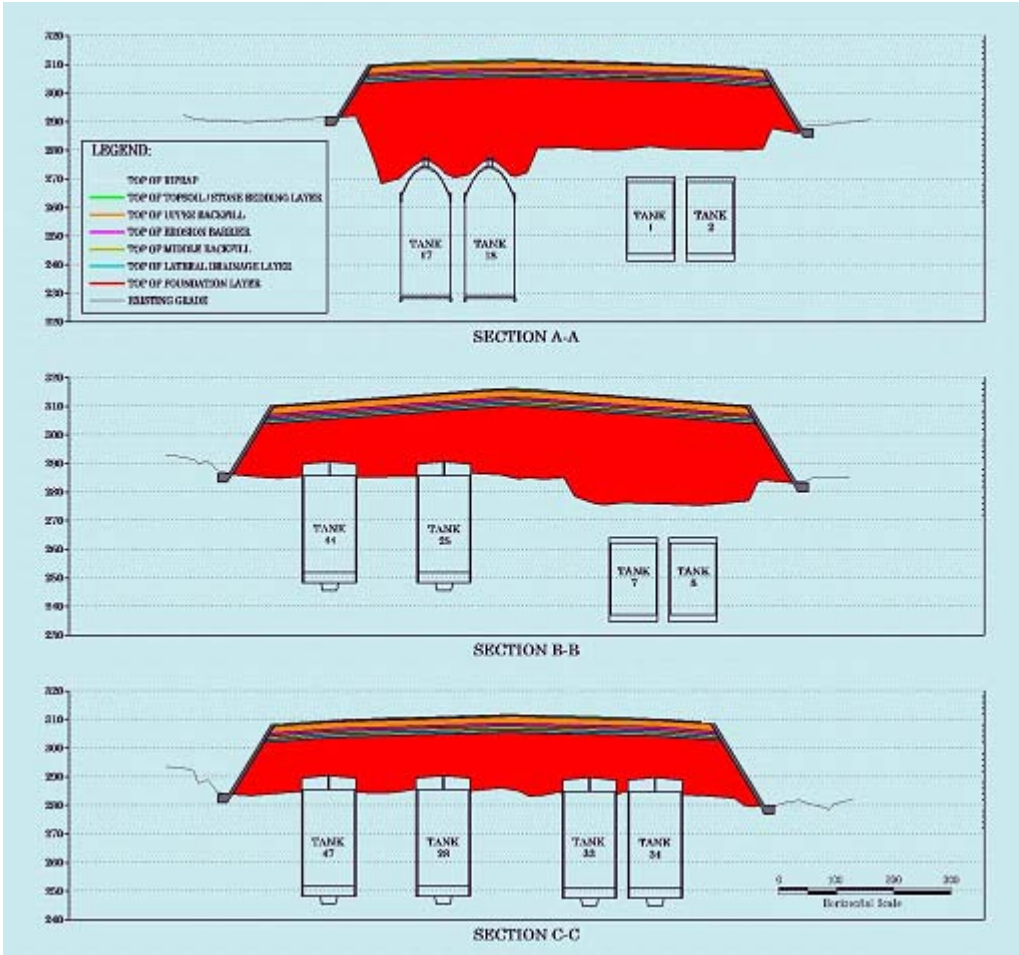
Note: Vertical scale of sections has been exaggerated 5 times

Figure 15.   FTF Closure Cap Scoping Level Cross-Sections A-A, B-B, and C-C
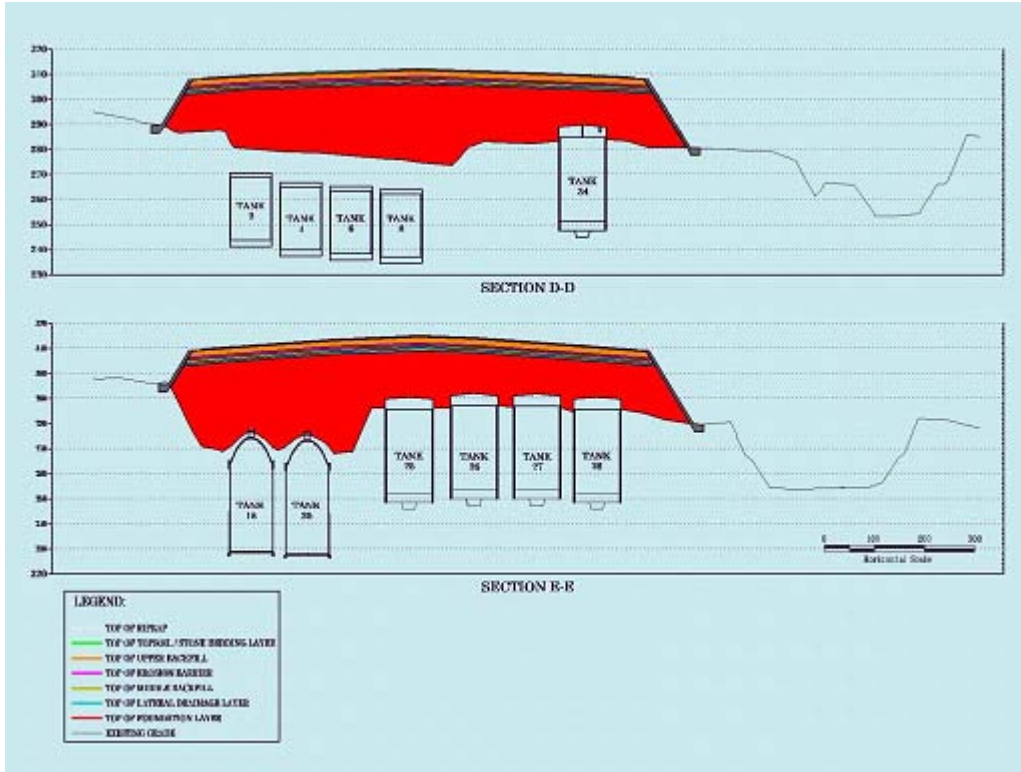
Note: Vertical scale of sections has been exaggerated 5 times

Figure 16.   FTF Closure Cap Scoping Level Cross-Sections D-D and E-E

4.4.1 Foundation Layer (Lower Backfill)

A foundation layer (lower backfill) will be placed over all tanks and significant ancillary equipment after site preparation (see above). The foundation layer will be designed to:

- Provide structural support for the rest of the overlying closure cap,
- Produce the required contours and a slope of 2 percent for the overlying layers,
- Produce the maximum 3:1 side slopes of the closure cap,
- Provide a suitable surface for installation of the GCL (i.e,. a soil with a moderately low permeability and a smooth surface free from deleterious materials),
- Promote drainage of infiltrating water away from and around the tanks and ancillary equipment, and
- Contain utilities, equipment, facilities, etc. that are not removed from above current grade prior to installation of the closure cap.

The thickness of this foundation layer will vary, but in all cases it will have a minimum thickness of 7 ft (84 in) over all tanks and significant ancillary equipment. The upper one foot of the foundation layer will consist of soil with a moderately low permeability (i.e., ≤1.0E-06 cm/s) and a smooth surface free from deleterious materials suitable for installation of the GCL. It is anticipated that the upper one foot of the foundation layer will consist of typical SRS backfill soil blended with a small weight percent bentonite to achieve the moderately low permeability (i.e., ≤1.0E-06 cm/s) and that it will be placed similar to that described for the middle backfill. The top lift of the foundation layer, upon which the GCL will be placed, shall be proof-rolled with a smooth drum roller to produce a surface satisfactory for placement of the GCL. It is anticipated that the foundation layer below the upper one foot will be control compacted backfill, placed similar to that described for the middle backfill, however the exact requirements for this portion of the layer, primarily in terms of its drainage, have not yet been determined. The maximum thickness of the foundation layer will depend upon the closure cap aerial geometry and the drainage paths.

4.4.2 Geosynthetic Clay Liner (GCL)

A Geosynthetic Clay Liner (GCL) will be placed directly on top of the finished foundation layer (lower backfill) at a slope of 2 percent. The GCL will form a composite hydraulic barrier in conjunction with an overlying HDPE geomembrane described below. The composite hydraulic barrier will be designed to promote lateral drainage through the overlying lateral drainage layer and to minimize infiltration to the tanks and ancillary equipment. As part of the composite hydraulic barrier the GCL is designed to hydraulically plug any holes that may develop in the HDPE geomembrane. The GCL shall have a minimum dry weight of sodium bentonite of 0.75 lbs/ft^2 and a "maximum through plane" saturated hydraulic conductivity of 5.0E-9 cm/s. The GCL shall conform to the requirements of GRI 2005. The GCL shall be obtained from the manufacturer in rolls, which are on the order of 15 ft wide by 150 ft long. The GCL rolls shall be stored flat and kept dry. The GCL shall be placed directly on top of the foundation layer, which would have been appropriately prepared to produce a smooth surface free from deleterious materials for GCL placement. Placement of the rolls of GCL shall consist of unrolling the GCL roll per the manufacturer's directions directly onto the surface of the foundation layer producing a GCL panel.

The GCL shall not be placed during periods of precipitation or under other conditions that could cause the bentonite to hydrate prematurely (i.e., prior to placement of the HDPE geomembrane and a minimum of 1 ft of sand on top of it). GCL panels shall be overlapped a minimum 12 in on panel edges and a minimum of 18 in on panel ends (Koerner and Koerner 2005). Only portions of the GCL containing bentonite shall be considered as part of the minimum required overlap. Portions of the GCL consisting of the geotextile only shall not be counted as part of the required minimum overlap. Loose granular bentonite shall be placed between overlapping panels at a rate of ¼ pound per linear foot. The GCL shall be inspected for rips, tears, displacement, and premature hydration prior to placement of the overlying HDPE geomembrane and sand. Any rips, tears, displacement, and premature hydration shall be repaired per the manufacturer's directions prior to placement of the HDPE geomembrane, geotextile fabric, and 1-ft coarse sand lateral drainage layer on top of it.

At the end of each working day, the uncovered edge of the GCL (i.e., that portion that does not have the sand on it) shall be protected with a waterproof sheet that is secured adequately with ballast to avoid premature hydration. (USEPA 2001; ASTM 2004a) All work in association with placement of the GCL shall be performed in accordance with the approved drawings, plans, and specifications of the final design, which will be produced near the end of the operational period.

4.4.3 High Density Polyethylene (HDPE) Geomembrane

A high density polyethylene (HDPE) geomembrane will be placed directly on top of the GCL at a slope of 2 percent. The HDPE geomembrane will form a composite hydraulic barrier in conjunction with the GCL described above. The composite hydraulic barrier will be designed to promote lateral drainage through the overlying lateral drainage layer and to minimize infiltration to the tanks and ancillary equipment. The HDPE is considered the primary hydraulic barrier with the GCL acting as a secondary hydraulic barrier by plugging any holes that may develop in the geomembrane.

The geomembrane shall be 60-mils thick (minimum) and shall conform to the requirements of GRI 2003. The geomembrane shall be obtained from the manufacturer in rolls, which are on the order of 22 ft wide by 500 ft long or greater. The geomembrane rolls shall be stored flat; kept dry; protected from puncture, abrasions, and excessive dirt; and protected from ultraviolet light exposure. Each geomembrane roll shall be numbered and a panel placement plot plan shall be developed that minimizes the total length of field seaming required and maximizes the length of seams oriented down slope versus those across slope. Placement of the geomembrane rolls shall consist of unrolling the geomembrane roll down slope per the manufacturer's directions directly onto the surface of the GCL producing a geotextile panel. Adjacent geomembrane panels shall be overlapped a minimum of 6 in and seamed using either extrusion welding or hot wedge welding methods per the manufacturer's directions. A quality assurance plan shall be developed and implemented that incorporates the following: 100-percent visual inspection of all rolls as they are laid down and of all seams; appropriate wrinkle control measures as the rolls are laid down, seamed, and covered; 100-percent non-destructive field testing of all seams by vacuum testing (ASTM 2006a) and/or air pressure testing (ASTM 2006b); and destructive testing (ASTM 2006c) on a frequency consistent with GRI 1998. Any seam or non-seam area that has been identified as defective and any holes created for destructive testing shall be repaired and non-destructively tested prior to acceptance. The emplaced geomembrane panels shall be held down with sandbags or approved equivalent that will not damage the geomembrane until replaced with the overlying geotextile fabric and sand layer to prevent wind uplift of the geomembrane. (USEPA 1989; Koerner 1990) All work in association with placement of the geomembrane shall be performed in accordance with the approved drawings, plans, and specifications of the final design, which will be produced near the end of the operational period.

4.4.4 Geotextile Fabric

A nonwoven geotextile fabric will be placed directly on top of the HDPE geomembrane to protect it from puncture or tear during placement of the overlying 1-ft thick coarse sand lateral drainage layer. The geotextile shall be selected primarily for its puncture and tear resistance and shall conform to the requirements of GRI 2002. The geotextile shall be obtained from the manufacturer in rolls, which are on the order of 15 ft wide by 300 ft long or greater. Placement of the rolls of geotextile shall consist of unrolling the geotextile roll down slope per the manufacturer's directions directly onto the surface of the HDPE geomembrane producing a geotextile panel. Adjacent geotextile panels shall be seamed using heat seaming or stitching methods per the manufacturer's directions in a manner that does not damage the underlying GCL and HDPE geomembrane. The emplaced geotextile panels shall be held down with sandbags or an approved equivalent until replaced with the overlying sand layer to prevent wind uplift of the geotextile. The emplaced geotextile panels shall not be exposed to direct sunlight for more than 7 days prior to placement of the overlying sand layer. The emplaced geotextile shall be inspected for rips, tears, wrinkling, and displacement prior to placement of the sand layer on top of it. Any rips, tears, wrinkling, and displacement shall be repaired per the manufacturer's directions prior to placement of the sand layer on top of it. The overlying sand layer shall be placed in a single 1-ft lift on top of the combined GCL, HDPE geomembrane, and geotextile fabric per the manufacturer's directions in order to avoiding damaging the GCL and HDPE geomembrane. No equipment used to place the sand shall come into direct contact with the GCL, HDPE geomembrane, or geotextile fabric. (Koerner 1990 Section 2.11; ASTM 1988)

All work in association with placement of this geotextile filter fabric shall be performed in accordance with the approved drawings, plans, and specifications of the final design, which will be produced near the end of the operational period.

4.4.5 Lateral Drainage Layer

A lateral drainage layer will be placed over the combined GCL, HDPE geomembrane, and geotextile fabric. The lateral drainage layer will be designed to:

- Divert infiltrating water away from the underlying tanks and ancillary equipment and transport the water to the perimeter drainage system in conjunction with the underlying composite hydraulic barrier (i.e., HDPE geomembrane and GCL), and
- Provide the necessary confining pressures to allow the underlying GCL to hydrate properly.

The lateral drainage layer will be sloped at the same slope as the foundation layer (i.e., 2 percent slope). The lateral drainage layer will be hydraulically connected to the overall facility drainage system in order to divert and transport as much infiltrating water as possible through the lateral drainage layer to the facility drainage system and away from the underlying waste tanks and ancillary equipment. The lateral drainage layer shall consist of a 1-ft thick layer of coarse sand with a minimum saturated hydraulic conductivity of 5.0E-02 cm/s and that is free of any materials deleterious to the underlying GCL, HDPE geomembrane, and geotextile fabric or overlying geotextile fabric. The sand layer shall be placed in a single 1-ft lift on top of the GCL, HDPE geomembrane, and geotextile fabric per the GCL and HDPE geomembrane manufacturer's directions in order to avoiding damaging the GCL and HDPE geomembrane. The sand layer will be fine graded to the required contours. No equipment used to place the sand shall come into direct contact with the GCL, HDPE geomembrane, and geotextile fabric; the equipment used to place and fine grade the sand shall be low ground pressure equipment that is driven on top of the previously placed foot thick sand layer. No compactive effort shall be applied to the sand layer other than that provided by the equipment used to place and fine grade it. All work in association with placement of the drainage layer shall be performed in accordance with the approved drawings, plans, and specifications of the final design, which will be produced near the end of the operational period.

4.4.6 Geotextile Filter Fabric

An appropriate geotextile filter fabric shall be placed on top of the 1-ft thick coarse sand lateral drainage layer to provide filtration between the underlying sand layer and the overlying middle backfill. Koerner 1990 (page 120) defines filtration with a geotextile as:

> "The equilibrium fabric-to-soil system that allows for free liquid flow (but no soil loss) across the plane of the fabric over an indefinitely long period of time."

The geotextile filter fabric shall have a minimum thickness of 0.1 in, a minimum through plane saturated hydraulic conductivity of 0.1 cm/s, and an apparent opening size small enough to appropriately filter the overlaying backfill. The geotextile shall be obtained from the manufacturer in rolls, which are on the order of 15 ft wide by 300 ft long or greater. The geotextile rolls shall be stored flat, kept dry, protected from ultraviolet light exposure. The geotextile shall be placed directly on top of the sand layer, which would have been appropriately contoured and determined to be free of materials deleterious to the geotextile. Placement of the rolls of geotextile shall consist of unrolling the geotextile roll down slope per the manufacturer's directions directly onto the surface of the sand producing a geotextile panel.

Adjacent geotextile panels shall be seamed using heat seaming or stitching methods per the manufacturer's directions. The emplaced geotextile panels shall be held down with sandbags or an approved equivalent until replaced with the overlying middle backfill to prevent wind uplift of the geotextile. The emplaced geotextile panels shall not be exposed to direct sunlight for more than 7 days prior to placement of the overlying middle backfill. The emplaced geotextile shall be inspected for rips, tears, wrinkling, and displacement prior to placement of the middle backfill on top of it. Any rips, tears, wrinkling, and displacement shall be repaired per the manufacturer's directions prior to placement of the middle backfill on top of it. The initial loose lift of the overlying middle backfill shall be placed in a single lift on top of the geotextile per the manufacturer's directions in order to avoid displacing or damaging the geotextile.

No equipment used to place the backfill shall come into direct contact with the geotextile. The feet of any compaction equipment used on the backfill shall be sized so that compaction of the backfill does not damage the geotextile. (Koerner 1990 Section 2.11; ASTM 1988) All work in association with placement of this geotextile filter fabric shall be performed in accordance with the approved drawings, plans, and specifications of the final design, which will be produced near the end of the operational period.

4.4.7 Middle Backfill

A backfill will be placed over the lateral drainage layer and associated geotextile filter fabric. The middle backfill will provide water storage for the promotion of evapotranspiration in the event that the topsoil and upper backfill are eroded away, since the overlying erosion barrier provides only minimal such water storage. The middle backfill soils will be obtained from on site sources. Only on-site soil classified as SC (clayey sands) shall be used. Borrow areas will be pre-qualified prior to use. The middle backfill shall be placed in lifts not to exceed 9 inches in uncompacted thickness in areas where hand operated mechanical compaction equipment is used and not to exceed 12 inches in uncompacted thickness in areas where self propelled or towed mechanical compaction equipment is used. Each lift shall be compacted to at least 90% of the maximum dry density per the Modified Proctor Density Test (ASTM 2002b) or 95% per the Standard Proctor Density Test (ASTM 2000). Each lift shall also be placed within specified tolerances of the optimum moisture content.

If the surface of a lift is smooth drum rolled for protection prior to placement of a subsequent lift, that lift will be scarified prior to placement of the subsequent lift to ensure proper bonding between lifts. The top lift, upon which an overlying geotextile fabric will be placed, shall be proof-rolled with a smooth drum roller to produce a surface satisfactory for placement of the geotextile fabric and erosion barrier. All work in association with placement of the lower backfill shall be performed in accordance with the approved drawings, plans, and specifications of the final design, which will be produced near the end of the operational period.

4.4.8 Geotextile Fabric

An appropriate geotextile fabric shall be placed on top of the middle backfill and below the erosion barrier to prevent the erosion barrier stone from penetrating into the middle backfill primarily during construction and as an additional measure to prevent piping of the middle backfill through the erosion barrier voids. The geotextile fabric material shall conform to the requirements of ASTM 2002a, AASHTO 2005, and GRI 2004. Although this geotextile fabric has a different material requirement and a different function than the previous geotextiles, the placement method of this geotextile is essentially identical to that of the previous geotextile filter fabric placed on top of the sand layer. The overlying erosion barrier shall be placed in a single lift on top of the geotextile per the manufacturer's directions in order to avoid displacing or damaging the geotextile. No equipment used to place the erosion barrier shall come into direct contact with the geotextile. All work in association with placement of this geotextile shall be performed in accordance with the approved drawings, plans, and specifications of the final design, which will be produced near the end of the operational period.

4.4.9 Erosion Barrier

An erosion barrier will be placed over the middle backfill and associated geotextile fabric. The erosion barrier will be designed to prevent riprap movement during a PMP event and will therefore form a barrier to further erosion and gully formation (i.e., provide closure cap physical stability). It will also be designed to act as a barrier to burrowing animals. It will also be used to maintain a minimum 10 ft of clean material above the tanks and significant ancillary equipment to act as an intruder deterrent. It also provides minimal water storage for the promotion of evapotranspiration. The erosion barrier rock has been sized based upon the Probable Maximum Precipitation (PMP) and the methodology outlined by Abt and Johnson 1991 and Johnson 2002 (see Appendix A for the calculations). Based upon these calculations a 1 ft thick layer of rock consistent with Type B riprap from Table F-3 of Johnson 2002 or Size R-20 riprap from Table 1 of ASTM 1997 has been determined to be suitable for use in the erosion barrier. The stone shall conform to one of these two stone gradations or equivalent. The exact gradation utilized shall be determined by availability and economics.

Quarries located near the SRS produce aggregate and rip rap consisting of granite, granite gneiss, gneiss, and mylonite (GDOT 2007). Granite aggregate and rip rap is typically utilized at SRS. However, the mylonitic quartzite reported available at an Augusta, Georgia quarry will be evaluated for durability versus the local granite. Consistent with the recommendations of Johnson 2002 and ASTM 1997, the rock utilized for the erosion barrier shall be angular, shall have a minimum specific gravity of 2.65, and shall be considered durable per the criteria outlined below.

- The rock shall be dense, sound, resistant to abrasion, free of clays, and free of cracks, seams, and other defects as determined by a petrographic examination (ASTM 2003a).

- Specific gravity (ASTM 2004b), absorption (ASTM 2004b), sodium sulfate soundness (ASTM 2005b), Los Angeles abrasion (ASTM 2003b), Schmidt Rebound Hardness-ISRM Method (Johnson 2002) tests shall be performed on the rock. Based upon these tests and the scoring methodology outlined by Johnson 2002, the rock shall have a quality score of 80 or greater.

Rock production and associated Quality Assurance/Quality Control (QA/QC) will be coordinated with the supplying quarry to assure the requisite rock size and mineralogical types are procured. The general approach will be to identify the highest-percent quartz rock type by quarry. Within the identified quarry, highly fractured, obviously weathered, and relatively feldspar-rich rock will be avoided, while "whole", fresh, and relatively quartz-rich rock will be preferentially selected. Visual selection of optimal rock may be supported by supplementary information (e.g., sulfate analyses and abrasion testing) available from the supplier. The final closure cap design will include a comprehensive QA/QC plan for selection and installation of all materials used to construct the cap.

The stone shall be handled, loaded, transported, stockpiled, and placed consistent with the requirements outlined in ASTM 2002a and Johnson 2002. In particular, the stone shall be handled, loaded, transported, stockpiled, and placed in a manner that prevents breakage and segregation of the stone into various sizes. The stone shall be placed in a single 1-ft lift on top of the middle backfill and overlying geotextile fabric by dumping and spreading with heavy equipment. The stone shall be placed in a manner that achieves a reasonably well-graded distribution of stones, a fairly consistent thickness (i.e., 0.9 to 1.25 ft), and a densely packed, wedged together, firmly interlocked layer. No equipment used to place the stone shall come into direct contact with the underlying geotextile; the equipment used to place the stone shall be low ground pressure equipment that is driven on top of the previously placed 1 ft thick stone. The only compactive effort applied to the stone shall be that provided by the equipment used to place it and a minimum of two passes of a Caterpillar D6 tracked bulldozer or equivalent.

Additionally as pointed out by NUREG (2006 and 1982) natural or archaeological analogs can be utilized to help demonstrate the long-term performance of closure cap materials. Prior to developing a final closure cap design, available literature and local natural or archaeological analogs for the erosion barrier stone will be researched and included as input for erosion barrier durability and degradation with time. As a starting point for the literature review, the literature review for long-term survivability of riprap presented in NUREG (1982) will be reviewed.

The rock utilized for the erosion barrier will be located below grade, while similar rock utilized for the side slopes (Section 4.4.14) and toe (Section 4.4.13) will be located above grade. Therefore the literature review and evaluation of local natural or archaeological analogs will include both those applicable to below grade and above grade weathering. Since the erosion barrier rock will likely be granite because of its durability, cost, and local availability, the following potential below grade local natural or archaeological analogs will be considered for evaluation:

- The Nature Conservancy's Heggie's Rock Preserve, located in Columbia County Georgia near the town of Appling, is a granite outcrop that is nearly 70 feet higher than the surrounding area (The Nature Conservancy 2007)
- Other granitic regoliths located in the southeastern United States
- Local granite quarries (GDOT 2007):
  – Martin Marietta Aggregates, Appling, Georgia
  – Rinker Materials, Dogwood Quarry, Appling, Georgia
- Granite quarries and manufacturing in Elberton, Georgia, which can be found through the Elberton Granite Association at www.egaonline.com/home/ (known as the "Granite Capital of the World" and located less than 100 miles from SRS).

In conjunction with the evaluation of below grade local natural or archaeological analogs for granite weathering, above grade analogs will also be evaluated for applicability to the side slope (Section 4.4.14) and toe (Section 4.4.13) rock:

- The Nature Conservancy's Heggie's Rock Preserve, located in Columbia county Georgia near the town of Appling, is a granite outcrop that is nearly 70 feet higher than the surrounding area (The Nature Conservancy 2007).
- Other granitic regoliths located in the southeastern United States
- Local granite quarries (GDOT 2007):
  – Martin Marietta Aggregates, Appling, Georgia
  – Rinker Materials, Dogwood Quarry, Appling, Georgia
- Granite quarries and manufacturing in Elberton, Georgia, which can be found through the Elberton Granite Association at www.egaonline.com/home/ (known as the "Granite Capital of the World" and located less than 100 miles from SRS).
- Elberton, Georgia High School facilities constructed of granite
- SRS and local area granite rip rap
- Local area granite head stones
- Georgia sites with petroglyphs including:
  – Forsyth County, Georgia granite boulder, which has been on display at the University of Georgia since 1963
  – Track Rock Gap, near Blairsville
  – The Reinhardt Rock, which originated near Keithsburg, Cherokee County, and is now on display at Reinhardt College

In addition to these local analogs for above grade granite, the National Institute of Standards and Technology (NIST) Stone Test Wall, located in Gaithersburg, MD (Stutzman 2001) will also be considered. This wall, constructed in 1948 as a cooperative study between the National Bureau of Standards and ASTM Committee C18 on Building Stone, contains 2,352 individual samples of over 30 distinct types of stone. The wall's purpose is to allow study of the performance of stone subjected to above-ground weathering. However, as of 1987, of the many stone types placed in the wall, "…only a few fossiliferous limestones permit a valid measurement of surface reduction in a polluted urban environment" (Winkler 1987). A web site (http://stonewall.nist.gov) is available for additional information (Stutzman 2001).

Based upon the results of the natural or archaeological analog evaluation, the required size of the emplaced stone and the thickness of the stone layer will be increased, if necessary, during final closure cap design to accommodate anticipated weathering in order to ensure closure cap physical stability with regards to erosion over 10,000 years. Weathering is discussed further in Section 7.4.1.

In order to prevent the loss of overlying material into the erosion barrier the voids within the rock mass will be filled. The material to be used to fill the voids within the rock mass has yet to be selected. An evaluation of potential materials will be conducted and will include at a minimum the following potential fill materials:

- Controlled low-strength material (CLSM) or Flowable Fill infilling
- Gravel and/or sand infilling
- Bituminous material infilling
- Other cementitious material infilling and placement similar to roller-compacted concrete

After placement of the stone infilling with CLSM or Flowable Fill, gravel and/or sand, or bituminous material shall be applied on top of the stone in a manner that allows the material to penetrate into all the voids within the stone layer. The evaluation of materials to infill the stone will consider the following favorably during the selection process:

- No negative impact on the layer's ability to adequately perform as an erosion barrier
- No negative impact upon weathering or preferably tending to decrease the weathering rate,
- Its ability to facilitate the layer's ability to act as a barrier to burrowing animals
- Its ability to facilitate the layer's ability to hinder root penetration
- Its projected durability (i.e. longevity)
- No negative impact upon other FTF Closure Cap layers, particularly the lateral drainage layer and GCL

All work in association with placement of the erosion barrier shall be performed in accordance with the approved drawings, plans, and specifications of the final design, which will be produced near the end of the operational period.

4.4.10 Upper Backfill

A backfill will be placed over the erosion barrier. The upper backfill will be a minimum 2.5-ft thick layer used to bring the elevation of the closure cap up to that necessary for placement of the topsoil. The upper backfill will also provide water storage to promote evapotranspiration. The materials and placement method for the upper backfill is essentially identical to that of the middle backfill. The initial loose lift of the upper backfill shall be placed in a single lift on top of the erosion control barrier in order to avoiding damaging the erosion control barrier. No equipment used to place the upper backfill shall come into direct contact with the erosion control barrier. It shall be driven only on top of previously placed backfill. The feet of any compaction equipment used on the backfill shall be sized so that during compaction of the backfill the feet do not directly run on the erosion control barrier. The upper backfill will be fine graded to the required contours. All work in association with placement of the upper backfill shall be performed in accordance with the approved drawings, plans, and specifications of the final design, which will be produced near the end of the operational period.

4.4.11 Topsoil

The upper most soil layer of the closure cap shall consist of minimum 6 inches of soils capable of supporting a vegetative cover (i.e., topsoil) obtained from onsite sources. It will be placed at a maximum 2.0 percent slope in order to promote runoff and to provide a stable slope that will prevent the initiation of gullying (see Appendix A for the calculations based upon the Probable Maximum Precipitation (PMP) and the methodology outlined by Johnson 2002). The topsoil in conjunction with the vegetative cover will store water and promote evapotranspiration. The topsoil shall be placed in a single 0.5-ft lift on top of the upper backfill. The equipment used to place and fine grade the topsoil shall be low ground pressure equipment. No compactive effort shall be applied to the topsoil other than that provided by the equipment used to place and fine grade it. Measures shall be taken to minimize erosion of the topsoil layer prior to the establishment of the vegetative cover. Any such erosion shall be repaired by the installation subcontractor until such time as the vegetative cover has been established and construction of the closure cap has been certified as complete. Certification of closure cap construction completion will be provided by a Professional Engineer who certifies that the closure cap has been constructed per the approved drawings, plans, and specifications. All work in association with placement of the topsoil shall be performed in accordance with the approved drawings, plans, and specifications of the final design, which will be produced near the end of the operational period.

4.4.12 Vegetative Cover

A vegetative cover will be established to promote runoff, minimize erosion, and promote evapotranspiration. The topsoil will be fertilized, seeded, and mulched to provide a vegetative cover. The initial vegetative cover shall be a persistent grass such as Bahia. During seeding and establishment of the initial grass, appropriate mulch, erosion control fabric, or similar substances will be used to protect the surface.

The area will be repaired through transplanting or replanting to ensure that a self maintaining cover is developed. If it is determined that bamboo is a climax species that prevents or greatly slows the intrusion of pine trees, it will be planted as the final vegetative cover at the end of the 100-year institutional control period. Pine trees are typically assumed to be the most deeply rooted naturally occurring climax plant species at SRS, which will degrade the GCL through root penetration. In contrast, bamboo is a shallow-rooted species, which will not degrade the GCL. Additionally bamboo evapotranspirates year-round in the SRS climate, minimizes erosion, and can sustain growth with minimal maintenance. A study conducted by the U.S. Department of Agriculture (USDA) Soil Conservation Service (SCS) has shown that two species of bamboo (Phyllostachys bissetii and Phyllostachys rubromarginata) will quickly establish a dense ground cover (Salvo and Cook 1993). All work in association with the vegetative cover shall be performed in accordance with the approved drawings, plans, and specifications of the final design, which will be produced near the end of the operational period.

4.4.13 Toe of Closure Cap Side Slopes

The toe of closure cap side slopes will consist of a riprap layer to stabilize the side slope rip rap, provide erosion protection at the toe, transition flow from the side slope to adjacent areas, and provide gully intrusion protection to the embankment. The toe riprap will extend from the toe of the side slope a minimum of 20 ft (Figure 12). The toe riprap has been sized based upon the Probable Maximum Precipitation (PMP) and the methodology outlined by Johnson 2002 (see Appendix A for the calculations). Based upon these calculations, a 42 in thick layer of rock consistent with Type D riprap from Table F-3 of Johnson 2002 or Size R-300 riprap from Table 1 of ASTM 1997 has been determined to be suitable for use on the toe. The stone shall conform to one of these two stone gradations or equivalent. The exact gradation utilized shall be determined by availability and economics.

Quarries located near the SRS produce aggregate and rip rap consisting of granite, granite gneiss, gneiss, and mylonite (GDOT 2007). Granite aggregate and rip rap is typically utilized at SRS. However, the mylonitic quartzite reported available at an Augusta, Georgia quarry will be evaluated for durability versus the local granite. Consistent with the recommendations of Johnson 2002 and ASTM 1997, the toe riprap shall be angular, shall have a minimum specific gravity of 2.65, and shall be considered durable per the criteria outlined below:

- The rock shall be dense, sound, resistant to abrasion, free of clays, and free of cracks, seams, and other defects as determined by a petrographic examination (ASTM 2003a).

- Specific gravity (ASTM 2004b), absorption (ASTM 2004b), sodium sulfate soundness (ASTM 2005b), Los Angeles abrasion (ASTM 2003b), Schmidt Rebound Hardness-ISRM Method (Johnson 2002) tests shall be performed on the rock. Based upon these tests and the scoring methodology outlined by Johnson 2002, the rock shall have a quality score of 80 or greater.

Rock production and associated Quality Assurance/Quality Control (QA/QC) will be coordinated with the supplying quarry to assure the requisite rock size and mineralogical types are procured. The general approach will be to identify the highest-percent quartz rock type by quarry. Within the identified quarry, highly fractured, obviously weathered, and relatively feldspar-rich rock will be avoided, while "whole", fresh, and relatively quartz-rich rock will be preferentially selected. Visual selection of optimal rock may be supported by supplementary information (e.g., sulfate analyses and abrasion testing) available from the supplier. The final closure cap design will include a comprehensive QA/QC plan for selection and installation of all materials used to construct the cap.

The toe riprap shall be handled, loaded, transported, stockpiled, and placed consistent with the requirements outlined in ASTM 2002a and Johnson 2002. In particular, the riprap shall be handled, loaded, transported, stockpiled, and placed in a manner that prevents breakage and segregation of the stone into various sizes. The riprap shall be placed in a single 42-in lift by dumping and spreading with heavy equipment. The stone shall be placed in a manner that achieves a reasonably well-graded distribution of stones, a fairly consistent thickness (i.e., 38 to 52 in.), and a densely packed, wedged together, firmly interlocked layer. The only compactive effort applied to the stone shall be that provided by the equipment used to place it and a minimum of two passes of a Caterpillar D6 tracked bulldozer or equivalent.

Weathering of the stone shall be considered as outlined in Sections 4.4.9 and 7.4.1. All work in association with placement of the toe riprap shall be performed in accordance with the approved drawings, plans, and specifications of the final design, which will be produced near the end of the operational period.

4.4.14 Closure Cap Side Slopes

The closure cap side slopes will be placed at a maximum 3 horizontal to 1 vertical (3H:1V, 33.3 percent, or 19.5 degrees) and have a riprap surface with an underlying gravel bedding layer to prevent gully formation on the side slopes and to provide long-term slope stability. The side slope riprap and underlying gravel bedding layer will extend from the toe of the side slope up the side slope to a minimum 10 ft onto the top slope (Figure 12). The stone bedding layer shall consist of a 6 in thick layer of well-graded crushed stone with either the gradation shown in Table F-4 of Johnson 2002 or that of Figure 8 of ASTM 1997 (i.e., FS-2 filter/bedding stone). The side slope riprap has been sized based upon the Probable Maximum Precipitation (PMP) and the methodology outlined by Abt and Johnson 1991 and Johnson 2002 (see Appendix A for the calculations). Based upon these calculations, a 24-in thick layer of rock consistent with Type D riprap from Table F-3 of Johnson 2002 or Size R-150 riprap from Table 1 of ASTM 1997 has been determined to be suitable for use on the side slopes. The stone shall conform to one of these two stone gradations or equivalent. The exact gradation utilized shall be determined by availability and economics.

Quarries located near the SRS produce aggregate and rip rap consisting of granite, granite gneiss, gneiss, and mylonite (GDOT 2007). Granite aggregate and rip rap is typically utilized at SRS. However, the mylonitic quartzite reported available at an Augusta, Georgia quarry will be evaluated for durability versus the local granite. Consistent with the recommendations of Johnson 2002 and ASTM 1997, both the bedding stone and riprap shall be angular, shall have a minimum specific gravity of 2.65, and shall be considered durable per the criteria outlined below:

- The rock shall be dense, sound, resistant to abrasion, free of clays, and free of cracks, seams, and other defects as determined by a petrographic examination (ASTM 2003a).

- Specific gravity (ASTM 2004b), absorption (ASTM 2004b), sodium sulfate soundness (ASTM 2005b), Los Angeles abrasion (ASTM 2003b), Schmidt Rebound Hardness-ISRM Method (Johnson 2002) tests shall be performed on the rock. Based upon these tests and the scoring methodology outlined by Johnson 2002, the rock shall have a quality score of 80 or greater.

Rock production and associated Quality Assurance/Quality Control (QA/QC) will be coordinated with the supplying quarry to assure the requisite rock size and mineralogical types are procured. The general approach will be to identify the highest-percent quartz rock type by quarry. Within the identified quarry, highly fractured, obviously weathered, and relatively feldspar-rich rock will be avoided, while "whole", fresh, and relatively quartz-rich rock will be preferentially selected. Visual selection of optimal rock may be supported by supplementary information (e.g., sulfate analyses and abrasion testing) available from the supplier. The final closure cap design will include a comprehensive QA/QC plan for selection and installation of all materials used to construct the cap.

Both the bedding stone and riprap shall be handled, loaded, transported, stockpiled, and placed consistent with the requirements outlined in ASTM 2002a and Johnson 2002. In particular, the bedding stone and riprap shall be handled, loaded, transported, stockpiled, and placed in a manner that prevents breakage and segregation of the stone into various sizes. The bedding stone shall be placed in a single 6-in compacted lift on the side slope from the bottom of the slope up the side slope by dumping, spreading, and compacting with a rubber-tired or smooth drum roller. The riprap shall be placed in a single 2-ft lift on top of the bedding stone from the bottom of the slope up the side slope by dumping and spreading with heavy equipment. The stone shall be placed in a manner that achieves a reasonably well-graded distribution of stones, a fairly consistent thickness (i.e., 1.8 to 2.5 ft), and a densely packed, wedged together, firmly interlocked layer. The only compactive effort applied to the stone shall be that provided by the equipment used to place it and a minimum of two passes of a Caterpillar D6 tracked bulldozer or equivalent.

Weathering of the stone shall be considered as outlined in Sections 4.4.9 and 7.4.1. All work in association with placement of the side slope bedding stone and riprap shall be performed in accordance with the approved drawings, plans, and specifications of the final design, which will be produced near the end of the operational period.

4.4.15 Integrated Drainage System

An integrated drainage system will be designed and built to handle the runoff from the closure cap and drainage from the closure cap lateral drainage layer. The runoff and lateral drainage will be directed to a system of riprap lined ditches, which will be designed in accordance with Johnson 2002. The riprap lined ditches will direct the water away from the FTF closure cap as a whole and will be constructed around the perimeter of the FTF closure cap. The ditches will discharge into sedimentation basins as necessary for sediment control. The riprap for the ditches has not been sized yet since the FTF is currently in the initial phase operational period. Due to the early phase and lack of a detailed closure cap layout, a detailed drainage system cannot yet be designed. Therefore drainage areas and flows cannot be currently assigned in order to size the riprap for various sized ditches.

5.0 INITIAL INFILTRATION ESTIMATES

Initial infiltration estimates have been made for the following potential FTF Closure Cap configurations:

- Configuration #1: The closure cap configuration described in Table 11 and Table 12 of Section 4.3, with the erosion barrier infilled with CLSM. (i.e. composite barrier, lateral drainage and erosion barrier with CLSM infill)

- Configuration #1a: Closure cap configuration described in Table 11 and Table 12 of Section 4.3, with sandy soil infilling the erosion barrier. (i.e. composite barrier, lateral drainage and erosion barrier with sandy soil infill)

- Configuration #2: Closure cap configuration #1 without the geosynthetic clay liner (GCL). (i.e. HDPE geomembrane as sole hydraulic barrier, lateral drainage and erosion barrier with CLSM infill).

- Configuration #3: Closure cap configuration #1 without the high density polyethylene (HDPE) geomembrane. (i.e. GCL as sole hydraulic barrier, lateral drainage and erosion barrier with CLSM infill).

- Configuration #4: Closure cap configuration #1 without the lateral drainage layer. (i.e., composite barrier and erosion barrier with CLSM infill)

- Configuration #5: Closure cap configuration #1 without the erosion barrier. (i.e., composite barrier and lateral drainage)

- Configuration #6: Closure cap configuration described in Table 11 and Table 12 of Section 4.3 where the GCL and HDPE geomembrane were eliminated and the material properties for lateral drainage layer and erosion barrier were replaced with those of backfill rather than eliminating the layers.(i.e. a soils closure cap only).

5.1 HELP MODEL USE AND DESCRIPTION

Within the FTF Performance Assessment (PA) the Hydrologic Evaluation of Landfill Performance (HELP) Model is used to provide the upper boundary condition for a 2-dimensional PORFLOW vadose zone flow model. The upper boundary condition provided by the HELP Model consists of the average annual infiltration through the composite barrier layer (i.e., HDPE geomembrane overlaying a GCL) of the FTF Closure Cap (see Figure 11) at each time step modeled.

The HELP model is a quasi-two-dimensional water balance model designed to conduct landfill water balance analyses. The model requires the input of weather, soil, and closure cap design data. It provides estimates of runoff, evapotranspiration, lateral drainage, vertical percolation (i.e., infiltration), hydraulic head, and water storage for the evaluation of various landfill designs.

United States Army Corps of Engineers (USACE) personnel at the Waterways Experiment Station (WES) in Vicksburg, Mississippi developed the HELP model, under an interagency agreement (DW21931425) with the U.S. Environmental Protection Agency (USEPA). As such the HELP model is a USEPA-sanctioned model for conducting landfill water balance analyses. HELP model version 3.07, issued on November 1, 1997, is the latest version of the model. It is public domain software available from the WES website at:

http://el.erdc.usace.army.mil/products.cfm?Topic=model&Type=landfill.

USEPA and the USACE have provided the following documentation associated with the HELP model:

- A user's guide (Schroeder et al. 1994a), which provides instructions for HELP model use.
- Engineering documentation (Schroeder et al. 1994b), which provides information on the source language used to write the code, the hardware necessary to operate the code, data generation methodologies available for use, and the methods of solution.
- Verification test reports comparing the model's drainage layer estimates to the results of large-scale physical models (Schroeder et al. 1987a) and comparing the model's water balance estimates to "field data from a total of 20 landfill cells at 7 sites in the United States" (Schroeder et al. 1987b).

The software quality assurance plan for the use of the HELP model in Performance Assessments (PA) is documented in Phifer 2006.

The National Research Council of the National Academies (NRC-NA 2007) conducted an assessment of waste barrier performance, which included information on the use of the HELP model. The NRC-NA concluded that the HELP model is probably the most widely used model to predict the water balance (infiltration in particular) of closure caps. They noted that the primary advantages of the HELP model over more sophisticated models for unsaturated flow (i.e., those solving Richard's equation and utilizing characteristic curves) are that the HELP model requires much less input data and requires significant less computational time. While the NRC-NA conceptually prefers the use of the more sophisticated models over the HELP model, their evaluation of the HELP model indicates that it over predicts infiltration in humid environments similar to that at SRS (see NRC-NA 2007 Table 5.5). Bonaparte, et al. (2002) came to conclusions consistent with the NRC-NA 2007 regarding the use of the HELP model. Bonaparte, et al. (2002) performed a literature review of the comparison of field derived landfill water balances to HELP model results. This evaluation concluded that "for a number of cases the HELP model analysis was shown to give reasonable predictions of cumulative longer-term water balances." In addition Bonaparte, et al. (2002) performed an evaluation of measured leachate collection and removal system (LCRS) flow rates for six landfill cells versus leachate generation rates estimated by HELP. Based upon this evaluation the authors concluded "that the HELP model can appropriately be employed as a tool to estimate long-term average leachate generation rates …"

Additionally a comparison of the Section 3.2 background SRS water balance and infiltration studies with HELP model results for FTF Closure Cap configuration #6 is presented in Section 5.6. It is concluded in Section 5.6 that the HELP model results compare very well with the background water balance and infiltration studies, indicating that the use of the HELP model produces reasonable and acceptable results. Based upon these evaluations, use of the HELP model to establish the upper boundary condition infiltration for a 2-dimensional PORFLOW vadose zone flow model seems appropriate.

The 2-dimensional PORFLOW vadose zone flow model, to which the HELP model infiltration results form the upper boundary condition, meets the preferred NRC-NA model requirements (i.e. solves Richard's equation and utilizing characteristic curves). The PORFLOW software package is a comprehensive mathematical model for simulating multi-phase fluid flow, heat transfer and mass transport in variably saturated porous and fractured media (Aleman 2007). It is a finite element code that solves Richard's equation utilizing characteristic curves to solve variably saturated flow problems. It can simulate transient or steady-state problems in Cartesian or cylindrical geometry. The porous medium may be anisotropic and heterogeneous and may contain discrete fractures or boreholes with the porous matrix. The theoretical models within the code provide a unified treatment of concepts relevant to fluid flow and transport.

The HELP and PORFLOW models are currently used in conjunction for the FTF PA. The HELP model considers precipitation, runoff, evapotranspiration, and lateral drainage in estimating infiltration through the composite barrier layer (i.e., HDPE geomembrane overlaying a GCL) of the FTF Closure Cap (see Figure 11). This infiltration forms the upper boundary condition for a 2-dimensional PORFLOW FTF vadose zone flow model. This PORFLOW model solves Richard's equation utilizing characteristic curves to solve variably saturated flow within the vadose zone consistent with the preferences of the NRC-NA. This combined use of the HELP and PORFLOW models appears reasonable.
However as indicated in Section 8.7.1, the HELP model is not capable of appropriately considering the results of the probability based root penetration model which has been developed to evaluate root penetration of the GCL through tensile stress cracks within the overlaying HDPE geomembrane. For this reason in the future other models will be evaluated as a replacement to the HELP model. The models to be considered may include but are not limited to FEHM, HYDRUS-2D, LEACHM, TOUGH-2, UNSAT-H, and VADOSE/W.

The initial infiltration estimates (i.e. at year 0) through the potential FTF Closure Cap configurations listed in Section 5.0 have been made utilizing the HELP Model and the results are provided in Section 5.6. Additionally infiltration estimates which account for closure cap degradation have been made for FTF Closure Cap configuration #1a over 10,000 years within Section 8.0.

5.2 HELP MODEL WEATHER INPUT DATA

The HELP model requires the input of evapotranspiration, precipitation, temperature, and solar radiation data. There are several input options for each type of weather data required. In general the options available for weather data input include (Phifer and Nelson 2003):

- Historical records from specific cities ("default")
- Synthetically generated data based upon the statistical characteristics of historic data from specific cities
- Synthetically generated data modified with average monthly precipitation and temperature data from the site in question
- Manual data entry (Schroeder et al. 1994a and Schroeder et al. 1994b)

The default weather databases included in the HELP model are very limited in terms of the period of time and cities covered in the database. A complete set of historic weather data is not available for the Savannah River Site (SRS) or Augusta, GA within the HELP model. However, the HELP model can generate synthetic weather data for up to a 100-year span and many more cities are included than in the default weather databases. In particular, synthetic weather data can be generated for Augusta; however it is not available for SRS. However average monthly data from SRS is available to modify the Augusta synthetically generated data. The manual input option requires data availability and placement of the data in a format acceptable to the HELP model, which is a very time consuming operation. Therefore for the purposes of this modeling, synthetic daily weather data for precipitation, temperature, and solar radiation over 100 years was generated based upon the HELP data for Augusta and modified with the SRS specific average monthly precipitation and temperature data. (Phifer and Nelson 2003)

The SRS collects meteorological data from a network of nine weather stations. The primary SRS precipitation data has been collected from the Savannah River National Laboratory (SRNL) (773-A) weather station between 1952 and 1995 and from the Central Climatology site (CLM) since 1995. However the closest weather station to the FTF is the 200-F weather station, from which daily precipitation data has been collected from a manual rain gauge from 1961 onward. Collection of temperature data at SRS began in 1968.

The primary SRS temperature data has been collected from the SRNL (773-A) weather station between 1968 and 1995 and from the Central Climatology site (CLM) since 1995. Temperature data is not collected at the 200-F weather station where the manual rain gauge is located. (Hunter 2006)

SRS-specific monthly precipitation and average monthly temperature data from the combined SRNL/CLM weather stations and precipitation data from the 200-F weather station were obtained from the SRNL Atmospheric Technologies Group (ATG) web site located at http://shweather.srs.gov/servlet/idg.Weather.Weather (SRNL – ATG 2006). Table 13 provides the monthly precipitation for years 1952 to 2006 obtained from the combined SRNL/CLM weather stations and the average monthly precipitation over the entire time span. Table 14 provides the monthly precipitation for the years 1961 to 2006 obtained from the 200-F weather station and the average monthly precipitation over the entire time span. As noted in Table 14, there are some missing precipitation data associated with the 200-F weather station. Therefore the monthly 200-F precipitation data for each month that has any missing data has been replaced with the primary SRS precipitation data obtained from the combined SRNL/CLM weather stations, if the combined SRNL/CLM precipitation data for that month is greater than that of the 200-F weather station. The combined SRNL/CLM data results in an average precipitation of 48.53 in/yr over the 55-year monitoring period; whereas, the revised 200-F data results in an average precipitation of 49.04 in/yr over its 46 year monitoring period. Table 15 provides the average monthly temperature for the years 1968 to 2006 obtained from the combined SRNL/CLM weather stations and the monthly average over the entire time span. A 100 year synthetic daily weather database for precipitation, temperature, and solar radiation was generated based upon the HELP data for Augusta that was modified with the SRS specific average monthly precipitation and temperature for the entire time spans from Table 14 and Table 15, respectively.

To generate the evapotranspiration data, the default option for Augusta, Georgia was utilized, since it is available and is considered constant from year to year. Additionally, the user must specify two values, the evaporative zone depth and maximum leaf area index. The evaporative zone depth is the maximum depth to which the HELP model will allow evapotranspiration to occur. An evaporative zone depth of 22 inches was selected based upon HELP model guidance, which lists this depth as a "fair" depth for Augusta, Georgia. This is considered a conservative maximum evaporative zone depth due to the anticipated capillarity associated with the surficial soil types (i.e. topsoil and upper backfill) and the anticipated root depths (see Section 7.2). The maximum leaf area index is a measure of the maximum active biomass that the HELP model will allow to be present. The actual leaf area index utilized by the HELP model is modified from the maximum based upon daily temperature, daily solar radiation, and the beginning and ending dates of the growing season. A maximum leaf area index of 3.5 was selected based upon HELP model guidance, which lists this value for a "good" stand of grass. (Schroeder et al. 1994b and Phifer and Nelson 2003) The HELP model methodology to estimate evapotranspiration is described in detail by Schroeder et al. (1994b). The methodology takes into consideration daily solar radiation, daily temperature, humidity, wind speed, vegetation type, leaf area index, growing season, surface and soil water content, maximum evaporative depth, soil water transport, and soil capillarity. As outlined previously (see Section 4.4) the initial vegetative cover of the FTF Closure Cap shall be a persistent grass such as Bahia. Bamboo shall be utilized as the final vegetative cover only if it is determined that bamboo is a climax species that prevents or greatly slows the intrusion of pine trees onto the closure cap. Therefore at this time the HELP modeling of the FTF closure cap will be based upon the use of a grass vegetative cover rather than bamboo.

The HELP model weather data input files, which were utilized for all HELP model runs, are provided in the following appendices:

- Appendix B, Augusta Synthetic Precipitation Modified with SRS Specific Average Monthly Precipitation Data over 100 Years (file name: Fprec.d4)
- Appendix C, Augusta Synthetic Temperature Modified with SRS Specific Average Monthly Temperature Data over 100 Years (file name: Ftemp.d7)
- Appendix D, Augusta Synthetic Solar Radiation Data over 100 Years (file name: Fsolar.d13)
- Appendix E, Augusta Evapotranspiration Data (file name: Fevap.d11)

A statistical evaluation of the precipitation data set (file name: Fprec.d4) is provided in Table 16 and Table 17 as an aid to the interpretation of the HELP model infiltration results provided in subsequent sections. The precipitation data set utilized represents 100 years of synthetic daily precipitation data, developed as described. Table 16 provides a statistical evaluation of this precipitation data set in terms of both annual and daily precipitation. The annual precipitation within the data set ranges from 29.81 to 68.60 inches/ year; while the daily precipitation ranges from 0 to 6.72 inches/day. Table 17 provides the percentage frequency of daily precipitation events for the data set in 0.5 inch increments from 0 to 7.0 inches/day. As seen no precipitation occurs on approximately 72.5 percent of the days, and on the days that precipitation does occur, the bulk of the precipitation (i.e., >99 percent) is in the 0 to 3 inch/day range.

Table 13. Combined SRNL/CLM Weather Stations Monthly and Annual Precipitation for Years 1952 to 2006

Year	Jan	Feb	March	April	May	June	July	August	Sept	October	Nov	Dec	Annual
1952	2.07	3.23	6.55	3.12	5.56	5.67	2.82	5.98	3.34	1.36	2.86	3.99	46.55
1953	2.69	5.48	3.83	2.96	4.42	5.38	3.63	3.61	8.53	0.11	1.04	7.51	49.19
1954	1.26	1.64	2.95	2.50	2.89	2.91	2.03	4.10	1.43	1.29	2.94	2.88	28.82
1955	4.75	2.62	2.21	5.57	4.53	3.31	3.94	5.07	3.42	1.32	2.93	0.46	40.13
1956	1.67	7.94	4.84	3.21	3.07	2.34	4.34	3.18	4.56	1.83	0.93	2.05	39.96
1957	2.05	1.58	4.29	2.75	8.02	4.17	3.51	2.41	5.04	6.12	6.46	2.24	48.64
1958	4.01	4.38	4.96	5.63	2.07	2.50	5.32	2.76	1.12	0.96	0.21	4.42	38.34
1959	3.54	6.06	6.44	2.03	3.81	4.06	5.80	2.93	8.71	10.86	1.97	3.54	59.75
1960	6.91	5.81	5.76	5.07	1.96	3.66	5.27	2.81	4.84	0.97	0.83	2.93	46.82
1961	3.59	5.76	7.23	8.20	3.88	3.01	3.09	7.15	1.00	0.07	1.83	6.60	51.41
1962	4.64	5.14	6.52	4.03	3.50	4.41	2.56	3.43	5.55	2.27	3.50	2.20	47.75
1963	5.96	3.64	3.34	3.70	2.98	8.42	3.18	1.04	5.37	0.00	3.68	4.47	45.78
1964	7.79	6.00	5.79	5.94	3.62	4.50	10.42	12.34	5.43	6.53	0.60	4.10	73.06
1965	1.83	6.19	10.18	2.81	1.63	5.14	9.57	1.29	2.36	2.95	1.99	1.69	47.63
1966	7.81	6.22	4.30	2.93	5.28	4.81	3.52	5.84	3.98	1.51	1.37	3.85	51.42
1967	3.91	4.43	7.54	2.60	5.94	4.06	7.23	8.48	0.99	0.31	2.81	3.37	51.67
1968	4.56	0.97	1.58	2.23	4.24	5.28	3.58	8.05	5.06	3.33	4.14	2.93	45.95
1969	2.20	2.47	3.42	4.71	2.57	4.26	1.94	4.38	4.05	2.00	0.40	4.42	36.82
1970	3.12	2.75	7.90	1.28	4.01	4.68	4.69	3.78	2.75	4.02	1.50	5.62	46.10
1971	5.01	3.80	9.71	2.57	3.62	4.81	13.71	9.98	4.74	5.27	2.16	2.79	68.17
1972	7.81	3.71	2.68	0.60	4.10	5.64	1.92	8.19	1.52	1.03	2.92	4.26	44.38
1973	5.50	4.47	6.67	4.55	4.91	12.97	6.86	3.90	4.38	1.72	0.98	3.99	60.90
1974	2.42	6.66	3.03	3.05	3.35	2.80	4.44	6.77	3.32	0.09	1.99	4.11	42.03
1975	4.98	6.64	5.92	4.42	5.15	3.83	8.55	3.83	5.18	1.74	3.41	2.03	55.68

Table 13. Combined SRNL/CLM Weather Stations Monthly and Annual Precipitation for Years 1952 to 2006 - continued

Year	Jan	Feb	March	April	May	June	July	August	Sept	October	Nov	Dec	Annual
1976	4.18	1.08	3.83	2.50	10.9	4.35	1.95	1.64	5.48	4.92	4.19	5.08	50.10
1977	3.72	1.62	6.86	1.27	1.79	2.47	3.42	7.30	5.50	4.27	1.63	3.86	43.71
1978	10.02	1.31	3.06	3.53	3.64	3.42	4.11	5.10	4.06	0.06	3.54	1.87	43.72
1979	3.59	7.74	3.09	6.49	8.94	1.54	7.85	2.12	6.13	1.35	3.95	2.17	54.96
1980	5.12	3.48	10.96	1.69	3.49	2.99	0.90	2.03	5.86	2.14	2.5	1.91	43.07
1981	0.89	5.02	4.72	2.07	6.90	4.29	3.96	5.79	0.54	2.81	1.00	9.55	47.54
1982	3.94	4.46	2.51	5.68	2.73	4.28	11.49	5.02	4.62	3.87	2.41	4.85	55.86
1983	3.75	7.22	6.62	5.77	1.67	6.57	4.85	6.32	3.56	1.92	5.39	4.15	57.79
1984	3.51	7.09	6.05	8.00	9.79	2.54	7.28	5.52	0.60	0.31	0.90	1.38	52.97
1985	3.01	6.92	1.31	0.84	1.70	4.62	8.10	4.38	0.49	6.34	6.36	2.48	46.55
1986	1.46	3.58	4.08	1.45	3.84	3.03	2.96	10.9	1.54	4.19	5.82	5.83	48.68
1987	7.39	7.55	4.97	0.70	3.57	5.64	4.87	4.93	3.56	0.29	2.74	1.42	47.63
1988	4.15	3.19	2.91	4.78	2.85	7.12	1.78	6.80	4.40	3.39	2.17	2.91	46.45
1989	1.42	3.59	5.52	4.89	2.60	6.67	11.46	3.27	4.87	3.36	3.00	4.41	55.06
1990	3.07	2.38	2.37	1.21	2.95	0.89	7.31	8.07	0.62	19.62	1.41	1.57	51.47
1991	7.03	1.84	7.89	4.73	3.06	2.17	7.89	9.26	4.40	0.99	1.55	3.32	54.13
1992	4.45	3.89	2.98	2.40	1.34	6.27	3.69	4.83	6.38	3.11	7.78	2.86	49.98
1993	7.45	3.62	8.37	1.74	1.43	3.27	3.12	2.23	7.29	0.99	1.87	1.81	43.19
1994	4.80	3.91	6.42	1.05	1.45	5.08	7.47	3.47	0.99	10.01	3.05	4.62	52.32
1995	6.96	7.97	0.92	1.28	1.77	8.15	5.71	6.92	5.75	2.64	2.38	4.47	54.92
1996	3.18	2.43	6.24	1.42	1.23	3.46	5.20	4.83	4.05	1.95	1.17	2.70	37.86
1997	4.42	5.35	2.88	3.05	2.23	9.58	6.00	4.00	5.59	3.90	4.76	7.91	59.67
1998	7.83	7.18	5.61	6.28	3.53	3.76	4.49	4.34	8.43	0.52	0.77	1.76	54.50
1999	5.71	2.75	2.55	1.66	2.82	5.21	4.97	3.86	5.02	2.38	1.04	1.47	39.44

Table 13. Combined SRNL/CLM Weather Stations Monthly and Annual Precipitation for Years 1952 to 2006 - continued

Year	Jan	Feb	March	April	May	June	July	August	Sept	October	Nov	Dec	Annual
2000	6.53	0.61	3.84	1.43	0.20	4.86	2.49	5.11	7.82	0.00	3.50	1.94	38.33
2001	2.80	2.52	7.27	0.96	4.79	4.87	5.42	1.60	3.34	0.12	1.16	1.20	36.05
2002	2.97	2.23	3.88	2.10	2.87	3.25	3.92	4.59	3.88	2.62	4.73	4.32	41.36
2003	2.32	5.03	8.65	9.19	7.17	9.47	5.94	5.16	4.29	3.31	1.52	1.92	63.97
2004	3.79	6.28	1.44	1.94	2.50	8.71	4.66	2.74	8.72	0.66	4.74	1.72	47.9
2005	1.78	4.87	5.42	2.16	3.22	5.56	6.28	3.86	0.05	3.35	2.79	4.77	44.11
2006	2.94	2.83	2.90	2.98	1.60	7.23	2.59	2.54	2.43	3.48	2.61	5.03	39.16
Monthly Average Precip.	4.26	4.31	4.98	3.30	3.70	4.80	5.16	4.91	4.13	2.85	2.65	3.49	48.53

Notes to Table 13:

- All precipitation values in inches
- The 1952 through 1995 precipitation data has been collected from the SRNL (773-A) weather station and since 1995 it has been collected from the Central Climatology site (CLM)
- The monthly data highlighted in grey represents months for which some precipitation data is missing from the 200-F weather station precipitation database. The Table 14 monthly 200-F precipitation data for each month that has any missing data has been replaced with the combined SRNL/CLM weather stations precipitation data, if the combined SRNL/CLM precipitation data for that month is greater than that of the 200-F weather station.

Table 14.   200-F Weather Station Monthly and Annual Precipitation for Years 1961 to 2006

Year	Jan	Feb	March	April	May	June	July	August	Sept	October	Nov	Dec	Annual
1961	3.55	5.53	7.57	7.23	4.21	2.00	2.94	8.55	0.56	0.02	1.80	6.20	50.16
1962	4.35	5.28	6.46	3.85	2.61	1.97	1.74	4.36	4.03	1.87	3.31	2.40	42.23
1963	6.05	3.59	3.15	3.18	2.37	7.04	2.00	1.54	5.05	0.00	3.24	4.11	41.32
1964	7.67	5.69	5.40	5.81	3.56	5.18	10.99	10.87	5.19	6.44	0.77	4.17	71.74
1965	2.12	6.24	8.13	2.45	1.70	4.28	9.63	1.75	2.11	3.00	2.18	1.31	44.90
1966	6.82	5.42	4.39	3.26	4.87	3.82	3.88	5.17	4.68	1.37	1.18	3.21	48.07
1967	3.56	3.71	7.54	2.60	4.56	2.13	6.28	7.31	1.02	0.53	2.37	2.83	44.44
1968	3.92	0.97	1.92	1.83	2.91	4.32	4.93	3.14	1.88	3.03	4.14	2.84	35.83
1969	1.85	2.13	3.43	4.20	3.41	4.36	1.99	5.43	5.96	1.96	0.34	3.83	38.89
1970	2.78	2.62	7.65	1.33	4.99	3.09	2.87	3.20	0.69	4.29	1.83	5.06	40.40
1971	5.01	3.97	8.70	2.85	2.03	6.73	11.52	9.40	2.33	4.91	2.16	3.03	62.64
1972	7.93	3.66	2.78	0.47	3.75	5.84	2.68	6.88	1.28	0.76	3.62	4.73	44.38
1973	5.31	4.82	6.48	4.97	5.17	8.52	4.50	5.83	3.22	1.22	0.35	4.69	55.08
1974	2.68	6.60	2.91	2.63	3.86	4.97	4.00	6.98	3.24	0.01	2.05	4.12	44.05
1975	5.45	6.19	5.97	3.98	5.48	3.24	7.65	3.95	7.86	1.00	4.43	4.00	59.20
1976	4.22	1.50	3.95	2.22	10.86	6.40	3.28	2.41	5.40	5.54	3.89	4.82	54.49
1977	3.86	2.20	7.90	1.02	2.61	3.79	4.02	8.43	4.66	5.44	2.07	5.14	51.14
1978	8.44	1.45	3.07	4.85	3.33	1.94	4.13	2.72	3.74	0.20	3.54	2.17	39.58
1979	3.41	9.31	3.95	5.37	7.44	1.55	7.55	9.14	7.77	1.38	7.34	2.29	66.50
1980	4.29	2.33	11.44	2.31	3.57	3.30	0.99	2.86	7.38	1.95	2.21	1.96	44.59
1981	0.93	3.91	3.87	2.71	4.51	5.05	4.39	5.92	0.85	2.88	0.91	8.45	44.38
1982	4.73	3.86	1.95	4.90	2.37	4.07	10.53	6.45	5.02	3.61	2.06	4.58	54.13
1983	4.00	8.06	5.49	4.71	3.00	2.77	3.71	6.21	3.52	2.21	4.98	3.66	52.32
1984	3.53	5.34	6.05	7.11	10.73	1.82	6.46	3.52	1.06	0.40	0.97	1.16	48.15
1985	2.98	6.36	1.06	0.83	3.49	4.88	9.82	2.90	0.90	3.77	7.51	2.74	47.24

Table 14.   200-F Weather Station Monthly and Annual Precipitation for Years 1961 to 2006 - continued

Year	Jan	Feb	March	April	May	June	July	August	Sept	October	Nov	Dec	Annual
1986	1.18	3.05	2.75	0.96	3.47	2.60	2.61	8.59	0.80	3.05	5.76	4.94	39.76
1987	6.79	7.50	4.35	0.75	1.86	5.02	5.68	4.20	2.91	0.32	2.28	1.37	43.03
1988	3.74	1.03	2.48	4.88	0.97	6.67	2.24	2.98	4.79	3.50	1.92	1.66	36.86
1989	1.24	2.91	4.83	5.89	3.36	5.82	9.51	0.39	4.84	5.51	3.65	3.35	51.30
1990	2.91	1.84	1.88	0.94	2.16	3.87	7.65	10.65	0.50	17.84	1.25	2.55	54.04
1991	6.73	1.80	7.86	5.43	3.93	3.35	14.4	9.79	2.05	0.80	1.47	3.19	60.80
1992	3.63	5.32	2.93	2.74	1.54	8.28	5.18	8.70	2.42	6.21	8.57	2.96	58.48
1993	8.90	5.09	8.48	1.37	1.56	6.03	2.87	3.48	6.56	0.61	2.29	1.79	49.03
1994	4.81	3.38	6.68	0.98	1.20	4.80	5.54	5.29	1.48	10.5	2.56	4.91	52.13
1995	5.97	7.50	0.83	0.93	2.10	12.73	4.27	6.69	5.42	2.31	2.13	3.90	54.78
1996	3.08	2.08	6.81	1.69	2.40	4.59	5.55	10.58	3.14	2.09	1.46	2.97	46.44
1997	4.20	5.56	2.32	3.88	2.42	6.77	7.02	2.33	5.80	5.54	5.49	7.57	58.90
1998	8.42	6.59	6.48	5.97	3.63	3.74	4.79	3.63	8.30	0.78	0.76	1.90	54.99
1999	5.82	2.60	3.04	1.34	2.55	8.67	4.70	2.87	5.66	2.24	0.65	1.35	41.49
2000	5.80	1.06	3.06	2.08	2.27	6.02	2.90	5.84	6.47	0.02	3.86	2.02	41.40
2001	3.21	3.55	6.88	1.44	4.00	6.29	5.30	1.78	5.70	0.04	0.97	0.68	39.84
2002	2.07	2.13	3.50	2.19	1.54	2.75	4.76	6.02	3.87	3.34	5.64	4.20	42.01
2003	1.62	5.97	8.10	9.67	6.60	7.28	5.86	3.09	2.32	3.10	1.30	2.27	57.18
2004	4.63	6.81	0.99	1.69	2.47	8.49	3.01	4.21	10.54	3.32	4.11	3.81	54.08
2005	2.88	3.96	6.57	1.35	3.82	7.78	5.09	6.00	0.20	4.80	2.42	6.33	51.20
2006	3.47	3.37	2.45	3.22	1.53	7.73	5.88	1.49	2.34	2.53	3.25	5.12	42.38
Monthly Average Precip.	4.36	4.21	4.88	3.18	3.54	5.05	5.38	5.29	3.82	2.96	2.85	3.53	49.04

Notes to Table 14:

- All precipitation values in inches
- All precipitation data taken from the 200-F Weather Station, except that as noted below
- No 200-F Weather Station precipitation data is available for the following dates in the SRS ATG Climate Data database:
    - 3/30/1967 and 3/31/1967
    - 4/1/1967 through 4/18/1967
    - 11/4/1968
    - 10/31/1970
    - 1/24/1971
    - 11/27/1971
    - 10/31/1998
- The monthly data highlighted in grey represents months for which some precipitation data is missing from the 200-F weather station precipitation database. The monthly 200-F precipitation data for each month that has any missing data has been replaced with the Table 13 combined SRNL/CLM weather stations precipitation data, if the combined SRNL/CLM precipitation data for that month is greater than that of the 200-F weather station. The following denotes the replacement status of the monthly data highlighted in grey:
    - March 1967: The monthly 200-F precipitation data point of 5.29 inches was replaced with the monthly combined SRNL/CLM data point of 7.54 inches
    - April 1967: The monthly 200-F precipitation data point of 2.58 inches was replaced with the monthly combined SRNL/CLM data point of 2.6 inches
    - November 1968: The monthly 200-F precipitation data point of 2.89 inches was replaced with the monthly combined SRNL/CLM data point of 4.14 inches
    - October 1970: The monthly 200-F precipitation data point of 4.29 inches was not replaced with the monthly combined SRNL/CLM data point of 4.02 inches
    - January 1971: The monthly 200-F precipitation data point of 4.47 inches was replaced with the monthly combined SRNL/CLM data point of 5.01 inches
    - November 1971: The monthly 200-F precipitation data point of 1.75 inches was replaced with the monthly combined SRNL/CLM data point of 2.16 inches
    - October 1998: The monthly 200-F precipitation data point of 0.78 inches was not replaced with the monthly combined SRNL/CLM data point of 0.52 inches

Table 15. SRS Monthly and Annual Average Temperatures for Years 1968 to 2005

Year	Jan	Feb	March	April	May	June	July	August	Sept	October	Nov	Dec	Annual
1968	43.5	43.4	57.1	66.5	71.3	80.0	83.1	82.8	77.0	67.0	55.4	45.9	64.4
1969	46.5	46.6	51.5	64.5	70.5	80.3	83.3	77.6	72.8	66.1	52.1	45.4	63.1
1970	39.0	47.2	55.9	66.8	74.2	79.0	81.1	80.8	78.6	67.0	51.6	49.3	64.2
1971	44.6	46.4	49.5	63.4	70.7	81.3	80.7	80.4	75.2	70.2	55.5	56.9	64.6
1972	51.7	45.6	57.6	67.4	72.4	75.3	79.7	80.6	77.2	64.8	54.4	53.2	65.0
1973	46.1	45.9	60.7	61.9	70.5	77.7	79.1	74.5	70.5	62.4	59.0	50.3	63.2
1974	59.6	50.8	62.2	66.2	75.3	77.5	81.5	80.9	75.3	64.5	56.6	49.0	66.6
1975	51.4	53.2	55.8	63.9	75.6	79.1	79.7	82.4	75.7	68.7	59.3	48.5	66.1
1976	44.2	55.7	61.5	64.8	68.9	75.6	80.4	78.0	73.1	60.1	48.7	44.8	63.0
1977	35.3	47.1	60.0	66.9	73.3	80.6	83.6	80.6	77.9	62.1	58.2	46.7	64.4
1978	39.3	41.3	54.2	65.7	70.9	79.7	82.1	81.2	77.1	65.6	60.7	49.6	64.0
1979	42.1	44.6	57.5	64.5	71.3	75.1	79.6	80.5	73.4	64.8	57.4	47.4	63.2
1980	45.9	44.3	52.6	63.5	71.2	78.3	83.8	82.5	79.2	62.7	52.8	46.0	63.6
1981	40.4	48.5	53.0	67.0	68.6	81.3	81.3	76.3	74.0	62.1	54.4	43.2	62.5
1982	43.0	50.0	58.9	62.4	75.7	78.8	80.9	80.1	75.0	66.2	58.7	54.8	65.4
1983	43.3	48.0	55.3	59.4	66.8	76.7	84.3	83.9	74.8	67.2	56.4	45.8	63.5
1984	45.0	51.7	56.5	62.6	71.9	80.1	80.1	80.8	74.0	73.4	53.4	56.9	65.5
1985	42.9	49.5	60.2	67.5	74.5	80.8	81.1	79.7	75.7	70.8	65.5	45.4	66.1
1986	45.4	54.6	57.9	66.4	74.4	82.7	86.9	80.1	78.4	67.1	61.3	49.3	67.0
1987	46.2	48.6	56.5	62.3	74.5	79.9	82.8	83.8	76.6	60.7	59.1	52.9	65.3
1988	42.3	47.8	56.8	64.2	70.4	76.8	81.6	81.4	75.4	61.2	58.0	49.1	63.8
1989	52.2	52.0	58.3	64.2	70.6	79.8	81.4	80.9	75.3	67.3	52.4	44.2	64.9

Table 15.   SRS Monthly and Annual Average Temperatures for Years 1968 to 2005 - continued

Year	Jan	Feb	March	April	May	June	July	August	Sept	October	Nov	Dec	Annual
1990	54.9	57.5	60.0	64.0	72.9	80.5	83.7	83.8	79.0	69.4	59.9	54.6	68.4
1991	47.9	54.1	60.3	69.2	76.9	79.5	83.6	81.2	77.4	68.1	55.4	54.0	67.3
1992	49.5	54.1	57.2	65.0	71.2	78.9	83.7	80.7	76.9	65.0	57.1	48.0	65.6
1993	51.7	47.8	53.2	58.9	69.7	78.2	83.6	80.0	75.2	62.8	55.2	43.6	63.3
1994	41.5	50.1	60.2	68.0	71.2	82.3	81.8	81.2	77.4	67.2	62.3	53.3	66.4
1995	45.5	49.9	58.6	65.9	73.5	75.0	79.9	79.0	71.8	65.9	50.8	43.8	63.3
1996	44.6	50.1	50.6	61.6	72.9	76.5	79.3	76.0	72.7	62.1	51.6	48.8	62.2
1997	48.2	52.9	63.3	61.2	68.5	74.0	80.2	79.0	75.0	64.1	51.6	47.0	63.7
1998	49.7	51.1	53.6	62.7	74.6	82.1	82.6	80.3	75.8	66.9	60.5	53.6	66.1
1999	51.9	51.6	53.4	67.2	69.7	76.6	80.7	82.9	73.8	64.3	58.1	48.6	64.9
2000	44.4	50.2	58.5	60.7	75.1	78.0	79.9	77.6	71.7	62.5	53.1	38.2	62.5
2001	43.8	52.4	53.0	63.9	71.3	75.3	77.7	78.8	71.2	62.2	60.0	52.4	63.5
2002	47.3	48.0	57.6	68.1	70.2	77.5	80.5	78.4	75.4	66.7	51.7	44.5	63.8
2003	42.0	47.5	57.6	61.6	70.6	75.2	77.3	77.7	71.9	63.7	58.2	42.9	62.2
2004	43.7	45.2	58.5	63.4	74.0	77.7	80.1	77.3	73.2	66.2	56.1	45.8	63.4
2005	47.9	49.0	53.1	60.9	68.0	75.4	79.4	78.8	77.0	64.7	56.1	44.3	62.9
2006	50.8	47.3	55.3	66.3	70.1	76.2	80.3	80.5	72.9	62.4	53.6	50.6	63.8
Average Monthly Temp	46.0	49.3	56.8	64.4	71.9	78.3	81.3	80.1	75.1	65.3	56.2	48.4	64.4

Notes to Table 15:

- All temperatures in degree Fahrenheit (°F)
- Temperature data collected from the SRNL (773-A) weather station between 1968 and 1995 and from the Central Climatology site (CLM) since 1995

Table 16.   Precipitation Data Set Annual and Daily Precipitation Statistics

Parameter	Annual Precipitation (inches/year)	Daily Precipitation (inches/day)
Maximum	68.60	6.72
Average	49.14	0.13
Median	48.83	0
Minimum	29.81	0
Standard Deviation	7.69	0.37

Table 17.   Precipitation Data Set Frequency of Daily Precipitation Events

Daily Precipitation Range (inches)	Percent of Total Days in Range	Cumulative Percent of Total Days	Percent of Days with Precipitation in Range	Cumulative Percent of Days with Precipitation
0	72.543	72.543	-	-
0 to 0.5	18.381	90.924	66.946	66.946
0.5 to 1.0	5.330	96.254	19.411	86.357
1.0 to 1.5	2.084	98.338	7.589	93.946
1.5 to 2.0	0.900	99.238	3.278	97.224
2.0 to 2.5	0.427	99.665	1.555	98.779
2.5 to 3.0	0.143	99.808	0.522	99.301
3.0 to 3.5	0.092	99.900	0.335	99.636
3.5 to 4.0	0.065	99.965	0.236	99.872
4.0 to 4.5	0.022	99.986	0.079	99.951
4.5 to 5.0	0.003	99.989	0.010	99.961
5.0 to 5.5	0.003	99.992	0.010	99.970
5.5 to 6.0	0.000	99.992	0.000	99.970
6.0 to 6.5	0.003	99.995	0.010	99.980
6.5 to 7.0	0.005	100.000	0.020	100.000

5.3 HELP MODEL GENERAL INPUT DATA

Table 18 provides a listing of the HELP model (Schroeder et al. 1994a and Schroeder et al. 1994b) general input parameters (i.e., HELP model query) and the associated values selected for the FTF Closure Cap. The reasoning for each of the selected values is discussed.

The landfill area was based upon the maximum closure cap slope length of 585 feet as discussed in Section 4.1 (Figure 10) and the 1-foot width as utilized in the Appendix A, Physical Stability Calculations. This results in a modeled landfill area of 0.0134 acres. The landfill area is only utilized by the HELP model to estimate overall landfill water volumes associated with precipitation, runoff, evapotranspiration, lateral drainage, percolation, and change in water storage. This type of volume information is not utilized as input to subsequent models and therefore use of the entire area of the FTF closure cap is not required.

As outlined in Section 4.1 (Figure 10) it is assumed that the FTF Closure Cap is appropriately sloped so that 100 percent of the cap allows runoff to occur (i.e., there are no depressions).

Table 18.   FTF Closure Cap HELP Model General Input Parameters and Values

Input Parameter (HELP Model Query)	Selected Input Parameter Value
Landfill area =	0.0134 acres
Percent of area where runoff is possible =	100%
Do you want to specify initial moisture storage? (Y/N)	Y
Amount of water or snow on surface =	0 in.

A "yes" response has been provided to the HELP model query, which asks, "Do you want to specify initial moisture storage? (Y/N)." Therefore the initial moisture storage has been specified for all soil layers. While the initial moisture storage is not a fixed value for all soil layers, a fixed method of selecting the initial moisture storage value has been utilized for consistency. The initial soil moisture storage value has been selected as follows:

- The initial moisture storage of soil layers designated as either a vertical percolation layer or a lateral drainage layer was set at the field capacity of the soil layer.
- The initial moisture storage of soil layers designated as a barrier soil liner was set at the porosity of the soil.

The amount of water or snow on the surface of the cap was assumed to be zero as the initial model condition.

5.4 HELP MODEL LAYER INPUT DATA

The HELP model requires the classification of each layer into one of the following classifications (Schroeder et al. 1994a; Schroeder et al. 1994b):

- <u>Vertical Percolation Layer:</u> Layers with this designation allow unsaturated downward water flux due to gravity and if the layer is within the evaporative zone depth of 22 inches as discussed in Section 5.2, upward water flux due to evapotranspiration.
- <u>Lateral Drainage Layer:</u> Layers with this designation allow unsaturated downward water flux due to gravity and saturated, down slope, lateral drainage due to the build up of positive head within the layer. A lateral drainage layer must be underlain by either a barrier soil liner or geomembrane liner.
- <u>Barrier Soil Liner:</u> Layers with this designation are those with lower saturated hydraulic conducitivites that are designed to restrict the downward flux of water. They are assumed to be saturated and allow saturated downward water flux due to positive head above the liner.
- <u>Geomembrane Liner:</u> Layers with this designation are synthetic membranes designed to restrict the downward flux of water. A saturated downward water flux due to positive head above the liner is allowed through these liners due to both holes in the liner and its saturated hydraulic conductivity.

Different HELP model inputs are required for each of the layer types as outlined in Table 19. Table 20 provides the thickness, maximum slope length, and top of layer slope associated with each of the FTF Closure Cap layers outlined in Sections 4.2 and 4.3 (Table 11). The three geotextile fabric layers outlined in Table 11 will not be included in the HELP modeling, since they act primarily to separate or protect layers rather than to perform a hydraulic function. Additionally, Table 20 provides the HELP model layer type associated with each layer. Development of the required inputs (Table 19) for each of the FTF Closure Cap layers modeled (Table 20) is discussed.

5.4.1 Topsoil HELP Model Inputs

As indicated in Table 19, total porosity, field capacity, wilting point, and saturated hydraulic conductivity input values are required for the topsoil. SRS soils, utilized as top soils, would generally be classified as silty sand (SM) materials under the Unified Soil Classification System (USCS) or typically as loamy sand (LS) or sometimes as sandy loams (SL) in the United States Department of Agriculture (USDA) soil textural classification (i.e., textural triangle). Yu et al. 1993 provides total porosity, water retention (suction head versus saturation), and saturated hydraulic conductivity data for two samples of SRS topsoil.

Table 19. HELP Model Required Input per Layer Type

Property	HELP Model Layer Type			
	Vertical Percolation Layer	**Lateral Drainage Layer**	**Barrier Soil Liner**	**Geomembrane Liner**
Thickness (in)	X	X	X	X
Total Porosity	X	X	X	na
Field Capacity [1]	X	X	X	na
Wilting Point [2]	X	X	X	na
Initial Moisture	X	X	X	na
Saturated Hydraulic Conductivity (cm/s)	X	X	X	X
Drainage Length (ft)	na	X	na	na
Drain Slope (%)	na	X	na	na
Geomembrane Pinhole Density (#/acre)	na	na	na	X
Geomembrane Installation Defects (#/acre)	na	na	na	X
Geomembrane Placement Quality	na	na	na	X

X = property input value required for that layer type

na = property input value is not applicable for that layer type

[1] The HELP model defines the field capacity as the volumetric water content (θ_v) at a soil suction head (Ψ) of 0.33 bars." (Schroeder et al. 1994a; Schroeder et al. 1994b) 0.33 bars ≈ 337 cm-H_2O (1 bar ≈ 1,020.7 cm-H_2O at 60°F)

[2] The HELP model defines the wilting point as the volumetric water content (θ_v) at a soil suction head (Ψ) of 15 bars." (Schroeder et al. 1994a; Schroeder et al. 1994b) 15 bars ≈ 15,310 cm-H_2O (1 bar ≈ 1,020.7 cm-H_2O at 60 °F)

Table 20. FTF Closure Cap Layer Thickness, Slope Length, Slope and Layer Type

Layer	Thickness (inches)	Maximum Slope Length (ft)	Top of Layer Slope (%)	HELP Model Layer Type
Topsoil	6	585	2	1
Upper Backfill	30	585	2	1
Erosion Barrier	12	585	2	1
Middle Backfill	12	585	2	1
Lateral Drainage Layer	12	585	2	2
High Density Polyethylene (HDPE) Geomembrane	0.06 (60 mil)	585	2	4
Geosynthetic Clay Liner (GCL)	0.2	585	2	3
Foundation Layer (Lower Backfill)	84 (minimum)	585	2	1

Within the HELP model the layer types are denoted by the following numeric designations:
1 = vertical percolation layer
2 = lateral drainage layer
3 = barrier soil liner
4 = geomembrane liner

Yu et al. 1993 (page 1-5) provides the saturated hydraulic conductivity and porosity for two SRS topsoil samples. The average values of saturated hydraulic conductivity and porosity of the two SRS topsoil samples were utilized in the HELP modeling:

Sample ID	Saturated Hydraulic Conductivity, K_{sat} (cm/s)	Porosity, η (vol/vol)
Top Soil – 1	3.06E-03	0.405
Top Soil – 2	3.13E-03	0.388
Average	3.1E-03	0.396

See the notes from Table 19 for the HELP model definition of field capacity and wilting point. Volumetric moisture content can be determined as follows (Hillel 1982):

$$\theta_v = \eta s, \quad \text{where } \theta_v = \text{volumetric moisture content; } \eta = \text{porosity; } s = \text{saturation}$$

The following information was obtained from the table on page 1-9 of Yu et al. 1993 for water retention (suction head versus saturation) testing of topsoil samples from which the field capacity (volumetric water content at 0.33 bars or 337 cm-H_2O) can be derived by linear interpolation:

Sample ID	Applied Pressure	
	4 psi (281.2 cm-H_2O)	8 psi (562.5 cm-H_2O)
Top Soil – 1	0.298	0.257
Top Soil – 2	0.266	0.239
Average	0.282	0.248

All values are saturations (*s*) in vol/vol format
1 psi $\approx$ 70.3087 cm-H_2O at 4°C

The following provides the linear interpolation used to determine the top soil field capacity based upon the above top soil water retention data, which will be used in the HELP modeling:

Field capacity = θ_v at 337 cm-H_2O = $\eta \times s$ at 337 cm-H_2O =

$$0.396 \times \left(0.248 + \left[\left(\frac{562.5 - 337}{562.5 - 281.2} \right)(0.282 - 0.248) \right] \right) = 0.109$$

Site specific data are not available for the determination of SRS top soil wilting point. Therefore the wilting point from a HELP model default soil that closely resembles the SRS top soil will be utilized. Table 1 of Schroeder 1994b provides HELP model default soils. The HELP model default soil #4, with a wilting point of 0.047, that is classified as a SM material (USCS) and a LS material (USDA) is considered the closest HELP model default soil to the SRS top soil. Therefore the SRS top soil will be assigned a wilting point of 0.047 for the HELP modeling.

A comparison of the SRS top soil with HELP model default soil #4 is provided:

Material	Porosity, η (vol/vol)	Field Capacity (vol/vol)	Wilting Point (vol/vol)	Saturated Hydraulic Conductivity, K_{sat} (cm/s)
HELP model default soil #4 [1]	0.437	0.105	0.047	1.7E-03
SRS top soil	0.396	0.109	-	3.1E-03

[1] Schroeder 1994b Table 1

5.4.2 Upper Backfill and Middle Backfill HELP Model Inputs

As indicated in Table 19, total porosity, field capacity, wilting point, and saturated hydraulic conductivity input values are required for the upper backfill and middle backfill. Phifer et al. 2006 provides recommended values of total porosity, characteristic curves (suction head, saturation, and relative permeability), and saturated hydraulic conductivity for control compacted backfill placed over the Old Radioactive Waste Burial Ground (643-G) and for remolded samples from Z-Area soils. The field capacity and wilting point can be derived from characteristic curve data. The 643-G and Z-Area materials represent typical SRS control compacted backfill, consisting of soils classified typically as clayey sands (SC) or sometimes silty sands (SM) materials under USCS or as sandy clay loam (SCL) in the USDA soil textural classification (i.e. textural triangle) that have been compacted to specified test standards.

From Table 5-18 of Phifer et al. 2006 the following recommended backfill property values were obtained, which will be utilized in the HELP modeling:

- Total porosity (η) = 0.35
- Vertical saturated hydraulic conductivity (K_{sat}) = 4.1E-05 cm/s

Use of the vertical saturated hydraulic conductivity within the HELP model for the backfill materials is considered appropriate, since the backfill has been designated as a vertical percolation layer within the model subject to vertical flow considerations only.

See the notes from Table 19 for the HELP model definition of field capacity and wilting point. Volumetric moisture content can be determined as follows (Hillel 1982):

$$\theta_v = \eta s, \quad \text{where } \theta_v = \text{volumetric moisture content; } \eta = \text{porosity; } s = \text{saturation}$$

Backfill characteristic curve data was obtained from the Phifer et al. 2006, Table 5-21. From this data the field capacity (volumetric water content at 0.33 bars or 337 cm-H$_2$O) and wilting point (volumetric water content at 15 bars or 15,310 cm-H$_2$O) of the backfill were derived by linear interpolation:

Suction Head Ψ (cm-H$_2$O)	Saturation s (vol/vol)
331	0.721
381	0.711
14,400	0.519
16,600	0.513

The following provides the linear interpolation used to determine the backfill field capacity and wilting point, respectively, based upon the above backfill characteristic curve data, which will be used in the HELP modeling:

Field capacity = θ_v at 337 cm-H$_2$O = $\eta \times s$ at 337 cm-H$_2$O =

$$0.35 \times \left(0.711 + \left[\left(\frac{381-337}{381-331} \right)(0.721-0.711) \right] \right) = 0.252$$

Wilting point = θ_v at 15,310 cm-H$_2$O = $\eta \times s$ at 15,310 cm-H$_2$O =

$$0.35 \times \left(0.513 + \left[\left(\frac{16,600-15,310}{16,600-14,400} \right)(0.519-0.513) \right] \right) = 0.181$$

5.4.3 Erosion Barrier HELP Model Inputs

As indicated in Table 19, total porosity, field capacity, wilting point, and saturated hydraulic conductivity input values are required for the erosion barrier. As outlined within Section 4.4.9, the erosion barrier shall consist of rock consistent with Type B riprap from Table F-3 of Johnson 2002 or Size R-20 riprap from Table 1 of ASTM 1997 that is filled with a yet to be determined material (see Section 4.4.9) to prevent the loss of overlying material into the erosion barrier. Configurations #1, #2, #3, and #4 (see Section 5.0) include an erosion barrier infilled with CLSM. Configuration #1a includes and erosion barrier infilled with a sandy soil.

This results in a combined material with the following properties for each of the infilling cases considered:

Erosion Barrier Infill Material	Porosity, η (vol/vol)	Field Capacity (vol/vol)	Wilting Point (vol/vol)	Saturated Hydraulic Conductivity, K_{sat} (cm/s)
Erosion barrier with CLSM infill	0.125	0.109	0.031	8.36E-07
Erosion barrier with sandy soil infill	0.15	0.10	0.07	1.3E-04

See Appendix F for the calculations associated with the soil properties for the erosion barrier.

5.4.4 Lateral Drainage Layer HELP Model Inputs

As indicated in Table 19, total porosity, field capacity, wilting point, and saturated hydraulic conductivity input values are required for the lateral drainage layer. As outlined within Section 4.4.5, the lateral drainage layer shall consist of a 1-foot thick layer of coarse sand. The sand utilized for the lateral drainage layer will be a procured material rather than a material obtained from a SRS borrow pit. Therefore a minimum saturated hydraulic conductivity of the sand will be a requirement in the specification for the procurement of the sand. Table 21 provides the saturated hydraulic conductivity of various sands. The saturated hydraulic conductivity of the natural sands in Table 21 ranges from 1E-04 to 1 cm/s. The saturated hydraulic conductivity of the procured sands in Table 21 ranges from 5.0E-02 to 4.5E-01 cm/s. Based upon this information, a minimum saturated hydraulic conductivity of 5.0E-02 cm/s will be specified for the lateral drainage layer sand. The total porosity, field capacity, and wilting point for the HELP modeling will be taken as that of the HELP model default soil #1 (i.e., natural coarse sand (USDA) or poorly graded sand (USCS)) as shown below (Schroeder 1994b):

- Total porosity (η) = 0.417
- Field capacity = 0.045
- Wilting point = 0.018

Table 21. Sand Saturated Hydraulic Conductivity

Material	Saturated Hydraulic Conductivity, K_{sat} (cm/s)	Source
SRS water table aquifer at the TNX Terrace	2.1E-02	Phifer et al. 2001 Table 5
Natural deposit of clean sand	<1E-03 to 1	Freeze and Cherry 1979 Table 2.2
Clean sand or sand and gravel	1E-03 to 1	Bear 1972 Table 5.5.1
Various natural sands	1E-04 to 2.0E-01	Lamb and Whitman 1969 Figure 19.5
Sedimentary deposit of well-sorted sand, glacial outwash	1E-03 to 1E-01	Fetter 1988 Table 4.5
Sandy soils	1E-03 to 1E-02	Hillel 1982
HELP model default soil #1 [1]	1E-02	Schroeder 1994b Table 1
Foster Dixianna FX-50 fine gravel pack	5.0E-02	Phifer et al. 2001 Table 7
Foster Dixianna FX-99 coarse gravel pack	4.5E-01	Phifer et al. 2001 Table 7
Fine gravel	1.5E-01	Phifer et al. 2006 Table 5-18 and Yu et al. 1993

Notes:
Materials in grey are natural sands and the other items are procured materials.
[1] HELP model default soil #1 is a natural coarse sand (USDA) or poorly graded sand (USCS)

5.4.5 High Density Polyethylene (HDPE) Geomembrane HELP Model Inputs

As indicated in Table 19, saturated hydraulic conductivity, geomembrane pinhole density, geomembrane installation defects, and geomembrane placement quality input values are required for the HDPE geomembrane. The permeability of water through HDPE geomembranes is not a hydraulic conductivity through interconnected pore space, but rather it is a water vapor diffusional process (Rumer and Mitchell 1995). Therefore the water permeability of HDPE geomembranes is not determined by standard hydraulic conductivity tests performed for porous materials but by a water vapor transmission (WVT) test (ASTM 2005a). A typical value of water vapor transmission through a 100 mil HDPE geomembrane is approximately 0.006 g/m^2-day, which equates to a saturated hydraulic conductivity of approximately 1.0E-13 cm/s (Koerner 1990; Rumer and Mitchell 1995). Schroeder 1994b Table 6 uses a saturated hydraulic conductivity of 2.0E-13 cm/s as the default value for HDPE geomembranes within the HELP model (HELP model default geosynthetic material #35). A saturated hydraulic conductivity of 2.0E-13 cm/s will be utilized for the 60 mil HDPE geomembrane within the HELP modeling, since it is the higher of those documented.

Layers designated as geomembrane liners (HELP model layer type #4) do not require the input of total porosity, field capacity, and wilting point as required for soil layers. However, geomembrane liners do require the additional input of geomembrane pinhole density (#/acre), geomembrane installation defects (#/acre), and geomembrane placement quality. Within the HELP model (Schroeder et al. 1994a; Schroeder et al. 1994b), geomembrane pinholes are defined as manufacturing defects such as polymerization deficiencies that result in holes estimated to be 1 mm in diameter (7.84E-03 cm^2).

The following is stated concerning pinholes (Schroeder et al. 1994b):

> "… Pinhole flaws are more commonly associated with the original, less sophisticated, geomembrane manufacturing techniques. Current manufacturing and polymerization techniques have made pinhole flaws less common."

Schroeder et al. 1994a recommends that "typical geomembranes may have about 0.5 to 1 pinhole per acre from manufacturing defects." Based upon this guidance, the as-installed FTF Closure Cap HDPE geomembrane will be assumed to have 1 pinhole/acre.

Within the HELP model (Schroeder et al. 1994a; Schroeder et al. 1994b), geomembrane installation defects are defined as geomembrane damage resulting from seaming errors, abrasion, and punctures occurring during installation that result in holes estimated to be 1 cm^2 in area (1.13 cm in diameter). Schroeder et al. 1994b recommends an installation defect density of 1 defect per acre for intensively monitored projects and 10 defects per acre or more "when quality assurance is limited to spot checks or when environmental difficulties are encountered during construction". In summary Schroeder et al. 1994a provide the following installation defect densities based upon the quality of installation:

Installation Quality	Installation Defect Density (#/acre)	Frequency [1] (percent)
Excellent	Up to 1	10
Good	1 to 4	40
Fair	4 to 10	40
Poor	10 to 20	10

[1] Provides the frequency of landfill installation built to that particular level of quality assurance.

As outlined within Section 4.4.3, the HDPE geomembrane quality assurance plan shall be developed and implemented for 100-percent visual inspection of all rolls as they are laid down and of all seams; appropriate wrinkle control measures as the rolls are laid down, seamed, and covered; 100-percent non-destructive field testing of all seams by vacuum testing (ASTM 2006a) and/or air pressure testing (ASTM 2006b); and destructive testing (ASTM 2006c) on a frequency consistent with GRI 1998. Any seam or non-seam area that has been identified as defective and any holes created for destructive testing shall be repaired and non-destructively tested prior to acceptance. Additionally a nonwoven geotextile fabric will be placed directly on top of the HDPE geomembrane to protect it from puncture or tear during placement of the overlying 1-foot thick coarse sand lateral drainage layer.

Based upon these FTF Closure Cap requirements and the guidance provided by Schroeder et al. 1994a and Schroeder et al. 1994b, the as-installed FTF Closure Cap HDPE geomembrane will be assumed to be installed with good quality assurance and will be assumed to have 4 installation defects/acre.

Within the HELP model (Schroeder et al. 1994a; Schroeder et al. 1994b), six geomembrane placement quality designations are provided. These geomembrane placement quality designations relate to the degree of contact between the geomembrane and the underlying soil and the potential for lateral flow along the boundary between the two layers. Schroeder et al. 1994b states the following regarding the geomembrane placement quality for geomembranes underlain by a GCL:

> "Excellent liner contact is achieved under three circumstances. Medium permeability soils and materials are typically cohesionless and therefore generally are able to conform to the geomembrane, providing excellent contact. The second circumstance is for very well prepared low permeability soil layer with exceptional geomembrane placement typically achievable in the laboratory, small lysimeters or small test plots. The third circumstance is by the use of a geosynthetic clay liner (GCL) adjacent to the geomembrane with a good foundation. The GCL, upon wetting, will swell to fill the gap between the geomembrane and the foundation, providing excellent contact."

Based upon the use of a GCL beneath the HDPE geomembrane for the FTF Closure Cap configurations #1, #1a, #4, and #5 and the guidance provided by Schroeder et al. 1994a and Schroeder et al. 1994b, an "excellent" (HELP model numerical designation 2) geomembrane placement quality designation will be utilized for these configurations. FTF Closure Cap configuration #2 involves the placement of the HDPE geomembrane directly on top of the Upper Foundation Layer. Under these conditions Schroeder et al. 1994a and Schroeder et al. 1994b recommend a "good" (HELP model numerical designation 3) geomembrane placement quality designation.

5.4.6 Geosynthetic Clay Liner (GCL) HELP Model Inputs

As indicated in Table 19 total porosity, field capacity, wilting point, and saturated hydraulic conductivity input values are required for the GCL. Schroeder et al. 1994a Table 4 and Schroeder et al. 1994b Table 2 provide the following default property values for bentonite mats (i.e. GCLs):

- Total porosity (η) = 0.750
- Field capacity = 0.747
- Wilting point = 0.400
- Saturated Hydraulic Conductivity (K_{sat}) = 3.0E-09 cm/s

GCL manufacturers typically list the maximum hydraulic conductivity of GCLs as 5.0E-09 cm/s. Dixon and Phifer 2006 reported the results of 9 saturated hydraulic conductivity measurements made on a GCL (BentoFix® Thermal Lock® NWL) manufactured by GSE Lining Technology, Inc., with simulated groundwater as the permeant. This GCL was utilized as part of the closure cap placed on the SRS Old Radioactive Waste Burial Ground (643-G).

The following provides the results of this testing:

GSE Lining Technology, Inc. BentoFix® Thermal Lock® NWL Saturated Hydraulic Conductivity		
GSE Specification	SRS Testing (Dixon and Phifer 2006)	
	Range	Average
5.0E-09 cm/s (maximum)	1.4E-09 to 4.1E-10 cm/s	6.81E-10 cm/s

All of the Dixon and Phifer 2006 saturated hydraulic conductivity values were well below the manufacture's specification of 5.0E-09 cm/s and the HELP model default value of 3.0E-09 cm/s. However, since the manufacturers typically list the maximum hydraulic conductivity of GCLs as 5.0E-09 cm/s, the manufacturers' value will be utilized for the FTF Closure Cap HELP modeling. The values of total porosity, field capacity, and wilting point recommended by Schroeder et al. 1994a and Schroeder et al. 1994b will also be utilized for the FTF Closure Cap HELP modeling.

5.4.7 Foundation Layer (Lower Backfill) HELP Model Inputs

As outlined within Section 4.4.1, it is anticipated that the upper one foot of the foundation layer will consist of soil with a moderately low permeability (i.e., ≤1.0E-06 cm/s) produced by blending typical SRS backfill with a small weight percent bentonite. Since it is anticipated that the upper one foot of the foundation layer will consist of typical SRS backfill with a small weight percent bentonite, the porosity, field capacity, and wilting point of typical SRS backfill from Section 5.4.2 will be utilized for this portion of the foundation layer as shown below:

- Total porosity (η) = 0.35
- Field capacity = 0.252
- Wilting point = 0.181
- Saturated Hydraulic Conductivity (Ksat) = 1.0E-06 cm/s

It is further anticipated that the lower portions of the foundation layer will need to promote drainage of infiltrating water away from and around the tanks and ancillary equipment, requiring a relatively high saturated hydraulic conductivity such as 1.0E-03 cm/s. A default HELP soil with a saturated hydraulic conductivity of approximately 1.0E-03 cm/s has been selected to represent this portion of the foundation layer. HELP model default soil #5 meets this criteria and has the following property values (Schroeder et al. 1994a; Schroeder et al. 1994b):

- Total porosity (η) = 0.457
- Field capacity = 0.131
- Wilting point = 0.058
- Saturated Hydraulic Conductivity (Ksat) = 1.0E-03 cm/s

5.4.8 HELP Model Layer Summary Input Data

Table 22 provides a summary of the initial intact HELP Model inputs for each of the FTF closure cap layers modeled.

Table 22. Initial Intact HELP Model Input Summary for the FTF Closure Cap Layers

Layer	HELP Model Layer Type	Thickness (in)	Total Porosity	Field Capacity	Wilting Point	Initial Moisture [1]	Saturated Hydraulic Conductivity (cm/s)	Drainage Length (ft)	Drain Slope (%)
Topsoil	1	6	0.396	0.109	0.047	0.109	3.1E-03	na	na
Upper Backfill	1	30	0.35	0.252	0.181	0.252	4.1E-05	na	na
Erosion Barrier: Configuration #1 with CLSM Infill	1	12	0.125	0.109	0.031	0.109	8.36E-07	na	na
Erosion Barrier: Configuration #1a with Sandy Soil Infill	1	12	0.15	0.10	0.07	0.10	1.3E-04	na	na
Middle Backfill	1	12	0.35	0.252	0.181	0.252	4.1E-05	na	na
Lateral Drainage Layer	2	12	0.417	0.045	0.018	0.045	5.0E-02	585	2
HDPE Geomembrane	4	0.06 (60 mil)	na	na	na	na	2.0E-13	na	na
GCL	3	0.2	0.750	0.747	0.400	0.750	5.0E-09	na	na
Upper Foundation Layer	1	12	0.35	0.252	0.181	0.252	1.0E-06	na	na
Lower Foundation Layer	1	72	0.457	0.131	0.058	0.131	1.0E-03	na	na

Layer	Geomembrane Pinhole Density (#/acre)		Geomembrane Installation Defects (#/acre)		Geomembrane Placement Quality	
HDPE Geomembrane	1		4		3	

[1] The initial soil moisture storage value has been selected as follows:

- The initial moisture storage of soil layers designated as either a vertical percolation layer or a lateral drainage layer was set at the field capacity of the soil layer.
- The initial moisture storage of soil layers designated as a barrier soil liner was set at the porosity of the soil.

5.5 HELP MODEL RUNOFF INPUT DATA

The Soil Conservation Service (SCS) runoff curve number (CN) is another required HELP model input parameter. The HELP model provides three options to specify the CN. The option that produces a HELP model computed curve number, based on surface slope and slope length, soil texture of the top layer, and vegetation, was utilized. Table 23 provides the input values of surface slope and slope length, soil texture of the top layer, and vegetation that were utilized to produce the HELP model computed curve number. The 2 percent slope at a maximum 585-foot slope length was derived within Section 4.2. The soil texture selected (i.e., HELP model default soil #4) was selected as outlined in Section 5.4.1 above as being the closest HELP model default soil to typical SRS top soil. The HELP model (Schroeder et al. 1994a; Schroeder et al. 1994b) provides the following entries for the vegetation for determination of the CN:

1. Bare ground
2. Poor stand of grass
3. Fair stand of grass
4. Good stand of grass
5. Excellent stand of grass

As outlined in Section 4.4.12, the FTF Closure Cap initial vegetative cover shall be established and maintained such that a persistent, self maintaining, grass cover is provided. Based upon this requirement a good stand of grass (i.e., HELP model designation 4) will be utilized in the modeling. Based upon these input parameter values the HELP model computed a CN of 46.2.

Table 23. HELP Model Computed Curve Number Input Parameters

CN Input Parameter (HELP Model Query)	CN Input Parameter Value
Slope =	2%
Slope length =	585 ft
Soil Texture =	4 (HELP model default soil texture)
Vegetation =	4 (i.e., a good stand of grass)
HELP Model Computed Curve Number = 46.2	

5.6 HELP MODEL RUNS AND RESULTS

Table 24 provides the FTF Closure Cap configurations for which initial, intact (i.e., Year 0) infiltration estimates have been made along with a description of the configuration and the associated HELP model input and output file names. The HELP model input associated with each of the Table 24 configurations is provided in Appendix G. One hundred HELP model simulations, with precipitation ranging from 29.8 to 68.6 inches/year, were produced for the initial, intact conditions (i.e., Year 0) of each configuration. The detailed water balance data by simulation for each of the configurations are provided in Appendix H. The following HELP model results are provided for each of the configurations modeled:

- A chart of the annual infiltration versus annual precipitation for precipitation ranging from 29.8 to 68.6 inches/year (including a linear regression for the precipitation-infiltration data set)
- A table of the annual water balance (precipitation, runoff, evapotranspiration, lateral drainage, infiltration, and change in water storage) statistics
- A figure of the annual average water balance

As seen in Figure 17 and Table 25, precipitation falling on a configuration #1 type closure cap under initial, intact conditions (i.e., Year 0) results in an average infiltration of 0.00016 inches/year thru the GCL with a very narrow range of 0.00006 to 0.00020 inches/year. The water balance for precipitation falling on this configuration (see Table 25 and Figure 18) is dominated by evapotranspiration (average of 34.37 inches/year), lateral drainage (average of 8.48 inches/year), and runoff (6.24 inches/year).

As seen in Figure 19 and Table 26, precipitation falling on a configuration #1a type closure cap under initial, intact conditions results in an average infiltration of 0.00088 inches/year thru the GCL with a range of 0.00009 to 0.005 inches/year. The water balance for precipitation falling on this configuration (see Table 26 and Figure 20) is dominated by evapotranspiration (average of 32.57 inches/year) and lateral drainage (average of 16.07 inches/year).

As seen in Figure 21 and Table 27, precipitation falling on a configuration #2 type closure cap (no GCL) under initial, intact conditions results in an average infiltration of 0.012 inches/year thru the HDPE geomembrane with a very narrow range of 0.005 to 0.014 inches/year. The water balance for precipitation falling on this configuration (see Table 27 and Figure 22) is dominated by evapotranspiration (average of 34.37 inches/year), lateral drainage (average of 8.46 inches/year), and runoff (6.24 inches/year).

As seen in Figure 23 and Table 28, precipitation falling on a configuration #3 type closure cap (no HDPE geomembrane) under initial, intact conditions results in an average infiltration of 0.74 inches/year thru the GCL with a very narrow range of 0.32 to 0.89 inches/year. The water balance for precipitation falling on this configuration (see Table 28 and Figure 24) is dominated by evapotranspiration (average of 34.37 inches/year), lateral drainage (average of 7.74 inches/year), and runoff (6.24 inches/year).

As seen in Figure 25 and Table 29, precipitation falling on a configuration #4 type closure cap (no lateral drainage layer) under initial, intact conditions results in an average infiltration of 0.019 inches/year thru the GCL with a very narrow range of 0.005 to 0.022 inches/year. The water balance for precipitation falling on this configuration (see Table 29 and Figure 26) is dominated by evapotranspiration (average of 37.00 inches/year) and runoff (10.94 inches/year).

As seen in Figure 27 and Table 30, precipitation falling on a configuration #5 type closure cap (no erosion barrier) under initial, intact conditions results in an average infiltration of 0.00086 inches/year thru the GCL with a range of 0.00008 to 0.0049 inches/year. The water balance for precipitation falling on this configuration (see Table 30 and Figure 28) is dominated by evapotranspiration (average of 32.60 inches/year) and lateral drainage (average of 15.39 inches/year).

As seen in Figure 29 and Table 31, precipitation falling on a configuration #6 type closure cap (soils only closure cap) under initial, intact conditions results in an average infiltration of 16.45 inches/year with a very wide range of 0.02 to 30.80 inches/year. The water balance for precipitation falling on this configuration (see Table 31 and Figure 30) is dominated by evapotranspiration (average of 32.55 inches/year) and infiltration (average of 15.39 inches/year). Configuration #6 is a soils only closure cap with no barrier, drainage, or erosion control layers. As such the HELP model water balance results from configuration #6 are most applicable for comparison to the background water balance and infiltration studies presented in Section 3.2, as a check on the HELP model. Table 32 provides a comparison of the configuration #6 HELP model water balance results with the background water balance median and range presented in Section 3.2 (see Table 9 and Table 10 of Section 3.2). As seen in Table 32, the HELP model, configuration #6, water balance compares very well with that of the background studies. The precipitation values, from which the water balances are derived, are essentially the same, with the average HELP model configuration #6 precipitation (49.14 inches/year) being slightly greater than the median of the background studies (47.79 inches/ year). Very little runoff is shown for either. The water balance evapotranspiration for both are essentially the same, with the average HELP model configuration #6 evapotranspiration (32.55 inches/year) deviating from the median evapotranspiration of the background studies (31.2 inches/year) by the same deviation between the respective precipitation values. As a bottom line, the average HELP model configuration #6 infiltration (16.45 inches/year) is slightly greater than the median infiltration of the background studies (14.85 inches/year); indicating that the HELP model infiltration results may be conservative. All in all the HELP model results compare very well with the background water balance and infiltration studies, indicating that the use of the HELP model produces reasonable and acceptable results.

Figure 31, Table 33, and Figure 32 provide a comparison of the various configurations. Figure 31 provides a comparison of the annual infiltration versus annual precipitation of the configurations. This comparison is based upon the linear regression previously produced for each configuration's precipitation-infiltration data-set. Table 33 provides a summary of the pertinent HELP model average annual water balance output associated with each of these configurations. Figure 32 provides the average annual water balance output associated with each of these configurations graphically.

As seen from Figure 31, Table 33, and Figure 32, under initial, intact conditions, the FTF Closure Cap configuration #1 (composite barrier, lateral drainage and erosion barrier with CLSM infill) results the least infiltration with a projected annual average infiltration of 0.00016 inches/year. Configurations #1a (composite barrier, lateral drainage and erosion barrier with sandy soil infill) and 5 (composite barrier and lateral drainage (no erosion barrier)) result in the next least infiltration with a projected annual average infiltration of 0.00088 and 0.00086, respectively. Configurations #1a and 5 have essentially the same average annual water balance. Elimination of the GCL (configuration #2), HDPE geomembrane (configuration #3), or lateral drainage layer (configuration #4) from configuration #1 results in a significant increase in projected annual average infiltration to 0.012, 0.74, 0.19 inches/year, respectively. Configuration #6 represents a soils only closure cap and has the highest initial, intact average annual infiltration at 16.45 inches/year, but the lowest assumed installation cost. The average annual infiltration of configuration #6 is at the upper end of typical SRS background infiltration levels.

The following configurations will be eliminated from further consideration for the reasons outlined below:

- Even though the initial, intact infiltration configuration #2 is relatively low, it will be eliminated from further consideration, since it does not include a GCL underlying the HDPE geomembrane. Without a GCL underlying the HDPE geomembrane, holes formed in the HDPE geomembrane over time due to HDPE degradation will not be plugged by a GCL, which will allow substantial increases in infiltration over time.
- Configuration #4 will be eliminated from further consideration, since the use of a composite hydraulic barrier (i.e., HDPE geomembrane overlying a GCL) without an overlying lateral drainage layer results in essentially complete saturation of all layers above the hydraulic barrier layers. Such complete saturation could be detrimental to the closure cap vegetation and increase erosion.
- Configuration #5 will be eliminated from further consideration, since its elimination is not considered feasible, because it is needed to provide long-term physical stability for the closure cap. One item of note associated with the results for configuration #5, for which the erosion barrier was eliminated, is that a comparison to configurations #1, #2, #3, and #4 demonstrates that an erosion barrier infilled with CLSM promotes runoff and evapotranspiration, due to its relatively low saturated hydraulic conductivity (i.e., 8.36E-07 cm/s). This indicates that an erosion barrier with a low saturated hydraulic conductivity could be of benefit to minimize infiltration.

Configuration #1 will receive further consideration, since it results in the lowest projected infiltration. Configuration #1a will also receive further consideration for comparison with Configuration #1. Configuration #3 will receive further consideration, since it is most similar to the projected Saltstone Disposal Facility (SDF) closure cap configuration. Configuration #6 will receive further consideration, since it represents the least assumed installation cost and highest infiltration.

The annual infiltration data versus annual precipitation data for configurations #1, #1a, #3, and #6 is provided in Figure 17, Figure 19, Figure 23, and Figure 29 respectively, while Figure 31 provides a comparison of each configuration's annual infiltration versus annual precipitation based upon the linear regression of the associated configuration data from Figure 17, Figure 19, Figure 23, and Figure 29. Summary statistics for the water balance data for configurations #1, #1a, #3, and #6 are provided in Table 25, Table 26, Table 28, and Table 31, respectively, while Table 33 and Figure 32 provide a comparison of each configuration's average water balance.

Over an annual precipitation range of approximately 30 to 70 in/yr, Figure 31 shows that configuration #1 initially reduces infiltration by more than four orders of magnitude over a soils only closure cap (i.e., configuration #6), while configuration #1a reduces it by more than three orders of magnitude. Figure 31 also shows that configuration #3 (i.e., GCL hydraulic barrier only) initially reduces infiltration slightly greater than one order of magnitude over a soils only closure cap (i.e., configuration #6). The water balance for configurations #1 and #1a differ primarily in that configuration #1a results in significantly less runoff and more lateral drainage than configuration #1 (Table 33 and Figure 32). The water balance for configurations #1 and #3 are essentially the same except that configuration #1 directs more water out the lateral drainage layer and less through the GCL (Table 33 and Figure 32). A soils-only closure cap (i.e., configuration #6) results in very little runoff, no lateral drainage, and the greatest infiltration (Table 33 and Figure 32).

A comparison of Figure 17 (configuration #1) and Figure 19 (configuration #1a) show a greater scatter in data points for configuration #1a than #1, reflecting the greater variability in moisture moving through the erosion barrier (and thus greater variability in head on the HDPE geomembrane) with a higher hydraulic conductivity erosion barrier infill. As expected, the infiltration rate for the composite hydraulic barrier with overlying lateral drainage layer configuration is higher for an erosion barrier with a sandy soil, rather than CLSM infill - in this case, by over one order of magnitude. This indicates the benefit of using a lower, rather than higher hydraulic conductivity infill for the erosion barrier.

Table 24. FTF Closure Cap Configurations Modeled

#	Configuration description	HELP Model Input File	HELP Model Output File
1	Closure cap configuration described in Table 11 and Table 12 of Section 4.3, with CLSM infilling the erosion barrier. (i.e., composite barrier, lateral drainage and erosion barrier with CLSM infill)	FC100.D10	FC100o
1a	Closure cap configuration described in Table 11 and Table 12 of Section 4.3, with sandy soil infilling the erosion barrier. (i.e., composite barrier, lateral drainage and erosion barrier with sandy soil infill)	FC1A00.D10	FC1A00o.OUT
2	Closure cap configuration #1 without the GCL. The GCL was simply eliminated and was not replaced with another material since it is so thin. (i.e., HDPE geomembrane as sole hydraulic barrier, lateral drainage and erosion barrier with CLSM infill).	FC200.D10	FC200o.OUT
3	Closure cap configuration #1 without the HDPE geomembrane. The HDPE geomembrane was simply eliminated and was not replaced with another material since it is so thin. (i.e., GCL as sole hydraulic barrier, lateral drainage and erosion barrier with CLSM infill).	FC300.D10	FC300o.OUT
4	Closure cap configuration #1 without the lateral drainage layer. The material properties for the lateral drainage layer were replaced with those of backfill rather than eliminating the layer. (i.e., composite barrier and erosion barrier with CLSM infill)	FC400.D10	FC400o.OUT
5	Closure cap configuration #1 without the erosion barrier. The material properties for the erosion barrier were replaced with those of backfill rather than eliminating the layer. (i.e., composite barrier and lateral drainage)	FC500.D10	FC500o.OUT
6	Closure cap configuration described in Table 11 and Table 12 of Section 4.3 where the GCL and HDPE geomembrane were eliminated and the material properties for lateral drainage layer and erosion barrier were replaced with those of backfill rather than eliminating the layers (i.e., soils only closure cap).	FC600.D10	FC600o.OUT
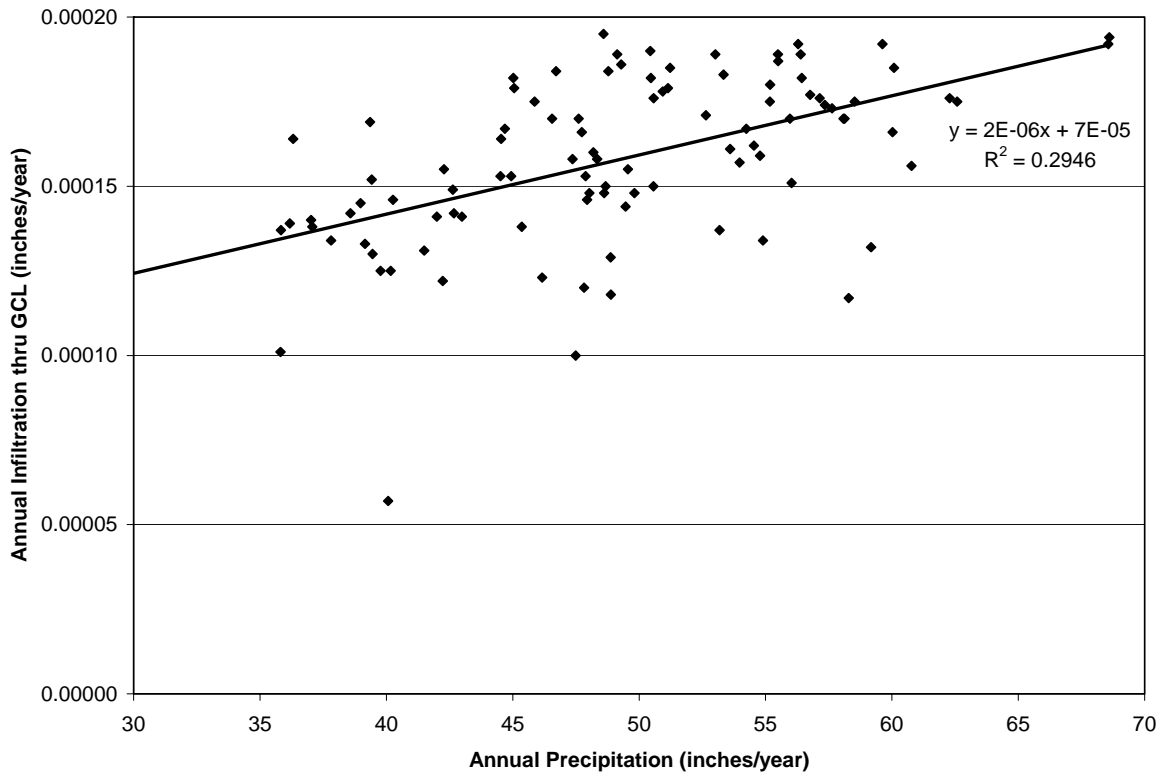
Figure 17.   Configuration #1 at Year 0 HELP Model Simulations - Annual Infiltration thru GCL versus Annual Precipitation

Table 25.   Configuration #1 at Year 0 HELP Model Simulations - Water Balance Statistics

Parameter	Precipitation (in/yr)	Runoff (in/yr)	Evapotrans-piration (in/yr)	Lateral Drainage (in/yr)	Infiltration thru GCL (in/yr)	Change in Water Storage (in/yr)
Count	100	100	100	100	100	100
Maximum	68.60	20.23	42.74	10.27	0.00020	5.63
Average	49.14	6.24	34.37	8.48	0.00016	0.06
Median	48.83	5.37	34.19	8.59	0.00016	0.23
Minimum	29.81	0.00	22.81	3.26	0.00006	-6.02
Std Dev	7.69	4.52	3.68	1.23	0.00002	2.56
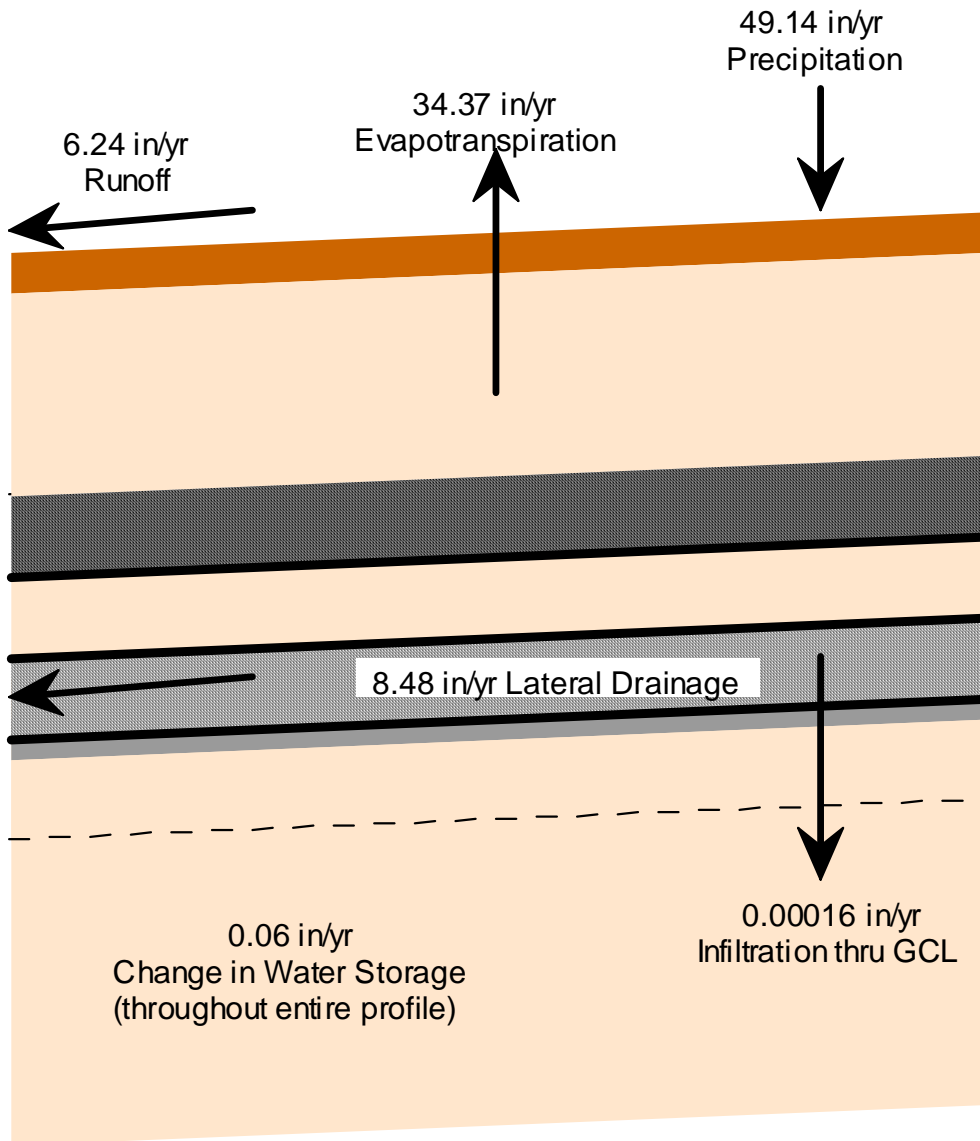
Figure 18.   Configuration #1 at Year 0 HELP Model Simulations – Average Water Balance
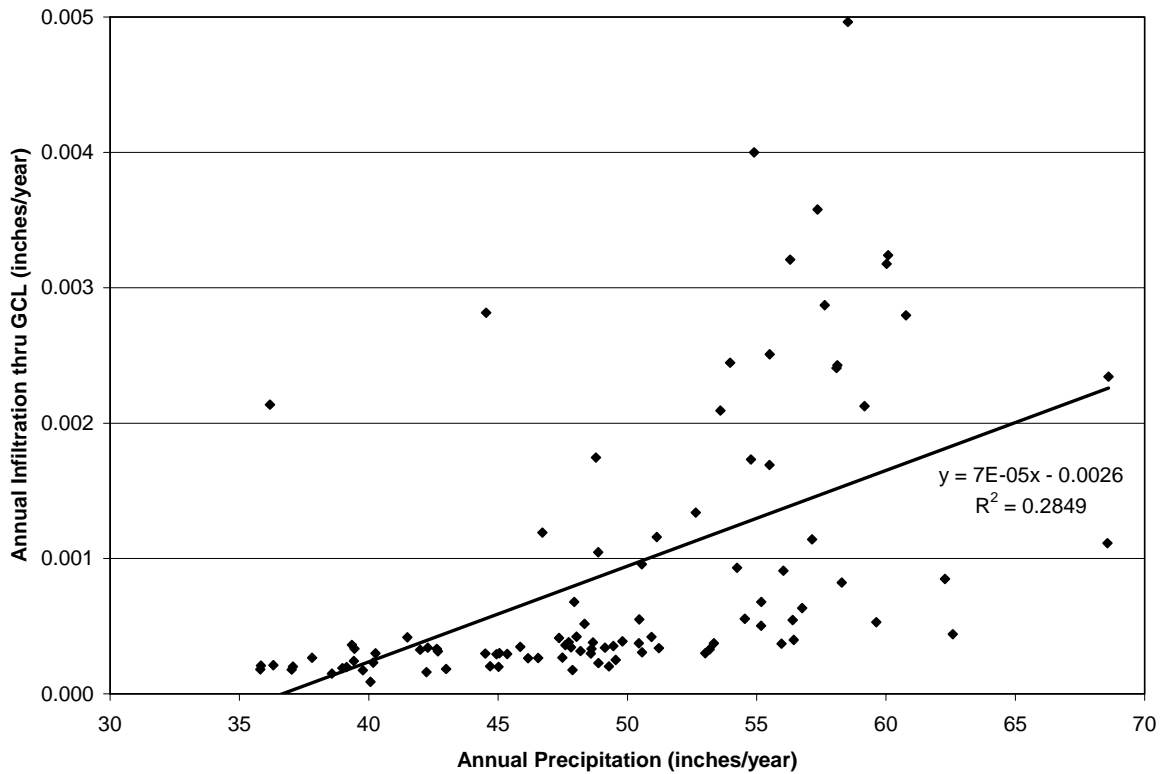
Figure 19. Configuration #1a at Year 0 HELP Model Simulations - Annual Infiltration thru GCL versus Annual Precipitation

Table 26. Configuration #1a at Year 0 HELP Model Simulations - Water Balance Statistics

Parameter	Precipitation (in/yr)	Runoff (in/yr)	Evapotrans-piration (in/yr)	Lateral Drainage (in/yr)	Infiltration thru GCL (in/yr)	Change in Water Storage (in/yr)
Count	100	100	100	100	100	100
Maximum	68.60	3.81	41.48	29.63	0.00496	5.26
Average	49.14	0.43	32.57	16.07	0.00088	0.06
Median	48.83	0.00	32.59	15.37	0.00037	0.26
Minimum	29.81	0.00	21.67	4.67	0.00009	-6.58
Std Dev	7.69	0.76	3.38	5.25	0.00102	2.63

Figure 20. Configuration #1a at Year 0 HELP Model Simulations – Average Water Balance
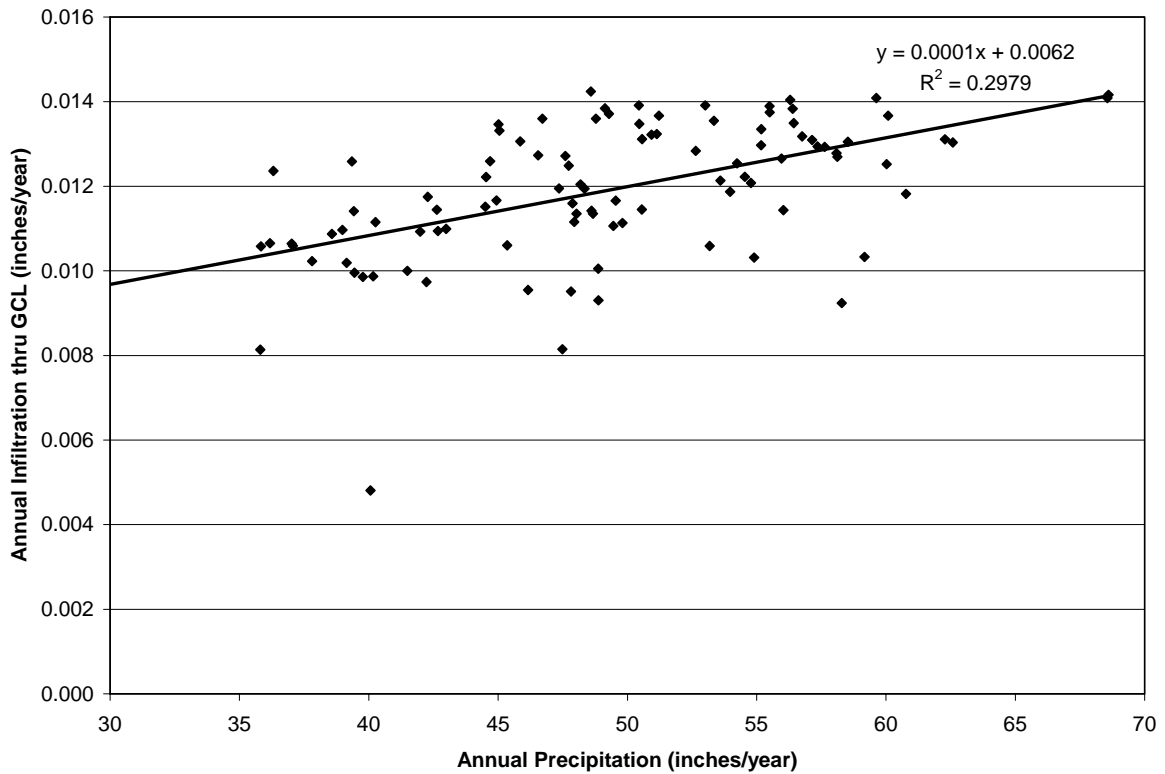
Figure 21. Configuration #2 at Year 0 HELP Model Simulations - Annual Infiltration thru HDPE Geomembrane versus Annual Precipitation

Table 27. Configuration #2 at Year 0 HELP Model Simulations - Water Balance Statistics

Parameter	Precipitation (in/yr)	Runoff (in/yr)	Evapotrans-piration (in/yr)	Lateral Drainage (in/yr)	Infiltration thru HDPE Geomem-brane (in/yr)	Change in Water Storage (in/yr)
Count	100.00	100.00	100.00	100.00	100.00	100.00
Maximum	68.60	20.23	42.74	10.25	0.014	5.63
Average	49.14	6.24	34.37	8.46	0.012	0.06
Median	48.83	5.37	34.19	8.58	0.012	0.24
Minimum	29.81	0.00	22.81	3.26	0.005	-6.03
Std Dev	7.69	4.52	3.68	1.22	0.002	2.56

49.14 in/yr
Precipitation

34.37 in/yr
Evapotranspiration

6.24 in/yr
Runoff

8.46 in/yr Lateral Drainage

0.06 in/yr
Change in Water Storage
(throughout entire profile)

0.012 in/yr
Infiltration thru HDPE
Geomembrane
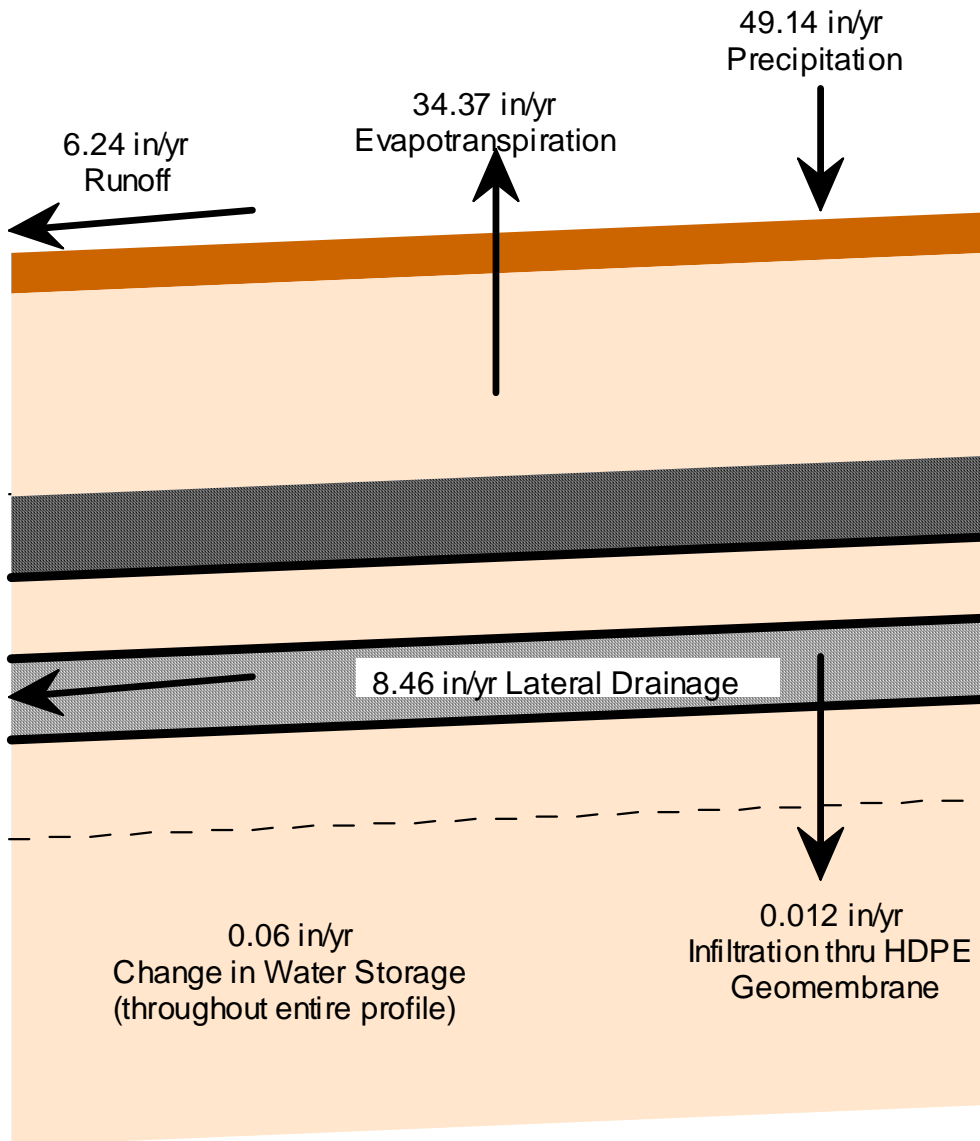
Figure 22. Configuration #2 at Year 0 HELP Model Simulations – Average Water Balance
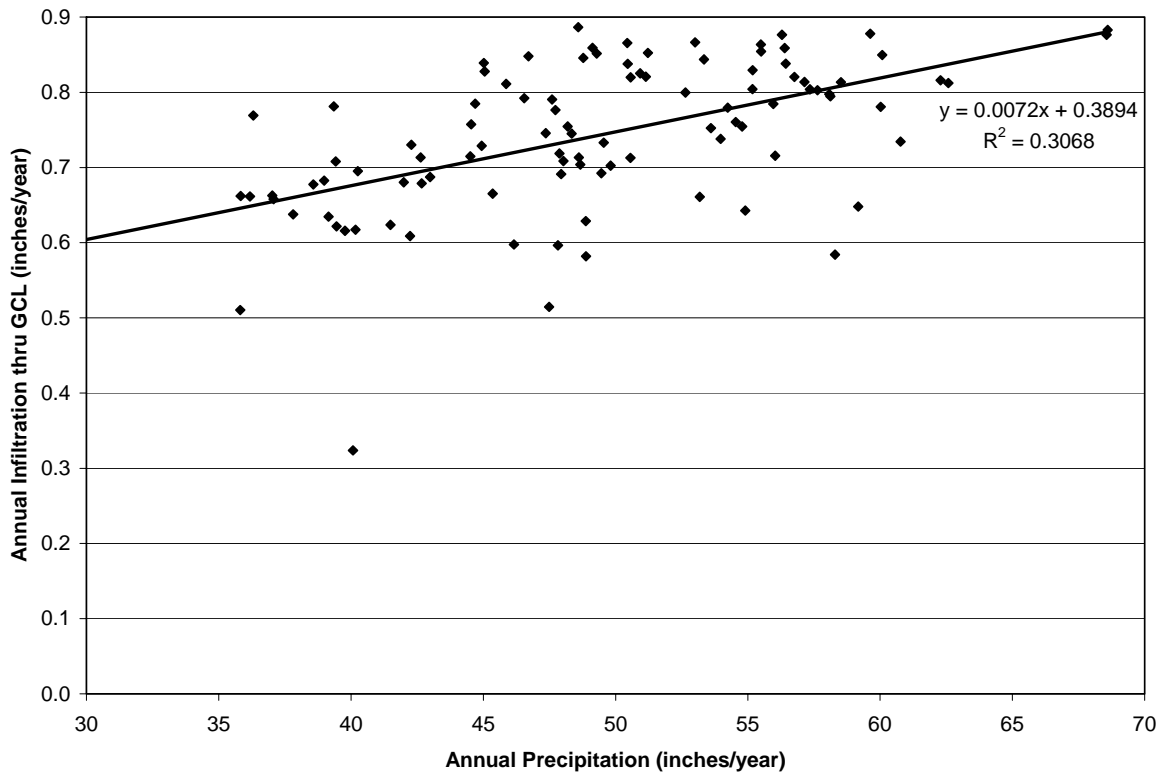
Figure 23. **Configuration #3 at Year 0 HELP Model Simulations - Annual Infiltration thru GCL versus Annual Precipitation**

Table 28. **Configuration #3 at Year 0 HELP Model Simulations - Water Balance Statistics**

Parameter	Precipitation (in/yr)	Runoff (in/yr)	Evapotrans-piration (in/yr)	Lateral Drainage (in/yr)	Infiltration thru GCL (in/yr)	Change in Water Storage (in/yr)
Count	100.00	100.00	100.00	100.00	100.00	100.00
Maximum	68.60	20.23	42.74	9.39	0.89	5.33
Average	49.14	6.24	34.37	7.74	0.74	0.10
Median	48.83	5.37	34.19	7.87	0.75	0.30
Minimum	29.81	0.00	22.81	3.01	0.32	-6.05
Std Dev	7.69	4.52	3.68	1.13	0.10	2.54
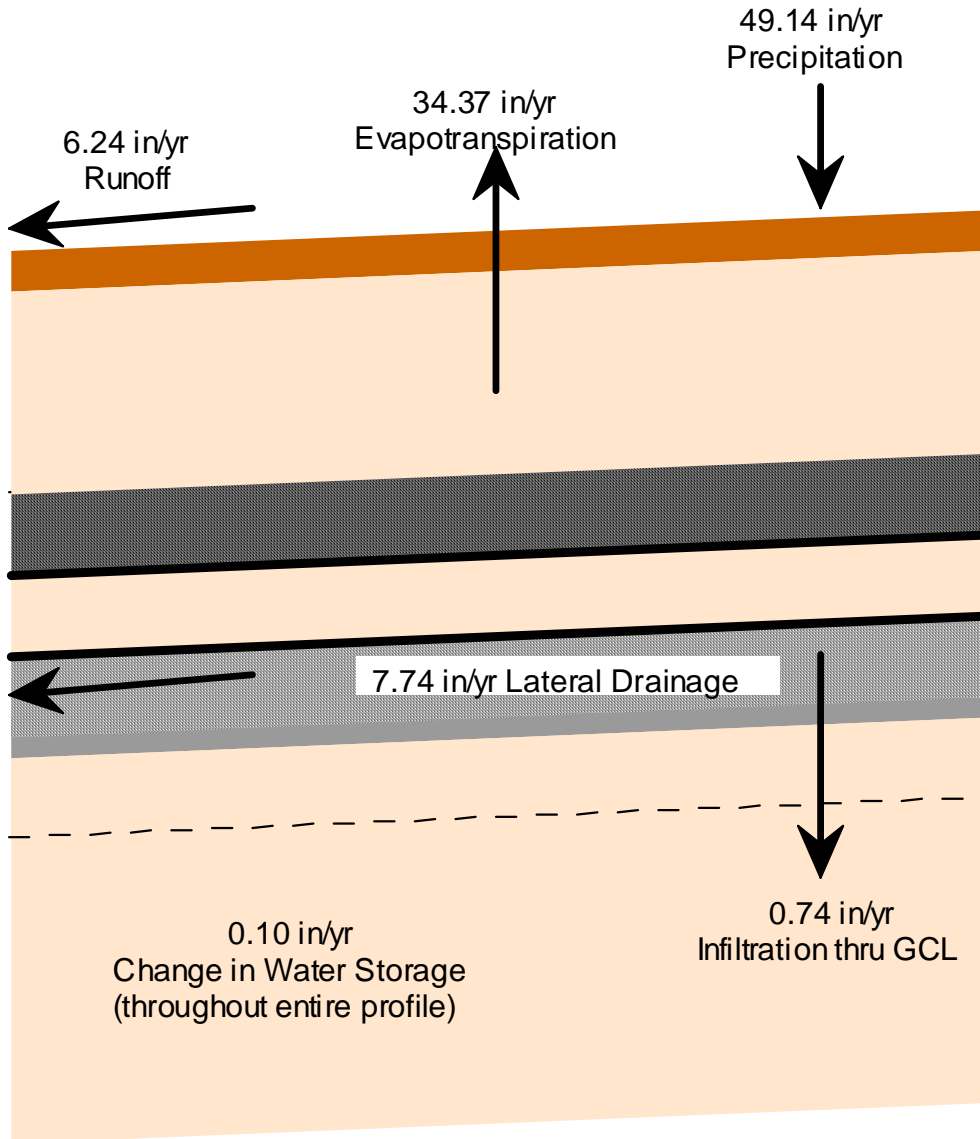
Figure 24. Configuration #3 at Year 0 HELP Model Simulations – Average Water Balance
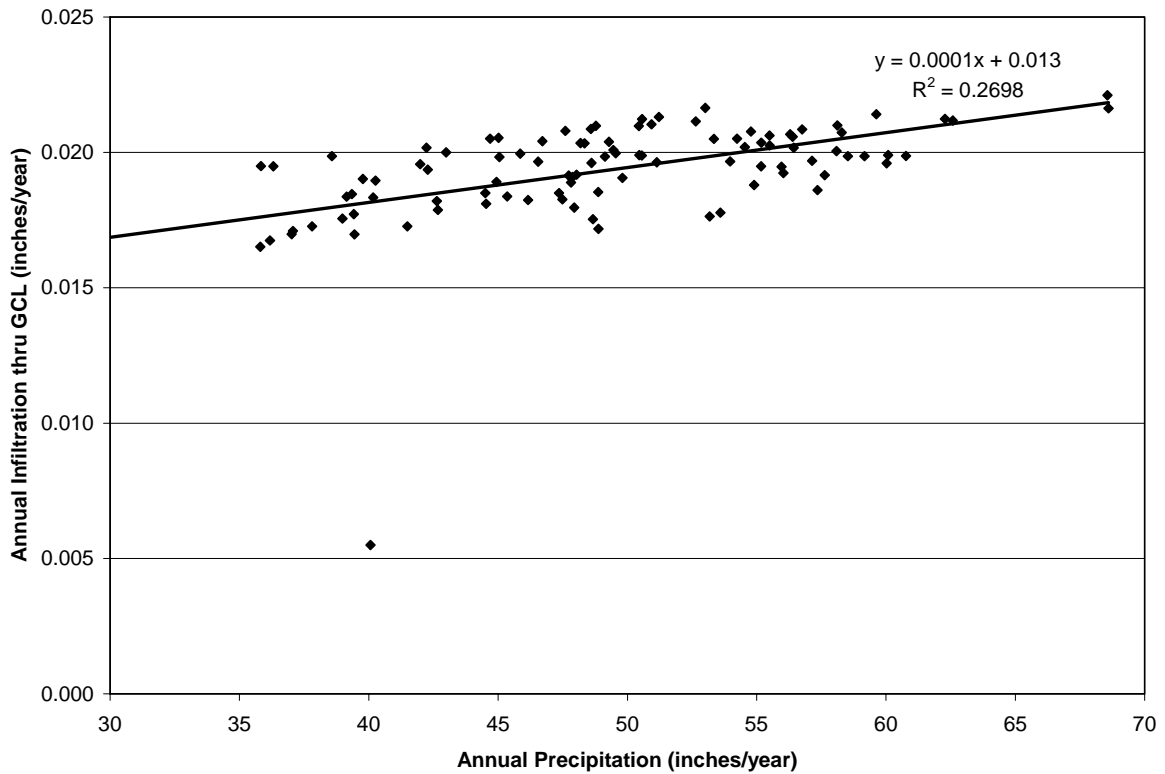
Figure 25. Configuration #4 at Year 0 HELP Model Simulations - Annual Infiltration thru GCL versus Annual Precipitation

Table 29. Configuration #4 at Year 0 HELP Model Simulations - Water Balance Statistics

Parameter	Precipitation (in/yr)	Runoff (in/yr)	Evapotrans-piration (in/yr)	Lateral Drainage (in/yr)	Infiltration thru GCL (in/yr)	Change in Water Storage (in/yr)
Count	100.00	100.00	100.00	100.00	100.00	100.00
Maximum	68.60	28.40	44.06	1.05	0.022	7.03
Average	49.14	11.84	36.51	0.70	0.019	0.07
Median	48.83	10.94	37.00	0.70	0.020	0.10
Minimum	29.81	0.80	24.00	0.16	0.005	-3.59
Std Dev	7.69	5.61	3.83	0.15	0.002	1.50

49.14 in/yr
Precipitation

36.514 in/yr
Evapotranspiration

11.84 in/yr
Runoff

0.70 in/yr Lateral Drainage

0.07 in/yr
Change in Water Storage
(throughout entire profile)

0.019 in/yr
Infiltration thru GCL
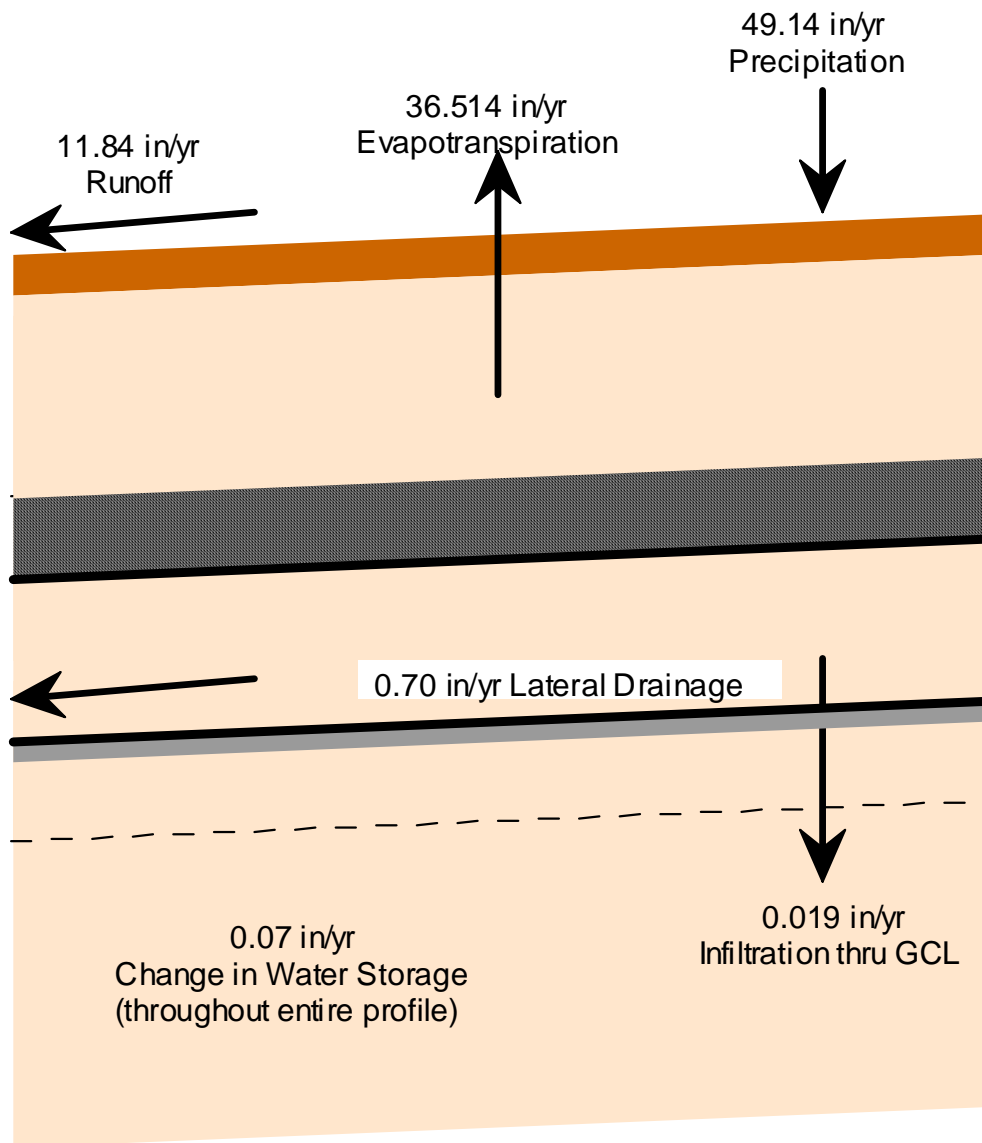
Figure 26. Configuration #4 at Year 0 HELP Model Simulations – Average Water Balance
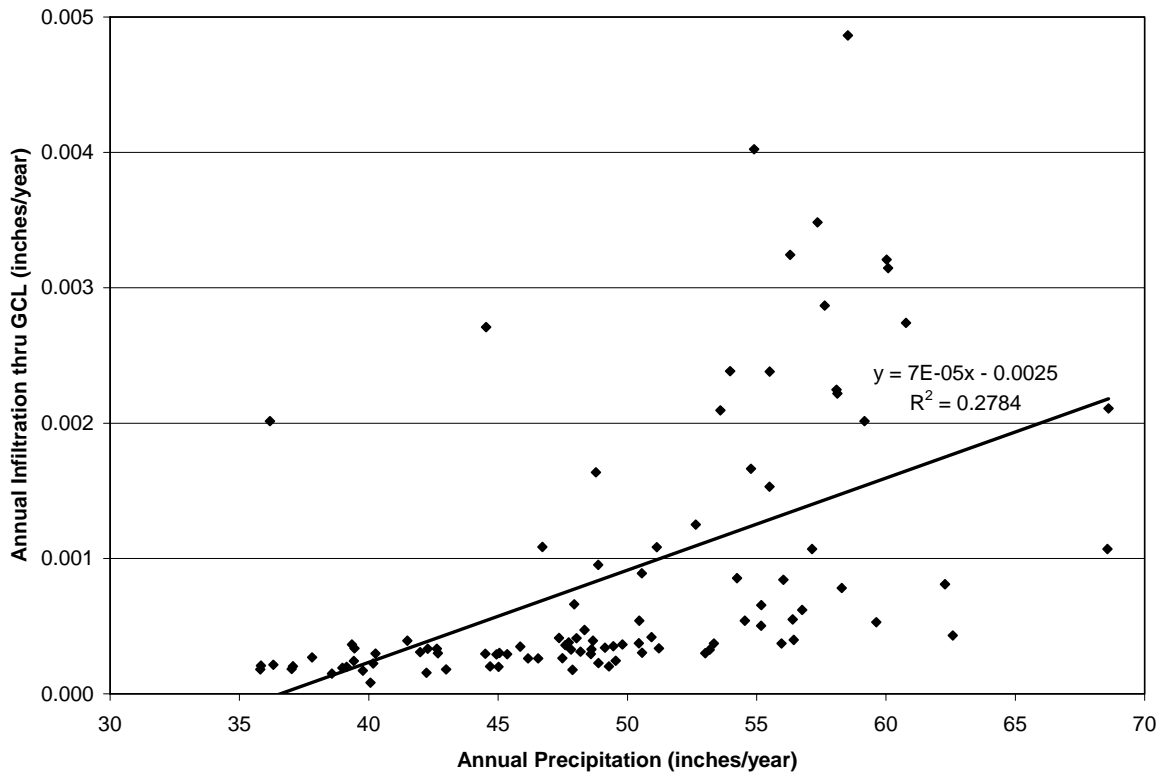
Figure 27. Configuration #5 at Year 0 HELP Model Simulations - Annual Infiltration thru GCL versus Annual Precipitation

Table 30. Configuration #5 at Year 0 HELP Model Simulations - Water Balance Statistics

Parameter	Precipitation (in/yr)	Runoff (in/yr)	Evapotrans-piration (in/yr)	Lateral Drainage (in/yr)	Infiltration thru GCL (in/yr)	Change in Water Storage (in/yr)
Count	100.00	100.00	100.00	100.00	100.00	100.00
Maximum	68.60	3.81	41.45	29.46	0.00487	5.34
Average	49.14	0.42	32.57	16.09	0.00086	0.07
Median	48.83	0.00	32.60	15.39	0.00037	0.28
Minimum	29.81	0.00	21.65	4.38	0.00008	-6.78
Std Dev	7.69	0.74	3.38	5.27	0.00099	2.71
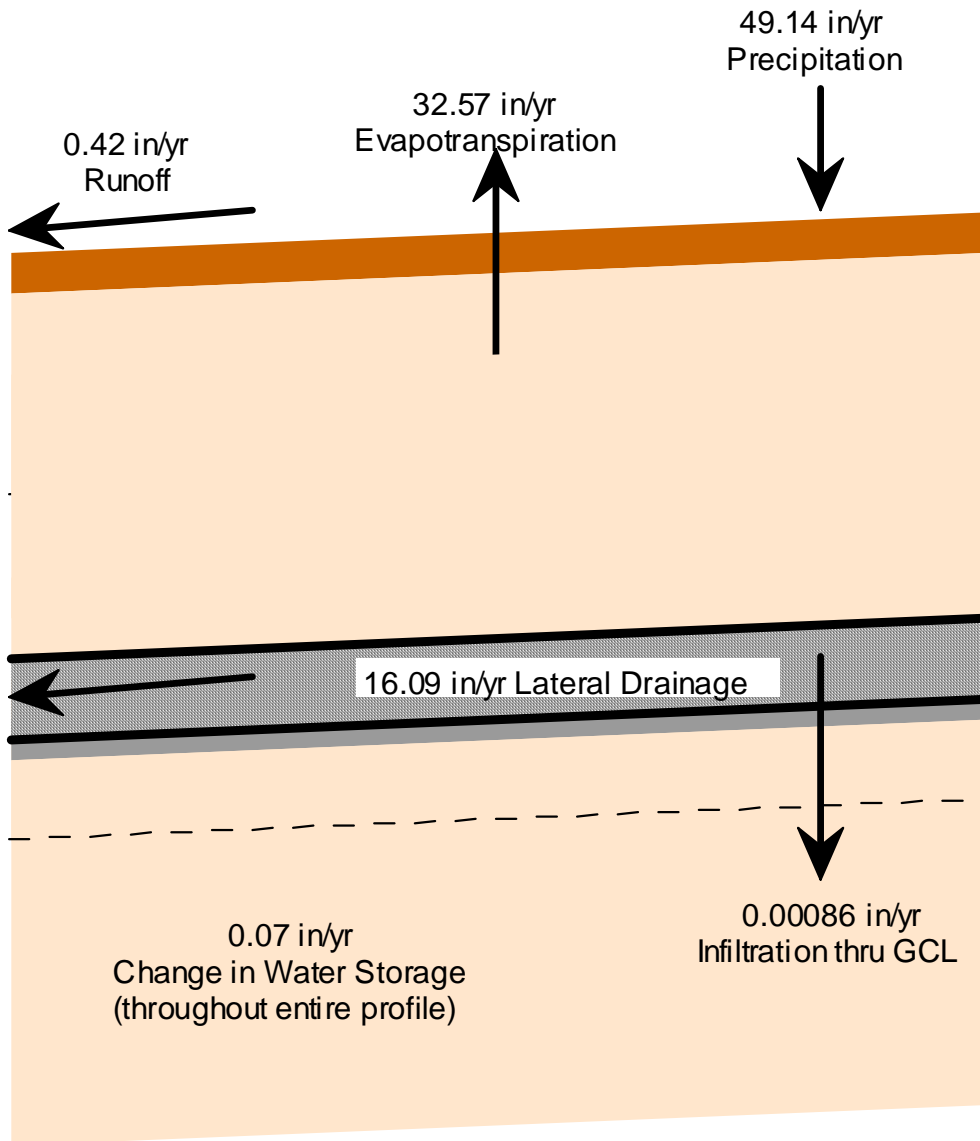
Figure 28. Configuration #5 at Year 0 HELP Model Simulations – Average Water Balance
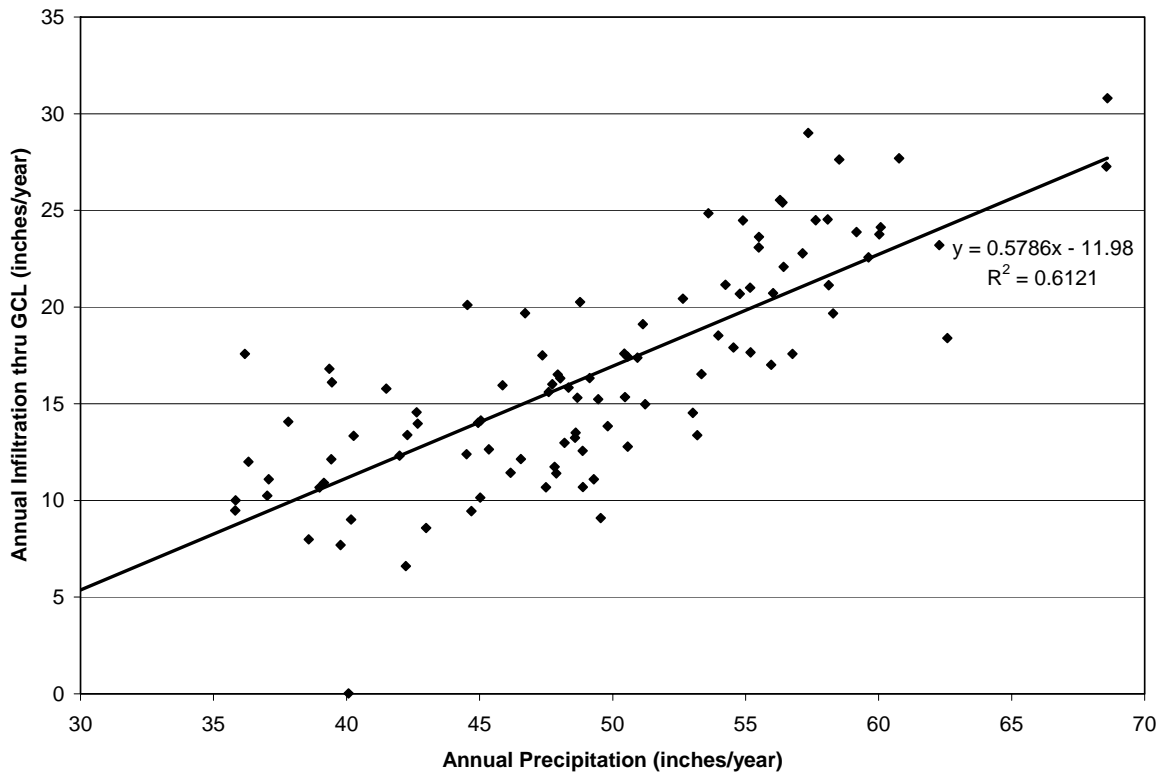
Figure 29. Configuration #6 at Year 0 HELP Model Simulations - Annual Infiltration versus Annual Precipitation

Table 31. Configuration #6 at Year 0 HELP Model Simulations - Water Balance Statistics

Parameter	Precipitation (in/yr)	Runoff (in/yr)	Evapotrans-piration (in/yr)	Lateral Drainage (in/yr)	Infiltration (in/yr)	Change in Water Storage (in/yr)
Count	100	100	100	na	100	100
Maximum	68.60	0.12	41.47	na	30.80	8.38
Average	49.14	0.00	32.55	na	16.45	0.14
Median	48.83	0.00	32.59	na	15.90	0.43
Minimum	29.81	0.00	21.66	na	0.02	-8.07
Std Dev	7.69	0.01	3.38	na	5.69	3.40
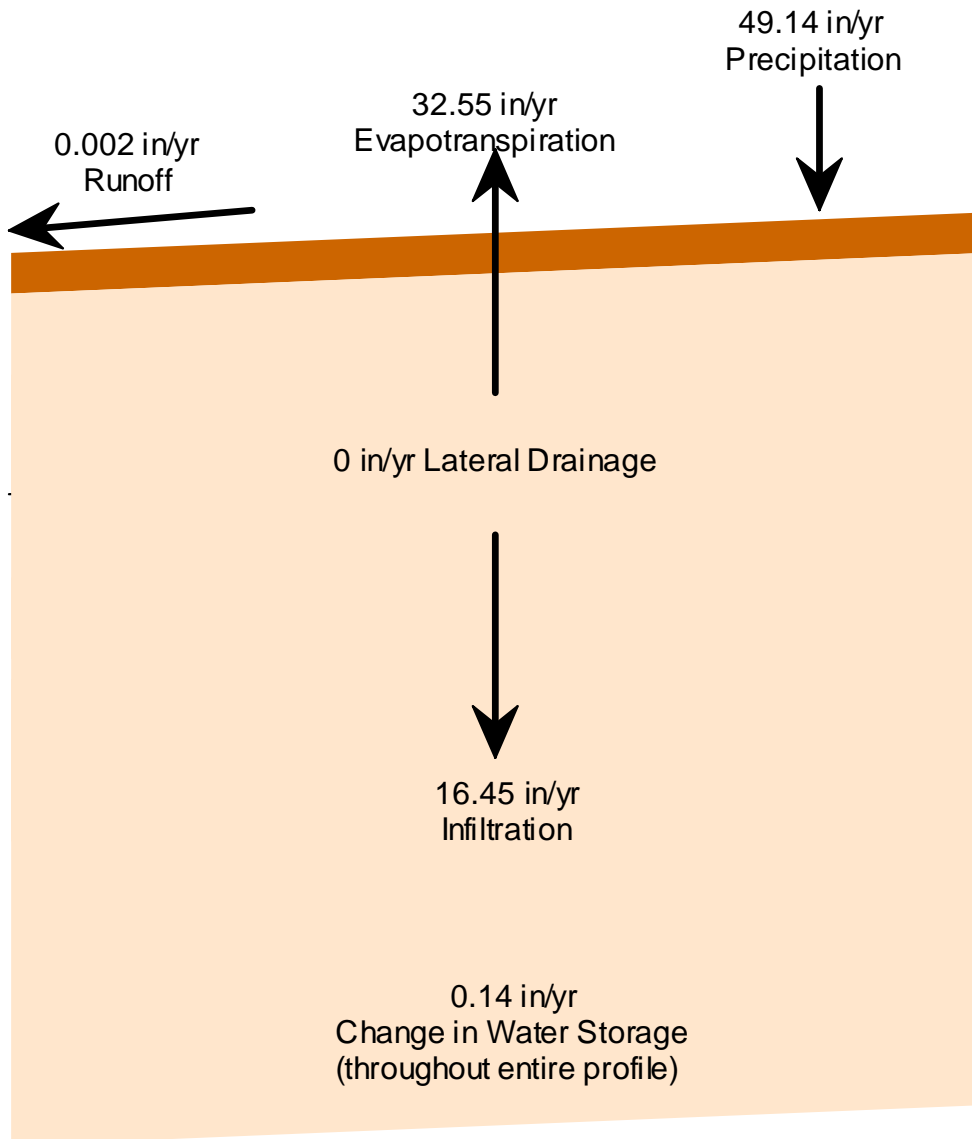
Figure 30. Configuration #6 at Year 0 HELP Model Simulations – Average Water Balance

Table 32. Water Balance Comparison: HELP Model Configuration #6 Results versus Background Studies (Section 3.2)

Source	Parameter	Precipitation (in/yr)	Runoff (in/yr)	Evapotrans-piration (in/yr)	Infiltration (in/yr)
HELP Model Configuration #6 [1]	Average	49.14	0	32.55	16.45
HELP Model Configuration #6 [1]	Range	29.81 to 68.6	0 to 0.12	21.66 to 41.47	0.02 to 30.8
Background Studies (Section 3.2) [2]	Median	47.79	1.6	31.2	14.85
Background Studies (Section 3.2) [3]	Range	34.7 to 71.9	0.1 to 4.1	29.1 to 35.9	5.0 to 32.1

[1] Taken from Table 31
[2] Taken from Section 3.2 Table 9
[3] Taken from Section 3.2 Table 10
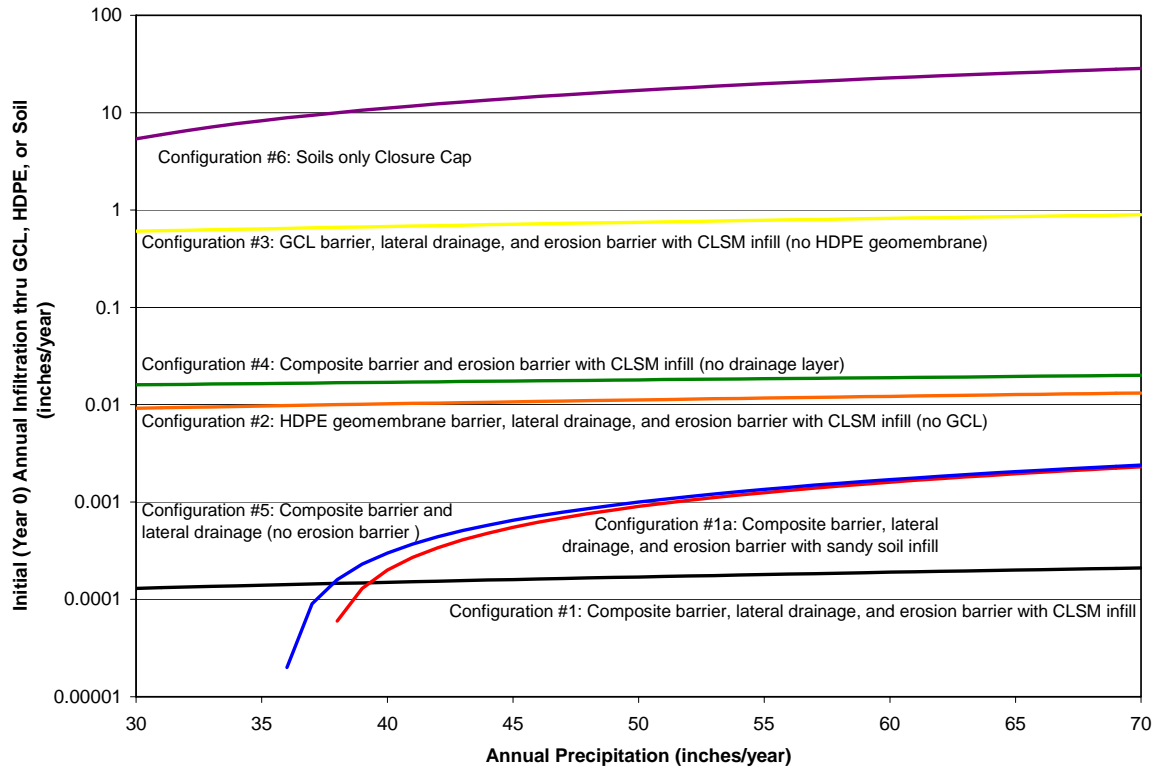
Figure 31.   Comparison of Configurations #1 thru #6 – Annual Infiltration versus Annual Precipitation

Table 33.   Comparison of Configurations #1 thru #6 – Average Water Balance

Configuration	Precipitation (inch)	Runoff (inch)	Evapotrans-piration (inch)	Lateral Drainage (inch)	Infiltration (inch)	Change in Water Storage (inch)
#1	49.14	6.24	34.37	8.48	0.00016	0.06
#1a	49.14	0.43	32.57	16.07	0.00088	0.06
#2	49.14	6.24	34.37	8.46	0.012	0.06
#3	49.14	6.24	34.37	7.74	0.74	0.10
#4	49.14	11.84	36.51	0.70	0.019	0.07
#5	49.14	0.42	32.57	16.09	0.00086	0.07
#6	49.14	0.002	32.55	na	16.45	0.14

na = not applicable
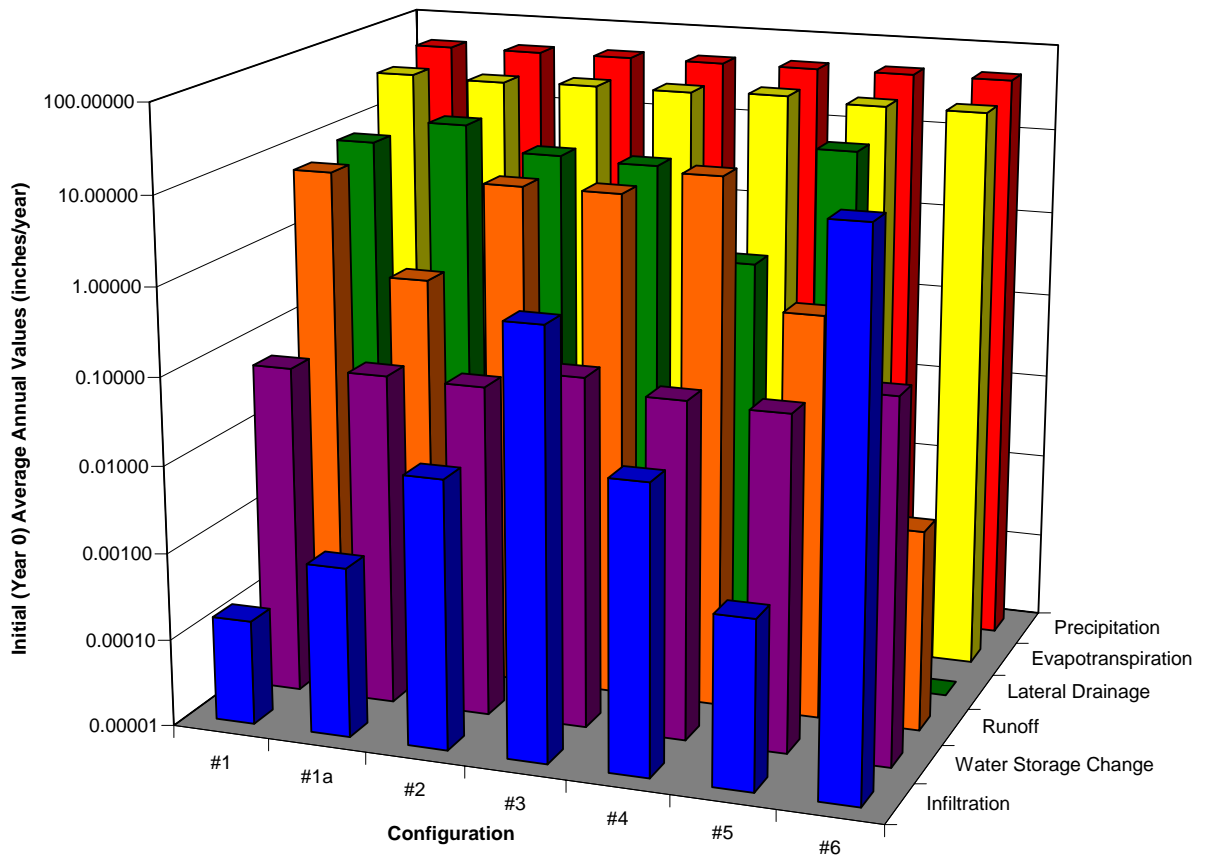
Figure 32.   Comparison of Configurations #1 thru #6 – Average Water Balance

6.0 RECOMMENDED FTF CLOSURE CAP CONFIGURATION

Based upon the average annual water balance and in particular the initial, intact infiltration, it is recommended that closure cap configuration #1 (or #1a, depending upon material selection process for filling erosion barrier stone voids, see Section 4.4.9), which consists of a composite hydraulic barrier with an overlaying lateral drainage layer and an erosion barrier, (i.e., that described in Table 11 and Table 12 of Section 4.3) be utilized as the FTF closure cap. This recommendation is being made for the following reasons:

- It results in the least infiltration to the tanks,
- The use of a composite hydraulic barrier (i.e., HDPE geomembrane underlain by a GCL) provides defense-in-depth by the providing a HDPE geomembrane with a significantly lower saturated hydraulic conductivity underlain by the GCL to plug any holes that may develop in the HDPE geomembrane, and
- The use of an erosion barrier provides long-term physical stability for the closure cap

For modeling of infiltration over time, configuration #1a should be used, since it is conservative relative to configuration #1 (i.e., infiltration through the composite barrier is greater), and selection of the material to infill the erosion barrier stone has yet to be determined. A detailed description of the function of each configuration #1 (or #1a) layer is found in Table 12.

This page intentionally left blank.

7.0 POTENTIAL FTF CLOSURE CAP DEGRADATION MECHANISMS

Potential FTF Closure Cap degradation mechanisms presented in this section are discussed in context of the base case land use scenario (i.e., institutional control to pine forest, land use scenario). This scenario assumes a 100-year institutional control period following FTF Closure Cap construction during which the closure cap is maintained (see Section 2.0). At the end of institutional control, it is assumed that a pine forest succeeds the cap's original vegetative cover.

Table 34 provides a listing of potential FTF Closure Cap degradation mechanisms that were taken into consideration for the estimation of infiltration through the closure cap over time. The table lists the potential degradation mechanisms associated with each of the major FTF Closure Cap layers, other than backfill layers located below the erosion barrier. Waste Layer subsidence is not considered an applicable degradation mechanism to the FTF Closure Cap, since the waste tanks and subsurface items containing significant void space will be filled with grout as outlined in Section 4.4. Additionally chemical degradation from contact with waste leachate is generally not applicable to closure caps, since they are located above the waste layer. For the FTF Closure Cap, in particular, waste is contained within waste tanks, ancillary equipment, and piping located a minimum of seven feet below any closure cap layer that could be significantly affected by leachate. Therefore chemical degradation of the FTF Closure Cap by leachate is not considered applicable.

Finally, degradation of sand layers due to mineral precipitation and microbial growth are primarily degradation mechanisms associated with leachate collection layers rather than closure cap lateral drainage layers. Leachate collection layers receive leachate containing both organic and inorganic degradation products from the waste; whereas closure cap lateral drainage layers only receive non-contaminated water from infiltration (in the case of SRS infiltrating water is very low in both mineral and organic content). Therefore mineral precipitation and microbial growth within the lateral drainage layer is not considered an applicable degradation mechanism. Since waste layer subsidence, chemical (waste leachate) degradation, and mineral precipitation and microbial growth within the lateral drainage layer are not applicable to the FTF Closure Cap, they will not receive further consideration. Subsequent sections will discuss the other potential FTF Closure Cap degradation mechanisms outlined in Table 34.

Table 34. Potential FTF Closure Cap Degradation Mechanisms

Affected Layer	Potential Degradation Mechanism
All	• Static loading induced settlement • Seismic induced liquefaction and subsequent settlement • Seismic induced slope instability • Seismic induced lateral spread • Seismic induced direct rupture due to faulting • Waste Layer Subsidence [1]
Vegetative cover	• Succession • Stressors (droughts, disease, fire, and biological)
Soil above the erosion barrier	• Erosion • Desiccation (wet-dry cycles)
Erosion barrier	• Weathering (Dissolution) • Biological (root penetration, burrowing animals) • Chemical (waste leachate) [2]
Lateral drainage layer	• Silting-in • Biological (root penetration)
High density polyethylene (HDPE) geomembrane	• Ultraviolet (UV) radiation • Antioxidant depletion • Thermal oxidation • High energy irradiation • Tensile stress cracking • Biological (microbial, root penetration, burrowing animals) • Chemical (waste leachate) [2]
Geosynthetic clay liner (GCL)	• Slope stability • Freeze-thaw cycles • Dissolution • Divalent cations (Ca^{+2}, Mg^{+2}, etc.) • Desiccation (wet-dry cycles) • Biological (root penetration, burrowing animals) • Chemical (waste leachate) [2]

[1] Waste Layer subsidence is not considered applicable to the FTF Closure Cap since the waste tanks and subsurface items containing significant void space will be filled with grout.
[2] Chemical degradation of the erosion barrier, HDPE geomembrane, and GCL from leachate associated with the waste tanks, ancillary equipment, and piping is not considered applicable to the FTF Closure Cap, since the erosion barrier, HDPE geomembrane, and GCL will be located above the waste tanks, ancillary equipment, and piping.

7.1 POTENTIAL STATIC LOADING AND SEISMIC INDUCED DEGRADATION

As outlined in Table 34, the following five, potential static loading and seismic induced degradation mechanisms will be considered versus their impact upon the overall closure cap:

- Static loading induced settlement
- Seismic induced liquefaction and subsequent settlement
- Seismic induced slope instability
- Seismic induced lateral spread
- Seismic induced direct rupture due to faulting

At the SRS, the first three potential degradation mechanisms above require attention during design. The latter two are of no consequence as the conditions at the SRS are not conducive to lateral spreading (at least not at the locations of the postulated cover system) and surface faulting is non-existent in the Southeast United States.

Settlement will occur due to two phenomena: first settlement due to the static load of the cap system itself, and second settlement due to seismic shaking (liquefaction or partial liquefaction). The current FTF closure cap concept indicates that the thickness of the cover system will be on the order of 30 feet over the existing tank tops. It is expected that static settlement due to this load (approximately 3,600 psf) would be on the order of 2 to 3 inches, based on previous analysis in F-Area. This amount of settlement would be expected to occur uniformly over the entire area of the cap, thus differential settlement would be negligible assuming the subsurface conditions are relatively uniform.

Settlement due to liquefaction or partial liquefaction is a result of the dissipation of excess porewater pressures that have been elevated due to a seismic event. Previous studies in F-Area (for PC-3 seismic events, return period of 2,500 years, peak ground acceleration (PGA) of 0.16 g, and a repeat of the 1886 Charleston event) indicate these settlements should be on the order of a few inches, and that they too should be rather uniform.

The stability of the FTF closure cap will depend on the final geometry of the system and the strength of the materials used. Given the types of soils used for construction of these systems global slope stability should not be an issue. Side slopes would vary probably between 3 horizontal (h) and 1 vertical (1) to 5 h to 1 v depending on the actual strength of the compacted soil, the final height of the embankment, the seismic coefficient used (for seismic design), and the actual subsurface conditions beneath the cover system. Closure of the 241-97F Cooling Water Basin and the 281-8F Basin will influence the design of the adjacent FTF Closure Cap side-slope relative to seismic considerations.

Interface stability can actually control the design of the system, particularly under seismic conditions. Interface stability refers to the stability between interfaces of various geosynthetic materials and between geosynthetic materials and soil. This can be a key issue and depends heavily on environmental conditions.

In both cases it is fully expected that a stable design can be achieved with reasonable slopes and grades given the known subsurface conditions in F-Area and the types of fill materials that would be utilized.

Since seismic induced lateral spreading and surface faulting are of no consequence at SRS they will not be considered as a FTF Closure Cap degradation mechanism for modeling purposes. The final design of the FTF Closure Cap will appropriately consider and handle static loading induced settlement, seismic induced liquefaction and subsequent settlement, and seismic induced slope instability, so that they are designed out as FTF Closure Cap degradation mechanisms; therefore they will not be considered as a FTF Closure Cap degradation mechanism for modeling purposes.

7.2 POTENTIAL VEGETATIVE COVER DEGRADATION MECHANISMS

As discussed in Table 12 and Section 4.4.12 a vegetative cover will be established on the FTF Closure Cap to promote runoff, minimize erosion, and promote evapotranspiration. The initial vegetative cover shall be a persistent turf grass consisting predominately of bahia (*Paspalum notatum*). As discussed in Section 2.0, it is assumed that a 100-year institutional control period will begin after installation of the closure cap, during which active FTF facility maintenance will be conducted. This active maintenance will sustain a self maintaining, healthy, vigorous cover of the bahia grass throughout the 100-year institutional control period. As part of the maintenance conducted during the institutional control period, the areas between the FTF Closure Cap and existing Roads 49-30, C, and E will be maintained in grass and the establishment of trees within this area will be prevented. Based upon this maintenance it will be assumed that mature pine tree exist at the edge of the maintenance boundary but that no pine trees exist within the area at the end of institutional control. This will result in the nearest mature pine tree stand being at least 600 feet from the FTF Closure Cap at the end of institutional control. After the institutional control period, it is assumed that a 10,000-year post-closure compliance period will begin, during which no active FTF facility maintenance will be conducted.

As outlined in Table 34 the following five potential degradation mechanisms will be considered for the vegetative cover:

- Succession
- Droughts
- Disease
- Fire
- Biological

The following provides a discussion of possible vegetation transition (succession) and stressors (droughts, disease, fire, and biological), based on typical events occurring in the SRS region, that are likely to occur after active FTF facility maintenance has ceased. The vegetative transition discussed is basically one from an old field community into an upland pine community (Odum, 1960; Pinder, 1975).

Bahia is a very hardy species in this region, and will continue to be a dominant ground cover for many years after active maintenance has ceased (McCarty, 2003). However, without active maintenance, the pattern of vegetation on the cap will begin to change over time. Because of the location of the closure cap relative to the surrounding landscape and the top soils routinely used in capping projects (see Section 7.3.2), the site is expected to not be extremely moist or fertile. The scenarios discussed reflect this aspect of the microenvironment that the cap provides.

After active maintenance ceases, over time there will likely be some deterioration of the bahia cover, from many possible disturbances. Bahia is a low-growing creeping perennial species of grass with stolons and stout rhizomes. The stolons typically grow along the ground, have short innernodes, and root freely from the nodes, thus forming a dense sod. The species is deeply rooted and contains thick branching rhizomes. Most roots occur in the top 6 inches, but some may extent to 12 inches in non-compact soils (Gates et al., 1999). The species is very drought hardy and does not require frequent fertilization, although it does benefit from applications. It will remain a primary component of the community after maintenance stops until it begins to be reduced due to light competition.

During this transition period, numerous biotic and abiotic factors will influence the exact nature and timing of succession. These could include drought, insects, diseases, fire, etc. The basic biology and ecology of bahia and many of the early invaders will typically be altered only slightly due to biotic factors. This can result in a minimum lengthening of the time sequence of advancement. The possible exception is the occurrence of fire during the early successional years. This would tend to delay the advancement of the shrub and pine community until an interval after the last fire occurrence. When the interval between fires is long enough for the encroaching pine saplings to become tall enough to withstand fire disturbance and survive, the successional pattern to a pine dominated stand will proceed. This is the normal successional pattern for the SRS region.

During the first 10 years after active maintenance ceases, a number of early successional herbaceous species will begin to colonize the site, as well as other grass species (Odum, 1960). Typical of the new herbaceous species are horseweed (*Erigeron canadense*), yellow aster *Haplopappus divaricatus*), and sheep sorrel (*Rumex acetosella*), and the grass broomsedge (*Andropogon* spp.). Also expected to begin invasion during this early transitional period are blackberry (*Rubus* spp.) and loblolly pine (*Pinus taeda*) (Golley, 1965; Golley and Gentry, 1966). The herbaceous and vine species that are early invaders typically have well developed root systems to take advantage of the soil resource, but rarely extend beyond 18 inches.

The closure cap will be an upland, better drained site due to cap construction techniques and become somewhat less diverse than mixed species upland hardwood sites. Loblolly pine is expected to become the dominant species over time. This will be a progression over time and produce a mixed age pine stand that will become self perpetuating. There will be a small component of mixed hardwoods in the understory and sapling layers of the forest, and would include turkey oak (*Quercus laevis*), sweetgum (*Liquidambar styraciflua*), and black cherry (*Prunus serotina*).

These species will not become dominant or co-dominant trees and remained suppressed in the understory. They typically have more evenly distributed root patterns and will not extent the six feet to the HDPE geomembrane in this community structure (Zutter et al., 1999). Shrubs and vines typical of this community type would also be present and would include sparkleberry (*Vaccinium* spp.), poison ivy (*Rhus radicans*), green briar (*Smilax* spp.) and grape (*Vitis* spp.) (Jones et al., 1981). As previously mentioned, the vine species can produce large root and tuber mass below ground, but typically do not extend more than 18 to 24 inches into the soil. Loblolly pine has a much deeper root system as described below that could potentially damage the composite hydraulic barrier of the FTF Closure Cap. Due to the potential closure cap damage caused by loblolly pine roots, the succession of pine trees is discussed in detail. Encroachment by loblolly pine would begin initially along the edges of the maintained area and progressively work towards the closure cap and eventually cover the cap.

Seed production of loblolly pine in the South East region is typically good to heavy, but can vary by individual year. Individual trees as young as 10 years old have produced viable seed, but the seed production typically increases from 30 to 50 years of age (40 years is taken as representative for this discussion) for dominant and co-dominant trees at an individual site (Fowells, 1965). Production continues at this maximum rate throughout the remaining life of the tree. Seed production can vary between 18,000 and 300,000 seeds per acre in natural stands.

Loblolly pine has a winged seed that is typically dispersed and disseminated by wind. The cones and seeds ripen to maturity during early October and seeds are released as the cones open in the upper portion of the canopy. When natural stands are cut, seed dispersal from the remaining edge of the forest generally results in 85% of the subsequent seeds being released falling within 200 feet of the boundary (Pomeroy and Korstian, 1949). Migration into old fields, where dispersal of seed is less restricted, establishment of less than 1000 seedlings per acre at 330 feet from the seed source have been noted (McQuilkin, 1940). Prevailing wind direction at the FTF closure site during the month of October is from the southwest, as recorded in historic SRS meteorological data base. According to the planned closure scenario, the distance from the nearest seed source to the southwest is approximately 800 feet, and the other nearby seed sources are in excess of 600 feet and not on the appropriate wind direction pathway for dispersal toward to closure cap.

According to the expected seed sources and dispersal of the seed, movement of loblolly pine across grassed areas towards the closure cap will be a sequential process. Seedlings will become established in harvested areas as institutional control is removed at a conservative rate of 400 feet the first seed dispersal event. These trees would subsequently mature and produce seed after 40 years, and begin to release seed towards the closure cap. As the new trees grow, the distance of dispersal from the original seed trees is reduced to an estimated 200 ft. The new trees then continue this process to occupy the open site between the remaining forest and the closure cap. Because the closure cap will be approximately 20 to 30 feet taller than the surrounding landscape, this will present an additional barrier to the wind dispersal of loblolly pine seeds.

Individual trees that provide the initial seeds upon the actual closure cap will have to be tall enough that the gravity/wind movement will allow them to fall on the cap itself. After active maintenance is ceased it is anticipated that at least 4 cycles of 40 years (i.e., 160 years from the end of institutional control) will be required begin establishment of pine seedlings on top of the closure cap. Once the seedlings become established on the closure cap, the migration to disperse seed over the entire cap area would probably be accomplished in the succeeding two 40 year periods (i.e., 240 years from the end of institutional control for establishment of pine seedlings over the entire closure cap). After that it would take another 40 year period for mature pine to be established over the entire closure cap (i.e., 280 years from the end of institutional control to produce a closed canopy). At this point, the natural pattern of pine forest cycling detailed below will become the normal.

The long-term continuance of a pine forest community on a closure cap has been previous discussed and referenced (Phifer and Nelson, 2003), and the relevant aspects are repeated here with appropriate modifications (Bohm (1979), Burns and Hondala (1990), Ludovici et al. (2002), Taylor (1974), Ulrich et al. (1981), Walkinshaw (1999), and Wilcox (1968)). Because of the age structure difference from edge to center and across the cap due to age of the overstory individuals, the second generation, and subsequent ones, will also probably be variable across the cap. Decline of individual loblolly trees will begin around 100 years of age. After the second establishment, the new seedlings will be established as "gaps" occur in the overstory, either through the decline or death of a dominant tree, or through abiotic occurrences (wind throw, lightning strikes, fire, insect outbreak, tornado, etc.). This will tend towards making the entire acreage an uneven age, constantly re-establishing forest. In this region, fire may be quite important in the long-term ecology of the cap. Fire will reduce the smaller understory individuals and seedlings, but will have minimal impact on the dominant individuals.

It is anticipated that tree density will remain fairly constant. For a natural regeneration stand over a 100-year period, the tree density is assumed to be approximately 550 dominant and co-dominant trees per acre with approximately 400 mature (i.e., 40 to 125 years old) trees per acre. It is assumed that complete turnover of the 400 mature trees per acre occurs every 100 years (i.e. 400 mature trees per acre die every 100 years in a staggered manner). Smaller trees will be suppressed and die.

It is assumed that mature pine will have 5 deep roots, mainly near the center of the tree spread (i.e., concentrated near main trunk). Of these 5 deep roots, four go to a depth of 6 feet and one to 12 feet. It is assumed that it takes approximately 30 years for the tap roots to reach a 6-foot depth and the remainder of the tree's life (i.e., 70 years) for the root to go its full depth. Deep roots have a diameter of 3 inches in the top foot of soil and taper with depth to 0.25 inches at depth. These roots will be maintained over the life of the tree and exhibit little turnover prior to death. They will enlarge with yearly growth, similar to branches, although anatomically different and at a slower rate. Smaller trees, which are suppressed and die, will not establish deep roots in excess of 4 to 5 feet, and primarily only 1 or 2 such roots. Hard layers and water-saturated layers will slow root penetration. A continuous water surface will stop elongation. Hard natural layers will eventually be penetrated. HDPE geomembranes can only be penetrated by root in locations of existing cracks or holes (see Section 7.6.6). GCLs are freely penetrated by roots (see Section 7.7.7).

Decomposition of roots near the ground surface should occur fairly quickly due to better microclimate for microbial populations than at depth. Decomposition of roots at depth will be fairly slow, depending on the soil environment and aeration. It is assumed that it will take 25 years for the decomposition of intermediate depth roots and 30 years at depth due to the soil environment. Some shrinkage of the deep roots may occur at depth and provide a channel for water or sediment movement along the surface. Very rapid yearly turnover of fine roots and feeder roots occurs in the soil, although these are primarily in the top 18 inches of soil and will not go vertically with any intensity or longevity.

Based upon the above discussion, vegetation transition (succession) from a bahia grass field to a pine forest will be considered as a FTF Closure Cap degradation mechanism for modeling purposes. Primarily such a succession will result in the deep roots of the pine tree penetrating various FTF Closure Cap layers resulting in degradation particularly of the composite hydraulic barrier. Vegetative stressors (droughts, disease, fire, and biological) primarily impact the FTF Closure Cap in terms of the rate of succession rather than as any long term degradation mechanism on their own. Therefore these vegetative stressors will not be considered as a FTF Closure Cap degradation mechanism for modeling purposes.

Based upon this discussion the following assumptions are made relative to the succession of a bahia grass field to a pine forest for this evaluation:

- A 100-year institutional control period begins after closure cap installation during which the bahia grass is maintained and pine trees are excluded.
- 160 years after the end of institutional control it is assumed that the establishment of pine seedlings on top of the closure cap will begin.
- Pine trees are considered mature once they reach 40 years old.
- It will take approximately 3 cycles of pine seedlings to mature pine trees (i.e., approximately 40 years per cycle) to establish mature pine over the entire closure cap.
- 280 years after the end of institutional control it is assumed that the entire cap is dominated by mature loblolly pine.
- Complete turnover of the 400 mature trees per acre occurs every 100 years (i.e., 400 mature trees per acre die every 100 years in a staggered manner).
- It will take approximately 30 years for the tap roots to reach a 6-foot depth and the remainder of the tree's life (i.e., 70 years) for the root to go its full depth.
- Each mature tree has 4 tap roots to 6 feet and 1 tap root to 12 feet. The roots are 3 inches in diameter at a depth of 1 foot and 0.25 inches in diameter at either 6 or 12 feet, whichever is applicable.
- Deep roots will freely penetrate the erosion barrier (see Section 7.4.2) and the geosynthetic clay liner (see Section 7.7.7).
- Deep roots will be unable to penetrate the intact HDPE geomembrane; roots that reach the HDPE geomembrane will only be able to penetrate in locations where holes in the geomembrane have already formed due to HDPE degradation (see Section 7.6.6).

Loblolly pine seedling development is very dependent on the availability of light for growth. These scenarios are for migration of pine across a grass landscape which allows for sufficient light to the developing seedling. If an alternative cap vegetation strategy is pursued to reduce the availability of light to the seedlings, such as use of bamboo as the final vegetation cover, the rate of migration and establishment of pine on the closure cap would be retarded. Preliminary reports indicate that pine succession can be markedly inhibited by dense bamboo cover at SRS in a natural landscape (Nelson, 2005).

7.3 POTENTIAL SOIL ABOVE THE EROSION BARRIER DEGRADATION MECHANISMS

As discussed in Table 12 and Sections 4.4.10 and 4.4.11, a 2.5-foot thick upper backfill to provide water storage for the promotion of evapotranspiration and a 6-inch thick topsoil capable of supporting a vegetative cover and promote evapotranspiration will be located above an erosion barrier in the FTF Closure Cap. As outlined in Table 34 the following two potential degradation mechanisms will be considered for this soil located above the erosion barrier:
- Erosion
- Desiccation (wet-dry cycles)

7.3.1 Erosion

As outlined in Section 4.2 the FTF Closure Cap vegetative soil cover (i.e., topsoil and upper backfill), erosion barrier, side slope, and toe of the side slope have been designed to be physically stable relative to erosion potential resulting from a SRS-specific probable maximum precipitation (PMP) event consistent with Abt and Johnson 1991 and Johnson 2002. A 2-percent slope over a 585-ft slope length for the vegetative soil cover is considered physically stable (i.e., prevents the initiation of gullying during a PMP event). An erosion barrier consisting of 12-in thick riprap with a D_{50} (median size) of 2.5 in on a 585-ft long, 2-percent slope is considered physically stable (i.e., prevents any riprap movement during a PMP event).

While the slope and slope length of topsoil and upper backfill layers have been specified to prevent the initiation of gullying during a PMP event, these layers are subject to erosion, since they are located above the erosion barrier. The erosion barrier has been designed to preclude further erosion into the FTF Closure Cap profile (see Section 4.2 and associated Appendix A). Therefore layers located below the erosion barrier are not subject to erosion. Since the soil layers located above the erosion barrier are subject to erosion, erosion of these layers will be considered as a FTF Closure Cap degradation mechanism for modeling purposes.

7.3.2 Desiccation (wet-dry cycles)

As outlined in Sections 4.4.11 and 5.4.1, the soil utilized as topsoil will be obtained from an on-site source and would typically be classified as silty sand (SM) materials under the Unified Soil Classification System (USCS) or as loamy sand (LS) or sandy loam (SL) in the United States Department of Agriculture (USDA) soil textural classification (i.e., textural triangle). As outlined in Sections 4.4.7, 4.4.10, and 5.4.2, only onsite soil classified as clayey sands (SC) under USCS or as sandy clay loam (SCL) in the USDA soil textural classification (i.e., textural triangle) will be utilized for the upper backfill. Table 35 presents the grain size distribution for typical SRS backfill from Phifer et al. (2006). As seen on average SRS backfill consists of 3% gravel, 61% sand, 10% silt, and 26% clay.

The surficial soils at SRS are highly leached and weathered. Looney et al. (1990) conducted a SRS soils geochemical and physical property investigation. Samples of unimpacted soil were obtained from six soil series considered representative of the 29 soil series at SRS. Table 36 presents a summary of the SRS soil mineralogy/composition as determined by Looney et al. (1990) for the 32 samples analyzed for mineralogy by x-ray diffraction (XRD). The samples were taken in intervals from the ground surface to a depth of 10 feet. As seen in Table 36 the soil mineralogy is dominated by quartz at an average of 93 wt%. The clay fraction is dominated by kaolinite at an average of 84 wt%. Kaolinite is one of the most stable phases in the weathering zone. The organic content of the soil is very low at an average of 0.22 wt%. Iron oxide minerals are also present in many of the SRS soils and give them their distinctive red coloration; however the iron oxide levels were below the XRD detection limits and are therefore not reported in Table 36. In summary SRS surficial soils are highly leached and consist predominately of quartz and kaolinite with a low organic and iron oxide content.

Table 35.   Typical SRS Backfill Grain Size Distribution (Phifer et al. 2006)

Statistical Parameter	% +3"	% Gravel	% Sand	% Silt	% Clay
Minimum	0.00	0.00	36.90	2.70	15.60
Average	0.00	3.38	60.73	9.42	26.46
Standard Deviation	0.00	6.98	9.02	3.67	4.52
Median	0.00	1.00	62.80	8.90	26.80
Maximum	0.00	34.90	73.90	18.30	35.90

Grain size distribution definitions: gravel > 4.45 mm; 4.45 mm < sand > 0.074 mm; 0.074 mm < silt > 0.005 mm; clay < 0.005

Table 36. SRS Soil Mineralogy/Composition (Looney et al. 1990)

Statistical Parameter	Quartz (wt%)	Clay (wt%)	TOC (wt%)	Total Quartz, Clay, & TOC (wt%)	Clay Mineralogy (wt%)		
					Vermiculite	Illite	Kaolinite
Minimum	82.00	0.00	0.02	89.03	0.70	0.00	62.60
Average	93.06	5.06	0.22	98.34	14.92	1.51	83.57
Standard Deviation	4.53	4.22	0.31	3.13	9.32	1.99	9.68
Median	94.00	3.50	0.09	99.08	15.60	0.90	83.05
Maximum	100.00	17.00	1.31	101.11	34.30	7.10	98.80

The potential for shrinkage of soils upon drying, which results in cracking of the soil, is influenced by the following (Dinauer 1977; Phifer et al. 1993; Chien et al. 2006):

- The type of clay present in the soil. Smectite clays (montmorillonite or bentonite) have an extremely high shrink/swell capacity. When such clays are present in the soil in a large fraction, it can lead to cracking of the soil upon drying. In general clay with a high cation exchange capacity (CEC), a high specific surface area, and monovalent exchangeable ions such as sodium are more likely to cause a soil to crack upon drying.
- Soils containing a large clay fraction are more likely to exhibit cracking upon drying, whereas soils containing a small clay fraction will likely not exhibit cracking upon drying.
- Soils that include a significant fraction of granular soils (sand and silts) are less likely to crack upon drying.
- Soils that have undergone greater compaction are less likely to crack upon drying, than those that have not undergone significant compaction.

As outlined above typical SRS topsoil consists predominately of sand with a very small clay fraction and would be classified as loamy sand (LS) or sandy loam (SL) per USDA. Typical SRS backfill consists predominately of sand with a smaller fraction of clay and would be classified as clayey sand (SC) under USCS or as sandy clay loam (SCL) under USDA. As shown in Table 36, the predominate clay mineral in SRS topsoil and backfill is kaolinite. Kaolinite is low plasticity clay with a low shrink/swell capacity, low cation exchange capacity (3 to 15 meq/100g) and a low specific surface area (10 to 20 m^2/g) (Lambe and Whitman 1969; Mitchell 1993; Phifer et al. 1993). Additionally since SRS soils are highly leached the presence of significant amounts of monovalent exchangeable ions such as sodium are highly unlikely. Finally as outlined in Sections 4.4.7 and 4.4.10 the backfill will be controlled compacted backfill. For all these reasons significant shrinkage of SRS topsoil and backfill upon drying that could lead to significant cracking is highly unlikely and will therefore not be considered as a FTF Closure Cap degradation mechanism for modeling purposes.

7.4 POTENTIAL EROSION BARRIER DEGRADATION MECHANISMS

As outlined within Section 4.4.9 the erosion barrier will be designed to form a barrier to erosion and gully formation and as a barrier to burrowing animals. It is likely that granite will be utilized for the stone within the erosion barrier due to its durability, cost, and local availability. Other potential rock types available locally include granite gneiss, gneiss, and mylonite (GDOT 2007). As outlined in Table 34 the following two potential degradation mechanisms will be considered for the erosion barrier:

- Weathering (Dissolution)
- Biological (root penetration, burrowing animals)

7.4.1 Weathering (Dissolution)

In humid environments, such as the southeastern United States, silicate rocks are more resistant to both mechanical and chemical weathering than are carbonates and many sandstones and mudstones. Studies have evaluated weathering rates for various silicate rocks. Granite is the most chemically durable plutonic silicate rock type, and pure quartzite is the most chemically durable metamorphic silicate rock type (Lindsey et al. 1982). Briefly, mineral weathering rates in granitic alluvium occur in the following decreasing order: hornblende > plagioclase > K-feldspar > quartz, with these minerals' loss resulting in increasing authigenic kaolinite and residual quartz (White et al. 1996). So, rocks containing relatively higher percentages of quartz (such as granite and quartzite) are desirable for resistance to chemical weathering. Well known examples of granite durability in the humid southeast include granitic monadnocks such as Stone Mountain, near Atlanta, Georgia, and Heggie's Rock, near Appling, Georgia.

As mentioned in Section 4.4.9, the likely material to be used for both the closure cap's erosion barrier and side slopes and toe is granite from nearby Georgia quarries. Another option may be a mylonitic quartzite from a nearby Georgia quarry. The rock utilized for the erosion barrier will be located below grade, while similar rock utilized for the side slopes (Section 4.4.14) and toe (Section 4.4.13) will be located above grade. Therefore both below grade and above grade weathering will be considered.

Below Grade Weathering

The most appropriate below grade analogs identified to date include the weathering of granitic regoliths. White et al. (1996) also indicate that changes in bulk density and volume occur with granitic soil age, with significant density increase and volume decrease taking place well beyond the 10,000-year timeframe. From granitic regoliths in the southeastern United States, White et al. (2000) identify weathering front propagation rates of $7 \text{ m}/10^6$ yr for the Panola regolith in Georgia, and $4 \text{ m}/10^6$ yr for the Davis Run regolith in Virginia. Using the faster rate yields a weathering front propagation of 0.07 m/10,000 yr (7 cm/10,000 yr or 2.8 in/10,000 yr). Other below-ground analogs will be evaluated as they are identified as outlined in Section 4.4.9. However, because granite weathers so slowly in the humid southeast compared to rocks such as carbonates, it is expected that natural analogs will provide the most reliable data for the 10,000-yr timeframe.

Above Grade Weathering

As indicated in Section 4.4.9 sites with petroglyphs can provide above grade archaeological examples of granite weathering. A 5th to 6th century mining site at Bir Umm Fawakhir in the Eastern Desert of Egypt (Meyer 1997) has "ancient graffiti scratched on granite boulders". The Lake Onega petroglyph, now on display at the State Hermitage Museum in Russia has an estimated age of 5,000 to 6,000 years (web site reference - www.hermitagemuseum.org/html_En/03/hm3_2_2c.html). Even older petroglyph ages are reported in Bednarik (2002), for locations in the Pilbara region of western Australia. Ages dating as old as just under 20,000 years are reported for openly exposed quartz monzonite rock (a granitic rock) using "microerosion analysis" for the Woodstock adamellite petroglyph. In a web site (http://mc2.vicnet.net.au/home/cognit/shared_files/cupules.pdf) article "Cupules – The Oldest Surviving Rock Art", the same author, Robert G. Bednarik, summarizes peer reviewed works citing minimum ages of Middle Paleolithic (200,000 – 150,000 years ago) and, arguably, even Lower Paleolithic age for cupules (simple anthropogenic indentations made on rock surfaces) from quartzite rocks in Auditorium Cave, located in central India. These oldest, simple petroglyphs provide context for maximum petroglyph age, but since they are from environments protected from the weather, provide limited information on weathering rates for the rock. Possible examples from the United States include Native American granite petroglyphs located in Grapevine Canyon, near Las Vegas, Nevada; in Picture Canyon, near Needles, California; or in the Coso Rock Art District National Historic Landmark in China Lake, California (though, per the National Park Service web site http://www.nps.gov/archeology/rockArt/arch1.htm, the latter site primarily has petroglyphs on basalt rocks and few on granite). In the humid southeastern United States, limestone stelae petroglyphs thought to be 2,100 years old can be found at Crystal River State Park, Florida (web site reference - http://www.public.asu.edu/~rexweeks/Public_Access_RA_Sites.htm). Closer to the SRS, granite petroglyphs are reported on a boulder that originated in Forsyth County, Georgia and has been on display at the University of Georgia in 1963. The petroglyphs may be over 800 years old (web site reference - http://abob.libs.uga.edu/bobk/rockpet.html). Other Georgia petroglyph sites include Track Rock Gap, near Blairsville, and the Reinhardt Rock, which originated near Keithsburg, Cherokee County, and is now on display at Reinhardt College. The Sprayberry Rock, on display at the Wachovia Bank, Sandy Plains Road, Marietta, is a soapstone source-rock with petroglyphs overlying soapstone bowl-removal scars, and an estimated age no earlier than Late Archaic (3,600 to 3,000 years; (Loubser et al. 2003). Overall, Georgia petroglyphs suggest ages between the Late Woodland (1,500 to 1,000 years ago) to Middle Mississippian (800 to 600 years ago) periods (Loubser et al. 2003). The evidence from above grade petroglyphs suggests very slow weathering rates for above grade granite, even in the humid southeast.

As indicated in Section 4.4.9, above grade weathering results from the NIST Stone Test Wall, located in Gaithersburg, MD (Stutzman 2001), will also be considered as they become available. Over a 40 year period ending in 1987 only a few limestones have had measurable weathering.

Additionally new information regarding rock weathering through efforts by the Weathering System Science Consortium (WSSC; recently proposed to be renamed the Critical Zone Exploration Network) may be available by the time final design for the closure cap is underway. WSSC has proposed an initiative to, "…predict how weathering rates… respond to climatic, tectonic, and anthropogenic forces over all temporal and spatial scales". WSSC is a coalition of geochemists, geomorpologists, soil scientists, and ecologists with the objective of developing integrated weathering research, including human impacts on and resulting from weathering (Anderson et al. 2004). The WSSC plans to develop three highly-instrumented "node" sites to investigate weathering at the soil profile and catchment scales, and also to establish a network of "backbone" soil sites to be measured for standard weathering parameters over a range of depths. The fourth of the four "Driving Questions" for the WSSC is, "…how do weathering processes change and evolve over human time scales and over geologic time, and what approaches are useful in predicting the temporal evolution of weathering products and elemental fluxes?" (Anderson et al. 2004). If WSSC is successful in integrating weathering research, new information pertinent to closure cap design may be forthcoming. More information regarding WSSC is available at http://www.wssc.psu.edu/index.html and at http://www.czen.org/wssc.

As outlined in Section 4.4.9 available literature and local natural or archaeological analogs for the erosion barrier and side-slope and toe stone will be researched and included as input for erosion barrier durability and degradation with time. Based upon these results, the required size of the emplaced stone and the thickness of the stone layer will be increased, if necessary, during final closure cap design to accommodate anticipated weathering in order to ensure closure cap physical stability with regards to erosion over 10,000 years. Additionally as discussed in Section 4.4.9 the voids within the erosion barrier rock mass will be filled with a yet-to-be determine materials in order to prevent the loss of overlying material into the erosion barrier. Selection of the material to infill the voids will consider the impact of the material upon weathering of the stone. A material which has either no impact upon weathering or preferably tends to decrease the weathering rate will be favored in the selection process. Based upon appropriate consideration of stone weathering during the final design phase of the FTF Closure Cap, weathering of the erosion barrier stone will not be considered as a FTF Closure Cap degradation mechanism for modeling purposes.

7.4.2 Biological (root penetration, burrowing animals)

Potential biological degradation mechanisms include plant root penetration and burrowing animals. As discussed in Section 7.2 it is anticipated that a pine forest will eventually succeed the initial bahia grass vegetative cover, and that pine trees will produce roots 6 to 12 feet deep, which will eventually penetrate hard layers such as the erosion barrier. As discussed in Section 4.4.9 one criterion for the selection of the material which will be used to infill the voids of the erosion barrier stone mass will be its ability to facilitate the layer's ability to hinder root penetration. However for modeling purposes, the erosion barrier will be assumed to not hinder root penetration and root penetration will be considered as a FTF Closure Cap degradation mechanism for modeling purposes for both the erosion barrier and underlying layers as appropriate.

As outlined in Section 6.0, FTF Closure Cap configuration #1a will form the basis for closure cap degradation and infiltration modeling over time. Configuration #1a includes an erosion barrier whose stone is infilled with a sand as outlined in Section 5.4.3, resulting in an erosion barrier with a fairly high saturated hydraulic conductivity as shown in Table 22. While it is assumed that roots can freely penetrate the erosion barrier, such penetration will not impact the layer's ability to function as an erosion barrier, since the roots will only minimally displace the stones. Additionally such root penetration will only minimally impact the saturated hydraulic conductivity of the sand infilled erosion barrier for the following reasons:

- Tap roots while alive will form an essentially impermeable barrier. However such roots will constitute a very small area of the erosion barrier resulting in very little impact to the overall saturated hydraulic conductivity. Ignoring this tends to be conservative, since considering it would tend to lower the saturated hydraulic conductivity of the erosion barrier resulting in lower infiltration through it.
- As tap roots die and decay over a 25 to 30 year period (see Section 7.2) the sand of the erosion barrier will tend to flow back into the void left by the slowly decaying roots. The sand will have very little cohesion to keep it in place.
- There is very little difference between the saturated hydraulic conductivity of the erosion barrier and the overlying and underlying backfill (i.e., a factor of 3 between the erosion barrier conductivity of 1.3E-04 cm/s versus that of the backfill at 4.1E-05 cm/s). Even if the overlying backfill were to fall into void created by slowly decaying roots, such fluffing up of the backfill caused by falling into the void would cause its saturated hydraulic conductivity to increase to near that of the sand (i.e., 3.3E-04 cm/s (see Appendix F)) of the erosion barrier.

For these reasons, although tap roots will be assumed to freely penetrate the erosion barrier and impact the hydraulic properties of underlying layers, the hydraulic properties of the erosion barrier will not be assumed to be appreciably impacted by root penetration.

Another consideration, in association with plant root penetration, is the potential impact on the erosion barrier of wind-thrown trees that have been uprooted. This is not considered a significant degradation mechanism in relation to the functionality of the erosion barrier due to the following reasons:

- The instances of uprooted wind-thrown trees tend to be isolated and infrequent and will therefore have minimal impact on the erosion barrier as a whole. If uprooted wind-thrown trees did result in localized damage to the erosion barrier, adjacent intact portions of the erosion barrier would still ensure the overall functionality of the erosion barrier. That is erosion in the localized damaged area could not proceed below the depth of the adjacent intact portions of the erosion barrier. This indicates that uprooted wind-thrown trees are not a significant degradation mechanism for the erosion barrier.

- As outlined in Section 4.3, three feet of soil will initially exist over the erosion barrier. Additionally as outlined in Section 4.2, the slope of the three feet of soil above the erosion barrier has been selected to promote physical stability (i.e. to prevent the initiation of gully erosion during a PMP event) consistent with Abt and Johnson 1991 and Johnson 2002 (i.e. per NRC guidance). Due to this shallow slope, erosion of the soil above the erosion barrier should proceed very slowly (see Section 8.2 for anticipated erosion rates). Finally as outlined in Section 7.2 the bulk of pine tree roots which could potentially hold and displace rocks from the erosion barrier are located in the upper 18 inches of the soil, well above the erosion barrier. There are an insufficient number of tap roots to hold and displace rocks from the erosion barrier. For these reasons uprooted wind-thrown trees are not considered an applicable degradation mechanism for the erosion barrier prior to the occurrence of significant erosion.
- As currently conceived the erosion barrier consists of 0.5 to 7.5 inch diameter rock infilled with sandy soil (configuration #1a). Such a configuration provides no cohesion between the individual particles of rock or sand, which will severely limit the ability of even the roots in the upper 18 inches of soil to hold and displace rocks from the erosion barrier. That is the finer material will quickly slip from the roots and more coarse material will tend to subsequently slip from the roots as openings become larger with the removal of finer materials. For these reasons uprooted wind-thrown trees are not considered a significant degradation mechanism for the erosion barrier.
- Finally the roots of uprooted wind-thrown trees rot more quickly than the rest of the tree and any material held in the roots tends to subsequently fall back into the hole from which it originated, tending to negate any lasting impacts on the erosion barrier (i.e. it is not a significant degradation mechanism for the erosion barrier).

Since root penetration has minimal impact on the erosion barrier either hydraulically or due to uprooted wind-thrown trees, root penetration of the erosion barrier will not be considered an FTF Closure Cap degradation mechanism for modeling purposes.

At SRS, burrowing animals include: oldfield mouse (*Peromyscus polionotus*); short tail shrew (*Blarine brevicauda*); eastern mole (*Scalopus aquiticus*); harvester ant (*Pogonomyrmex badius*); pyramid ant (*Dorymyrmex pyramicus*); imported red fire ant (Solenopsis invicta); and earthworms (Mcdowell-Boyer et al. 2000). As discussed in Section 4.4.9 the erosion barrier will be designed to act as a barrier to burrowing animals. Also as discussed selection of the material used to infill the stone will consider its ability to facilitate the layer's ability to act as a barrier to burrowing animals. The use of rock layers to preclude burrowing animals is discussed in Jacobs (1988), Koerner (1990), IAEA (2001), and Link et al., (1995). Therefore, animal burrowing into and below the erosion barrier will not be considered as a FTF Closure Cap degradation mechanism for modeling purposes.

7.5 POTENTIAL LATERAL DRAINAGE LAYER DEGRADATION MECHANISMS

As outlined in Table 12 and Section 4.4.5 a one-foot thick lateral drainage layer with a minimum saturated hydraulic conductivity of 5.0E-02 cm/s will be provided in conjunction with a composite hydraulic barrier to divert infiltrating water away from the underlying tanks and ancillary equipment. As outlined in Table 34 the following two potential degradation mechanisms will be considered for the lateral drainage layer:

- Silting-in
- Biological (root penetration)

7.5.1 Silting-in

As outlined in Table 12 and Sections 4.4.5 and 4.4.6 the lateral drainage layer will be overlain with a geotextile filter fabric to prevent the migration of soil from the middle backfill into the lateral drainage layer. As outlined in Section 4.4.6 the apparent opening size of this filter fabric will be appropriately designed to provide filtration between the underlying sand drainage layer and the overlying middle backfill (i.e., free liquid flow but no soil loss). Sufficient data is not currently available to estimate the service life of the filter fabric. However it will degrade due to oxidation and root penetration, both of which will tend to increase its already high through plane saturated hydraulic conductivity. It is unlikely that the filter fabric will become clogged, since there is very little organic matter in SRS soils to promote the formation of a biofilm and since SRS soils consist predominately of quartz and non-swelling clays (see Section 7.3.2). Any potential clogging of the filter fabric will be more than compensated for by the formation of root penetrations over time. Therefore for modeling purposes the presence of the filter fabric will be ignored.

Since such a fabric will degrade over time and is unlikely to completely preclude the migration of colloidal clay, the lateral drainage layer will be assumed to silt-up over time with colloidal clay that migrates from the overlying middle backfill as a FTF Closure Cap degradation mechanism for modeling purposes. It will be assumed that colloidal clay migrates from the overlying middle backfill and accumulates in the lateral drainage layer reducing its saturated hydraulic conductivity over time. The clay minerals (in order of predominance) at SRS are shown in Table 37 along with the average clay mineral fraction and typical range in particle size for each. Colloids can be mineral grains such as clays, which have particle sizes between 0.01 and 10 μm (Looney and Falta 2000). Colloidal clay can exist in groundwater in concentrations up to 63 mg/L as measured by suspended solids (Puls and Powell 1992). Based upon this information and the previous assumption, it will be assumed that water flux driven colloidal clay migration at a concentration of 63 mg/L occurs from the overlying middle backfill layer to the lateral drainage layer.

Table 37. SRS Soil Clay Minerals

Clay Mineral	SRS Soil Average Clay Mineral Fraction [1] (%)	Typical Particle Size Range [2] (μm)
Kaolinite	83.57	0.1 to 4
Vermiculite	14.92	0.1 to 2
Illite	1.51	0.1 to 2

[1] See Table 23 (Looney et al. 1990)
[2] Mitchell (1993)

It is assumed that colloidal clay migration from the 1-foot-thick middle backfill to the underlying 1-foot-thick lateral drainage layer causes the middle backfill saturated hydraulic conductivity to increase over time and that of the lateral drainage layer to decrease over time. It will be assumed that half the clay content of the middle backfill migrates into the lateral drainage layer, at which point the two layers essentially become the same material and material property changes cease. Based upon this it will be assumed that the endpoint saturated hydraulic conductivity of the layers will become that of the log mid-point between the initial middle backfill and lateral drainage layer conditions. It will be assumed that the clay migrates out of the middle backfill into the lateral drainage layer with the water flux containing 63 mg/L of colloidal clay. It will also be assumed that the time to achieve the endpoint conditions will be based upon the estimated water flux into the lateral drainage layer and migration of half the clay content of the middle backfill layer.

It will be assumed that the saturated hydraulic conductivity of the middle backfill layer is increasing log linearly with time until half it clay content has migrated out at which point the saturated hydraulic conductivity becomes static. Conversely it will be assumed that the saturated hydraulic conductivity of the lateral drainage layer is decreasing log linearly with time until half the middle backfill clay content has migrated out at which point the saturated hydraulic conductivity becomes static. (Phifer and Nelson 2003)

These assumptions are analogous to the formation of the B soil horizon as documented in the soil science literature. Clay translocation is a very slow process where discrete clay particles are washed out in slightly acidic conditions and deposited lower in the soil profile (McRae 1988). Evidence has been found that the B-horizon where the translocated clay is deposited may form at a rate of 10 inches per 5,000 years (Buol et al. 1973).

7.5.2 Biological (root penetration)

As discussed in Section 7.2, it is anticipated that a pine forest will eventually succeed the initial bahia grass vegetative cover. As discussed, it is anticipated that the closure cap will eventually be covered with approximately 400 mature trees per acre over a 100-year period, each with five deep roots that can penetrate through the one foot thick lateral drainage layer (i.e., deep roots).

The bulk of the roots associated with the closure cap vegetation will be located within 24 inches of the ground surface (see Section 7.2) and therefore cannot impact the lateral drainage layer, since the erosion barrier will always maintain at least 24 inches of material between the top of the lateral drainage layer and the ground surface. Deep roots will be maintained and enlarge with yearly growth over the life of the tree.

Trees are expected to die at approximately 100 years, and it is anticipated that decomposition of deep roots will occur over a 30 year period. Prior to decomposition the roots represent an impermeable volume within the lateral drainage layer. The presence of roots within the lateral drainage layer will be considered as a FTF closure cap degradation mechanism for modeling purposes.

7.6 POTENTIAL HDPE GEOMEMBRANE DEGRADATION MECHANISMS

High density polyethylene (HDPE) is one of the most common polymers utilized in the production of geomembranes (Koerner 1998). HDPE geomembranes consist of 95-98% resin, 2-3% carbon black, and 0.25-1% antioxidants. HDPE geomembranes have a minimum sheet density of 0.940 g/cm^3 (GRI 2003; Koerner and Hsuan 2003; Needham et al. 2004). It has an extremely low permeability (2.0E-13 cm/s) (Schroeder et al. 1994a; Schroeder et al. 1994b) and an extremely low water vapor diffusional flux (~0.006 g/m^2-day) (Rumer and Mitchell 1995). Rumer and Mitchell (1995) report that "diffusion of water or solvent through HDPE geomembranes can only occur in a vapor state".

As outlined Table 12 and Sections 4.4.3 and 4.4.2, a HDPE geomembrane will be utilized in conjunction with a GCL to form a composite hydraulic barrier to infiltration. The potential HDPE geomembrane degradation mechanism discussion presented below was primarily extracted from Phifer 2005. HDPE geomembranes can degrade over time through the following mechanisms (also see Table 34), which are discussed in detail in the succeeding sections (Koerner 1998; Needham et al. 2004; Rowe 2004):

- Ultraviolet (UV) radiation
- Antioxidant Depletion
- Thermal Oxidation
- High Energy Irradiation
- Tensile Stress Cracking
- Biological (root penetration, burrowing animals)

7.6.1 Ultraviolet (UV) Degradation
HDPE geomembrane degradation due to short-wavelength ultraviolet (UV) radiation (i.e. sunlight) exposure has been extensively studied both in the laboratory and field (Koerner 1998; Koerner and Hsuan 2003). Exposure to UV radiation and subsequent penetration of UV radiation into the polymer structure causes polymer degradation by chain scission and bond breaking. Additionally, photo-oxidation due to UV radiation and atmospheric exposure causes significantly faster antioxidant depletion than thermal oxidation (Needham et al. 2004).

However current HDPE geomembrane formulations typically contain 2 to 3% carbon black and may contain other ultraviolet chemical stabilizers to minimize ultraviolet degradation. Due to carbon black usage, UV radiation is not considered a significant degradation mechanism for short-term exposures associated with construction, where the geomembrane is covered in a timely manner. Typically exposures of less than several years is not considered a concern, since manufacturers' warranties for up to 20 years are available for exposed geomembranes. (Koerner 1998; Needham et al. 2004) Additionally UV degradation is not autocatalytic, that is after burial UV degradation does not continue to occur (Bonaparte et al. 2002). Therefore UV degradation of the HDPE geomembrane will not be considered as a FTF Closure Cap degradation mechanism for modeling purposes.

7.6.2 Antioxidant Depletion

Antioxidants are added to HDPE geomembranes primarily to prevent thermal oxidative degradation (see Section 7.6.3). As long as significant antioxidants are present within a HDPE geomembrane, as measured by Oxidative Induction Time (OIT) tests, thermal oxidative degradation will be prevented and the mechanical properties of the geomembrane will remain essentially unchanged. However after the antioxidants have been depleted, thermal oxidation of the geomembrane can begin. Typical antioxidants packages consist of a phosphite and a hindered phenol at 0.1 to 1.0 weight percent of the geomembrane. Phosphites are most effective at higher temperatures and are used as manufacturing process stabilizers, whereas hindered phenols are effective over a wide temperature range and are used as long-term field stabilizers. (Koerner 1998; Hsuan and Koerner 1998; Sangam and Rowe 2002; Mueller and Jakob 2003; Rowe 2004; Needham 2004)

The OIT time determined from OIT tests is related to the quantity and type of antioxidants in the polymer. OIT tests use a differential scanning calorimeter with a special testing cell capable of sustaining pressure. In the standard OIT test (ASTM 2007) a 5 mg specimen is brought to a temperature of 200°C and a pressure of 35 kPa under a nitrogen atmosphere. Oxygen is then introduced and the test is terminated when an exothermal peak is reached. The OIT time is the time from oxygen introduction to the exothermal peak. The high pressure OIT (HP-OIT) test (ASTM 2006d) is conducted similar to the standard test except it is conducted at a temperature of 150°C and a pressure of 3,500 kPa are utilized.

Three major antioxidant depletion studies have been performed: Hsuan and Koerner 1998; Sangam and Rowe 2002; and Mueller and Jakob 2003. Each of these studies is discussed in the succeeding sections.

7.6.2.1 Hsuan and Koerner (1998) Antioxidant Depletion Study

Hsuan and Koerner (1998) reported on twenty-four months of HDPE geomembrane antioxidant depletion testing. The HDPE geomembrane tested was taken from a single roll of commercially available 60 mil thick HDPE. The primary antioxidants in this geomembrane were probably phosphites and hindered phenols (Hsuan and Guan 1997). OIT tests, which provide a relative measure of the total antioxidants within the geomembrane, were initially performed.

The following were the initial OIT measurements for this geomembrane:
- Standard-OIT = 80.5 min (The Std-OIT value for pure unstabilized (no antioxidants) HDPE resin was found to be 0.5 min)
- High Pressure-OIT = 210 min (The HP-OIT value for pure unstabilized (no antioxidants) HDPE resin was found to be 20 min)

Four sets of five columns for a total of twenty were maintained at elevated temperatures of 85, 75, 65, and 55°C and under a static normal load of 260 kPa and a 300 mm head of tap water. The top surface of the HDPE was saturated sand and the bottom surface was dry sand vented to the atmosphere. Samples were retrieved at various time intervals over a two year period and analyzed for numerous physical, mechanical, and chemical properties including OIT.

Although the OIT value decreased with time, the testing was not conducted to antioxidant depletion. Therefore no significant changes in physical and mechanical properties (i.e., density, melt flow index, yield stress, yield strain, break stress, and break strain) were noted over the 24 month period, since these properties remain unchanged as long as antioxidants exist in the geomembrane (i.e., OIT values greater than that of unstabilized HDPE resin).

Hsuan and Koerner (1998) plotted both the standard and high pressure OIT data for each of the four test temperatures as the natural logarithm of OIT versus incubation time. This produced a linear response for each test temperature for each OIT methodology, where the OIT depletion rate for each temperature is the slope of its respective line and the y-intercept is the natural logarithm of the initial geomembrane OIT value.

The equation for the line then becomes:

$\ln(OIT) = \ln(P) - St$, where OIT = OIT (minutes); S = OIT depletion rate (minutes/month);
t = incubation time (months); and
P = the initial geomembrane OIT value (i.e., a constant)

Based upon these plots Hsuan and Koerner (1998) determined the antioxidant depletion rates for each OIT methodology for each test temperature as shown in Table 38.

Table 38. Hsuan and Koerner (1998) Antioxidant Depletion Rates

Temperature (°C)	S Std-OIT (min/month)	S HP-OIT (min/month)
85	0.1404	0.0661
75	0.0798	0.0387
65	0.0589	0.0284
55	0.0217	0.0097

Hsuan and Koerner (1998) then used the Arrhenius equation to extrapolate the OIT depletion rate to lower temperatures more representative of typical field condition. The Arrhenius equation can be use to expressed by:

$$S = Ae^{-E/RT}$$

$\ln(S) = \ln(A) + (-E_a / R)(1/T)$, where S = OIT depletion rate (see Table 38); E_a = activation energy of the antioxidant depletion reaction (kJ/mol); R = universal gas constant (8.31 j/mol); T = test temperature in absolute Kelvin (K); and A = constant.

A plot of ln(S) versus 1/T results in a linear plot as shown in Figure 33. The activation energy of the antioxidant depletion reaction is obtained from the slope of the line. From the Arrhenius plot Hsuan and Koerner (1998) determined the Arrhenius equation associated with each OIT test method and the associated activation energy as shown in Table 39. Table 39 equations were utilized to determine the OIT depletion rate (S) associated with various temperatures (see Table 40). Then the time to antioxidant depletion was determined for select temperatures (see Table 40) using the following equation:

$\ln(OIT) = \ln(P) - St$, where OIT = antioxidant depleted OIT value (minutes) taken as the OIT value of pure unstabilized (no antioxidants) HDPE resin; S = OIT depletion rate (minutes/month) (see Table 40); t = time to antioxidant depletion (months); and P = the original value of OIT of the geomembrane (i.e. a constant)
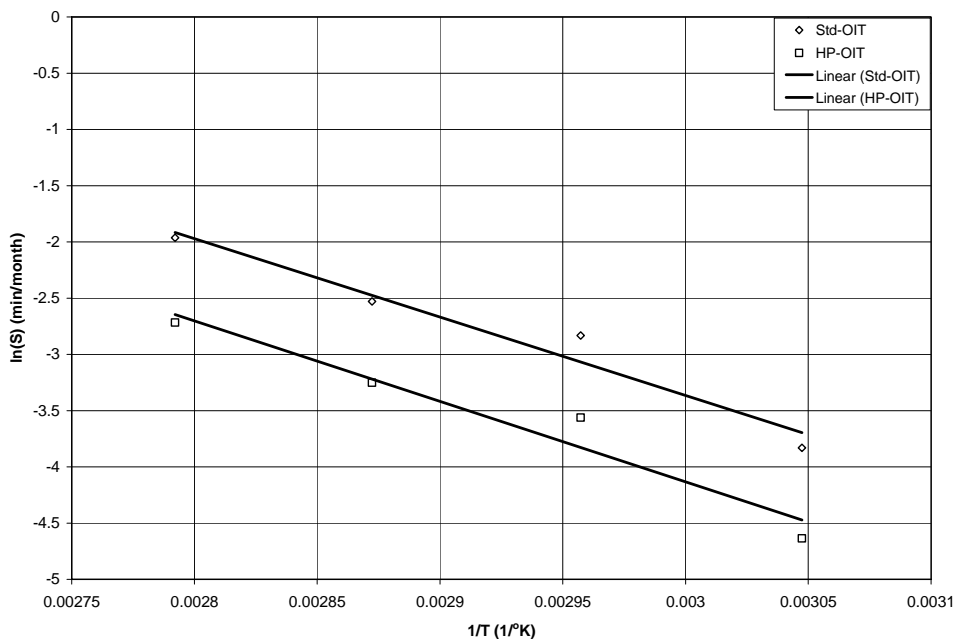
Figure 33. Hsuan and Koerner (1998) Arrhenius Plot

Table 39. Hsuan and Koerner (1998) Arrhenius Equations and Activation Energy

OIT Test Method	Arrhenius equation	E_a (kJ/mol)
Std-OIT	Ln(S) = 17.045 – 6798/T	56
HP-OIT	Ln(S) = 16.850 – 6989/T	58

Table 40. Hsuan and Koerner (1998) OIT depletion Rate (S) and Time to Antioxidant Depletion

Temperature (^{o}C)	$S_{std\text{-}OIT}$ (minute/month)	$t_{std\text{-}OIT}$ (yrs)	$S_{HP\text{-}OIT}$ (minute/month)	$t_{HP\text{-}OIT}$ (yrs)
13	0.0012	348.1	0.0005	381.6
15	0.0014	295.2	0.0006	322.1
20	0.0021	197.4	0.0009	213.0
25	0.0032	133.8	0.0014	142.8
33	0.0057	73.7	0.0025	77.4
40	0.0094	44.9	0.0042	46.5

Based upon their 24 months of testing, Hsuan and Koerner (1998) postulated that HDPE degradation due to thermal oxidation occurs in the following three stages:

- Stage A: Antioxidant depletion period
- Stage B: Induction period
- Stage C: Polymer thermal oxidation period

After 24 months of testing, the HDPE degradation was still in the antioxidant depletion period, based upon this data Hsuan and Koerner (1998) estimated that the antioxidant depletion period would last approximately 200 years at a temperature of 20 °C. Koerner (1998) has additionally estimated that the induction period (i.e., the time between antioxidant depletion and onset of thermal oxidation) would last from 20 to 30 years based upon the examination of exhumed HDPE milk containers at the bottom of a landfill. Thus in a buried environment at 20 °C, they estimate a time span of approximately 220 years with essentially no degradation of physical and mechanical properties.

7.6.2.2 Sangam and Rowe (2002) Antioxidant Depletion Study

Sangam and Rowe (2002) reported on approximately thirty-three months of HDPE geomembrane antioxidant depletion testing. The HDPE geomembrane tested was a GSE Lining Technology, Inc. 80-mil thick smooth HDPE manufactured from a copolymer resin with a density of 0.940 g/cm^3, a carbon black content of 2.54%, and an initial standard OIT of 133 minutes. It was assumed that the primary antioxidants in this geomembrane were phosphites and hindered phenols based upon the previous work of Hsuan and Guan (1997).

HDPE coupons were immersed in air, tap water, and synthetic landfill leachate (i.e., exposed on both sides), each at temperatures of 22 ± 2, 40, 55, 70, and 85°C. Samples were retrieved at various time intervals over a 33-month period and analyzed for primarily standard OIT. The synthetic landfill leachate consisted of approximately 15,000 mg/L inorganic ions, 7,500 mg/L volatile fatty acids, 5000 mg/L of a surfactant, and less than 10 mg/L trace heavy metals.

Sangam and Rowe (2002) plotted the standard OIT data for each of the immersion medium (i.e., air, tap water, and synthetic landfill leachate) at each of the five test temperatures as the natural logarithm of OIT versus incubation time. This produced a straight line for each test exposure condition (i.e., immersion medium and temperature) suggesting that the antioxidant depletion follows first-order decay, with the OIT depletion rate represented by the slope of the line. At any time (t), the OIT value which represents the remaining amount of antioxidants the geomembrane can be expressed as:

$$OIT(t) = OIT_0 \, e^{-St},$$

where OIT(t) = OIT at any time, t, in minutes; OIT_0 = initial OIT in minutes; S = rate of antioxidant depletion in month^{-1}.; t = time in months

This resulted in the inferred depletion rates provided in Table 41.

Table 41. Sangam and Rowe (2002) Inferred Depletion Rates (S = month^{-1})

Temperature (°C)	Air	Water	Leachate
85	0.1094	0.1746	0.4074
70	0.0497	0.1050	-
55	0.0226	0.0470	0.1504
40	0.0152	0.0362	0.0886
22	0.0023	0.0043	0.0188

The Table 41 depletion rates determined at elevated temperatures can be extrapolated to typical field temperatures using the Arrhenius equation (a time-temperature superposition principal) in order to estimate the field service life.

$$S = A \, e^{-E_a / RT}$$

$$\ln(S) = \ln(A) + (-E_a / R)(1/T),$$

S = OIT depletion rate (see Table 41); E_a = activation energy in J/mol; R = 8.314 J/mol K (universal gas constant); T = absolute temperature in K; A = constant (collisional factor)

A plot of ln(S) versus 1/T results in a linear plot as shown in Figure 34. The activation energy of the antioxidant depletion reaction is obtained from the slope of the line. From the Arrhenius plot Sangam and Rowe (2002) determined the Arrhenius equation associated with each immersion medium (i.e., air, water, and leachate) and the associated activation energy. However Sangam and Rowe (2002) appear to have made a mistake in their calculations. Rather than using the temperature 40°C in their calculations they appeared to have used50 °C. Making this correction, the derived Arrhenius equation and the inferred activation energy (E_a) for each immersion medium are summarized in Table 42.

The Table 42 equations were utilized to determine the OIT depletion rate (S) associated with various temperatures (see Table 43). Then the time to antioxidant depletion was determined for select temperatures (see Table 43) using the following equation and assuming the OIT of an unstabilized HDPE to be 0.5 minute:

$\ln(OIT_D) = \ln(OIT_o) - St$, where OIT_D = antioxidant depleted OIT value of 0.5 minutes;
S = OIT depletion rate (minutes/month) (see Table 40);
t = time to antioxidant depletion (months); and P = the original value of OIT of the geomembrane (i.e., a constant)
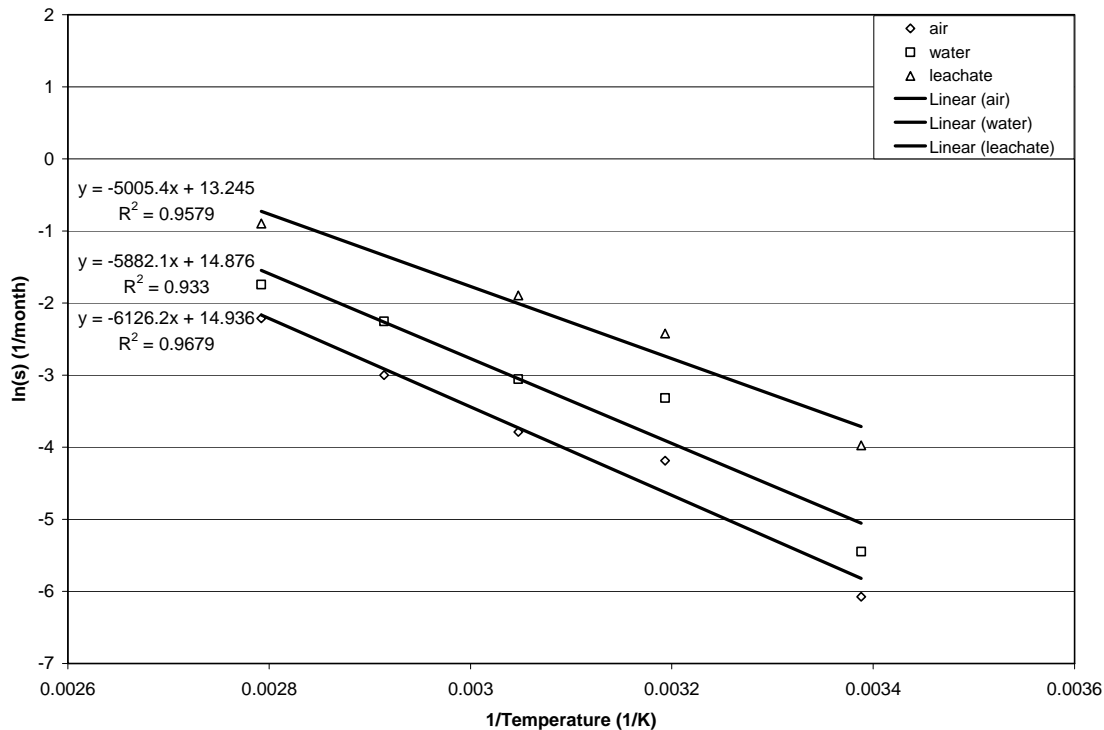
Figure 34. Sangam and Rowe (2002) Arrhenius Plot

Table 42.   Sangam and Rowe (2002) Arrhenius Equations and Activation Energy

Exposure Medium	Arrhenius equation $(S = month^{-1}; T = month)$	E_a (kJ/mol)	R^2
Air	Ln(s) = 14.936 – 6126.2/T	50.93	0.9679
Water	Ln(s) = 14.876 – 5882.1/T	48.90	0.933
Leachate	Ln(s) = 13.245 – 5005.4/T	41.61	0.9579

Table 43.   Sangam and Rowe (2002) OIT Depletion Rate (S) and Time to Antioxidant Depletion

Temp. (°C)	S (month⁻¹)	Air (yrs)	S (month⁻¹)	Water (yrs)	S (month⁻¹)	Leachate (yrs)
13	0.0015	301.3	0.0034	136.3	0.0143	32.5
15	0.0018	259.7	0.0039	118.2	0.0162	28.8
20	0.0026	180.7	0.0056	83.4	0.0217	21.4
25	0.0037	127.3	0.0078	59.6	0.0289	16.1
33	0.0063	74.4	0.0131	35.6	0.0448	10.4
40	0.0098	47.6	0.0201	23.2	0.0646	7.2

As seen in Table 43, antioxidant depletion for the range of temperatures 13 to 33°C is estimated to be approximately twice as fast in tap water than in air and four times faster in high organic content leachate than in tap water. Sangam and Rowe (2002) state that the following regarding these estimates of antioxidant depletion:

- The Table 43 time to antioxidant depletion estimates represent a lower bound to the time and the time in the field would be expected to be longer under these exposure conditions.

- The Table 43 time to antioxidant depletion estimates are based upon having the immersion medium on both sides of the geomembrane and must be adjusted for actual field conditions (i.e., leachate is not typically located on both sides of the membrane).

7.6.2.3 Mueller and Jakob (2003) Antioxidant Depletion Study

Mueller and Jakob (2003) report on 13.6 years of HDPE geomembrane antioxidant depletion testing for immersion in air and 6 years for immersion in de-ionized water. The HDPE geomembranes tested by Mueller and Jakob (2003) consisted of nine commercially available HDPE geomembranes made by five different manufacturers from seven different resins. The geomembranes were 100-mil thick, had densities ranging from 0.940 to 0.950 g/cm^3, contained 2 to 2.5 weight percent carbon black and a few thousand ppm phenolic and phosphite antioxidants, and had an initial OIT (Al-pan at 200°C) from 11 to 138 min.

HDPE samples were immersed in air and de-ionized water (i.e., exposed on both sides) at 80°C. The samples immersed in air were in an oven with substantially less than 10 air changes per hour. The samples were immersed in water in glass flasks, which were opened and shook every four weeks. The water was completely changed every three months. At various times samples were removed and tested for OIT and tensile strength and elongation.

During accelerated aging in heated air, the OIT slowly decreased in a steady, exponential-like, fashion. After 13.6 years of accelerated aging in heated air, no significant changes in mechanical properties due to oxidation were detected. For aging in heated air it was found that "the relative OIT values (i.e., OIT/OIT$_{intial}$) showed roughly a common decline as a function of aging time, independent of the resin or the OIT testing temperature".

During accelerated aging in heated water, the OIT decreased rapidly at first and then leveled off. Mueller and Jakob (2003) looked at this as a two step exponential decline with a short-term high antioxidant depletion rate and a long-term low antioxidant depletion rate. After 6 years of accelerated aging in heated water, it was found that most samples approached very low OIT values after 200 days (i.e. the antioxidant depletion rate was initially fairly high), that the antioxidant depletion rate decreased significantly after 200 days, and that oxidation of the polymer itself started after 5 years, and that deterioration proceeded quite rapidly after oxidation began at the elevated test temperature (80°C). Since the phosphite stabilizer substantially determines the initial OIT and since it constitutes the bulk of the stabilizer in the HDPE geomembranes, Mueller and Jakob (2003) assume that depletion especially of the phosphite component is seen in the initial rapid OIT decrease. "The long-term antioxidant depletion time would then be determined by the migration of the remaining phenolic stabilizer. Therefore, a high initial OIT does not necessarily correlate with good long-term oxidation stability."

Short-term antioxidant depletion rates were estimated at 0.15 to 0.3 minute/month (approximately 0.2) in water at 80°C (100-200 days) and long-term antioxidant depletion rates at 0.015 to 0.03 minute/month (1000-2000 days). Most of the data appeared to be in the 0.15 minute/month (200 days) range for the short-term antioxidant depletion rate and 0.015 minute/month (2000 days) for long-term antioxidant depletion rate.

Mueller and Jakob (2003) could not estimate the antioxidant depletion time (i.e., time it takes to deplete the antioxidants and begin oxidation) at typical field temperatures using the Arrhenius equation, since they did not perform their testing at multiple temperature as required for use of the Arrhenius equation. Therefore they utilized the van't Hoff rule for the temperature dependence of antioxidant depletion time, their measured antioxidant depletion time of 5 years for HDPE GMs immersed in 80°C de-ionized water, and assumed activation energies from other studies.

$$t_1(T) = t_1(T') \, e^{\frac{E_a}{R}\left[\frac{1}{T} - \frac{1}{T'}\right]},$$

where $t_1(T)$ = antioxidant depletion period in years at the ambient temperature of the HDPE; $t_1(T')$ = antioxidant depletion period in years at test temperature of 80°C (i.e., 5 years); E_a = depletion process activation energy; R = universal gas constant (8.319 J/mol K); T = ambient temperature of the HDPE in K (K = 273.15 + °C); T' = test temperature in K = 273.15 + 80°C = 353.15

Table 44 provides various antioxidant depletion process activation energies that have been determined by others. These activation energies have been utilized with the van't Hoff rule to calculate estimated antioxidant depletion times per Mueller and Jakob's (2003) methodology (see Table 45). As seen in Table 45 the estimated antioxidant depletion time varies widely with the assumed activation energy. At a temperature of 33°C the antioxidant depletion time varies from 45 to 930 years with the utilization of activation energies of 42 and 100 kJ/mol, respectively.

Mueller and Jakob (2003) believe that an activation energy of 60 kJ/mol is a very low activation energy which is expected to represent the lower limit of antioxidant depletion time. At a temperature of 33°C and an activation energy of 60 kJ/mol the antioxidant depletion time would be approximately 103.6 years.

Table 44.   Antioxidant Depletion Process Activation Energies

Source	Media	E_a (kJ/mol)	Comment
Hsuan-Koerner (1998)	Sand-water-air	56	Using Std-OIT test; didn't take test out to antioxidant depletion
		58	Using HP-OIT test; didn't take test out to antioxidant depletion
Sangam-Rowe (2002)	Air	51	Using Std-OIT test; didn't take test out to antioxidant depletion
	Water	49	
	Synthetic Leachate	42	
Smith et al. (1992)	Water	100	-

Table 45.   Estimated Antioxidant Depletion Times (Mueller and Jakob 2003)

Temperature (°C)	E_a = 42 kJ/mol Antioxidant Depletion Time (years)	E_a = 49 kJ/mol Antioxidant Depletion Time (years)	E_a = 51 kJ/mol Antioxidant Depletion Time (years)
13	142.1	248.3	291.2
15	125.8	215.2	251.0
20	93.3	151.9	174.6
25	69.9	108.4	123.0
33	44.9	64.7	71.8
40	31.0	42.1	45.9
Temperature (°C)	E_a = 56 kJ/mol Antioxidant Depletion Time (years)	E_a = 58 kJ/mol Antioxidant Depletion Time (years)	E_a = 100 kJ/mol Antioxidant Depletion Time (years)
13	433.8	508.8	14,462.3
15	368.4	429.6	10,804.6
20	247.4	284.3	5,303.9
25	168.3	190.8	2,666.5
33	93.3	103.6	929.8
40	57.1	62.3	386.6

Mueller and Jakob (2003) determined that antioxidant depletion occurs due to diffusion out of the HDPE geomembrane and oxidative consumption. It was also determined that under conditions of low temperature and low oxygen levels, diffusion is the predominant antioxidant depletion mechanism as with typical field conditions. The diffusion rate is higher with immersion in water rather than in air. Oxidative consumption is the predominant mechanism, under conditions of high temperature and high oxygen levels. Additionally, Mueller and Jakob (2003) determined that the mechanical properties of HDPE geomembrane are not significantly degraded as long as a significant OIT value is measurable.

7.6.2.4 Summary of Antioxidant Depletion Studies

Both Hsuan and Koerner (1998) and Mueller and Jakob (2003) determined that no significant changes in physical and mechanical properties of the HDPE geomembrane occur until the antioxidants are essentially depleted. Sangam and Rowe (2002) and Mueller and Jakob (2003) determined that the antioxidant depletion rate is dependent upon the medium within which the HDPE geomembrane is immersed. Sangam and Rowe (2002) determined that the antioxidant depletion rate increases in order with immersion in the following media: air, tap water, and high organic content leachate. Mueller and Jakob (2003) confirmed that the antioxidant depletion rate is greater with immersion in water than with air. Both Sangam and Rowe (2002) and Mueller and Jakob (2003) immersed their HDPE geomembrane samples in the immersion medium such that both side of the samples were in contact with the medium.

Mueller and Jakob (2003) observed a two-stage antioxidant depletion process with immersion in water. The two-stage process was seen to consist of initial short-term antioxidant depletion at a high rate followed by long-term antioxidant depletion at a low rate. They assume that the initial short-term depletion during their testing at 80°C was the phosphite stabilizer, which constitutes the bulk of the antioxidant, diffusing out over 200 days at a rate of 0.15 minute/month as determined by OIT measurement. They further assume that the long-term depletion during their testing at 80°C was the hindered phenols diffusing out over 2000 days at a rate of 0.015 minute/month as determined by OIT measurement. They further observed that oxidation of the polymer itself started after 5 years and that deterioration proceeded quite rapidly after oxidation began at the elevated test temperature (80°C). This was not observed in the testing conducted by Hsuan and Koerner (1998) nor Sangam and Rowe (2002), since their testing was of a much shorter duration than that of Mueller and Jakob (2003). Additionally testing by Hsuan and Koerner (1998) nor Sangam and Rowe (2002) were not conducted to antioxidant depletion as with Mueller and Jakob (2003); therefore they did not observe oxidative degradation and associated degradation of the physical and mechanical properties.

Mueller and Jakob (2003) determined that antioxidant depletion occurs over time due to diffusion out of the HDPE geomembrane and oxidative consumption within the geomembrane. It was also determined that under conditions of low temperature and low oxygen levels, diffusion is the predominant antioxidant depletion mechanism as with typical field conditions. Oxidative consumption is the predominant mechanism, under conditions of high temperature and high oxygen levels.

Hsuan and Koerner (1998) postulated that HDPE degradation due to thermal oxidation occurs in the following three stages:
- Stage A: Antioxidant depletion period
- Stage B: Induction period
- Stage C: Polymer thermal oxidation period

Koerner (1998) has additionally estimated that the induction period (i.e., the time between antioxidant depletion and onset of thermal oxidation) would last from 20 to 30 years based upon the examination of exhumed HDPE milk containers at the bottom of a landfill.

Table 46 presents the estimated antioxidant depletion times at temperatures of 33 and 40°C based upon the testing by Hsuan and Koerner (1998) and Sangam and Rowe (2002). Additionally the times based upon the methodology of Mueller and Jakob (2003) are provided utilizing the corresponding activation energies determined by Hsuan and Koerner (1998) and Sangam and Rowe (2002). In general the antioxidant depletion times estimated by the methodology of Mueller and Jakob (2003) are greater than those determined by Hsuan and Koerner (1998) and Sangam and Rowe (2002) for the same activation energies. It is likely that the antioxidant depletion times provided in Table 46 are low (i.e., conservative), since they are probably based upon activation energies associated with the initial short-term depletion of the phosphite stabilizer rather than the long-term depletion of the hindered phenols.

A final item of note is the fact that the studies utilized different HDPE geomembranes with potentially different antioxidant packages. All three studies assumed that the antioxidant packages of the HDPE geomembranes they tested included phosphites and hindered phenols, however the quantity of each was unknown. The antioxidant packages are typically treated as proprietary information, by the HDPE geomembrane manufacturers, and therefore the information is not generally available to the public. Differences in the makeup of the antioxidant packages could have a significant impact on the on the estimated antioxidant depletion times derived from each study.

Table 46. Summary of Estimated Antioxidant Depletion Times

Temperature (°C)	Hsuan and Koerner (1998) Water/Air/Sand (yrs)	Mueller and Jakob (2003) E_a = 56 kJ/mol Antioxidant Depletion Time (years)	Sangam and Rowe (2002) Air (yrs)	Mueller and Jakob (2003) E_a = 51 kJ/mol Antioxidant Depletion Time (years)
33	73.7	93.3	74.4	71.8
40	44.9	57.1	47.6	45.9
Temperature (°C)	Sangam and Rowe (2002) Water (yrs)	Mueller and Jakob (2003) E_a = 49 kJ/mol Antioxidant Depletion Time (years)	Sangam and Rowe (2002) Leachate (yrs)	Mueller and Jakob (2003) E_a = 42 kJ/mol Antioxidant Depletion Time (years)
33	35.6	64.7	10.4	44.9
40	23.2	42.1	7.2	31.0

Needham et al. (2004) performed an extensive review of these studies and came to the following primary conclusions:

- The antioxidant depletion times of HDPE geomembranes may be significantly longer than that estimated by Hsuan and Koerner (1998) and Sangam and Rowe (2002), based upon the two-stage depletion seen by Mueller and Jakob (2003). Additionally it may also be longer due to the following:
  - The leachate strength in testing by Sangam and Rowe (2002) remained constant, whereas it will likely decrease with time and the rate of antioxidant depletion will probably also decrease with time,
  - The presence of soil particles in contact with the geomembrane in the field reduces its contact area with air, water, and/or leachate.
  - Antioxidant depletion due to oxidative consumption would be low, since only limited oxygen levels would be present due to the partially saturated or saturated surrounding materials and the reducing conditions often associated with landfills.
- Mueller and Jakob (2003) took samples for OIT measurement from the center of the geomembrane thickness, whereas Hsuan and Koerner (1998) and Sangam and Rowe (2002) tested the entire geomembrane thickness. This could have had an impact on the antioxidant depletion times estimated, since a greater concentration of antioxidants should be located in the center than at the surface over time.

WSRC-STI-2007-00184, REVISION 2

- "The activation energy reflects the necessary minimum energy of the antioxidant depletion process and will depend on the characteristics of the polyethylene resin, the antioxidant package, and the exposure conditions in which the antioxidant loss is occurring." The rate of antioxidant depletion is exponentially dependent upon the activation energy. "It is tentatively inferred that the lower activation energies found by Hsuan and Koerner (1998) and Sangam and Rowe (2002) reflect faster diffusion of more easily depleted antioxidants, rather than slower diffusion of the residual antioxidants, which provide the very long-term antioxidant protection." "Values of activation energy of 60-75 kJ/mol appear a reasonable, conservative estimate."

- "As noted by Mueller and Jakob (2003), the overall rate of antioxidant loss from a geosynthetic is proportional to its surface area and the total amount of stabilizer in the geosynthetic is proportional to its volume. Thus, the antioxidant depletion time should be proportional to the thickness of the material." However due to the limited available data sets, it is not yet possible to draw quantitative conclusions with regard to geomembrane thickness.

- High initial OIT values do not necessarily result in long-term oxidation stability. For example, phosphites can produce high initial OIT values but do not greatly contribute to long-term oxidative stability at typical field temperatures. Therefore HDPE geomembrane specifications should not only stipulate an initial OIT value.

- Needham et al. (2004) believe that a reasonable estimation of the antioxidant depletion time can be derived from the following:
  – Slow long-term OIT depletion rates from Mueller and Jakob (2003),
  – Increased rate of depletion for leachate exposure found by Sangam and Rowe (2002),
  – Effects of a confined sample under compressive stress sandwiched between saturated sand and dry sand, as investigated by Hsuan and Koerner (1998), and
  – Measuring durability of the geomembrane in terms of the tensile test (but not service life as a hydraulic barrier).

Based upon the above discussion antioxidant depletion of the HDPE geomembrane will be considered as a FTF Closure Cap degradation mechanism for modeling purposes using the Needham et al. (2004) model discussed in Section 7.6.7.

7.6.3 Thermal Oxidative Degradation

Thermal oxidative degradation is the principal degradation mechanism for HDPE geomembranes in landfills (Rowe 2004). Thermal oxidative degradation of a HDPE geomembrane can begin only after the antioxidants have been depleted and only if oxygen is available. (Koerner 1998; Mueller and Jakob 2003; Needham et al. 2004). Thermal oxidative degradation is initiated with the production of free radicals ($R^\bullet$) within the polymer structure due to elevated temperatures, high energy irradiation, etc (Koerner 1998; Needham et al. 2004). If oxygen is available the free radicals rapidly combine with oxygen producing peroxide free radicals ($ROO^\bullet$). These peroxide free radicals can then react with intact portions of the polymer to form additional free radicals and hydroperoxides (i.e., oxidized polymer chains (ROOH)).

The hydroperoxides can then decompose to produce additional free radicals. This progression leads to accelerated polymer chain reactions, resulting in polymeric main chain scission (i.e., breakage of covalent bonds within the polymer structure) (Koerner 1998; Koerner and Hsuan 2003; Needham et al. 2004). The following are the primary thermal oxidative degradation reactions:

$$RH + energy \ R^\bullet + H^\bullet$$
$$R^\bullet + O_2 \rightarrow ROO^\bullet$$
$$ROO^\bullet + RH + energy \rightarrow ROOH + R^\bullet,$$

where RH = polymer chain, $R^\bullet$ = free radical, $ROO^\bullet$ = peroxide free radical; ROOH = hydroperoxides (i.e. oxidized polymer chains)
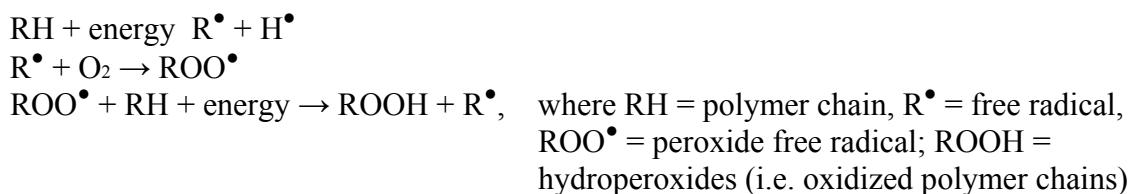
Polymeric main chain scission caused by oxidation results in embrittlement of the HDPE geomembrane and degradation of its mechanical properties (Koerner and Hsuan 2003; Mueller and Jakob 2003). However, even after the HDPE geomembrane becomes brittle it remains intact and can withstand high pressure (Mueller and Jakob 2003). Oxidation only occurs in amorphous regions of an HDPE geomembrane, since oxygen can not enter the crystalline regions. Therefore the overall rate of oxidation is inversely proportional to the degree of crystallinity (Needham et al. 2004). Elevated temperatures and the presence of transition metals (e.g. manganese, copper, aluminum, and iron) increase the rate of oxidation (Needham et al. 2004). However complete oxidation of a HDPE geomembrane will take an extended period of time. It has been estimated by Albertsson and Banhidi (1980) that a 60-mil thick HDPE geomembrane would take 10,000,000 years for complete oxidation based upon a mass loss of 0.00001% per year once oxidation starts (Needham et al. 2004).

However if oxygen is not available, the production of free radicals ($R^\bullet$) leads to polymer crosslinking (i.e., combining polymer molecules) rather than polymer chain scission. Polymer crosslinking up to a point in general improves the mechanical properties of the HDPE geomembrane (Kresser 1957; Frados 1976; Schnabel 1981; Sangster 1993; Koerner 1998).

Based upon this information it has been concluded (Koerner 1998; Needham et al. 2004) that HDPE geomembranes in landfill service will slowly degrade by thermal oxidation. Oxidation will generally be limited by the availability of oxygen within the subsurface, and such slow oxidative degradation will not result in the disintegration or disappearance of the geomembrane within a timeframe of interest (i.e., 10,000 years). Thermal oxidative degradation is of no concern where oxygen has been removed from the surface of the geomembrane.

Based upon the above discussion thermal oxidative degradation of the HDPE geomembrane in conjunction with tensile stress cracking degradation (see Section 7.6.5) will be considered as a FTF Closure Cap degradation mechanism for modeling purposes using the Needham et al. (2004) model discussed in Section 7.6.7.

7.6.4 High Energy Irradiation Degradation

HDPE degradation by high energy irradiation can be similar to degradation by UV radiation (Needham et al. 2004). It has often been cited that the basic mechanical properties of a typical polymer start to change due to irradiation degradation by main chain scission at a total dose greater than 1 to 10 Mrad (Phillips 1988; Koerner et al., 1990; Koerner 1998; Nimitz et al. 2001; Needham et al., 2004). However, as discussed below, the impact of irradiation on polymers, and on high density polyethylene (HDPE) in particular, is determined primarily by the total absorbed dose and the presence or absence of oxygen.

The absorption of high energy ionizing radiation such as gamma rays (γ-rays) by polymers primarily results in the production of free cation radicals and the ejection of electrons within the polymer. The ejected electrons can induce additional ionizations or produce electronic excitation in surrounding molecules. Secondary reactions can include the production of ions (both cations and anions) and free anion radicals. These products of radiation absorption are unstable and are reactive toward surrounding intact molecules resulting in both crosslinking (combining polymer molecules) and main-chain scission (breakage of polymer molecules). For polyethylene the extent of irradiation induced crosslinking or main chain scission appears to be independent of the type of radiation within a factor of 2 (i.e., alpha particles, beta particles, gamma-rays, X-rays, protons). Crosslinking predominates in the absence of oxygen and main chain scission predominates in the presence of oxygen. (Schnabel 1981; Sangster 1993; Harper 1996; Kudoh et al. 1996)

Irradiation of polyethylene in the absence of oxygen at relatively low doses (i.e. less than 10 Mrad) primarily results in crosslinking, which improves temperature and chemical resistance, increases the elastic modulus, tensile strength, and hardness, reduces the solubility, and improves the weatherability of the polyethylene (Kresser 1957; Frados 1976; Schnabel 1981; Sangster 1993). However, at high absorbed doses polyethylene becomes very hard and brittle (Kresser 1957; Kane and Widmayer 1989; Sangster 1993). For high density polyethylene (HDPE) the ultimate strength half-dose value in vacuum has been measured at greater than 5000 Mrad and the ultimate elongation half-dose value in vacuum has been measured at between 10 to 30 Mrad (Brandrup and Immergut 1989). The half-dose value is the absorbed dose required to reduce a particular mechanical property of the polymer by half under a defined environment (Brandrup and Immergut 1989). (Schnabel 1981)

However during irradiation in the presence of oxygen (i.e., in the presence of air) polyethylene undergoes predominately main-chain scission, which results in a rapid deterioration and subsequent deleterious impact upon mechanical properties. Main-chain scission can occur during reactions involving peroxyl and oxyl radicals. Since the oxidation of free cation radicals, produced during irradiation, results in peroxyl and oxyl radicals, the presence of oxygen during irradiation results in the occurrence of more main-chain scission. Additionally oxygen can react with lateral macroradicals, which would otherwise crosslink, thus reducing the occurrence of crosslinking. Finally radiation can provide the activation energy necessary for oxidation to occur, if oxygen is available. (Schnabel 1981; Sangster 1993; Sun et al. 1996; Badu-Tweneboah et al. 1999)

In the absence of oxygen the dose rate does not appear to influence the impact of irradiation on polyethylene (Brandrup et al. 1999). However in the presence of oxygen the following are two apparent dose rate effects (Schnabel 1981; Brandrup and Immergut 1989):

- High dose rates can result in the rapid depletion of oxygen within a polymer. This can result in further polymer deterioration, due to the combined effect of irradiation and oxidation which produces main-chain scission, being limited by oxygen diffusion into the polymer. In the case of polyethylene this can actually lead to increased crosslinking due to further irradiation once the interior oxygen has been depleted and an actual improvement in mechanical properties. In this case main-chain scission only occurs at the surface of the polymer where oxygen is available. This, therefore, produces an apparent dose rate effect upon polymer deterioration at high dose rates. (Brandrup et al. 1999). At low dose rates polymer deterioration due to main-chain scission produced by irradiation and oxidation is not limited by oxygen diffusion into the polymer. Therefore at these low dose rates the full impact of combined irradiation and oxidation is realized. Therefore at lower dose rates, dose rate does not appear to impact degradation due to irradiation but it appears to be dependent upon total dose and the presence of oxygen. Polymer thickness also impacts the influence of oxygen on the polymer, since the thicker the polymer the longer the diffusion path for oxygen diffusion into the polymer (Brandrup et al. 1999). Figure 35 and Table 47 provide the impact of dose rate on the half-dose values for ultimate strength and ultimate elongation of HDPE in air (Brandrup and Immergut 1989). From Figure 35 it is seen that dose rates above about 5000 Rad/hr have an apparent dose rate effect while dose rates below 5000 Rad/hr do not.
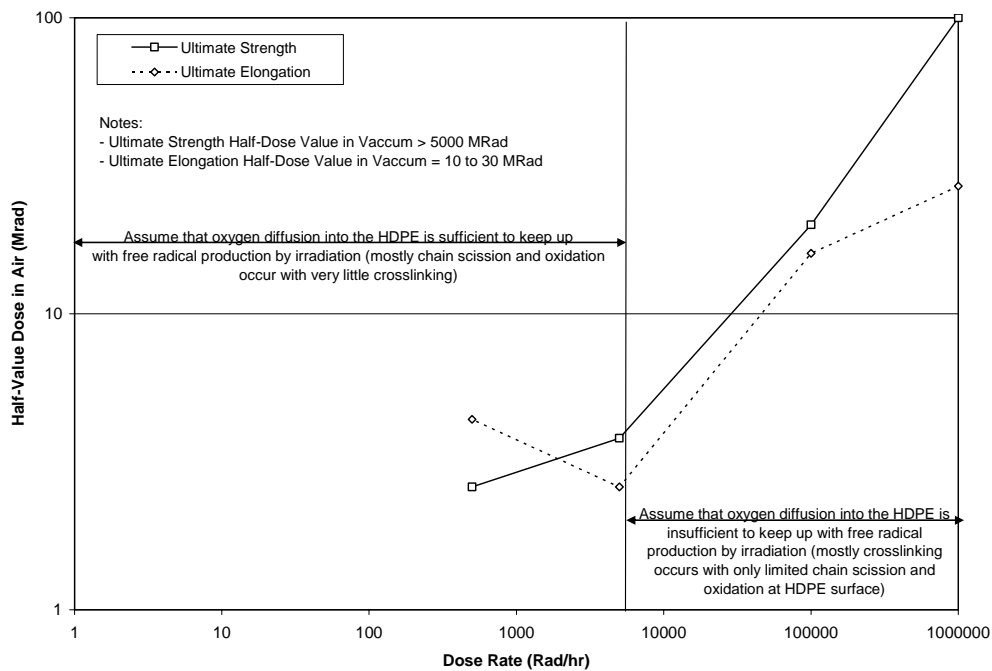
Figure 35. Dose Rate Impact on HDPE Ultimate Strength and Elongation Half-Value Dose in Air (Brandrup and Immergut 1989)

Table 47.   Dose Rate Impact on HDPE Ultimate Strength and Elongation Half-Value Dose in Air (Brandrup and Immergut 1989)

Dose Rate (Rad/hr)	Ultimate Strength Half-Value Dose in Air (Mrad)	Ultimate Elongation Half-Value Dose in Air (Mrad)
1000000	100	27
100000	20	16
5000	3.8	2.6
500	2.6	4.4

- High dose rates can also result in an increase in the polymer's temperature. Many chemical reactions have fairly high activation energies, which can be overcome with the irradiation induced temperature increase and lead to reactions which might not otherwise occur (Brandrup et al. 1999).

Mechanical stress combined with irradiation is also known to accelerate radiation-induced degradation. (Hamilton et al. 1996).

7.6.4.1 Mitigating Irradiation Impacts on HDPE

The impacts of irradiation on HDPE can be mitigated by one or a combination of the following:

- The radiation dose rate can be lowered through the use of shielding to reduce the total dose absorbed by the HDPE over the period of concern,
- The level of oxygen to which the HDPE is exposed over the period of concern can be lowered so that the level and rate of degradation is oxygen dependent,
- Antioxidants (prevents oxidative chain reactions and scavenges free radicals) and carbon black (acts as an energy sink) can be incorporated into the HDPE to lower the impact of the presence of oxygen and radiation (Schnabel 1981; Brandrup et al. 1999),
- Thicker HDPE, such as 100 mil (2.5 mm) rather than 60 mil (1.5 mm), can be utilized to limit degradation to the surface of the sheet rather than to its interior, and/or
- Tensile stress on the HDPE can be minimized.

In most cases it is recommended that all of the mitigation means be employed.

7.6.4.2 Nuclear Regulatory Commission Recommendations

Staff from the Nuclear Regulatory Commission (NRC) recommended the following within Kane and Widmayer 1989:

"To compensate for the uncertainties associated with the long-term performance of geosynthetics, and to provide the level of confidence that is required by federal regulations, the use of geosynthetics alone (e.g., as a low-permeability geomembrane or as a geotextile filter fabric) is not recommended by the NRC staff. However, the use of geosynthetics to complement and improve the performance of natural soils and rocks or other proven construction materials is recommended by the staff."

A "100 Mrad regulatory guideline was established to promote selection of polyethylene materials with extremely low risk of degradation under the exposure conditions expected in the high integrity containers." (Badu-Tweneboah et al. 1999)

7.6.4.3 HDPE Irradiation Examples

Several HDPE irradiation examples are provided below particularly those dealing with its use in low-level radioactive waste disposal service:

- Whyatt and Fansworth (1990) evaluated a 60-mil HDPE geomembrane in simulated short-term (up to 120 days) chemical compatible tests with a high pH (~14) inorganic solution at 90°C and subjected them to radiation doses ranging from 0.6 to 38.9 Mrad. The solution consisted predominately of the following in descending order: sodium, nitrite, nitrate, aluminum, potassium, and sulfate. With immersion in the solution and an applied radiation dose, the break strength and elongation decreased (i.e. properties degraded), while yield and puncture strengths and their associated elongations all increased (i.e., properties improved). The 38.9 dose was slightly greater than the break elongation half-dose value (see Section 7.6.4 for the definition of the half-dose value) of the HDPE geomembrane under the conditions tested. No other properties tested were near the half-dose value.
- Badu-Tweneboah et al. 1999 performed an evaluation that demonstrated that the polyethylene components of a low-level radioactive waste disposal landfill in Barnwell South Carolina would perform their intended function of containment during at least the 500-year design period. The two polyethylene components were a 60 mil HDPE geomembrane in the cover system and 3/8 inch thick Linear Medium Density Polyethylene (LMDPE) inner liners within concrete high integrity containers for the disposal of low-level radioactive waste.
- Compatibility testing was performed on the 60-mil smooth HDPE geomembrane planned for the Hanford Grout facility. HDPE samples were exposed to a dose rate of 740,000 rads per hour until a total radiation dose of 16 Mrad or 37 Mrad was reached. The total dose of 37 Mrad resulted in a greater than 25% decrease in geomembrane strength and elasticity. Then the HDPE was immersed in a 194°F solution with a pH of 9.2 and a concentration of inorganics of 368,336 mg/L. It was stated that under these conditions the HDPE showed no unacceptable effects. (INEEL 2004)
- Traditional radiation sterilization of polymers for medical implants is performed to a dose of 2.5 Mrad (Deng et al. 1996).

7.6.4.4 High Energy Irradiation Degradation Applicability to FTF Closure Cap HDPE Geomembrane

Rosenberger (2007) has determined that the dose rate to the FTF Closure Cap HDPE geomembrane would be less than 0.1 mR/hr and that the total dose over 10,000 years would be less than 9,000 rad. This dose rate is significantly below the 5000 Rad/hr dose rate above which an apparent dose rate effect in HDPE is seen (see Section 7.6.4). Therefore the irradiation impact upon the HDPE geomembrane is assumed to be due to only total dose and not dose rate. From Table 47 the HDPE ultimate strength half-value dose in air at a dose rate of 500 Rad/hr was 2.6 Mrad (Brandrup and Immergut 1989). The basic mechanical properties of a typical polymer start to change due to irradiation degradation at a total dose greater than 1 to 10 Mrad (Phillips 1988; Koerner et al., 1990; Koerner 1998; Nimitz et al. 2001; Needham et al., 2004), with levels as high as 100 Mrad being listed as acceptable (Badu-Tweneboah et al. 1999). Therefore a total dose of 2.6 Mrad appears to be a reasonable limit for total dose to the HDPE geomembrane utilized as part of the FTF Closure Cap. This limit of 2.6 Mrad is approximately 290 times greater than the maximum dose of 9,000 rad over 10,000 years to which the FTF Closure Cap geomembrane could potentially be exposed. Based upon this discussion, high energy irradiation of the FTF Closure Cap HDPE geomembrane is considered an insignificant degradation mechanism.

7.6.5 Tensile Stress Cracking Degradation

After the antioxidants in a HDPE geomembrane have been depleted, thermal oxidation of the geomembrane commences if oxygen is present causing embrittlement and degradation of mechanical properties over time. However the geomembrane will remain an effective hydraulic barrier unless it is physically damaged or develops holes or cracks. Holes or cracks can develop from the following two types of tensile stress cracking in a HDPE geomembrane (Needham et al. 2004):

- Ductile tensile failure is a ductile failure where the applied tensile stress exceeds the short-term tensile break strength of the geomembrane
- Brittle stress cracking is a brittle failure where the applied long-term tensile stress is less than the short-term tensile break strength of the geomembrane

In general, HDPE geomembrane installations should be designed so that the short-term tensile break strength of the geomembrane is not exceeded. However subgrade settlement and geomembrane downdrag by waste settlement on the side slopes can occur and cause exceedance of the geomembrane's tensile break strength. (Needham et al. 2004)

Brittle stress cracking, on the other hand, can occur as oxidation of the HDPE geomembrane proceeds and causes increased embrittlement and degradation of its mechanical properties over time. As thermal oxidation proceeds brittle stress cracking will occur where the geomembrane is under stress at lower and lower stresses over time. However as cracking occurs stresses are relieved thus reducing the likelihood of further cracking. Brittle stress cracking can be exasperated by elevated temperatures and contact with agents such as detergents, alcohols (e.g., methanol, ethanol, and propanol), acids and chlorinated solvents (i.e., environmental stress cracking).

The extent of brittle stress cracking is dependent upon the geomembrane stress crack resistance (SCR), the local and global stress over the geomembrane, the geomembrane temperature, the fluid in contact with the geomembrane, and the extent of thermal oxidative degradation. However as long as the geomembrane is not subjected to tensile or shear stresses, it should not fragment and disintegrate, but it should remain intact, for practical considerations, indefinitely. (Needham et al. 2004)

Based upon the above discussion tensile stress cracking degradation of the HDPE geomembrane in conjunction with thermal oxidative degradation (see Section 7.6.3) will be considered as a FTF Closure Cap degradation mechanism for modeling purposes using the Needham et al. (2004) model discussed in Section 7.6.7.

7.6.6 Biological Degradation (microbial, root penetration, burrowing animals)

Biological degradation of HDPE geomembranes could potentially be caused by microbial biodegradation, root penetration, or burrowing animals. Limited investigations have been performed relative to the microbial degradation of HDPE geomembranes. Koerner (1998) stated that the high-molecular-weight polymers used for geomembranes are judged insensitive to microbial (i.e., fungi or bacteria) biodegradation.

Information regarding root penetration of HDPE geomembranes is present in the literature. Available references, including field experience at SRS, indicate HDPE membranes of the thickness used for landfill liners typically preclude root penetration and cause roots to follow laterally atop the geomembrane surface. Landreth (1991) describes a USEPA test using four membranes "that might be used in waste management facilities for landfill cover systems", including polyethylene. The results were that although root mass achieved maximum density atop the membranes, "there was no evidence of root penetration". Badu-Tweneboah et al. (1999) confirm this with their statement that roots are not likely to penetrate an intact geomembrane, they are likely to develop laterally above the geomembrane, and they are not known to enlarge existing geomembrane defects. Additionally Carson (2001) indicated that roots do not penetrate geomembranes. An investigation conducted by Serrato (2004) at SRS showed that roots from overlying pine trees turned horizontally and followed along the top of the geomembrane upon reaching a HDPE geomembrane without damaging or penetrating it. Newman et al. (2004) describe the thirty-year durability of a 20-mil thick polyvinylchloride (PVC) geomembrane used as an aquaculture pond liner. They interpreted the lack of holes to indicate resistance to both microorganisms and root penetration from the dense stand of cattails, trees, and other vegetation. In general, polymer sheets such as polyethylene, polypropylene, and PVC are impervious to roots, and are commercially marketed as root barriers. For example, the Henry Company markets various polypropylene root barrier sheets for "green roofs" and other horticultural applications. "Root Stop HD (Heavy Duty)" is a commercially available 27-mil thick HDPE root barrier distributed by Hydrotech, Inc., also designed for rooftop gardens.

Based upon this information, it will be assumed that roots reaching intact portions of the HDPE geomembrane will be unable to penetrate it. Such roots upon reaching intact portions of the HDPE geomembrane will instead turn and continue growth laterally along the top of the geomembrane in a down slope direction. Roots that reach the HDPE geomembrane will only be able to penetrate it in locations where holes in the geomembrane have already formed due to HDPE degradation. Such root penetration through existing holes within the HDPE geomembrane and subsequent penetration of the underlying GCL (see Section 7.7.7) will be considered as a FTF Closure Cap degradation mechanism for modeling purposes.

Very little information is available relative to the potential for geomembrane damage due to burrowing animals. A geomembrane would have to be harder than the burrowing animals' teeth or claws to avoid the potential for damage. Therefore geomembranes are potentially vulnerable to burrowing animals. Logically it is assumed that stronger, harder, and thicker geomembranes are more resistant to burrowing animals. (Koerner 1998) While burrowing animals can potentially damage unprotected HDPE geomembranes in general, damage of the FTF Closure Cap HDPE geomembrane is not considered a threat due to the presence of the overlying erosion barrier, which will be designed to preclude burrowing animals (see Table 12 and Section 4.4.9) from reaching the HDPE geomembrane. Therefore burrowing animals will not be considered as a FTF Closure Cap HDPE geomembrane degradation mechanism for modeling purposes.

7.6.7 Environment Agency Degradation Model

Based upon an extensive literature of HDPE geomembrane degradation mechanisms, Needham et al. (2004) has produced a long-term degradation HDPE geomembrane degradation model for use by the Environment Agency of England and Wales in the preparation of Performance Assessments (PA) for landfill. Needham et al. (2004) tie all degradation mechanisms to the generation of holes or cracks in the HDPE geomembrane through time. From this they have produced a six-stage model for generation of holes over time. They take generation of holes from initial installation of the geomembrane to long-term generation of holes as the geomembrane becomes increasingly more susceptible to brittle stress cracking. The following are the six stages considered by Needham et al. (2004):

- Stage 1 is the period of disposal facility construction and considers the holes produced by construction.
- Stage 2 is the operational period and considers the holes produced by waste placement.
- Stage 3 is a 10 to 50 year period immediately following closure cap construction during which no additional holes are assumed to be produced.
- Stage 4 is a combination of the antioxidant depletion and induction periods during which holes are assumed to be produced at low rates relative to subsequent stages due to tensile stresses.
- Stage 5 is the oxidation stage, which is assumed to last 50 years, during which embrittlement and further stress cracking will occur relatively rapidly due to any significant remaining tensile stress.
- Stage 6 is the terminal stage, during which it is assumed that the total number of holes present at the end of Stage 5 are reproduced as new holes every 100 years.

For each of the stages Needham et al. (2004) the generation of holes is divided into an excellent, good, and fair case with the number of holes produced increasing from the excellent to fair case. They also provide different hole sizes divided into the categories of pin holes, holes, tears, and cracks. The model produced by Needham et al. (2004) is based upon the most current research conducted concerning HDPE geomembrane degradation. They have converted that research into a form (i.e., generation of holes over time) that can be utilized in Performance Assessment (PA) contaminant transport modeling.

This model will be used for the consideration of antioxidant depletion (Section 7.6.2), thermal oxidation (Section 7.6.3), and tensile stress cracking (Section 7.6.5) as a FTF Closure Cap degradation mechanism for modeling purposes.

7.7 POTENTIAL GCL DEGRADATION MECHANISMS

A geosynthetic clay liner GCL consists of "bentonite sandwiched between two geotextiles" (USEPA 2001) or bentonite mixed with an adhesive and attached to a geomembrane (Bonaparte et al. 2002). Bentonite, the hydraulically functional portion of a GCL, is a mixture of minerals typically dominated by swelling-type montmorillonite clays, which is formed as the stable alteration product of volcanic ash (Worrall 1975). The bentonite used is generally sodium or calcium bentonite. Sodium bentonite is used more frequently because of its superior swelling capacity and lower initial permeability. Calcium bentonite has a smaller swelling capacity and a somewhat higher initial hydraulic conductivity (Witt and Siegmund 2001). The following is the definition of a Geotextile GCL as defined by the Environmental Protection Agency (USEPA 2001):

> A Geotextile GCL "is a relatively thin layer of processed" bentonite … "fixed between two sheets of geotextile. … A geotextile is a woven or nonwoven sheet material … resistant to penetration." … "Adhesives, stitchbonding, needlepunching, or a combination of the three" are used to affix the bentonite to the geotextile. "Although stitchbonding and needlepunching create small holes in the geotextile, these holes are sealed when the installed GCL's clay layer hydrates."

A GCL was first used in a landfill in 1986 (Bonaparte et al. 2002). Major advantages of GCLs over compacted clay liners (CCL) include an extremely low hydraulic conductivity (1 to 5E-09 cm/s), low infiltration rate, ability to withstand differential settlement and assimilate deformations, ability to self-heal after desiccation, resistance to the potentially damaging effects of freezing temperatures, relatively low cost, simple and quick construction, and its thinness (Benson 1999; Bonaparte et al. 2002; Witt and Siegmund 2001). GCLs, which have not been hydrated, are on the order of 0.2 inches thick, much thinner than the typical 2-foot CCL. Some primary potential disadvantages associated with GCLs relative to CCL are related to the thinness of GCLs. These include increased thinning due to excessive or unevenly applied pressure such as that resulting from overlying gravel intrusion (Chien et al. 2006), increased vulnerability to puncture from construction equipment, less capacity to adsorb and attenuate chemicals, and less resistance to chemical diffusion (Bonaparte et al. 2002). For the FTF Closure Cap these potential disadvantages relative to CCLs are mitigated by the following:

- The GCL will be only be overlain by six feet of material, therefore the total applied pressure will be relatively low. It will be immediately overlain (from bottom to top) by a 60-mil HDPE geomembrane (see Section 4.4.3), a geotextile fabric (see Section 4.4.4), and a sand drainage layer (see Section 4.4.5); all of which will tend to produce even application of the overburden pressure on the GCL. Therefore potential thinning due to excessive or unevenly applied pressure will be mitigated.
- The GCL will be overlain by a 60-mil HDPE geomembrane (see Section 4.4.3) and a geotextile fabric (see Section 4.4.4) which will provide GCL protection from puncture (see Section 4.4.2).
- As outlined in Section 7.0 the GCL will be located in the FTF Closure Cap above the waste tanks, ancillary equipment, and piping and is therefore not subject to chemical degradation from leachate associated with the waste tanks, ancillary equipment, and piping. Therefore the GCL is not designed to attenuate chemicals or provide resistance to chemical diffusion from any such leachate as it might be if it were located in a bottom liner.

These items will receive no further consideration as potential GCL degradation mechanisms based upon the above discussion.

As outlined Table 12 and Sections 4.4.2 and 4.4.3, a GCL will be utilized in conjunction with a HDPE geomembrane to form a composite hydraulic barrier to infiltration. As outlined in Table 34 the following potential degradation mechanisms will be considered for the GCL:

- Slope stability
- Freeze-thaw cycles
- Dissolution
- Divalent cations (Ca^{+2}, Mg^{+2}, etc.)
- Desiccation (wet-dry cycles)
- Biological (root penetration, burrowing animals)

7.7.1 Slope Stability

Hydrated sodium bentonite within GCLs has both low shear strength and bearing capacity. Fully hydrated sodium bentonite may have internal friction angles as low as 4 to 10° (Benson 1999; Bonaparte et al. 2002). GCLs can generally be safely placed on slopes of 10H:1V (5.7° or 10%) or flatter without the need for internal reinforcement or slope stability analysis (Bonaparte et al. 2002). Internally-reinforced GCLs can be safely placed on greater than 10% slopes. Bonaparte et al. (2002) report on slope stability monitoring of final cover system test plots that include internally-reinforced GCLs. The results demonstrate acceptable performance on 3H:1V (33%) slopes but not on 2H:1V (50%) slopes. The failures were due to inadequate interface strength and not inadequate internal shear strength, clearly indicating that proper characterization of GCL interface shear strength is an important design step.

As outlined in Section 4.4.2, the GCL will be placed at a 2% slope and it is not anticipated that the GCL would be placed on the side-slopes. This is well below the 10% to 33% slopes upon which GCLs can be safely placed. Therefore slope failure due to the GCL on a 2% will not be considered as a FTF Closure Cap degradation mechanism for modeling purposes.

7.7.2 Freeze-Thaw Cycles

Field studies indicate that GCLs are resistant to damage from freezing temperatures, are undamaged by freeze-thaw cycling, and do not need to be protected from frost (Benson 1999: Bonaparte et al. 2002). These studies "indicate that GCLs are not damaged by frost because the hydrated bentonite is soft, and readily consolidates around ice lenses and other defects during thawing" (Benson 1999).

DeGaetano and Wilks (2001) produced a map of extreme-value maximum soil freezing depths for the United States (see Figure 36). As seen in the figure most of South Carolina has a maximum frost depth of between 0 and 25 cm (0 and 10 inches). Interpolation to SRS yields a maximum frost depth of approximately 5 inches, which is well above the FTF Closure cap's GCL depth of burial (i.e., 6 feet) thereby precluding freeze-thaw cycles as a degradation mechanism. Therefore freeze-thaw will not be considered as a FTF Closure Cap GCL degradation mechanism for modeling purposes.
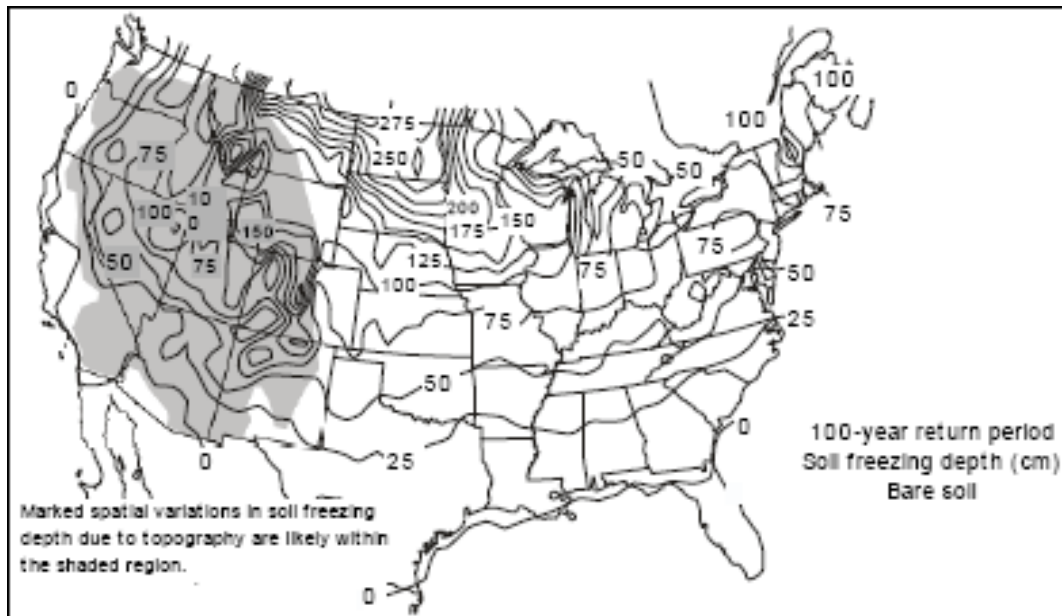
Figure 36.   United States Extreme-Value Maximum Soil Freezing Depth Map

7.7.3 Dissolution

Bentonite is a mixture of minerals typically dominated by montmorillonite clays, with sodium-bentonite dominated by sodium-montmorillonite. Thus, degradation of sodium - bentonite depends on how sodium-montmorillonite degrades. As with many clay minerals, sodium-montmorillonite has a variable formula. For the purposes of this discussion and selection of thermodynamic data the formula will be assumed to be:

$Na_{0.33}Mg_{0.33}Al_{1.67}Si_4O_{10}(OH)_2$,   where Na is the interlayer, easily exchangeable cation and Mg substitutes for Al in octahedral sheets.
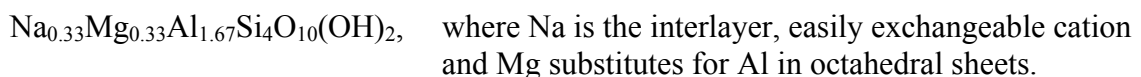
Sodium-montmorillonite dissolves incongruently. If it is assumed that all Na and Mg stays in solution, the dissolution reaction can be written as:

Sodium-montmorillonite + $0.99H^+$ + $0.175H_2O$ = $0.33Mg^{+2}$ + $0.33Na^+$ + 0.835 Kaolinite + 2.33 Quartz,
where kaolinite and quartz are the products.
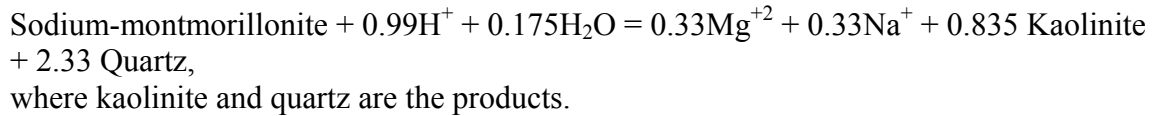
Based on a log K of 6.12 for this reaction (Bethke, 2005), 1.8×10^{-5} moles of sodium-montmorillonite would dissolve in 1 liter of relatively clean water under equilibrium conditions (i.e., assuming no kinetic limitations). For a bentonite quantity of 0.75 lbs/ft^2 and assuming the bentonite consists of 90% sodium-montmorillonite, 46,364 liters of water would have to pass through a square foot to dissolve all of the bentonite under equilibrium conditions. The infiltration rate through a soils only closure cap (i.e., configuration #6 of Table 24 without the composite hydraulic barrier, lateral drainage layer, and erosion control layer) of 16.45 in/yr) can be used to represent the infiltration rate at complete failure of the closure cap.

Assuming this complete closure cap failure infiltration rate of 16.45 in/yr, it would take approximately 1,200 years to completely convert the sodium-montmorillonite to kaolinite and quartz. Under slowly degrading closure cap conditions, it would take significantly longer for the conversion to occur. Additionally while montmorillonite can weather directly to kaolinite and quartz (Borchardt, 1977), it more commonly weathers through a series of predominately clay minerals. The low solubility of sodium-montmorillonite, the large volume of water and extended time required to convert it to kaolinite and quartz under equilibrium conditions, and the fact that it more commonly weathers through a series of clays suggest that sodium-bentonite dissolution is probably not its predominate degradation mechanism versus infiltration. Therefore dissolution of the bentonite in the GCL will not be considered as a major FTF Closure Cap degradation mechanism over a 10,000 year period and will therefore not be modeled.

7.7.4 Divalent Cations (Ca^{+2}, Mg^{+2}, etc.)

The bentonite used in GCLs is generally sodium or calcium bentonite. Sodium bentonite is used more frequently than calcium bentonite because of its superior swelling capacity and lower initial permeability (Witt and Siegmund 2001). However within closure caps, sodium bentonite GCLs that are not protected by an overlying geomembrane are susceptible to exchange of sodium with divalent cations such as calcium and magnesium particularly when calcium and magnesium rich soils overly the GCL (Benson 1999; Bonaparte et al. 2002; Egloffstein 2001). The conversion of hydrated sodium bentonite to calcium bentonite results in a decrease in the swell potential or potential volume of water bound to the mineral surface (i.e., immobile water) and a subsequent increase in the saturated hydraulic conductivity of the GCL particularly under conditions of low confining or overburden stress such as found in closure caps (Bonaparte et al. 2002; Egloffstein 2001; Jo et al. 2005).

The free swell index (ASTM 2006e) of sodium bentonite is typically greater than 24 ml/2 g (GSE 2006a), while that of calcium bentonite is on the order of 12 ml/2 g (CIMBAR 2001). Studies and case histories have shown that permeation of a sodium bentonite GCL with solutions containing a large fraction of divalent cations can cause the hydraulic conductivity of the GCL to increase 1 order of magnitude or more (Benson 1999; Jo et al. 2005).

One of the most comprehensive studies regarding the impact of divalent cation solutions on sodium bentonite GCLs has been conducted by Jo et al. (2005). Jo et al. (2005) permeated sodium bentonite GCL samples with deionized water, 100 mM sodium chloride (NaCl) and potassium chloride (KCl) solutions, and calcium chloride (CaCl$_2$) solutions ranging from 5 to 500 mM until further changes in saturated hydraulic conductivity were not detected (in some cases this took more than 2.5 years and up to 686 pore volumes). Table 48 presents a summary of the results from Jo et al. (2005). The following are the primary conclusions drawn by Jo et al. (2005):

- Permeation of the sodium bentonite GCL with DI water from a practical perspective resulted in essentially no change in the saturated hydraulic conductivity of approximately 3.0E-09 cm/s (see Table 48).
- Permeation of the sodium bentonite GCL with either NaCl or KCl solutions from a practical perspective resulted in essentially no change in the saturated hydraulic conductivity (i.e., within a factor of 2 of those obtained using DI water) even though Na and K have different hydrated radii.
- Permeation of the sodium bentonite GCL with weak divalent solutions (i.e., CaCl$_2$ ≤ 20 mM), resulted in an initially low saturated hydraulic conductivity (~2.0E−09 cm/s), which did not change for some time. Subsequently, the saturated hydraulic conductivity gradually increased by approximately one order of magnitude (~2.0E−08 cm/s). Measurements of the exchange complex after testing showed that exchange of Ca^{+2} for Na^{+} was essentially complete regardless of which weak divalent solution was used.
- Permeation of the sodium bentonite GCL with strong divalent solutions (CaCl$_2$ ≥ 50 mM) resulted in an almost immediate (<1 day) increase in saturated hydraulic conductivity of approximately 3 orders of magnitude (~1.0E−06 cm/s) than that of GCLs permeated with DI water. The high Ca^{+2} concentration resulted in rapid Na^{+} exchange and saturated hydraulic conductivity increase.
- CaCl$_2$ solutions should be representative of the behavior of sodium bentonite GCLs to solutions containing divalent cations in general.

Table 48. GCL Average Saturated Hydraulic Conductivity from Jo et al. (2005)

Permeant	DI Water		5 to 20 mM CaCl$_2$ [1]		50 to 500 mM CaCl$_2$ [2]	
Period	Initial	Final	Initial	Final	Initial	Final
K$_{sat}$ (cm/s)	2.1E-09	3.0E-09	2.3E-09	1.8E-08	1.2E-06	1.3E-06
K$_{sat}$ / Initial DI Water K$_{sat}$	1	1.4	1.1	8.6	571	619

Source: Jo et al. (2005) Table 2
Samples were under either an effective stress of 2.3 or 3.4 psi
[1] 209 to 848 mg/L Ca^{+2}
[2] 1,985 to 19,400 mg/L Ca^{+2}

Based upon the above literature concerning the impact of the exchangeable cations on the saturated hydraulic conductivity of sodium bentonite, geochemical simulations using Geochemist's Workbench® (Bethke, 2005) have been performed to evaluate the potential changes to the sodium bentonite from likely SRS permeants. The following two potential SRS permeants were modeled: 1) rainwater equilibrated with SRS soil; 2) rainwater equilibrated with portlandite (Ca(OH)$_2$).

The composition of rainwater equilibrated with SRS soil used in the simulation was taken as that of uncontaminated SRS background monitoring well (P27D) in the vicinity of the General Separations Area (Strom and Kaback, 1992). The well is screened in the water table aquifer and is assumed to be an approximation of rainwater equilibrated with SRS soil. The composition of rainwater equilibrated with portlandite (Ca(OH)$_2$) is an approximation of the composition of infiltration passing through typical CLSM containing portland cement.

The compositions of the two waters used in the simulations are shown in Table 49. Reaction of the infiltrating water with an initial 306 grams of sodium-montmorillonite was simulated. This is the estimated mass in a sodium-bentonite composed of 90 wt% sodium-montmorillonite and incorporated into the GCL at 0.75 lbs/ft^2. Thus, the simulations are for liters of infiltrating water that pass through this hypothetical square foot of GCL. Figure 37 shows the geochemical simulation of sodium-montmorillonite degradation with infiltrating water representing rainwater equilibrated with SRS soil. Figure 38 shows the geochemical simulation of sodium-montmorillonite degradation with infiltrating water representing rainwater equilibrated with a typical CLSM (i.e., portlandite (Ca(OH)$_2$))

Table 49. Chemical Compositions of Infiltrating Water used for Sodium-Montmorillonite Degradation Geochemical Simulations

Constituent	P27D Groundwater	Water Equilibrated with Portlandite
pH	5.4	12.3
Ca	2.5 mg/L	641 mg/L
Mg	0.4 mg/L	99.6 mg/L
Na	1.0 mg/L	1.0 mg/L
Cl	3.3 mg/L	3.3 mg/L
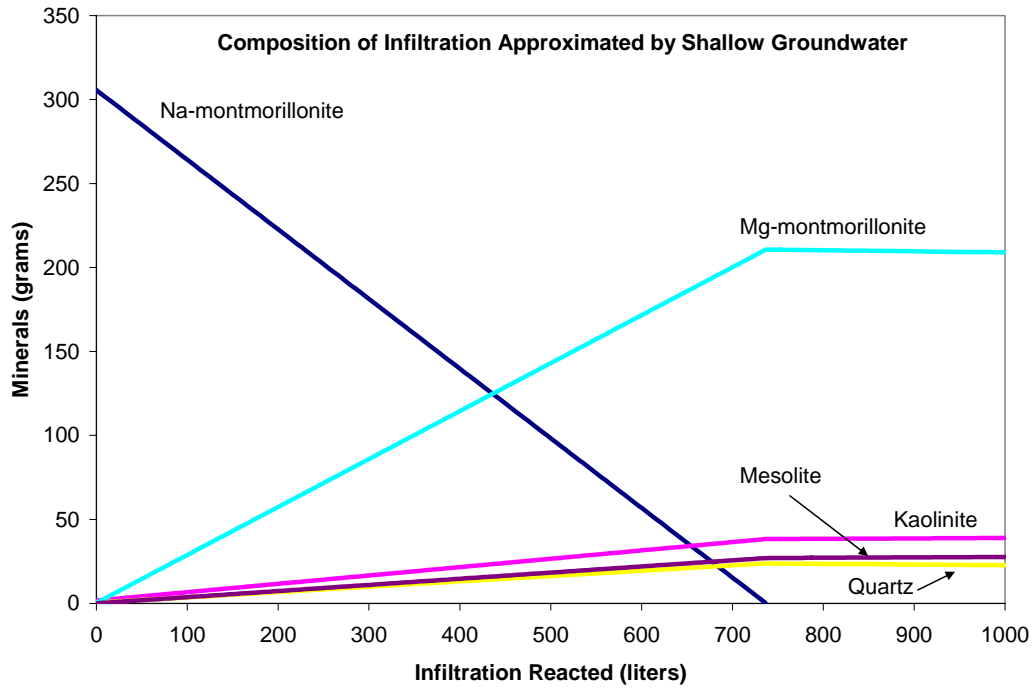
Figure 37. **Geochemical Simulation of the Alteration of Sodium-Montmorillonite by Infiltrating Water Equilibrated with SRS Soil**
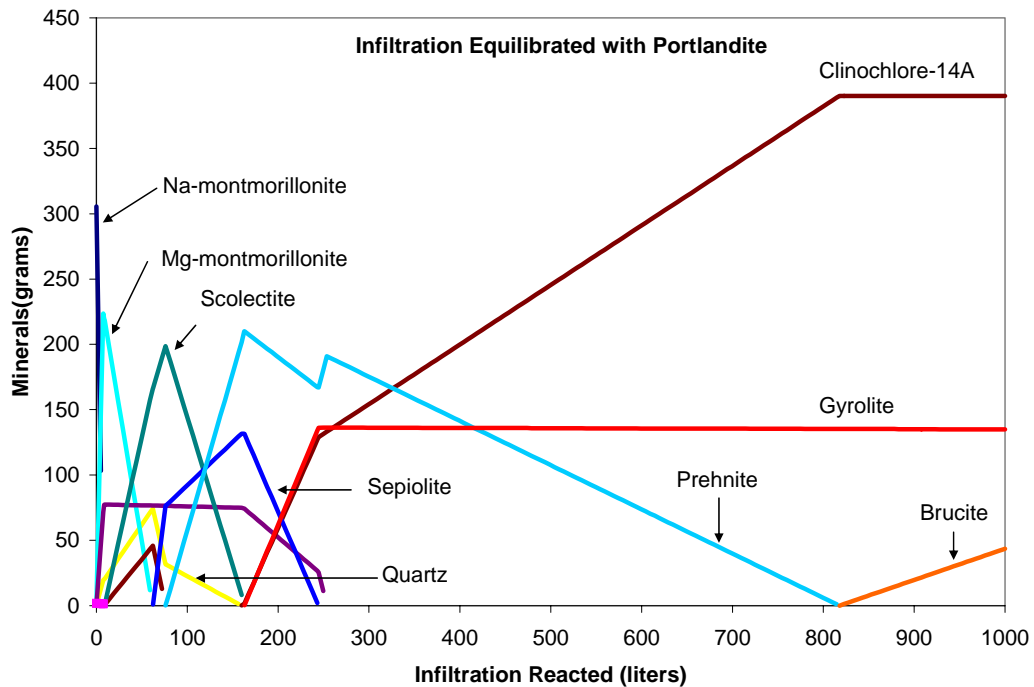
Figure 38. **Geochemical Simulation of the Alteration of Sodium-Montmorillonite by Infiltrating Water Equilibrated with Typical CLSM**

For infiltration equilibrated with SRS soil, sodium-montmorillonite completely degrades to magnesium-montmorillonite after passage of about 740 liters of water through a square foot containing 0.75 lbs of bentonite. Between 740 and 1000 liters the assemblage of minerals replacing sodium-montmorillonite is magnesium-montmorillonite, kaolinite, mesolite (a calcium zeolite), and quartz.

Infiltration equilibrated with portlandite has a much higher pH and concentrations of Ca and Mg (for these simulations the Mg/Ca ratio was assumed to be the same in both waters). This causes much quicker and more complicated degradation of sodium-montmorillonite. The sodium-montmorillonite is initially converted to magnesium-montmorillonite after fewer than 5 liters of infiltration have passed. This is followed by alteration of the magnesium-montmorillonite to various clays, zeolites, and other minerals. At 1000 liters of infiltration the mineral assemblage is clinochlore-14A (a chlorite clay), gyrolite (a Ca silicate), and brucite ($Mg(OH)_2$).

The different mechanisms and environments of degradation result in very different rates of sodium-montmorillonite removal. The fastest rate is when infiltration has equilibrated with portlandite. In none of these cases is the mineral layer in the GCL completely removed, rather it is altered to different minerals.

Some information on long-term degradation rates of bentonite has been garnered from study of bentonites in their natural settings. Ohe et al. (1998) concluded that the alteration rate of a Japanese sodium-bentonite to calcium-magnesium-bentonite for a layer below the water table was about 1 cm/1000 years. Based on study of another Japanese bentonite, Kamei et al. (2005) concluded that if this material was used in a geologic storage system complete conversion to illite would require greater than 10,000 years. While these studies do not allow a prediction of the life-time of a GCL in the closure cap, they do suggest the processes of bentonite degradation are slow.

Based upon this discussion, it will be assumed that if a sodium bentonite GCL with a saturated hydraulic conductivity of 5.0E-09 cm/s (see Section 5.4.6) is utilized, it will be eventually converted to a calcium or magnesium bentonite with a saturated hydraulic conductivity one order of magnitude lower (i.e. 5.0E-08 cm/s). Additionally if it is determined that a sodium bentonite GCL will be utilized, selection of the material utilized to fill the voids in the erosion barrier stone will consider its impact upon the sodium bentonite GCL. In particular materials such as CLSM, which typically contain cement with significant calcium content, would likely not be utilized.

Use of a calcium bentonite GCL or bagged calcium bentonite as a substitute for a sodium bentonite GCL will be evaluated. If calcium bentonite is utilized a saturated hydraulic conductivity of 5.0E-08 cm/s will also be assigned to this layer at this time pending further investigation. This is considered conservative relative to the information provided in Section 7.7.5 concerning the saturated hydraulic conductivity of 4.0E-09 cm/s determined for a 45 year old calcium bentonite field installation at SRS (Serrato 2007). Therefore degradation of the bentonite GCL by cation exchange will be considered as a FTF Closure Cap degradation mechanism for modeling purposes, with the assignment of a degraded saturated hydraulic conductivity of 5.0E-08 cm/s whether sodium or calcium bentonite is utilized for the GCL.

Since it is currently difficult to assign timing to conversion of sodium bentonite to calcium or magnesium bentonite, it will be assumed that during the 100-year institutional period that the GCL has a saturated hydraulic conductivity of 5.0E-09 cm/s and thereafter it has a saturated hydraulic conductivity of 5.0E-08 cm/s for modeling purposes.

7.7.5 Desiccation (wet-dry cycles)

One often reported advantage of GCLs over compacted clay liners (CCL) is the ability of GCLs to self-heal after desiccation (Boardman and Daniel 1996; Carson 2001; Egloffstein 2001; Witt and Siegmund 2001). However the following must be taken into consideration in relation to the potential desiccation self-healing properties of GCLs:

- After desiccation and subsequent cracking of a GCL, it can take a significant period of time (i.e., potentially days) upon rewetting to seal the cracks and re-achieve the initially low saturated hydraulic conductivity. This delay in crack sealing can allow preferential saturated flow through the cracks rather than through the GCL matrix during the resealing period (Bonaparte et al. 2002; Witt and Siegmund 2001).
- The alteration of sodium-bentonite to calcium-magnesium-bentonite can potentially reduce the swell potential of the bentonite to such an extent that cracks formed during desiccation can not completely swell shut upon rewetting thus increasing the saturated hydraulic conductivity of the GCL by several orders of magnitude (Benson 1999; Chien et al. 2006; Egloffstein 2001; Lin and Benson 2000; Witt and Siegmund 2001).

The following can preclude or reduce the impact of GCL desiccation and desiccation combined with the alteration of sodium-bentonite to calcium-magnesium-bentonite on the saturated hydraulic conductivity of the GCL and potential infiltration:

- A sufficient thickness of soil overlying the GCL can be provided to prevent desiccation and maintain constant water content. The thicker the overlying soil, the less likely desiccation cracks will form within the GCL. There is little danger of desiccation at all for GCLs overlain by 6 feet or more of soil and located in humid environments with a relatively uniform annual precipitation. (Egloffstein 2001; Witt and Siegmund 2001)
- The GCL can be overlain by both a geomembrane and a minimum of several feet of soil to prevent desiccation, maintain constant water content, and preclude or reduce the rate of alteration of sodium-bentonite to calcium-magnesium-bentonite (Benson 1999; GSE 2006b; Lin and Benson, 2000). Benson 1999 takes this further by stating that "GCLs should not be used without being overlain by a geomembrane."
- The soil overlying the GCL should not contain an abnormally high concentration of soluble salts containing divalent cations such as Ca^{+2} or Mg^{+2} (GSE 2006b; Jo et al. 2005).
- Calcium bentonite can be used rather than sodium bentonite. While calcium bentonite has a smaller swelling capacity and a somewhat higher initial hydraulic conductivity, it more resistance to degradation due to exchange with external cations and therefore will maintain its self-healing capacity and a more constant saturated hydraulic conductivity (Egloffstein 2001; Witt and Siegmund 2001).

Hawkins (1962) reports on a series of laboratory to field scale tests to investigate the use of bentonite at SRS to limit soil moisture movement into buried radioactive waste. The bentonite utilized was a southeastern calcium bentonite (American Colloid Company Panther Creek bentonite (Serrato 2006)). The tests included an evaluation of the impact of desiccation on the bentonite. Hawkins (1962) reported the following concerning the tests conducted at SRS:

- A laboratory saturated hydraulic conductivity of 3.0E-08 cm/s was determined for the bentonite.
- A laboratory test was conducted where dry bentonite was placed between two 4-inch layers of clayey sand, the bentonite was hydrated, the system was allowed to dry under atmospheric conditions for three weeks, and then the system was rewetted. During the drying phase cracks completely penetrating the bentonite developed which were rapidly (<1 hour) resealed upon rewetting. It was estimated that approximately 5% of the rewetting water past through the cracked bentonite before it resealed.
- Lysimeter testing in the field was conducted from November 1960 through March 1962, during which a 3-month drought occurred in the fall of 1961. The lysimeters consisted of bentonite layers overlain by 1 or 2 feet of soil in addition to soils only lysimeters. A total rainfall of 74.71 inches was recorded during this period. No percolation occurred through any of the lysimeters with bentonite, whereas an average of 27.51 inches of percolation was recorded through the soils-only lysimeters. Noticeable settling of the surface soil of the lysimeters containing bentonite overlain by 1-foot of soil was observed after the 3-month drought; this was not observed in the lysimeters containing bentonite overlain by 2-foot of soil. It was concluded that cracking of the bentonite overlain by only 1-foot of soil resulted in the settling; however the bentonite subsequently resealed upon rewetting.
- Based upon the previous testing, a 50-foot by 50-foot field test area (Test Facility – Bentonite Unbrella Test (TFBUT)) was completed in November 1961 that consisted of 3 to 4 inches of dry calcium bentonite (Serrato 2006) overlain by 2-feet of soil. Active maintenance of the field test site to maintain natural grasses and prevent the establishment of trees was conducted until 1989. Since 1989 no active maintenance of the area has been conducted.

In 2006 (45 years after installation) a Shelby tube sample of the bentonite within TFBUT was taken and the saturated hydraulic conductivity of the bentonite layer was determined to be 4.0E-09 cm/s (Serrato 2007). This is a lower saturated hydraulic conductivity than that determined by Hawkins (1962); indicating that no degradation of the bentonite in relation to the saturated hydraulic conductivity of the matrix is evident after 45 years.

As outlined in Table 11, the FTF Closure Cap GCL will be overlain by a 60-mil HDPE geomembrane (see Section 7.7.6 below for information on the benefits of composite hydraulic barriers) and 6-feet of soil materials. This conforms to the requirements laid out by Benson (1999), Egloffstein (2001), GSE (2006b), Lin and Benson (2000), and Witt and Siegmund (2001) for closure cap systems that preclude desiccation damage of the GCL.

Additionally as outlined in Section 7.7.4 if it is determined that a sodium bentonite GCL will be utilized, selection of the material utilized to fill the voids in the erosion barrier stone will consider its impact upon the sodium bentonite GCL. In particular materials such as CLSM, which typically contain cement with significant calcium content, would likely not be utilized. Use of a calcium bentonite GCL or bagged calcium bentonite as a substitute for a sodium bentonite GCL will also be evaluated. Therefore GCL desiccation damage will not be considered as a FTF Closure Cap degradation mechanism for modeling purposes.

7.7.6 Composite Hydraulic Barriers versus Divalent Cations and Desiccation

Composite hydraulic barriers typically consist of a geosynthetic clay liner (GCL) or compacted clay liner (CCL) overlain by a geomembrane. The use of a GCL or CCL as the sole hydraulic barrier results in infiltration through the barrier over its entire surface area when subjected to a positive hydraulic head. Additionally experience has shown that closure caps that rely solely on GCLs and particularly CCLs as the hydraulic barrier are prone to failure, whereas composite barriers appear to function extremely well. The use of a geomembrane as the sole hydraulic barrier placed over a permeable soil results in flow through any geomembrane holes that "can approach the rate of flow through a similarly-sized orifice".

Whereas, since geomembranes are nearly impervious, the use of a composite hydraulic barrier results in percolation essentially only occurring at the location of geomembrane holes, where such leakage is subsequently impeded by the presence of the GCL or CCL (i.e., flow will be much slower than flow through an orifice). In particular, experimentation has shown that when water migrates through a geomembrane hole in a geomembrane/GCL composite that interface flow between the geomembrane and GCL is of only minor consequence, while it may be more important with a geomembrane/CCL composite. While GCLs, CCLs, or geomembranes can be used as a sole hydraulic barrier, the combination of components in a composite hydraulic barrier has proven (both theoretically and through field performance) to be most effective in terms of minimizing percolation (i.e. infiltration) through the barrier. (Benson 1999; Bonaparte et al. 2002; Chien et al. 2006)

Benson 1999 reported on several field studies that evaluated the performance of geomembrane/CCL composite hydraulic barriers in closure cap situations and made the following observations:

* At a site in Hamburg, Germany a closure cap profile consisting of from top to bottom a 2-foot vegetative soil layer, a 1-foot sand drainage layer, and a composite hydraulic barrier consisting of a 60-mil HDPE geomembrane overlying a 2-foot compacted clay liner (CCL) was tested. Percolation through this closure cap with a composite hydraulic barrier leveled off between 0.08 and 0.12 in/yr. This percolation was nearly two orders of magnitude less than percolation through a closure cap profile with a CCL as the sole hydraulic barrier at the same location (~ 8 in/yr). "Test pits excavated in the composite cover test sections showed that the geomembrane prevented desiccation cracking of the clay. The compacted clay beneath the geomembrane was moist, pliable, and homogeneous even after the cover had been exposed to drought." (Benson 1999)

- 161 -

- At the Kettleman Hills hazardous waste landfill in southern California (semi-arid climate) a closure cap profile consisting of from top to bottom a 2-foot vegetative soil layer and a composite hydraulic barrier consisting of a 60-mil HDPE geomembrane overlying a 3-foot compacted clay liner (CCL) constructed with highly plastic clay was evaluated. "After six months of exposure to ambient conditions, test pits were excavated to examine the condition of the clay in each test pad. The compacted clay barrier in the composite cover was devoid of cracks. The clay was moist, soft, and pliable as if it had just been placed." (Benson 1999)
- At a site in Steamboat Springs, Colorado test pits were dug three years after construction into a closure cap profile with a composite hydraulic barrier. The compacted clay in the composite cover was still moist and un-cracked. (Benson 1999)

Based upon concerns with the potential impacts of divalent cation exchange and desiccation on sodium bentonite GCLs and the favorable field experience of CCLs overlain with geomembranes, Benson (1999) concludes that "GCLs should not be used without being overlain by a geomembrane."

As outlined in Sections 4.4.2, 4.4.3, and 7.7.5, the FTF Closure Cap includes a composite hydraulic barrier consisting of a GCL overlain by a HDPE geomembrane, both beneath 6-feet of soil materials. This conforms to the best practices to limit divalent cation and desiccation damage to the GCL.

7.7.7 Biological (root penetration, burrowing animals)

Plant roots can freely penetrate unprotected GCLs and results in increases in the hydraulic conductivity of the GCL (Bonaparte et al. 2002; Carson 2001; Witt and Siegmund 2001). Since plant roots can freely penetrate GCLs but not HDPE geomembranes except in locations of existing holes within the HDPE geomembrane (see Section 7.6.6), root penetration of the GCL in locations of existing holes within the HDPE geomembrane will be considered as a FTF Closure Cap degradation mechanism for future modeling purposes.

While burrowing animals can potentially damage unprotected GCLs in general, damage of the FTF Closure Cap GCL is not considered a threat due to the presence of the overlying erosion barrier, which will be designed to preclude burrowing animals (see Table 12 and Section 4.4.9) from reaching the GCL. Therefore burrowing animals will not be considered as a FTF Closure Cap GCL degradation mechanism for modeling purposes.

7.8 FTF CLOSURE CAP DEGRADATION MECHANISM SUMMARY

A summary of the applicability of the potential degradation mechanisms from Table 34 to the FTF closure cap is provided in Table 50. Table 50 lists the potential degradation mechanisms per closure cap layer, provides the section which discusses the potential degradation mechanism and its applicability to the FTF Closure Cap, and provides a summary statement concerning its applicability. The summary statement of each potential degradation mechanism's applicability lists the mechanisms in one or more of the following categories:

- **Not applicable**: for the reason(s) provided the potential degradation mechanism has been deemed not applicable to the FTF Closure Cap. Therefore it will not be considered a FTF Closure Cap degradation mechanism for modeling purposes.
- **Not significant**: for the reason(s) provided the potential degradation mechanism has been deemed not a significant degradation mechanism for the FTF Closure Cap. Therefore it will not be considered a FTF Closure Cap degradation mechanism for modeling purposes.
- **Incorporate in system design**: for the potential degradation mechanism sufficient design measures exist and will be taken as necessary to preclude that mechanism from being a FTF Closure Cap degradation mechanism. Therefore it will not be considered a FTF Closure Cap degradation mechanism for modeling purposes.
- **Applicable**: this potential degradation mechanism is considered a significant FTF Closure Cap degradation mechanism that will be taken into account during modeling.

Table 51 provides a listing of open issues related to the FTF Closure Cap concept particularly in regard to potential degradation mechanisms.

Table 50. FTF Closure Cap Degradation Mechanism Summary

Affected Layer	Potential Degradation Mechanism	Section	Summary of the Applicability to the FTF Closure Cap
All	Static loading induced settlement	7.1	**Not significant**: Settlement due static loading is anticipated to be on the order of 2 to 3 inches and expected to occur uniformly over the entire area of the cap. Differential settlement, from which degradation could result, is anticipated to be negligible.
	Seismic induced liquefaction and subsequent settlement	7.1	**Not significant**: Settlement due seismic loading and resulting liquefaction is anticipated to be on the order of a few inches and expected to occur uniformly over the entire area of the cap. Differential settlement, from which degradation could result, is anticipated to be negligible.
	Seismic induced slope instability	7.1	**Incorporate in system design**: The side-slopes will be designed for seismic stability.
	Seismic induced lateral spread	7.1	**Not applicable**: Conditions at SRS are not conducive to lateral spreading.
	Seismic induced direct rupture due to faulting	7.1	**Not applicable**: Surface faulting is non-existent in the Southeast United States.
	Waste Layer Subsidence	7.1	**Not applicable**: Waste Layer subsidence is not considered applicable to the closure cap, since the waste tanks and subsurface items containing significant void space will be filled with grout.
Vegetative cover	Succession	7.2	**Applicable**: Vegetation succession from a bahia grass field to a pine forest will be considered a closure cap degradation mechanism, resulting in deep pine tree roots penetrating various closure cap layers resulting in degradation particularly of the composite hydraulic barrier.
	Stressors (droughts, disease, fire, and biological)	7.2	**Not significant**: Vegetative stressors (droughts, disease, fire, and biological) primarily impact the closure cap in terms of the rate of succession rather than as any long term degradation mechanism on their own.

Table 50. FTF Closure Cap Degradation Mechanism Summary - continued

Affected Layer	Potential Degradation Mechanism	Section	Applicability to the FTF Closure Cap
Soil above the erosion barrier	Erosion	7.3.1	**Applicable**: Erosion of the soil layers above the erosion barrier will be considered a closure cap degradation mechanism.
	Desiccation (wet-dry cycles)	7.3.2	**Not significant**: Significant cracking of SRS topsoil and backfill upon drying is highly unlikely since the soils consist predominately of quartz sand, the clay content is predominately kaolinite, SRS soils are highly leached, and the backfill is compacted.
Erosion barrier	Weathering (Dissolution)	7.4.1	**Incorporate in system design**: The erosion barrier stone size will be designed considering the applicable weathering rate over 10,000 years. materials used to infill the stone voids will be selected such that it has either no impact upon weathering or preferably tends to decrease the weathering rate of the stone.
	Biological: – Root penetration – Burrowing animals	7.4.2	**Applicable**: It is assumed that deep pine tree roots will penetrate the erosion barrier. **Incorporate in system design**: The erosion barrier will be designed to act as a barrier to burrowing animals.
	Chemical (waste leachate)	7.0	**Not applicable**: Chemical degradation of the erosion barrier from leachate associated with the waste tanks, ancillary equipment, and piping is not considered applicable, since the erosion barrier will be located above the waste tanks, ancillary equipment, and piping.
Lateral drainage layer	Silting-in	7.5.1	**Applicable**: It will be assumed that the lateral drainage layer silts up over time with colloidal clay that migrates from the overlying middle backfill.
	Biological (root penetration)	7.5.2	**Applicable**: It is assumed that deep pine tree roots will penetrate into the lateral drainage layer and act as an impermeable volume until they decay.

Table 50. FTF Closure Cap Degradation Mechanism Summary - continued

Affected Layer	Potential Degradation Mechanism	Section	Applicability to the FTF Closure Cap
HDPE geomembrane	Ultraviolet (UV) radiation	7.6.1	**Incorporate in system design**: The HDPE geomembrane will contain carbon black which acts as a UV stabilizer and HDPE geomembrane exposure to sunlight during closure cap construction will be limited in duration.
	Antioxidant depletion	7.6.2	**Applicable**: Antioxidant depletion of the HDPE geomembrane will occur through oxidation of the antioxidants and diffusion out of the geomembrane.
	Thermal oxidation	7.6.3	**Applicable**: Thermal oxidation of the HDPE geomembrane will occur after depletion of the antioxidants and it is assumed in conjunction with tensile stress cracking will cause degradation of the geomembrane.
	High energy irradiation	7.6.4	**Not significant**: high energy irradiation of the FTF Closure Cap HDPE geomembrane is considered an insignificant degradation mechanism
	Tensile stress cracking	7.6.5	**Applicable**: It is assumed that tensile stress cracking of the HDPE geomembrane will occur in conjunction with thermal oxidation.
	Biological: – Microbial – Root penetration – Burrowing animals	7.6.6	**Not significant**: The high-molecular-weight polymers used for geomembranes seem insensitive to microbial biodegradation **Applicable**: Intact HDPE geomembranes preclude root penetration and cause the roots to follow laterally atop the geomembrane surface; however it will be assumed that roots can penetrate the geomembrane in locations where holes have already formed due to other degradation mechanisms. **Incorporate in system design**: The overlying erosion barrier will be designed to act as a barrier to burrowing animals and preclude their reaching the HDPE geomembrane.
	Chemical (waste leachate)	7.0	**Not applicable**: Chemical degradation of the HDPE geomembrane from leachate associated with the waste tanks, ancillary equipment, and piping is not considered applicable, since the HDPE geomembrane will be located above the waste tanks, ancillary equipment, and piping.

Table 50. FTF Closure Cap Degradation Mechanism Summary - continued

Affected Layer	Potential Degradation Mechanism	Section	Applicability to the FTF Closure Cap
GCL	Slope stability	7.7.1	**Incorporate in system design**: The GCL will be placed at a 2% slope and it is not anticipated that the GCL would be placed on the side-slopes. This is well below the 10% to 33% slopes upon which GCLs can be safely placed.
	Freeze-thaw cycles	7.7.2	**Incorporate in system design**: GCLs are resistant to damage from freeze-thaw cycling and the closure cap GCL will be well below the SRS maximum frost depth of approximately 5 inches.
	Dissolution	7.7.3	**Not significant**: Sodium-montmorillonite has a low solubility and a large volume of water and extended time are required to weather it through a series of clays.
	Divalent cations (Ca^{+2}, Mg^{+2}, etc.)	7.7.4	**Applicable**: It will be assumed that sodium bentonite is converted to calcium-magnesium-bentonite, resulting in an order of magnitude increase in saturated hydraulic conductivity
	Desiccation (wet-dry cycles)	7.7.5	**Incorporate in system design**: The GCL will be located beneath a 60-mil HDPE geomembrane and 6-feet of soil materials in order to preclude desiccation damage. Additionally the material utilized to fill the stone voids of the erosion barrier will be selected so that it does not negatively impact the underlying GCL.
	Biological: – Root penetration – Burrowing animals	7.7.7	**Applicable**: The GCL will be overlain by a HDPE geomembrane. Intact HDPE geomembranes preclude root penetration; however it will be assumed that roots can penetrate the GCL in locations where holes have already formed in the HDPE geomembrane due to other degradation mechanisms. **Incorporate in system design**: The overlying erosion barrier will be designed to act as a barrier to burrowing animals and preclude their reaching the GCL.
	Chemical (waste leachate)	7.0	**Not applicable**: Chemical degradation of the GCL from leachate associated with the waste tanks, ancillary equipment, and piping is not considered applicable, since the GCL will be located above the waste tanks, ancillary equipment, and piping.

Table 51. FTF Closure Cap Concept Open Design Issues Not Affecting Modeling

Issue #	Section(s)	Open Design Issues
1	2.0 4.4.12 7.2	Is bamboo a climax species that prevents or greatly slows the intrusion of pine trees?
2	4.4.1 5.4.7	What are the requirements for the foundation layer particularly in terms of its ability to drain water away from and around the tanks and ancillary equipment?
3	4.4.9 4.4.13 4.4.14 5.4.3 7.4.1	What is the estimated weathering rate of the erosion barrier, toe of side slopes, and side slopes stone (assumed granite) based upon natural or archaeological analogs and available literature?
4	4.4.9 5.4.3 7.4.1 7.4.4 Appendix F	What material should be used to fill the stone voids of the erosion barrier to prevent loss of overlying material into the erosion barrier?
5	4.1 7.1	How will the 241-97F Cooling Water Basin and 281-8F Basin be closed? Closure of these basins can influence the surface drainage from the FTF Closure Cap and the design of the side-slope relative to seismic considerations.
6	7.7.4 7.7.5	Should a sodium bentonite or calcium bentonite GCL be utilized?
7	4.4	The definition of a significant void requiring grouting in order to eliminate subsidence needs to be determined.
8	4.1	Is the 50-foot extension of the closure cap beyond the sides of the tanks sufficient to prevent infiltration at the side-slopes, the perimeter drainage system, or the natural surrounding land surface from impacting contaminant transport out of the tanks?
9	4.3 4.4.5 4.4.14	The final design must allow the free transport of water out of the lateral drainage layer into the side-slope rip rap, while at the same time preventing sand movement from the lateral drainage layer into the side-slope rip rap.
10	4.4.3 7.6 8.5	The final design will considered the practicality and benefit of conducting an electrical leak detection survey of the HDPE geomembrane as an additional QA/QC measure.

8.0 FTF CLOSURE CAP DEGRADATION AND INFILTRATION MODELING

As outlined in Section 6.0, FTF Closure Cap configuration #1a will be utilized for the purposes of modeling infiltration over time. FTF Closure Cap configuration #1a is described in Table 11, Table 12, and Table 24 and Figure 11. Potential FTF Closure Cap degradation mechanisms are discussed in detail in Section 7.0. Section 7.0 culminates with Table 50, which lists all the degradation mechanisms evaluated and provides an evaluation of the applicability and significance of each degradation mechanism to the FTF Closure Cap.

Based upon the Section 7.0 evaluation of degradation mechanisms, the degradation mechanisms and affected closure cap layers selected for modeling along with a brief description of the method of modeling are provided in Table 52. The following sections (Sections 8.1 through 8.7) discuss the application of degradation mechanisms in more detail and the development of HELP model inputs based upon the impact of the degradation mechanisms on the various closure cap layers. Root penetration of the erosion barrier receives no further discussion than that provided in previous Section 7.4.2 and Table 52. Root penetration of the HDPE geomembrane and underlying GCL have been considered together as together they form a composite hydraulic barrier. Appendix I provides the associated FTF Closure Cap degraded property value calculations. Based upon the development of generally conservative degraded HELP model inputs, an estimate of FTF Closure Cap Infiltration over 10,000 years has been made.

Table 52. FTF Closure Cap Degradation Mechanisms Applicable to Infiltration Modeling

Affected Layer	Applicable Degradation Mechanism	Method of Modeling
Vegetative cover	Succession	Vegetation succession from a bahia grass field to a pine forest will be assumed to begin at the end of the 100-year institutional control period as outlined in Section 7.2
Soil above the erosion barrier	Erosion	Erosion of the soil layers above the erosion barrier will be assumed to begin immediately following closure cap construction as outlined in Section 7.3.1
Erosion barrier	Root penetration	Pine tree roots will be assumed to freely penetrate the erosion barrier consistent with the rate of root production as outlined in Section 7.2, however such penetration will be assumed to have no impact on the hydraulic properties of the erosion barrier as outlined in Section 7.4.2
Lateral drainage layer	Silting-in	Upon closure cap construction accumulation of colloidal clay, which migrates from the middle backfill into the underlying lateral drainage layer, will be assumed to begin and reduce the saturated hydraulic conductivity of the drainage layer over time as outlined in Section 7.5.1
	Root penetration	Pine tree roots will be assumed to freely penetrate the erosion barrier consistent with the rate of root production as outlined in Section 7.2 and to reduce the saturated hydraulic conductivity of the layer as outlined in Section 7.5.2
High density polyethylene (HDPE) geomembrane	Antioxidant depletion, thermal oxidation, & tensile stress cracking	The Mueller and Jakob (2003) methodology (see Section 7.6.2.3) for antioxidant depletion and the Needham et al. (2004) methodology (see Section 7.6.7) for combining these degradation mechanisms into hole generation over time will be utilized
	Root penetration	It will be assumed that every HDPE geomembrane hole generated over time is penetrated by a root that subsequently penetrates the GCL, once significant roots are available to penetrate
Geosynthetic clay liner (GCL)	Divalent cations (Ca^{+2}, Mg^{+2}, etc.)	It will be assumed that the GCL consists of sodium bentonite with a saturated hydraulic conductivity of 5.0E-09 cm/s during the 100-year institutional control period and that it consists of calcium bentonite with a conductivity of 5.0E-08 cm/s thereafter
	Root penetration	It will be assumed that every HDPE geomembrane hole generated over time is penetrated by a root that subsequently penetrates the GCL, once significant roots are available to penetrate

8.1 PINE TREE SUCCESSION OF THE VEGETATIVE COVER

As outlined in Section 7.2 and Table 52 vegetation succession from a bahia grass field to a pine forest is assumed to be a degradation mechanism that is both applicable and significant to degradation of the FTF Closure Cap. The following assumptions associated with pine tree succession discussed in Section 7.2 affect the timing of pine tree succession on the FTF Closure Cap:

- A 100-year institutional control period begins after closure cap installation during which the initial bahia grass vegetative cover is maintained and pine trees are excluded.
- 160 years after the end of institutional control it is assumed that the establishment of pine seedlings on top of the closure cap will begin.
- It will take approximately 30 years for the tap roots to reach a 6-foot depth and the remainder of the tree's life (i.e., 70 years) for the root to go its full depth.
- It will take approximately 3 cycles of pine seedling to mature pine trees (i.e., approximately 40 years each cycle) to establish mature pine over the entire cap
- 280 years after the end of institutional control it is assumed that the entire cap is dominated by mature loblolly pine.
- Complete turnover of the 400 mature trees per acre occurs every 100 years (i.e., 400 mature trees per acre die every 100 years in a staggered manner).

The pine tree succession assumptions result in the vegetative cover pine tree succession timeline presented in Table 53. Along with the Table 53 vegetative cover pine tree succession timeline, the assumption that there are 400 mature trees per acre with 4 roots to 6 feet and 1 root to 12 feet as discussed in Section 7.2 impact the number of pine roots at any one time and the cumulative number of roots produced over time. Within Appendix I, the Table 53 timeline has been converted into an accounting of pine root accumulation over time as shown in Figure 39.

Table 53. Vegetative Cover Pine Tree Succession Timeline

Year	Occurrence
0	Construction of FTF Closure Cap
100	End of 100-year institutional control period
260	Pine tree seedlings begin to invade the FTF Closure Cap
290	Pine tree roots first start to reach HDPE geomembrane
300	Mature pine trees established over a third of the FTF Closure Cap
340	Mature pine trees established over two-thirds and pine tree seedlings established over the entire FTF Closure Cap
380	Mature pine trees established over the entire FTF Closure Cap
380 to 10,000	Complete turnover of mature trees occurs every 100 years

Figure 39.   Pine Root Accumulation over Time

8.2 EROSION OF THE SOIL ABOVE THE EROSION BARRIER

As outlined in Section 7.3.1 and Table 52 erosion of the soil layers above the erosion barrier (i.e. topsoil and upper backfill) is assumed to be a degradation mechanism that is both applicable and significant to degradation of the FTF Closure Cap. For this institutional control to pine forest land use scenario, it is assumed that the closure cap will be vegetated with bahia grass during the institutional control period (see Sections 4.4.12 and 7.2), with a combination of bahia and pine trees for a period immediately following the institutional control period, and with a pine forest thereafter.

The projected erosion rate for both the topsoil and upper backfill layers has been determined utilizing the Universal Soil Loss Equation (Goldman et al. 1986) for both vegetative cover conditions (i.e. bahia grass and pine forest) within Appendix I. Table 54 provides a summary of the estimated FTF Closure Cap vegetative soil cover (i.e. topsoil and upper backfill) soil losses due to erosion. In order to maximize the erosion rate utilized, the bahia grass erosion rate, which is higher, will be used until the projected time that mature pine trees are assumed to cover the entire closure cap (i.e., at year 380 per Table 53). Based upon these erosion rates, the thickness of the topsoil and upper backfill layers over time was calculated within Appendix I. The summary Appendix I results are provided in Table 55.

Table 54. Estimated FTF Closure Cap Vegetative Soil Cover Soil Losses

Soil-Vegetation Condition	Estimated Soil Loss (tons/acre/year)	Estimated Soil Loss (inches/year)
Topsoil with a bahia grass vegetative cover	0.099	5.2E-04
Topsoil with a pine forest	0.025	1.3E-04
Backfill with a bahia grass vegetative cover	0.071	3.7E-04
Backfill with a pine forest	0.018	9.3E-05

Table 55. Topsoil and Upper Backfill Thickness over Time

Year	Topsoil Thickness (inches)	Upper Backfill Thickness (inches)
0	6	30
100	5.95	30
180	5.91	30
290	5.85	30
300	5.84	30
340	5.82	30
380	5.80	30
560	5.78	30
1,000	5.72	30
1,800	5.62	30
2,623	5.51	30
3,200	5.44	30
5,600	5.12	30
10,000	4.55	30

8.3 SILTING-IN OF THE LATERAL DRAINAGE LAYER

As outlined in Section 7.5.1 and Table 52 silting-in of the lateral drainage layer is assumed to be a degradation mechanism that is both applicable and significant to degradation of the FTF Closure Cap. As outlined in Section 7.5.1 silting-in of the lateral drainage layer is assumed to occur as follows:

- Over time colloidal clay migrates with the water flux from the 1-foot-thick middle backfill to the underlying 1-foot-thick lateral drainage layer at a concentration of 63 mg of colloidal clay per liter of water flux.
- Once half the clay content of the backfill has migrated to the drainage layer, the two layers essentially become the same material and material property changes cease with an endpoint saturated hydraulic conductivity that of the log mid-point between the initial backfill and drainage layer conditions.

- It will be assumed that the saturated hydraulic conductivity of the middle backfill layer is increasing log linearly with time, and conversely it will be assumed that the saturated hydraulic conductivity of the drainage layer is decreasing log linearly with time.

It will also be assumed that the endpoint porosity, field capacity, and wilting point will become the arithmetic average of the backfill and upper drainage layer.

Based upon these assumptions, the hydraulic properties of the middle backfill and lateral drainage layer were calculated within Appendix I. Table 56 and Table 57 provide the Appendix I calculated values of saturated hydraulic conductivity, porosity, field capacity, and wilting point for the middle backfill and lateral drainage, respectively, based upon the above silting-in assumptions.

Table 56. Middle Backfill Saturated Hydraulic Conductivity, Porosity, Field Capacity, and Wilting Point

Year	Saturated Hydraulic Conductivity (cm/s)	Porosity	Field Capacity	Wilting Point
0	4.10E-05	0.350	0.252	0.181
100	4.69E-05	0.351	0.248	0.178
180	5.22E-05	0.352	0.245	0.175
290	6.06E-05	0.353	0.241	0.172
300	6.14E-05	0.353	0.240	0.172
340	6.48E-05	0.354	0.239	0.171
380	6.84E-05	0.354	0.237	0.169
560	8.71E-05	0.356	0.230	0.164
1,000	1.58E-04	0.361	0.212	0.150
1,800	4.62E-04	0.371	0.181	0.125
2,623	1.40E-03	0.380	0.148	0.100
3,200	1.40E-03	0.380	0.148	0.100
5,600	1.40E-03	0.380	0.148	0.100
10,000	1.40E-03	0.380	0.148	0.100

Table 57.   Lateral Drainage Layer Saturated Hydraulic Conductivity, Porosity, Field Capacity, and Wilting Point

Year	Saturated Hydraulic Conductivity (cm/s)	Porosity	Field Capacity	Wilting Point
0	5.00E-02	0.417	0.045	0.018
100	4.36E-02	0.416	0.049	0.021
180	3.91E-02	0.414	0.052	0.024
290	3.37E-02	0.413	0.056	0.027
300	3.32E-02	0.413	0.057	0.027
340	3.15E-02	0.412	0.058	0.029
380	2.98E-02	0.412	0.060	0.030
560	2.33E-02	0.409	0.067	0.036
1,000	1.28E-02	0.403	0.084	0.049
1,800	4.30E-03	0.392	0.116	0.074
2,623	1.40E-03	0.380	0.148	0.100
3,200	1.40E-03	0.380	0.148	0.100
5,600	1.40E-03	0.380	0.148	0.100
10,000	1.40E-03	0.380	0.148	0.100

8.4 ROOT PENETRATION OF THE LATERAL DRAINAGE LAYER

As outlined in Section 7.5.2 and Table 52 root penetration of the lateral drainage layer is assumed to be a degradation mechanism that is both applicable and significant to degradation of the FTF Closure Cap. For this institutional control to pine forest land use scenario, it is assumed that the closure cap will be vegetated with bahia grass during the institutional control period (see Sections 4.4.12 and 7.2), with a combination of bahia and pine trees for a period immediately following the institutional control period, and with a pine forest thereafter. From the calculations above it is assumed that mature pine trees will be established over a third of the FTF Closure Cap by year 300; over two-thirds of the cap by year 340; and over the entire cap by year 380. As discussed in Section 7.5.2, roots will represent an impermeable volume within the lateral drainage layer prior to their decomposition.

From Section 7.2, the following assumptions were made relative to the establishment of a pine forest on the closure cap that results in root penetration through the lateral drainage layer and a subsequent impermeable volume in the layer due to roots:

- The closure cap will eventually be covered with approximately 400 mature trees per acre.
- Each mature tree will have 4 roots to 6 feet and 1 root to 12 feet. The roots are 3 inches in diameter at a depth of 1 foot and 0.25 inches in diameter at either 6 or 12 feet, whichever is applicable.
- Deep roots will be maintained and enlarge with yearly growth over the life of the tree.
- Trees are expected to die at approximately 100 years, and it is anticipated that decomposition of deep roots will occur over a 30 year period.
- Prior to decomposition the roots represent an impermeable volume within the lateral drainage layer

Based upon these assumptions, the impermeable volume that roots represent within the lateral drainage layer was calculated within Appendix I. Based upon the Appendix I calculations the roots within the lateral drainage layer will represent an impermeable volume at any time that ranges from 0.032 to 0.17 percent, depending upon the extent of erosion above the erosion barrier. In order to compensate for the presence of the roots within the lateral drainage layer the saturated hydraulic conductivity of the layer will be reduced by multiplying by 0.998 once the pine forest has been established on the closure cap. The conductivity will be reduced at year 300 when a third of the FTF Closure Cap is anticipated to be covered in mature pine trees. This factor is based upon the worse case percent volume of roots in the layer (i.e., approximately 0.2 percent). Table 58 provides the resulting saturated hydraulic conductivity of the lateral drainage layer over time based upon the use of this factor.

Table 58.   Lateral Drainage Layer Saturated Hydraulic Conductivity Modification due to Root Penetration

Year	Table 57 Saturated Hydraulic Conductivity (cm/s)	Modified Saturated Hydraulic Conductivity (cm/s)
0	5.00E-02	5.00E-02
100	4.36E-02	4.36E-02
180	3.91E-02	3.91E-02
290	3.37E-02	3.37E-02
300	3.32E-02	3.32E-02
340	3.15E-02	3.14E-02
380	2.98E-02	2.97E-02
560	2.33E-02	2.33E-02
1,000	1.28E-02	1.28E-02
1,800	4.30E-03	4.29E-03
2,623	1.40E-03	1.40E-03
3,200	1.40E-03	1.40E-03
5,600	1.40E-03	1.40E-03
10,000	1.40E-03	1.40E-03

8.5 ANTIOXIDANT DEPLETION, THERMAL OXIDATION, AND TENSILE STRESS CRACKING OF THE HDPE

As outlined in Table 52 antioxidant depletion (see Section 7.6.2), thermal oxidation (see Section 7.6.3), and tensile stress cracking (see Section 7.6.5) of the HDPE geomembrane are assumed to be degradation mechanisms that are both applicable and significant to degradation of the FTF Closure Cap. These HDPE geomembrane degradation mechanisms have been equated to geomembrane hole generation over time within Appendix I utilizing the Mueller and Jakob (2003) methodology (see Section 7.6.2.3) for antioxidant depletion and the Needham et al. (2004) methodology (see Section 7.6.7) for combining these degradation mechanisms into hole generation over time. The resulting HDPE geomembrane hole generation summary is provided in Table 59 and depicted in Figure 40.

Table 59.   Summary HDPE Geomembrane Hole Generation over Time

Year	Total Cumulative # of Holes (#/acre)	Total Cumulative Hole Size (cm²/acre)
0	12	4
100	26	50
180	39	90
290	56	146
300	63	170
340	111	334
380	158	479
560	370	1115
1,000	886	2669
1,800	1825	5496
2,623	2791	8403
3,200	3468	10442
5,600	6285	18921
10,000	11448	34466

Figure 40. Summary HDPE Geomembrane Hole Generation over Time

8.6 DIVALENT CATION DEGRADATION OF THE GCL

As outlined in Section 7.7.4 and Table 52 divalent cation degradation of the GCL is assumed to be a degradation mechanism that is both applicable and significant to degradation of the FTF Closure Cap. As outlined in Section 7.7.4, it will be assumed that the sodium bentonite GCL is converted to calcium-magnesium-bentonite GCL, resulting in an order of magnitude increase in saturated hydraulic conductivity. During the 100-year institutional period, it will be assumed the GCL consists of sodium bentonite with a saturated hydraulic conductivity of 5.0E-09 cm/s. After the 100-year institutional period, it will be assumed the GCL consists of calcium-magnesium-bentonite with a saturated hydraulic conductivity of 5.0E-08 cm/s.

8.7 ROOT PENETRATION OF THE COMPOSITE HYDRAULIC BARRIER

As outlined in Table 52 root penetration of the HDPE geomembrane (see Section 7.6.6), and GCL (see Section 7.7.7) are assumed to be degradation mechanisms that are both applicable and significant to degradation of the FTF Closure Cap. The HDPE geomembrane and immediately underlying GCL together form a composite hydraulic barrier. For conservatism it will be assumed that every HDPE geomembrane hole generated over time is penetrated by a root that subsequently penetrates the GCL, once significant roots are available to penetrate. As with the drainage layer (see Section 8.4), it will be assumed that significant roots are available for penetration at year 300 and beyond (at year 300 a third of the closure cap is assumed to be covered by mature trees).

Figure 41 provides a comparison of the number of pine tree roots (see Section 8.1 and Figure 39) versus the number of holes in the HDPE geomembrane (see Section 8.5 and Figure 40) over time as derived from Appendix I. As seen there are significantly more pine tree roots than HDPE geomembrane holes. The HELP model allows the input of up to 999,999 one square centimeter installation defects per acre for a geomembrane liner; therefore the total cumulative hole size provided in Table 59 for each year to be modeled will be used as the number of one square centimeter installation defects per acre for input into the HELP model. This results in more holes than determined but maintains the area of holes determined.

Since the HELP model can not handle holes in a barrier soil liner (i.e., the GCL), the GCL must either be ignored in the HELP modeling or combined with the HDPE geomembrane for all cases at year 300 and beyond. Due to this the HELP model will be run with the following representations of the composite hydraulic barrier (i.e., combined HDPE geomembrane and GCL) as determined in Appendix I:

- At or before year 100, the HDPE geomembrane and GCL will be modeled as separate layers with holes in the HDPE geomembrane and an intact GCL with a Ksat = 5.0E-09 cm/s.
- After year 100 but before year 300, the HDPE geomembrane and GCL will be modeled as separate layers with holes in the HDPE geomembrane and an intact GCL with a Ksat = 5.0E-08 cm/s.
- At and beyond year 300, the HDPE geomembrane and GCL will be modeled as a combined layer with holes all the way through and with a Ksat = 8.7E-13 cm/s and a thickness of 0.260" for intact portions
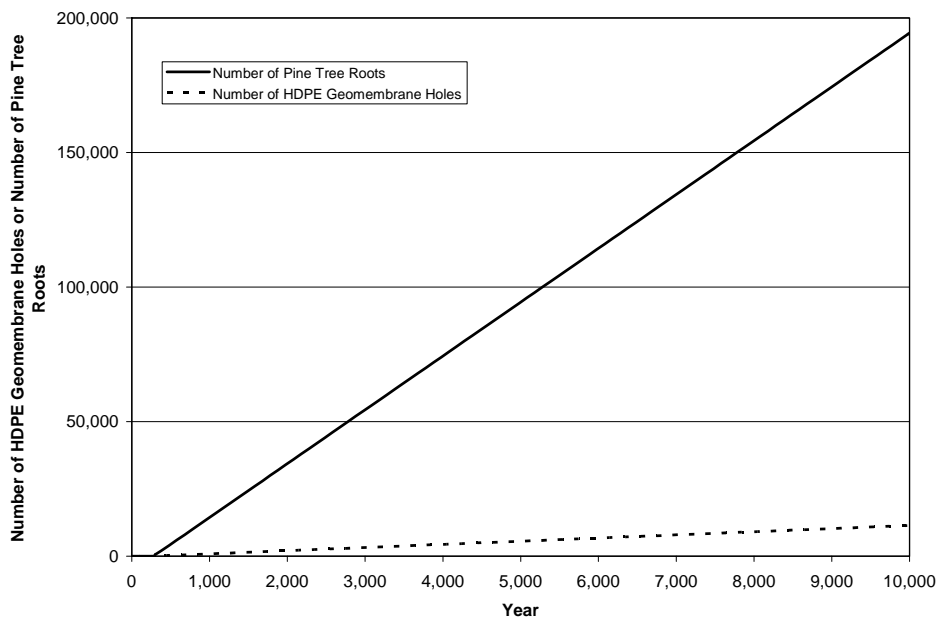
Figure 41.   Pine Tree Roots versus HDPE geomembrane holes

8.7.1 Probability Based Root Penetration Model

A probability based root penetration model has been produced to estimate the probability of pine tree roots penetrating cracks in the HDPE geomembrane and subsequently producing a hole in the underlying GCL (Shine 2007). This probability model demonstrates the conservative nature of infiltration estimates produced under the assumption that every HDPE geomembrane hole generated over time is penetrated by a root that subsequently penetrates the GCL, once significant roots are available to penetrate (i.e., assumed at 300 years) (see Section 8.7). This probability based root penetration model is described in detail in Appendix L.

Thirty-three probability based simulations of root penetration through the HDPE/GCL composite barrier have been run with the probability model, resulting in the root/hole averages for the years of interest shown in Table 60. Figure 42 and Figure 43 provide the average results of the root penetration probability model graphically. Figure 42 provides the number of pine tree roots, HDPE geomembrane cracks, and GCL penetrations over time, and Figure 43 provides a close-up to better see the number of HDPE geomembrane cracks and GCL penetrations over time. As seen in Table 60, no roots penetrate HDPE geomembrane holes (and subsequently the underlying GCL) until year 560. As seen in Table 60 and Figure 42 and Figure 43 the number of GCL penetrations is significantly less than the number of HDPE geomembrane cracks over time, demonstrating the conservative nature of infiltration estimates made with the assumptions outlined in Section 8.7.

The simulations of root penetration through the composite barrier results in the following four areas of consideration for the composite barrier:

- Areas comprised of both intact HDPE geomembrane and intact GCL
- Areas comprised of holes in the HDPE geomembranes and intact GCL
- Areas comprised of holes in both the HDPE geomembrane and GCL with a live root in the hole
- Areas comprised of holes in both the HDPE geomembrane and GCL with a dead root which is assumed to immediately disappear upon death of the tree

The HELP model is capable of handling the first two types of areas outlined above, but it is not capable of handling all four of these conditions together. The HELP model does not allow holes in barrier soil liners such as the GCL, and it does not allow the placement of two geomembrane liners, which can have holes, directly on top of one another. Due to this the HELP model is not suitable to appropriately incorporate the results of the probability model.

Table 60. Root Penetration Probability Simulation Average

Year	Cumulative Number of Tap Roots (# / acre)	Total Number of HDPE Geomembrane Holes (# / acre)	Total Number of Live Tap Roots in HDPE Geomembrane Holes (# / acre)	Total Number of Dead Tap Roots in HDPE Geomembrane Holes (# / acre)	Total Number of HDPE Geomembrane Holes without Roots (# / acre)
0	0	12	0	0	12
100	0	26	0	0	26
180 [1]	0	39	0	0	39
290 [2]	665	56	0	0	56
300	665	63	0	0	63
340	1335	111	0	0	111
380	2000	158	0	0	157
560	5600	370	0	2	367
1000	14400	886	2	15	870
1800	30400	1825	4	64	1758
2623	46800	2791	4	154	2633
3200	58400	3468	8	234	3227
5600	106400	6285	12	738	5535
10000	194400	11449 [3]	20	2272	9157

[1] HDPE geomembrane hole values for year 180 interpolated from years 175 and 182:

175	0	38	0	0	38
182	0	39	0	0	39

[2] HDPE geomembrane hole values for year 290 interpolated from years 289 and 291; and cumulative number of tap roots taken as that of year 291.

289	0	56	0	0	56
291	665	56	0	0	56

[3] The previously determined total cumulative number of holes per acre in the HDPE geomembrane at 10,000 years was 11448, which is one less than the value of 11449 produced by the probability based root penetration model simulations.
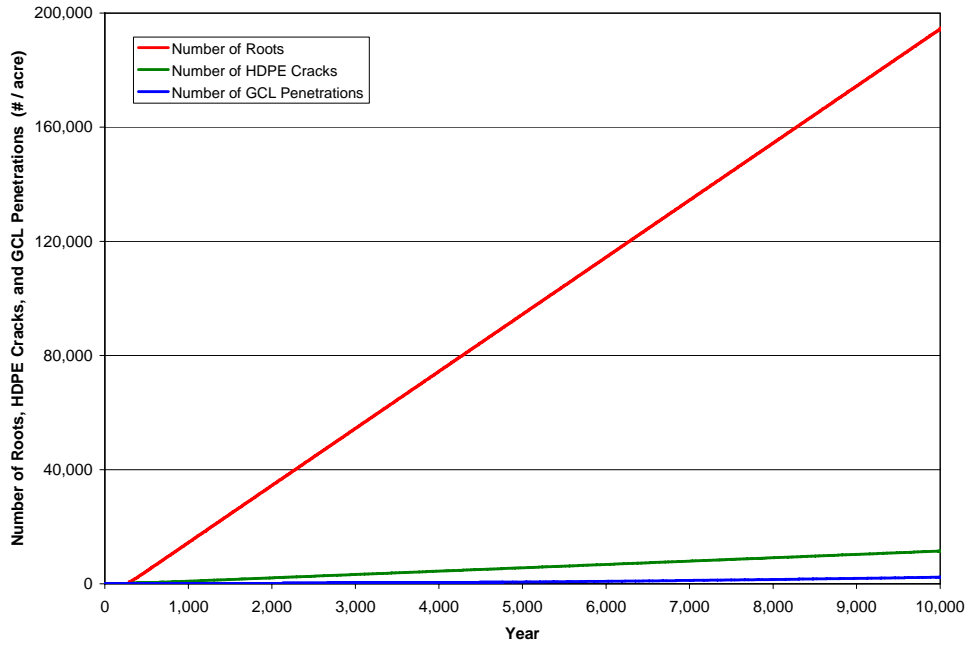
Figure 42. Root Penetration Probability Simulation Average (Roots, Cracks, and Penetrations)
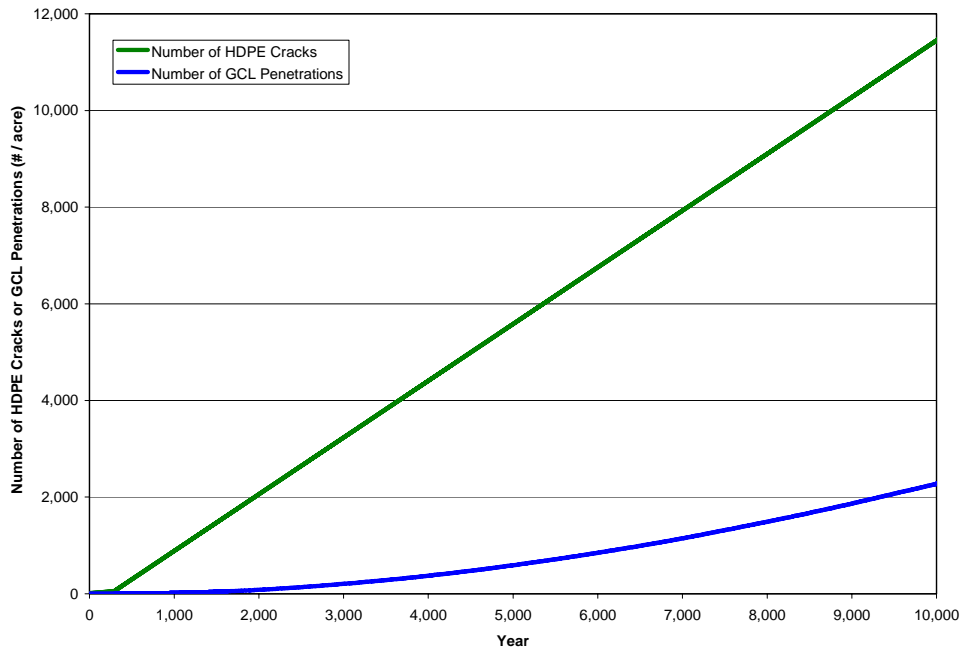
Figure 43. Root Penetration Probability Simulation Average (Cracks and Penetrations)

8.8 SUMMARY HELP MODEL INPUT

Development of the HELP model weather data input files were discussed in Section 5.2, and the files, which were utilized for all HELP model runs, are provided in the following appendices:

- Appendix B, Augusta Synthetic Precipitation Modified with SRS Specific Average Monthly Precipitation Data over 100 Years (file name: Fprec.d4)
- Appendix C, Augusta Synthetic Temperature Modified with SRS Specific Average Monthly Temperature Data over 100 Years (file name: Ftemp.d7)
- Appendix D, Augusta Synthetic Solar Radiation Data over 100 Years (file name: Fsolar.d13)
- Appendix E, Augusta Evapotranspiration Data (file name: Fevap.d11)

Development of the HELP model general input data and runoff input data were discussed in Sections 5.3 and 5.5, respectively. Both the general and runoff input data developed in these sections is applicable to both the initial, intact and the degraded FTF Closure Cap conditions. Development of initial, intact HELP model layer input data were discussed in Section 5.4. Table 22 of Section 5.4.8 provides a summary of the initial, intact HELP model input for the FTF Closure Cap layers. Sections 8.1 through 8.7 discuss the application of closure cap degradation mechanisms and the development of HELP model inputs based upon the impact of the degradation mechanisms on the various closure cap layers. Appendix I provides the associated FTF Closure Cap degraded property value calculations. The following tables provide the degraded HELP model inputs used to produce, an estimate of FTF Closure Cap Infiltration over 10,000 years:

- Table 61 provides the reduction in topsoil thickness over time.
- Table 62 provides the change in the middle backfill's hydraulic properties over time,
- Table 63 provides the change in the lateral drainage layer's hydraulic properties over time.
- Table 64 provides the change in the saturated hydraulic conductivity and number of holes over time in the composite hydraulic barrier (i.e., combined HDPE geomembrane and underlying GCL).

The degraded HELP model inputs presented in Table 61 through Table 64 along with the initial, intact HELP model inputs presented in Table 22 were utilized to develop the Appendix J HELP model inputs for the FTF Closure Cap configuration #1a for each year modeled.

Table 61.   Topsoil Thickness over Time

Year	Topsoil Thickness (inches)
0	6
100	5.95
180	5.91
290	5.85
300	5.84
340	5.82
380	5.80
560	5.78
1,000	5.72
1,800	5.62
2,623	5.51
3,200	5.44
5,600	5.12
10,000	4.55

Table 62.   Middle Backfill Saturated Hydraulic Conductivity, Porosity, Field Capacity, and Wilting Point

Year	Saturated Hydraulic Conductivity (cm/s)	Porosity	Field Capacity	Wilting Point
0	4.10E-05	0.350	0.252	0.181
100	4.69E-05	0.351	0.248	0.178
180	5.22E-05	0.352	0.245	0.175
290	6.06E-05	0.353	0.241	0.172
300	6.14E-05	0.353	0.240	0.172
340	6.48E-05	0.354	0.239	0.171
380	6.84E-05	0.354	0.237	0.169
560	8.71E-05	0.356	0.230	0.164
1,000	1.58E-04	0.361	0.212	0.150
1,800	4.62E-04	0.371	0.181	0.125
2,623	1.40E-03	0.380	0.148	0.100
3,200	1.40E-03	0.380	0.148	0.100
5,600	1.40E-03	0.380	0.148	0.100
10,000	1.40E-03	0.380	0.148	0.100

Table 63.   Lateral Drainage Layer Saturated Hydraulic Conductivity, Porosity, Field Capacity, and Wilting Point

Year	Saturated Hydraulic Conductivity (cm/s)	Porosity	Field Capacity	Wilting Point
0	5.00E-02	0.417	0.045	0.018
100	4.36E-02	0.416	0.049	0.021
180	3.91E-02	0.414	0.052	0.024
290	3.37E-02	0.413	0.056	0.027
300	3.32E-02	0.413	0.057	0.027
340	3.14E-02	0.412	0.058	0.029
380	2.97E-02	0.412	0.060	0.030
560	2.33E-02	0.409	0.067	0.036
1,000	1.28E-02	0.403	0.084	0.049
1,800	4.29E-03	0.392	0.116	0.074
2,623	1.40E-03	0.380	0.148	0.100
3,200	1.40E-03	0.380	0.148	0.100
5,600	1.40E-03	0.380	0.148	0.100
10,000	1.40E-03	0.380	0.148	0.100

Table 64.   Composite Barrier Saturated Hydraulic Conductivity and Number of Holes

Year	GCL [1] Saturated Hydraulic Conductivity (cm/s)	HDPE Geomembrane [2]		Composite Barrier [3] (i.e., combined GCL and HDPE geomembrane)	
		Saturated Hydraulic Conductivity (cm/s)	Number of One cm^2 Holes (#/acre)	Saturated Hydraulic Conductivity (cm/s)	Number of One cm^2 Holes (#/acre)
0	5.0E-09	2.0E-13	4	na	na
100	5.0E-09	2.0E-13	50	na	na
180	5.0E-08	2.0E-13	90	na	na
290	5.0E-08	2.0E-13	146	na	na
300	na	na	na	8.7E-13	170
340	na	na	na	8.7E-13	334
380	na	na	na	8.7E-13	479
560	na	na	na	8.7E-13	1115
1,000	na	na	na	8.7E-13	2669
1,800	na	na	na	8.7E-13	5496
2,623	na	na	na	8.7E-13	8403
3,200	na	na	na	8.7E-13	10442
5,600	na	na	na	8.7E-13	18921
10,000	na	na	na	8.7E-13	34466

na = not applicable
[1] The thickness of the GCL alone is taken as 0.20 inches
[2] The thickness of the HDPE geomembrane alone is taken as 0.060 inches
[3] The thickness of the composite barrier is taken as 0.260 inches

8.9 SUMMARY HELP MODEL RESULTS

The following are measures, which have been taken to try and ensure conservative tending HELP Model infiltration results:

- The precipitation data utilized included maximum daily precipitation up to 6.7 inches (i.e. significant pulses of water).
- The use of bamboo to preclude or delay pine forest succession is not currently considered, even though current research indicates that the use of bamboo would be beneficial in this regard.
- Physical stability of the top surface of the closure cap is obtained by both the use of an erosion barrier designed to preclude any movement due to a PMP event and surficial soil designed to preclude gully erosion due to a PMP event. Such design could be considered redundant, and the use of a surficial slope greater than 2 percent would result in greater runoff.
- The maximum slope length of the closure cap (i.e., 585 feet) was utilized to determine both runoff and lateral drainage for the entire cap.
- A maximum evaporative zone depth of 22 inches, which is considered conservative due to the anticipated capillarity of the surficial soils, was utilized.
- The erosion barrier is assumed to be infilled with a sandy soil; the use of a less permeable infill would reduce infiltration.
- No lateral drainage is assumed to occur over the erosion barrier; however such lateral drainage could occur particularly if a low permeable infill were utilized.
- The lateral drainage layer was assumed to have the same 2 percent slope as specified for the vegetative soil cover for physical stability purposes; the lateral drainage layer slope could be greater without impacting the closure cap's physical stability.
- The initial saturated hydraulic conductivity of the sand used for the lateral drainage layer was taken as 5.0E-02 cm/s, which is well be low the maximum literature value of sand conductivity of 1 cm/s.
- Silting-in of the lateral drainage layer is assumed to begin immediately upon construction; it is assumed to result from the migration of elevated levels of colloidal clay within infiltrating water; the use of the overlying filter fabric is assumed not to reduce colloidal clay movement; and all colloidal clay that enters the layer is assumed to remain in the layer thus reducing its hydraulic conductivity.
- A saturated hydraulic conductivity was assigned to the intact portions of the HDPE geomembrane even though water transport through HDPE is a vapor diffusional process.
- The HDPE geomembrane antioxidant depletion time has been calculated using a conservative estimate of activation energy (i.e. 60 kJ/mol).
- The production of holes in the HDPE geomembrane over time has been estimated using the "fair" case outlined by Needham et al. (2004), which results in many more holes than the use of either the "good" or "excellent" cases. Since installation of the closure cap over the FTF will undergo a high level of QA/QC and the HDPE geomembrane will be under relative low stress conditions (i.e. emplaced on a 2 percent slope), the applicability of the "good" case and possibly the "excellent" case could potentially be supported.

- It has been assumed that every HDPE geomembrane hole generated over time is penetrated by a pine root that subsequently penetrates the GCL. However the results of the probability based root penetration model demonstrate that this is not the case and that most of the HDPE geomembrane holes are not penetrated by roots over the time period of interest.
- The initial saturated hydraulic conductivity of the GCL was taken as 5.0E-09 cm/s even though test results indicate that the value could be significantly lower.
- It has been assumed that the GCL saturated hydraulic conductivity increases to 5.0E-08 cm/s at the end of the 100-year institutional control period. This is not likely since infiltrating water at SRS should be very low in dissolved calcium and other divalent cations.
- The saturated hydraulic conductivity of the Upper Foundation Layer, which will be a soil-bentonite blend, was taken as 1.0E-06 cm/s even though significantly lower conductivities can be obtained with soil-bentonite blends.

The Appendix J HELP model inputs for the FTF Closure Cap configuration #1a for years 0, 100, 180, 290, 300, 340, 380, 560, 1,000, 1,800, 2,623, 3,200, 5,600, and 10,000 were run in the HELP model in order to produce an estimate of FTF Closure Cap Infiltration over 10,000 years. Table 65 provides input and output files names for each of the years modeled. Appendix J provides the HELP model input for each of the configuration #1a years modeled. One hundred HELP model simulations, with precipitation ranging from 29.8 to 68.6 inches/year, were produced for each of the configuration #1a years modeled. The detailed water balance data by simulation for each of the configuration #1a years modeled are provided in Appendix K. The following HELP model results are provided for each of the configuration #1a years modeled:

- A chart of the annual infiltration versus annual precipitation for precipitation ranging from 29.8 to 68.6 inches/year (including a linear regression for the precipitation-infiltration data-set),
- A table summarizing the annual water balance (precipitation, runoff, evapotranspiration, lateral drainage, infiltration, and change in water storage) statistics, and
- A figure depicting the annual average water balance.

As seen in Figure 44 and Table 66, precipitation falling on a configuration #1a type closure cap under initial, intact conditions at year 0 results in an average infiltration of 0.00088 inches/year thru the GCL with a range of 0.00009 to 0.005 inches/year. The water balance for precipitation falling on the cap at year 0 (see Table 66 and Figure 45) is dominated by evapotranspiration (average of 32.57 inches/year) and lateral drainage (average of 16.07 inches/year).

As seen in Figure 46 and Table 67, precipitation falling on a configuration #1a type closure cap under degraded conditions at year 100 results in an average infiltration of 0.010 inches/year thru the GCL with a range of 0.001 to 0.054 inches/year. The water balance for precipitation falling on the cap at year 100 (see Table 67 and Figure 47) is dominated by evapotranspiration (average of 32.59 inches/year) and lateral drainage (average of 15.98 inches/year).

As seen in Figure 48 and Table 68, precipitation falling on a configuration #1a type closure cap under degraded conditions at year 180 results in an average infiltration of 0.17 inches/year thru the GCL with a range of 0.01 to 0.81 inches/year. The water balance for precipitation falling on the cap at year 180 (see Table 68 and Figure 49) is dominated by evapotranspiration (average of 32.58 inches/year) and lateral drainage (average of 15.76 inches/year).

As seen in Figure 50 and Table 69, precipitation falling on a configuration #1a type closure cap under degraded conditions at year 290 results in an average infiltration of 0.37 inches/year thru the GCL with a range of 0.01 to 1.82 inches/year. The water balance for precipitation falling on the cap at year 290 (see Table 69 and Figure 51) is dominated by evapotranspiration (average of 32.58 inches/year) and lateral drainage (average of 15.44 inches/year).

As seen in Figure 52 and Table 70, precipitation falling on a configuration #1a type closure cap under degraded conditions at year 300 results in an average infiltration of 0.50 inches/year thru the GCL with a range of 0.07 to 1.76 inches/year. The water balance for precipitation falling on the cap at year 300 (see Table 70 and Figure 53) is dominated by evapotranspiration (average of 32.59 inches/year) and lateral drainage (average of 15.28 inches/year).

As seen in Figure 54 and Table 71, precipitation falling on a configuration #1a type closure cap under degraded conditions at year 340 results in an average infiltration of 1.00 inches/year thru the GCL with a range of 0.14 to 3.42 inches/year. The water balance for precipitation falling on the cap at year 340 (see Table 71 and Figure 55) is dominated by evapotranspiration (average of 32.58 inches/year), lateral drainage (average of 14.81 inches/year), and infiltration through the GCL (average of 1.00 inches/year).

As seen in Figure 56 and Table 72, precipitation falling on a configuration #1a type closure cap under degraded conditions at year 380 results in an average infiltration of 1.46 inches/year thru the GCL with a range of 0.21 to 4.92 inches/year. The water balance for precipitation falling on the cap at year 380 (see Table 72 and Figure 57) is dominated by evapotranspiration (average of 32.58 inches/year), lateral drainage (average of 14.36 inches/year), and infiltration through the GCL (average of 1.46 inches/year).

As seen in Figure 58 and Table 73, precipitation falling on a configuration #1a type closure cap under degraded conditions at year 560 results in an average infiltration of 3.23 inches/year thru the GCL with a range of 0.52 to 8.16 inches/year. The water balance for precipitation falling on the cap at year 560 (see Table 73 and Figure 59) is dominated by evapotranspiration (average of 32.59 inches/year), lateral drainage (average of 12.46 inches/year), and infiltration through the GCL (average of 3.23 inches/year).

As seen in Figure 60 and Table 74, precipitation falling on a configuration #1a type closure cap under degraded conditions at year 1,000 results in an average infiltration of 7.01 inches/year thru the GCL with a range of 1.43 to 11.15 inches/year. The water balance for precipitation falling on the cap at year 1,000 (see Table 74 and Figure 61) is dominated by evapotranspiration (average of 32.69 inches/year), lateral drainage (average of 8.07 inches/year), infiltration through the GCL (average of 7.01 inches/year), and runoff (1.29 inches/year).

As seen in Figure 62 and Table 75, precipitation falling on a configuration #1a type closure cap under degraded conditions at year 1,800 results in an average infiltration of 10.65 inches/year thru the GCL with a range of 2.92 to 12.45 inches/year. The water balance for precipitation falling on the cap at year 1,800 (see Table 75 and Figure 63) is dominated by evapotranspiration (average of 32.99 inches/year), infiltration through the GCL (average of 10.65 inches/year), lateral drainage (average of 3.35 inches/year), and runoff (2.08 inches/year).

As seen in Figure 64 and Table 76, precipitation falling on a configuration #1a type closure cap under degraded conditions at year 2,623 results in an average infiltration of 11.47 inches/year thru the GCL with a range of 3.78 to 12.45 inches/year. The water balance for precipitation falling on the cap at year 2,623 (see Table 76 and Figure 65) is dominated by evapotranspiration (average of 33.16 inches/year), infiltration through the GCL (average of 11.47 inches/year), runoff (2.49 inches/year), and lateral drainage (average of 1.96 inches/year).

As seen in Figure 66 and Table 77, precipitation falling on a configuration #1a type closure cap under degraded conditions at year 3,200 results in an average infiltration of 11.53 inches/year thru the GCL with a range of 3.99 to 12.45 inches/year. The water balance for precipitation falling on the cap at year 3,200 (see Table 77 and Figure 67) is dominated by evapotranspiration (average of 33.14 inches/year), infiltration through the GCL (average of 11.53 inches/year), runoff (2.47 inches/year), and lateral drainage (average of 1.93 inches/year).

As seen in Figure 68 and Table 78, precipitation falling on a configuration #1a type closure cap under degraded conditions at year 5,600 results in an average infiltration of 11.63 inches/year thru the GCL with a range of 4.38 to 12.45 inches/year. The water balance for precipitation falling on the cap at year 5,600 (see Table 78 and Figure 69) is dominated by evapotranspiration (average of 33.10 inches/year), infiltration through the GCL (average of 11.63 inches/year), runoff (2.46 inches/year), and lateral drainage (average of 1.88 inches/year).

As seen in Figure 70 and Table 79, precipitation falling on a configuration #1a type closure cap under degraded conditions at year 10,000 results in an average infiltration of 11.67 inches/year thru the GCL with a range of 4.53 to 12.45 inches/year. The water balance for precipitation falling on the cap at year 10,000 (see Table 79 and Figure 71) is dominated by evapotranspiration (average of 33.03 inches/year), infiltration through the GCL (average of 11.67 inches/year), runoff (2.53 inches/year), and lateral drainage (average of 1.84 inches/year).

Figure 72 provides a comparison of the annual infiltration through the GCL for FTF Closure Cap configuration #1a versus annual precipitation for all the modeled years. As outlined in Section 5.2, the precipitation data set used to produce the 100 annual simulations for each year modeled ranged from 29.8 to 68.6 inches/year with daily precipitation ranging from 0 to 6.7 inches/year. No precipitation occurs on approximately 72.5 percent of the days. On days that precipitation does occur (i.e., approximately 100 days per year), the range in daily precipitation consisted of 86.4 percent (i.e., approximately 86 days per year) ranging from 0.01 to 1.0 inches/day; 12.9 percent (i.e., approximately 13 days per year) ranging from 1.0 to 3.0 inches/day; and 0.7 percent (i.e., approximately 1 day per year) ranging from 3.0 to 7.0 inches/day. Based upon the precipitation data set used to produce the 100 annual simulation for each year modeled, it is evident that the modeling took into account large pulses of precipitation in the annual infiltrations shown in Figure 72.

A previous evaluation (WSRC 2005), which looked at the relationship between daily precipitation ranging from 0 to 6.9 inches/day and daily infiltration through a closure cap drew the following conclusions:

- "No discernable functional relationship could be established between precipitation and infiltration on a daily basis, as could be determined on an annual basis, due to the many processes which are very dynamic on a daily basis as compared to an annual basis."
- Infiltration increases "with daily precipitation events greater than about one inch and/or multiple consecutive days of precipitation".

Additionally it is evident from WSRC 2005 that under intact closure cap conditions the infiltration variations produced by variations in precipitation remain fairly small even with large pulses of precipitation up to 6.9 inches/day. Under intact conditions the closure cap lateral drainage layer and barrier layer can effectively remove even large pulses of precipitation with very little increases in infiltration. However under degraded conditions the infiltration variations produced by variations in precipitation are much larger and could result in daily infiltration rates approaching 1.5 inches/day with large pulses of precipitation up to 6.9 inches/day. The infiltration under such conditions is still much less than the precipitation (i.e. muted), since increased runoff and soil water storage occur under conditions of heavy precipitation. It is evident that while large pulses of precipitation do impact daily infiltration, there is little impact under intact closure cap conditions, and the daily infiltration is much less than precipitation, even under degraded closure cap conditions. Therefore the use of average annual infiltration rates based upon the precipitation data set utilized is considered appropriate.

Also as clearly seen in Figure 72, infiltration increases with time of closure cap degradation. Under initial, intact conditions (i.e., year 0) very little infiltration occurs, however as closure cap degradation proceeds, the infiltration increases until at year 2,623 and thereafter the infiltration appears to stabilize at an approximate average of 11.5 inches/year.

Table 80 and Figure 73 provide a comparison of the average water balance for FTF Closure Cap configuration #1a for all the modeled years. As seen for an average annual precipitation of 49.14 inches/year the average water balance changes as follows with closure cap degradation:

- Evapotranspiration remains fairly constant over time at an average ranging from 32.57 to 33.16 inches/year.
- Lateral drainage starts out at 16.07 inches/year under initial, intact conditions and decreases to less than 2 inches/year at year 2,623 and thereafter as the lateral layer silts-in.
- Runoff starts out at 0.43 inches/year under initial, intact conditions and increases to about 2.5 inches/year at year 2,623 and thereafter as pluggage of the lateral drainage layer results in somewhat slower soil water drainage in the soil layers above it.
- Infiltration through the GCL starts out at 0.00088 inches/year under initial, intact conditions and increases to about 11.5 inches/year at year 2,623 and thereafter as increasing holes through the composite hydraulic barrier (HDPE geomembrane and underlying GCL) result in increased infiltration through the GCL.

The resulting average annual infiltration through the GCL, which will be utilized as an upper boundary condition for the FTF PorFlow vadose zone modeling is provided in Table 81.

The closure cap design and infiltration information provided herein is preliminary and conceptual in nature, being consistent with a scoping level concept. In other words, it provides sufficient information for planning purposes, to evaluate the closure cap configuration relative to its constructability and functionality, and to estimate infiltration over time through modeling. It is not intended to constitute final design. Final design and a re-evaluation of infiltration will be performed near the end of the operational period. Technological advances, increased knowledge, and improved modeling capabilities are all likely and will result in improvements in both the closure cap design and infiltration estimates.

Table 65. HELP Model Input and Output File Names

Year	HELP Model Input File	HELP Model Output File
0	FC1A00.D10	FC1A00o.OUT
100	FC1A01.D10	FC1A01o.OUT
180	FC1A02.D10	FC1A02o.OUT
290	FC1A03.D10	FC1A03o.OUT
300	FC1A04.D10	FC1A04o.OUT
340	FC1A05.D10	FC1A05o.OUT
380	FC1A06.D10	FC1A06o.OUT
560	FC1A07.D10	FC1A07o.OUT
1,000	FC1A08.D10	FC1A08o.OUT
1,800	FC1A09.D10	FC1A09o.OUT
2,623	FC1A10.D10	FC1A10o.OUT
3,200	FC1A11.D10	FC1A11o.OUT
5,600	FC1A12.D10	FC1A12o.OUT
10,000	FC1A13.D10	FC1A13o.OUT
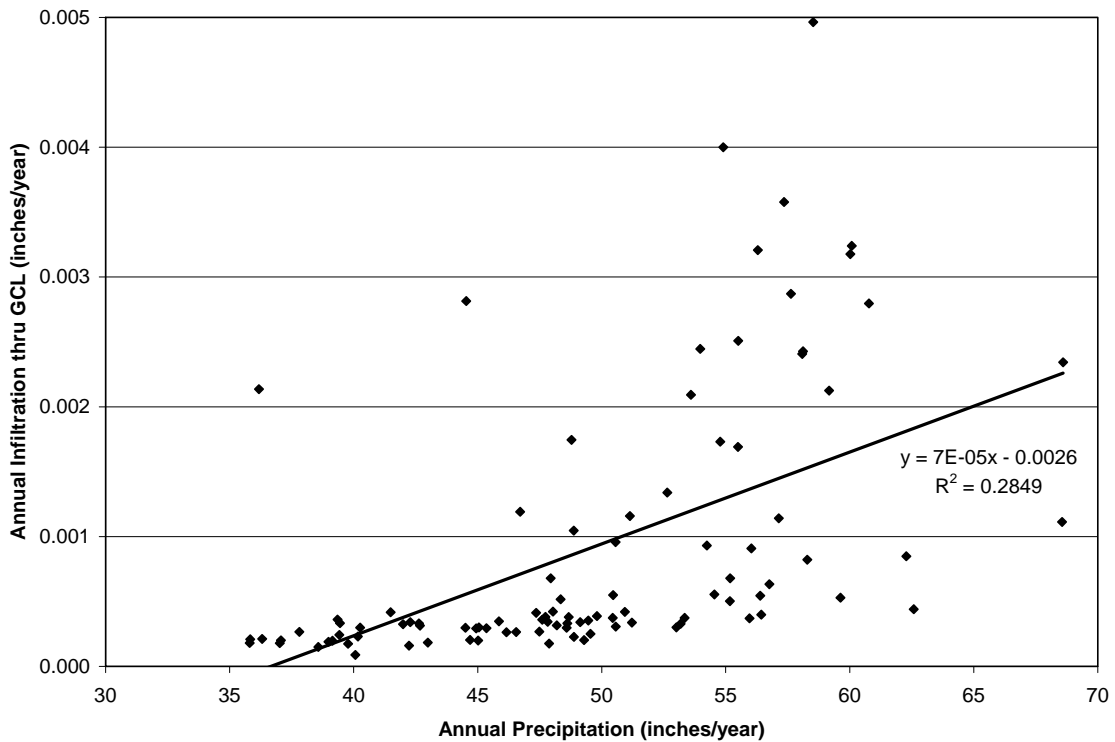
Figure 44. Configuration #1a at Year 0 HELP Model Simulations - Annual Infiltration thru GCL versus Annual Precipitation

Table 66. Configuration #1a at Year 0 HELP Model Simulations - Water Balance Statistics

Parameter	Precipitation (in/yr)	Runoff (in/yr)	Evapotrans-piration (in/yr)	Lateral Drainage (in/yr)	Infiltration thru GCL (in/yr)	Change in Water Storage (in/yr)
Count	100	100	100	100	100	100
Maximum	68.60	3.81	41.48	29.63	0.00496	5.26
Average	49.14	0.43	32.57	16.07	0.00088	0.06
Median	48.83	0.00	32.59	15.37	0.00037	0.26
Minimum	29.81	0.00	21.67	4.67	0.00009	-6.58
Std Dev	7.69	0.76	3.38	5.25	0.00102	2.63

Figure 45. Configuration #1a at Year 0 HELP Model Simulations – Average Water Balance
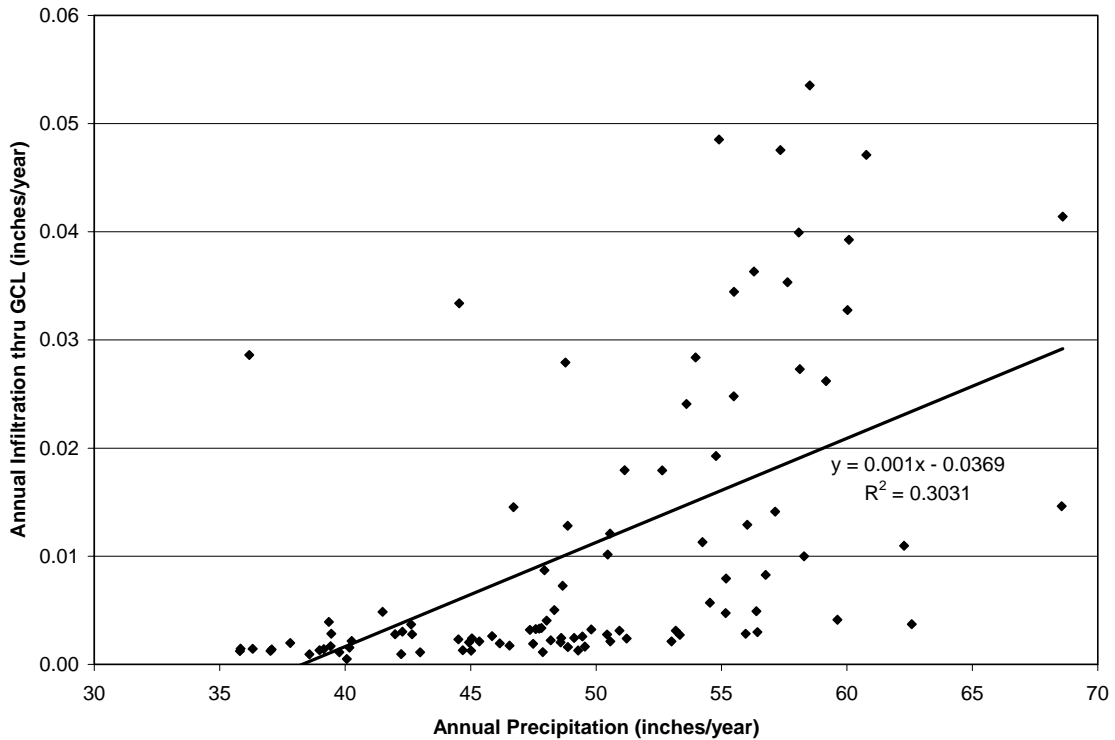
**Figure 46. Configuration #1a at Year 100 HELP Model Simulations - Annual
Infiltration thru GCL versus Annual Precipitation**

**Table 67. Configuration #1a at Year 100 HELP Model Simulations - Water Balance
Statistics**

Parameter	Precipitation (in/yr)	Runoff (in/yr)	Evapotrans-piration (in/yr)	Lateral Drainage (in/yr)	Infiltration thru GCL (in/yr)	Change in Water Storage (in/yr)
Count	100.00	100.00	100.00	100.00	100.00	100.00
Maximum	68.60	3.82	41.45	28.50	0.054	5.68
Average	49.14	0.50	32.59	15.98	0.010	0.07
Median	48.83	0.03	32.59	15.37	0.003	0.32
Minimum	29.81	0.00	21.66	4.53	0.001	-6.84
Std Dev	7.69	0.88	3.39	5.05	0.013	2.75

49.14 in/yr
Precipitation

32.59 in/yr
Evapotranspiration

0.50 in/yr
Runoff

15.98 in/yr Lateral Drainage

0.07 in/yr
Change in Water Storage
(throughout entire profile)

0.010 in/yr
Infiltration thru GCL
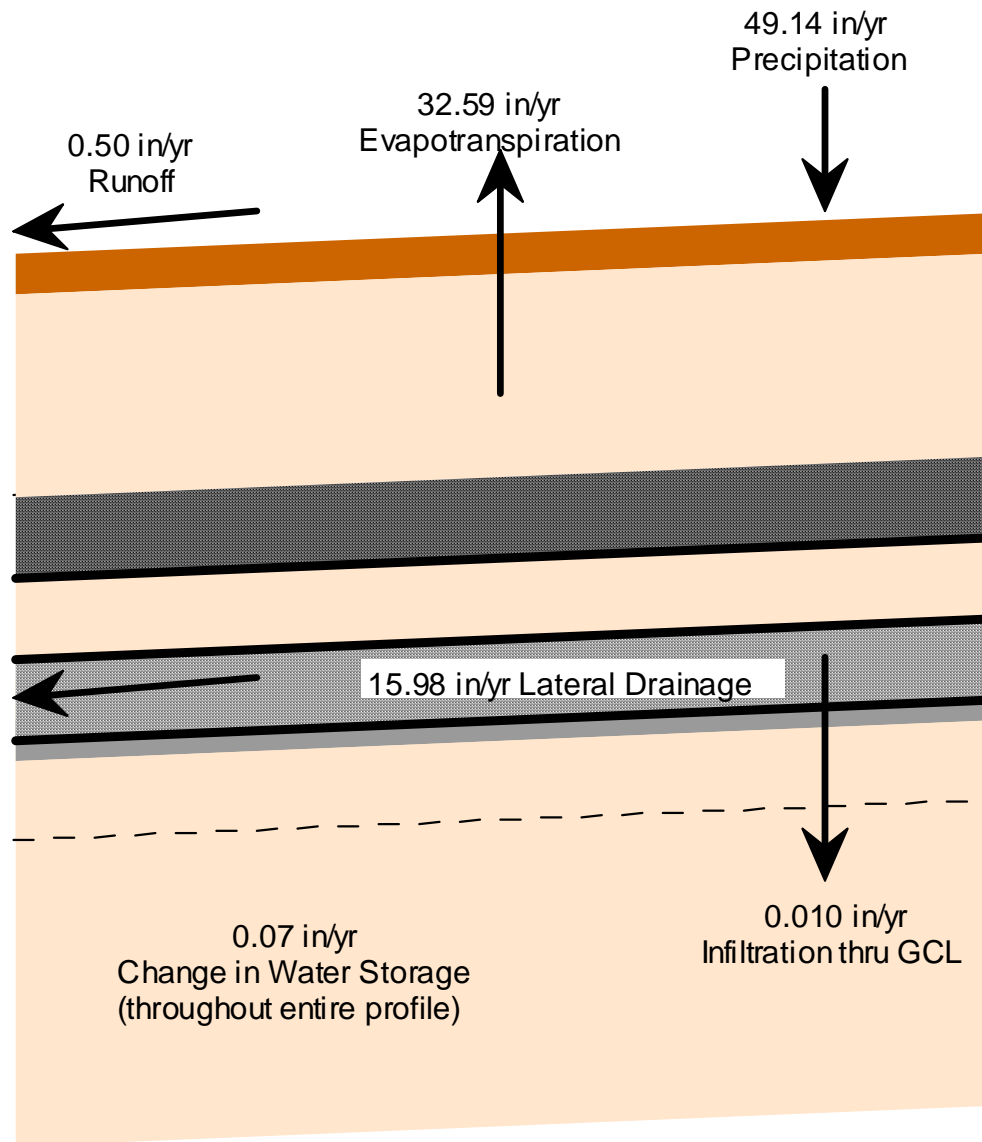
Figure 47.   Configuration #1a at Year 100 HELP Model Simulations – Average Water Balance
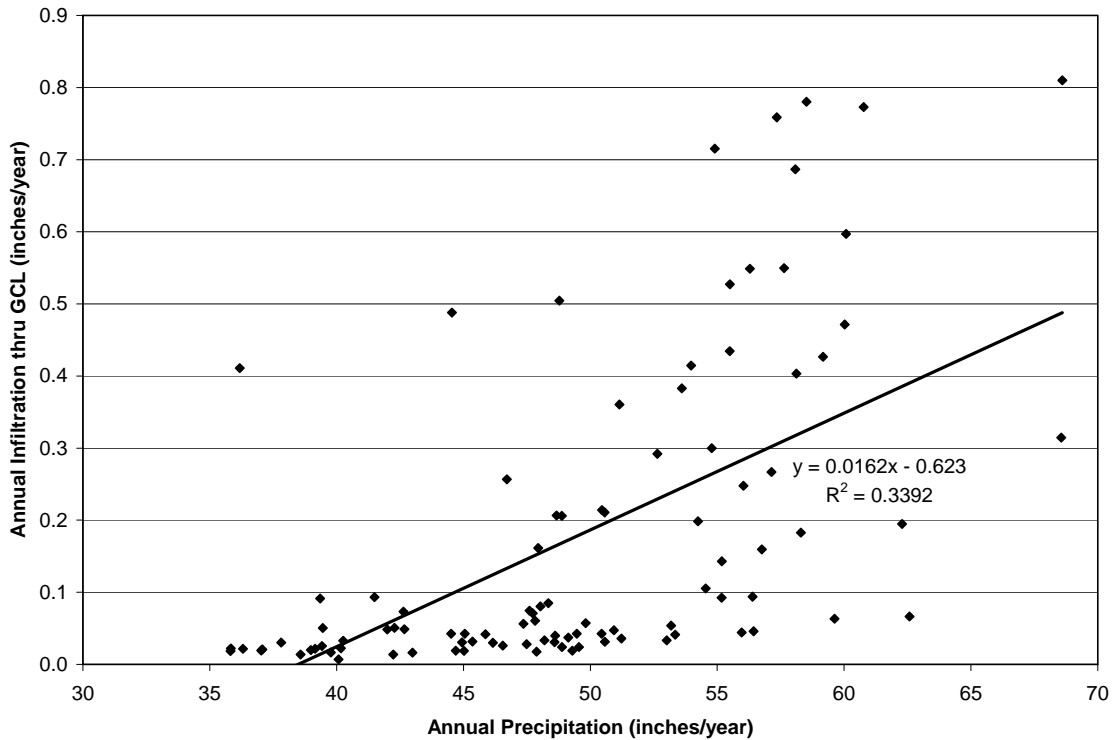
Figure 48.   Configuration #1a at Year 180 HELP Model Simulations - Annual Infiltration thru GCL versus Annual Precipitation

Table 68.   Configuration #1a at Year 180 HELP Model Simulations - Water Balance Statistics

Parameter	Precipitation (in/yr)	Runoff (in/yr)	Evapotrans-piration (in/yr)	Lateral Drainage (in/yr)	Infiltration thru GCL (in/yr)	Change in Water Storage (in/yr)
Count	100.00	100.00	100.00	100.00	100.00	100.00
Maximum	68.60	3.84	41.44	27.22	0.81	5.99
Average	49.14	0.56	32.58	15.76	0.17	0.09
Median	48.83	0.07	32.56	15.31	0.06	0.38
Minimum	29.81	0.00	21.65	4.40	0.01	-6.93
Std Dev	7.69	0.96	3.39	4.77	0.21	2.83
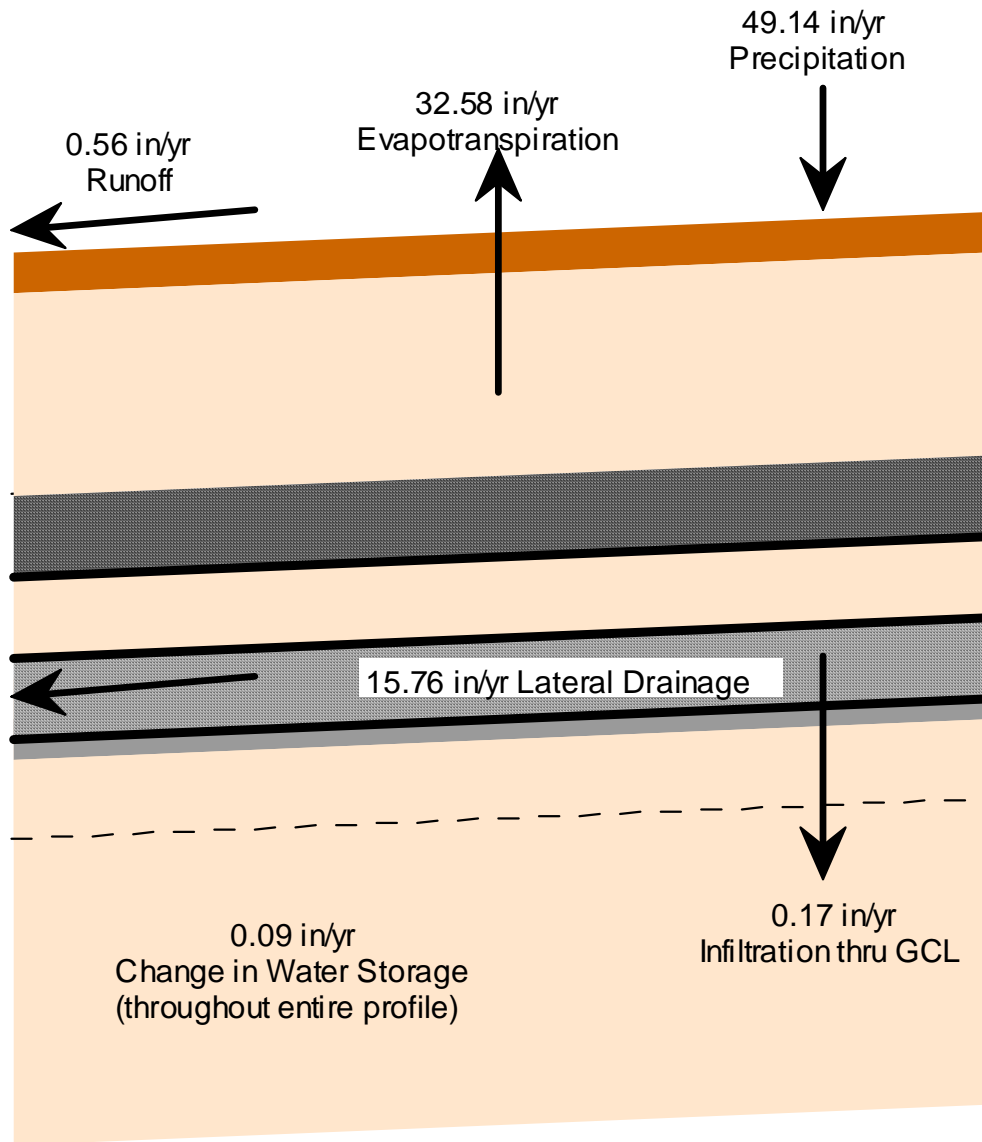
Figure 49. Configuration #1a at Year 180 HELP Model Simulations – Average Water Balance
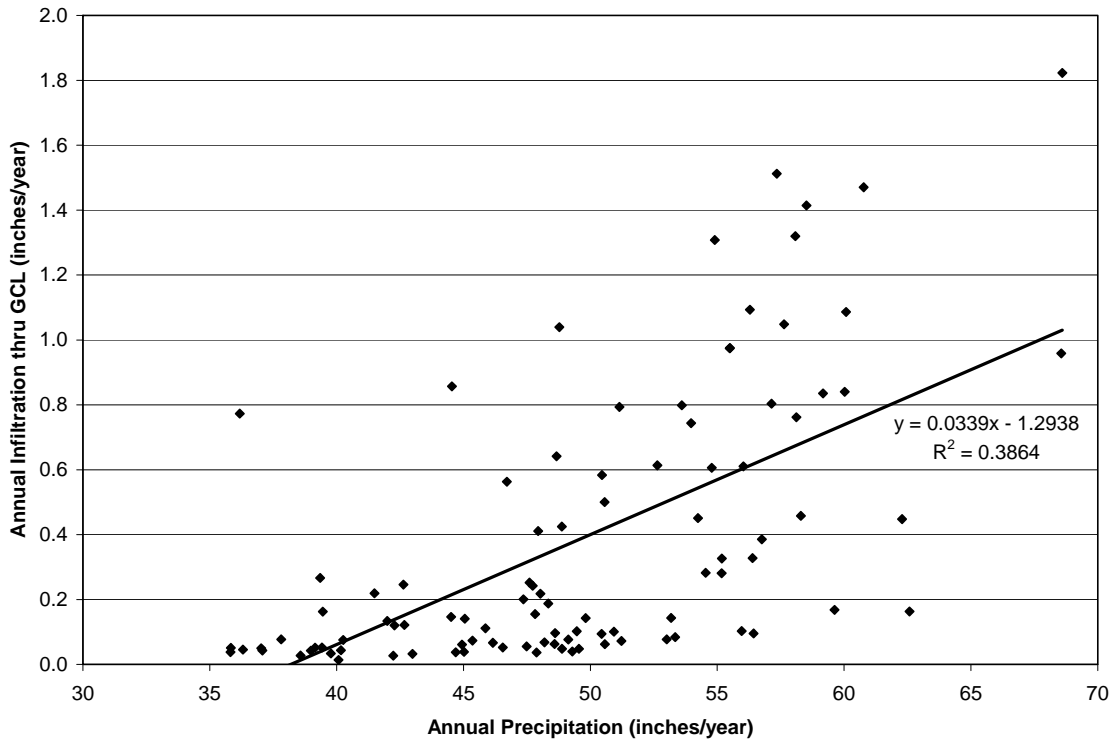
Figure 50. Configuration #1a at Year 290 HELP Model Simulations - Annual Infiltration thru GCL versus Annual Precipitation

Table 69. Configuration #1a at Year 290 HELP Model Simulations - Water Balance Statistics

Parameter	Precipitation (in/yr)	Runoff (in/yr)	Evapotrans-piration (in/yr)	Lateral Drainage (in/yr)	Infiltration thru GCL (in/yr)	Change in Water Storage (in/yr)
Count	100.00	100.00	100.00	100.00	100.00	100.00
Maximum	68.60	4.51	41.44	25.32	1.82	6.62
Average	49.14	0.68	32.58	15.44	0.37	0.10
Median	48.83	0.09	32.58	15.18	0.16	0.25
Minimum	29.81	0.00	21.63	4.18	0.01	-7.05
Std Dev	7.69	1.13	3.40	4.39	0.42	2.96
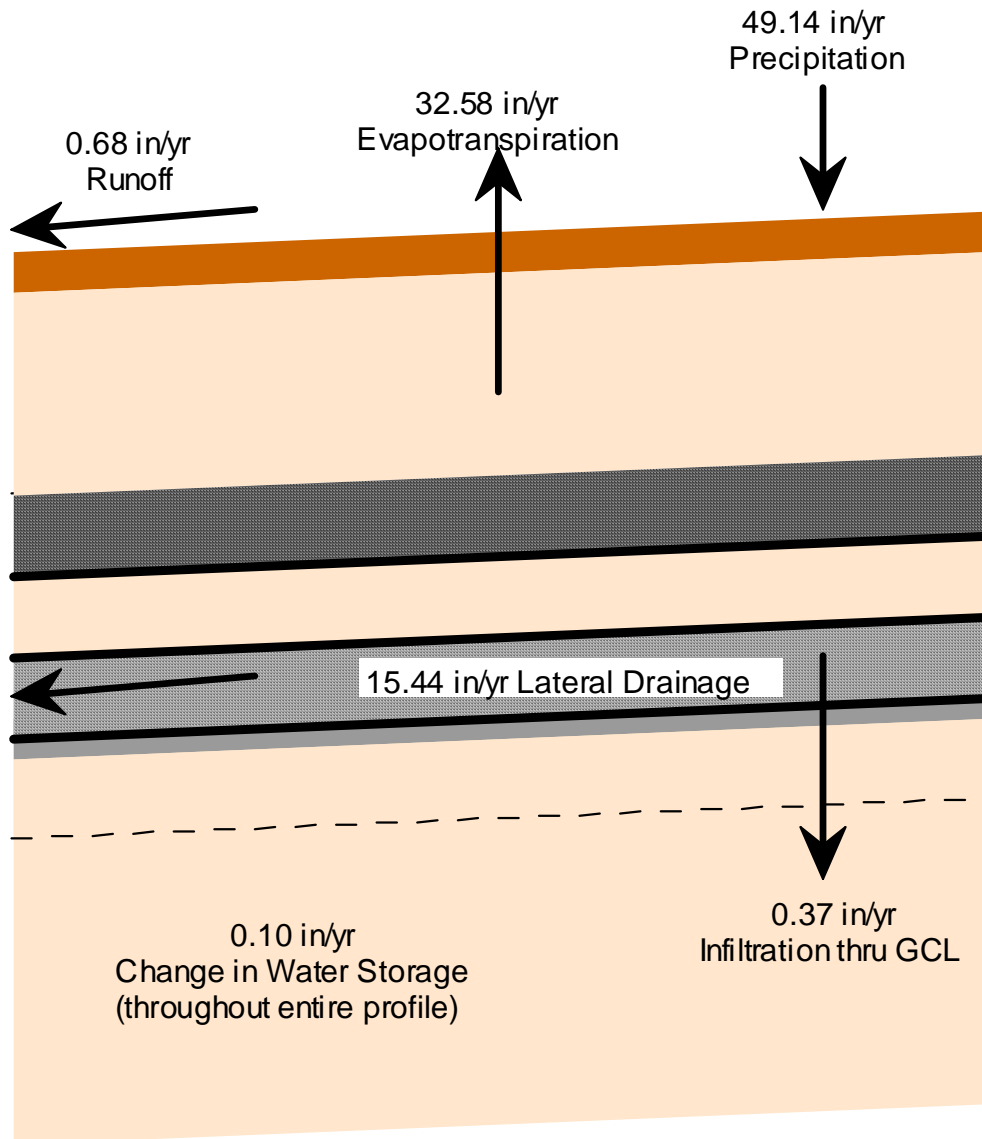
Figure 51. Configuration #1a at Year 290 HELP Model Simulations – Average Water Balance
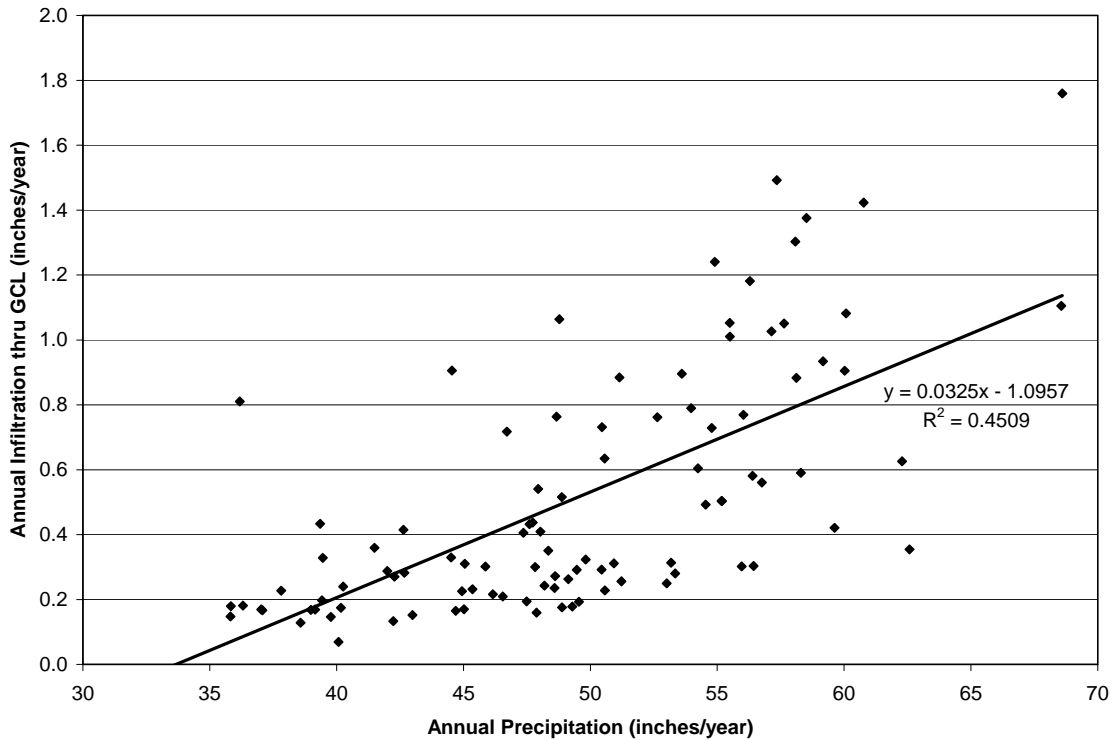
Figure 52. **Configuration #1a at Year 300 HELP Model Simulations - Annual Infiltration thru GCL versus Annual Precipitation**

Table 70. **Configuration #1a at Year 300 HELP Model Simulations - Water Balance Statistics**

Parameter	Precipitation (in/yr)	Runoff (in/yr)	Evapotrans-piration (in/yr)	Lateral Drainage (in/yr)	Infiltration thru GCL (in/yr)	Change in Water Storage (in/yr)
Count	100.00	100.00	100.00	100.00	100.00	100.00
Maximum	68.60	4.60	41.43	25.08	1.76	6.61
Average	49.14	0.71	32.59	15.28	0.50	0.10
Median	48.83	0.09	32.57	15.01	0.33	0.16
Minimum	29.81	0.00	21.65	4.10	0.07	-6.85
Std Dev	7.69	1.16	3.40	4.36	0.37	2.96

49.14 in/yr
Precipitation

32.59 in/yr
Evapotranspiration

0.71 in/yr
Runoff

15.28 in/yr Lateral Drainage

0.10 in/yr
Change in Water Storage
(throughout entire profile)

0.50 in/yr
Infiltration thru GCL
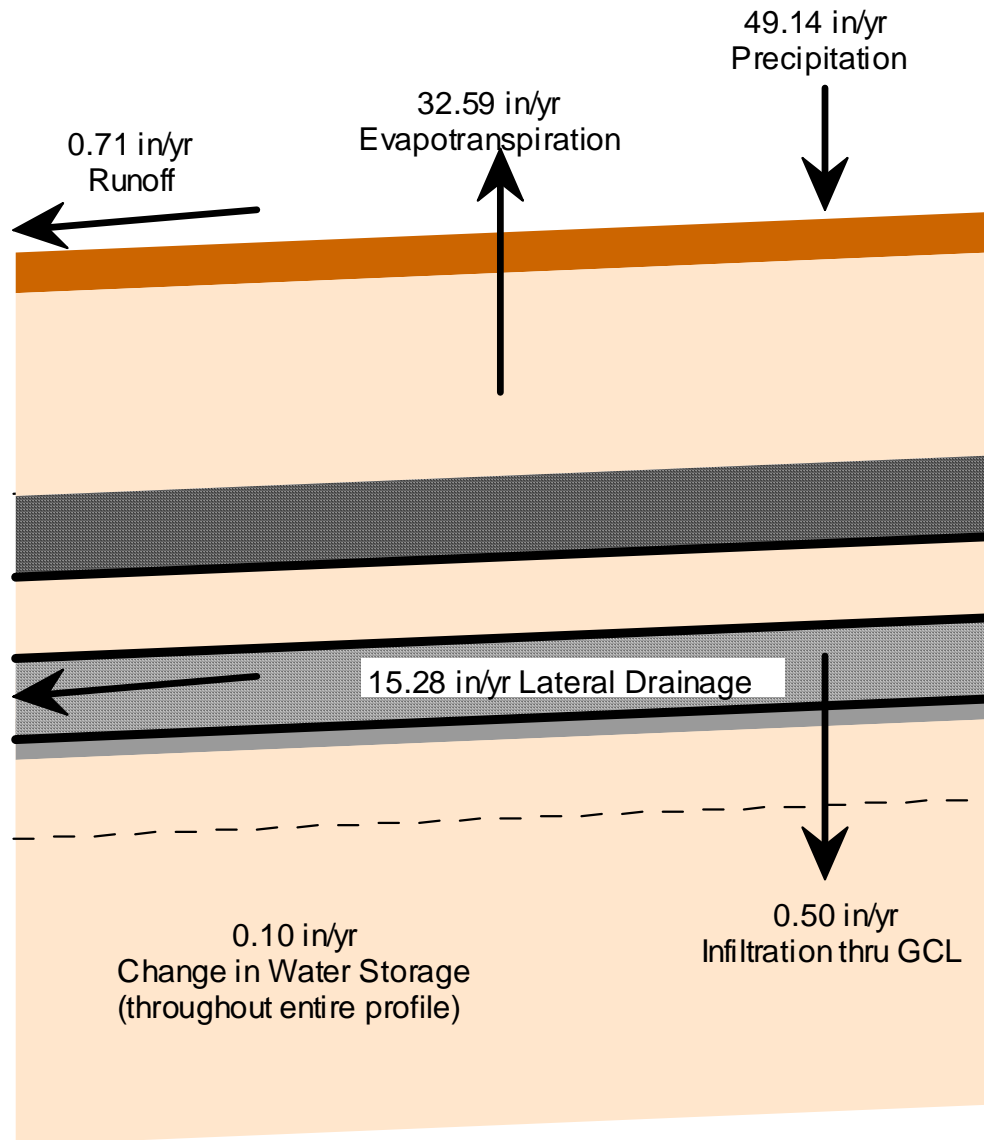
Figure 53. Configuration #1a at Year 300 HELP Model Simulations – Average Water Balance
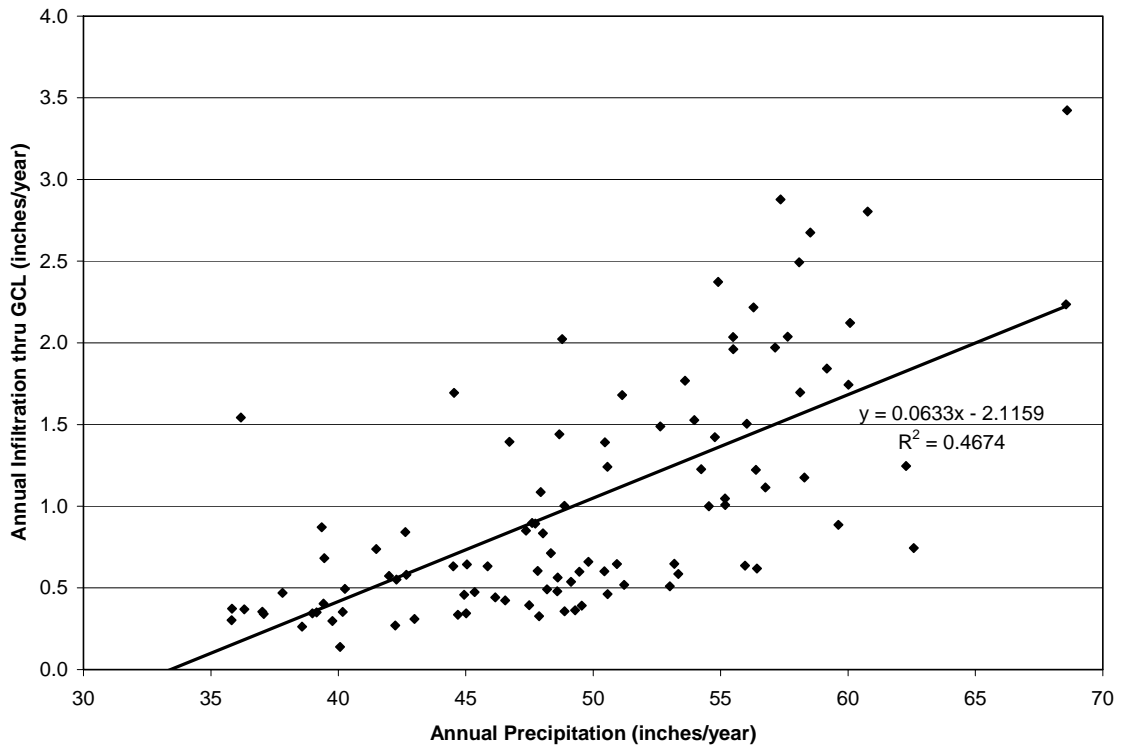
Figure 54. **Configuration #1a at Year 340 HELP Model Simulations - Annual Infiltration thru GCL versus Annual Precipitation**

Table 71. **Configuration #1a at Year 340 HELP Model Simulations - Water Balance Statistics**

Parameter	Precipitation (in/yr)	Runoff (in/yr)	Evapotrans-piration (in/yr)	Lateral Drainage (in/yr)	Infiltration thru GCL (in/yr)	Change in Water Storage (in/yr)
Count	100.00	100.00	100.00	100.00	100.00	100.00
Maximum	68.60	4.60	41.45	23.84	3.42	7.26
Average	49.14	0.69	32.58	14.81	1.00	0.10
Median	48.83	0.09	32.55	14.63	0.67	0.16
Minimum	29.81	0.00	21.66	3.98	0.14	-6.76
Std Dev	7.69	1.13	3.40	4.09	0.71	3.04
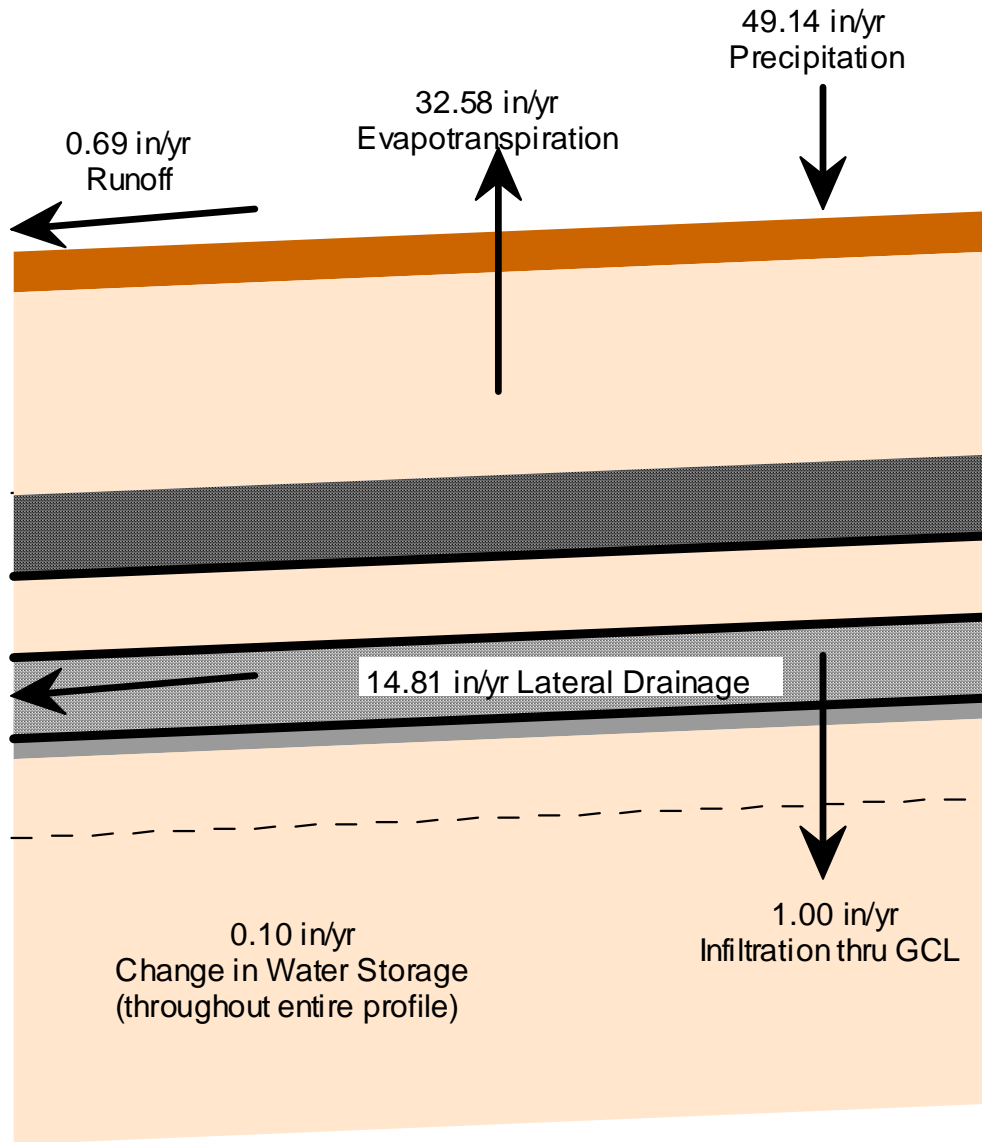
Figure 55. Configuration #1a at Year 340 HELP Model Simulations – Average Water Balance
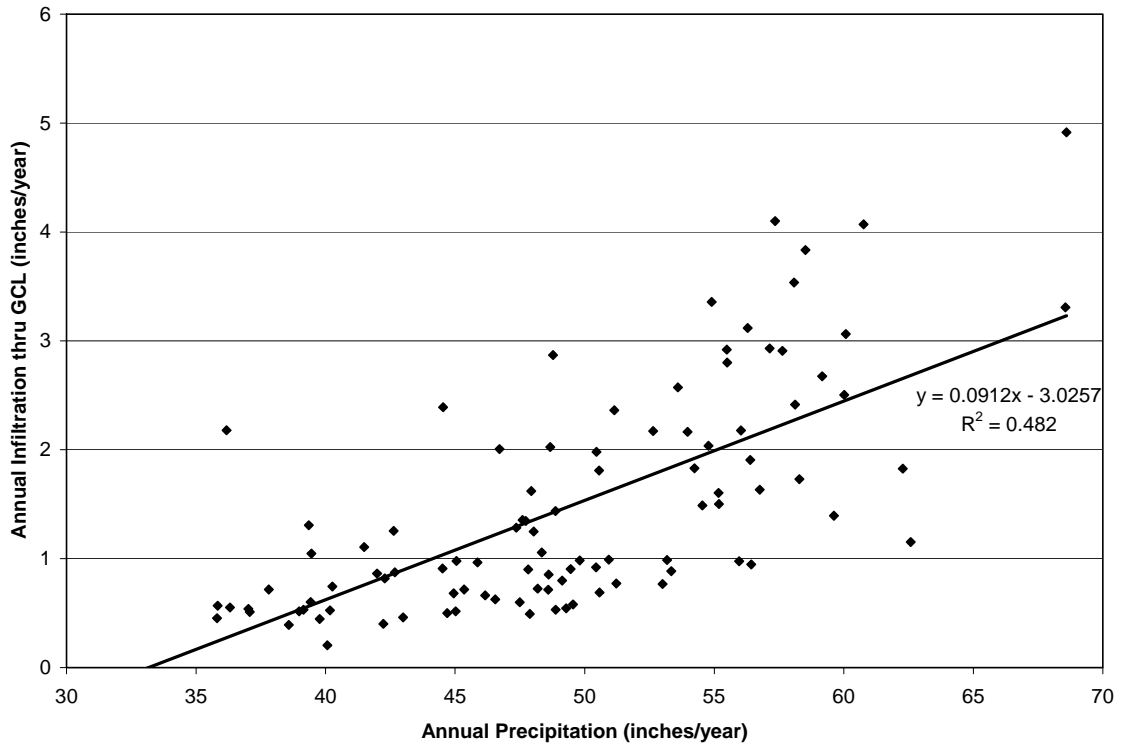
Figure 56. **Configuration #1a at Year 380 HELP Model Simulations - Annual Infiltration thru GCL versus Annual Precipitation**

Table 72. **Configuration #1a at Year 380 HELP Model Simulations - Water Balance Statistics**

Parameter	Precipitation (in/yr)	Runoff (in/yr)	Evapotrans-piration (in/yr)	Lateral Drainage (in/yr)	Infiltration thru GCL (in/yr)	Change in Water Storage (in/yr)
Count	100.00	100.00	100.00	100.00	100.00	100.00
Maximum	68.60	4.62	41.42	22.68	4.92	7.92
Average	49.14	0.68	32.58	14.36	1.46	0.11
Median	48.83	0.09	32.55	14.21	1.02	0.01
Minimum	29.81	0.00	21.66	3.89	0.21	-7.08
Std Dev	7.69	1.12	3.40	3.85	1.01	3.16
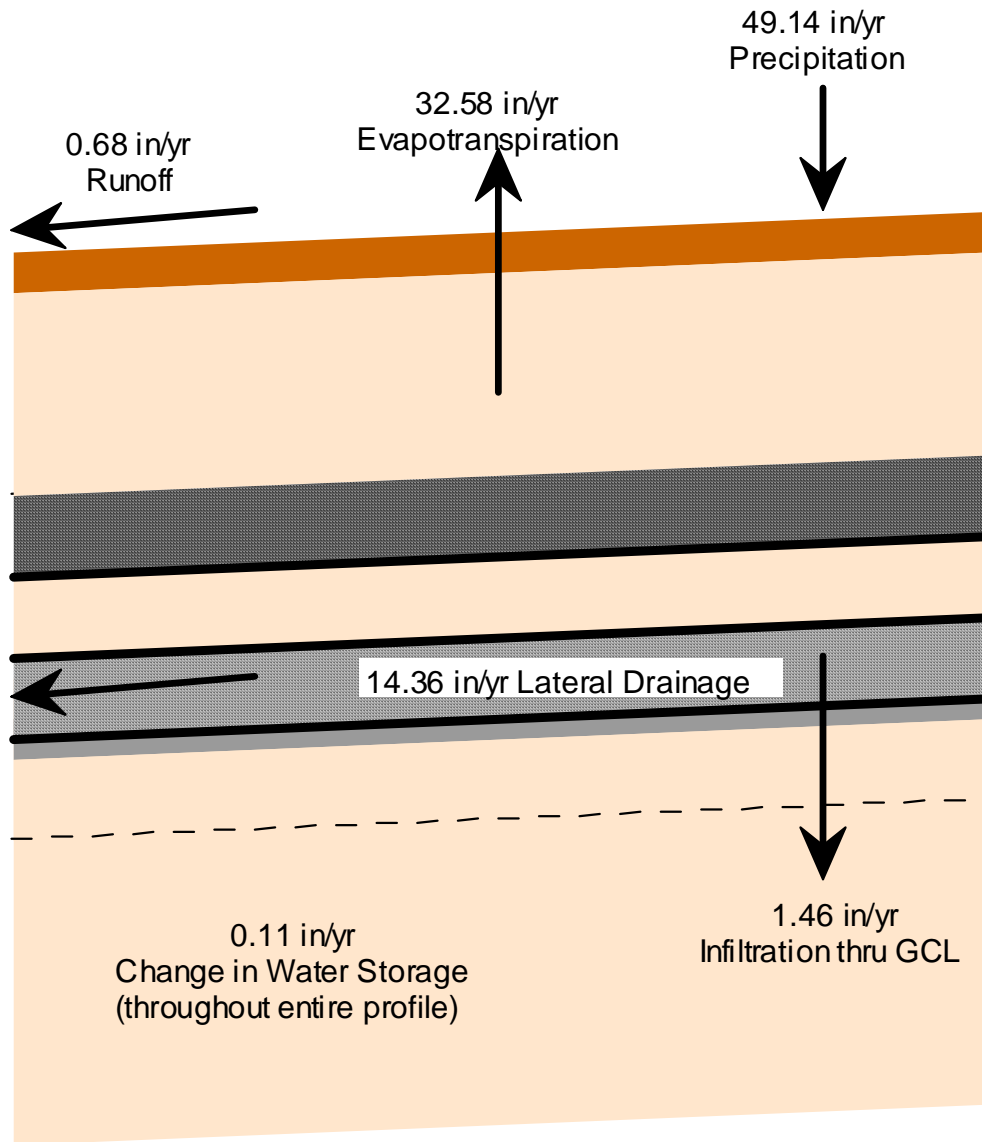
Figure 57. Configuration #1a at Year 380 HELP Model Simulations – Average Water Balance

The chart shows: $y = 0.1576x - 4.5151$, $R^2 = 0.5641$
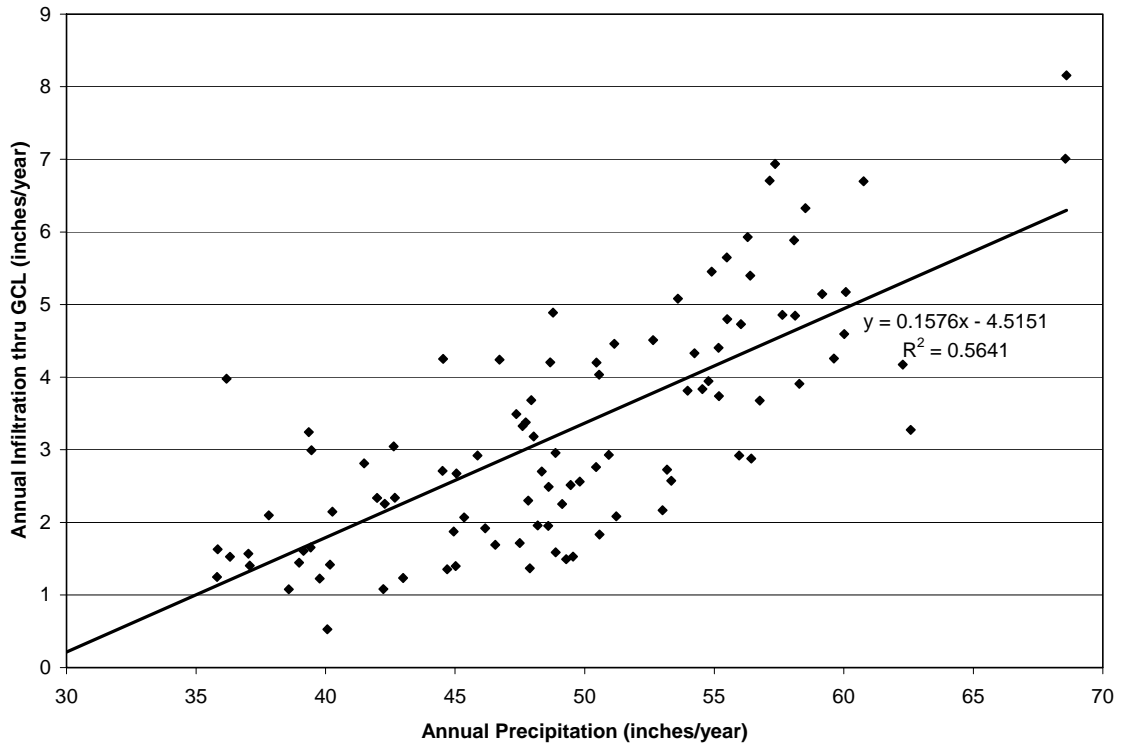
Figure 58. Configuration #1a at Year 560 HELP Model Simulations - Annual Infiltration thru GCL versus Annual Precipitation

Table 73. Configuration #1a at Year 560 HELP Model Simulations - Water Balance Statistics

Parameter	Precipitation (in/yr)	Runoff (in/yr)	Evapotrans-piration (in/yr)	Lateral Drainage (in/yr)	Infiltration thru GCL (in/yr)	Change in Water Storage (in/yr)
Count	100.00	100.00	100.00	100.00	100.00	100.00
Maximum	68.60	4.85	41.44	18.57	8.16	8.34
Average	49.14	0.79	32.59	12.46	3.23	0.12
Median	48.83	0.12	32.55	12.43	2.92	0.12
Minimum	29.81	0.00	21.63	3.33	0.52	-8.40
Std Dev	7.69	1.27	3.41	3.03	1.61	3.53
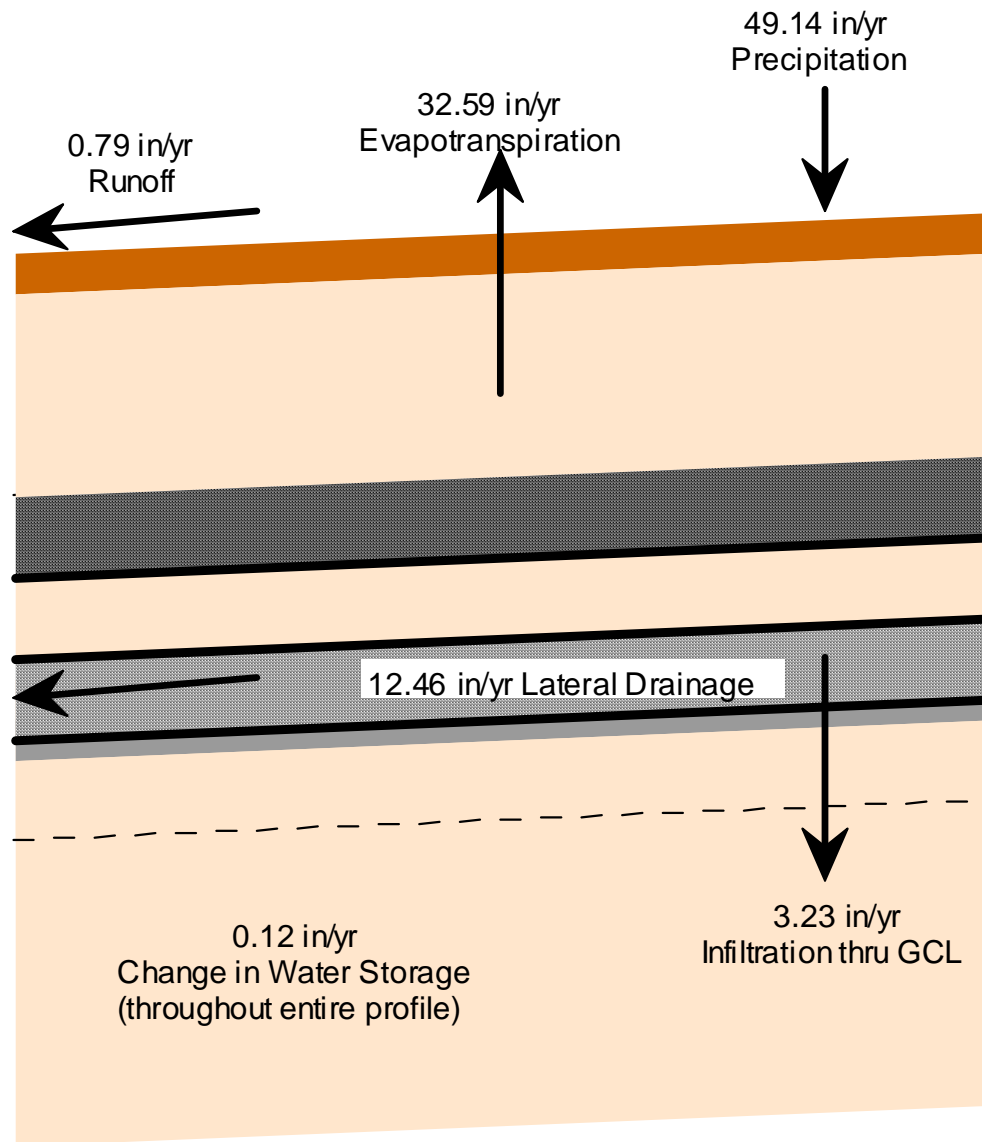
Figure 59. Configuration #1a at Year 560 HELP Model Simulations – Average Water Balance
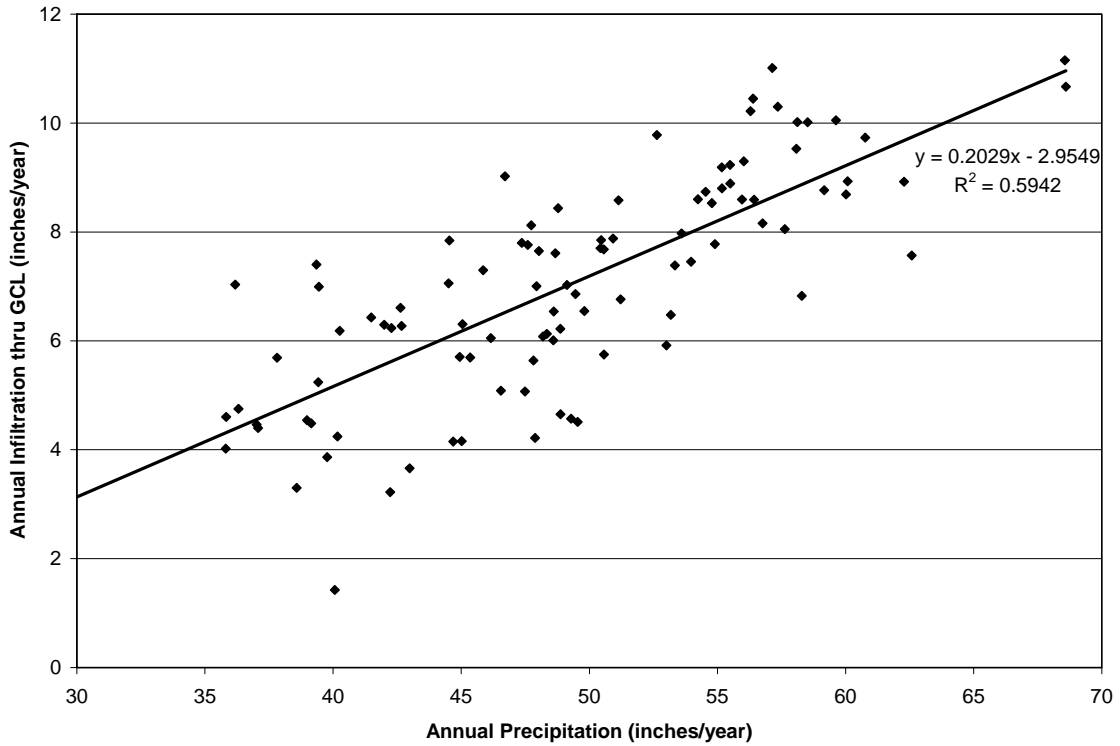
Figure 60. **Configuration #1a at Year 1,000 HELP Model Simulations - Annual Infiltration thru GCL versus Annual Precipitation**

Table 74. **Configuration #1a at Year 1,000 HELP Model Simulations - Water Balance Statistics**

Parameter	Precipitation (in/yr)	Runoff (in/yr)	Evapotrans-piration (in/yr)	Lateral Drainage (in/yr)	Infiltration thru GCL (in/yr)	Change in Water Storage (in/yr)
Count	100.00	100.00	100.00	100.00	100.00	100.00
Maximum	68.60	7.10	41.40	11.31	11.15	7.93
Average	49.14	1.29	32.69	8.07	7.01	0.14
Median	48.83	0.36	32.65	8.22	7.03	0.09
Minimum	29.81	0.00	21.67	2.07	1.43	-9.56
Std Dev	7.69	1.96	3.47	1.78	2.02	3.93
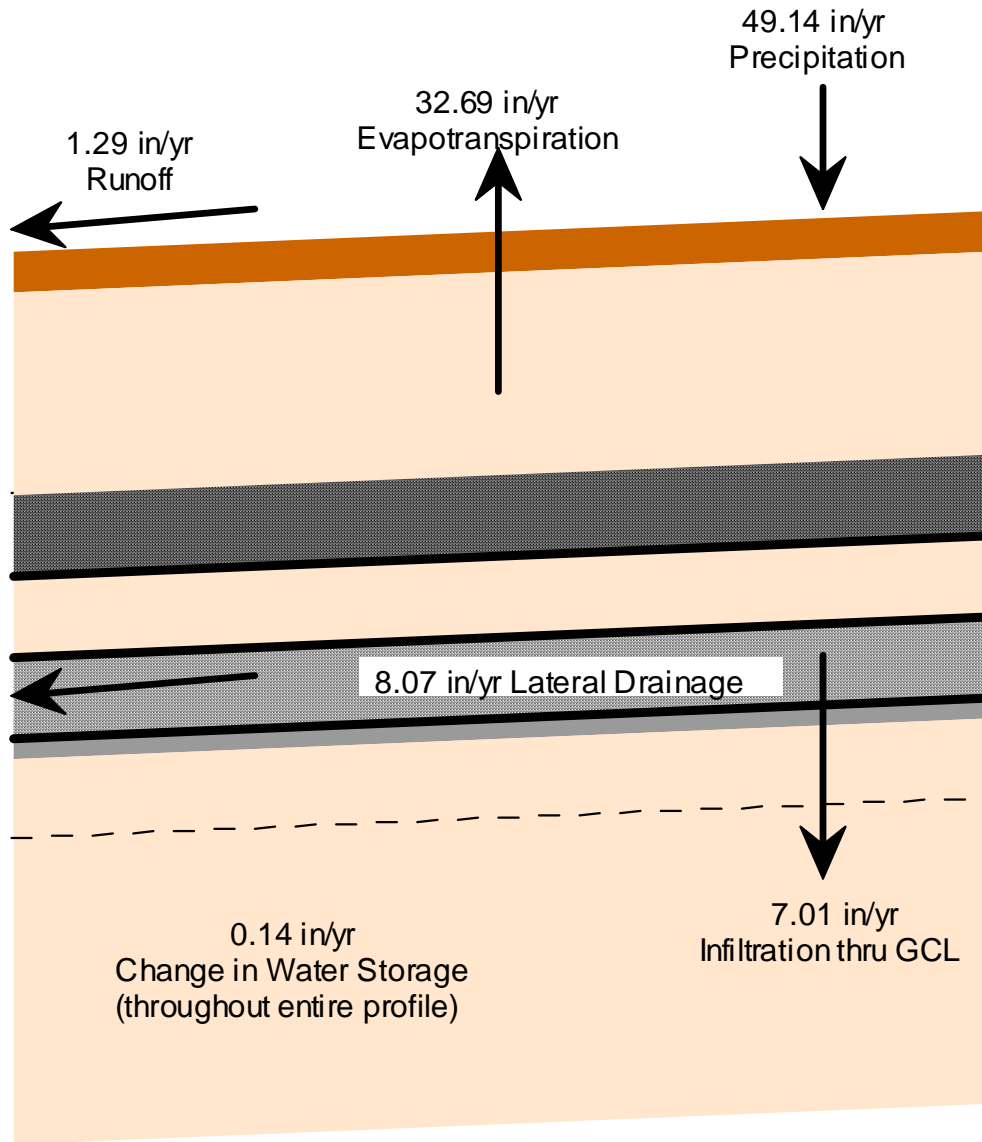
Figure 61. Configuration #1a at Year 1,000 HELP Model Simulations – Average Water Balance
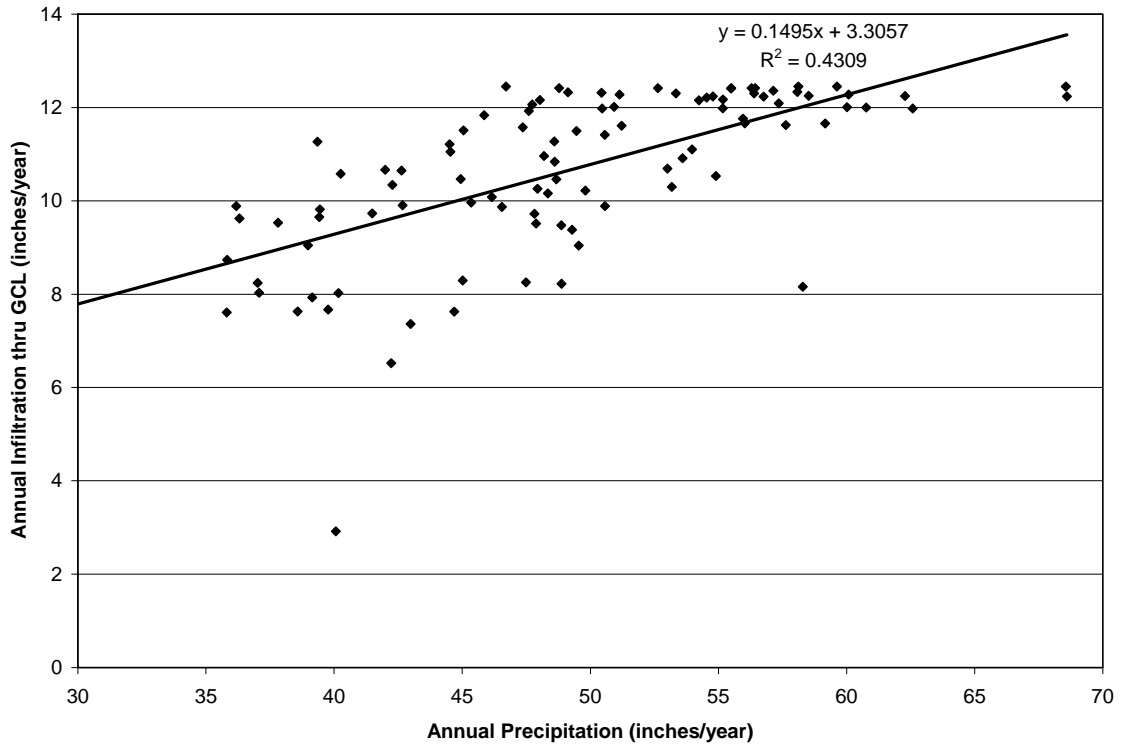
Figure 62. Configuration #1a at Year 1,800 HELP Model Simulations - Annual Infiltration thru GCL versus Annual Precipitation

Table 75. Configuration #1a at Year 1,800 HELP Model Simulations - Water Balance Statistics

Parameter	Precipitation (in/yr)	Runoff (in/yr)	Evapotrans-piration (in/yr)	Lateral Drainage (in/yr)	Infiltration thru GCL (in/yr)	Change in Water Storage (in/yr)
Count	100.00	100.00	100.00	100.00	100.00	100.00
Maximum	68.60	11.00	42.08	4.79	12.45	8.74
Average	49.14	2.08	32.99	3.35	10.65	0.15
Median	48.83	0.67	32.75	3.47	11.08	0.00
Minimum	29.81	0.00	21.77	0.69	2.92	-10.51
Std Dev	7.69	2.85	3.63	0.84	1.75	4.08
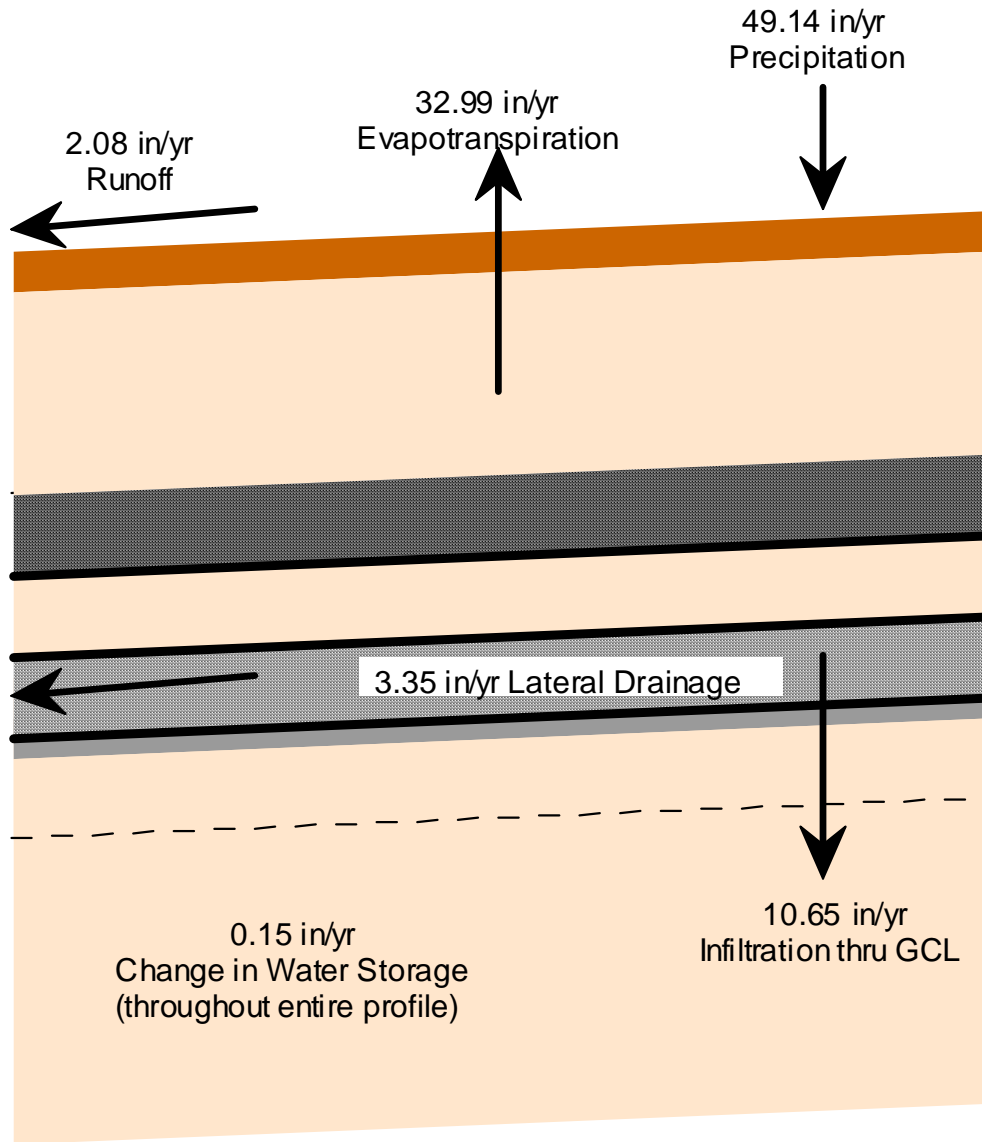
Figure 63. Configuration #1a at Year 1,800 HELP Model Simulations – Average Water Balance
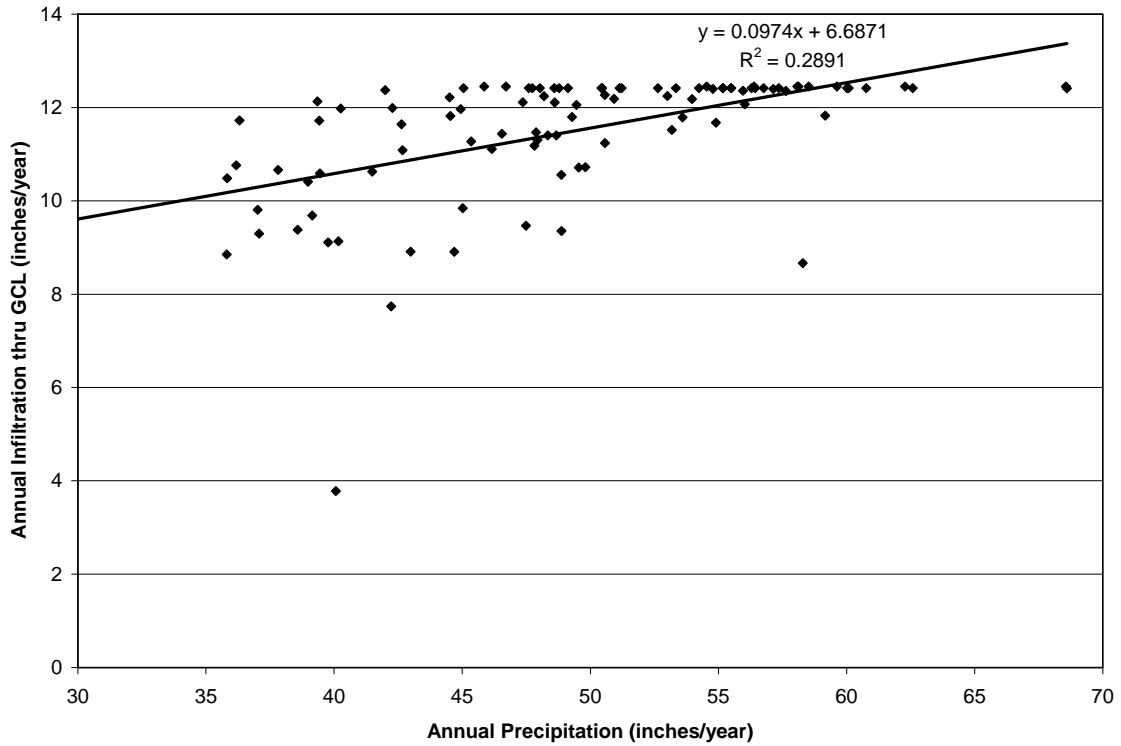
Figure 64. Configuration #1a at Year 2,623 HELP Model Simulations - Annual Infiltration thru GCL versus Annual Precipitation

Table 76. Configuration #1a at Year 2,623 HELP Model Simulations - Water Balance Statistics

Parameter	Precipitation (in/yr)	Runoff (in/yr)	Evapotrans-piration (in/yr)	Lateral Drainage (in/yr)	Infiltration thru GCL (in/yr)	Change in Water Storage (in/yr)
Count	100.00	100.00	100.00	100.00	100.00	100.00
Maximum	68.60	12.33	42.19	3.10	12.45	9.34
Average	49.14	2.49	33.16	1.96	11.47	0.15
Median	48.83	1.13	32.85	2.06	12.11	0.30
Minimum	29.81	0.00	22.41	0.19	3.78	-10.73
Std Dev	7.69	3.20	3.63	0.66	1.39	4.10
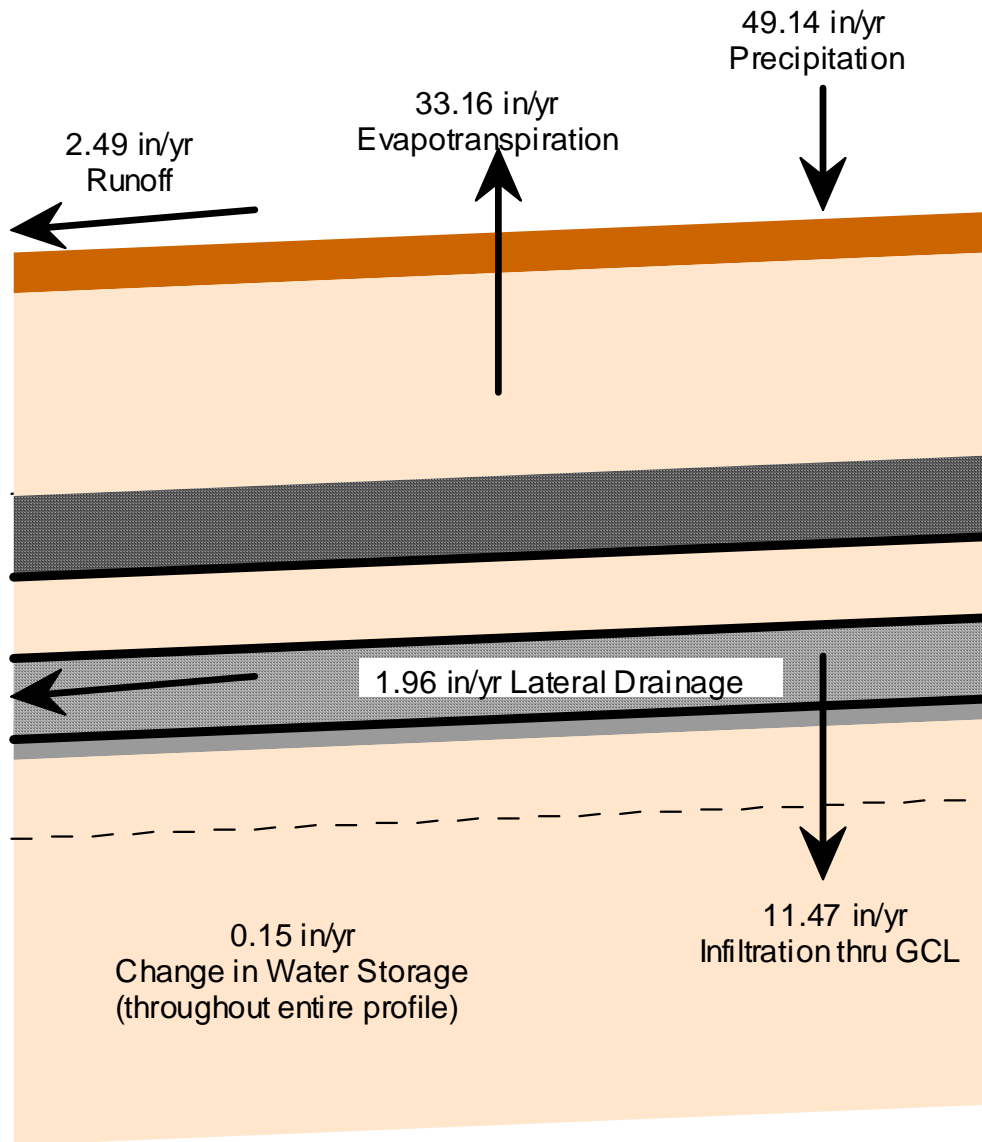
Figure 65.   Configuration #1a at Year 2,623 HELP Model Simulations – Average Water Balance

49.14 in/yr Precipitation

33.16 in/yr Evapotranspiration

2.49 in/yr Runoff

1.96 in/yr Lateral Drainage

0.15 in/yr Change in Water Storage (throughout entire profile)

11.47 in/yr Infiltration thru GCL

$$y = 0.0933x + 6.9434$$
$$R^2 = 0.2779$$
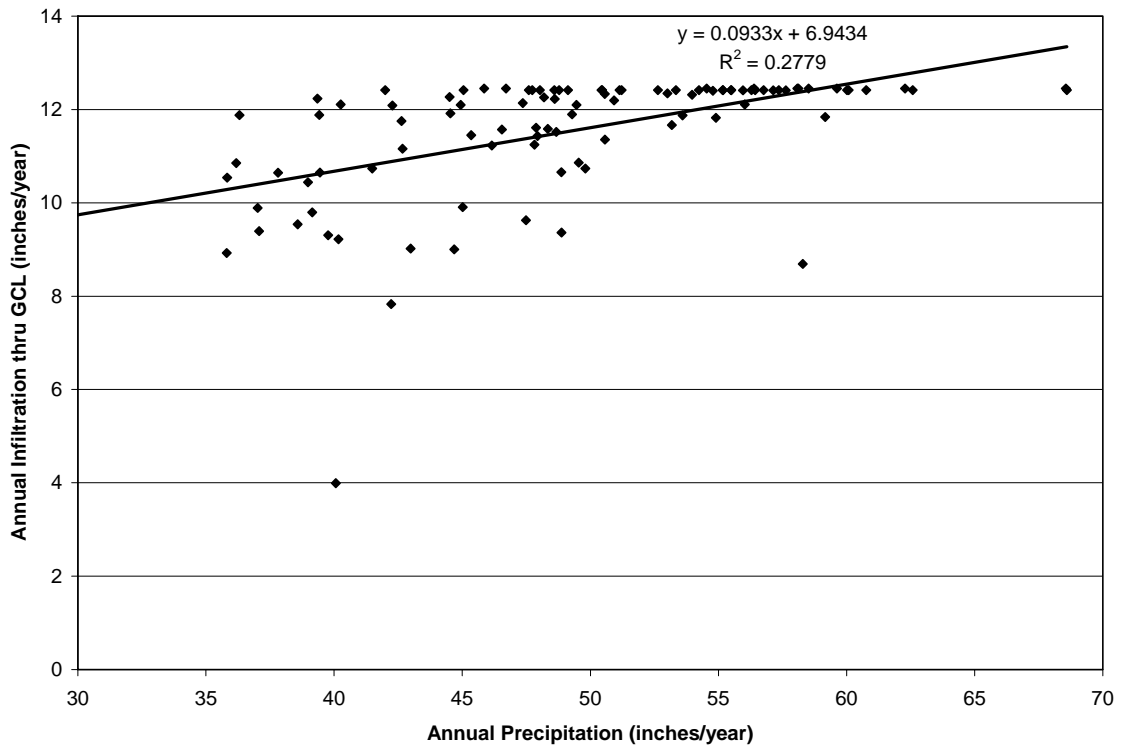
Figure 66. Configuration #1a at Year 3,200 HELP Model Simulations - Annual Infiltration thru GCL versus Annual Precipitation

Table 77. Configuration #1a at Year 3,200 HELP Model Simulations - Water Balance Statistics

Parameter	Precipitation (in/yr)	Runoff (in/yr)	Evapotrans-piration (in/yr)	Lateral Drainage (in/yr)	Infiltration thru GCL (in/yr)	Change in Water Storage (in/yr)
Count	100.00	100.00	100.00	100.00	100.00	100.00
Maximum	68.60	12.36	42.14	3.09	12.45	9.42
Average	49.14	2.47	33.14	1.93	11.53	0.15
Median	48.83	1.09	32.81	2.05	12.17	0.33
Minimum	29.81	0.00	22.41	0.17	3.99	-10.80
Std Dev	7.69	3.19	3.62	0.68	1.36	4.10

49.14 in/yr
Precipitation

33.14 in/yr
Evapotranspiration

2.47 in/yr
Runoff

1.93 in/yr Lateral Drainage

11.53 in/yr
Infiltration thru GCL

0.15 in/yr
Change in Water Storage
(throughout entire profile)
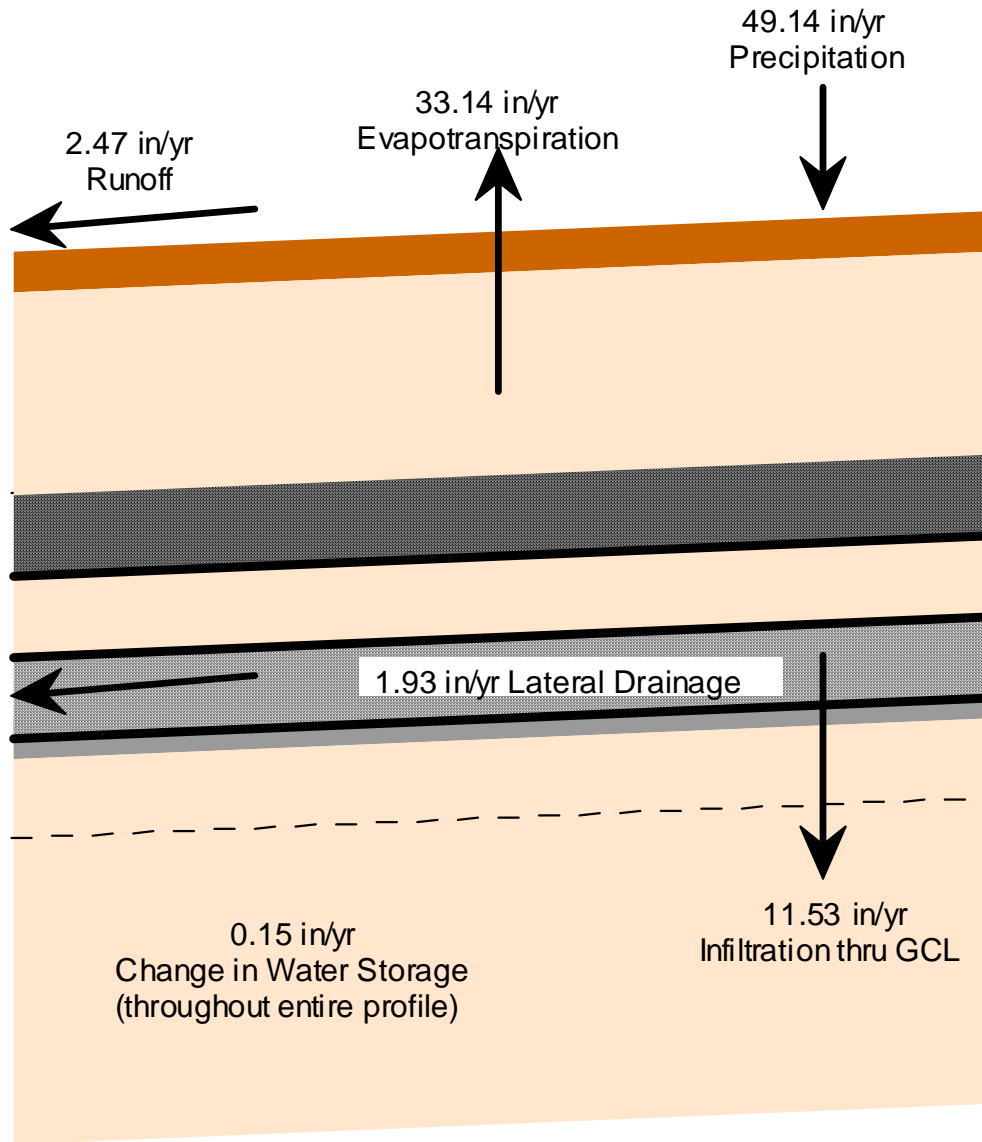
**Figure 67.   Configuration #1a at Year 3,200 HELP Model Simulations – Average
Water Balance**
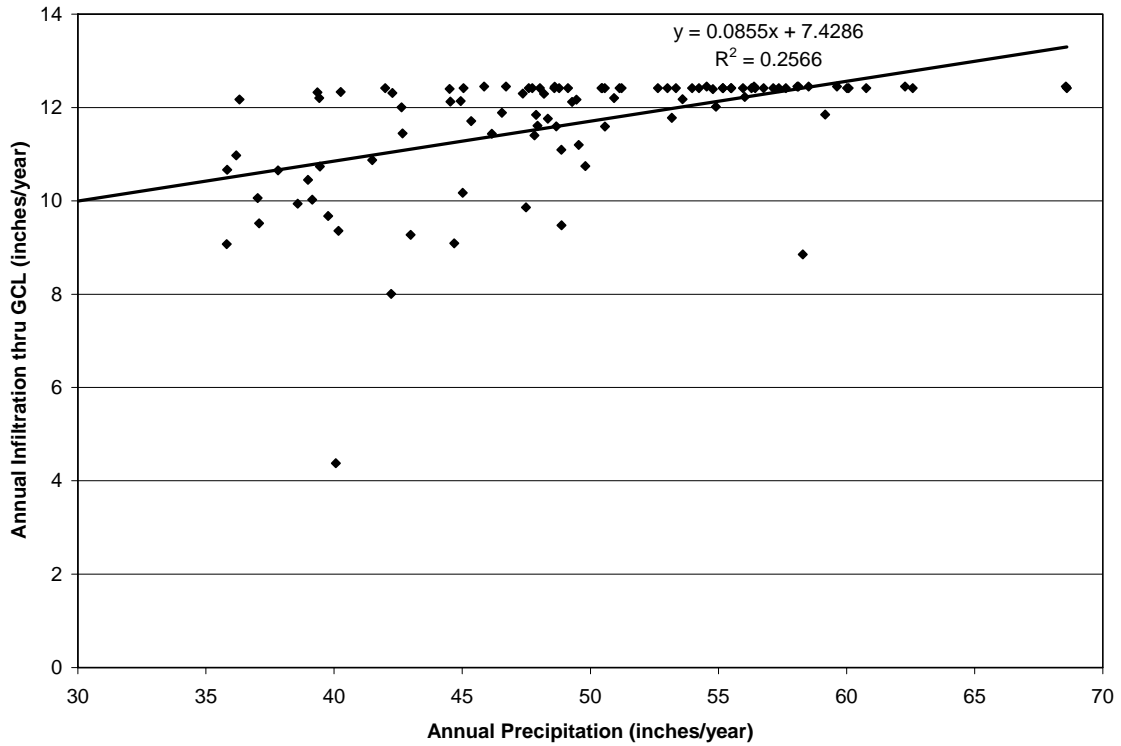
Figure 68. Configuration #1a at Year 5,600 HELP Model Simulations - Annual Infiltration thru GCL versus Annual Precipitation

Table 78. Configuration #1a at Year 5,600 HELP Model Simulations - Water Balance Statistics

Parameter	Precipitation (in/yr)	Runoff (in/yr)	Evapotrans-piration (in/yr)	Lateral Drainage (in/yr)	Infiltration thru GCL (in/yr)	Change in Water Storage (in/yr)
Count	100.00	100.00	100.00	100.00	100.00	100.00
Maximum	68.60	12.47	42.15	3.05	12.45	9.35
Average	49.14	2.46	33.10	1.88	11.63	0.15
Median	48.83	1.12	32.76	1.98	12.30	0.27
Minimum	29.81	0.00	22.34	0.14	4.38	-10.62
Std Dev	7.69	3.19	3.63	0.70	1.30	4.09

49.14 in/yr
Precipitation

33.10 in/yr
Evapotranspiration

2.46 in/yr
Runoff

1.88 in/yr Lateral Drainage

11.63 in/yr
Infiltration thru GCL

0.15 in/yr
Change in Water Storage
(throughout entire profile)
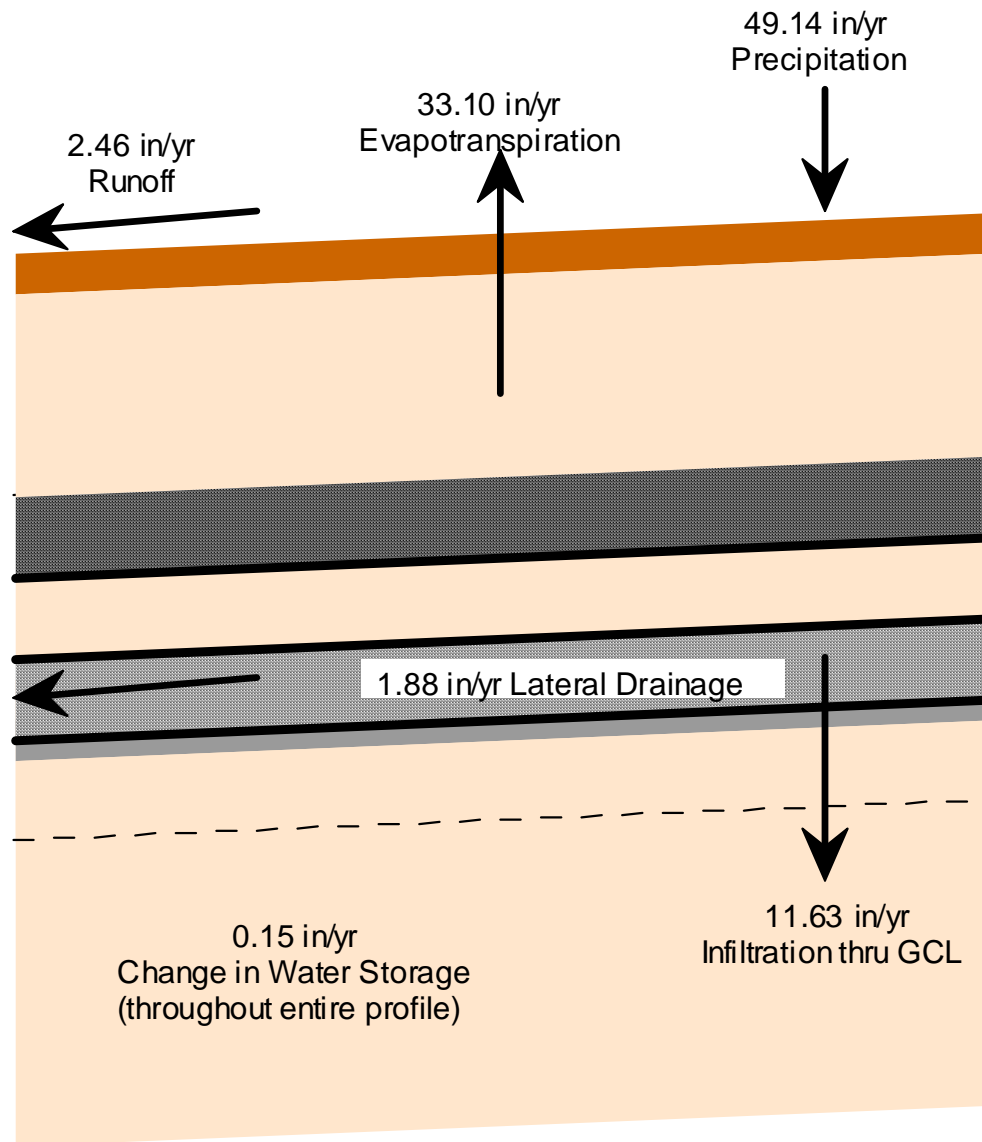
**Figure 69.   Configuration #1a at Year 5,600 HELP Model Simulations – Average
Water Balance**
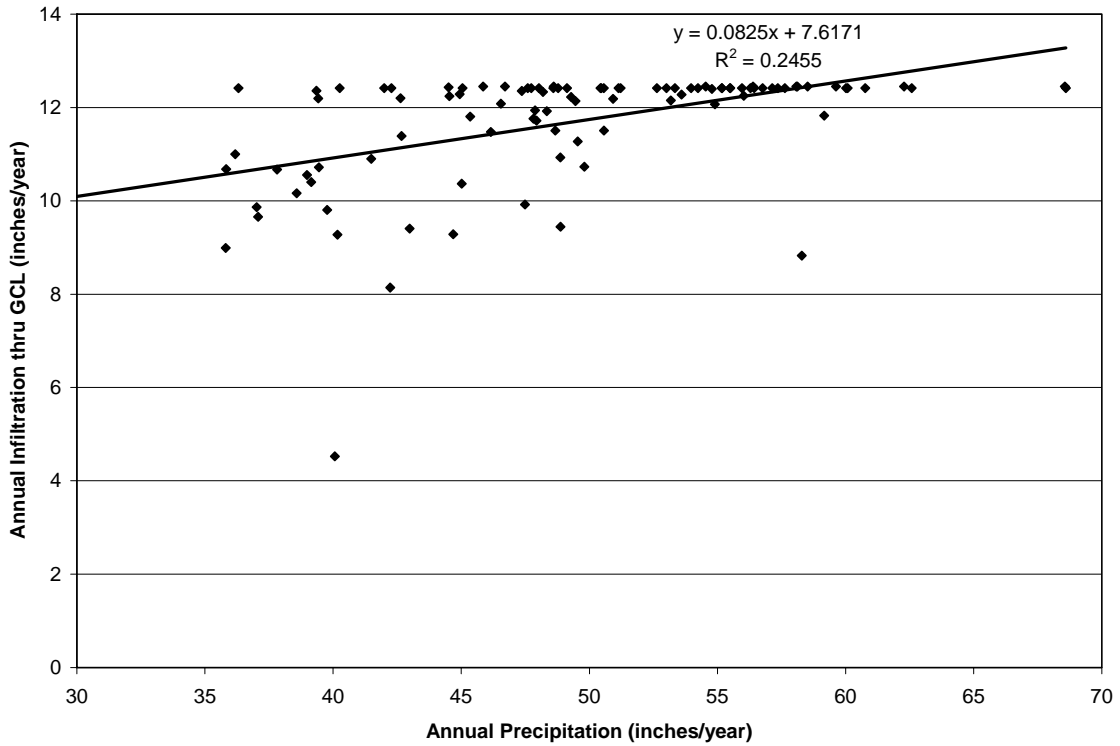
Figure 70. **Configuration #1a at Year 10,000 HELP Model Simulations - Annual Infiltration thru GCL versus Annual Precipitation**

Table 79. **Configuration #1a at Year 10,000 HELP Model Simulations - Water Balance Statistics**

Parameter	Precipitation (in/yr)	Runoff (in/yr)	Evapotrans-piration (in/yr)	Lateral Drainage (in/yr)	Infiltration thru GCL (in/yr)	Change in Water Storage (in/yr)
Count	100.00	100.00	100.00	100.00	100.00	100.00
Maximum	68.60	12.54	42.12	2.98	12.45	9.44
Average	49.14	2.53	33.03	1.84	11.67	0.15
Median	48.83	1.18	32.78	1.94	12.38	0.38
Minimum	29.81	0.00	22.29	0.11	4.53	-10.39
Std Dev	7.69	3.23	3.61	0.70	1.28	4.08
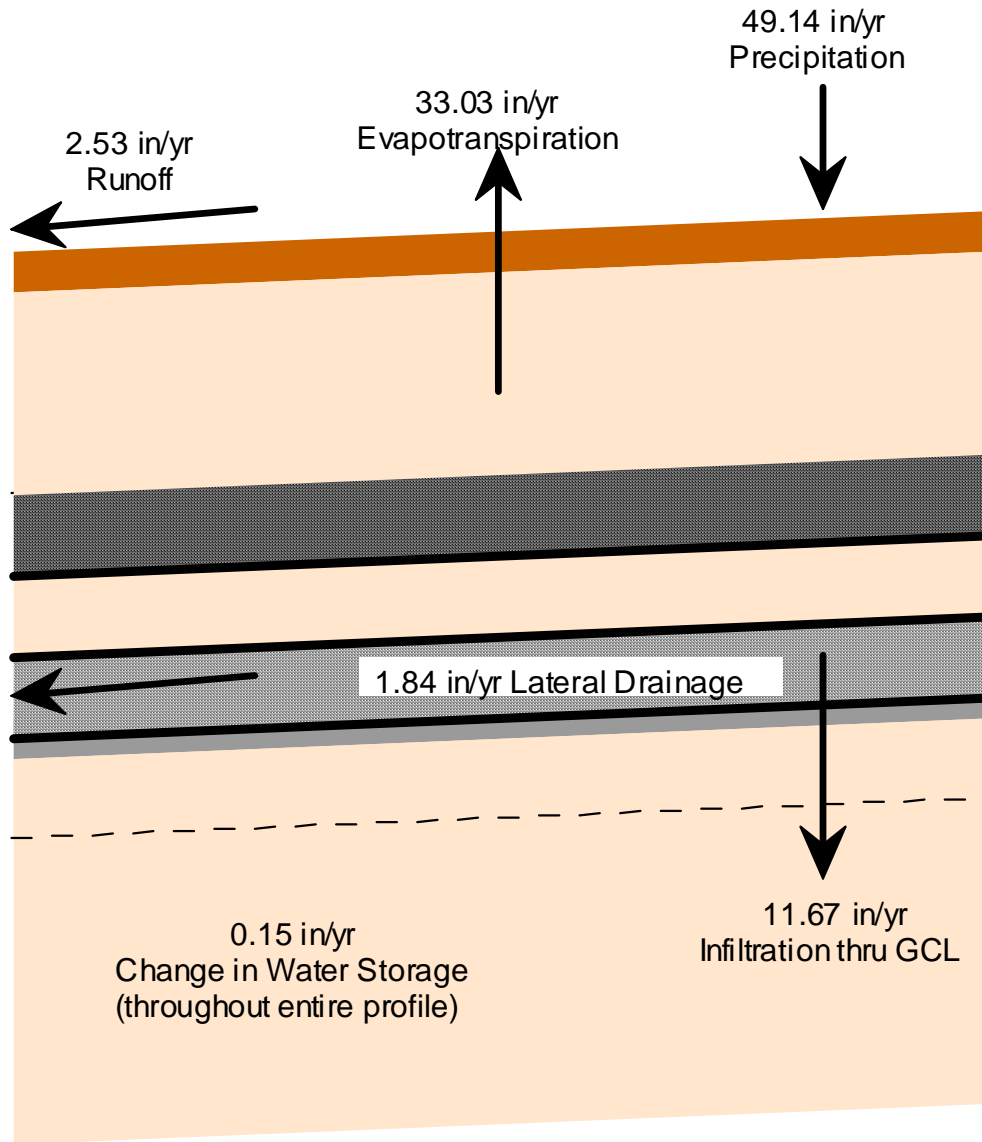
Figure 71. Configuration #1a at Year 10,000 HELP Model Simulations – Average Water Balance
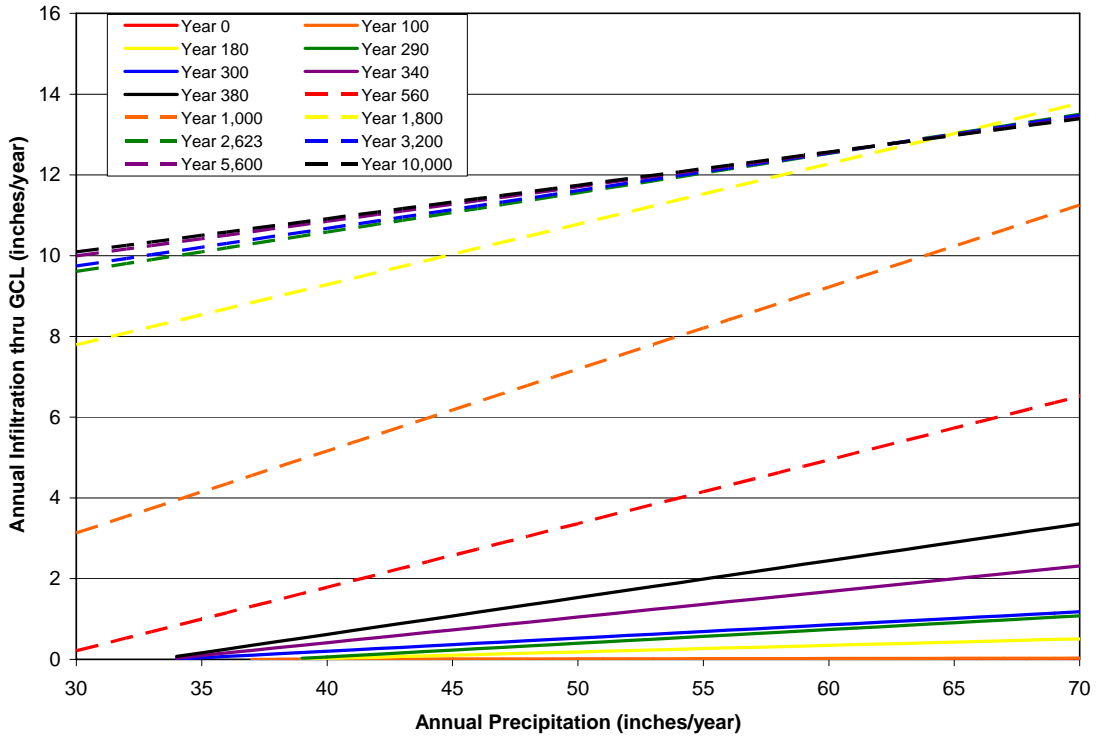
Figure 72. Configuration #1a Comparison of Modeled Time Steps - Annual Infiltration thru GCL versus Annual Precipitation

Table 80. Configuration #1a Comparison of Modeled Time Steps - Average Water Balance

Year	Precipitation (inch)	Runoff (inch)	Evapotrans-piration (inch)	Lateral Drainage (inch)	Infiltration thru GCL (inch)	Change in Water Storage (inch)
0	49.14	0.43	32.57	16.07	0.00088	0.06
100	49.14	0.50	32.59	15.98	0.010	0.07
180	49.14	0.56	32.58	15.76	0.17	0.09
290	49.14	0.68	32.58	15.44	0.37	0.10
300	49.14	0.71	32.59	15.28	0.50	0.10
340	49.14	0.69	32.58	14.81	1.00	0.10
380	49.14	0.68	32.58	14.36	1.46	0.11
560	49.14	0.79	32.59	12.46	3.23	0.12
1000	49.14	1.29	32.69	8.07	7.01	0.14
1800	49.14	2.08	32.99	3.35	10.65	0.15
2623	49.14	2.49	33.16	1.96	11.47	0.15
3200	49.14	2.47	33.14	1.93	11.53	0.15
5600	49.14	2.46	33.10	1.88	11.63	0.15
10000	49.14	2.53	33.03	1.84	11.67	0.15
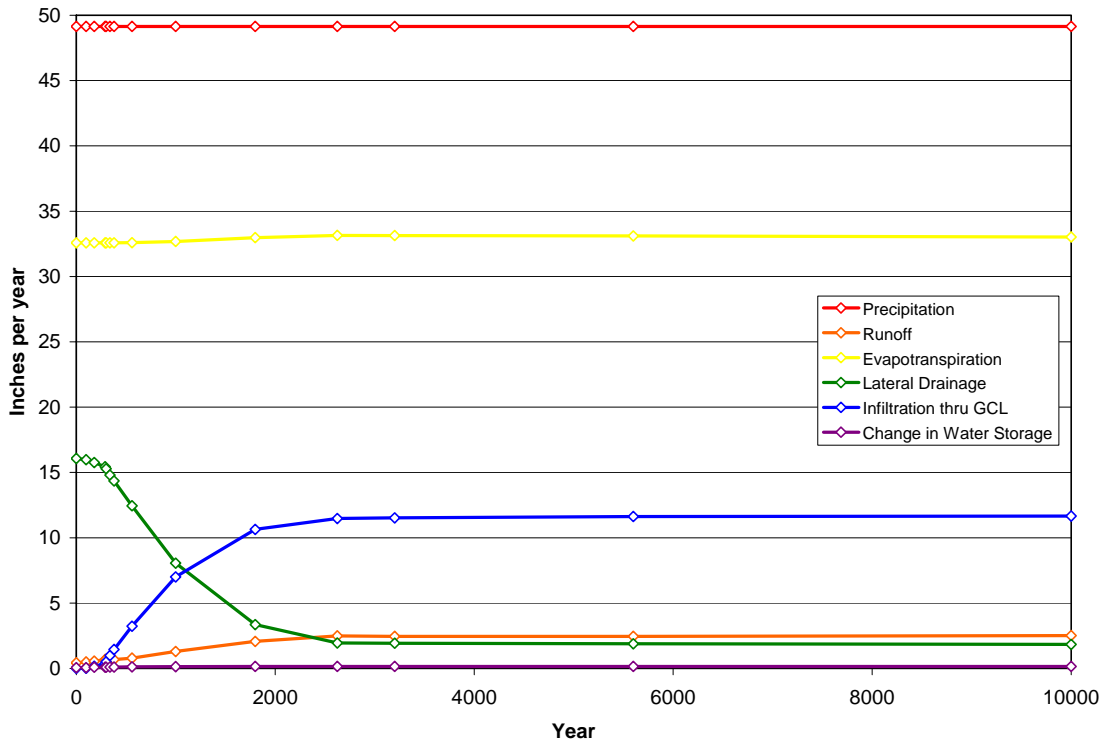
Figure 73.   Configuration #1a Comparison of Modeled Time Steps - Average Water Balance

Table 81.   PorFlow Model Upper Boundary Condition Input

Year	Average Annual Infiltration thru the GCL (in/yr)
0	0.00088
100	0.010
180	0.17
290	0.37
300	0.50
340	1.00
380	1.46
560	3.23
1000	7.01
1800	10.65
2623	11.47
3200	11.53
5600	11.63
10000	11.67

9.0 REFERENCES

Note to references: These references also include those cited in the appendices.

AASHTO (American Association of State Highway and Transportation Officials). 2005. Geotextile Specifications for Highway Applications. AASHTO M 288-05. American Association of State Highway and Transportation Officials, Washington DC. 2005

Abt, S. R. and Johnson, T. L. 1991. Riprap Design for Overtopping Flow. Journal of Hydraulic Engineering, Volume 117, Number 8, pp. 959-972. August 1991.

Albertsson and Banhidi (1980). Microbial and oxidative effects in degradation of polyethylene. Albertsson, A. C. and Banhidi, Z. G. Journal Applied Polymer Science, John Wiley & sons, New York, vol. 25, pp. 1655-1671.

Aleman, S. E. 2007. PORFLOW Testing and Verification Document, WSRC-STI-2007-00150, revision 0. Washington Savannah River Company, Aiken, SC. June 2007.

Anderson, S., Blum, J., Brantley, S. L., Chadwick, O., Chorover, J., Derry, L. A., Drever, J. I., Hering, J. G., Kirchner, J. W., Kump, L. R., Richter, D., and White, A. F. 2004. *Proposed Initiative Would Study Earth's Weathering Engine*, EOS, Transactions, American Geophysical Union, Vol. 85, No. 28, July 2004, pages 265-272.

ASTM International. 1988. *Standard Guide for Identification, Storage, and Handling of Geotextiles*. ASTM D-4873-88. ASTM International, West Conshohocken, PA. November 25, 1988.

ASTM International. 1997. *Standard Practice for Specifying Standard Sizes of Stone for Erosion Control*. ASTM D-6092-97. ASTM International, West Conshohocken, PA. March 10, 1997.

ASTM International. 2000. *Standard Test Methods for Laboratory Compaction Characteristics of Soil Using Standard Effort* (12,400 ft-lbf/ft^3 (600 kN-m/m^3)). ASTM D-698-00. ASTM International, West Conshohocken, PA. June 10, 2000.

ASTM International. 2002a. *Standard Guide for Placement of Riprap Revetments*. ASTM D-6825-02. ASTM International, West Conshohocken, PA. August 10, 2002.

ASTM International. 2002b. *Standard Test Methods for Laboratory Compaction Characteristics of Soil Using Modified Effort* (56,000 ft-lbf/ft^3 (2,700 kN-m/m^3)). ASTM D-1557-02. ASTM International, West Conshohocken, PA. November 10, 2002.

ASTM International. 2003a. *Standard Guide for Petrographic examination of Aggregates for Concrete*. ASTM C-295-03. ASTM International, West Conshohocken, PA. January 10, 2003.

ASTM International. 2003b. *Standard Test Method for Resistance to Degradation of Small-Size Coarse Aggregate by Abrasion and Impact in the Los Angeles Machine.* ASTM C-131-03. American Society of Testing and Materials, West Conshohocken, PA. March 10, 2003.

ASTM International. 2004a. *Standard Guide for Installation of Geosynthetic Clay Liners*, ASTM D-6102-04. ASTM International, West Conshohocken, PA. 2004.

ASTM International. 2004b. *Standard Test Method for Density, Relative Density (Specific Gravity), and Absorption of Coarse Aggregate*. ASTM C-127-04. ASTM International, West Conshohocken, PA. August 1, 2004.

ASTM International. 2005a. *Standard Test Methods for Water Vapor Transmission of Materials*. ASTM E-96/E 96M-05. ASTM International, West Conshohocken, PA. June 2005.

ASTM International. 2005b. *Standard Test Method for Soundness of Aggregates by Use of Sodium Sulfate or Magnesium Sulfate*. ASTM C-88-05. ASTM International, West Conshohocken, PA. July 15, 2005.

ASTM International. 2006a. *Standard Practice for Geomembrane Seam Evaluation by Vacuum Chamber*. ASTM D-5641-94 (Reapproved 2006). ASTM International, West Conshohocken, PA. June 2006.

ASTM International. 2006b. *Standard Practice for Pressurized Air Channel Evaluation of Dual Seamed Geomembranes.* ASTM D-5820-95 (Reapproved 2006). ASTM International, West Conshohocken, PA. June 2006.

ASTM International. 2006c. *Standard Test Method for Determining the Integrity of Nonreinforced Geomembrane Seams Produced Using Thermo-Fusion Methods*. ASTM D-6392-99 (Reapproved 2006) ASTM International, West Conshohocken, PA. June 2006.

ASTM International. 2006d. *Standard Test Method for Oxidative Induction Time of Polyolefin Geosynthetics by High-Pressure Differential Scanning Calorimetry*. ASTM D 5885-06. ASTM International, West Conchohocken, PA. November 2006.

ASTM International. 2006e. *Standard Test Method for Swell Index of Clay Mineral Component of Geosynthetic Clay Liners*. ASTM D 5890-06. ASTM International, West Conchohocken, PA. February 2006.

Badu-Tweneboah, K., Tisinger, L.G., Giroud, J. P., Smith, B. S., 1999. Assessment of the Long-Term Performance of Polyethylene Geomembrane and Containers in a Low-Level Radioactive Waste Disposal Landfill, Geosynthetics '99 Conference Proceedings, Vol. 2, pp. 1055-1070, Industrial Fabrics Association International, Roseville, MN, 55113.

Bear, J. 1972. Dynamics of Fluids in Porous Media. Dover Publications, Inc., New York.

Bednarik, R. G. 2002. *First Dating of Pilbara Petroglyphs*, Records of the Western Australian Museum, Vol. 20, pages 414-429.

Benson, C. H. 1999. Final Covers for Waste Containment Systems: A North American Perspective. XVII Conference of Geotechnics of Torino: "Control and Management of Subsoil Pollutants". Torino, Italy. November 23-25, 1999.

Bethke, C.M., 2005, The Geochemist's Workbench®, Release 6.0. University of Illinois, Urbana, IL.

Bohm, W. 1979. Methods of Studying Root Systems, Springer-Verlag, page 188.

Boardman, B.T. and Daniel, D.E. 1996. Hydraulic Conductivity of Desiccated Geosynthetic Clay Liners, Journal of Geotechnical Engineering, Volume 122, No. 3, pp 204-208.

Bonaparte, R., Daniel, D. E., and Koerner, R. M. 2002. Assessment and Recommendations for Improving the Performance of Waste Containment Systems. EPA/600/R-02/099, United States Environmental Protection Agency, Office of Research and Development, Cincinnati, OH. December 2002.

Borchardt, G.A., 1977, Montmorillonite and Other Smectite Minerals. In Minerals in Soil Environments, J.B. Dixon and S.B. Weed editors. Soil Science Society of America, Madison, WI.

Brandrup and Immergut (1989). Polymer Handbook, 3th edition, Brandrup, J., and Immergut, E. H. (editors). John Wiley & Sons, Inc., New York.

Brandrup et al. (1999). Polymer Handbook, 4th edition, Brandrup, J., Immergut, E. H., and Grulke, E. A. (editors). John Wiley & Sons, Inc., New York.

Buol, S. W., Hole, F. D., and McCracken, R. J. 1973. Soil Genesis and Classification. The Iowa University Press, Ames.

Burns, R. M., and B. H. Hondala (Technical Coordinators). 1990. Silvics of North America, Volume 1. Conifers, Agriculture Handbook 654, USDA.

Cahill, J. M., 1982, Hydrology of the Low-Level Radioactive-Solid-Waste Burial Site and Vicinity near Barnwell, South Carolina, Open-File Report 82-863: Columbia, South Carolina, U. S. Geological Survey, 101 p.

Carson, D. A. 2001. Geosynthetic Clay Liners in Waste Containment. Presentation found at www.epa.gov/tio/tsp/download/2001_meet/prez/carson.pdf. Office of Research and Development, US Environmental Protection Agency, Cincinnati, OH.

Chien C. C., Inyang, H. I., and Everett, L. G. (editors). 2006. Barrier Systems for Environmental Contaminant Containment and Treatment. CRC Press, Taylor & Fracncis Group, LLC, Boca Raton, FL.

CIMBAR 2001. Cal-Ben^{TM} (Calcium Bentonite). CIMBAR Performance Minerals, www.cimbar.com. June 2001.

DeGaetano, A.T. and Wilks, D.S. 2001. Extreme-value climatology of maximum soil freezing depths in the United States, Journal of Cold Regions Engineering, Vol. 16, pp. 51-71.

Deng et al. (1996). Effects of Gamma-ray Irradiation on Thermal and Tensile Properties of Ultrahigh-Molecular-Weight Polyethylene Systems. Deng, M., Johnson, R. A., Latour, Jr., R. A., Shalaby, S. W. Irradiation of Polymers – Fundamentals and Technological Applications. Clough R. L. and Shalaby, S. W. (editors). ACS Symposium Series 620, pp 293-301. American Chemical Society, Washington, DC.

Dennehy, K. F. and McMahon, P. B. 1989. Water Movement in the Unsaturated Zone at a Low-Level Radioactive-Waste Burial Site near Barnwell, South Carolina, United States Geological Survey Water-Supply Paper 2345: Denver, Colorado, U. S. Geological Survey, United States Government Printing Office, 40 p.

Dinauer, R. C. (managing editor). 1977. Mineral in Soil Environments. Soil Science Society of America, Madison, Wisconsin.

Dixon, K. L. and Phifer, M. A. 2006. Geosynthetic Clay Liner Compatibility with Saltstone Leachate, WSRC-STI-2006-00018, Revision 0. Washington Savannah River Company, Aiken, SC. September 2006.

Egloffstein, T. A. 2001. Natural bentonites—influence of the ion exchange and partial desiccation on permeability and self-healing capacity of bentonites used in GCLs. Geotextiles and Geomembranes, Volume 19, Issue 7, September 2001, Pages 427-444.

Feddes, R. A., Kowalik, P. J., and Zaradny, H. 1978. Simulation of Field Water Use and Crop Yield, John Wiley and Sons, New York, NY.

Fetter, C. W. 1988. Applied Hydrogeology, second edition. Macmillan Publishing Company, New York.

Fowells, H. A. 1965. Silvics of forest trees of the United States. USDA, Forest Service. Ag. Handbook No. 271, 762 p.

Frados (1976). Plastics Engineering Handbook of the Society of the Plastics Industry, Inc., 4th edition, Frados, J. (ed.). Van Nostrand Reinhold Company, New York.

Freeze, R. A. and Cherry, J. A. 1979. Groundwater. Prentice-Hall, Inc., Englewood Cliffs, New Hersey.

Gates, R. N., G. M. Hill and G.W. Burton. 1999. Response of selected and unselected bahia grass populations to defoliation. Agron. J. 91:787-795.

GDOT 2007. Qualified Products List – APL-2 – Coarse Aggregate Sources – Section A "Standard Sources List". Pits and Quarry Control Branch, Office of Materials and Research, Georgia Department of Transportation, Forest Park, GA. May 2, 2007. (http://www.dot.state.ga.us/dot/construction/materials-research/qpl-catlist.shtml)

Glover, T. J. 2001.Pocket Ref. Sequoia Publishing, Inc. Littleton, CO. June 2001.

Goldman, S. J., Jackson, K., and Bursztynsky, T. A. 1986. Erosion and Sediment Control Handbook, McGraw-Hill Publishing Company, New York.

Golley, F. B. 1965. Structure and function of an old-field broomsedge community. Ecol. Monogr 35:113-131.

Golley, F. B. and J. B. Gentry. 1966. A comparison of variety and standing crop of vegetation on a one-year and twelve-year abandoned field. Oikos 15:185-199.

GRI 1998. Selecting Variable Intervals for Taking Geomembrane Destructive Seam Samples Using the Method of Attributes, GRI Test Method GM14, Geosynthetic Research Institute, Folsom, PA. March 27, 1998.

GRI 2002. Test Methods and Properties for Geotextiles Used as Protection (or Cushioning Materials, GRI Test Method GT12(a) - ASTM Version, Geosynthetic Research Institute, Folsom, PA. February 18, 2002.

GRI 2003. Test Properties, Testing Frequency and Recommended Warranty for High Density Polyethylene (HDPE) Smooth and Textured Geomembranes, GRI Test Method GM13, Geosynthetic Research Institute, Folsom, PA. June 23, 2003.

GRI 2004. Test Methods and Properties for Nonwoven Geotextiles Used as Separation between Subgrade Soil and Aggregate, GRI Test Method GT13, Geosynthetic Research Institute, Folsom, PA. March 10, 2004.

GRI 2005. Test Methods, Required Properties, and Testing Frequencies of Geosynthetic Clay Liners (GCLs), GRI-GCL3. Geosynthetic Research Institute, Folsom, PA. May 16, 2005.

GSE 2006a. Product Data Sheet: GSE GundSeal GCL (Smooth HDPE). GSE Lining Technology, Inc., www.gseworld.com. 03/09/06

GSE 2006b. Technical Note: Bentofix® GCL Resistance to Cation Exchange. GSE Lining Technology, Inc., www.gseworld.com. 03/16/06.

Hamilton et al. (1996). Anisotropic Properties in Ultrahigh-Molecular-Weight Polyethylene after Cobalt-60 Irradiation. Hamilton, J. V., Greer, K. W., Ostiguy, P., and Pai, P. N. Irradiation of Polymers – Fundamentals and Technological Applications. Clough R. L. and Shalaby, S. W. (editors). ACS Symposium Series 620, pp 81-93. American Chemical Society, Washington, DC.

Hansen, E. M., Schreiner, L. C. and Miller, J. F. 1982. Application of Probable Maximum Precipitation Estimates, United States East of the 105th Meridian, Hydrometeorological Report 52. National Oceanic and Atmospheric Administration, National Weather Service, Office of Hydrology, Hydrometeorological Branch and U.S. Army Corps of Engineers. 168 p.

Harper (1996). Handbook of Plastics, Elastomers, and Composites, 3rd edition, Harper, C. A. (ed.). McGraw-Hill, New York.

Hawkins, R. H. 1962. Bentonite as a Protective Cover for Buried Radioactive Waste, DPSPU 62-30-3A, E. I. du Pont de Nemours and Company, Aiken, SC. May 1962.

Hillel, D. 1982. Introduction to Soil Physics. Academic Press, Inc., San Diego, California.

Horton, J. H. and Wilhite, E. L. 1978. Estimated Erosion Rate at the SRP Burial Ground, DP-1493, E. I. du Pont de Nemours and Company, Aiken, South Carolina. April 1978.

Hubbard, J. E. and Emslie, R. H. 1984. Water Budget for SRP Burial Ground Area, DPST-83-742. E. I. du Pont de Nemours and Company, Savannah River Plant, Aiken, South Carolina, March 19, 1984.

Hubbard, J. E. 1986. An Update on the SRP Burial Ground Area Water Balance and Hydrology, DPST-85-958. E. I. du Pont de Nemours and Company, Savannah River Plant, Aiken, South Carolina, January 9, 1986.

Hubbard, J. E. and Englehardt M. 1987. Calculation of Groundwater Recharge at the old SRP Burial Ground Using the CREAMS Model (1961-1986), State University of New York, Brockport, New York, Summer 1987 (report prepared for E. I. du Pont de Nemours and Company, Savannah River Plant, Aiken, South Carolina and given DuPont document number DP-MS-87-126)

Hunter, C. H. 2005. Probable Maximum Precipitation for the Z-area Saltstone Facility. SRNL-ATG-2005-00022, Westinghouse Savannah River Company, Aiken, South Carolina. September 2005.

Hsuan and Guan (1997). Evaluation of the Oxidation Behavior of Polyethylene Geomembranes Using Oxidative Induction Time Tests. Hsuan, Y. G. and Guan, Z. Oxidative Behavior of Materials by Thermal analytical Techniques, ASTM STP 1326, Riga, A. T. and Patterson, G. H. (editors). American Society of Testing and Materials (ASTM), Philadelphia, PA, pp. 76-90.

Hsuan and Koerner (1998). Antioxidant depletion lifetime in high density polyethylene geomembranes. Hsuan, Y. G. and Koerner, R. M. Journal of Geotechnical and Geoenvironmental Engineering, ASCE, Vol. 124, No. 6, pp. 532-541.

Hunter, C. H. 2006. Savannah River Site Annual Meteorology Report for 2005 (U), WSRC-RP-2006-00445. Westinghouse Savannah River Company, Aiken, SC. March 30, 2006.

IAEA, (2001). Procedures and Techniques for Closure of Near Surface Disposal Facilities for Radioactive Waste, IAEA-TECDOC-1260, International Atomic Energy Agency, Vienna, Austria, December 2001.

INEEL (2004). Engineering Design File Project No. 23350 Liner/Leachate Compatibility Study. EDF-ER-278, Revision 2, Idaho National Engineering and Environmental Laboratory (INEEL), 6/18/04.

Jacobs, 1988. Special Study on Vegetative Covers, final report for vegetative cover special study for UMTRA Project Office by Jacobs Engineering Group, November 1998, Albuquerque, NM,

Jo, H. Y., Benson, C. H., Shackelford, C. D., Lee, J., and Edil, T. E. 2005. Long-Term Hydraulic Conductivity of a Geosynthetic Clay Liner Permeated with Inorganic Salt Solutions. Journal of Geotechnical and Geoenvironmental Engineering, Vol. 131, No. 4, pp. 405-417, April 2005.

Johnson, T. L. 2002. Design of Erosion Protection for Long-Term Stabilization, NUREG-1623. U.S. Nuclear Regulatory Commission, Washington, DC. 139 p.

Jones, S. M., D. H. VanLear, and S. K. Cox. 1981. Major forest community types of the Savannah River Plant: A field guide. SRO-NERP-9, Savannah River National Environmental Research Park Program, Aiken, SC, 79 p.

Kamei, G., M.S. Mitsui, K. Futakuchi, S. Hashimoto, and Y. Sakuramoto, 2005, Kinetics of long-term illitization of montmorillonite – a natural analogue of thermal alteration of bentonite in the radioactive waste disposal system, *Journal of Physics and Chemistry of Solids*, 66, 612-614.

Kane and Widmayer (1989). Consideration for the Long-Term Performance of Geosynthetics at Radioactive Waste Disposal Facilities. Durability and Aging of Geosynthetics, ed. R. M. Koerner, London: Elsevier, 1989, pp. 13-27.

Koerner, R. M. 1990. *Designing with Geosynthetics, Second Edition*. Prentice Hall, Englewood Cliffs, New Jersey. 1990.

Koerner et al. (1990). Long-Term Durability and Aging of Geomembranes. Koerner, R. M., Halse, Y. H., and Lord, Jr., A. E. Waste Containment Systems: Construction, Regulation, and Performance, Bonaparte R. (editor), Geotechnical Special Publication No. 26, American Society of Civil Engineers, San Francisco, CA. pp. 106-134.

Koerner, R. M. 1998. Designing with Geosythetics, 4th edition. Prentice Hall, Upper Saddle River, New Jersey.

Koerner and Hsuan 2003. Lifetime Prediction of Polymeric Geomembranes Used in New Dam Construction and Dam Rehabilitation. Koerner, R. M. and Hsuan, Y. G. Proceedings of the Association of State Dam Safety Officials Conference, Lake Harmony, Pennsylvania, June 4-6, 2003.

Koerner, R. M. and Koerner, G. R. 2005. In-Situ Separation of GCL Panels Beneath Exposed Geomembranes, GRI White Paper #5. Geosynthetic Institute, Folsom, PA. April 15, 2005.

Kresser (1957). Reinhold Plastics Application Series 1. Polyethylene. Kresser, T. O. J. Reinhold Publishing Corporation, New York.

Kudoh et al. (1996). High-Energy Ion Irradiation Effects on Polymer Materials. Kudoh, H., Sasuga, T., and Seguchi, T. Irradiation of Polymers – Fundamentals and Technological Applications. Clough R. L. and Shalaby, S. W. (editors). ACS Symposium Series 620, pp 2-10. American Chemical Society, Washington, DC.

Lamb, T. W. and Whitman, R. V. 1969. Soil Mechanics. John Wiley & Sons, New York.

Landreth, R. E., 1991. The Resistance of Membranes in Cover Systems to Root Penetration by Grass and Trees, EPA/600/A-92/202, presented at Geosynthetics '91 Conference, Atlanta, GA.

Lin, L. and Benson, C. H. 2000. Effect of Wet-Dry Cycling on Swelling and Hydraulic Conductivity of GCLs. Journal of Geotechnical and Geoenvironmental Engineering, Vol. 126, No. 1, January 2000, pp. 40-49.

Lindsey, C. G., Long, L. W., Begej, C. W. 1982. *Long-Term Survivability of Riprap for Armoring Uranium Mill Tailings and Covers: A Literature Review*, prepared for U. S. Nuclear Regulatory Commission, Pacific Northwest Laboratory, Richland, WA 99352.

Link, S. O., Cadwell, L. L., Petersen, K. L., Sackschewsky, M. R., and Landeen, D. S., 1995. The role of Plants and Animals in Isolation Barriers at Hanford, Washington, PNL-10788, Pacific Northwest Laboratory, Richland, WA 99352.

Looney, B. B., Eddy, C. A., Ramdeen, M., Pickett, J., Rogers, V., Scott, M. T., and Shirley, P. A. 1990. Geochemical and Physical Properties of Soils and Shallow Sediments at the Savannah River Site (U), WSRC-RP-90-1031, Westinghouse Savannah River Company, Aiken, South Carolina. August 31, 1990.

Looney, B. B. and Falta, R. W. 2000. Vadose Zone Science and Technology Solutions, Volume II, Battelle Press, Columbus, Ohio. pp. 852-853.

Loubser, J., Hudson, T., and Greiner, T. 2003. *The Recent Recording of Petroglyphs in Georgia*, in The Profile, The Newsletter of the Society for Georgia Archaeology, No. 117, Winter 2002-2003, pages 3-5.

Ludovici, K. H., S. J. Zarnoch, and D. D. Richter. 2002. "Modeling In-situ Pine Root Decomposition Using Data from a 60-year Chronosequence", Can. J. For. Res. 32:1675-1684.

McCarty, B. (Ed.). 2003. Southern lawns: best management practices for the selection, establishment and maintenance of southern lawngrasses. EC 707, Clemson University, Clemson, SC, 566 p.

McDowell-Boyer, L., Yu, A. D., Cook, J. R., Kocher, D. C., Wilhite, E. L., Holmes-Burns, H., and Young, K. E. 2000. Radiological Performance Assessment for the E-Area Low-Level Waste Facility, Revision 1, WSRC-RP-94-218. Westinghouse Savannah River Company, Aiken, South Carolina. January 31, 2000.

McQuilkin, W. E. 1940. The natural establishment of pine in abandoned fields in the Piedmont Plateau region. Ecology 21:135-147.

McRae, S. G. 1988. Practical Pedology Studying Soils in the Field, Halsted Press: a division of John Wiley & Sons, New York.

Meyer, C. 1997. Bir Umm Fawakhir: Insights Into Ancient Egyptian Mining, Journal of the Minerals, Metals and Materials Society, Vol. 49, No. 3, 1997, pages 64-68.

Mitchell, J. K. 1993. Fundamentals of Soil Behavior, Second Edition. John Wiley & Sons, Inc. New York.

Mueller and Jakob (2003). Oxidative resistance of High-Density Polyethylene Geomembranes. Mueller, W. and Jakob, I. Polymer Degradation and Stability, Elsevier Science Ltd. Vol. 79 (2003) pp. 161-172.

Needham et al. (2004). The likely medium to long-term generation of defects in geomembrane liners. Needham, A., Gallagher, E., Peggs, I., Howe, G, and Norris, J. R&D Technical Report P1-500/1/TR, Environment Agency, Bristol, England.

Nelson, E. A. 2005. Assessment of the biological basis of bamboo as the final vegetation option for closure caps at SRS. WSRC-TR-2005-00424, Savannah River National Laboratory, 22p.

Nelson, J. D., Abt, S. R., Volpe, R. L., van Zyl, D., Hinkle, N. E., and Staub, W. P. 1986. Methodologies for Evaluating Long-Term Stabilization Designs of Uranium Mill Tailing Impoundments, NUREG/CR-4620, U.S. Nuclear Regulatory Commission, Washington, D.C. June 1986.

Newman, E. J., Stark, T. D., Rohe, F. P., and Diebel, P., 2004. Thirty-Year Durability of a 20-mil PVC Geomembrane, Journal of Vinyl and Additive Technology, V. 10, Issue 4, pp. 168-173.

Nimitz et al. (2001). Chemical Compatibility Testing Final Report Including Test Plan and Procedures. Nimitz, J. S., Allred, R. E., and Gordon, B. W. SAND2001-1988, Sandia National Laboratories.

NRC-NA 2007. Assessment of the Performance of Engineered Waste Containment Barriers. Prepublication Copy. National Research Council of the National Academies (NRC-NA), The National Academies Press, Washington, D.C.

Odum, E. P. 1960. Organic production and turnover in old field succession. Ecology 41:34-49.

Ohe, T., M. Itoh, T. Ishii, H. Nakashima, Y. Hirata, and H. Yoshida. 1998. The long-term alteration rate of Na-smectite in natural bentonite formation, *Journal of Contaminant Hydrology*, 35, 285-294.

NCSU (North Carolina State University). 1991. *Erosion and Sediment Control – Field Manual*, State of North Carolina. February 1991.

NUREG 1982. *Long-Term Survivability of Riprap for Armoring Uranium-Mill Tailings and Covers: A Literature Review,* NUREG/CR-2642, U. S. Nuclear Regulatory Commission, Washington, D. C. 20555-0001.

NUREG 2006. *Consolidated Decommissioning Guidance Characterization, Survey and Determination of Radiological Criteria,* Final Report, NUREG-1757, Vol. 2, Rev. 1, U. S. Nuclear Regulatory Commission, Washington, D. C. 20555-0001.

Parizek, R. R. and Root, R. W. 1986. Development of a Ground-Water Velocity Model for the Radioactive Waste Management Facility Savannah River Plant, South Carolina, The Pennsylvania State University, University Park, Pennsylvania, June 1986 (report prepared for E. I. du Pont de Nemours and Company, Savannah River Plant, Aiken, South Carolina and given DuPont document number DPST-86-658)

Phifer, M. A., Drumm, E. C., and Wilson, G. V. 1993. Effects of Post Compaction Water Content Variation on Saturated Conductivity, *Hydraulic Conductivity and Waste Contaminant Transport in Soils, ASTM STP 1142*, David E. Daniel and Stephen J. Trautwein, Eds., American Society for Testing and Materials, Philadelphia, PA.

Phifer, M. A., Nichols, R. L., Sappington, F. C., Steimke, J. L., and Jones, W. E. 2001. TNX GeoSiphon^{TM} Summary Report (U), WSRC-TR-2001-00015, Revision 0. Westinghouse Savannah River Company, Aiken, SC. January 19, 2001.

Phifer, M. A. and Nelson, E. A. 2003. Saltstone Disposal Facility Closure Cap Configuration and Degradation Base Case: Institutional Control to Pine Forest Scenario (U), WSRC-TR-2003-00436, Revision 0. Westinghouse Savannah River Company, Aiken, SC. September 22, 2003.

Phifer, M. A., Milllings, M. R., and Flach, G. P. 2006. Hydraulic Property Data Package for the E-Area and Z-Area Soils, Cementitious Materials, and Waste Zones, WSRC-STI-2006-00198, Revision 0. Washington Savannah River Company, Aiken, SC. September 2006.

Phifer, M. A. 2005. Scoping Study: High Density Polyethylene (HDPE) in Saltstone Service, WSRC-TR-2005-00101, Revision 0. Westilnghouse Savannah River Company, Aiken, SC. February 2005.

Phifer, M. A. 2006. Software Quality Assurance Plan for the Hydrologic Evaluation of Landfill Performance (HELP) Model, Q-SQA-A-00005, Revision 0. Washington Savannah River Company, Aiken, SC. October 2006.

Phillips (1988). Effects of Radiation on Polymers. Phillips, D. C. Materials Science and Technology, Vol. 4, pp. 85-91.

Pinder, J. E. III. 1975. Effects of species removal on an old-field plant community. Ecology 56:747-751.

Pomeroy, K. B. and C. F. Korstian. 1949. Further results of loblolly pine seed production and dispersal. J. Forestry 47:968-970.

Puls, R. S. and Powell, R. M. 1992. "Chapter 4, Surface-Charge Repulsive Effects on the Mobility of Inorganic Colloids in Subsurface System", Sabatini, D. A. and Knox, R. C. (editors), Transport and Remediation of Subsurface Contaminants Colloidal, Interfacial, and Surfactant Phenomena, American Chemical Society, Washington, DC.

Rosenberger, K. 2007. Subject: Potential Dose to F-Tank Farm Closure Cap Geomembrane, SRS-REG-2007-00001. Washington Savannah River Company, Aiken, SC. June 1, 2007.

Rowe (2004). Resolving Some of the Outstanding Issues in Landfill Barrier Design. Rowe, R. K. 3rd Asian Regional Conference on Geosynthetics.

Rumer, R. R. and Mitchell, J. K. (editors). 1995. Assessment of Barrier Containment Technologies A Comprehensive Treatment for Environmental Remediation Applications. International Containment Technology Workshop, Baltimore, Maryland. August 29-31, 1995.

Salvo and Cook 1993. Selection and Cultivation of Final Vegetative Cover for Closed Waste Sites at the Savannah River Site, SC (WSRC-MS-92-513). Salvo, S. K. and Cook, J. R. Westinghouse Savannah River Company, Aiken, South Carolina, 1993.

Sangam and Rowe (2002). Effects of exposure conditions on the depletion of antioxidants from HDPE geomembranes. Sangam, H. P. and Rowe, R. K. Canadian Geotechnical Journal, National Research Council Canada, Vol. 39, No. 6, pp. 1221-1230.

Sangster (1993). Applications of Radiation Treatment of Ultradrawn Polyethylene. Sangster, D. F. Irradiation of Polymeric Materials – Processes, Mechanisms, and Applications. Reichmanis, E., Frank, C. W., and O'Donnell, J. H. (editors). ACS Symposium Series 527, pp 95-101. American Chemical Society, Washington, DC.

Sappington, F. C., Phifer, M. A., Denham, M. E., Millings, M. R., Turick, C. E., and McKinsey, P. C. 2005. D-Area Sulfate Reduction Study Comprehensive Final Report (U), WSRC-TR-2005-00017. Westinghouse Savannah River Company, Aiken, SC. February 11, 2005.

Schnabel (1981). Polymer Degradation Principles and Practical Applications. Schnabel, W. Hanser International, Germany (distributed by Macmillan Publishing Co., Inc., New York)

Schreiner, L. C. and Riedel, J. T. 1978. Probable Maximum Precipitation Estimates, United States East of the 105th Meridian, Hydrometeorological Report 51. National Oceanic and Atmospheric Administration, National Weather Service, Office of Hydrology, Hydrometeorological Branch and U.S. Army Corps of Engineers. 87 p.

Schroeder, P. R. and Peyton, R. L. 1987a. Verification of the Lateral Drainage Component of the HELP Model Using Physical Models. EPA/600/2-87/049. Office of Research and Development, United States Environmental Protection Agency (EPA), Cincinnati, Ohio. July 1987.

Schroeder, P. R. and Peyton, R. L. 1987b. Verification of the Hydrologic Evaluation of Landfill Performance (HELP) Model Using Field Data. EPA/600/2-87/050. Office of Research and Development, United States Environmental Protection Agency (EPA), Cincinnati, Ohio. July 1987.

Schroeder, P. R., Lloyd, C. M., Zappi, P. A., and Aziz, N. M. 1994a. The Hydrologic Evaluation of Landfill Performance (HELP) Model User's Guide for Version 3. EPA/600/R-94/168a. Office of Research and Development, United States Environmental Protection Agency (EPA), Cincinnati, Ohio. September 1994.

Schroeder, P. R., Dozier, T. S., Zappi, P. A., McEnroe, B. M., Sjostrom, J. W., and Peyton, R. L. 1994b. The Hydrologic Evaluation of Landfill Performance (HELP) Engineering Documentation for Version 3. EPA/600/R-94/168b. Office of Research and Development, United States Environmental Protection Agency (EPA), Cincinnati, Ohio. September 1994.

SCS (Soil Conservation Service). 1984. Engineering Field Manual, fourth printing, U.S. Department of Agriculture, Soil Conservation Service. 1984.

Serrato, M. G., 2004. Field Observation Summary for Tree Extractions at the SRS E-Area Test Pads (U), SRNL-2004-00063, Westinghouse Savannah River Company, Aiken, SC 29808.

Serrato M. G. 2006. Meeting Summary – Visit with Richard Hawkins on December 6, 2005, IRD-TFBUT Project File. Washington Savannah River Company, Aiken, SC. January 23, 2006.

Serrato M. G. 2007. GeoTesting Express unpublished data sheets. Washington Savannah River Company, Aiken, SC. October 3, 2006.

Shine, E. P. 2007. F-area Tank Farm Closure Cap Probability Model of Pine Tree Tap Root Penetrations of HDPE Geomembrane (U), WSRC-TR-2007-00369, Washington Savannah River Company, Aiken, SC.

Smith, G.D., Karlsson, K., and Gedde, U.W. 1992. Modelling of antioxidant loss from polyolefins in hot water applications – 1. Model and application to medium density polyethylene pipes. *Polymer Eng. and Science*, Vol. 32, No. 10, 658-667.

Strom, R. N. and Kaback, D. S. 1992. SRP Baseline Hydrogeologic Investigation: Aquifer Characterization - Groundwater Geochemistry of the Savannah River Site and Vicinity (U), WSRC-RP-92-450. Westinghouse Savannah River Company, Aiken SC. March 31, 1992.

Stutzman, P. 2001. *Contributions of NIST/NBS Researchers to the Crystallography of Construction Minerals*, Journal of Research of the National Institute of Standards and Technology, Vol. 106, No. 6, November-December 2001, pages 1051-1061.

Sun et al. (1996). Development of an Accelerated Aging Method for Evaluation of Long-Term Irradiation Effects on Ultrahigh-Molecular-Weight Polyethylene Implants. Sun, D. C., Stark, C., and Dumbleton, J. H. Irradiation of Polymers – Fundamentals and Technological Applications. Clough R. L. and Shalaby, S. W. (editors). ACS Symposium Series 620, pp 340-349. American Chemical Society, Washington, DC.

SRNL – ATC (Savannah River National Laboratory (SRNL) – Atmosphere Technology Center (ATC)) 2006. Web site: http://shweather.srs.gov/servlet/idg.Weather.Weather

Taylor, H. M. 1974. "Root Behavior as Affected by Soil Structure and Strength," The Plant Root and Its Environment, University of Virginia Press, p. 271-292.

The Nature Conservancy 2007. Heggie's Rock.
(http://www.nature.org/wherewework/northamerica/states/georgia/preserves/art6696.html)

Ulrich, B., B. Benechi, W. F. Harris, P. K. Dhanna, and R. Mayer. 1981. "Chapter 5. Soil Processes," Dynamic Properties of Forest Ecosystems, IBP, Cambridge University Press.

USEPA (United States Environmental Protection Agency) 1989. Seminar Publication: Requirements for Hazardous Waste Landfill Design, Construction, and Closure, EPA/625/4-89/022, United States Environmental Protection Agency, Washington, DC. August 1989.

USEPA (United States Environmental Protection Agency) 2001. *Geosynthetic Clay Liners Used in Municipal Solid Waste Landfills*. Solid Waste and Emergency Response, EPA530-F-97-002, United States Environmental Protection Agency, Washington, DC. December 2001.

Walkinshaw, C. H. 1999. "Death of Root Tissues in Standing (Live) and Felled Loblolly Pines", 10th Biennial So. Silv. Res. Conf. pp. 573-577.

White, A. F., Blum, A. E., Schulz, M. S., Bullen, T. D., Harden, J.W., and Peterson, M. L., 1996. Chemical Weathering Rates of a Soil Chronosequence on Granitic Alluvium: I. Quantification of Mineralogical and Surface Area Changes and Calculation of Primary Silicate Reaction Rates, Geochimica et Cosmochimica Acta, Vol. 60, No. 14, pp. 2533-2550.

White, A. F., Bullen, T. D., Schulz, M. S., Blum, A. E., Huntington, T. G., and Peters, N. E., 2000. Differential Rates of Feldspar Weathering in Granitic Regoliths, Geochimica et Cosmochimica Acta, Vol. 65, No. 6, pp. 847-869.

Whyatt and Fansworth (1990). The High pH Chemical and Radiation Compatibility of Various Liner Materials. Whyatt, G. A. and Farnsworth, R. K. Geosynthetic Testing for Waste Containment Applications. Koerner, R. M. (editor). STP 1081, pp110-124. American Society of Testing and Materials, Philadelphia, PA.

Wilcox, H. 1968. "Morphological Studies of the Root of Red Pine, Pinus resinosa, Growth Characteristics and Patterns of Branching", Amer. J. Bot. 55:247-254.

Winkler, E. M. 1987. *Weathering and Weathering Rates of Natural Stone*, Environmental Geology, Vol. 9, No. 2, June, 1987, pages 85-92.

Witt, K. J. and Siegmund, M. 2001. Laboratory Testing of GCL under Changing Humidity. Proceedings of the 8th International waste Management and Landfill Symposium, Sardinia Second Conference, Euro Waste, Sardinia 2001.

WSRC 2005. Response to Action Items from Public Meetings between NRC and DOE to Discuss RAI for the Savannah River Site. CBU-PIT-2005-00203, revision 1. Westinghouse Savannah River Company, Aiken, SC. September 2005.

Worrall, W. E. 1975. Clays and Ceramic Raw Materials, John Wiley and Sons, Inc. New York.

Young, M. H. and Pohlmann, K. F. 2001. Analysis of Vadose Zone Monitoring System: Computer Simulation of Water Flux: E-Area Disposal Trenches, Task Order GA0074 (KG43360-0). Division of Hydrologic Sciences, Desert Research Institute, Las Vegas, NV. August 2001.

Young, M. H. and Pohlmann, K. F. 2003. Analysis of Vadose Zone Monitoring System: Computer Simulation of Water Flux under Conditions of Variable Vegetative Cover: E-Area Disposal Trenches, Publication No. 41188. Division of Hydrologic Sciences, Desert Research Institute, Las Vegas, NV. August 2001.

Yu, A. D., Langton, C. A., and Serrato, M. G. 1993. Physical Properties Measurement Program (U), WSRC-RP-93-894. Westinghouse Savannah River Company, Aiken, SC. June 30, 1993

Zutter, B. R., R. J. Mitchell, G. R. Glover and D. H. Gjerstad. 1999. Root length and biomass in mixtures of broomsedge with loblolly pine or sweetgum. Can. J. Forest Res. 29:926-933.

Web site reference - http://abob.libs.uga.edu/bobk/rockpet.html

Web site reference - www.hermitagemuseum.org/html_En/03/hm3_2_2c.html

Web site reference - http://mc2.vicnet.net.au/home/cognit/shared_files/cupules.pdf

Web site reference - http://www.nps.gov/archeology/rockArt/arch1.htm

Web site reference - http://www.public.asu.edu/~rexweeks/Public_Access_RA_Sites.htm

Web site reference - http://www.wssc.psu.edu/index.htm

Web site reference - http://www.czen.org/wssc

This page intentionally left blank.

APPENDIX A. PHYSICAL STABILITY CALCULATIONS

Scoping level calculations and/or estimations have been made in order to ensure that a physically stable closure cap configuration relative to erosion can be provided. Calculations and/or estimations for the following key items are provided below:

- Probable maximum precipitation (PMP) estimation
- Vegetative soil cover slope
- Erosion barrier riprap sizing
- Side slope riprap sizing
- Toe riprap sizing

Probable Maximum Precipitation Estimation
Estimates of the SRS-specific probable maximum precipitation (PMP) for storm (drainage) areas ranging from 1 to 1000 square miles and rainfall durations from 5 minutes to 72 hours have been made. A PMP is defined as the theoretically greatest depth of precipitation for a give duration that is physically possible over a given storm size area at a particular geographic location. These estimates are summarized in Table A- 1. The SRS-specific PMP estimates for storm areas of 10 square miles, 200 square miles, and 1,000 square miles and rainfall durations of 6 to 72 hours were based on interpolation from standard maps of generalized, all-season isohyets of PMP presented in Hydrometeorological Report (HMR)-51 (Schreiner and Riedel 1978). The PMP estimates for a 1 square mile area and for rainfall durations less than 6 hours were based on procedures outlined in HMR-52 (Hansen et al. 1982). The 1-hour duration rainfall over storm areas from 1 to 1000 square mile was obtained through interpolation from the standard PMP isohyetal maps. Additional maps presented in HMR-52 were used to obtain SRS-specific scaling factors that were then applied to the 1-hour PMP value to determine 5 and 15-minute amounts. The 1 square mile PMP is considered by HMR-52 equivalent to the rainfall at any point within that area. Therefore the 1 square mile PMP has been utilized in the subsequent riprap sizing calculations (see below). (Hunter 2005)

Table A- 1. Estimated Probable Maximum Precipitation for the Savannah River Site (SRS)

Duration	Area (square miles)			
	One	Ten	Two Hundred	One Thousand
5 min	6.2	5.1	2.9	NA
15 min	9.7	8.0	4.6	NA
1 hr	19.2	15.7	9.1	5.1
6 hr	NA	31	23	16.8
12 hr	NA	37	28	22.7
24 hr	NA	43.5	35	31
48 hr	NA	48	38	33
72 hr	NA	51.5	42	36

All precipitation values are in inches
Table taken from Hunter 2005
NA = not applicable

Vegetative Soil Cover Slope
The slope of the vegetative soil cover has been evaluated using the permissible velocity method as outlined by Johnson 2002 Appendix A. The following are the initial vegetative soil cover slope assumptions which were evaluated for acceptability:

- Maximum slope length = 585 ft
- Maximum slope = 1.5% = 0.015

Calculate the drainage area in acres of the maximum slope length of the 1.5% vegetative soil cover on a foot-width basis:

$$A = (585 \ ft \times 1 \ ft)/43560 \ ft^2/acre = 0.0134 \ acres$$

Calculate the time of concentration for the 1.5% vegetative soil cover using the Kirpich Method (Nelson et al. 1986 and Johnson 2002):

$$t_c = (11.9L^3/H)^{0.385}, \quad \text{where } t_c = \text{time of concentration in hours; } L = \text{drainage length in miles; } H = \text{elevation difference in ft}$$

L = 585 ft / 5280 ft/mile = 0.1108 miles
H (elevation difference) = 585 ft × 0.015 = 8.775 ft

$$t_c = (11.9 (0.1108)^3/8.775)^{0.385} = 0.0886 \ hrs = 5.3 \ \text{min}$$

Calculate the rainfall intensity for the 1.5% vegetative soil cover:

Rainfall intensities of 6.2 inches in five minutes and of 9.7 inches in 15 minutes are taken from Table A- 1. The rainfall intensity at the time of concentration of 5.3 will be determined by linear interpolation between those from Table A- 1 at 5 and 15 minutes and converted to inches per hour.

$$I_{5.3 \ min} = \left(6.2 \ in + \left[\left(\frac{5.3 \ min - 5 \ min}{15 \ min - 5 \ min}\right) \times (9.7 \ in - 6.2 \ in)\right]\right) \times \frac{60 \ min/hr}{5.3 \ min} = 71.4 \ in/hr$$

Calculate the peak flow rate using the rational formula and a flow concentration factor of 3 for the 1.5% vegetative soil cover:

$$Q_{cal} = FCIA, \quad \text{where } Q_{cal} = \text{calculated flow in cfs; } F = \text{flow concentration factor (unitless); } C = \text{runoff coefficient (unitless); } I = \text{precipitation in in/hr; } A = \text{drainage area in acres}$$

A flow concentration factor (F) of 3 is recommended by Johnson 2002.
The runoff coefficient (C) will be taken as the upper end of that for pasture and woodlands (i.e. $C = 0.45$) (Goldman et al. 1986 Table 4.1).
$I_{5.3min} = 71.4$ in/hr
$A = 0.0134$ acres

$$Q_{cal} = FCIA = 3(0.45)(71.4\ in/hr)(0.0134\ acres) = 1.29\ cfs$$

Calculate the flow depth using the Manning Equation for the 1.5% vegetative soil cover:

$$y^{5/3} = \frac{Q_{cal}n}{1.486\ S^{1/2}},$$ where y = depth in ft; Q_{cal} = flow in cfs (see value above);

n = Manning coefficient of roughness (unitless);
S = slope in fraction form

It is planned that the slope of the vegetative soil cover will be between 0 and 5 percent and that it will be vegetated with Bahia grass or equivalent (bamboo and pine trees are considered better than Bahia grass in terms of erosion protection). Based on the use of Bahia grass and a 0 to 5 percent slope, a maximum permissible velocity (MPV) of 5 fps has been obtained from Exhibit 7-3 of SCS 1984. Based upon Bahia grass, a retardance classification of C has been obtained from Exhibit 7-2 of SCS 1984. Determine the product of velocity (V) and hydraulic radius (R) based upon a unit width of flow of 1-ft (this is equal to the R since there are no sides in this case) and a MPV of 5 fps:

$$VR = 1\ ft \times 5\ ft/s = 5\ ft^2/s$$

Based upon a VR of 5 ft^2/s and a retardance classification of C, a Manning coefficient of roughness (n) of 0.039 has been obtained from Exhibit 7-1 of SCS 1984.

$Q_{cal} = 1.29$ cfs
$S = 0.015$

$$y^{5/3} = \frac{Q_{cal}n}{1.486\ S^{1/2}} = \frac{(1.29\ cfs)(0.039)}{1.486\ (0.015)^{1/2}} = 0.2764$$
$$y = (0.2764)^{3/5} = 0.46\ ft$$

Calculate permissible velocity (V_p) for the 1.5% vegetative soil cover based upon the depth of flow using the velocity correction factors provided by Johnson 2002 on page A-5:

For a depth of flow of 0.46 ft, the velocity correction factor (CF) will be interpolated from the following values provided by Johnson 2002 on page A-5:

Depth of Flow (ft)	Velocity Correction Factor (CF)
0.4	0.6
0.65	0.7

$$CF = 0.6 + \left[\left(\frac{0.46 \; ft - 0.4 \; ft}{0.65 \; ft - 0.4 \; ft} \right) \times (0.7 - 0.6) \right] = 0.624$$

$V_p = CF \times MPV = 0.624 \times 5 \text{ fps} = 3.12 \text{ fps}$

Calculate the actual velocity (V_a) for the 1.5% vegetative soil cover and compare to the permissible velocity (V_p):

$V_a = Q_{cal}/(y \times 1 \text{ ft}) = 1.29 \text{ cfs} / (0.46 \text{ ft} \times 1 \text{ ft}) = 2.80 \text{ fps}$

$V_a = 2.80 \text{ fps} < V_p = 3.12 \text{ fps}$, therefore the 1.5 percent slope is considered a stable slope to prevent the initiation of gullying for the precipitation considered (i.e., 71.4 in/hr).

Since a maximum slope length of 585 ft with a maximum slope of 1.5% is acceptable, a 2% vegetative soil cover slope will also be evaluated for acceptability:

- Maximum slope length = 585 ft
- Maximum slope = 2.0% = 0.020

The drainage area remains the same as previously calculated for the 1.5% slope vegetative soil cover at 0.0134 acres.

Calculate the time of concentration for a 2% vegetative soil cover using the Kirpich Method (Nelson et al. 1986 and Johnson 2002):

$t_c = \left(11.9L^3/H \right)^{0.385}$,   where t_c = time of concentration in hours; L = drainage length in miles; H = elevation difference in ft

L = 585 ft / 5280 ft/mile = 0.1108 miles
H (elevation difference) = 585 ft × 0.020 = 11.7 ft

$t_c = \left(11.9 \, (0.1108)^3 /11.7 \right)^{0.385} = 0.0793 \; hrs = 4.8 \text{ min}$

Calculate the rainfall intensity for the 2% vegetative soil cover:

From Table A- 1, a rainfall intensity of 6.2 inches in five minutes is provided. The rainfall intensity at the time of concentration of 4.8 will be determined by linear interpolation between that at 5 minutes and an intensity of 0 in at time zero and then converted to inches per hour.

$$I_{4.8\,min} = \left(0\ in + \left[\left(\frac{4.8\ min - 0\ min}{5\ min - 0\ min}\right) \times (6.2\ in - 0\ in)\right]\right) \times \frac{60\ min/hr}{4.8\ min} = 74.4\ in/hr$$

Calculate the peak flow rate using the rational formula and a flow concentration factor of 3 for the 2% vegetative soil cover:

$Q_{cal} = FCIA$, where Q_{cal} = calculated flow in cfs; F = flow concentration factor (unitless); C = runoff coefficient (unitless); I = precipitation in in/hr; A = drainage area in acres

A flow concentration factor (F) of 3 is recommended by Johnson 2002. The runoff coefficient (C) will be taken as the upper end of that for pasture and woodlands (i.e. $C = 0.45$) (Goldman et al. 1986 Table 4.1).
$I_{4.8min}$ = 74.4 in/hr
$A = 0.0134$ acres

$$Q_{cal} = FCIA = 3(0.45)(74.4\ in/hr)(0.0134\ acres) = 1.35\ cfs$$

Calculate the flow depth using the Manning Equation for the 2% vegetative soil cover:

$$y^{5/3} = \frac{Q_{cal}n}{1.486\ S^{1/2}}\,,$$ where y = depth in ft; Q_{cal} = flow in cfs (see value above); n = Manning coefficient of roughness (unitless); S = slope in fraction form

The following remain the same as previously determined for the 1.5% slope:

– Maximum permissible velocity (MPV) of 5 fps for Bahia grass on a 0 to 5 percent slope (Exhibit 7-3 of SCS 1984)
– A retardance classification of C for Bahia grass (Exhibit 7-2 of SCS 1984)
– The product of velocity (V) and hydraulic radius (R) of 5 ft^2/s remain
– Manning coefficient of roughness (n) of 0.039 (Exhibit 7-1 of SCS 1984)

$Q_{cal} = 1.35$ cfs
$S = 0.020$

$$y^{5/3} = \frac{Q_{cal}n}{1.486\ S^{1/2}} = \frac{(1.35\ cfs)(0.039)}{1.486\ (0.020)^{1/2}} = 0.2505$$
$$y = (0.2505)^{3/5} = 0.44\ ft$$

Calculate permissible velocity (V_p) for the 2% vegetative soil cover based upon the depth of flow using the velocity correction factors provided by Johnson 2002 on page A-5:

For a depth of flow of 0.44 ft, the velocity correction factor (CF) will be interpolated from the following values provided by Johnson 2002 on page A-5:

Depth of Flow (ft)	Velocity Correction Factor (CF)
0.4	0.6
0.65	0.7

$$CF = 0.6 + \left[\left(\frac{0.44\ ft - 0.4\ ft}{0.65\ ft - 0.4\ ft} \right) \times (0.7 - 0.6) \right] = 0.616$$

$V_p = CF \times MPV = 0.616 \times 5$ fps $= 3.08$ fps

Calculate the actual velocity (V_a) for the vegetative soil cover and compare to the permissible velocity (V_p):

$V_a = Q_{cal}/(y \times 1\ ft) = 1.35$ cfs $/ (0.44\ ft \times 1\ ft) = 3.07$ fps

$V_a = 3.07$ fps $< V_p = 3.08$ fps, therefore the 2 percent slope is considered a stable slope that prevents the initiation of gullying for the precipitation considered (i.e. 74.4 in/hr).

Based upon the above a maximum 585-ft slope length at a maximum 2 percent slope will be considered acceptable for the FTF closure cap vegetative soil cover. Maximum acceptable slopes for portions of the closure cap with slope lengths less than 585 ft may be greater than 2 percent, if it is determined that they are considered stable slopes that prevent the initiation of gullying versus a PMP event during the actual closure cap design process.

Erosion Barrier Riprap Sizing

The riprap for the erosion barrier (i.e. riprap on the top slope which is located 3 ft deep) has been sized per the Abt and Johnson Method (Abt and Johnson 1991 and Johnson 2002 Appendix D Section 2). It will be assumed that the erosion barrier is placed at the same slope length and slope as the overlying vegetative soil cover (i.e. the erosion barrier and overlying vegetative soil cover are parallel). Therefore the following are the erosion barrier slope length and slope which were utilized to determine the riprap size:

- Maximum slope length = 585 ft
- Maximum slope = 2% = 0.020

The erosion barrier drainage area on a foot-width basis (A), time of concentration in hours (t_c), and rainfall intensity ($I_{4.8min}$) are the same as that previously calculated for the 2% vegetative soil cover:

- $A = 0.0134$ acres
- $t_c = 4.8$ min
- $I_{4.8min} = 74.4$ in/hr

Calculate the peak flow rate using the rational formula and a flow concentration factor of 5:

$Q_{cal} = FCIA$, where Q_{cal} = calculated flow in cfs; F = flow concentration factor (unitless); C = runoff coefficient (unitless); I = precipitation in in/hr; A = drainage area in acres

A conservative flow concentration factor (F) of 5 has been utilized for the erosion barrier. The factor of 5 has been used for the erosion barrier since it is overlain by a 3-ft thick soil layer, which could potentially be subject to gully erosion. However the vegetative soil cover has been designed to prevent the initiation of gullying due to a PMP event. Designing both the vegetative soil cover and erosion barrier in consideration of a PMP event provides defense-in-depth and additional assurance of physical stability.

The voids within the stone of the erosion barrier will be filled with a yet to be determined material. In order to be conservative the runoff coefficient (C) will be taken as the lower end of that for concrete (i.e. $C = 0.8$) (Goldman et al. 1986 Table 4.1).

$Q_{cal} = FCIA = 5(0.8)(74.4\ in/hr)(0.0134\ acres) = 3.99\ cfs$

Calculate the required size of the riprap using the Abt and Johnson Method (Abt and Johnson 1991 and Johnson 2002 Appendix D Section 2):

$$D_{50} = 5.23 \, S^{0.43} \, Q_{design}^{0.56}, \qquad \text{where } D_{50} = \text{median size of riprap in inches; } S = \text{slope}$$

in fraction form; $Q_{design} = 1.35 \, Q_{failure}$; $Q_{failure} = Q_{cal}$ (flow calculated above in cfs)

The flow at failure ($Q_{failure}$) is the flow required to move the riprap such that the underlying filter fabric or bedding stone is exposed. In order to design for no movement of the riprap the design flow (Q_{design}) is utilized, which increases the failure flow ($Q_{failure}$) by a factor that represents the experimental ratio of "the unit discharge at movement to unit discharge at failure" (Abt and Johnson 1991).

$Q_{design} = 1.35 \, Q_{cal} = 1.35 \, (3.99 \text{ cfs}) = 5.39 \text{ cfs}$
$S = 0.020$

$$D_{50} = 5.23 \, S^{0.43} \, Q_{design}^{0.56} = 5.23 \, (0.02)^{0.43} \, (5.39 \, cfs)^{0.56} = 2.5 \; inches$$

Side Slope Riprap Sizing
The riprap for the side slopes have been sized per the Abt and Johnson Method (Abt and Johnson 1991 and Johnson 2002 Appendix D Section 2).

Calculate the drainage area of the side slope on a foot-width basis:

Assume a maximum slope = 3H:1V (33.3% or 0.333)
Assume a maximum 40 ft elevation difference between the south edge of the FTF closure cap (assume an elevation of ~310 ft-msl) and the 281-8F and 241-97F lined basins after they have been closed (assume a closed elevation of ~270 ft-msl) (i.e. H = 40 ft)
Slope length = 40 ft / 0.333 = 120 ft

$$A = (120 \; ft \times 1 \; ft)/43560 \; ft^2 / acre = 0.0028 \; acres$$

Calculate the time of concentration for the side slope using the Kirpich Method (Nelson et al. 1986 and Johnson 2002):

$$t_c = (11.9 L^3 / H)^{0.385}, \quad \text{where } t_c = \text{time of concentration in hours; } L = \text{drainage length}$$

in miles; H = elevation difference in ft

The time of concentration for the side slope is the summation of the time of concentration for the vegetative soil cover plus that of the side slope itself.

t_c for vegetative soil cover was previously calculated as 0.0793 hrs
L = 120 ft / 5280 ft/mile = 0.0227 miles
H = 40 ft

$$t_c = 0.0793 + \left(11.9 \left(0.0227\right)^3 / 40\right)^{0.385} = 0.0872 \; hrs = 5.2 \; min$$

Calculate the rainfall intensity for the side slope:

Rainfall intensities of 6.2 inches in five minutes and of 9.7 inches in 15 minutes are taken from Table A- 1. The rainfall intensity at the time of concentration of 5.2 will be determined by linear interpolation between those from Table A- 1 at 5 and 15 minutes and converted to inches per hour.

$$I_{5.2 \; min} = \left(6.2 \; in + \left[\left(\frac{5.2 \; min - 5 \; min}{15 \; min - 5 \; min}\right) \times \left(9.7 \; in - 6.2 \; in\right)\right]\right) \times \frac{60 \; min/hr}{5.2 \; min} = 72.3 \; in/hr$$

Calculate the peak flow rate using the rational formula and a flow concentration factor of 5:

$Q_{cal} = FCIA$, where Q_{cal} = calculated flow in cfs; F = flow concentration factor (unitless); C = runoff coefficient (unitless); I = precipitation in in/hr; A = drainage area in acres

A conservative flow concentration factor (F) of 5 has been utilized for the side slope. The factor of 5 has been used for the side slope, since the top slope feeds into the side slope.

The runoff coefficient for the side slope will be taken as 0.8, since it is on a barren steep slope (Goldman et al. 1986 Table 4.1).

$I_{5.2min}$ = 72.3 in/hr
The area (A) is equal to the side slope area itself (i.e. 0.0028 acres) plus the upgradient area of the erosion barrier or vegetative soil cover (i.e. 0.0134 acres)
A = 0.0028 acres + 0.0134 acres = 0.0162 acres

$$Q_{cal} = FCIA = 5(0.8)(72.3 \; in/hr)(0.0162 \; acres) = 4.69 \; cfs$$

Calculate the required size of the riprap using the Abt and Johnson Method (Abt and Johnson 1991 and Johnson 2002 Appendix D Section 2):

$D_{50} = 5.23 \; S^{0.43} \; Q_{design}^{0.56}$,   where D_{50} = median size of riprap in inches; S = slope in fraction form; Q_{design} = 1.35 $Q_{failure}$; $Q_{failure}$ = Q_{cal} (flow calculated above in cfs)

The flow at failure ($Q_{failure}$) is the flow required to move the riprap such that the underlying filter fabric or bedding stone is exposed. In order to design for no movement of the riprap the design flow (Q_{design}) is utilized, which increases the failure flow ($Q_{failure}$) by a factor that represents the experimental ratio of "the unit discharge at movement to unit discharge at failure" (Abt and Johnson 1991).

$$Q_{design} = 1.35 \, Q_{cal} = 1.35 \, (4.69 \text{ cfs}) = 6.33 \text{ cfs}$$
$$D_{50} = 5.23 \, S^{0.43} \, Q_{design}^{0.56} = 5.23 \, (0.33)^{0.43} \, (6.33 \, cfs)^{0.56} = 9.1 \, inches$$

Toe Riprap Sizing

The riprap for the toe has been sized per the Abt Method (Johnson 2002 Appendix D Section 6).

Calculate the peak flow rate off the combined erosion barrier or vegetative soil cover and side slope using the rational formula and a flow concentration factor of 3:

$$Q_{cal} = FCIA, \text{ where } Q_{cal} = \text{calculated flow in cfs; } F = \text{flow concentration factor}$$
(unitless); C = runoff coefficient (unitless); I = precipitation in in/hr; A = drainage area in acres

A flow concentration factor of 3 is recommended by Johnson 2002. A flow concentration factor of 5 is not used for the toe riprap although it is used for the erosion barrier and side slope riprap. Since the side riprap has been designed using a flow concentration factor of 5 and designed to prevent movement of its riprap, therefore channeling and the formation of gullies in the side slope which feed into the toe should be prevented. Therefore a flow concentration factor of 3 is deemed appropriate for the toe.

The runoff coefficient (i.e. 0.8), precipitation (i.e. 72.3 in/yr), and drainage area (0.0162) are the same as that of the side slope.

$$Q_{cal} = FCIA = 3(0.8)(72.3 \, in \, / \, hr)(0.0162 \, acres) = 2.81 \, cfs$$

Calculate the required size of the riprap using the Abt Method (Johnson 2002 Appendix D Section 6):

$$D_{50} = 10.46 \, S^{0.43} \, Q_{cal}^{0.56}, \quad \text{where } D_{50} = \text{median size of riprap in inches; } S = \text{slope in}$$
fraction form = 0.33 (see above for side slope); Q_{cal} = flow calculated above in cfs

$$D_{50} = 10.46 \, (0.33)^{0.43} \, (2.81 \, cfs)^{0.56} = 11.58 \, inches$$

Erosion Barrier, Side Slope, and Toe Riprap Summary

Using the Abt and Johnson 1991 method, the required D_{50} (median size) of the erosion barrier riprap was determined to be 2.5 in. Therefore the erosion barrier will consist of rock consistent with Type B riprap from Table F-3 of Johnson 2002 or Size R-20 riprap from Table 1 of ASTM 1997. Johnson 2002 recommends a riprap layer thickness of not "less than 1.5 times the mean stone diameter (D_{50}) or the D_{100} whichever is greater." NCSU 1991 recommends that the riprap layer thickness be at least 1.5 times the maximum stone diameter (D_{100}). Since the NCSU 1991 criterion is more conservative, it will be utilized.

Calculate the thickness of the erosion barrier:

The D_{100} for Type B riprap ≈ 5" and for Size R-20 ≈ 7.5 in

Thickness = 1.5 (D_{100}) = 1.5 (7.5 in) = 11.25 in ≈ 12 in

Using the Abt and Johnson 1991 method, the required D_{50} (median size) of the side slope riprap was determined to be 9.1 in. Therefore the side slope riprap will consist of rock consistent with Type D riprap from Table F-3 of Johnson 2002 or Size R-150 riprap from Table 1 of ASTM 1997. As stated above the more conservative NCSU 1991 criterion that requires a riprap layer thickness at least 1.5 times the maximum stone diameter (D_{100}) will be utilized.

Calculate the thickness of the side slope riprap:

The D_{100} for Type D riprap is between 12 and 18 in and for Size R-150 ≈ 14 in

Thickness = 1.5 (D_{100}) = 1.5 (14 in) = 21 in

However a 21 in placement is not typical, therefore a 24 in layer will be utilized.

Using the Abt and Johnson 1991 method, the required D_{50} (median size) of the toe riprap was determined to be 11.58 in. Therefore the toe riprap will consist of rock consistent with Type D riprap from Table F-3 of Johnson 2002 or Size R-300 riprap from Table 1 of ASTM 1997. Johnson 2002 recommends a toe riprap thickness of 3 times the mean stone diameter (D_{50}) and a toe width of 15 times the mean stone diameter (D_{50}).

Calculate the thickness and width of the toe riprap:

The D_{50} for Type D riprap is between 10 and 12 in and for Size R-300 ≈ 14 in

Thickness = 3 (D_{50}) = 3 (14 in) = 42 in

Calculate the toe width:

Width = 15 (D_{50}) = 15 (14 in) = 210 ins = 17.5 ft

A 20 ft toe width will be utilized.

Table A- 2 provides a summary of the erosion barrier, side slope, and toe riprap requirements. Erosion barrier, side slope, and toe riprap size may be smaller for portions of the closure cap with shorter slope lengths than those used to determine the requirements outlined in Table A- 2, if it is determined that the smaller sized riprap is stable versus a PMP event during the actual closure cap design process.

Table A- 2. Erosion Barrier, Side Slope, and Toe Riprap Requirements Summary

Location	Riprap Requirements
Erosion barrier	A 1 ft thick layer of rock consistent with Type B riprap from Table F-3 of Johnson 2002 or Size R-20 riprap from Table 1 of ASTM 1997. Voids within the stone layer shall be filled.
Side slope	A 2 ft thick layer of rock consistent with Type D riprap from Table F-3 of Johnson 2002 or Size R-150 riprap from Table 1 of ASTM 1997. The riprap shall be underlain with a stone bedding layer consisting of a 6 in thick layer of well-graded crushed stone with either the gradation shown in Table F-4 of Johnson 2002 or that of Figure 8 of ASTM 1997 (i.e. FS-2 filter/bedding stone).
Toe	A 3-ft 6-in thick layer of rock consistent with Type D riprap from Table F-3 of Johnson 2002 or Size R-300 riprap from Table 1 of ASTM 1997, which extends out 20 ft from the bottom of the side slope.

APPENDIX B. AUGUSTA SYNTHETIC PRECIPITATION MODIFIED WITH SRS SPECIFIC AVERAGE MONTHLY PRECIPITATION DATA OVER 100 YEARS

This appendix is available in CD format due to its size - (file name: Fprec.d4)

This page intentionally left blank.

APPENDIX C. AUGUSTA SYNTHETIC TEMPERATURE MODIFIED WITH SRS SPECIFIC AVERAGE MONTHLY TEMPERATURE DATA OVER 100 YEARS

This appendix is available in CD format due to its size - (file name: Ftemp.d7)

This page intentionally left blank.

APPENDIX D. AUGUSTA SYNTHETIC SOLAR RADIATION DATA OVER 100 YEARS

This appendix is available in CD format due to its size - (file name: Fsolar.d13)

This page intentionally left blank.

APPENDIX E. AUGUSTA EVAPOTRANSPIRATION

(file name: Fevap.d11)

```
1
AUGUSTA                 GEORGIA
33.22         68 323 3.5    22.    6.5  68.0 70.0 77.0 73.0
```

This page intentionally left blank.

APPENDIX F.
EROSION BARRIER MATERIAL PROPERTY CALCULATIONS

Erosion Barrier with CLSM as Infill

Determine the combined soil material properties for the Type B riprap from Table F-3 of Johnson 2002 or Size R-20 riprap from Table 1 of ASTM 1997 filled with a Controlled Low Strength Material (CLSM) or Flowable Fill (Phifer and Nelson 2003):

Type B riprap consists of stone ranging in size from a maximum of 5% by weight less than ½-inches to a maximum size of approximately 8-inches. Size R-20 riprap consists of stone ranging in size from a maximum of 15% by weight less than 3-inches to a maximum size of approximately 8-inches.

The following are porosity references for coarse grained materials:

Material	Porosity, η (vol/vol)	Source
Gravel	0.25 to 0.40	Freeze and Cherry 1979 Table 2.4
Well sorted sand or gravel	0.25 to 0.50	Fetter 1988 Table 4.2
Ottawa sand	0.33 to 0.44	Lamb and Whitman 1969 Table 3.2
HELP model default soil #21 (gravel or poorly graded gravel)	0.397	Schroeder 1994b Table 1

It is assumed that the rock that will be utilized will be granite from regional quarries. The table on Weights and Properties of Materials in Glover 2001 provides a broken granite specific gravity of 1.65 and a weight per cubic foot of 103 (this specific gravity and weight per cubic foot represent the bulk density of the broken granite). As outlined in Section 4.4.9 the stone shall have a minimum specific gravity of 2.65 (this specific gravity represents the particle density of the granite stone). Based upon this bulk density of 1.65 g/cm^3 and particle density of 2.65 g/cm^3, a porosity of the stone can be determined as follows (Hillel 1982):

$$\eta = 1 - \frac{\rho_b}{\rho_p}, \quad \text{where } \eta = \text{porosity; } \rho_b = \text{dry bulk density of 1.65 g/cm}^3\text{; } \rho_p = \text{particle}$$

density as 2.65 g/cm^3

$$\eta = 1 - \frac{1.65 \ g/cm^3}{2.65 \ g/cm^3} = 0.38$$

The 0.38 calculated stone porosity falls within that of the above referenced porosity ranges for coarse materials and is very close to the HELP model default soil #21 (gravel or poorly graded gravel) porosity of 0.397 (Schroeder 1994b Table 1). Therefore a porosity of 0.38 will be assumed for the erosion barrier stone.

From Table 6-27 of Phifer et al. 2006 the following recommended CLSM property values were obtained, which will be utilized in determining the combined rip rap/CLSM properties:

- Effective porosity (η) = 0.328
- Saturated hydraulic conductivity (K_{sat}) = 2.2E-06 cm/s

See the notes from Table 19 for the HELP model definition of field capacity and wilting point. Volumetric moisture content can be determined as follows (Hillel 1982):

$$\theta_v = \eta s, \quad \text{where } \theta_v = \text{volumetric moisture content; } \eta = \text{porosity; } s = \text{saturation}$$

CLSM curve data was obtained from the Phifer et al. 2006, Table 6-48. From this data the field capacity (volumetric water content at 0.33 bars or 337 cm-H_2O) and wilting point (volumetric water content at 15 bars or 15,310 cm-H_2O) of the CLSM were derived by linear interpolation:

Suction Head Ψ (cm-H_2O)	Saturation s (vol/vol)
300	0.8888
400	0.8401
14,200	0.2517
16,400	0.2443

The following provides the linear interpolation used to determine the CLSM field capacity and wilting point, respectively, based upon the above CLSM characteristic curve data, which will be utilized in determining the combined rip rap/CLSM properties:

Field capacity = θ_v at 337 cm-H_2O = $\eta \times s$ at 337 cm-H_2O =

$$0.328 \times \left(0.8401 + \left[\left(\frac{400 - 337}{400 - 300} \right) (0.8888 - 0.8401) \right] \right) = 0.286$$

Wilting point = θ_v at 15,310 cm-H_2O = $\eta \times s$ at 15,310 cm-H_2O =

$$0.328 \times \left(0.2443 + \left[\left(\frac{16,400 - 15,310}{16,400 - 14,200} \right) (0.2517 - 0.2443) \right] \right) = 0.081$$

The following table provides the summary CLSM properties:

Property	Property Value
Porosity, η (vol/vol)	0.328
Field capacity (vol/vol)	0.286
Wilting point (vol/vol)	0.081
Saturated hydraulic conductivity (K_{sat})	2.2E-06 cm/s

The matrix of an individual granite stone itself is considered impermeable and non-porous. The porosity of a layer of granite stone is considered to be 0.38 as outlined above. When the granite stone porosity is filled with CLSM, the resultant hydraulic properties, which are area or volume based, become that of the CLSM times the granite stone porosity. The resultant hydraulic properties are shown below:

Property	Property Value
Porosity, η (vol/vol)	$0.328 \times 0.38 = 0.125$
Field capacity (vol/vol)	$0.286 \times 0.38 = 0.109$
Wilting point (vol/vol)	$0.081 \times 0.38 = 0.031$
Saturated hydraulic conductivity (K_{sat})	2.2E-06 cm/s $\times$ 0.38 = 8.36E-07 cm/s

Erosion Barrier with Sandy Soil as Infill

Configuration #1a differs from Configuration #1 in using sandy soil properties rather than CLSM properties for the Erosion Barrier infill. Since the material finally selected for the erosion barrier could be something other than CLSM, this configuration is presented to contrast the infiltration results of using a higher hydraulic conductivity infill material with those of a lower hydraulic conductivity, e.g., CLSM infill. The sandy soil properties will be taken as those of the lower vadose zone (LVZ) from Phifer et al. (2006). This represents an SRS sandy soil which can be obtained on-site for use in closure cap construction.

Determine the combined soil material properties for the Type B riprap from Table F-3 of Johnson 2002 or Size R-20 riprap from Table 1 of ASTM 1997 filled with LVZ soil (Phifer et al., 2006):

Type B riprap consists of stone ranging in size from a maximum of 5% by weight less than ½-inches to a maximum size of approximately 8-inches. Size R-20 riprap consists of stone ranging in size from a maximum of 15% by weight less than 3-inches to a maximum size of approximately 8-inches.

The following are porosity references for coarse grained materials:

Material	Porosity, η (vol/vol)	Source
Gravel	0.25 to 0.40	Freeze and Cherry 1979 Table 2.4
Well sorted sand or gravel	0.25 to 0.50	Fetter 1988 Table 4.2
Ottawa sand	0.33 to 0.44	Lamb and Whitman 1969 Table 3.2
HELP model default soil #21 (gravel or poorly graded gravel)	0.397	Schroeder 1994b Table 1

It is assumed that the rock used will be granite from regional quarries. The table on Weights and Properties of Materials in Glover 2001 provides a broken granite specific gravity of 1.65 and a weight per cubic foot of 103 (this specific gravity and weight per cubic foot represent the bulk density of the broken granite). As outlined in Section 4.4.9 the stone shall have a minimum specific gravity of 2.65 (this specific gravity represents the particle density of the granite stone). Based upon this bulk density of 1.65 g/cm^3 and particle density of 2.65 g/cm^3, a porosity of the stone can be determined as follows (Hillel 1982):

$$\eta = 1 - \frac{\rho_b}{\rho_p}, \quad \text{where } \eta = \text{porosity}; \rho_b = \text{dry bulk density of 1.65 g/cm}^3; \rho_p = \text{particle}$$

$$\text{density as 2.65 g/cm}^3$$

$$\eta = 1 - \frac{1.65 \ g/cm^3}{2.65 \ g/cm^3} = 0.38$$

The 0.38 calculated stone porosity falls within that of the above referenced porosity ranges for coarse materials and is very close to the HELP model default soil #21 (gravel or poorly graded gravel) porosity of 0.397 (Schroeder 1994b Table 1). Therefore a porosity of 0.38 will be assumed for the erosion barrier stone.

From Table 5-18 of Phifer et al. 2006 the following recommended LVZ soil property values were obtained, which will be utilized in determining the combined rip rap/sandy soil properties:

- Effective porosity (η) = 0.39
- Saturated hydraulic conductivity (K_{sat}) = 3.3E-04 cm/s

See the notes from Table 19 for the HELP model definition of field capacity and wilting point. Volumetric moisture content can be determined as follows (Hillel 1982):

$$\theta_v = \eta s, \quad \text{where } \theta_v = \text{volumetric moisture content; } \eta = \text{porosity; } s = \text{saturation}$$

LVZ soil curve data was obtained from the Phifer et al. 2006, Table 5-19. From this data the field capacity (volumetric water content at 0.33 bars or 337 cm-H_2O) and wilting point (volumetric water content at 15 bars or 15,310 cm-H_2O) of the LVZ soil were derived by linear interpolation:

Suction Head Ψ (cm-H_2O)	Saturation s (vol/vol)
331	0.650
381	0.637
14,400	0.467
16,600	0.463

The following provides the linear interpolation used to determine the LVZ soil field capacity and wilting point, respectively, based upon the above LVZ soil characteristic curve data, which will be utilized in determining the combined rip rap/CLSM properties:

Field capacity = θ_v at 337 cm-H_2O = $\eta \times s$ at 337 cm-H_2O =

$$0.39 \times \left(0.637 + \left[\left(\frac{381 - 337}{381 - 331} \right)(0.650 - 0.637) \right] \right) = 0.253$$

Wilting point = θ_v at 15,310 cm-H_2O = $\eta \times s$ at 15,310 cm-H_2O =

$$0.39 \times \left(0.463 + \left[\left(\frac{16,600 - 15,310}{16,600 - 14,400} \right)(0.467 - 0.463) \right] \right) = 0.181$$

The following table provides the summary LVZ soil properties:

Property	Property Value
Porosity, η (vol/vol)	0.39
Field capacity (vol/vol)	0.253
Wilting point (vol/vol)	0.181
Saturated hydraulic conductivity (K_{sat})	3.3E-04 cm/s

The matrix of an individual granite stone itself is considered impermeable and non-porous. The porosity of a layer of granite stone is considered to be 0.38 as outlined above. When the granite stone porosity is filled with sandy soil, the resultant hydraulic properties, which are area or volume based, become that of the sandy soil porosity times the granite stone porosity. The resultant hydraulic properties are shown below:

Property	Property Value
Porosity, η (vol/vol)	$0.39 \times 0.38 = 0.15$
Field capacity (vol/vol)	$0.253 \times 0.38 = 0.10$
Wilting point (vol/vol)	$0.181 \times 0.38 = 0.07$
Saturated hydraulic conductivity (K_{sat})	3.3E-04 cm/s $\times$ 0.38 = 1.3E-04 cm/s

APPENDIX G.
HELP MODEL INPUT FOR INITIAL INFILTRATION OF FTF CLOSURE CAP CONFIGURATIONS #1 THROUGH #6

HELP Model Input Data for Configuration #1 (Year 0):

Input Parameter (HELP Model Query)	Generic Input Parameter Value
Landfill area =	0.0134 acres
Percent of area where runoff is possible =	100%
Do you want to specify initial moisture storage? (Y/N)	Y
Amount of water or snow on surface =	0 inches
CN Input Parameter (HELP Model Query)	CN Input Parameter Value
Slope =	2 %
Slope length =	585 ft
Soil Texture =	4 (HELP model default soil texture)
Vegetation =	4 (i.e., a good stand of grass)
HELP Model Computed Curve Number = 46.2	

Layer	Layer Number	Layer Type
Topsoil	1	1 (vertical percolation layer)
Upper Backfill	2	1 (vertical percolation layer)
Erosion Barrier	3	1 (vertical percolation layer)
Middle Backfill	4	1 (vertical percolation layer)
Lateral Drainage Layer	5	2 (lateral drainage layer)
HDPE Geomembrane	6	4 (geomembrane liner)
GCL	7	3 (barrier soil liner)
Foundation Layer (1.0E-06)	8	1 (vertical percolation layer)
Foundation Layer (1.0E-03)	9	1 (vertical percolation layer)

	Layer Type	Layer Thickness (in)	Soil Texture No.	Total Porosity (Vol/Vol)	Field Capacity (Vol/Vol)	Wilting Point (Vol/Vol)	Initial Moisture (Vol/Vol)
1	1	6		0.396	0.109	0.047	0.109
2	1	30		0.35	0.252	0.181	0.252
3	1	12		0.125	0.109	0.031	0.109
4	1	12		0.35	0.252	0.181	0.252
5	2	12		0.417	0.045	0.018	0.045
6	4	0.06					
7	3	0.2		0.750	0.747	0.400	0.750
8	1	12		0.35	0.252	0.181	0.252
9	1	72		0.457	0.131	0.058	0.131

HELP Model Input Data for Configuration #1 (Year 0) – continued:

	Layer Type	Sat. Hyd. Conductivity (cm/sec)	Drainage Length (ft)	Drain Slope (%)	Leachate Recirc. (%)	Recirc. to Layer (#)	Subsurface Inflow (in/yr)
1	1	3.1E-03					
2	1	4.1E-05					
3	1	8.36E-07					
4	1	4.1E-05					
5	2	5.0E-02	585	2			
6	4	2.0E-13					
7	3	5.0E-09					
8	1	1.0E-06					
9	1	1.0E-03					

	Layer Type	Geomembrane Pinhole Density (#/acre)	Geomembrane Instal. Defects (#/acre)	Geomembrane Placement Quality	Geotextile Transmissivity (cm^2/sec)
1	1				
2	1				
3	1				
4	1				
5	2				
6	4	1	4	2	
7	3				
8	1				
9	1				

The lack of values in the table for particular parameters in particular layers denotes that no HELP model input was required for that parameter in that layer. No data are missing from the table.

Configuration #1: Closure cap configuration described in Table 11 and Table 12 of Section 4.3, with CLSM infilling the erosion barrier. (i.e. composite barrier, lateral drainage and erosion barrier with CLSM infill)

HELP Model Input Data for Configuration #1a (Erosion Barrier with Sandy Soil Infill; Year 0):

Input Parameter (HELP Model Query)	Generic Input Parameter Value
Landfill area =	0.0134 acres
Percent of area where runoff is possible =	100%
Do you want to specify initial moisture storage? (Y/N)	Y
Amount of water or snow on surface =	0 inches
CN Input Parameter (HELP Model Query)	CN Input Parameter Value
Slope =	2 %
Slope length =	585 ft
Soil Texture =	4 (HELP model default soil texture)
Vegetation =	4 (i.e., a good stand of grass)
HELP Model Computed Curve Number = 46.2	

Layer	Layer Number	Layer Type
Topsoil	1	1 (vertical percolation layer)
Upper Backfill	2	1 (vertical percolation layer)
Erosion Barrier	3	1 (vertical percolation layer)
Middle Backfill	4	1 (vertical percolation layer)
Lateral Drainage Layer	5	2 (lateral drainage layer)
HDPE Geomembrane	6	4 (geomembrane liner)
GCL	7	3 (barrier soil liner)
Foundation Layer 1.0E-06)	8	1 (vertical percolation layer)
Foundation Layer 1.0E-03)	9	1 (vertical percolation layer)

	Layer Type	Layer Thickness (in)	Soil Texture No.	Total Porosity (Vol/Vol)	Field Capacity (Vol/Vol)	Wilting Point (Vol/Vol)	Initial Moisture (Vol/Vol)
1	1	6		0.396	0.109	0.047	0.109
2	1	30		0.35	0.252	0.181	0.252
3	1	12		0.15	0.10	0.07	0.10
4	1	12		0.35	0.252	0.181	0.252
5	2	12		0.417	0.045	0.018	0.045
6	4	0.06					
7	3	0.2		0.750	0.747	0.400	0.750
8	1	12		0.35	0.252	0.181	0.252
9	1	72		0.457	0.131	0.058	0.131

HELP Model Input Data for Configuration #1a (Year 0) – continued:

	Layer Type	Sat. Hyd. Conductivity (cm/sec)	Drainage Length (ft)	Drain Slope (%)	Leachate Recirc. (%)	Recirc. to Layer (#)	Subsurface Inflow (in/yr)
1	1	3.1E-03					
2	1	4.1E-05					
3	1	1.3E-04					
4	1	4.1E-05					
5	2	5.0E-02	585	2			
6	4	2.0E-13					
7	3	5.0E-09					
8	1	1.0E-06					
9	1	1.0E-03					

	Layer Type	Geomembrane Pinhole Density (#/acre)	Geomembrane Instal. Defects (#/acre)	Geomembrane Placement Quality	Geotextile Transmissivity (cm^2/sec)
1	1				
2	1				
3	1				
4	1				
5	2				
6	4	1	4	2	
7	3				
8	1				
9	1				

The lack of values in the table for particular parameters in particular layers denotes that no HELP model input was required for that parameter in that layer. No data are missing from the table.

Configuration #1a: Closure cap configuration described in Table 11 and Table 12 of Section 4.3, with sandy soil as infill rather than CLSM . (i.e. composite barrier, lateral drainage and erosion barrier with sandy soil infill)

HELP Model Input Data for Configuration #2 (Year 0):

Input Parameter (HELP Model Query)	Generic Input Parameter Value
Landfill area =	0.0134 acres
Percent of area where runoff is possible =	100%
Do you want to specify initial moisture storage? (Y/N)	Y
Amount of water or snow on surface =	0 inches
CN Input Parameter (HELP Model Query)	CN Input Parameter Value
Slope =	2 %
Slope length =	585 ft
Soil Texture =	4 (HELP model default soil texture)
Vegetation =	4 (i.e., a good stand of grass)
HELP Model Computed Curve Number = 46.2	

Layer	Layer Number	Layer Type
Topsoil	1	1 (vertical percolation layer)
Upper Backfill	2	1 (vertical percolation layer)
Erosion Barrier	3	1 (vertical percolation layer)
Middle Backfill	4	1 (vertical percolation layer)
Lateral Drainage Layer	5	2 (lateral drainage layer)
HDPE Geomembrane	6	4 (geomembrane liner)
Foundation Layer (1.0E-06)	7	1 (vertical percolation layer)
Foundation Layer (1.0E-03)	8	1 (vertical percolation layer)

	Layer Type	Layer Thickness (in)	Soil Texture No.	Total Porosity (Vol/Vol)	Field Capacity (Vol/Vol)	Wilting Point (Vol/Vol)	Initial Moisture (Vol/Vol)
1	1	6		0.396	0.109	0.047	0.109
2	1	30		0.35	0.252	0.181	0.252
3	1	12		0.125	0.109	0.031	0.109
4	1	12		0.35	0.252	0.181	0.252
5	2	12		0.417	0.045	0.018	0.045
6	4	0.06					
7	1	12		0.35	0.252	0.181	0.252
8	1	72		0.457	0.131	0.058	0.131

HELP Model Input Data for Configuration #2 (Year 0) – continued:

	Layer Type	Sat. Hyd. Conductivity (cm/sec)	Drainage Length (ft)	Drain Slope (%)	Leachate Recirc. (%)	Recirc. to Layer (#)	Subsurface Inflow (in/yr)
1	1	3.1E-03					
2	1	4.1E-05					
3	1	8.36E-07					
4	1	4.1E-05					
5	2	5.0E-02	585	2			
6	4	2.0E-13					
7	1	1.0E-06					
8	1	1.0E-03					

	Layer Type	Geomembrane Pinhole Density (#/acre)	Geomembrane Instal. Defects (#/acre)	Geomembrane Placement Quality	Geotextile Transmissivity (cm^2/sec)
1	1				
2	1				
3	1				
4	1				
5	2				
6	4	1	4	3	
7	1				
8	1				

The lack of values in the table for particular parameters in particular layers denotes that no HELP model input was required for that parameter in that layer. No data are missing from the table.

Configuration #2: Closure cap configuration #1 without the GCL. The GCL was simply eliminated and was not replaced with another material since it is so thin. (i.e. HDPE geomembrane as sole hydraulic barrier, lateral drainage and erosion barrier with CLSM infill).

HELP Model Input Data for Configuration #3 (Year 0):

Input Parameter (HELP Model Query)	Generic Input Parameter Value
Landfill area =	0.0134 acres
Percent of area where runoff is possible =	100%
Do you want to specify initial moisture storage? (Y/N)	Y
Amount of water or snow on surface =	0 inches
CN Input Parameter (HELP Model Query)	CN Input Parameter Value
Slope =	2 %
Slope length =	585 ft
Soil Texture =	4 (HELP model default soil texture)
Vegetation =	4 (i.e., a good stand of grass)
HELP Model Computed Curve Number = 46.2	

Layer	Layer Number	Layer Type
Topsoil	1	1 (vertical percolation layer)
Upper Backfill	2	1 (vertical percolation layer)
Erosion Barrier	3	1 (vertical percolation layer)
Middle Backfill	4	1 (vertical percolation layer)
Lateral Drainage Layer	5	2 (lateral drainage layer)
GCL	6	3 (barrier soil liner)
Foundation Layer (1.0E-06)	7	1 (vertical percolation layer)
Foundation Layer (1.0E-03)	8	1 (vertical percolation layer)

	Layer Type	Layer Thickness (in)	Soil Texture No.	Total Porosity (Vol/Vol)	Field Capacity (Vol/Vol)	Wilting Point (Vol/Vol)	Initial Moisture (Vol/Vol)
1	1	6		0.396	0.109	0.047	0.109
2	1	30		0.35	0.252	0.181	0.252
3	1	12		0.125	0.109	0.031	0.109
4	1	12		0.35	0.252	0.181	0.252
5	2	12		0.417	0.045	0.018	0.045
6	3	0.2		0.750	0.747	0.400	0.750
7	1	12		0.35	0.252	0.181	0.252
8	1	72		0.457	0.131	0.058	0.131

HELP Model Input Data for Configuration #3 (Year 0) – continued:

	Layer Type	Sat. Hyd. Conductivity (cm/sec)	Drainage Length (ft)	Drain Slope (%)	Leachate Recirc. (%)	Recirc. to Layer (#)	Subsurface Inflow (in/yr)
1	1	3.1E-03					
2	1	4.1E-05					
3	1	8.36E-07					
4	1	4.1E-05					
5	2	5.0E-02	585	2			
6	3	5.0E-09					
7	1	1.0E-06					
8	1	1.0E-03					

	Layer Type	Geomembrane Pinhole Density (#/acre)	Geomembrane Instal. Defects (#/acre)	Geomembrane Placement Quality	Geotextile Transmissivity (cm^2/sec)
1	1				
2	1				
3	1				
4	1				
5	2				
6	3				
7	1				
8	1				

The lack of values in the table for particular parameters in particular layers denotes that no HELP model input was required for that parameter in that layer. No data are missing from the table.

Configuration #3: Closure cap configuration #1 without the HDPE geomembrane. The HDPE geomembrane was simply eliminated and was not replaced with another material since it is so thin. (i.e. GCL as sole hydraulic barrier, lateral drainage and erosion barrier with CLSM infill).

HELP Model Input Data for Configuration #4 (Year 0):

Input Parameter (HELP Model Query)	Generic Input Parameter Value
Landfill area =	0.0134 acres
Percent of area where runoff is possible =	100%
Do you want to specify initial moisture storage? (Y/N)	Y
Amount of water or snow on surface =	0 inches
CN Input Parameter (HELP Model Query)	CN Input Parameter Value
Slope =	2 %
Slope length =	585 ft
Soil Texture =	4 (HELP model default soil texture)
Vegetation =	4 (i.e., a good stand of grass)
HELP Model Computed Curve Number = 46.2	

Layer	Layer Number	Layer Type
Topsoil	1	1 (vertical percolation layer)
Upper Backfill	2	1 (vertical percolation layer)
Erosion Barrier	3	1 (vertical percolation layer)
Middle Backfill	4	1 (vertical percolation layer)
Lateral Drainage Layer with Backfill Properties	5	2 (lateral drainage layer)
HDPE Geomembrane	6	4 (geomembrane liner)
GCL	7	3 (barrier soil liner)
Foundation Layer (1.0E-06)	8	1 (vertical percolation layer)
Foundation Layer (1.0E-03)	9	1 (vertical percolation layer)

	Layer Type	Layer Thickness (in)	Soil Texture No.	Total Porosity (Vol/Vol)	Field Capacity (Vol/Vol)	Wilting Point (Vol/Vol)	Initial Moisture (Vol/Vol)
1	1	6		0.396	0.109	0.047	0.109
2	1	30		0.35	0.252	0.181	0.252
3	1	12		0.125	0.109	0.031	0.109
4	1	12		0.35	0.252	0.181	0.252
5	2	12		0.35	0.252	0.181	0.252
6	4	0.06					
7	3	0.2		0.750	0.747	0.400	0.750
8	1	12		0.35	0.252	0.181	0.252
9	1	72		0.457	0.131	0.058	0.131

HELP Model Input Data for Configuration #4 (Year 0) – continued:

	Layer Type	Sat. Hyd. Conductivity (cm/sec)	Drainage Length (ft)	Drain Slope (%)	Leachate Recirc. (%)	Recirc. to Layer (#)	Subsurface Inflow (in/yr)
1	1	3.1E-03					
2	1	4.1E-05					
3	1	8.36E-07					
4	1	4.1E-05					
5	2	4.1E-05	585	2			
6	4	2.0E-13					
7	3	5.0E-09					
8	1	1.0E-06					
9	1	1.0E-03					

	Layer Type	Geomembrane Pinhole Density (#/acre)	Geomembrane Instal. Defects (#/acre)	Geomembrane Placement Quality	Geotextile Transmissivity (cm^2/sec)
1	1				
2	1				
3	1				
4	1				
5	2				
6	4	1	4	2	
7	3				
8	1				
9	1				

The lack of values in the table for particular parameters in particular layers denotes that no HELP model input was required for that parameter in that layer. No data are missing from the table.

Configuration #4: Closure cap configuration #1 without the lateral drainage layer. The material properties for the lateral drainage layer were replaced with those of backfill rather than eliminating the layer. (i.e. composite barrier and erosion barrier with CLSM infill)

HELP Model Input Data for Configuration #5 (Year 0):

Input Parameter (HELP Model Query)	Generic Input Parameter Value
Landfill area =	0.0134 acres
Percent of area where runoff is possible =	100%
Do you want to specify initial moisture storage? (Y/N)	Y
Amount of water or snow on surface =	0 inches
CN Input Parameter (HELP Model Query)	CN Input Parameter Value
Slope =	2 %
Slope length =	585 ft
Soil Texture =	4 (HELP model default soil texture)
Vegetation =	4 (i.e., a good stand of grass)
HELP Model Computed Curve Number = 46.2	

Layer	Layer Number	Layer Type
Topsoil	1	1 (vertical percolation layer)
Backfill	2	1 (vertical percolation layer)
Lateral Drainage Layer	3	2 (lateral drainage layer)
HDPE Geomembrane	4	4 (geomembrane liner)
GCL	5	3 (barrier soil liner)
Foundation Layer (1.0E-06)	6	1 (vertical percolation layer)
Foundation Layer (1.0E-03)	7	1 (vertical percolation layer)

	Layer Type	Layer Thickness (in)	Soil Texture No.	Total Porosity (Vol/Vol)	Field Capacity (Vol/Vol)	Wilting Point (Vol/Vol)	Initial Moisture (Vol/Vol)
1	1	6		0.396	0.109	0.047	0.109
2	1	54		0.35	0.252	0.181	0.252
3	2	12		0.417	0.045	0.018	0.045
4	4	0.06					
5	3	0.2		0.750	0.747	0.400	0.750
6	1	12		0.35	0.252	0.181	0.252
7	1	72		0.457	0.131	0.058	0.131

HELP Model Input Data for Configuration #5 (Year 0) – continued:

	Layer Type	Sat. Hyd. Conductivity (cm/sec)	Drainage Length (ft)	Drain Slope (%)	Leachate Recirc. (%)	Recirc. to Layer (#)	Subsurface Inflow (in/yr)
1	1	3.1E-03					
2	1	4.1E-05					
3	2	5.0E-02	585	2			
4	4	2.0E-13					
5	3	5.0E-09					
6	1	1.0E-06					
7	1	1.0E-03					
	Layer Type	Geomembrane Pinhole Density (#/acre)	Geomembrane Instal. Defects (#/acre)	Geomembrane Placement Quality	Geotextile Transmissivity (cm^2/sec)
1	1				
2	1				
3	2				
4	4	1	4	2	
5	3				
6	1				
7	1				

The lack of values in the table for particular parameters in particular layers denotes that no HELP model input was required for that parameter in that layer. No data are missing from the table.

Configuration #5: Closure cap configuration #1 without the erosion barrier. The material properties for the erosion barrier were replaced with those of backfill rather than eliminating the layer. (i.e. composite barrier and lateral drainage)

HELP Model Input Data for Configuration #6 (Year 0):

Input Parameter (HELP Model Query)	Generic Input Parameter Value
Landfill area =	0.0134 acres
Percent of area where runoff is possible =	100%
Do you want to specify initial moisture storage? (Y/N)	Y
Amount of water or snow on surface =	0 inches
CN Input Parameter (HELP Model Query)	CN Input Parameter Value
Slope =	2 %
Slope length =	585 ft
Soil Texture =	4 (HELP model default soil texture)
Vegetation =	4 (i.e., a good stand of grass)
HELP Model Computed Curve Number = 46.2	

Layer	Layer Number	Layer Type
Topsoil	1	1 (vertical percolation layer)
Backfill	2	1 (vertical percolation layer)
Foundation Layer (Lower Backfill)	3	1 (vertical percolation layer)

	Layer Type	Layer Thickness (in)	Soil Texture No.	Total Porosity (Vol/Vol)	Field Capacity (Vol/Vol)	Wilting Point (Vol/Vol)	Initial Moisture (Vol/Vol)
1	1	6		0.396	0.109	0.047	0.109
2	1	66		0.35	0.252	0.181	0.252
3	1	84		0.457	0.131	0.058	0.131

	Layer Type	Sat. Hyd. Conductivity (cm/sec)	Drainage Length (ft)	Drain Slope (%)	Leachate Recirc. (%)	Recirc. to Layer (#)	Subsurface Inflow (in/yr)
1	1	3.1E-03					
2	1	4.1E-05					
3	1	1.0E-03					

	Layer Type	Geomembrane Pinhole Density (#/acre)	Geomembrane Instal. Defects (#/acre)	Geomembrane Placement Quality	Geotextile Transmissivity (cm^2/sec)
1	1				
2	1				
3	1				

The lack of values in the table for particular parameters in particular layers denotes that no HELP model input was required for that parameter in that layer. No data are missing from the table.

Configuration #6: The closure cap configuration described in Table 11 and Table 12 of Section 4.3 where the GCL and HDPE geomembrane were eliminated and the material properties for lateral drainage layer and erosion barrier were replaced with those of backfill rather than eliminating the layers (i.e., soils only closure cap).

This page intentionally left blank.

APPENDIX H.
CONFIGURATIONS #1, THRU #6 DETAILED HELP MODEL ANNUAL WATER BALANCE DATA

Detailed HELP Model Annual Water Balance Data for Configuration #1 (Year 0):

Simulation	Prec (in/yr)	Runoff (in/yr)	Evap (in/yr)	Lateral Drainage (in/yr)	Infiltration thru GCL (in/yr)	Change in Water Storage (in/yr)
1	40.07	0.000	32.108	3.262	0.00006	4.699
2	57.14	10.188	36.785	9.382	0.00018	0.785
3	52.64	10.810	32.399	9.178	0.00017	0.253
4	47.88	1.668	39.835	8.250	0.00015	-1.874
5	50.57	3.045	35.513	9.395	0.00018	2.617
6	42.28	5.478	29.095	8.359	0.00016	-0.652
7	39.35	3.495	32.397	9.001	0.00017	-5.543
8	49.46	4.499	33.930	7.832	0.00014	3.199
9	48.59	0.623	36.983	10.266	0.00020	0.719
10	53.97	9.084	35.054	8.455	0.00016	1.378
11	57.63	14.277	33.712	9.258	0.00017	0.383
12	46.71	5.758	32.364	9.765	0.00018	-1.177
13	38.58	0.000	30.376	7.711	0.00014	0.493
14	41.49	7.135	29.109	7.072	0.00013	-1.826
15	44.94	2.963	35.954	8.292	0.00015	-2.269
16	54.78	9.023	33.664	8.602	0.00016	3.491
17	29.81	3.590	22.806	6.842	0.00013	-3.428
18	49.55	0.000	37.356	8.309	0.00016	3.885
19	55.50	9.985	37.170	9.882	0.00019	-1.537
20	68.56	16.812	39.028	10.142	0.00019	2.578
21	51.14	4.640	37.089	9.497	0.00018	-0.087
22	51.22	3.379	38.252	9.821	0.00019	-0.231
23	47.94	7.765	37.552	7.914	0.00015	-5.290
24	59.17	13.188	33.073	7.278	0.00013	5.631
25	47.73	6.356	32.835	8.918	0.00017	-0.379
26	50.56	8.943	33.205	8.128	0.00015	0.284
27	37.02	0.000	33.148	7.552	0.00014	-3.680
28	56.03	9.220	39.440	8.131	0.00015	-0.762
29	39.77	0.845	30.212	6.917	0.00013	1.795
30	46.55	1.413	35.834	9.099	0.00017	0.204
31	39.45	5.740	30.567	7.044	0.00013	-3.901
32	45.35	3.459	32.281	7.502	0.00014	2.108
33	42.23	0.000	32.202	6.815	0.00012	3.213
34	37.81	4.091	28.963	7.245	0.00013	-2.490
35	48.19	2.225	37.883	8.587	0.00016	-0.504
36	62.28	12.766	35.801	9.389	0.00018	4.324

Detailed HELP Model Annual Water Balance Data for Configuration #1 (Year 0) – Continued:

Simulation	Prec (in/yr)	Runoff (in/yr)	Evap (in/yr)	Lateral Drainage (in/yr)	Infiltration thru GCL (in/yr)	Change in Water Storage (in/yr)
37	55.96	5.346	42.442	9.059	0.00017	-0.887
38	40.26	3.126	29.542	7.911	0.00015	-0.319
39	60.02	12.980	37.725	8.939	0.00017	0.376
40	59.62	9.726	39.365	10.142	0.00019	0.387
41	47.60	5.982	32.378	9.096	0.00017	0.145
42	50.44	4.593	35.465	10.012	0.00019	0.370
43	39.42	3.854	28.374	8.128	0.00015	-0.936
44	48.61	3.991	35.775	8.090	0.00015	0.754
45	57.35	15.378	38.227	9.271	0.00017	-5.526
46	47.49	3.285	33.353	5.649	0.00010	5.202
47	38.98	1.888	32.952	7.795	0.00015	-3.654
48	42.99	0.000	33.953	7.761	0.00014	1.275
49	53.01	4.727	35.466	10.008	0.00019	2.809
50	55.17	8.286	39.548	9.294	0.00018	-1.958
51	46.16	5.359	32.491	6.718	0.00012	1.592
52	42.63	3.218	35.605	8.113	0.00015	-4.306
53	50.93	3.849	34.992	9.476	0.00018	2.613
54	54.24	13.430	30.556	8.963	0.00017	1.291
55	50.46	5.965	34.055	9.670	0.00018	0.770
56	56.39	8.145	41.882	9.952	0.00019	-3.589
57	41.99	3.151	29.793	7.727	0.00014	1.319
58	68.60	20.226	36.767	10.204	0.00019	1.403
59	48.67	5.585	35.146	8.079	0.00015	-0.141
60	58.12	9.448	38.952	9.082	0.00017	0.639
61	54.90	15.234	32.485	7.290	0.00013	-0.109
62	56.29	10.574	36.179	10.111	0.00019	-0.574
63	49.13	3.983	37.979	9.961	0.00019	-2.793
64	54.54	8.457	33.656	8.709	0.00016	3.718
65	45.05	2.984	34.216	9.544	0.00018	-1.695
66	37.07	1.556	30.928	7.491	0.00014	-2.906
67	40.17	3.130	25.868	6.933	0.00013	4.239
68	58.08	12.570	36.741	9.133	0.00017	-0.363
69	36.31	0.303	28.811	8.822	0.00016	-1.626
70	42.67	5.372	33.624	7.740	0.00014	-4.066
71	48.88	2.405	36.826	6.514	0.00012	3.135
72	47.36	5.955	35.680	8.504	0.00016	-2.780
73	35.81	2.229	27.617	5.652	0.00010	0.311
74	49.81	2.855	33.982	7.928	0.00015	5.044

Detailed HELP Model Annual Water Balance Data for Configuration #1 (Year 0) –
Continued:

Simulation	Prec (in/yr)	Runoff (in/yr)	Evap (in/yr)	Lateral Drainage (in/yr)	Infiltration thru GCL (in/yr)	Change in Water Storage (in/yr)
75	56.43	8.611	38.039	9.687	0.00018	0.093
76	45.86	4.655	34.215	9.350	0.00018	-2.360
77	56.76	5.345	41.200	9.445	0.00018	0.770
78	39.15	2.648	30.395	7.212	0.00013	-1.105
79	48.87	6.721	31.963	7.075	0.00013	3.111
80	58.52	13.654	36.403	9.340	0.00018	-0.877
81	53.34	5.708	37.293	9.727	0.00018	0.612
82	55.18	8.205	36.882	9.576	0.00018	0.517
83	53.60	13.155	36.072	8.657	0.00016	-4.284
84	47.82	3.668	35.654	6.665	0.00012	1.833
85	44.69	2.269	30.932	8.991	0.00017	2.498
86	60.77	15.597	37.628	8.414	0.00016	-0.870
87	48.34	7.753	30.372	8.504	0.00016	1.711
88	36.18	7.118	27.543	7.541	0.00014	-6.022
89	58.29	10.713	36.844	6.469	0.00012	4.264
90	60.08	17.086	32.161	9.820	0.00019	1.013
91	55.49	8.581	37.370	9.994	0.00019	-0.455
92	44.51	2.707	33.871	8.198	0.00015	-0.266
93	35.83	1.677	29.759	7.471	0.00014	-3.078
94	45.02	0.000	34.169	9.661	0.00018	1.190
95	44.54	8.222	29.852	8.732	0.00016	-2.267
96	53.18	5.039	37.255	7.479	0.00014	3.407
97	48.03	5.875	34.013	8.053	0.00015	0.089
98	62.58	9.148	42.737	9.332	0.00018	1.363
99	48.78	6.878	32.762	9.766	0.00018	-0.627
100	49.29	0.881	38.234	9.853	0.00019	0.322
Summary Statistics						
Count	100	100	100	100	100	100
Maximum	68.60	20.226	42.737	10.266	0.00020	5.631
Average	49.14	6.235	34.370	8.476	0.00016	0.062
Median	48.83	5.366	34.192	8.594	0.00016	0.229
Minimum	29.81	0.000	22.806	3.262	0.00006	-6.022
Std Dev	7.69	4.525	3.682	1.226	0.00002	2.565

Configuration #1: Closure cap configuration described in Table 11 and Table 12 of Section 4.3, with CLSM infilling the erosion barrier. (i.e., composite barrier, lateral drainage and erosion barrier with CLSM infill)

Detailed HELP Model Annual Water Balance Data for Configuration #1a (Year 0):

Simulation	Prec (in/yr)	Runoff (in/yr)	Evap (in/yr)	Lateral Drainage (in/yr)	Infiltration thru GCL (in/yr)	Change in Water Storage (in/yr)
1	40.07	0.000	31.653	4.674	0.00009	3.743
2	57.14	0.000	32.094	25.219	0.00114	-0.175
3	52.64	0.000	31.091	21.130	0.00134	0.417
4	47.88	0.952	38.428	9.002	0.00018	-0.503
5	50.57	0.000	34.394	14.093	0.00031	2.083
6	42.28	0.000	27.895	13.158	0.00034	1.227
7	39.35	0.515	30.611	14.807	0.00036	-6.584
8	49.46	0.509	31.514	15.519	0.00035	1.917
9	48.59	0.000	33.583	14.013	0.00030	0.994
10	53.97	0.000	33.906	19.125	0.00245	0.936
11	57.63	2.054	32.433	21.871	0.00287	1.269
12	46.71	0.000	29.208	20.020	0.00119	-2.519
13	38.58	0.000	30.409	7.619	0.00015	0.552
14	41.49	0.375	27.779	13.369	0.00042	-0.033
15	44.94	1.022	32.623	13.451	0.00029	-2.156
16	54.78	0.403	32.090	21.261	0.00173	1.024
17	29.81	0.000	21.667	9.165	0.00020	-1.022
18	49.55	0.000	34.895	11.998	0.00025	2.657
19	55.50	0.731	33.774	21.918	0.00251	-0.926
20	68.56	0.000	37.426	27.170	0.00111	3.963
21	51.14	0.000	33.876	19.158	0.00116	-1.895
22	51.22	0.000	36.715	15.447	0.00034	-0.942
23	47.94	0.000	36.529	14.831	0.00068	-3.421
24	59.17	1.199	31.240	23.092	0.00213	3.637
25	47.73	0.026	30.420	16.247	0.00038	1.037
26	50.56	0.194	31.935	17.538	0.00096	0.892
27	37.02	0.000	32.181	8.539	0.00018	-3.701
28	56.03	0.788	35.960	20.278	0.00091	-0.997
29	39.77	0.000	29.485	8.588	0.00017	1.697
30	46.55	0.299	33.864	12.716	0.00026	-0.328
31	39.45	0.060	28.844	13.692	0.00033	-3.146
32	45.35	0.375	29.807	13.016	0.00029	2.151
33	42.23	0.000	31.905	8.297	0.00016	2.027
34	37.81	0.000	27.339	11.779	0.00027	-1.307
35	48.19	0.286	34.212	14.470	0.00032	-0.778
36	62.28	3.520	34.056	20.336	0.00085	4.367

Detailed HELP Model Annual Water Balance Data for Configuration #1a (Year 0) – Continued:

Simulation	Prec (in/yr)	Runoff (in/yr)	Evap (in/yr)	Lateral Drainage (in/yr)	Infiltration thru GCL (in/yr)	Change in Water Storage (in/yr)
37	55.96	0.000	40.483	16.055	0.00037	-0.579
38	40.26	0.000	28.229	13.330	0.00030	-1.299
39	60.02	2.338	35.097	22.212	0.00318	0.369
40	59.62	0.734	37.281	21.810	0.00053	-0.207
41	47.60	0.000	31.582	15.355	0.00036	0.663
42	50.44	0.521	34.130	16.392	0.00037	-0.603
43	39.42	0.061	26.350	11.449	0.00024	1.559
44	48.61	0.000	33.998	14.369	0.00033	0.243
45	57.35	0.931	34.969	27.145	0.00358	-5.699
46	47.49	0.000	31.999	11.887	0.00027	3.604
47	38.98	0.000	31.666	9.265	0.00019	-1.951
48	42.99	0.000	32.694	9.297	0.00018	0.999
49	53.01	1.660	34.281	13.805	0.00030	3.264
50	55.17	0.038	38.102	20.038	0.00050	-3.008
51	46.16	0.000	31.248	11.786	0.00026	3.126
52	42.63	0.000	33.721	13.951	0.00033	-5.043
53	50.93	0.000	32.529	18.186	0.00042	0.215
54	54.24	0.582	28.380	20.018	0.00093	5.259
55	50.46	0.218	33.032	16.939	0.00055	0.270
56	56.39	1.117	38.507	21.660	0.00055	-4.894
57	41.99	0.000	27.957	13.188	0.00033	0.845
58	68.60	0.196	35.690	29.632	0.00234	3.079
59	48.67	0.089	33.998	14.821	0.00038	-0.239
60	58.12	0.000	34.682	23.126	0.00243	0.310
61	54.90	2.184	31.315	21.428	0.00400	-0.032
62	56.29	0.885	33.384	25.216	0.00321	-3.198
63	49.13	0.373	34.348	15.382	0.00034	-0.974
64	54.54	0.357	32.296	18.810	0.00056	3.077
65	45.05	0.000	32.908	13.493	0.00030	-1.351
66	37.07	0.000	29.770	9.605	0.00020	-2.305
67	40.17	0.000	25.014	10.780	0.00023	4.376
68	58.08	0.000	35.387	24.503	0.00241	-1.812
69	36.31	0.000	27.124	10.264	0.00021	-1.078
70	42.67	0.996	31.917	13.057	0.00031	-3.300
71	48.88	0.000	35.418	10.344	0.00023	3.118
72	47.36	0.511	32.766	17.179	0.00041	-3.096
73	35.81	0.000	26.571	8.543	0.00018	0.696
74	49.81	0.686	29.647	16.006	0.00039	3.472

Detailed HELP Model Annual Water Balance Data for Configuration #1a (Year 0) –
Continued:

Simulation	Prec (in/yr)	Runoff (in/yr)	Evap (in/yr)	Lateral Drainage (in/yr)	Infiltration thru GCL (in/yr)	Change in Water Storage (in/yr)
75	56.43	3.806	34.455	17.456	0.00040	0.713
76	45.86	0.000	32.561	15.138	0.00035	-1.839
77	56.76	0.000	39.129	18.383	0.00063	-0.753
78	39.15	0.000	29.546	8.964	0.00020	0.639
79	48.87	0.000	30.932	13.743	0.00105	4.194
80	58.52	0.982	33.493	27.411	0.00496	-3.371
81	53.34	0.000	35.510	16.525	0.00037	1.305
82	55.18	0.000	35.585	18.264	0.00068	1.331
83	53.60	2.607	34.853	20.405	0.00209	-4.267
84	47.82	0.000	34.139	12.820	0.00034	0.861
85	44.69	0.000	30.905	10.088	0.00020	3.697
86	60.77	0.000	35.879	27.609	0.00280	-2.721
87	48.34	1.123	29.579	14.361	0.00052	3.277
88	36.18	0.000	26.171	15.954	0.00214	-5.947
89	58.29	2.732	35.148	17.826	0.00082	2.583
90	60.08	1.421	30.575	23.354	0.00324	4.726
91	55.49	0.000	35.936	22.105	0.00169	-2.553
92	44.51	0.202	32.165	13.119	0.00030	-0.977
93	35.83	0.000	29.650	9.732	0.00021	-3.553
94	45.02	0.000	32.964	10.173	0.00020	1.883
95	44.54	0.000	27.674	18.660	0.00282	-1.797
96	53.18	0.108	35.755	13.943	0.00033	3.375
97	48.03	0.359	31.471	16.924	0.00042	-0.724
98	62.58	1.090	41.484	16.928	0.00044	3.078
99	48.78	0.684	31.561	20.295	0.00175	-3.762
100	49.29	0.000	35.882	10.372	0.00020	3.036
Summary Statistics						
Count	100	100	100	100	100	100
Maximum	68.60	3.806	41.484	29.632	0.00496	5.259
Average	49.14	0.429	32.573	16.075	0.00088	0.065
Median	48.83	0.000	32.592	15.368	0.00037	0.257
Minimum	29.81	0.000	21.667	4.674	0.00009	-6.584
Std Dev	7.69	0.765	3.383	5.255	0.00102	2.635

Configuration #1a: Closure cap configuration described in Table 11 and Table 12 of Section 4.3, with sandy soil infilling the erosion barrier. (i.e., composite barrier, lateral drainage and erosion barrier with sandy soil infill)

Detailed HELP Model Annual Water Balance Data for Configuration #2 (Year 0):

Simulation	Prec (in/yr)	Runoff (in/yr)	Evap (in/yr)	Lateral Drainage (in/yr)	Infiltration thru GCL (in/yr)	Change in Water Storage (in/yr)
1	40.07	0.000	32.108	3.259	0.00481	4.702
2	57.14	10.188	36.785	9.369	0.01309	0.798
3	52.64	10.810	32.399	9.166	0.01283	0.265
4	47.88	1.668	39.835	8.238	0.01160	-1.863
5	50.57	3.045	35.513	9.383	0.01312	2.629
6	42.28	5.478	29.095	8.347	0.01175	-0.643
7	39.35	3.495	32.397	8.988	0.01259	-5.532
8	49.46	4.499	33.930	7.822	0.01106	3.205
9	48.59	0.623	36.983	10.252	0.01424	0.730
10	53.97	9.084	35.054	8.443	0.01187	1.382
11	57.63	14.277	33.712	9.245	0.01293	0.387
12	46.71	5.758	32.364	9.752	0.01360	-1.172
13	38.58	0.000	30.376	7.699	0.01088	0.493
14	41.49	7.135	29.109	7.061	0.01000	-1.828
15	44.94	2.963	35.954	8.281	0.01167	-2.268
16	54.78	9.023	33.664	8.590	0.01208	3.493
17	29.81	3.590	22.806	6.831	0.00967	-3.430
18	49.55	0.000	37.356	8.299	0.01166	3.885
19	55.50	9.985	37.170	9.868	0.01375	-1.532
20	68.56	16.812	39.028	10.128	0.01409	2.583
21	51.14	4.640	37.089	9.484	0.01324	-0.085
22	51.22	3.379	38.252	9.808	0.01367	-0.228
23	47.94	7.765	37.552	7.902	0.01116	-5.293
24	59.17	13.188	33.073	7.269	0.01033	5.626
25	47.73	6.356	32.835	8.906	0.01249	-0.378
26	50.56	8.943	33.205	8.117	0.01145	0.283
27	37.02	0.000	33.148	7.541	0.01065	-3.683
28	56.03	9.220	39.440	8.120	0.01144	-0.763
29	39.77	0.845	30.212	6.908	0.00986	1.791
30	46.55	1.413	35.834	9.087	0.01273	0.206
31	39.45	5.740	30.567	7.033	0.00996	-3.905
32	45.35	3.459	32.281	7.492	0.01060	2.105
33	42.23	0.000	32.202	6.806	0.00974	3.209
34	37.81	4.091	28.963	7.234	0.01023	-2.492
35	48.19	2.225	37.883	8.576	0.01205	-0.504
36	62.28	12.766	35.801	9.376	0.01311	4.327

Detailed HELP Model Annual Water Balance Data for Configuration #2 (Year 0) –
Continued:

Simulation	Prec (in/yr)	Runoff (in/yr)	Evap (in/yr)	Lateral Drainage (in/yr)	Infiltration thru GCL (in/yr)	Change in Water Storage (in/yr)
37	55.96	5.346	42.442	9.046	0.01266	-0.885
38	40.26	3.126	29.542	7.900	0.01115	-0.321
39	60.02	12.980	37.725	8.927	0.01252	0.377
40	59.62	9.726	39.365	10.129	0.01409	0.391
41	47.60	5.982	32.378	9.083	0.01272	0.145
42	50.44	4.593	35.465	9.998	0.01391	0.373
43	39.42	3.854	28.374	8.116	0.01141	-0.939
44	48.61	3.991	35.775	8.079	0.01142	0.750
45	57.35	15.378	38.227	9.258	0.01294	-5.525
46	47.49	3.285	33.353	5.642	0.00815	5.192
47	38.98	1.888	32.952	7.783	0.01097	-3.656
48	42.99	0.000	33.953	7.751	0.01099	1.273
49	53.01	4.727	35.466	9.994	0.01391	2.812
50	55.17	8.286	39.548	9.280	0.01297	-1.957
51	46.16	5.359	32.491	6.708	0.00955	1.586
52	42.63	3.218	35.605	8.102	0.01144	-4.308
53	50.93	3.849	34.992	9.463	0.01322	2.616
54	54.24	13.430	30.556	8.950	0.01254	1.292
55	50.46	5.965	34.055	9.657	0.01347	0.772
56	56.39	8.145	41.882	9.938	0.01383	-3.587
57	41.99	3.151	29.793	7.716	0.01093	1.315
58	68.60	20.226	36.767	10.191	0.01416	1.406
59	48.67	5.585	35.146	8.067	0.01135	-0.144
60	58.12	9.448	38.952	9.070	0.01270	0.638
61	54.90	15.234	32.485	7.279	0.01031	-0.114
62	56.29	10.574	36.179	10.098	0.01404	-0.572
63	49.13	3.983	37.979	9.947	0.01384	-2.790
64	54.54	8.457	33.656	8.697	0.01222	3.716
65	45.05	2.984	34.216	9.531	0.01331	-1.694
66	37.07	1.556	30.928	7.480	0.01060	-2.911
67	40.17	3.130	25.868	6.923	0.00987	4.232
68	58.08	12.570	36.741	9.121	0.01278	-0.363
69	36.31	0.303	28.811	8.809	0.01236	-1.626
70	42.67	5.372	33.624	7.729	0.01094	-4.069
71	48.88	2.405	36.826	6.504	0.00930	3.128
72	47.36	5.955	35.680	8.493	0.01195	-2.780
73	35.81	2.229	27.617	5.644	0.00814	0.303
74	49.81	2.855	33.982	7.919	0.01113	5.043

Detailed HELP Model Annual Water Balance Data for Configuration #2 (Year 0) – Continued:

Simulation	Prec (in/yr)	Runoff (in/yr)	Evap (in/yr)	Lateral Drainage (in/yr)	Infiltration thru GCL (in/yr)	Change in Water Storage (in/yr)
75	56.43	8.611	38.039	9.674	0.01350	0.097
76	45.86	4.655	34.215	9.337	0.01306	-2.357
77	56.76	5.345	41.200	9.432	0.01318	0.772
78	39.15	2.648	30.395	7.201	0.01019	-1.109
79	48.87	6.721	31.963	7.065	0.01005	3.106
80	58.52	13.654	36.403	9.328	0.01305	-0.875
81	53.34	5.708	37.293	9.714	0.01355	0.615
82	55.18	8.205	36.882	9.563	0.01335	0.519
83	53.60	13.155	36.072	8.645	0.01214	-4.285
84	47.82	3.668	35.654	6.655	0.00951	1.826
85	44.69	2.269	30.932	8.979	0.01259	2.498
86	60.77	15.597	37.628	8.402	0.01182	-0.871
87	48.34	7.753	30.372	8.493	0.01194	1.710
88	36.18	7.118	27.543	7.529	0.01065	-6.025
89	58.29	10.713	36.844	6.461	0.00924	4.257
90	60.08	17.086	32.161	9.807	0.01367	1.016
91	55.49	8.581	37.370	9.980	0.01389	-0.451
92	44.51	2.707	33.871	8.186	0.01152	-0.268
93	35.83	1.677	29.759	7.461	0.01058	-3.082
94	45.02	0.000	34.169	9.648	0.01346	1.192
95	44.54	8.222	29.852	8.720	0.01222	-2.266
96	53.18	5.039	37.255	7.468	0.01059	3.402
97	48.03	5.875	34.013	8.042	0.01135	0.087
98	62.58	9.148	42.737	9.320	0.01304	1.365
99	48.78	6.878	32.762	9.753	0.01360	-0.625
100	49.29	0.881	38.234	9.839	0.01371	0.324
Summary Statistics						
Count	100	100	100	100	100	100
Maximum	68.60	20.226	42.737	10.252	0.01424	5.626
Average	49.14	6.235	34.370	8.464	0.01189	0.062
Median	48.83	5.366	34.192	8.583	0.01206	0.236
Minimum	29.81	0.000	22.806	3.259	0.00481	-6.025
Std Dev	7.69	4.525	3.682	1.224	0.00163	2.564

Configuration #2: Closure cap configuration #1 without the GCL. The GCL was simply eliminated and was not replaced with another material since it is so thin. (i.e. HDPE geomembrane as sole hydraulic barrier, lateral drainage and erosion barrier with CLSM infill).

Detailed HELP Model Annual Water Balance Data for Configuration #3 (Year 0):

Simulation	Prec (in/yr)	Runoff (in/yr)	Evap (in/yr)	Lateral Drainage (in/yr)	Infiltration thru GCL (in/yr)	Change in Water Storage (in/yr)
1	40.07	0.000	32.108	3.011	0.32360	4.951
2	57.14	10.188	36.785	8.563	0.81381	1.603
3	52.64	10.810	32.399	8.401	0.79955	1.030
4	47.88	1.668	39.835	7.479	0.71877	-1.102
5	50.57	3.045	35.513	8.631	0.81976	3.369
6	42.28	5.478	29.095	7.612	0.73026	-0.155
7	39.35	3.495	32.397	8.191	0.78111	-5.521
8	49.46	4.499	33.930	7.176	0.69223	3.050
9	48.59	0.623	36.983	9.391	0.88650	0.950
10	53.97	9.084	35.054	7.700	0.73799	1.350
11	57.63	14.277	33.712	8.438	0.80282	0.344
12	46.71	5.758	32.364	8.951	0.84799	-1.140
13	38.58	0.000	30.376	7.011	0.67751	0.432
14	41.49	7.135	29.109	6.399	0.62378	-1.974
15	44.94	2.963	35.954	7.596	0.72886	-2.376
16	54.78	9.023	33.664	7.885	0.75445	3.637
17	29.81	3.590	22.806	6.166	0.60337	-3.387
18	49.55	0.000	37.356	7.642	0.73297	3.624
19	55.50	9.985	37.170	9.026	0.85444	-1.146
20	68.56	16.812	39.028	9.276	0.87654	2.652
21	51.14	4.640	37.089	8.641	0.82067	-0.084
22	51.22	3.379	38.252	9.004	0.85247	-0.286
23	47.94	7.765	37.552	7.168	0.69130	-5.331
24	59.17	13.188	33.073	6.674	0.64816	5.328
25	47.73	6.356	32.835	8.138	0.77644	-0.140
26	50.56	8.943	33.205	7.411	0.71263	0.272
27	37.02	0.000	33.148	6.841	0.66260	-3.724
28	56.03	9.220	39.440	7.443	0.71565	-0.926
29	39.77	0.845	30.212	6.309	0.61592	1.831
30	46.55	1.413	35.834	8.317	0.79217	0.333
31	39.45	5.740	30.567	6.374	0.62158	-3.901
32	45.35	3.459	32.281	6.868	0.66517	1.843
33	42.23	0.000	32.202	6.227	0.60873	3.276
34	37.81	4.091	28.963	6.557	0.63771	-2.359
35	48.19	2.225	37.883	7.890	0.75466	-0.603
36	62.28	12.766	35.801	8.585	0.81586	4.596

Detailed HELP Model Annual Water Balance Data for Configuration #3 (Year 0) – Continued:

Simulation	Prec (in/yr)	Runoff (in/yr)	Evap (in/yr)	Lateral Drainage (in/yr)	Infiltration thru GCL (in/yr)	Change in Water Storage (in/yr)
37	55.96	5.346	42.442	8.229	0.78446	-0.825
38	40.26	3.126	29.542	7.211	0.69508	-0.474
39	60.02	12.980	37.725	8.185	0.78064	0.374
40	59.62	9.726	39.365	9.292	0.87796	0.543
41	47.60	5.982	32.378	8.297	0.79043	0.154
42	50.44	4.593	35.465	9.153	0.86553	0.388
43	39.42	3.854	28.374	7.358	0.70799	-0.991
44	48.61	3.991	35.775	7.418	0.71339	0.539
45	57.35	15.378	38.227	8.450	0.80385	-5.351
46	47.49	3.285	33.353	5.154	0.51454	4.852
47	38.98	1.888	32.952	7.067	0.68242	-3.479
48	42.99	0.000	33.953	7.120	0.68731	1.176
49	53.01	4.727	35.466	9.163	0.86642	3.093
50	55.17	8.286	39.548	8.453	0.80408	-1.872
51	46.16	5.359	32.491	6.099	0.59745	1.363
52	42.63	3.218	35.605	7.418	0.71340	-4.418
53	50.93	3.849	34.992	8.693	0.82517	2.776
54	54.24	13.430	30.556	8.173	0.77954	1.430
55	50.46	5.965	34.055	8.838	0.83791	0.775
56	56.39	8.145	41.882	9.074	0.85881	-3.525
57	41.99	3.151	29.793	7.043	0.68034	1.156
58	68.60	20.226	36.767	9.350	0.88284	1.473
59	48.67	5.585	35.146	7.311	0.70389	-0.132
60	58.12	9.448	38.952	8.341	0.79449	0.468
61	54.90	15.234	32.485	6.614	0.64265	-0.052
62	56.29	10.574	36.179	9.278	0.87653	-0.559
63	49.13	3.983	37.979	9.080	0.85915	-2.604
64	54.54	8.457	33.656	7.952	0.76031	3.629
65	45.05	2.984	34.216	8.720	0.82760	-1.701
66	37.07	1.556	30.928	6.788	0.65793	-2.981
67	40.17	3.130	25.868	6.324	0.61723	3.976
68	58.08	12.570	36.741	8.374	0.79733	-0.186
69	36.31	0.303	28.811	8.053	0.76898	-1.495
70	42.67	5.372	33.624	7.026	0.67888	-4.132
71	48.88	2.405	36.826	5.922	0.58193	2.881
72	47.36	5.955	35.680	7.784	0.74554	-2.662
73	35.81	2.229	27.617	5.107	0.51037	0.247
74	49.81	2.855	33.982	7.296	0.70251	4.863

Detailed HELP Model Annual Water Balance Data for Configuration #3 (Year 0) –
Continued:

Simulation	Prec (in/yr)	Runoff (in/yr)	Evap (in/yr)	Lateral Drainage (in/yr)	Infiltration thru GCL (in/yr)	Change in Water Storage (in/yr)
75	56.43	8.611	38.039	8.840	0.83813	0.554
76	45.86	4.655	34.215	8.531	0.81112	-2.306
77	56.76	5.345	41.200	8.640	0.82050	0.744
78	39.15	2.648	30.395	6.521	0.63453	-1.201
79	48.87	6.721	31.963	6.453	0.62857	2.883
80	58.52	13.654	36.403	8.557	0.81341	-0.755
81	53.34	5.708	37.293	8.903	0.84362	0.815
82	55.18	8.205	36.882	8.741	0.82942	0.571
83	53.60	13.155	36.072	7.861	0.75215	-4.340
84	47.82	3.668	35.654	6.084	0.59634	1.562
85	44.69	2.269	30.932	8.232	0.78468	2.600
86	60.77	15.597	37.628	7.659	0.73446	-0.773
87	48.34	7.753	30.372	7.778	0.74489	1.666
88	36.18	7.118	27.543	6.827	0.66151	-6.046
89	58.29	10.713	36.844	5.947	0.58417	3.931
90	60.08	17.086	32.161	8.971	0.84961	1.406
91	55.49	8.581	37.370	9.129	0.86347	-0.305
92	44.51	2.707	33.871	7.433	0.71475	-0.351
93	35.83	1.677	29.759	6.835	0.66210	-3.285
94	45.02	0.000	34.169	8.850	0.83900	1.282
95	44.54	8.222	29.852	7.919	0.75722	-2.119
96	53.18	5.039	37.255	6.821	0.66105	3.173
97	48.03	5.875	34.013	7.365	0.70861	0.072
98	62.58	9.148	42.737	8.547	0.81233	1.538
99	48.78	6.878	32.762	8.925	0.84552	-0.534
100	49.29	0.881	38.234	8.992	0.85162	0.366
Summary Statistics						
Count	100	100	100	100	100	100
Maximum	68.60	20.226	42.737	9.391	0.88650	5.328
Average	49.14	6.235	34.370	7.736	0.74116	0.102
Median	48.83	5.366	34.192	7.873	0.75330	0.303
Minimum	29.81	0.000	22.806	3.011	0.32360	-6.046
Std Dev	7.69	4.525	3.682	1.131	0.09936	2.542

Configuration #3: Closure cap configuration #1 without the HDPE geomembrane. The HDPE geomembrane was simply eliminated and was not replaced with another material since it is so thin. (i.e. GCL as sole hydraulic barrier, lateral drainage and erosion barrier with CLSM infill).

Detailed HELP Model Annual Water Balance Data for Configuration #4 (Year 0):

Simulation	Prec (in/yr)	Runoff (in/yr)	Evap (in/yr)	Lateral Drainage (in/yr)	Infiltration thru GCL (in/yr)	Change in Water Storage (in/yr)
1	40.07	0.800	32.082	0.161	0.00550	7.027
2	57.14	17.552	38.669	0.767	0.01969	0.152
3	52.64	18.454	33.623	0.948	0.02115	-0.385
4	47.88	5.363	41.502	0.616	0.01909	0.399
5	50.57	10.858	38.709	0.904	0.02123	0.098
6	42.28	11.103	30.798	0.716	0.01936	-0.339
7	39.35	6.381	35.508	0.568	0.01846	-3.110
8	49.46	11.021	34.400	0.742	0.02009	3.292
9	48.59	9.547	38.085	0.818	0.02087	0.133
10	53.97	17.241	36.257	0.798	0.01967	-0.337
11	57.63	19.342	37.272	0.639	0.01916	0.363
12	46.71	11.491	35.096	0.840	0.02042	-0.731
13	38.58	4.608	32.756	0.801	0.01986	0.398
14	41.49	10.448	30.320	0.510	0.01727	0.190
15	44.94	8.654	37.730	0.618	0.01891	-2.082
16	54.78	16.242	35.708	0.841	0.02077	1.971
17	29.81	7.087	24.002	0.475	0.01653	-1.777
18	49.55	6.865	39.955	0.677	0.01997	2.033
19	55.50	16.045	38.656	0.772	0.02026	0.007
20	68.56	27.503	40.130	1.052	0.02211	-0.144
21	51.14	10.774	39.484	0.682	0.01963	0.178
22	51.22	9.868	40.456	0.910	0.02131	-0.034
23	47.94	10.456	39.715	0.567	0.01796	-2.821
24	59.17	21.071	34.578	0.789	0.01986	2.710
25	47.73	13.127	33.987	0.604	0.01914	-0.011
26	50.56	14.548	35.171	0.837	0.01988	-0.017
27	37.02	1.880	35.475	0.500	0.01698	-0.858
28	56.03	15.465	41.034	0.665	0.01924	-1.156
29	39.77	4.693	32.512	0.578	0.01902	1.967
30	46.55	8.489	38.023	0.669	0.01966	-0.651
31	39.45	10.582	31.135	0.521	0.01697	-2.811
32	45.35	7.786	35.120	0.564	0.01837	1.860
33	42.23	3.388	36.687	0.594	0.02017	1.541
34	37.81	7.280	30.549	0.489	0.01727	-0.530
35	48.19	6.719	40.547	0.714	0.02035	0.191
36	62.28	23.621	37.072	0.946	0.02124	0.622

Detailed HELP Model Annual Water Balance Data for Configuration #4 (Year 0) – Continued:

Simulation	Prec (in/yr)	Runoff (in/yr)	Evap (in/yr)	Lateral Drainage (in/yr)	Infiltration thru GCL (in/yr)	Change in Water Storage (in/yr)
37	55.96	11.839	43.578	0.713	0.01948	-0.191
38	40.26	7.399	32.326	0.630	0.01896	-0.117
39	60.02	19.318	39.872	0.723	0.01960	0.085
40	59.62	16.637	41.789	0.956	0.02141	0.219
41	47.60	13.208	33.693	0.901	0.02080	-0.223
42	50.44	11.214	38.142	0.840	0.02097	0.222
43	39.42	7.976	30.920	0.587	0.01772	-0.087
44	48.61	9.757	38.065	0.687	0.01961	0.079
45	57.35	19.702	40.050	0.651	0.01861	-3.075
46	47.49	9.970	34.095	0.600	0.01827	2.804
47	38.98	4.256	35.145	0.476	0.01756	-0.919
48	42.99	4.694	36.749	0.613	0.02000	0.915
49	53.01	14.271	37.649	0.859	0.02164	0.213
50	55.17	12.354	42.911	0.668	0.01949	-0.786
51	46.16	11.065	33.594	0.644	0.01824	0.835
52	42.63	6.124	37.686	0.540	0.01820	-1.742
53	50.93	11.442	37.522	0.837	0.02104	1.110
54	54.24	21.934	31.281	0.884	0.02051	0.121
55	50.46	12.233	37.026	0.679	0.01990	0.501
56	56.39	12.946	43.710	0.720	0.02058	-1.008
57	41.99	10.072	30.414	0.712	0.01957	0.770
58	68.60	28.398	39.554	0.978	0.02163	-0.350
59	48.67	9.851	37.714	0.494	0.01753	0.587
60	58.12	16.944	40.483	0.791	0.02100	-0.120
61	54.90	20.579	33.664	0.726	0.01880	-0.092
62	56.29	16.368	38.930	0.841	0.02067	0.130
63	49.13	7.623	41.860	0.655	0.01985	-1.030
64	54.54	16.568	36.097	0.820	0.02020	1.033
65	45.05	6.625	37.938	0.711	0.01983	-0.246
66	37.07	5.101	33.145	0.462	0.01710	-1.660
67	40.17	8.714	28.920	0.598	0.01833	1.915
68	58.08	18.095	39.582	0.848	0.02005	-0.465
69	36.31	4.130	30.703	0.628	0.01948	0.829
70	42.67	10.855	34.865	0.518	0.01788	-3.590
71	48.88	5.689	40.183	0.403	0.01718	2.583
72	47.36	11.409	38.060	0.555	0.01850	-2.684
73	35.81	5.334	29.849	0.456	0.01652	0.151
74	49.81	9.542	36.981	0.575	0.01906	2.693

Detailed HELP Model Annual Water Balance Data for Configuration #4 (Year 0) – Continued:

Simulation	Prec (in/yr)	Runoff (in/yr)	Evap (in/yr)	Lateral Drainage (in/yr)	Infiltration thru GCL (in/yr)	Change in Water Storage (in/yr)
75	56.43	15.969	39.284	0.751	0.02018	0.407
76	45.86	8.473	36.608	0.701	0.01996	0.059
77	56.76	14.144	42.383	0.861	0.02085	-0.648
78	39.15	6.362	31.784	0.617	0.01837	0.365
79	48.87	14.370	33.527	0.621	0.01854	0.331
80	58.52	19.428	38.880	0.787	0.01986	-0.595
81	53.34	11.999	40.168	0.789	0.02050	0.364
82	55.18	14.694	39.463	0.841	0.02036	0.160
83	53.60	15.439	39.139	0.556	0.01777	-1.555
84	47.82	9.326	36.721	0.676	0.01889	1.075
85	44.69	9.010	34.339	0.810	0.02051	0.511
86	60.77	21.851	38.340	0.881	0.01987	-0.323
87	48.34	14.183	31.939	0.833	0.02033	1.364
88	36.18	9.497	29.526	0.464	0.01675	-3.329
89	58.29	16.387	39.277	0.778	0.02074	1.828
90	60.08	24.130	34.738	0.705	0.01990	0.487
91	55.49	14.245	40.644	0.870	0.02062	-0.290
92	44.51	7.260	36.417	0.651	0.01850	0.160
93	35.83	3.208	32.171	0.693	0.01949	-0.263
94	45.02	4.441	39.478	0.693	0.02054	0.388
95	44.54	13.743	32.194	0.561	0.01810	-1.979
96	53.18	10.617	40.129	0.548	0.01763	1.864
97	48.03	10.750	36.418	0.736	0.01917	0.105
98	62.58	17.599	44.056	0.904	0.02118	0.003
99	48.78	12.215	35.732	0.908	0.02098	-0.095
100	49.29	7.940	40.520	0.713	0.02039	0.096
Summary Statistics						
Count	100	100	100	100	100	100
Maximum	68.60	28.398	44.056	1.052	0.02211	7.027
Average	49.14	11.839	36.514	0.698	0.01933	0.072
Median	48.83	10.940	37.004	0.697	0.01966	0.097
Minimum	29.81	0.800	24.002	0.161	0.00550	-3.590
Std Dev	7.69	5.608	3.827	0.150	0.00191	1.500

Configuration #4: Closure cap configuration #1 without the lateral drainage layer. The material properties for the lateral drainage layer were replaced with those of backfill rather than eliminating the layer. (i.e. composite barrier and erosion barrier with CLSM infill)

Detailed HELP Model Annual Water Balance Data for Configuration #5 (Year 0):

Simulation	Prec (in/yr)	Runoff (in/yr)	Evap (in/yr)	Lateral Drainage (in/yr)	Infiltration thru GCL (in/yr)	Change in Water Storage (in/yr)
1	40.07	0.000	31.653	4.377	0.00008	4.040
2	57.14	0.000	32.094	25.218	0.00107	-0.174
3	52.64	0.000	31.091	21.072	0.00125	0.475
4	47.88	0.952	38.428	9.094	0.00018	-0.595
5	50.57	0.000	34.394	13.999	0.00030	2.177
6	42.28	0.000	27.895	13.135	0.00033	1.250
7	39.35	0.515	30.611	15.008	0.00036	-6.784
8	49.46	0.509	31.514	15.474	0.00035	1.963
9	48.59	0.000	33.583	13.910	0.00029	1.097
10	53.97	0.000	33.864	19.120	0.00238	0.983
11	57.63	1.890	32.454	22.074	0.00287	1.209
12	46.71	0.000	29.263	19.937	0.00109	-2.490
13	38.58	0.000	30.417	7.618	0.00015	0.545
14	41.49	0.375	27.783	13.502	0.00039	-0.171
15	44.94	1.022	32.633	13.440	0.00029	-2.155
16	54.78	0.403	32.037	21.208	0.00166	1.130
17	29.81	0.000	21.653	9.372	0.00021	-1.214
18	49.55	0.000	34.890	11.778	0.00024	2.882
19	55.50	0.731	33.797	21.931	0.00238	-0.961
20	68.56	0.000	37.422	27.067	0.00107	4.070
21	51.14	0.000	33.873	19.241	0.00108	-1.975
22	51.22	0.000	36.724	15.397	0.00034	-0.901
23	47.94	0.000	36.558	14.977	0.00066	-3.596
24	59.17	1.198	31.171	23.065	0.00202	3.734
25	47.73	0.026	30.408	16.270	0.00038	1.026
26	50.56	0.194	31.931	17.458	0.00089	0.976
27	37.02	0.000	32.178	8.754	0.00018	-3.912
28	56.03	0.788	35.928	20.301	0.00084	-0.988
29	39.77	0.000	29.488	8.475	0.00017	1.807
30	46.55	0.299	33.879	12.651	0.00026	-0.279
31	39.45	0.060	28.859	13.885	0.00034	-3.355
32	45.35	0.375	29.797	12.953	0.00029	2.225
33	42.23	0.000	31.954	8.109	0.00016	2.167
34	37.81	0.000	27.326	12.002	0.00027	-1.519
35	48.19	0.286	34.206	14.292	0.00031	-0.595
36	62.28	3.520	34.055	20.254	0.00081	4.449

Detailed HELP Model Annual Water Balance Data for Configuration #5 (Year 0) – Continued:

Simulation	Prec (in/yr)	Runoff (in/yr)	Evap (in/yr)	Lateral Drainage (in/yr)	Infiltration thru GCL (in/yr)	Change in Water Storage (in/yr)
37	55.96	0.000	40.485	16.160	0.00037	-0.686
38	40.26	0.000	28.231	13.300	0.00030	-1.271
39	60.02	2.158	35.072	22.396	0.00321	0.391
40	59.62	0.734	37.197	21.841	0.00053	-0.153
41	47.60	0.000	31.580	15.386	0.00036	0.633
42	50.44	0.521	34.130	16.457	0.00037	-0.669
43	39.42	0.061	26.348	11.468	0.00024	1.543
44	48.61	0.000	34.011	14.313	0.00033	0.286
45	57.35	0.807	34.944	27.434	0.00348	-5.839
46	47.49	0.000	31.999	11.729	0.00026	3.761
47	38.98	0.000	31.706	9.348	0.00019	-2.074
48	42.99	0.000	32.706	9.204	0.00018	1.079
49	53.01	1.660	34.260	13.749	0.00030	3.342
50	55.17	0.038	38.085	20.111	0.00050	-3.065
51	46.16	0.000	31.223	11.798	0.00026	3.138
52	42.63	0.000	33.704	14.049	0.00033	-5.123
53	50.93	0.000	32.528	18.123	0.00042	0.278
54	54.24	0.582	28.380	19.939	0.00086	5.338
55	50.46	0.218	33.032	16.949	0.00054	0.259
56	56.39	1.117	38.507	21.830	0.00055	-5.064
57	41.99	0.000	27.957	13.121	0.00031	0.912
58	68.60	0.196	35.690	29.458	0.00211	3.253
59	48.67	0.089	33.998	15.054	0.00039	-0.471
60	58.12	0.000	34.682	23.002	0.00222	0.434
61	54.90	1.986	31.315	21.617	0.00402	-0.022
62	56.29	0.676	33.384	25.452	0.00324	-3.225
63	49.13	0.373	34.348	15.442	0.00034	-1.034
64	54.54	0.357	32.296	18.712	0.00054	3.175
65	45.05	0.000	32.908	13.516	0.00030	-1.374
66	37.07	0.000	29.770	9.764	0.00020	-2.464
67	40.17	0.000	25.014	10.645	0.00023	4.511
68	58.08	0.000	35.387	24.457	0.00225	-1.767
69	36.31	0.000	27.124	10.417	0.00022	-1.231
70	42.67	0.996	31.917	13.060	0.00030	-3.303
71	48.88	0.000	35.418	10.365	0.00023	3.097
72	47.36	0.511	32.766	17.180	0.00041	-3.097
73	35.81	0.000	26.571	8.549	0.00018	0.690
74	49.81	0.686	29.647	15.818	0.00036	3.659

Detailed HELP Model Annual Water Balance Data for Configuration #5 (Year 0) – Continued:

Simulation	Prec (in/yr)	Runoff (in/yr)	Evap (in/yr)	Lateral Drainage (in/yr)	Infiltration thru GCL (in/yr)	Change in Water Storage (in/yr)
75	56.43	3.806	34.455	17.476	0.00040	0.692
76	45.86	0.000	32.561	15.211	0.00035	-1.912
77	56.76	0.000	39.129	18.329	0.00062	-0.699
78	39.15	0.000	29.546	9.044	0.00020	0.559
79	48.87	0.000	30.932	13.652	0.00095	4.285
80	58.52	0.952	33.474	27.434	0.00487	-3.345
81	53.34	0.000	35.521	16.476	0.00037	1.342
82	55.18	0.000	35.593	18.272	0.00066	1.314
83	53.60	2.437	34.840	20.796	0.00210	-4.475
84	47.82	0.000	34.131	12.686	0.00033	1.003
85	44.69	0.000	30.872	10.041	0.00020	3.777
86	60.77	0.000	35.881	27.651	0.00274	-2.765
87	48.34	1.123	29.576	14.365	0.00047	3.276
88	36.18	0.000	26.160	16.145	0.00202	-6.128
89	58.29	2.732	35.149	17.634	0.00078	2.774
90	60.08	1.279	30.559	23.519	0.00315	4.719
91	55.49	0.000	35.926	22.084	0.00153	-2.522
92	44.51	0.202	32.171	13.187	0.00030	-1.051
93	35.83	0.000	29.652	9.795	0.00021	-3.618
94	45.02	0.000	32.953	10.163	0.00020	1.904
95	44.54	0.000	27.646	18.803	0.00271	-1.912
96	53.18	0.108	35.750	13.863	0.00033	3.459
97	48.03	0.359	31.468	16.846	0.00041	-0.643
98	62.58	1.090	41.453	16.905	0.00043	3.132
99	48.78	0.684	31.550	20.329	0.00164	-3.784
100	49.29	0.000	35.899	10.420	0.00020	2.971
Summary Statistics						
Count	100	100	100	100	100	100
Maximum	68.60	3.806	41.453	29.458	0.00487	5.338
Average	49.14	0.417	32.570	16.088	0.00086	0.067
Median	48.83	0.000	32.597	15.391	0.00037	0.282
Minimum	29.81	0.000	21.653	4.377	0.00008	-6.784
Std Dev	7.69	0.744	3.381	5.271	0.00099	2.707

Configuration #5: Closure cap configuration #1 without the erosion barrier. The material properties for the erosion barrier were replaced with those of backfill rather than eliminating the layer. (i.e. composite barrier and lateral drainage)

Detailed HELP Model Annual Water Balance Data for Configuration #6 (Year 0):

Simulation	Prec (in/yr)	Runoff (in/yr)	Evap (in/yr)	Lateral Drainage (in/yr)	Infiltration thru GCL (in/yr)	Change in Water Storage (in/yr)
1	40.07	0.000	31.670	na	0.02018	8.380
2	57.14	0.000	32.020	na	22.77775	2.342
3	52.64	0.000	31.025	na	20.43955	1.175
4	47.88	0.000	38.407	na	11.40097	-1.928
5	50.57	0.000	34.360	na	12.78641	3.424
6	42.28	0.000	27.913	na	13.38747	0.980
7	39.35	0.000	30.605	na	16.81047	-8.066
8	49.46	0.000	31.615	na	15.24271	2.603
9	48.59	0.000	33.559	na	13.24079	1.790
10	53.97	0.000	33.921	na	18.53501	1.514
11	57.63	0.000	32.606	na	24.49066	0.533
12	46.71	0.000	28.943	na	19.68068	-1.913
13	38.58	0.000	30.403	na	7.99099	0.186
14	41.49	0.000	27.716	na	15.78027	-2.007
15	44.94	0.000	32.582	na	14.02064	-1.663
16	54.78	0.000	31.934	na	20.69179	2.154
17	29.81	0.000	21.663	na	11.24358	-3.096
18	49.55	0.000	34.793	na	9.09013	5.667
19	55.50	0.000	33.818	na	23.63476	-1.952
20	68.56	0.000	37.415	na	27.27379	3.872
21	51.14	0.000	33.641	na	19.11489	-1.615
22	51.22	0.000	36.732	na	14.97796	-0.490
23	47.94	0.000	36.528	na	16.51801	-5.106
24	59.17	0.022	31.063	na	23.88545	4.200
25	47.73	0.000	30.415	na	16.01341	1.302
26	50.56	0.000	31.711	na	17.44236	1.406
27	37.02	0.000	32.254	na	10.24329	-5.477
28	56.03	0.004	35.949	na	20.72605	-0.650
29	39.77	0.000	29.460	na	7.69103	2.619
30	46.55	0.000	33.954	na	12.14368	0.452
31	39.45	0.000	28.858	na	16.10760	-5.515
32	45.35	0.000	29.806	na	12.64460	2.899
33	42.23	0.000	31.938	na	6.61023	3.682
34	37.81	0.000	27.336	na	14.07468	-3.601
35	48.19	0.000	34.214	na	12.98185	0.994
36	62.28	0.116	34.068	na	23.20636	4.889

Detailed HELP Model Annual Water Balance Data for Configuration #6 (Year 0) – Continued:

Simulation	Prec (in/yr)	Runoff (in/yr)	Evap (in/yr)	Lateral Drainage (in/yr)	Infiltration thru GCL (in/yr)	Change in Water Storage (in/yr)
37	55.96	0.000	40.446	na	17.01797	-1.504
38	40.26	0.000	28.260	na	13.34111	-1.341
39	60.02	0.000	35.133	na	23.76736	1.120
40	59.62	0.000	37.107	na	22.56993	-0.057
41	47.60	0.000	31.586	na	15.60678	0.407
42	50.44	0.000	34.014	na	17.59638	-1.170
43	39.42	0.000	26.339	na	12.13255	0.949
44	48.61	0.000	34.204	na	13.49996	0.907
45	57.35	0.000	34.894	na	29.00128	-6.545
46	47.49	0.000	32.003	na	10.68740	4.800
47	38.98	0.000	31.723	na	10.67319	-3.417
48	42.99	0.000	32.671	na	8.57583	1.743
49	53.01	0.000	34.329	na	14.53249	4.148
50	55.17	0.000	38.050	na	21.00276	-3.883
51	46.16	0.000	31.253	na	11.43159	3.475
52	42.63	0.000	33.774	na	14.56718	-5.712
53	50.93	0.000	32.373	na	17.38144	1.176
54	54.24	0.000	28.377	na	21.15454	4.708
55	50.46	0.000	33.070	na	15.35229	2.038
56	56.39	0.000	38.088	na	25.41062	-7.108
57	41.99	0.000	27.892	na	12.31284	1.785
58	68.60	0.000	35.629	na	30.80434	2.167
59	48.67	0.000	33.895	na	15.31592	-0.541
60	58.12	0.000	34.662	na	21.13368	2.325
61	54.90	0.000	31.333	na	24.48006	-0.914
62	56.29	0.000	33.484	na	25.53459	-2.729
63	49.13	0.000	34.689	na	16.32857	-1.888
64	54.54	0.000	32.268	na	17.91214	4.360
65	45.05	0.000	32.701	na	14.14012	-1.792
66	37.07	0.000	29.708	na	11.09997	-3.738
67	40.17	0.000	24.966	na	9.01362	6.190
68	58.08	0.000	35.054	na	24.53912	-1.513
69	36.31	0.000	27.070	na	12.00630	-2.766
70	42.67	0.000	31.911	na	13.97297	-3.214
71	48.88	0.000	35.612	na	10.69246	2.576
72	47.36	0.000	32.783	na	17.50533	-2.928
73	35.81	0.000	26.558	na	9.47852	-0.226
74	49.81	0.000	29.619	na	13.83831	6.353

Detailed HELP Model Annual Water Balance Data for Configuration #6 (Year 0) – Continued:

Simulation	Prec (in/yr)	Runoff (in/yr)	Evap (in/yr)	Lateral Drainage (in/yr)	Infiltration thru GCL (in/yr)	Change in Water Storage (in/yr)
75	56.43	0.014	34.368	na	22.08089	-0.033
76	45.86	0.000	32.521	na	15.96036	-2.621
77	56.76	0.000	39.042	na	17.57841	0.139
78	39.15	0.000	29.493	na	10.90812	-1.251
79	48.87	0.000	30.987	na	12.56270	5.320
80	58.52	0.000	33.327	na	27.62755	-2.435
81	53.34	0.000	35.508	na	16.54020	1.292
82	55.18	0.000	35.808	na	17.66267	1.709
83	53.60	0.000	34.872	na	24.85195	-6.124
84	47.82	0.000	34.261	na	11.73842	1.821
85	44.69	0.000	30.778	na	9.45557	4.457
86	60.77	0.000	35.817	na	27.69293	-2.740
87	48.34	0.000	29.568	na	15.83772	2.934
88	36.18	0.000	26.173	na	17.58125	-7.574
89	58.29	0.043	35.151	na	19.67283	3.423
90	60.08	0.000	30.445	na	24.13214	5.503
91	55.49	0.000	36.042	na	23.09059	-3.643
92	44.51	0.000	32.234	na	12.39264	-0.117
93	35.83	0.000	29.651	na	10.00157	-3.822
94	45.02	0.000	32.909	na	10.15040	1.961
95	44.54	0.000	27.502	na	20.10647	-3.069
96	53.18	0.000	35.766	na	13.37279	4.041
97	48.03	0.000	31.406	na	16.31575	0.308
98	62.58	0.000	41.468	na	18.40235	2.710
99	48.78	0.000	31.667	na	20.26097	-3.148
100	49.29	0.000	35.925	na	11.09578	2.270
Summary Statistics						
Count	100	100	100	na	100	100
Maximum	68.60	0.116	41.468	na	30.80434	8.380
Average	49.14	0.002	32.551	na	16.45404	0.135
Median	48.83	0.000	32.594	na	15.89904	0.430
Minimum	29.81	0.000	21.663	na	0.02018	-8.066
Std Dev	7.69	0.013	3.384	na	5.68556	3.403

Configuration #6: Closure cap configuration described in Table 11 and Table 12 of Section 4.3 where the GCL and HDPE geomembrane were eliminated and the material properties for lateral drainage layer and erosion barrier were replaced with those of backfill rather than eliminating the layers (i.e., soils only closure cap).

This page intentionally left blank.

APPENDIX I.
FTF CLOSURE CAP DEGRADED PROPERTY VALUE CALCULATIONS

Pine Tree Succession of the Vegetative Cover

The following assumptions associated with pine tree succession discussed in Section 7.2 affect the timing of pine tree succession on the FTF Closure Cap:

- A 100-year institutional control period begins after closure cap installation during which the initial bahia grass vegetative cover is maintained and pine trees are excluded.
- 160 years after the end of institutional control it is assumed that the establishment of pine seedlings on top of the closure cap will begin.
- It will take approximately 30 years for the tap roots to reach a 6-foot depth and the remainder of the tree's life (i.e. 70 years) for the root to go its full depth.
- It will take approximately 3 cycles of pine seedling to mature pine trees (i.e. approximately 40 years each cycle) to establish mature pine over the entire cap
- 280 years after the end of institutional control it is assumed that the entire cap is dominated by mature loblolly pine.
- Complete turnover of the 400 mature trees per acre occurs every 100 years (i.e. 400 mature trees per acre die every 100 years in a staggered manner).

These pine tree succession assumptions discussed in Section 7.2 result in the following vegetative cover pine tree succession time-line:

Year	Occurrence
0	Construction of FTF Closure Cap
100	End of 100-year institutional control period
260	Pine tree seedlings begin to invade the FTF Closure Cap
290	Pine tree roots first start to reach HDPE geomembrane
300	Mature pine trees established over a third of the FTF Closure Cap
340	Mature pine trees established over two-thirds and pine tree seedlings established over the entire FTF Closure Cap
380	Mature pine trees established over the entire FTF Closure Cap
380 to 10,000	Complete turnover of mature trees occurs every 100 years

Along with the above vegetative cover pine tree succession time-line, the assumption that there are 400 mature trees per acre with 4 roots to 6 feet and 1 root to 12 feet as discussed in Section 7.2 impact the number of pine roots at any one time and the cumulative number of roots produced over time. These assumptions result in the following table of pine root accumulation over time.

Year	Live Mature Pine Trees (#/acre)	Live Mature 6-foot Roots (#/acre)	Cumulative Number of 6-foot Roots Produced (#/acre)	Live Mature 12-foot Roots (#/acre)	Cumulative Number of 12-foot Roots Produced (#/acre)
0	0	0	0	0	0
100	0	0	0	0	0
260	0	0	0	0	0
290 [1]	133	532	532	133	133
300	133	532	532	133	133
340	267	1068	1068	267	267
380	400	1600	1600	400	400
480	400	1600	3200	400	800
580	400	1600	4800	400	1200
680	400	1600	6400	400	1600
780	400	1600	8000	400	2000
880	400	1600	9600	400	2400
980	400	1600	11200	400	2800
1080	400	1600	12800	400	3200
1180	400	1600	14400	400	3600
1280	400	1600	16000	400	4000
1380	400	1600	17600	400	4400
1480	400	1600	19200	400	4800
1580	400	1600	20800	400	5200
1680	400	1600	22400	400	5600
1780	400	1600	24000	400	6000
1880	400	1600	25600	400	6400
1980	400	1600	27200	400	6800
2080	400	1600	28800	400	7200
2180	400	1600	30400	400	7600
2280	400	1600	32000	400	8000
2380	400	1600	33600	400	8400
2480	400	1600	35200	400	8800
2580	400	1600	36800	400	9200
2680	400	1600	38400	400	9600
2780	400	1600	40000	400	10000
2880	400	1600	41600	400	10400
2980	400	1600	43200	400	10800
3080	400	1600	44800	400	11200
3180	400	1600	46400	400	11600
3280	400	1600	48000	400	12000
3380	400	1600	49600	400	12400

[1] It is assumed that the tap roots of a 30 year old tree reach a depth of 6 feet

- 302 -

Year	Live Mature Pine Trees (#/acre)	Live Mature 6-foot Roots (#/acre)	Cumulative Number of 6-foot Roots Produced (#/acre)	Live Mature 12-foot Roots (#/acre)	Cumulative Number of 12-foot Roots Produced (#/acre)
3480	400	1600	51200	400	12800
3580	400	1600	52800	400	13200
3680	400	1600	54400	400	13600
3780	400	1600	56000	400	14000
3880	400	1600	57600	400	14400
3980	400	1600	59200	400	14800
4080	400	1600	60800	400	15200
4180	400	1600	62400	400	15600
4280	400	1600	64000	400	16000
4380	400	1600	65600	400	16400
4480	400	1600	67200	400	16800
4580	400	1600	68800	400	17200
4680	400	1600	70400	400	17600
4780	400	1600	72000	400	18000
4880	400	1600	73600	400	18400
4980	400	1600	75200	400	18800
5080	400	1600	76800	400	19200
5180	400	1600	78400	400	19600
5280	400	1600	80000	400	20000
5380	400	1600	81600	400	20400
5480	400	1600	83200	400	20800
5580	400	1600	84800	400	21200
5680	400	1600	86400	400	21600
5780	400	1600	88000	400	22000
5880	400	1600	89600	400	22400
5980	400	1600	91200	400	22800
6080	400	1600	92800	400	23200
6180	400	1600	94400	400	23600
6280	400	1600	96000	400	24000
6380	400	1600	97600	400	24400
6480	400	1600	99200	400	24800
6580	400	1600	100800	400	25200
6680	400	1600	102400	400	25600
6780	400	1600	104000	400	26000
6880	400	1600	105600	400	26400
6980	400	1600	107200	400	26800
7080	400	1600	108800	400	27200
7180	400	1600	110400	400	27600

Year	Live Mature Pine Trees (#/acre)	Live Mature 6-foot Roots (#/acre)	Cumulative Number of 6-foot Roots Produced (#/acre)	Live Mature 12-foot Roots (#/acre)	Cumulative Number of 12-foot Roots Produced (#/acre)
7280	400	1600	112000	400	28000
7380	400	1600	113600	400	28400
7480	400	1600	115200	400	28800
7580	400	1600	116800	400	29200
7680	400	1600	118400	400	29600
7780	400	1600	120000	400	30000
7880	400	1600	121600	400	30400
7980	400	1600	123200	400	30800
8080	400	1600	124800	400	31200
8180	400	1600	126400	400	31600
8280	400	1600	128000	400	32000
8380	400	1600	129600	400	32400
8480	400	1600	131200	400	32800
8580	400	1600	132800	400	33200
8680	400	1600	134400	400	33600
8780	400	1600	136000	400	34000
8880	400	1600	137600	400	34400
8980	400	1600	139200	400	34800
9080	400	1600	140800	400	35200
9180	400	1600	142400	400	35600
9280	400	1600	144000	400	36000
9380	400	1600	145600	400	36400
9480	400	1600	147200	400	36800
9580	400	1600	148800	400	37200
9680	400	1600	150400	400	37600
9780	400	1600	152000	400	38000
9880	400	1600	153600	400	38400
9980	400	1600	155200	400	38800
10080	400	1600	156800	400	39200

Erosion of the Soil above the Erosion Barrier

For the institutional control to pine forest land use scenario, it is assumed that the closure cap will be vegetated with bahia grass during the institutional control period (see Sections 4.4.12 and 7.2), with a combination of bahia and pine trees for a period immediately following the institutional control period, and with a pine forest thereafter. The projected erosion rate for both the topsoil and upper backfill layers has been determined utilizing the Universal Soil Loss Equation (Goldman et al. 1986). The Universal Soil Loss Equation is expressed as:

$A = R \times K \times LS \times C \times P$, where A = soil loss (tons/acre/year); R = rainfall erosion index (100 ft·ton/acre per in/hr); K = soil erodability factor, tons/acre per unit of R; LS = slope length and steepness factor, dimensionless; C = vegetative cover factor, dimensionless; P = erosion control practice factor, dimensionless

The following are estimated parameter values based upon Goldman et al. 1986 and Horton and Wilhite 1978:

- From Figure 5.2 of Goldman et al. (1986), R is seen to be slightly greater than 250 but significantly less than 300 100 ft·ton/acre per in/hr for the SRS location. Horton and Wilhite (1978) utilized an R value of 260 100 ft·ton/acre per in/hr for previous SRS Burial Grounds erosion estimates. Therefore an R value of 260 100 ft·ton/acre per in/hr will be utilized.
- As outlined in Section 5.4.1, typical SRS topsoil would generally be classified as silty sand (SM) materials under the Unified Soil Classification System (USCS) or as loamy sand (LS) or sandy loam (SL) in the United States Department of Agriculture (USDA) soil textural classification (i.e., textural triangle). If it is assumed that the topsoil is a sandy loam that consists of 70% sand, 25% silt, and 5% clay, the K is seen to equal approximately 0.28 tons/acre per unit of R from Figure 5.6 of Goldman et al. (1986).
- As outlined in Section 5.4.2, typical SRS control compacted backfill would generally be classified as clayey sand (SC) materials under USCS or as sandy clay loam (SCL) in the USDA soil textural classification (i.e. textural triangle). If it is assumed that the backfill is a sandy clay loam that consists of 50% sand, 30% clay, and 20% silt, the K is seen to equal approximately 0.20 tons/acre per unit of R from Figure 5.6 of Goldman et al. (1986).
- With a slope length of 585 feet and a slope of 2% (see Section 4.2) the LS value equals 0.34 as determined from Table 5.5 of Goldman et al. (1986).
- For a bahia grass vegetative cover, the C factor will be taken as that of a meadow at 0.004 (Horton and Wilhite 1978).
- For a pine forest, the C factor will be taken as that of a natural successional forest at 0.001 (Horton and Wilhite 1978).
- No supporting practices are associated with the closure cap therefore P equals 1.

Based upon the Universal Soil Loss Equation and the parameter values listed above the following are the estimated soil losses:

- Topsoil with a bahia grass vegetative cover has an estimated soil loss of 0.099 tons/acre/year ($A = 260 \times 0.28 \times 0.34 \times 0.004 \times 1$).
- Topsoil with a pine forest has an estimated soil loss of 0.025 tons/acre/year ($A = 260 \times 0.28 \times 0.34 \times 0.001 \times 1$).
- Backfill with a bahia grass vegetative cover has an estimated soil loss of 0.071 tons/acre/year ($A = 260 \times 0.20 \times 0.34 \times 0.004 \times 1$).
- Backfill with a pine forest has an estimated soil loss of 0.018 tons/acre/year ($A = 260 \times 0.20 \times 0.34 \times 0.001 \times 1$).

Based upon the dry bulk density the estimated soil loss can be converted to a loss in terms of depth of loss per year. Yu et al. (1993) provides the following information, from which the average dry bulk density (i.e. approximately 1.67 g/cm^3 or 104 lbs/ft^3) of the two SRS topsoil samples tested can be determined:

Parameter	Top Soil – 1 [1]	Top Soil – 2 [2]
Sample length (cm)	7.59	7.59
Sample area (cm^2)	11.76	11.76
Sample dry weight (g)	148.81	149.75
Sample dry bulk density (g/cm^3)	1.667	1.678

[1] Yu et al. (1993) page 2-72
[2] Yu et al. (1993) page 2-84

Phifer et al. (2006) Table 5-18 provides a dry bulk density value of 1.71 g/cm^3 or 107 lbs/ft^3 for control compacted backfill. Based upon these dry bulk densities the estimated soil loss calculated above was converted to a depth of loss per year as follows:

- Topsoil with a bahia grass vegetative cover has an estimated depth of soil loss of approximately 5.2E-04 inches/year
$$(Loss = \frac{0.099 \; tons / acre / year \times 2000 \; lbs / ton \times 12 \; inches / foot}{43560 \; ft^2 / acre \times 104 \; lbs / ft^3}$$

- Topsoil with a pine forest has an estimated depth of soil loss of approximately 1.3E-04 inches/year $(Loss = \dfrac{0.025 \; tons / acre / year \times 2000 \; lbs / ton \times 12 \; inches / foot}{43560 \; ft^2 / acre \times 104 \; lbs / ft^3}$

- Backfill with a bahia grass vegetative cover has an estimated depth of soil loss of approximately 3.7E-04 inches/year
$$(Loss = \frac{0.071 \; tons / acre / year \times 2000 \; lbs / ton \times 12 \; inches / foot}{43560 \; ft^2 / acre \times 107 \; lbs / ft^3}$$

- Backfill with a pine forest has an estimated depth of soil loss of approximately 9.3E-05 inches/year $(Loss = \dfrac{0.018 \; tons / acre / year \times 2000 \; lbs / ton \times 12 \; inches / foot}{43560 \; ft^2 / acre \times 107 \; lbs / ft^3}$

The following provides a summary of the estimated topsoil and upper backfill soil losses due to erosion for both bahia grass and pine forest vegetative cover:

Soil-Vegetation Condition	Estimated Soil Loss	Estimated Soil Loss

	(tons/acre/year)	(inches/year)
Topsoil with a bahia grass vegetative cover	0.099	5.2E-04
Topsoil with a pine forest	0.025	1.3E-04
Backfill with a bahia grass vegetative cover	0.071	3.7E-04
Backfill with a pine forest	0.018	9.3E-05

In order to maximize the erosion rate utilized the bahia erosion rate, which is higher, will be used until it is assumed that mature pine trees cover the entire closure cap at year 380.

Topsoil Thickness over Time Calculation:

Year	Thickness
0	6" – (0 years × 5.2E-04 inches/year) = 6"
100	6" – (100 years × 5.2E-04 inches/year) = 5.95"
180	6" – (180 years × 5.2E-04 inches/year) = 5.91"
290	6" – (290 years × 5.2E-04 inches/year) = 5.85"
300	6" – (300 years × 5.2E-04 inches/year) = 5.84"
340	6" – (340 years × 5.2E-04 inches/year) = 5.82"
380	6" – (380 years × 5.2E-04 inches/year) = 5.80"
560	5.80" – [(560 years – 380 years) × 1.3E-04 inches/year)] = 5.78"
1,000	5.80" – [(1,000 years – 380 years) × 1.3E-04 inches/year)] = 5.72"
1,800	5.80" – [(1,800 years – 380 years) × 1.3E-04 inches/year)] = 5.62"
2,623	5.80" – [(2,623 years – 380 years) × 1.3E-04 inches/year)] = 5.51"
3,200	5.80" – [(3,200 years – 380 years) × 1.3E-04 inches/year)] = 5.44"
5,600	5.80" – [(5,600 years – 380 years) × 1.3E-04 inches/year)] = 5.12"
10,000	5.80" – [(10,000 years – 380 years) × 1.3E-04 inches/year)] = 4.55"

Since the topsoil does not completely erode away within the 10,000 years of interest, no reduction in the upper backfill layer occurs.

Silting-in of the Lateral Drainage Layer

As outlined in Section 7.5.1 silting-in of the lateral drainage layer will be assumed to occur as follows:

- Over time colloidal clay migrates with the water flux from the 1-foot-thick middle backfill to the underlying 1-foot-thick lateral drainage layer at a concentration of 63 mg of colloidal clay per liter of water flux.
- Once half the clay content of the backfill has migrated to the drainage layer, the two layers essentially become the same material and material property changes cease with an endpoint saturated hydraulic conductivity that of the log mid-point between the initial backfill and drainage layer conditions.
- It will be assumed that the saturated hydraulic conductivity of the middle backfill layer is increasing log linearly with time, and conversely it will be assumed that the saturated hydraulic conductivity of the drainage layer is decreasing log linearly with time.

It will also be assumed that the endpoint porosity, field capacity, and wilting point will become the arithmetic average of the backfill and upper drainage layer.

The following are the intact hydraulic properties of the middle backfill and lateral drainage layer:

Hydraulic Parameter	Middle Backfill	Lateral Drainage Layer
K_{sat} (cm/s)	4.1E-05	5.0E-02
η	0.35	0.417
FC	0.252	0.045
WP	0.181	0.018

Endpoint saturated hydraulic conductivity:

- Middle backfill: K_{MB} = 0.000041; log K_{MB} = -4.39
- Lateral drainage layer: K_{LDL} = 0.05; log K_{UDL} = -1.3
- Log mid-point: $\dfrac{Log\ K_{MB} + Log\ K_{LDL}}{2} = \dfrac{-4.39 + (-1.3)}{2} = -2.84$
- $K_E = 10^{-2.84}$ = 1.4E-03 cm/s

Endpoint n, FC, and WP:

- n = (0.35 + 0.417)/2 = 0.38
- FC = (0.252 + 0.045)/2 = 0.148
- WP = (0.181 + 0.018)/2 = 0.100

As outlined above the time to achieve the endpoint conditions will be based upon migration of half the clay content from the middle backfill into the lateral drainage layer from the estimated water flux containing 63 mg/L colloidal clay.

Determine available clay mass in the middle backfill layer and half the clay mass:
- From Section 7.3.2 and Table 35 will assume that the middle backfill layer consists of 3 wt% gravel, 61 wt% sand, 10 wt% silt, and 26 wt% clay.
- From Phifer et al. (2006) will assume that the middle backfill has a dry bulk density of 1.71 g/cm^3.
- Clay mass = 1.71 g/cm^3 × 0.26 × 28316.8 cm^3/ft^3
- Clay mass = 12,589.6 g/ft^3
- ½ the backfill clay mass = ½ × 12,589.6 g/ft^3
- ½ the backfill clay mass = 6,294.8 g/ft^3

Determine the flux of water into the lateral drainage layer from the following results of the HELP model run for the initial configuration #1a conditions (see Section 5.6):
- Precipitation = 49.14 in/yr
- Runoff = 0.429 in/yr
- Evapotranspiration = 32.572 in/yr
- Flux of water into lateral drainage layer = Precipitation – (Runoff + Evapotranspiration)
- Flux of water into lateral drainage layer = 49.14 in/yr – (0.429 in/yr + 32.572 in/yr)
- Flux of water into lateral drainage layer = 16.139 in/yr

Determine the yearly clay migration into the lateral drainage layer:
- Flux of water into lateral drainage layer = 16.139 in/yr
- Colloidal clay concentration = 63 mg/L
- Flux through a 1 ft^2 area = 16.139 in/yr × ft/12 in × 1 ft^2
- Flux through a 1 ft^2 area = 1.34 ft^3/yr
- Clay flux = 1.34 ft^3/yr × 63 mg/L × 2.831685E-02 m^3/ft^3 × 1000 L/m^3
- Clay flux = 2,390 mg/yr = 2.4 g/yr

Determine the time it takes the 6,294.8 g of clay to migrate from the middle backfill to the lateral drainage layer:
- Time = 6,294.8 g ÷ 2.4 g/yr
- Time = 2,623 yr

Determine middle backfill and lateral drainage layer hydraulic property variation with time:
- It will be assumed that the K$_{sat}$ of the middle backfill increases log linearly with time from 4.1E-05 cm/s to 1.4E-03 cm/s, until year 2,623 at which time the K becomes static. Conversely it will be assumed that the K$_{sat}$ of the lateral drainage layer decreases log linearly with time from 5.0E-02 cm/s to 1.4E-03 cm/s, until year 2,623 at which time the K becomes static. Porosity (n), FC, and WP will be assumed to behave similarly but in an arithmetic linear manner.
- The following are the initial and end state hydraulic properties of the middle backfill and lateral drainage layer:

Hydraulic Parameter	Initial Middle Backfill	Initial Lateral Drainage Layer	End State at 2,623 years
K_{sat} (cm/s)	4.1E-05	5.0E-02	1.4E-03
η	0.35	0.417	0.38
FC	0.252	0.045	0.148
WP	0.181	0.018	0.100

- Determine fraction change for each year:

Year	Fraction
0	$0 \div 2{,}623 = 0$
100	$100 \div 2{,}623 = 0.038$
180	$180 \div 2{,}623 = 0.069$
290	$290 \div 2{,}623 = 0.111$
300	$300 \div 2{,}623 = 0.114$
340	$340 \div 2{,}623 = 0.130$
380	$380 \div 2{,}623 = 0.145$
560	$560 \div 2{,}623 = 0.213$
1,000	$1000 \div 2{,}623 = 0.381$
1,800	$1800 \div 2{,}623 = 0.686$
2,623	$2623 \div 2{,}623 = 1.0$
3,200	1.0
5,600	1.0
10,000	1.0

Determine variation in K, n, FC, and WP with time in the middle backfill:

Year	Fraction, F	K_{sat} (cm/s) [1]	n [2]	FC [3]	WP [4]
0	0	4.10E-05	0.350	0.252	0.181
100	0.038	4.69E-05	0.351	0.248	0.178
180	0.069	5.22E-05	0.352	0.245	0.175
290	0.111	6.06E-05	0.353	0.241	0.172
300	0.114	6.14E-05	0.353	0.240	0.172
340	0.130	6.48E-05	0.354	0.239	0.171
380	0.145	6.84E-05	0.354	0.237	0.169
560	0.213	8.71E-05	0.356	0.230	0.164
1,000	0.381	1.58E-04	0.361	0.212	0.150
1,800	0.686	4.62E-04	0.371	0.181	0.125
2,623	1.0	1.40E-03	0.380	0.148	0.100
3,200	1.0	1.40E-03	0.380	0.148	0.100
5,600	1.0	1.40E-03	0.380	0.148	0.100
10,000	1.0	1.40E-03	0.380	0.148	0.100

[1] $K_{sat} = 10^{[Log_{10}(4.1E-05) + (Log_{10}(1.4E-03) - Log_{10}(4.1E-05)) \times F]}$

[2] $n = 0.35 + (0.38 - 0.35) \times F$

[3] $FC = 0.252 - (0.252 - 0.148) \times F$

[4] $WP = 0.181 - (0.181 - 0.100) \times F$

Determine variation in K, n, FC, and WP with time in the lateral drainage layer:

Year	Fraction, F	K_{sat} (cm/s) [1]	n [2]	FC [3]	WP [4]
0	0	5.00E-02	0.417	0.045	0.018
100	0.038	4.36E-02	0.416	0.049	0.021
180	0.069	3.91E-02	0.414	0.052	0.024
290	0.111	3.37E-02	0.413	0.056	0.027
300	0.114	3.32E-02	0.413	0.057	0.027
340	0.130	3.15E-02	0.412	0.058	0.029
380	0.145	2.98E-02	0.412	0.060	0.030
560	0.213	2.33E-02	0.409	0.067	0.036
1,000	0.381	1.28E-02	0.403	0.084	0.049
1,800	0.686	4.30E-03	0.392	0.116	0.074
2,623	1.0	1.40E-03	0.380	0.148	0.100
3,200	1.0	1.40E-03	0.380	0.148	0.100
5,600	1.0	1.40E-03	0.380	0.148	0.100
10,000	1.0	1.40E-03	0.380	0.148	0.100

[1] $K_{sat} = 10^{[Log_{10}(5.0E-02) + (Log_{10}(1.4E-03) - Log_{10}(5.0E-02)) \times F]}$

[2] $n = 0.417 - (0.417 - 0.38) \times F$

[3] $FC = 0.045 + (0.148 - 0.045) \times F$

[4] $WP = 0.018 + (0.100 - 0.018) \times F$

Root Penetration of the Lateral Drainage Layer

For the institutional control to pine forest land use scenario, it is assumed that the closure cap will be vegetated with bahia grass during the institutional control period (see Sections 4.4.12 and 7.2), with a combination of bahia and pine trees for a period immediately following the institutional control period, and with a pine forest thereafter. From the calculations above it is assumed that mature pine trees will be established over a third of the FTF Closure Cap by year 300; over two-thirds of the cap by year 340; and over the entire cap by year 380. As discussed in Section 7.5.2, roots will represent an impermeable volume within the lateral drainage layer prior to their decomposition.

From Section 7.2, the following assumptions were made relative to the establishment of a pine forest on the closure cap that results in root penetration through the lateral drainage layer and a subsequent impermeable volume in the layer due to roots:

- The closure cap will eventually be covered with approximately 400 mature trees per acre.
- Each mature tree will have 4 roots to 6 feet and 1 root to 12 feet. The roots are 3 inches in diameter at a depth of 1 foot and 0.25 inches in diameter at either 6 or 12 feet, whichever is applicable.
- Deep roots will be maintained and enlarge with yearly growth over the life of the tree.
- Trees are expected to die at approximately 100 years, and it is anticipated that decomposition of deep roots will occur over a 30 year period.
- Prior to decomposition the roots represent an impermeable volume within the lateral drainage layer

The following two impermeable root volume cases will be considered:

- No erosion (in which case the lateral drainage layer will be located 5 to 6 feet below the ground surface)
- All material above the erosion barrier eroded away (in which case the lateral drainage layer will be located 2 to 3 feet below the ground surface)

General calculations applicable to both cases:

Maximum number of trees/acre with deep roots:
    Considering both live and dead trees prior to decomposition of roots
    Number = 400 live trees/acre + [(30 yrs/100 yrs) × 400 dead trees/acre]
    Number = 520 trees/acre with deep roots

Taper of 6' root per foot:
    3" diameter at 1' depth and 0.25" at 6'
    $(3"-0.25")/(6'-1') = 0.55"/ft$

Taper of 12' root per foot:
    3" diameter at 1' depth and 0.25" at 12'
    $(3"-0.25")/(12'-1') = 0.25"/ft$

No erosion case volume calculation:

Root Diameter for 6' roots at 5':
    Diameter = 0.25" + [(6' − 5') × 0.55"/ft] = 0.80"
Area of 6' roots at 5':
    Area = ¼πD^2 = ¼π(0.80")^2 = 0.50 in^2
Root Diameter for 6' roots at 6':
    Diameter = 0.25" + [(6' − 6') × 0.55"/ft] = 0.25"
Area of for 6' roots at 6':
    Area = ¼πD^2 = ¼π(0.25")^2 = 0.05 in^2
Average Area of 6' roots between 5' and 6':
    Average Area = (0.50 in^2 + 0.05 in^2)/2 = 0.28 in^2
Volume of 6' roots between 5' and 6' within the lateral drainage layer:
    Volume = (0.28 in^2/144 in^2/ft^2) × 1 ft = 1.94E-03 ft^3
Volume of 6' roots between 5' and 6'/acre within the lateral drainage layer:
    Volume = 520 trees/acre × 4-6' roots/tree × 1.94E-03 ft^3/6' root
    Volume = 4.04 ft^3/acre

Root Diameter for 12' roots at 5':
    Diameter = 0.25" + [(12' − 5') × 0.25"/ft] = 2.0"
Area of 12' roots at 5':
    Area = ¼πD^2 = ¼π(2.0")^2 = 3.14 in^2
Root Diameter for 12' roots at 6':
    Diameter = 0.25" + [(12' − 6') × 0.25"/ft] = 1.75"
Area of for 12' roots at 6':
    Area = ¼πD^2 = ¼π(1.75")^2 = 2.41 in^2
Average Area of 12' roots between 5' and 6':
    Average Area = (3.14 in^2 + 2.41 in^2)/2 = 2.78 in^2
Volume of 12' roots between 5' and 6' within the lateral drainage layer:
    Volume = (2.78 in^2/144 in^2/ft^2) × 1 ft = 1.93E-02 ft^3
Volume of 12' roots between 5' and 6'/acre within the lateral drainage layer:
    Volume = 520 trees/acre × 1-12' root/tree × 1.93E-02 ft^3/12' root
    Volume = 10.04 ft^3/acre

Total Volume of impermeable roots in the lateral drainage layer:
    Total Volume = 4.04 ft^3/acre + 10.04 ft^3/acre = 14.08 ft^3/acre

Volume of lateral drainage layer per acre:
    Volume = 43560 ft^2/acre × 1-foot thick lateral drainage layer
    Volume = 43560 ft^3/acre

Volume percent of lateral drainage layer occupied by impermeable roots:
    Volume percent = (14.08 ft^3/acre / 43560 ft^3/acre) × 100 = 0.032%

All material above the erosion barrier eroded away case volume calculation:

Root Diameter for 6' roots at 2':
   Diameter = 0.25" + [(6' − 2') × 0.55"/ft] = 2.45"
Area of for 6' roots at 2':
   Area = ¼πD^2 = ¼π(2.45")^2 = 4.71 in^2
Root Diameter for 6' roots at 3':
   Diameter = 0.25" + [(6' − 3') × 0.55"/ft] = 1.90"
Area of for 6' roots at 3':
   Area = ¼πD^2 = ¼π(1.90")^2 = 2.84 in^2
Average Area of 6' roots between 2' and 3':
   Average Area = (4.71 in^2 + 2.84 in^2)/2 = 3.78 in^2
Volume of 6' roots between 2' and 3' within the lateral drainage layer:
   Volume = (3.78 in^2/144 in^2/ft^2) × 1 ft = 2.63E-02 ft^3
Volume of 6' roots between 2' and 3'/acre within the lateral drainage layer:
   Volume = 520 trees/acre × 4-6' roots/tree × 2.63E-02 ft^3/6' root
   Volume = 54.70 ft^3/acre

Root Diameter for 12' roots at 2':
   Diameter = 0.25" + [(12' − 2') × 0.25"/ft] = 2.75"
Area of for 12' roots at 2':
   Area = ¼πD^2 = ¼π(2.75")^2 = 5.94 in^2
Root Diameter for 12' roots at 3':
   Diameter = 0.25" + [(12' − 3') × 0.25"/ft] = 2.50"
Area of for 12' roots at 3':
   Area = ¼πD^2 = ¼π(2.50")^2 = 4.91 in^2
Average Area of 12' roots between 2' and 3':
   Average Area = (5.94 in^2 + 4.91 in^2)/2 = 5.43 in^2
Volume of 12' roots between 2' and 3' within the lateral drainage layer:
   Volume = (5.43 in^2/144 in^2/ft^2) × 1 ft = 3.77E-02 ft^3
Volume of 12' roots between 5' and 6'/acre within the lateral drainage layer:
   Volume = 520 trees/acre × 1-6' root/tree × 3.77E-02 ft^3/12' root
   Volume = 19.60 ft^3/acre

Total Volume of impermeable roots in the lateral drainage layer:
   Total Volume = 54.70 ft^3/acre + 19.60 ft^3/acre = 74.30 ft^3/acre

Volume of lateral drainage layer per acre:
   Volume = 43560 ft^2/acre × 1-foot thick lateral drainage layer
   Volume = 43560 ft^3/acre

Volume percent of lateral drainage layer occupied by impermeable roots:
   Volume percent = (74.30 ft^3/acre / 43560 ft^3/acre) × 100 = 0.17%

Based upon the above calculations the roots within the lateral drainage layer will represent an impermeable volume at any time that ranges from 0.032 to 0.17 percent, depending upon the extent of erosion above the erosion barrier. In order to compensate for the presence of the roots within the lateral drainage layer the saturated hydraulic conductivity of the layer will be reduced by multiplying by 0.998 once the pine forest has been established on the closure cap. The conductivity will be reduced at year 300 when a third of the FTF Closure Cap is anticipated to be covered in mature pine trees. This factor is based upon the worse case percent volume of roots in the layer (i.e. approximately 0.2 percent).

Antioxidant Depletion, Thermal Oxidation, and Tensile Stress Cracking of the HDPE

HDPE Geomembrane Antioxidant Depletion

Antioxidant time of depletion for the HDPE within the FTF Closure Cap has been estimated utilizing the methodology of Mueller and Jakob (2003). They utilized the van't Hoff rule for the temperature dependence of antioxidant depletion time and their measured antioxidant depletion time of 5 years for HDPE geomembranes immersed in 80°C de-ionized water.

van't Hoff rule:

$$t_1(T) = t_1(T') \, e^{\frac{E_a}{R}\left[\frac{1}{T}-\frac{1}{T'}\right]},$$

where $t_1(T)$ = antioxidant depletion period in years at the ambient temperature of the HDPE; $t_1(T')$ = antioxidant depletion period in years at test temperature of 80°C (i.e. 5 years); E_a = depletion process activation energy; R = universal gas constant (8.319 J/mol K); T = ambient temperature of the HDPE in K (K = 273.15 + °C); T' = test temperature in K = 273.15 + 80°C = 353.15

van't Hoff rule with substitution of 5 year time of depletion in 80°C de-ionized water:

$$t_1(T) = 5 \; yrs \; e^{\frac{E_a}{8.319 \, J/mol \, K}\left[\frac{1}{T}-\frac{1}{353.15 \, K}\right]},$$

where $t_1(T)$ = antioxidant depletion period in years at the ambient temperature of the HDPE; E_a = depletion process activation energy; T = ambient temperature of the HDPE in K (K = 273.15 + °C)

As outlined in Section 7.6.2.4, Needham et al. (2004) concluded that, "Values of activation energy of 60-75 kJ/mol appear a reasonable, conservative estimate." Therefore for determination of a conservative antioxidant time of depletion for a HDPE geomembrane within the FTF Closure Cap, an activation energy of 60 kJ/mol will be utilized. This results in the following equation:

$$t_1(T) = 5 \; yrs \; e^{\frac{60,000 \, J/mol}{8.319 \, J/mol \, K}\left[\frac{1}{T}-\frac{1}{353.15 \, K}\right]},$$

where $t_1(T)$ = antioxidant depletion period in years at the ambient temperature of the HDPE; T = ambient temperature of the HDPE in K (K = 273.15 + °C)

Sappington et al. (2005) determined the subsurface temperatures within a well (DIW-1-2) screened within a shallow water table aquifer (approximately 10 feet to the water table surface) at SRS. The average monthly temperature measurements taken by Sappington et al. (2005) during 2002, 2003, and 2004 are provided below along with the yearly average (21.64°C) and median (21.03 °C). These subsurface temperatures are considered representative of that that the FTF Closure Cap HDPE geomembrane will experience since it is located at a comparable shallow depth of 6 feet below ground surface (see Table 11). Therefore the antioxidant depletion period for the FTF Closure Cap HDPE geomembrane has been estimated based upon an average subsurface temperature of approximately 22 °C.

Month	DIW-1-2 Average Monthly Temperature (°C)
January	19.52
February	19.40
March	17.54
April	19.46
May	21.20
June	20.79
July	24.43
August	25.26
September	24.92
October	23.56
November	22.70
December	20.87
Average	21.64
Median	21.03

As seen in the calculation below antioxidant depletion is anticipated to occur in the FTF Closure Cap HDPE geomembrane in 275 years after burial.

$$K = 273.15 + \text{°C}$$
$$K = 273.15 + 22\,\text{°C}$$
$$K = 295.15$$

$$t_1(T) = 5\ yrs\ e^{\frac{60,000\ J/mol}{8.319\ J/mol\ K}\left[\frac{1}{T}-\frac{1}{353.15\ K}\right]},$$ where $t_1(T)$ = antioxidant depletion period in years at the ambient temperature of the HDPE; T = ambient temperature of the HDPE in K (K = 295.15)

$$t_1(T) = 5\ yrs\ e^{\frac{60,000\ J/mol}{8.319\ J/mol\ K}\left[\frac{1}{295.15}-\frac{1}{353.15\ K}\right]}$$
$$t_1(T) = 5\ yrs\ e^{4.01}$$
$$t_1(T) = 276.66\ yrs \approx 275\ yrs$$

Needham et al. (2004) Model of HDPE Geomembrane Hole Generation due to Antioxidant Depletion, Thermal Oxidation, and Tensile Stress Cracking

It is assumed that the HDPE geomembrane will degrade over time consistent with the "fair" case degradation outlined by Needham et al. (2004). HDPE degradation results in holes in the HDPE, while the intact portion of the HDPE is assumed to maintain it initial effective hydraulic conductivity of 2.0E-13 cm/s (see Section 5.4.5).

Estimation of Duration of Different Stages of Defect Generation in the FTF Closure Cap HDPE geomembrane based upon the Methodology of Needham et al. (2004):

Stage	Duration (years)	Cumulative (years)	Comments - Assumptions
1	0	0	FTF Closure Cap construction
2	0	0	No operations anticipated on the FTF Closure Cap after construction; only monitoring and maintenance activities anticipated
3	10	10	No hole generation during this stage; minimum recommended period (Needham et al., 2004)
4	285	295	Oxidation estimated to commence after 275 year antioxidant depletion period plus 20 year induction period (i.e. 295 years) after construction
5	50	345	Period of further stress cracking during oxidation; recommended period (Needham et al., 2004)
6	9,655	10,000	Continuing deterioration through 10,000 years

Estimation of Hole Type and Size per Stage of Defect Generation in the FTF Closure Cap HDPE geomembrane based upon the Methodology of Needham et al. (2004):

Hole Type	Individual Hole Size (mm^2)	Stage					
		1 [1]		2 [2]		3	
		# of holes	holes size	# of holes	holes size	# of holes	holes size
pinholes	2.5	20	50	0	0	0	0
holes	50	10	500	0	0	0	0
tears	5000	0	0	0	0	0	0
small cracks	10	0	0	0	0	0	0
large cracks	1000	0	0	0	0	0	0
total (# of holes/stage)		30	total	0	total	0	-
total (mm^2/hectare)		550	total	0	total	0	

Hole Type	Individual Hole Size (mm^2)	Stage					
		4		5		6 [3]	
		# of holes	holes size	# of holes	holes size	# of holes	holes size
pinholes	2.5	0	0	0	0	20	50
holes	50	0	0	0	0	10	500
tears	5000	0	0	0	0	0	0
small cracks	10	75	750	100	1000	175	1750
large cracks	1000	35	35000	50	50000	85	85000
total (# of holes/stage)		110	total	150	total	290	-
total (mm^2/hectare)		35750	total	51000	total	87300	

The individual hole size for pinholes, holes, and tears is taken as the midpoint in the range provided by Needham et al. (2004)

The individual hole size for small cracks and large cracks is taken as that recommended by Needham et al. (2004)

The number of holes is the most likely number or average number from Needham et al. (2004) for the "fair" case except where noted below:

[1] The anticipated FTF Closure Cap configuration with the HDPE geomembrane on a maximum 2% slope and associated construction methodology and quality assurance (see Section 4.4.3) seem to preclude the generation of tears during construction.

[2] No operations at the F-Area Tank Farm are anticipated after installation of the FTF Closure Cap. Only monitoring and maintenance activities are anticipated. Therefore no holes, tears, or cracks generation due to operations are anticipated.

[3] # of holes and holes size is per 100 years

Estimation of Number and Size of Holes Generated per Stage for the Needham et al. (2004)
Fair Case:

Stage	Cumulative (years)	Number of Holes Generated for the Needham et al. (2004) Fair Case (#)	Size of Holes Generated for the Needham et al. (2004) Fair Case (mm^2 / Hectare)
1	0	30	550
2	0	0	0
3	10	0	0
4	295	110	35,750
5	345	150	51,000
6	10,000	290 / 100 years	87,300 / 100 years

This results in the following cumulative number and area of holes over time in the HDPE

Stage	Year	Total Stage # of Holes (#/hectare)	Total Cumulative # of Holes (#/hectare)	Total Cumulative # of Holes (#/acre)	Total Stage Hole Size (mm^2/hectare)	Total Cumulative Hole Size (mm^2/hectare)	Total Cumulative Hole Size (cm^2/acres)	Average Single Hole Size (cm^2)
1	0	30	30	12	550	550	2	0.2
2	0	0	30	12	0	550	2	0.2
3	10	0	30	12	0	550	2	0.2
4	295	110	140	57	35,750	36300	147	2.6
5	345	150	290	117	51,000	87300	353	3.0
6	445	290	580	235	87,300	174600	707	3.0
6	545	290	870	352	87,300	261900	1060	3.0
6	645	290	1160	469	87,300	349200	1413	3.0
6	745	290	1450	587	87,300	436500	1766	3.0
6	845	290	1740	704	87,300	523800	2120	3.0
6	945	290	2030	822	87,300	611100	2473	3.0
6	1045	290	2320	939	87,300	698400	2826	3.0
6	1145	290	2610	1056	87,300	785700	3180	3.0
6	1245	290	2900	1174	87,300	873000	3533	3.0
6	1345	290	3190	1291	87,300	960300	3886	3.0
6	1445	290	3480	1408	87,300	1047600	4240	3.0
6	1545	290	3770	1526	87,300	1134900	4593	3.0
6	1645	290	4060	1643	87,300	1222200	4946	3.0
6	1745	290	4350	1760	87,300	1309500	5299	3.0
6	1845	290	4640	1878	87,300	1396800	5653	3.0
6	1945	290	4930	1995	87,300	1484100	6006	3.0
6	2045	290	5220	2113	87,300	1571400	6359	3.0
6	2145	290	5510	2230	87,300	1658700	6713	3.0
6	2245	290	5800	2347	87,300	1746000	7066	3.0
6	2345	290	6090	2465	87,300	1833300	7419	3.0
6	2445	290	6380	2582	87,300	1920600	7773	3.0

Stage	Year	Total Stage # of Holes (#/hectare)	Total Cumulative # of Holes (#/hectare)	Total Cumulative # of Holes (#/acre)	Total Stage Hole Size (mm^2/hectare)	Total Cumulative Hole Size (mm^2/hectare)	Total Cumulative Hole Size (cm^2/acres)	Average Single Hole Size (cm^2)
6	2545	290	6670	2699	87,300	2007900	8126	3.0
6	2645	290	6960	2817	87,300	2095200	8479	3.0
6	2745	290	7250	2934	87,300	2182500	8832	3.0
6	2845	290	7540	3051	87,300	2269800	9186	3.0
6	2945	290	7830	3169	87,300	2357100	9539	3.0
6	3045	290	8120	3286	87,300	2444400	9892	3.0
6	3145	290	8410	3403	87,300	2531700	10246	3.0
6	3245	290	8700	3521	87,300	2619000	10599	3.0
6	3345	290	8990	3638	87,300	2706300	10952	3.0
6	3445	290	9280	3756	87,300	2793600	11306	3.0
6	3545	290	9570	3873	87,300	2880900	11659	3.0
6	3645	290	9860	3990	87,300	2968200	12012	3.0
6	3745	290	10150	4108	87,300	3055500	12365	3.0
6	3845	290	10440	4225	87,300	3142800	12719	3.0
6	3945	290	10730	4342	87,300	3230100	13072	3.0
6	4045	290	11020	4460	87,300	3317400	13425	3.0
6	4145	290	11310	4577	87,300	3404700	13779	3.0
6	4245	290	11600	4694	87,300	3492000	14132	3.0
6	4345	290	11890	4812	87,300	3579300	14485	3.0
6	4445	290	12180	4929	87,300	3666600	14839	3.0
6	4545	290	12470	5047	87,300	3753900	15192	3.0
6	4645	290	12760	5164	87,300	3841200	15545	3.0
6	4745	290	13050	5281	87,300	3928500	15898	3.0
6	4845	290	13340	5399	87,300	4015800	16252	3.0
6	4945	290	13630	5516	87,300	4103100	16605	3.0
6	5045	290	13920	5633	87,300	4190400	16958	3.0
6	5145	290	14210	5751	87,300	4277700	17312	3.0
6	5245	290	14500	5868	87,300	4365000	17665	3.0

Stage	Year	Total Stage # of Holes (#/hectare)	Total Cumulative # of Holes (#/hectare)	Total Cumulative # of Holes (#/acre)	Total Stage Hole Size (mm²/hectare)	Total Cumulative Hole Size (mm²/hectare)	Total Cumulative Hole Size (cm²/acres)	Average Single Hole Size (cm²)
6	5345	290	14790	5985	87,300	4452300	18018	3.0
6	5445	290	15080	6103	87,300	4539600	18372	3.0
6	5545	290	15370	6220	87,300	4626900	18725	3.0
6	5645	290	15660	6338	87,300	4714200	19078	3.0
6	5745	290	15950	6455	87,300	4801500	19431	3.0
6	5845	290	16240	6572	87,300	4888800	19785	3.0
6	5945	290	16530	6690	87,300	4976100	20138	3.0
6	6045	290	16820	6807	87,300	5063400	20491	3.0
6	6145	290	17110	6924	87,300	5150700	20845	3.0
6	6245	290	17400	7042	87,300	5238000	21198	3.0
6	6345	290	17690	7159	87,300	5325300	21551	3.0
6	6445	290	17980	7276	87,300	5412600	21904	3.0
6	6545	290	18270	7394	87,300	5499900	22258	3.0
6	6645	290	18560	7511	87,300	5587200	22611	3.0
6	6745	290	18850	7628	87,300	5674500	22964	3.0
6	6845	290	19140	7746	87,300	5761800	23318	3.0
6	6945	290	19430	7863	87,300	5849100	23671	3.0
6	7045	290	19720	7981	87,300	5936400	24024	3.0
6	7145	290	20010	8098	87,300	6023700	24378	3.0
6	7245	290	20300	8215	87,300	6111000	24731	3.0
6	7345	290	20590	8333	87,300	6198300	25084	3.0
6	7445	290	20880	8450	87,300	6285600	25437	3.0
6	7545	290	21170	8567	87,300	6372900	25791	3.0
6	7645	290	21460	8685	87,300	6460200	26144	3.0
6	7745	290	21750	8802	87,300	6547500	26497	3.0
6	7845	290	22040	8919	87,300	6634800	26851	3.0
6	7945	290	22330	9037	87,300	6722100	27204	3.0
6	8045	290	22620	9154	87,300	6809400	27557	3.0

Stage	Year	Total Stage # of Holes (#/hectare)	Total Cumulative # of Holes (#/hectare)	Total Cumulative # of Holes (#/acre)	Total Stage Hole Size (mm^2/hectare)	Total Cumulative Hole Size (mm^2/hectare)	Total Cumulative Hole Size (cm^2/acres)	Average Single Hole Size (cm^2)
6	8145	290	22910	9272	87,300	6896700	27911	3.0
6	8245	290	23200	9389	87,300	6984000	28264	3.0
6	8345	290	23490	9506	87,300	7071300	28617	3.0
6	8445	290	23780	9624	87,300	7158600	28970	3.0
6	8545	290	24070	9741	87,300	7245900	29324	3.0
6	8645	290	24360	9858	87,300	7333200	29677	3.0
6	8745	290	24650	9976	87,300	7420500	30030	3.0
6	8845	290	24940	10093	87,300	7507800	30384	3.0
6	8945	290	25230	10210	87,300	7595100	30737	3.0
6	9045	290	25520	10328	87,300	7682400	31090	3.0
6	9145	290	25810	10445	87,300	7769700	31444	3.0
6	9245	290	26100	10563	87,300	7857000	31797	3.0
6	9345	290	26390	10680	87,300	7944300	32150	3.0
6	9445	290	26680	10797	87,300	8031600	32503	3.0
6	9545	290	26970	10915	87,300	8118900	32857	3.0
6	9645	290	27260	11032	87,300	8206200	33210	3.0
6	9745	290	27550	11149	87,300	8293500	33563	3.0
6	9845	290	27840	11267	87,300	8380800	33917	3.0
6	9945	290	28130	11384	87,300	8468100	34270	3.0
6	10045	290	28420	11501	87,300	8555400	34623	3.0

Determine total cumulative number of holes and hole size per acre for the years to be modeled by linear interpolation from adjacent values:

Year (Yr$_x$)	Total Cumulative # of Holes [1] (#/acre)	Total Cumulative Hole Size [2] (cm^2/acres)	Adjacent Values from which Linear Interpolation Made		
			Adjacent Years	Adjacent Total Cumulative # of Holes (#/acre)	Adjacent Total Cumulative Hole Size (cm^2/acres)
			Yr$_1$	#H$_1$	HS$_1$
			Yr$_2$	#H$_2$	HS$_2$
0	12	2	0	12	2
			0	12	2
100	26	48	10	12	2
			295	57	147
180	39	88	10	12	2
			295	57	147
290	56	144	10	12	2
			295	57	147
300	63	168	295	57	147
			345	117	353
340	111	332	295	57	147
			345	117	353
380	158	477	345	117	353
			445	235	707
560	370	1113	545	352	1060
			645	469	1413
1,000	886	2667	945	822	2473
			1045	939	2826
1,800	1825	5494	1745	1760	5299
			1845	1878	5653
2,623	2791	8401	2545	2699	8126
			2645	2817	8479
3,200	3468	10440	3145	3403	10246
			3245	3521	10599
5,600	6285	18919	5545	6220	18725
			5645	6338	19078
10,000	11448	34464	9945	11384	34270
			10045	11501	34623

[1] Total Cumulative # of Holes (#/acre) = #H$_1$ + (((Yr$_x$ − Yr$_1$) / (Yr$_2$ − Yr$_1$)) × (#H$_2$ - #H$_1$))

[2] Total Cumulative Hole Size (cm^2/acres) = HS$_1$ + (((Yr$_x$ − Yr$_1$) / (Yr$_2$ − Yr$_1$)) × (HS$_2$ - HS$_1$))

Divalent Cation Degradation of the GCL

As outlined in Section 7.7.4 and Table 48, it will be assumed that the sodium bentonite GCL is converted to calcium-magnesium-bentonite GCL, resulting in an order of magnitude increase in saturated hydraulic conductivity. During the 100-year institutional period, it will be assumed the GCL consists of sodium bentonite with a saturated hydraulic conductivity of 5.0E-09 cm/s. After the 100-year institutional period, it will be assumed the GCL consists of calcium-magnesium-bentonite with a saturated hydraulic conductivity of 5.0E-08 cm/s.

Root Penetration of the Composite Hydraulic Barrier

The chart below provides a comparison of the number of holes in the HDPE geomembrane versus the number of pine tree roots over time. As seen there are significantly more pine tree roots than HDPE geomembrane holes.

HDPE Geomembrane Holes vs Pine Tree Roots
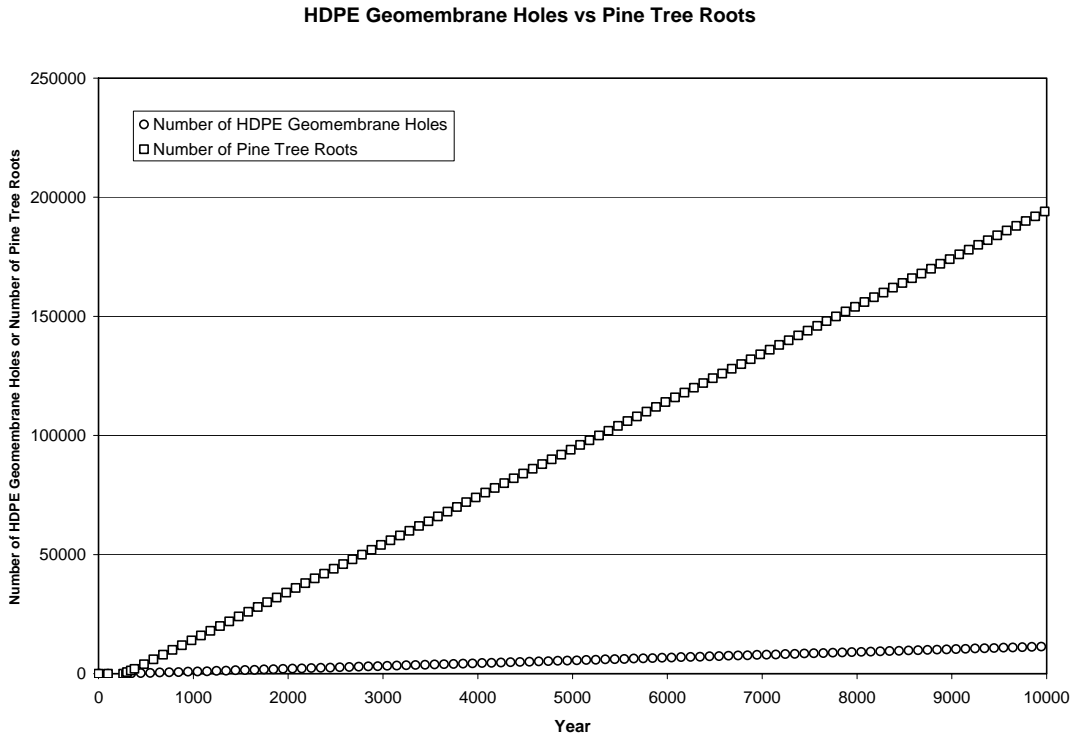
As a conservative estimation of root penetration through the GCL, it will be assumed that every HDPE geomembrane hole generated over time is penetrated by a root that subsequently penetrates the GCL, once significant roots are available to penetrate. As with the drainage layer, it will be assumed that significant roots are available for penetration at year 300 and beyond (at year 300 a third of the closure cap is assumed to be covered by mature trees).

Determine average projected area of roots at the depth of the HDPE geomembrane as though the HDPE geomembrane was not present:

The root area at the depth of the HDPE geomembrane will be determine based upon its depth at year 10,000, since this will result in the maximum root area. From the topsoil erosion calculations above the thickness of topsoil at 10,000 years is reduced from 6 to 4.55 inches. Therefore the thickness of materials above the HDPE geomembrane at year 10,000 is:

Thickness = 6' – ((6" – 4.55")/12"/ft) = 5.88'

Root Diameter for 6' roots at 5.88':
  Diameter = 0.25" + [(6' − 5.88') × 0.55"/ft] = 0.32"
Area of 6' roots at 5.88':
  Area = ¼πD² = ¼π(0.32")² = 0.08 in² × 6.4516 cm²/in² = 0.52 cm²

Root Diameter for 12' roots at 5.88':
  Diameter = 0.25" + [(12' − 5.88') × 0.25"/ft] = 1.78"
Area of 12' roots at 5.88':
  Area = ¼πD² = ¼π(1.78")² = 2.49 in² × 6.4516 cm²/in² = 16.06 cm²

Average root area at 5.88':
  4-6' roots per tree
  1-12' root per tree
  Average = ((4 × 0.52 cm²) + (1 × 16.06 cm²))/(4 + 1) = 3.63 cm²

As seen in the HDPE hole generation calculations above, at 340 years the average hole diameter in the HDPE geomembrane is 3.0 cm², which is near the average root area of 3.63 cm² at the depth of the HDPE geomembrane. The average root area was determined as though the HDPE geomembrane was not present. As outlined in Section 7.6.6, roots are not known to enlarge existing geomembrane defects (Badu-Tweneboah et al. 1999). Therefore the size of hole produced in the composite barrier (HDPE and GCL) through root penetration will be assumed to be that of the average hole diameter in the HDPE geomembrane (i.e., 3.0 cm²).

Based upon the conservative assumption that every HDPE hole is penetrated by a root at year 300 and beyond and assuming that such holes produced by root penetration are 3.0 cm², only the following two composite barrier conditions will be assumed:

- HDPE geomembrane with holes overlying an intact GCL prior to year 300, or
- HDPE geomembrane and underlying GCL with holes (GCL holes produced by root penetration through all HDPE geomembrane holes) at year 300 and beyond.

The HELP model allows the input of up to 999,999 one square centimeter installation defects per acre for a geomembrane liner; therefore the total cumulative hole size shown below for each year to be modeled will be used as the number of one square centimeter installation defects per acre for input into the HELP model. This results in more holes than determined but maintains the area of holes determined.

Year	Total Cumulative # of Holes (#/acre)	Total Cumulative Hole Size (cm^2/acre)
0	12	2
100	26	48
180	39	88
290	56	144
300	63	168
340	111	332
380	158	477
560	370	1113
1,000	886	2667
1,800	1825	5494
2,623	2791	8401
3,200	3468	10440
5,600	6285	18919
10,000	11448	34464

Based upon recommendations from Schroeder et al. (1994a) and Schroeder et al. (1994b) discussed in Section 5.4.5, the initial hole size utilized for year 0 HELP modeling of the FTF Closure Cap was taken as 4 geomembrane installation defects at a total area of 4 cm^2/acre (additionally it included 1 pinhole with an area of 7.84E-03 cm^2/acre). Based upon this, the number and size of holes shown above using the Needham et al. (2004) methodology will be modified. The greater number of holes and greater area of holes for the initial condition (i.e., year 0) produced by the Needham et al. (2004) methodology or based upon the Section 5.4.5 initial assumptions will be utilized. For the initial conditions this results in 12 holes/acre with an area of 4 cm^2. Therefore the total cumulative hole size shown above will be increased by 2 cm^2/acre for each time period considered as shown below.

Year	Total Cumulative # of Holes (#/acre)	Total Cumulative Hole Size (cm^2/acre)
0	12	4
100	26	50
180	39	90
290	56	146
300	63	170
340	111	334
380	158	479
560	370	1115
1,000	886	2669
1,800	1825	5496
2,623	2791	8403
3,200	3468	10442
5,600	6285	18921
10,000	11448	34466

Since the HELP model can not handle holes in a barrier soil liner (i.e., the GCL), the GCL must either be ignored in the HELP modeling or combined with the HDPE geomembrane for all cases at year 300 and beyond.

Based upon the above will run the HELP model with the following representations of the composite hydraulic barrier (HDPE geomembrane and GCL):

- At or before year 100, the HDPE geomembrane and GCL will be modeled as separate layers with holes in the HDPE geomembrane and an intact GCL with a Ksat = 5.0E-09 cm/s.
- After year 100 but before year 300, the HDPE geomembrane and GCL will be modeled as separate layers with holes in the HDPE geomembrane and an intact GCL with a Ksat = 5.0E-08 cm/s.
- At and beyond year 300, the HDPE geomembrane and GCL will be modeled as a combined layer with holes all the way through and with a Ksat = 8.7E-13 cm/s and a thickness of 0.260" for intact portions (calculations for the combined Ksat are shown below – the HELP model input field limits the number of digits to 14 and does not allow the input of scientific notation)

Determine the equivalent K_{sat} for the intact portions of the combined HDPE geomembrane and GCL for year 300 and beyond:

– Intact HDPE geomembrane assumed to always have a K_{sat} = 2E-13 cm/s and a thickness of 0.060 inches
– Beyond 100 years the intact GCL is assumed to have a K_{sat} = 5E-08 cm/s and a thickness of 0.20 inches

Equivalent K_{sat} for flow perpendicular to layering (Freeze and Cherry 1979):

$$K_v = \frac{d}{\sum_{i=1}^{n} d_i / K_i} \,,$$ where K_v = combined saturated hydraulic conductivity of

combined layers; d = total thickness of all layers combined; di = thickness of ith layer; K_i = saturated hydraulic conductivity of ith layer

At 300 years and beyond:

$$K_v = \frac{0.20" + 0.060"}{\dfrac{0.20"}{5E-08\ cm/s} + \dfrac{0.060"}{2E-13\ cm/s}} = 8.7E-13\ cm/s$$

Summary FTF Closure Cap Degraded Property Values for Entry into the HELP Model

Topsoil Thickness over Time:

Year	Thickness
0	6"
100	5.95"
180	5.91"
290	5.85"
300	5.84"
340	5.82"
380	5.80"
560	5.78"
1,000	5.72"
1,800	5.62"
2,623	5.51"
3,200	5.44"
5,600	5.12"
10,000	4.55"

Middle backfill K_{sat}, n, FC, and WP with time:

Year	K_{sat} (cm/s)	n	FC	WP
0	4.10E-05	0.350	0.252	0.181
100	4.69E-05	0.351	0.248	0.178
180	5.22E-05	0.352	0.245	0.175
290	6.06E-05	0.353	0.241	0.172
300	6.14E-05	0.353	0.240	0.172
340	6.48E-05	0.354	0.239	0.171
380	6.84E-05	0.354	0.237	0.169
560	8.71E-05	0.356	0.230	0.164
1,000	1.58E-04	0.361	0.212	0.150
1,800	4.62E-04	0.371	0.181	0.125
2,623	1.40E-03	0.380	0.148	0.100
3,200	1.40E-03	0.380	0.148	0.100
5,600	1.40E-03	0.380	0.148	0.100
10,000	1.40E-03	0.380	0.148	0.100

Lateral drainage layer K_{sat}, n, FC, and WP with time:

Year	K_{sat} (cm/s)	n	FC	WP
0	5.00E-02	0.417	0.045	0.018
100	4.36E-02	0.416	0.049	0.021
180	3.91E-02	0.414	0.052	0.024
290	3.37E-02	0.413	0.056	0.027
300	3.32E-02 (3.32E-02)	0.413	0.057	0.027
340	3.14E-02 (3.15E-02)	0.412	0.058	0.029
380	2.97E-02 (2.98E-02)	0.412	0.060	0.030
560	2.33E-02 (2.33E-02)	0.409	0.067	0.036
1,000	1.28E-02 (1.28E-02)	0.403	0.084	0.049
1,800	4.29E-03 (4.30E-03)	0.392	0.116	0.074
2,623	1.40E-03 (1.40E-03)	0.380	0.148	0.100
3,200	1.40E-03 (1.40E-03)	0.380	0.148	0.100
5,600	1.40E-03 (1.40E-03)	0.380	0.148	0.100
10,000	1.40E-03 (1.40E-03)	0.380	0.148	0.100

In order to compensate for the presence of the roots within the lateral drainage layer, the saturated hydraulic conductivity of the layer will be reduced by a factor of 0.998 at year 300 and beyond due to the presence of mature pine trees on the FTF Closure Cap. The original K_{sat} prior to reduction by the 0.998 factor is shown in parenthesis.

GCL K_{sat} with time:

Year	K_{sat} (cm/s)
0	5.0E-09
100	5.0E-09
180	5.0E-08
290	5.0E-08

Number of 1 cm^2 holes per acre in the HDPE Geomembrane with time for input to the HELP model:

Year	Number of 1 cm^2 Holes (#/acre)
0	4
100	50
180	90
290	146

Number of 1 cm^2 holes per acre in the composite hydraulic barrier (HDPE Geomembrane and GCL) with time for input to the HELP model:

Year	Number of 1 cm^2 Holes (#/acre)
300	170
340	334
380	479
560	1115
1,000	2669
1,800	5496
2,623	8403
3,200	10442
5,600	18921
10,000	34466

Will run the HELP model with the following representations of the intact composite hydraulic barrier at year 300 and beyond:

- Ksat = 8.7E-13 cm/s with a thickness of 0.260"

HELP Model Input Data Tables below are set up for representation of the intact composite hydraulic barrier at year 300 and beyond with Ksat = 8.7E-13 cm/s with a thickness of 0.260".

This page intentionally left blank.

APPENDIX J.
HELP MODEL INPUT OF FTF CLOSURE CAP
CONFIGURATION #1A OVER 10,000 YEARS

HELP Model Input Data for Configuration #1a (Year 0):

Input Parameter (HELP Model Query)	Generic Input Parameter Value
Landfill area =	0.0134 acres
Percent of area where runoff is possible =	100%
Do you want to specify initial moisture storage? (Y/N)	Y
Amount of water or snow on surface =	0 inches
CN Input Parameter (HELP Model Query)	CN Input Parameter Value
Slope =	2 %
Slope length =	585 ft
Soil Texture =	4 (HELP model default soil texture)
Vegetation =	4 (i.e., a good stand of grass)
HELP Model Computed Curve Number = 46.2	

Layer	Layer Number	Layer Type
Topsoil	1	1 (vertical percolation layer)
Upper Backfill	2	1 (vertical percolation layer)
Erosion Barrier	3	1 (vertical percolation layer)
Middle Backfill	4	1 (vertical percolation layer)
Lateral Drainage Layer	5	2 (lateral drainage layer)
HDPE Geomembrane	6	4 (geomembrane liner)
GCL	7	3 (barrier soil liner)
Foundation Layer (1E-06)	8	1 (vertical percolation layer)
Foundation Layer (1E-03)	9	1 (vertical percolation layer)

	Layer Type	Layer Thickness (in)	Soil Texture No.	Total Porosity (Vol/Vol)	Field Capacity (Vol/Vol)	Wilting Point (Vol/Vol)	Initial Moisture (Vol/Vol)
1	1	6		0.396	0.109	0.047	0.109
2	1	30		0.35	0.252	0.181	0.252
3	1	12		0.15	0.10	0.07	0.10
4	1	12		0.35	0.252	0.181	0.252
5	2	12		0.417	0.045	0.018	0.045
6	4	0.06					
7	3	0.2		0.750	0.747	0.400	0.750
8	1	12		0.35	0.252	0.181	0.252
9	1	72		0.457	0.131	0.058	0.131

HELP Model Input Data for Configuration #1a (Year 0) – continued:

	Layer Type	Sat. Hyd. Conductivity (cm/sec)	Drainage Length (ft)	Drain Slope (%)	Leachate Recirc. (%)	Recirc. to Layer (#)	Subsurface Inflow (in/yr)
1	1	3.1E-03					
2	1	4.1E-05					
3	1	1.3E-04					
4	1	4.1E-05					
5	2	5.0E-02	585	2			
6	4	2.0E-13					
7	3	5.0E-09					
8	1	1.0E-06					
9	1	1.0E-03					

	Layer Type	Geomembrane Pinhole Density (#/acre)	Geomembrane Instal. Defects (#/acre)	Geomembrane Placement Quality	Geotextile Transmissivity (cm^2/sec)
1	1				
2	1				
3	1				
4	1				
5	2				
6	4	1	4	2	
7	3				
8	1				
9	1				

The lack of values in the table for particular parameters in particular layers denotes that no HELP model input was required for that parameter in that layer. No data are missing from the table.

Input File: FC1A00.D10; Output File: FC1A00o.OUT

HELP Model Input Data for Configuration #1a (Year 100):

Input Parameter (HELP Model Query)	Generic Input Parameter Value
Landfill area =	0.0134 acres
Percent of area where runoff is possible =	100%
Do you want to specify initial moisture storage? (Y/N)	Y
Amount of water or snow on surface =	0 inches
CN Input Parameter (HELP Model Query)	CN Input Parameter Value
Slope =	2 %
Slope length =	585 ft
Soil Texture =	4 (HELP model default soil texture)
Vegetation =	4 (i.e., a good stand of grass)

HELP Model Computed Curve Number = 46.2		
Layer	Layer Number	Layer Type
Topsoil	1	1 (vertical percolation layer)
Upper Backfill	2	1 (vertical percolation layer)
Erosion Barrier	3	1 (vertical percolation layer)
Middle Backfill	4	1 (vertical percolation layer)
Lateral Drainage Layer	5	2 (lateral drainage layer)
HDPE Geomembrane	6	4 (geomembrane liner)
GCL	7	3 (barrier soil liner)
Foundation Layer (1E-06)	8	1 (vertical percolation layer)
Foundation Layer (1E-03)	9	1 (vertical percolation layer)

	Layer Type	Layer Thickness (in)	Soil Texture No.	Total Porosity (Vol/Vol)	Field Capacity (Vol/Vol)	Wilting Point (Vol/Vol)	Initial Moisture (Vol/Vol)
1	1	5.95		0.396	0.109	0.047	0.109
2	1	30		0.35	0.252	0.181	0.252
3	1	12		0.15	0.10	0.07	0.10
4	1	12		0.351	0.248	0.178	0.248
5	2	12		0.416	0.049	0.021	0.049
6	4	0.06					
7	3	0.2		0.750	0.747	0.400	0.750
8	1	12		0.35	0.252	0.181	0.252
9	1	72		0.457	0.131	0.058	0.131

HELP Model Input Data for Configuration #1a (Year 100) – continued:

	Layer Type	Sat. Hyd. Conductivity (cm/sec)	Drainage Length (ft)	Drain Slope (%)	Leachate Recirc. (%)	Recirc. to Layer (#)	Subsurface Inflow (in/yr)
1	1	3.1E-03					
2	1	4.1E-05					
3	1	1.3E-04					
4	1	4.69E-05					
5	2	4.36E-02	585	2			
6	4	2.0E-13					
7	3	5.0E-09					
8	1	1.0E-06					
9	1	1.0E-03					

	Layer Type	Geomembrane Pinhole Density (#/acre)	Geomembrane Instal. Defects (#/acre)	Geomembrane Placement Quality	Geotextile Transmissivity (cm^2/sec)
1	1				
2	1				
3	1				
4	1				
5	2				
6	4	1	50	2	
7	3				
8	1				
9	1				

The lack of values in the table for particular parameters in particular layers denotes that no HELP model input was required for that parameter in that layer. No data are missing from the table.
Input File: FC1A01.D10; Output File: FC1A01o.OUT

HELP Model Input Data for Configuration #1a (Year 180):

Input Parameter (HELP Model Query)	Generic Input Parameter Value
Landfill area =	0.0134 acres
Percent of area where runoff is possible =	100%
Do you want to specify initial moisture storage? (Y/N)	Y
Amount of water or snow on surface =	0 inches
CN Input Parameter (HELP Model Query)	CN Input Parameter Value
Slope =	2 %
Slope length =	585 ft
Soil Texture =	4 (HELP model default soil texture)
Vegetation =	4 (i.e., a good stand of grass)

HELP Model Computed Curve Number = 46.2		

Layer	Layer Number	Layer Type
Topsoil	1	1 (vertical percolation layer)
Upper Backfill	2	1 (vertical percolation layer)
Erosion Barrier	3	1 (vertical percolation layer)
Middle Backfill	4	1 (vertical percolation layer)
Lateral Drainage Layer	5	2 (lateral drainage layer)
HDPE Geomembrane	6	4 (geomembrane liner)
GCL	7	3 (barrier soil liner)
Foundation Layer (1E-06)	8	1 (vertical percolation layer)
Foundation Layer (1E-03)	9	1 (vertical percolation layer)

	Layer Type	Layer Thickness (in)	Soil Texture No.	Total Porosity (Vol/Vol)	Field Capacity (Vol/Vol)	Wilting Point (Vol/Vol)	Initial Moisture (Vol/Vol)
1	1	5.91		0.396	0.109	0.047	0.109
2	1	30		0.35	0.252	0.181	0.252
3	1	12		0.15	0.10	0.07	0.10
4	1	12		0.352	0.245	0.175	0.245
5	2	12		0.414	0.052	0.024	0.052
6	4	0.06					
7	3	0.2		0.750	0.747	0.400	0.750
8	1	12		0.35	0.252	0.181	0.252
9	1	72		0.457	0.131	0.058	0.131

HELP Model Input Data for Configuration #1a (Year 180) – continued:

	Layer Type	Sat. Hyd. Conductivity (cm/sec)	Drainage Length (ft)	Drain Slope (%)	Leachate Recirc. (%)	Recirc. to Layer (#)	Subsurface Inflow (in/yr)
1	1	3.1E-03					
2	1	4.1E-05					
3	1	1.3E-04					
4	1	5.22E-05					
5	2	3.91E-02	585	2			
6	4	2.0E-13					
7	3	5.0E-08					
8	1	1.0E-06					
9	1	1.0E-03					

	Layer Type	Geomembrane Pinhole Density (#/acre)	Geomembrane Instal. Defects (#/acre)	Geomembrane Placement Quality	Geotextile Transmissivity (cm^2/sec)
1	1				
2	1				
3	1				
4	1				
5	2				
6	4	1	90	2	
7	3				
8	1				
9	1				

The lack of values in the table for particular parameters in particular layers denotes that no HELP model input was required for that parameter in that layer. No data are missing from the table.

Input File: FC1A02.D10; Output File: FC1A02o.OUT

HELP Model Input Data for Configuration #1a (Year 290):

Input Parameter (HELP Model Query)	Generic Input Parameter Value
Landfill area =	0.0134 acres
Percent of area where runoff is possible =	100%
Do you want to specify initial moisture storage? (Y/N)	Y
Amount of water or snow on surface =	0 inches
CN Input Parameter (HELP Model Query)	CN Input Parameter Value
Slope =	2 %
Slope length =	585 ft
Soil Texture =	4 (HELP model default soil texture)
Vegetation =	4 (i.e., a good stand of grass)

HELP Model Computed Curve Number = 46.2		

Layer	Layer Number	Layer Type
Topsoil	1	1 (vertical percolation layer)
Upper Backfill	2	1 (vertical percolation layer)
Erosion Barrier	3	1 (vertical percolation layer)
Middle Backfill	4	1 (vertical percolation layer)
Lateral Drainage Layer	5	2 (lateral drainage layer)
HDPE Geomembrane	6	4 (geomembrane liner)
GCL	7	3 (barrier soil liner)
Foundation Layer (1E-06)	8	1 (vertical percolation layer)
Foundation Layer (1E-03)	9	1 (vertical percolation layer)

	Layer Type	Layer Thickness (in)	Soil Texture No.	Total Porosity (Vol/Vol)	Field Capacity (Vol/Vol)	Wilting Point (Vol/Vol)	Initial Moisture (Vol/Vol)
1	1	5.85		0.396	0.109	0.047	0.109
2	1	30		0.35	0.252	0.181	0.252
3	1	12		0.15	0.10	0.07	0.10
4	1	12		0.353	0.241	0.172	0.241
5	2	12		0.413	0.056	0.027	0.056
6	4	0.06					
7	3	0.2		0.750	0.747	0.400	0.750
8	1	12		0.35	0.252	0.181	0.252
9	1	72		0.457	0.131	0.058	0.131

HELP Model Input Data for Configuration #1a (Year 290) – continued:

	Layer Type	Sat. Hyd. Conductivity (cm/sec)	Drainage Length (ft)	Drain Slope (%)	Leachate Recirc. (%)	Recirc. to Layer (#)	Subsurface Inflow (in/yr)
1	1	3.1E-03					
2	1	4.1E-05					
3	1	1.3E-04					
4	1	6.06E-05					
5	2	3.37E-02	585	2			
6	4	2.0E-13					
7	3	5.0E-08					
8	1	1.0E-06					
9	1	1.0E-03					

	Layer Type	Geomembrane Pinhole Density (#/acre)	Geomembrane Instal. Defects (#/acre)	Geomembrane Placement Quality	Geotextile Transmissivity (cm^2/sec)
1	1				
2	1				
3	1				
4	1				
5	2				
6	4	1	146	2	
7	3				
8	1				
9	1				

The lack of values in the table for particular parameters in particular layers denotes that no HELP model input was required for that parameter in that layer. No data are missing from the table.

Input File: FC1A03.D10; Output File: FC1A03o.OUT

HELP Model Input Data for Configuration #1a (Year 300):

Input Parameter (HELP Model Query)	Generic Input Parameter Value
Landfill area =	0.0134 acres
Percent of area where runoff is possible =	100%
Do you want to specify initial moisture storage? (Y/N)	Y
Amount of water or snow on surface =	0 inches
CN Input Parameter (HELP Model Query)	CN Input Parameter Value
Slope =	2 %
Slope length =	585 ft
Soil Texture =	4 (HELP model default soil texture)
Vegetation =	4 (i.e., a good stand of grass)

HELP Model Computed Curve Number = 46.2		
Layer	Layer Number	Layer Type
Topsoil	1	1 (vertical percolation layer)
Upper Backfill	2	1 (vertical percolation layer)
Erosion Barrier	3	1 (vertical percolation layer)
Middle Backfill	4	1 (vertical percolation layer)
Lateral Drainage Layer	5	2 (lateral drainage layer)
HDPE Geomembrane & GCL	6	4 (geomembrane liner)
Foundation Layer (1E-06)	7	1 (vertical percolation layer)
Foundation Layer (1E-03)	8	1 (vertical percolation layer)

	Layer Type	Layer Thickness (in)	Soil Texture No.	Total Porosity (Vol/Vol)	Field Capacity (Vol/Vol)	Wilting Point (Vol/Vol)	Initial Moisture (Vol/Vol)
1	1	5.84		0.396	0.109	0.047	0.109
2	1	30		0.35	0.252	0.181	0.252
3	1	12		0.15	0.10	0.07	0.10
4	1	12		0.353	0.240	0.172	0.240
5	2	12		0.413	0.057	0.027	0.057
6	4	0.26					
7	1	12		0.35	0.252	0.181	0.252
8	1	72		0.457	0.131	0.058	0.131

HELP Model Input Data for Configuration #1a (Year 300) – continued:

	Layer Type	Sat. Hyd. Conductivity (cm/sec)	Drainage Length (ft)	Drain Slope (%)	Leachate Recirc. (%)	Recirc. to Layer (#)	Subsurface Inflow (in/yr)
1	1	3.1E-03					
2	1	4.1E-05					
3	1	1.3E-04					
4	1	6.14E-05					
5	2	3.32E-02	585	2			
6	4	8.7E-13					
7	1	1.0E-06					
8	1	1.0E-03					

	Layer Type	Geomembrane Pinhole Density (#/acre)	Geomembrane Instal. Defects (#/acre)	Geomembrane Placement Quality	Geotextile Transmissivity (cm^2/sec)
1	1				
2	1				
3	1				
4	1				
5	2				
6	4	1	170	2	
7	1				
8	1				

The lack of values in the table for particular parameters in particular layers denotes that no HELP model input was required for that parameter in that layer. No data are missing from the table.

Input File: FC1A04.D10; Output File: FC1A04o.OUT

HELP Model Input Data for Configuration #1a (Year 340):

Input Parameter (HELP Model Query)	Generic Input Parameter Value
Landfill area =	0.0134 acres
Percent of area where runoff is possible =	100%
Do you want to specify initial moisture storage? (Y/N)	Y
Amount of water or snow on surface =	0 inches
CN Input Parameter (HELP Model Query)	CN Input Parameter Value
Slope =	2 %
Slope length =	585 ft
Soil Texture =	4 (HELP model default soil texture)
Vegetation =	4 (i.e., a good stand of grass)
HELP Model Computed Curve Number = 46.2	

Layer	Layer Number	Layer Type
Topsoil	1	1 (vertical percolation layer)
Upper Backfill	2	1 (vertical percolation layer)
Erosion Barrier	3	1 (vertical percolation layer)
Middle Backfill	4	1 (vertical percolation layer)
Lateral Drainage Layer	5	2 (lateral drainage layer)
HDPE Geomembrane & GCL	6	4 (geomembrane liner)
Foundation Layer (1E-06)	7	1 (vertical percolation layer)
Foundation Layer (1E-03)	8	1 (vertical percolation layer)

	Layer Type	Layer Thickness (in)	Soil Texture No.	Total Porosity (Vol/Vol)	Field Capacity (Vol/Vol)	Wilting Point (Vol/Vol)	Initial Moisture (Vol/Vol)
1	1	5.82		0.396	0.109	0.047	0.109
2	1	30		0.35	0.252	0.181	0.252
3	1	12		0.15	0.10	0.07	0.10
4	1	12		0.354	0.239	0.171	0.239
5	2	12		0.412	0.058	0.029	0.058
6	4	0.26					
7	1	12		0.35	0.252	0.181	0.252
8	1	72		0.457	0.131	0.058	0.131

HELP Model Input Data for Configuration #1a (Year 340) – continued:

	Layer Type	Sat. Hyd. Conductivity (cm/sec)	Drainage Length (ft)	Drain Slope (%)	Leachate Recirc. (%)	Recirc. To Layer (#)	Subsurface Inflow (in/yr)
1	1	3.1E-03					
2	1	4.1E-05					
3	1	1.3E-04					
4	1	6.48E-05					
5	2	3.15E-02	585	2			
6	4	8.7E-13					
7	1	1.0E-06					
8	1	1.0E-03					

	Layer Type	Geomembrane Pinhole Density (#/acre)	Geomembrane Instal. Defects (#/acre)	Geomembrane Placement Quality	Geotextile Transmissivity (cm^2/sec)
1	1				
2	1				
3	1				
4	1				
5	2				
6	4	1	334	2	
7	1				
8	1				

The lack of values in the table for particular parameters in particular layers denotes that no HELP model input was required for that parameter in that layer. No data are missing from the table.
Input File: FC1A05.D10; Output File: FC1A05o.OUT

HELP Model Input Data for Configuration #1a (Year 380):

Input Parameter (HELP Model Query)	Generic Input Parameter Value
Landfill area =	0.0134 acres
Percent of area where runoff is possible =	100%
Do you want to specify initial moisture storage? (Y/N)	Y
Amount of water or snow on surface =	0 inches
CN Input Parameter (HELP Model Query)	CN Input Parameter Value
Slope =	2 %
Slope length =	585 ft
Soil Texture =	4 (HELP model default soil texture)
Vegetation =	4 (i.e., a good stand of grass)
HELP Model Computed Curve Number = 46.2	

Layer	Layer Number	Layer Type
Topsoil	1	1 (vertical percolation layer)
Upper Backfill	2	1 (vertical percolation layer)
Erosion Barrier	3	1 (vertical percolation layer)
Middle Backfill	4	1 (vertical percolation layer)
Lateral Drainage Layer	5	2 (lateral drainage layer)
HDPE Geomembrane & GCL	6	4 (geomembrane liner)
Foundation Layer (1E-06)	7	1 (vertical percolation layer)
Foundation Layer (1E-03)	8	1 (vertical percolation layer)

	Layer Type	Layer Thickness (in)	Soil Texture No.	Total Porosity (Vol/Vol)	Field Capacity (Vol/Vol)	Wilting Point (Vol/Vol)	Initial Moisture (Vol/Vol)
1	1	5.80		0.396	0.109	0.047	0.109
2	1	30		0.35	0.252	0.181	0.252
3	1	12		0.15	0.10	0.07	0.10
4	1	12		0.354	0.237	0.169	0.237
5	2	12		0.412	0.060	0.030	0.060
6	4	0.26					
7	1	12		0.35	0.252	0.181	0.252
8	1	72		0.457	0.131	0.058	0.131

HELP Model Input Data for Configuration #1a (Year 380) – continued:

	Layer Type	Sat. Hyd. Conductivity (cm/sec)	Drainage Length (ft)	Drain Slope (%)	Leachate Recirc. (%)	Recirc. to Layer (#)	Subsurface Inflow (in/yr)
1	1	3.1E-03					
2	1	4.1E-05					
3	1	1.3E-04					
4	1	6.84E-05					
5	2	2.98E-02	585	2			
6	4	8.7E-13					
7	1	1.0E-06					
8	1	1.0E-03					
	Layer Type	Geomembrane Pinhole Density (#/acre)		Geomembrane Instal. Defects (#/acre)	Geomembrane Placement Quality		Geotextile Transmissivity (cm^2/sec)
1	1						
2	1						
3	1						
4	1						
5	2						
6	4	1		479	2		
7	1						
8	1						

The lack of values in the table for particular parameters in particular layers denotes that no HELP model input was required for that parameter in that layer. No data are missing from the table.
Input File: FC1A06.D10; Output File: FC1A06o.OUT

HELP Model Input Data for Configuration #1a (Year 560):

Input Parameter (HELP Model Query)	Generic Input Parameter Value
Landfill area =	0.0134 acres
Percent of area where runoff is possible =	100%
Do you want to specify initial moisture storage? (Y/N)	Y
Amount of water or snow on surface =	0 inches
CN Input Parameter (HELP Model Query)	CN Input Parameter Value
Slope =	2 %
Slope length =	585 ft
Soil Texture =	4 (HELP model default soil texture)
Vegetation =	4 (i.e., a good stand of grass)

HELP Model Computed Curve Number = 46.2		
Layer	Layer Number	Layer Type
Topsoil	1	1 (vertical percolation layer)
Upper Backfill	2	1 (vertical percolation layer)
Erosion Barrier	3	1 (vertical percolation layer)
Middle Backfill	4	1 (vertical percolation layer)
Lateral Drainage Layer	5	2 (lateral drainage layer)
HDPE Geomembrane & GCL	6	4 (geomembrane liner)
Foundation Layer (1E-06)	7	1 (vertical percolation layer)
Foundation Layer (1E-03)	8	1 (vertical percolation layer)

	Layer Type	Layer Thickness (in)	Soil Texture No.	Total Porosity (Vol/Vol)	Field Capacity (Vol/Vol)	Wilting Point (Vol/Vol)	Initial Moisture (Vol/Vol)
1	1	5.78		0.396	0.109	0.047	0.109
2	1	30		0.35	0.252	0.181	0.252
3	1	12		0.15	0.10	0.07	0.10
4	1	12		0.356	0.230	0.164	0.230
5	2	12		0.409	0.067	0.036	0.067
6	4	0.26					
7	1	12		0.35	0.252	0.181	0.252
8	1	72		0.457	0.131	0.058	0.131

HELP Model Input Data for Configuration #1a (Year 560) – continued:

	Layer Type	Sat. Hyd. Conductivity (cm/sec)	Drainage Length (ft)	Drain Slope (%)	Leachate Recirc. (%)	Recirc. to Layer (#)	Subsurface Inflow (in/yr)
1	1	3.1E-03					
2	1	4.1E-05					
3	1	1.3E-04					
4	1	8.71E-05					
5	2	2.33E-02	585	2			
6	4	8.7E-13					
7	1	1.0E-06					
8	1	1.0E-03					

	Layer Type	Geomembrane Pinhole Density (#/acre)	Geomembrane Instal. Defects (#/acre)	Geomembrane Placement Quality	Geotextile Transmissivity (cm^2/sec)
1	1				
2	1				
3	1				
4	1				
5	2				
6	4	1	1,115	2	
7	1				
8	1				

The lack of values in the table for particular parameters in particular layers denotes that no HELP model input was required for that parameter in that layer. No data are missing from the table.

Input File: FC1A07.D10; Output File: FC1A07o.OUT

HELP Model Input Data for Configuration #1a (Year 1,000):

Input Parameter (HELP Model Query)	Generic Input Parameter Value
Landfill area =	0.0134 acres
Percent of area where runoff is possible =	100%
Do you want to specify initial moisture storage? (Y/N)	Y
Amount of water or snow on surface =	0 inches
CN Input Parameter (HELP Model Query)	CN Input Parameter Value
Slope =	2 %
Slope length =	585 ft
Soil Texture =	4 (HELP model default soil texture)
Vegetation =	4 (i.e., a good stand of grass)
HELP Model Computed Curve Number = 46.2	

Layer	Layer Number	Layer Type
Topsoil	1	1 (vertical percolation layer)
Upper Backfill	2	1 (vertical percolation layer)
Erosion Barrier	3	1 (vertical percolation layer)
Middle Backfill	4	1 (vertical percolation layer)
Lateral Drainage Layer	5	2 (lateral drainage layer)
HDPE Geomembrane & GCL	6	4 (geomembrane liner)
Foundation Layer (1E-06)	7	1 (vertical percolation layer)
Foundation Layer (1E-03)	8	1 (vertical percolation layer)

	Layer Type	Layer Thickness (in)	Soil Texture No.	Total Porosity (Vol/Vol)	Field Capacity (Vol/Vol)	Wilting Point (Vol/Vol)	Initial Moisture (Vol/Vol)
1	1	5.72		0.396	0.109	0.047	0.109
2	1	30		0.35	0.252	0.181	0.252
3	1	12		0.15	0.10	0.07	0.10
4	1	12		0.361	0.212	0.150	0.212
5	2	12		0.403	0.084	0.049	0.084
6	4	0.26					
7	1	12		0.35	0.252	0.181	0.252
8	1	72		0.457	0.131	0.058	0.131

HELP Model Input Data for Configuration #1a (Year 1,000) – continued:

	Layer Type	Sat. Hyd. Conductivity (cm/sec)	Drainage Length (ft)	Drain Slope (%)	Leachate Recirc. (%)	Recirc. To Layer (#)	Subsurface Inflow (in/yr)
1	1	3.1E-03					
2	1	4.1E-05					
3	1	1.3E-04					
4	1	1.58E-04					
5	2	1.28E-02	585	2			
6	4	8.7E-13					
7	1	1.0E-06					
8	1	1.0E-03					

	Layer Type	Geomembrane Pinhole Density (#/acre)	Geomembrane Instal. Defects (#/acre)	Geomembrane Placement Quality	Geotextile Transmissivity (cm^2/sec)
1	1				
2	1				
3	1				
4	1				
5	2				
6	4	1	2,669	2	
7	1				
8	1				

The lack of values in the table for particular parameters in particular layers denotes that no HELP model input was required for that parameter in that layer. No data are missing from the table.
Input File: FC1A08.D10; Output File: FC1A08o.OUT

HELP Model Input Data for Configuration #1a (Year 1,800):

Input Parameter (HELP Model Query)	Generic Input Parameter Value
Landfill area =	0.0134 acres
Percent of area where runoff is possible =	100%
Do you want to specify initial moisture storage? (Y/N)	Y
Amount of water or snow on surface =	0 inches
CN Input Parameter (HELP Model Query)	CN Input Parameter Value
Slope =	2 %
Slope length =	585 ft
Soil Texture =	4 (HELP model default soil texture)
Vegetation =	4 (i.e., a good stand of grass)

HELP Model Computed Curve Number = 46.2		
Layer	Layer Number	Layer Type
Topsoil	1	1 (vertical percolation layer)
Upper Backfill	2	1 (vertical percolation layer)
Erosion Barrier	3	1 (vertical percolation layer)
Middle Backfill	4	1 (vertical percolation layer)
Lateral Drainage Layer	5	2 (lateral drainage layer)
HDPE Geomembrane & GCL	6	4 (geomembrane liner)
Foundation Layer (1E-06)	7	1 (vertical percolation layer)
Foundation Layer (1E-03)	8	1 (vertical percolation layer)

	Layer Type	Layer Thickness (in)	Soil Texture No.	Total Porosity (Vol/Vol)	Field Capacity (Vol/Vol)	Wilting Point (Vol/Vol)	Initial Moisture (Vol/Vol)
1	1	5.62		0.396	0.109	0.047	0.109
2	1	30		0.35	0.252	0.181	0.252
3	1	12		0.15	0.10	0.07	0.10
4	1	12		0.371	0.181	0.125	0.181
5	2	12		0.392	0.116	0.074	0.116
6	4	0.26					
7	1	12		0.35	0.252	0.181	0.252
8	1	72		0.457	0.131	0.058	0.131

HELP Model Input Data for Configuration #1a (Year 1,800) – continued:

	Layer Type	Sat. Hyd. Conductivity (cm/sec)	Drainage Length (ft)	Drain Slope (%)	Leachate Recirc. (%)	Recirc. to Layer (#)	Subsurface Inflow (in/yr)
1	1	3.1E-03					
2	1	4.1E-05					
3	1	1.3E-04					
4	1	4.62E-04					
5	2	4.30E-03	585	2			
6	4	8.7E-13					
7	1	1.0E-06					
8	1	1.0E-03					

	Layer Type	Geomembrane Pinhole Density (#/acre)	Geomembrane Instal. Defects (#/acre)	Geomembrane Placement Quality	Geotextile Transmissivity (cm^2/sec)
1	1				
2	1				
3	1				
4	1				
5	2				
6	4	1	5,496	2	
7	1				
8	1				

The lack of values in the table for particular parameters in particular layers denotes that no HELP model input was required for that parameter in that layer. No data are missing from the table.
Input File: FC1A09.D10; Output File: FC1A09o.OUT

HELP Model Input Data for Configuration #1a (Year 2,623):

Input Parameter (HELP Model Query)	Generic Input Parameter Value
Landfill area =	0.0134 acres
Percent of area where runoff is possible =	100%
Do you want to specify initial moisture storage? (Y/N)	Y
Amount of water or snow on surface =	0 inches
CN Input Parameter (HELP Model Query)	CN Input Parameter Value
Slope =	2 %
Slope length =	585 ft
Soil Texture =	4 (HELP model default soil texture)
Vegetation =	4 (i.e., a good stand of grass)
HELP Model Computed Curve Number = 46.2	

Layer	Layer Number	Layer Type
Topsoil	1	1 (vertical percolation layer)
Upper Backfill	2	1 (vertical percolation layer)
Erosion Barrier	3	1 (vertical percolation layer)
Lateral Drainage Layer (including Middle Backfill)	4	2 (lateral drainage layer)
HDPE Geomembrane & GCL	5	4 (geomembrane liner)
Foundation Layer (1E-06)	6	1 (vertical percolation layer)
Foundation Layer (1E-03)	7	1 (vertical percolation layer)

	Layer Type	Layer Thickness (in)	Soil Texture No.	Total Porosity (Vol/Vol)	Field Capacity (Vol/Vol)	Wilting Point (Vol/Vol)	Initial Moisture (Vol/Vol)
1	1	5.51		0.396	0.109	0.047	0.109
2	1	30		0.35	0.252	0.181	0.252
3	1	12		0.15	0.10	0.07	0.10
4	2	24		0.380	0.148	0.100	0.148
5	4	0.26					
6	1	12		0.35	0.252	0.181	0.252
7	1	72		0.457	0.131	0.058	0.131

	Layer Type	Sat. Hyd. Conductivity (cm/sec)	Drainage Length (ft)	Drain Slope (%)	Leachate Recirc. (%)	Recirc. to Layer (#)	Subsurface Inflow (in/yr)
1	1	3.1E-03					
2	1	4.1E-05					
3	1	1.3E-04					
4	2	1.40E-03	585	2			
5	4	8.7E-13					
6	1	1.0E-06					
7	1	1.0E-03					

	Layer Type	Geomembrane Pinhole Density (#/acre)	Geomembrane Instal. Defects (#/acre)	Geomembrane Placement Quality	Geotextile Transmissivity (cm^2/sec)
1	1				
2	1				
3	1				
4	2				
5	4	1	8,403	2	
6	1				
7	1				

The lack of values in the table for particular parameters in particular layers denotes that no HELP model input was required. No data are missing from the table.
Input File: FC1A10.D10; Output File: FC1A10o.OUT

HELP Model Input Data for Configuration #1a (Year 3,200):

Input Parameter (HELP Model Query)	Generic Input Parameter Value
Landfill area =	0.0134 acres
Percent of area where runoff is possible =	100%
Do you want to specify initial moisture storage? (Y/N)	Y
Amount of water or snow on surface =	0 inches
CN Input Parameter (HELP Model Query)	CN Input Parameter Value
Slope =	2 %
Slope length =	585 ft
Soil Texture =	4 (HELP model default soil texture)
Vegetation =	4 (i.e., a good stand of grass)
HELP Model Computed Curve Number = 46.2	

Layer	Layer Number	Layer Type
Topsoil	1	1 (vertical percolation layer)
Upper Backfill	2	1 (vertical percolation layer)
Erosion Barrier	3	1 (vertical percolation layer)
Lateral Drainage Layer (including Middle Backfill)	4	2 (lateral drainage layer)
HDPE Geomembrane & GCL	5	4 (geomembrane liner)
Foundation Layer (1E-06)	6	1 (vertical percolation layer)
Foundation Layer (1E-03)	7	1 (vertical percolation layer)

	Layer Type	Layer Thickness (in)	Soil Texture No.	Total Porosity (Vol/Vol)	Field Capacity (Vol/Vol)	Wilting Point (Vol/Vol)	Initial Moisture (Vol/Vol)
1	1	5.44		0.396	0.109	0.047	0.109
2	1	30		0.35	0.252	0.181	0.252
3	1	12		0.15	0.10	0.07	0.10
4	2	24		0.380	0.148	0.100	0.148
5	4	0.26					
6	1	12		0.35	0.252	0.181	0.252
7	1	72		0.457	0.131	0.058	0.131

	Layer Type	Sat. Hyd. Conductivity (cm/sec)	Drainage Length (ft)	Drain Slope (%)	Leachate Recirc. (%)	Recirc. to Layer (#)	Subsurface Inflow (in/yr)
1	1	3.1E-03					
2	1	4.1E-05					
3	1	1.3E-04					
4	2	1.40E-03	585	2			
5	4	8.7E-13					
6	1	1.0E-06					
7	1	1.0E-03					

	Layer Type	Geomembrane Pinhole Density (#/acre)	Geomembrane Instal. Defects (#/acre)	Geomembrane Placement Quality	Geotextile Transmissivity (cm^2/sec)
1	1				
2	1				
3	1				
4	2				
5	4	1	10,442	2	
6	1				
7	1				

The lack of values in the table for particular parameters in particular layers denotes that no HELP model input was required. No data are missing from the table.
Input File: FC1A11.D10; Output File: FC1A11o.OUT

HELP Model Input Data for Configuration #1a (Year 5,600):

Input Parameter (HELP Model Query)	Generic Input Parameter Value
Landfill area =	0.0134 acres
Percent of area where runoff is possible =	100%
Do you want to specify initial moisture storage? (Y/N)	Y
Amount of water or snow on surface =	0 inches
CN Input Parameter (HELP Model Query)	CN Input Parameter Value
Slope =	2 %
Slope length =	585 ft
Soil Texture =	4 (HELP model default soil texture)
Vegetation =	4 (i.e., a good stand of grass)
HELP Model Computed Curve Number = 46.2	

Layer	Layer Number	Layer Type
Topsoil	1	1 (vertical percolation layer)
Upper Backfill	2	1 (vertical percolation layer)
Erosion Barrier	3	1 (vertical percolation layer)
Lateral Drainage Layer (including Middle Backfill)	4	2 (lateral drainage layer)
HDPE Geomembrane & GCL	5	4 (geomembrane liner)
Foundation Layer (1E-06)	6	1 (vertical percolation layer)
Foundation Layer (1E-03)	7	1 (vertical percolation layer)

	Layer Type	Layer Thickness (in)	Soil Texture No.	Total Porosity (Vol/Vol)	Field Capacity (Vol/Vol)	Wilting Point (Vol/Vol)	Initial Moisture (Vol/Vol)
1	1	5.12		0.396	0.109	0.047	0.109
2	1	30		0.35	0.252	0.181	0.252
3	1	12		0.15	0.10	0.07	0.10
4	2	24		0.380	0.148	0.100	0.148
5	4	0.26					
6	1	12		0.35	0.252	0.181	0.252
7	1	72		0.457	0.131	0.058	0.131

	Layer Type	Sat. Hyd. Conductivity (cm/sec)	Drainage Length (ft)	Drain Slope (%)	Leachate Recirc. (%)	Recirc. to Layer (#)	Subsurface Inflow (in/yr)
1	1	3.1E-03					
2	1	4.1E-05					
3	1	1.3E-04					
4	2	1.40E-03	585	2			
5	4	8.7E-13					
6	1	1.0E-06					
7	1	1.0E-03					

	Layer Type	Geomembrane Pinhole Density (#/acre)	Geomembrane Instal. Defects (#/acre)	Geomembrane Placement Quality	Geotextile Transmissivity (cm^2/sec)
1	1				
2	1				
3	1				
4	2				
5	4	1	18,921	2	
6	1				
7	1				

The lack of values in the table for particular parameters in particular layers denotes that no HELP model input was required. No data are missing from the table.
Input File: FC1A12.D10; Output File: FC1A12o.OUT

HELP Model Input Data for Configuration #1a (Year 10,000):

Input Parameter (HELP Model Query)	Generic Input Parameter Value
Landfill area =	0.0134 acres
Percent of area where runoff is possible =	100%
Do you want to specify initial moisture storage? (Y/N)	Y
Amount of water or snow on surface =	0 inches
CN Input Parameter (HELP Model Query)	CN Input Parameter Value
Slope =	2 %
Slope length =	585 ft
Soil Texture =	4 (HELP model default soil texture)
Vegetation =	4 (i.e., a good stand of grass)

HELP Model Computed Curve Number = 46.2

Layer	Layer Number	Layer Type
Topsoil	1	1 (vertical percolation layer)
Upper Backfill	2	1 (vertical percolation layer)
Erosion Barrier	3	1 (vertical percolation layer)
Lateral Drainage Layer (including Middle Backfill)	4	2 (lateral drainage layer)
HDPE Geomembrane & GCL	5	4 (geomembrane liner)
Foundation Layer (1E-06)	6	1 (vertical percolation layer)
Foundation Layer (1E-03)	7	1 (vertical percolation layer)

	Layer Type	Layer Thickness (in)	Soil Texture No.	Total Porosity (Vol/Vol)	Field Capacity (Vol/Vol)	Wilting Point (Vol/Vol)	Initial Moisture (Vol/Vol)
1	1	4.55		0.396	0.109	0.047	0.109
2	1	30		0.35	0.252	0.181	0.252
3	1	12		0.15	0.10	0.07	0.10
4	2	24		0.380	0.148	0.100	0.148
5	4	0.26					
6	1	12		0.35	0.252	0.181	0.252
7	1	72		0.457	0.131	0.058	0.131

	Layer Type	Sat. Hyd. Conductivity (cm/sec)	Drainage Length (ft)	Drain Slope (%)	Leachate Recirc. (%)	Recirc. to Layer (#)	Subsurface Inflow (in/yr)
1	1	3.1E-03					
2	1	4.1E-05					
3	1	1.3E-04					
4	2	1.40E-03	585	2			
5	4	8.7E-13					
6	1	1.0E-06					
7	1	1.0E-03					

	Layer Type	Geomembrane Pinhole Density (#/acre)	Geomembrane Instal. Defects (#/acre)	Geomembrane Placement Quality	Geotextile Transmissivity (cm^2/sec)
1	1				
2	1				
3	1				
4	2				
5	4	1	34,466	2	
6	1				
7	1				

The lack of values in the table for particular parameters in particular layers denotes that no HELP model input was required. No data are missing from the table.
Input File: FC1A13.D10; Output File: FC1A13o.OUT

APPENDIX K.
CONFIGURATION #1A DETAILED HELP MODEL ANNUAL WATER BALANCE DATA OVER TIME

Detailed HELP Model Annual Water Balance Data for Configuration #1a (Year 0):

Simulation	Precip-itation (in/yr)	Runoff (in/yr)	Evapotrans-piration (in/yr)	Lateral Drainage (in/yr)	Infiltration thru GCL (in/yr)	Change in Water Storage (in/yr)
1	40.07	0.000	31.653	4.674	0.00009	3.743
2	57.14	0.000	32.094	25.219	0.00114	-0.175
3	52.64	0.000	31.091	21.130	0.00134	0.417
4	47.88	0.952	38.428	9.002	0.00018	-0.503
5	50.57	0.000	34.394	14.093	0.00031	2.083
6	42.28	0.000	27.895	13.158	0.00034	1.227
7	39.35	0.515	30.611	14.807	0.00036	-6.584
8	49.46	0.509	31.514	15.519	0.00035	1.917
9	48.59	0.000	33.583	14.013	0.00030	0.994
10	53.97	0.000	33.906	19.125	0.00245	0.936
11	57.63	2.054	32.433	21.871	0.00287	1.269
12	46.71	0.000	29.208	20.020	0.00119	-2.519
13	38.58	0.000	30.409	7.619	0.00015	0.552
14	41.49	0.375	27.779	13.369	0.00042	-0.033
15	44.94	1.022	32.623	13.451	0.00029	-2.156
16	54.78	0.403	32.090	21.261	0.00173	1.024
17	29.81	0.000	21.667	9.165	0.00020	-1.022
18	49.55	0.000	34.895	11.998	0.00025	2.657
19	55.50	0.731	33.774	21.918	0.00251	-0.926
20	68.56	0.000	37.426	27.170	0.00111	3.963
21	51.14	0.000	33.876	19.158	0.00116	-1.895
22	51.22	0.000	36.715	15.447	0.00034	-0.942
23	47.94	0.000	36.529	14.831	0.00068	-3.421
24	59.17	1.199	31.240	23.092	0.00213	3.637
25	47.73	0.026	30.420	16.247	0.00038	1.037
26	50.56	0.194	31.935	17.538	0.00096	0.892
27	37.02	0.000	32.181	8.539	0.00018	-3.701
28	56.03	0.788	35.960	20.278	0.00091	-0.997
29	39.77	0.000	29.485	8.588	0.00017	1.697
30	46.55	0.299	33.864	12.716	0.00026	-0.328
31	39.45	0.060	28.844	13.692	0.00033	-3.146
32	45.35	0.375	29.807	13.016	0.00029	2.151
33	42.23	0.000	31.905	8.297	0.00016	2.027
34	37.81	0.000	27.339	11.779	0.00027	-1.307
35	48.19	0.286	34.212	14.470	0.00032	-0.778
36	62.28	3.520	34.056	20.336	0.00085	4.367

Detailed HELP Model Annual Water Balance Data for Configuration #1a (Year 0) –
Continued:

Simulation	Precip-itation (in/yr)	Runoff (in/yr)	Evapotrans-piration (in/yr)	Lateral Drainage (in/yr)	Infiltration thru GCL (in/yr)	Change in Water Storage (in/yr)
37	55.96	0.000	40.483	16.055	0.00037	-0.579
38	40.26	0.000	28.229	13.330	0.00030	-1.299
39	60.02	2.338	35.097	22.212	0.00318	0.369
40	59.62	0.734	37.281	21.810	0.00053	-0.207
41	47.60	0.000	31.582	15.355	0.00036	0.663
42	50.44	0.521	34.130	16.392	0.00037	-0.603
43	39.42	0.061	26.350	11.449	0.00024	1.559
44	48.61	0.000	33.998	14.369	0.00033	0.243
45	57.35	0.931	34.969	27.145	0.00358	-5.699
46	47.49	0.000	31.999	11.887	0.00027	3.604
47	38.98	0.000	31.666	9.265	0.00019	-1.951
48	42.99	0.000	32.694	9.297	0.00018	0.999
49	53.01	1.660	34.281	13.805	0.00030	3.264
50	55.17	0.038	38.102	20.038	0.00050	-3.008
51	46.16	0.000	31.248	11.786	0.00026	3.126
52	42.63	0.000	33.721	13.951	0.00033	-5.043
53	50.93	0.000	32.529	18.186	0.00042	0.215
54	54.24	0.582	28.380	20.018	0.00093	5.259
55	50.46	0.218	33.032	16.939	0.00055	0.270
56	56.39	1.117	38.507	21.660	0.00055	-4.894
57	41.99	0.000	27.957	13.188	0.00033	0.845
58	68.60	0.196	35.690	29.632	0.00234	3.079
59	48.67	0.089	33.998	14.821	0.00038	-0.239
60	58.12	0.000	34.682	23.126	0.00243	0.310
61	54.90	2.184	31.315	21.428	0.00400	-0.032
62	56.29	0.885	33.384	25.216	0.00321	-3.198
63	49.13	0.373	34.348	15.382	0.00034	-0.974
64	54.54	0.357	32.296	18.810	0.00056	3.077
65	45.05	0.000	32.908	13.493	0.00030	-1.351
66	37.07	0.000	29.770	9.605	0.00020	-2.305
67	40.17	0.000	25.014	10.780	0.00023	4.376
68	58.08	0.000	35.387	24.503	0.00241	-1.812
69	36.31	0.000	27.124	10.264	0.00021	-1.078
70	42.67	0.996	31.917	13.057	0.00031	-3.300
71	48.88	0.000	35.418	10.344	0.00023	3.118
72	47.36	0.511	32.766	17.179	0.00041	-3.096
73	35.81	0.000	26.571	8.543	0.00018	0.696
74	49.81	0.686	29.647	16.006	0.00039	3.472

Detailed HELP Model Annual Water Balance Data for Configuration #1a (Year 0) – Continued:

Simulation	Precip- itation (in/yr)	Runoff (in/yr)	Evapotrans- piration (in/yr)	Lateral Drainage (in/yr)	Infiltration thru GCL (in/yr)	Change in Water Storage (in/yr)
75	56.43	3.806	34.455	17.456	0.00040	0.713
76	45.86	0.000	32.561	15.138	0.00035	-1.839
77	56.76	0.000	39.129	18.383	0.00063	-0.753
78	39.15	0.000	29.546	8.964	0.00020	0.639
79	48.87	0.000	30.932	13.743	0.00105	4.194
80	58.52	0.982	33.493	27.411	0.00496	-3.371
81	53.34	0.000	35.510	16.525	0.00037	1.305
82	55.18	0.000	35.585	18.264	0.00068	1.331
83	53.60	2.607	34.853	20.405	0.00209	-4.267
84	47.82	0.000	34.139	12.820	0.00034	0.861
85	44.69	0.000	30.905	10.088	0.00020	3.697
86	60.77	0.000	35.879	27.609	0.00280	-2.721
87	48.34	1.123	29.579	14.361	0.00052	3.277
88	36.18	0.000	26.171	15.954	0.00214	-5.947
89	58.29	2.732	35.148	17.826	0.00082	2.583
90	60.08	1.421	30.575	23.354	0.00324	4.726
91	55.49	0.000	35.936	22.105	0.00169	-2.553
92	44.51	0.202	32.165	13.119	0.00030	-0.977
93	35.83	0.000	29.650	9.732	0.00021	-3.553
94	45.02	0.000	32.964	10.173	0.00020	1.883
95	44.54	0.000	27.674	18.660	0.00282	-1.797
96	53.18	0.108	35.755	13.943	0.00033	3.375
97	48.03	0.359	31.471	16.924	0.00042	-0.724
98	62.58	1.090	41.484	16.928	0.00044	3.078
99	48.78	0.684	31.561	20.295	0.00175	-3.762
100	49.29	0.000	35.882	10.372	0.00020	3.036
Summary Statistics						
Count	100	100	100	100	100	100
Maximum	68.60	3.806	41.484	29.632	0.00496	5.259
Average	49.14	0.429	32.573	16.075	0.00088	0.065
Median	48.83	0.000	32.592	15.368	0.00037	0.257
Minimum	29.81	0.000	21.667	4.674	0.00009	-6.584
Std Dev	7.69	0.765	3.383	5.255	0.00102	2.635

Detailed HELP Model Annual Water Balance Data for Configuration #1a (Year 100):

Simulation	Precip- itation (in/yr)	Runoff (in/yr)	Evapotrans- piration (in/yr)	Lateral Drainage (in/yr)	Infiltration thru GCL (in/yr)	Change in Water Storage (in/yr)
1	40.07	0.000	31.622	4.528	0.00051	3.919
2	57.14	0.000	32.071	25.087	0.01413	-0.022
3	52.64	0.000	31.087	21.123	0.01794	0.423
4	47.88	0.961	38.433	9.197	0.00115	-0.720
5	50.57	0.000	34.365	13.935	0.00213	2.261
6	42.28	0.000	27.905	13.097	0.00302	1.270
7	39.35	0.524	30.609	15.048	0.00392	-6.838
8	49.46	0.520	31.585	15.359	0.00257	1.989
9	48.59	0.000	33.589	13.968	0.00204	1.025
10	53.97	0.139	33.980	18.819	0.02839	1.026
11	57.63	2.964	32.491	20.951	0.03534	1.216
12	46.71	0.000	29.259	19.903	0.01453	-2.461
13	38.58	0.000	30.409	7.627	0.00093	0.533
14	41.49	0.382	27.789	13.504	0.00486	-0.196
15	44.94	1.028	32.636	13.395	0.00204	-2.129
16	54.78	0.427	32.315	20.832	0.01927	1.198
17	29.81	0.000	21.660	9.391	0.00147	-1.252
18	49.55	0.000	34.895	11.810	0.00164	2.836
19	55.50	0.748	33.766	21.937	0.03446	-0.958
20	68.56	0.000	37.436	26.629	0.01463	4.487
21	51.14	0.000	33.822	19.682	0.01796	-2.375
22	51.22	0.000	36.709	15.343	0.00239	-0.844
23	47.94	0.000	36.557	15.036	0.00871	-3.665
24	59.17	1.208	31.513	22.464	0.02620	3.974
25	47.73	0.033	30.409	16.467	0.00331	0.808
26	50.56	0.202	31.905	17.393	0.01208	1.048
27	37.02	0.000	32.189	8.809	0.00126	-3.992
28	56.03	0.795	35.900	20.245	0.01291	-0.921
29	39.77	0.000	29.472	8.615	0.00113	1.669
30	46.55	0.308	33.981	12.504	0.00174	-0.254
31	39.45	0.068	28.850	13.812	0.00284	-3.290
32	45.35	0.384	29.792	12.977	0.00212	2.187
33	42.23	0.000	31.930	8.156	0.00095	2.135
34	37.81	0.000	27.326	11.949	0.00197	-1.473
35	48.19	0.295	34.210	14.366	0.00222	-0.689
36	62.28	3.530	34.020	20.129	0.01096	4.594

Detailed HELP Model Annual Water Balance Data for Configuration #1a (Year 100) – Continued:

Simulation	Precip- itation (in/yr)	Runoff (in/yr)	Evapotrans- piration (in/yr)	Lateral Drainage (in/yr)	Infiltration thru GCL (in/yr)	Change in Water Storage (in/yr)
37	55.96	0.000	40.431	16.330	0.00284	-0.809
38	40.26	0.000	28.241	13.314	0.00216	-1.304
39	60.02	3.055	35.017	21.463	0.03276	0.478
40	59.62	0.749	37.243	21.672	0.00413	-0.052
41	47.60	0.000	31.597	15.522	0.00328	0.473
42	50.44	0.512	34.097	16.457	0.00277	-0.635
43	39.42	0.070	26.341	11.529	0.00169	1.472
44	48.61	0.000	33.994	14.326	0.00245	0.282
45	57.35	1.867	34.988	26.180	0.04755	-5.691
46	47.49	0.000	32.007	11.667	0.00190	3.805
47	38.98	0.000	31.695	9.486	0.00130	-2.211
48	42.99	0.000	32.715	9.238	0.00113	1.027
49	53.01	1.669	34.188	13.797	0.00212	3.348
50	55.17	0.051	38.078	19.890	0.00474	-2.856
51	46.16	0.000	31.247	11.937	0.00194	2.968
52	42.63	0.000	33.781	13.993	0.00370	-5.152
53	50.93	0.000	32.529	18.042	0.00313	0.352
54	54.24	0.598	28.389	19.571	0.01131	5.677
55	50.46	0.226	33.024	17.307	0.01017	-0.104
56	56.39	1.133	38.540	21.750	0.00491	-5.040
57	41.99	0.000	27.952	13.247	0.00278	0.783
58	68.60	0.206	35.683	28.501	0.04141	4.206
59	48.67	0.080	33.999	15.908	0.00727	-1.328
60	58.12	0.022	34.682	22.897	0.02730	0.509
61	54.90	2.671	31.351	20.730	0.04852	0.134
62	56.29	1.433	33.363	24.818	0.03632	-3.343
63	49.13	0.395	34.398	15.384	0.00245	-1.069
64	54.54	0.365	32.290	18.656	0.00570	3.211
65	45.05	0.000	32.934	13.584	0.00241	-1.485
66	37.07	0.000	29.785	9.699	0.00138	-2.430
67	40.17	0.000	24.990	10.649	0.00155	4.517
68	58.08	0.000	35.398	24.369	0.03994	-1.698
69	36.31	0.000	27.112	10.442	0.00144	-1.260
70	42.67	1.005	31.955	13.061	0.00278	-3.365
71	48.88	0.000	35.448	10.329	0.00160	3.089
72	47.36	0.519	32.768	17.117	0.00320	-3.054
73	35.81	0.000	26.593	8.595	0.00124	0.611
74	49.81	0.696	29.606	15.765	0.00323	3.733

Detailed HELP Model Annual Water Balance Data for Configuration #1a (Year 100) – Continued:

Simulation	Precip- itation (in/yr)	Runoff (in/yr)	Evapotrans- piration (in/yr)	Lateral Drainage (in/yr)	Infiltration thru GCL (in/yr)	Change in Water Storage (in/yr)
75	56.43	3.823	34.430	17.558	0.00299	0.611
76	45.86	0.000	32.552	15.221	0.00261	-1.923
77	56.76	0.000	39.060	18.384	0.00827	-0.692
78	39.15	0.000	29.523	9.098	0.00142	0.520
79	48.87	0.000	30.961	13.594	0.01281	4.307
80	58.52	2.222	33.492	26.040	0.05354	-3.242
81	53.34	0.000	35.532	16.429	0.00272	1.365
82	55.18	0.000	35.581	18.326	0.00795	1.262
83	53.60	3.240	34.826	19.974	0.02409	-4.450
84	47.82	0.000	34.214	12.645	0.00337	0.947
85	44.69	0.000	30.866	10.018	0.00130	3.791
86	60.77	0.000	36.719	26.692	0.04712	-2.651
87	48.34	1.138	29.583	14.306	0.00502	3.298
88	36.18	0.096	26.146	16.140	0.02862	-6.219
89	58.29	2.740	35.162	17.378	0.01000	2.995
90	60.08	2.122	30.612	22.640	0.03926	4.690
91	55.49	0.000	35.918	21.736	0.02480	-2.182
92	44.51	0.208	32.159	13.628	0.00231	-1.508
93	35.83	0.000	29.641	9.879	0.00147	-3.711
94	45.02	0.000	32.931	10.194	0.00126	1.877
95	44.54	0.087	27.619	18.679	0.03340	-1.860
96	53.18	0.117	35.730	13.920	0.00312	3.396
97	48.03	0.365	31.447	16.871	0.00405	-0.668
98	62.58	1.108	41.454	16.711	0.00372	3.294
99	48.78	0.691	31.566	20.427	0.02791	-3.916
100	49.29	0.000	35.879	10.476	0.00128	2.919
Summary Statistics						
Count	100	100	100	100	100	100
Maximum	68.60	3.823	41.454	28.501	0.05354	5.677
Average	49.14	0.498	32.585	15.983	0.01045	0.066
Median	48.83	0.028	32.594	15.372	0.00322	0.317
Minimum	29.81	0.000	21.660	4.528	0.00051	-6.838
Std Dev	7.69	0.882	3.388	5.054	0.01345	2.745

Detailed HELP Model Annual Water Balance Data for Configuration #1a (Year 180):

Simulation	Precip-itation (in/yr)	Runoff (in/yr)	Evapotrans-piration (in/yr)	Lateral Drainage (in/yr)	Infiltration thru GCL (in/yr)	Change in Water Storage (in/yr)
1	40.07	0.000	31.616	4.398	0.00707	4.056
2	57.14	0.000	32.011	24.763	0.26696	0.361
3	52.64	0.000	31.116	20.878	0.29195	0.636
4	47.88	0.969	38.369	9.367	0.01753	-0.831
5	50.57	0.000	34.402	13.698	0.03141	2.470
6	42.28	0.000	27.883	13.075	0.05075	1.303
7	39.35	0.532	30.588	15.149	0.09131	-6.933
8	49.46	0.529	31.580	15.250	0.04255	2.062
9	48.59	0.000	33.567	13.932	0.03080	1.060
10	53.97	0.391	33.985	18.132	0.41441	1.430
11	57.63	3.460	32.408	20.081	0.54970	1.638
12	46.71	0.000	29.268	19.608	0.25688	-2.200
13	38.58	0.000	30.390	7.652	0.01365	0.537
14	41.49	0.373	27.700	13.626	0.09348	-0.291
15	44.94	1.033	32.588	13.378	0.03062	-2.267
16	54.78	0.452	32.354	20.351	0.29996	1.417
17	29.81	0.000	21.652	9.572	0.02274	-1.574
18	49.55	0.000	34.892	11.634	0.02407	2.923
19	55.50	1.203	33.782	21.022	0.52728	-0.668
20	68.56	0.000	37.412	25.879	0.31441	5.203
21	51.14	0.000	33.802	19.819	0.36035	-2.622
22	51.22	0.000	36.721	15.195	0.03596	-0.803
23	47.94	0.000	36.528	15.102	0.16137	-4.038
24	59.17	1.215	31.619	21.694	0.42657	4.366
25	47.73	0.038	30.408	16.577	0.07080	0.548
26	50.56	0.209	31.926	17.053	0.21066	1.165
27	37.02	0.000	32.196	8.994	0.01946	-4.358
28	56.03	0.801	35.897	19.941	0.24770	-0.863
29	39.77	0.000	29.478	8.619	0.01663	1.464
30	46.55	0.315	33.941	12.467	0.02604	-0.339
31	39.45	0.074	28.840	13.863	0.05051	-3.513
32	45.35	0.391	29.799	12.884	0.03180	2.088
33	42.23	0.000	31.908	8.099	0.01361	2.055
34	37.81	0.000	27.344	12.018	0.03024	-1.679
35	48.19	0.302	34.153	14.299	0.03342	-0.692
36	62.28	3.536	34.024	19.758	0.19488	4.843

Detailed HELP Model Annual Water Balance Data for Configuration #1a (Year 180) – Continued:

Simulation	Precip-itation (in/yr)	Runoff (in/yr)	Evapotrans-piration (in/yr)	Lateral Drainage (in/yr)	Infiltration thru GCL (in/yr)	Change in Water Storage (in/yr)
37	55.96	0.000	40.403	16.488	0.04438	-1.048
38	40.26	0.000	28.216	13.339	0.03288	-1.396
39	60.02	3.393	34.990	20.632	0.47132	0.920
40	59.62	0.761	37.219	21.495	0.06343	0.070
41	47.60	0.000	31.584	15.598	0.07468	0.401
42	50.44	0.505	34.095	16.453	0.04252	-0.642
43	39.42	0.078	26.342	11.564	0.02554	1.360
44	48.61	0.000	34.007	14.244	0.03987	0.248
45	57.35	2.279	34.967	25.071	0.75887	-5.119
46	47.49	0.000	32.005	11.499	0.02811	3.921
47	38.98	0.000	31.703	9.663	0.02000	-2.455
48	42.99	0.000	32.703	9.188	0.01639	0.900
49	53.01	1.676	34.181	13.720	0.03330	3.235
50	55.17	0.060	38.075	19.668	0.09255	-2.818
51	46.16	0.000	31.214	12.067	0.02997	2.707
52	42.63	0.000	33.787	13.994	0.07308	-5.294
53	50.93	0.000	32.532	17.871	0.04737	0.404
54	54.24	0.610	28.370	19.174	0.19841	5.987
55	50.46	0.234	33.027	17.276	0.21401	-0.179
56	56.39	1.147	38.477	21.823	0.09378	-5.133
57	41.99	0.000	27.960	13.176	0.04862	0.811
58	68.60	0.213	35.708	27.221	0.81007	5.401
59	48.67	0.073	33.986	16.272	0.20649	-1.754
60	58.12	0.200	34.689	22.170	0.40346	1.017
61	54.90	3.005	31.427	19.615	0.71542	0.711
62	56.29	1.827	33.387	23.967	0.54870	-3.307
63	49.13	0.409	34.441	15.362	0.03723	-1.755
64	54.54	0.373	32.291	18.448	0.10544	2.919
65	45.05	0.000	32.919	13.646	0.04263	-1.852
66	37.07	0.000	29.780	9.771	0.02084	-2.735
67	40.17	0.000	25.008	10.442	0.02230	4.504
68	58.08	0.000	35.590	23.530	0.68671	-1.251
69	36.31	0.000	27.111	10.526	0.02169	-1.393
70	42.67	1.012	31.941	13.069	0.04888	-3.471
71	48.88	0.000	35.442	10.323	0.02399	2.900
72	47.36	0.524	32.752	17.028	0.05638	-3.145
73	35.81	0.000	26.535	8.679	0.01864	0.404
74	49.81	0.732	29.609	15.502	0.05709	3.806

Detailed HELP Model Annual Water Balance Data for Configuration #1a (Year 180) – Continued:

Simulation	Precip-itation (in/yr)	Runoff (in/yr)	Evapotrans-piration (in/yr)	Lateral Drainage (in/yr)	Infiltration thru GCL (in/yr)	Change in Water Storage (in/yr)
75	56.43	3.836	34.418	17.571	0.04609	0.478
76	45.86	0.000	32.524	15.261	0.04183	-2.057
77	56.76	0.000	39.083	18.170	0.15951	-0.612
78	39.15	0.000	29.549	9.169	0.02157	0.310
79	48.87	0.000	30.924	13.338	0.20593	4.523
80	58.52	2.860	33.432	24.655	0.78027	-2.509
81	53.34	0.000	35.542	16.333	0.04132	1.441
82	55.18	0.000	35.597	18.209	0.14301	1.308
83	53.60	3.521	34.951	19.380	0.38285	-4.454
84	47.82	0.000	34.195	12.538	0.06047	1.000
85	44.69	0.000	30.865	9.931	0.01901	3.702
86	60.77	0.406	36.879	25.368	0.77291	-2.149
87	48.34	1.150	29.570	14.175	0.08486	3.355
88	36.18	0.618	26.160	15.467	0.41088	-6.363
89	58.29	2.746	35.237	16.710	0.18277	3.371
90	60.08	2.659	30.603	21.729	0.59698	4.756
91	55.49	0.000	35.950	21.073	0.43458	-1.793
92	44.51	0.212	32.143	13.895	0.04274	-2.101
93	35.83	0.000	29.622	9.985	0.02228	-4.147
94	45.02	0.000	32.916	10.175	0.01866	1.583
95	44.54	0.315	27.606	18.069	0.48800	-1.771
96	53.18	0.124	35.705	13.872	0.05390	3.351
97	48.03	0.371	31.451	16.725	0.08052	-0.701
98	62.58	1.120	41.440	16.478	0.06651	3.317
99	48.78	0.696	31.558	20.082	0.50457	-3.788
100	49.29	0.000	35.887	10.520	0.01907	2.822
Summary Statistics						
Count	100	100	100	100	100	100
Maximum	68.60	3.836	41.440	27.221	0.81007	5.987
Average	49.14	0.556	32.584	15.763	0.17264	0.087
Median	48.83	0.067	32.560	15.311	0.05674	0.381
Minimum	29.81	0.000	21.652	4.398	0.00707	-6.933
Std Dev	7.69	0.959	3.392	4.774	0.21371	2.828

Detailed HELP Model Annual Water Balance Data for Configuration #1a (Year 290):

Simulation	Precip-itation (in/yr)	Runoff (in/yr)	Evapotrans-piration (in/yr)	Lateral Drainage (in/yr)	Infiltration thru GCL (in/yr)	Change in Water Storage (in/yr)
1	40.07	0.000	31.624	4.182	0.01340	4.265
2	57.14	0.000	32.013	23.990	0.80353	1.131
3	52.64	0.000	31.085	20.630	0.61350	0.909
4	47.88	0.979	38.422	9.541	0.03687	-1.062
5	50.57	0.000	34.380	13.462	0.06245	2.724
6	42.28	0.000	27.892	13.079	0.12014	1.275
7	39.35	0.542	30.596	15.112	0.26641	-7.051
8	49.46	0.545	31.427	15.241	0.10231	2.178
9	48.59	0.000	33.561	13.856	0.06269	1.088
10	53.97	0.788	33.997	17.341	0.74391	1.673
11	57.63	4.169	32.398	18.971	1.04807	2.017
12	46.71	0.000	29.224	19.254	0.56289	-2.265
13	38.58	0.000	30.393	7.716	0.02756	-0.249
14	41.49	0.375	27.702	13.630	0.21905	-0.739
15	44.94	1.041	32.627	13.242	0.06114	-2.267
16	54.78	0.489	32.376	19.778	0.60631	1.839
17	29.81	0.000	21.633	9.864	0.05088	-1.799
18	49.55	0.000	34.849	11.423	0.04774	3.005
19	55.50	1.736	33.747	20.138	0.97530	-0.382
20	68.56	0.000	37.430	24.502	0.95829	6.316
21	51.14	0.940	33.792	19.194	0.79357	-3.422
22	51.22	0.000	36.728	14.986	0.07242	-1.437
23	47.94	0.000	36.548	15.082	0.41129	-4.245
24	59.17	1.755	31.639	20.352	0.83550	5.168
25	47.73	0.047	30.382	16.678	0.24257	0.270
26	50.56	0.218	31.880	16.670	0.50010	1.330
27	37.02	0.000	32.226	9.235	0.05009	-5.038
28	56.03	0.809	35.872	19.463	0.61045	-0.564
29	39.77	0.000	29.456	8.689	0.03367	1.379
30	46.55	0.326	33.944	12.317	0.05211	-0.438
31	39.45	0.083	28.826	13.931	0.16272	-3.747
32	45.35	0.402	29.791	12.772	0.07353	2.146
33	42.23	0.000	31.934	7.976	0.02673	2.117
34	37.81	0.000	27.326	12.120	0.07727	-1.791
35	48.19	0.313	34.074	14.229	0.06800	-0.598
36	62.28	3.543	34.034	19.177	0.44787	5.345

Detailed HELP Model Annual Water Balance Data for Configuration #1a (Year 290) – Continued:

Simulation	Precip-itation (in/yr)	Runoff (in/yr)	Evapotrans-piration (in/yr)	Lateral Drainage (in/yr)	Infiltration thru GCL (in/yr)	Change in Water Storage (in/yr)
37	55.96	0.000	40.431	16.745	0.10258	-1.326
38	40.26	0.000	28.222	13.283	0.07509	-1.289
39	60.02	3.984	35.087	19.462	0.84029	1.358
40	59.62	0.781	37.178	21.202	0.16794	0.368
41	47.60	0.000	31.581	15.666	0.25230	0.012
42	50.44	0.494	34.098	16.415	0.09402	-0.818
43	39.42	0.088	26.336	11.647	0.05250	1.041
44	48.61	0.000	34.000	14.150	0.09672	0.195
45	57.35	2.921	34.942	23.628	1.51247	-4.360
46	47.49	0.000	31.979	11.380	0.05574	3.765
47	38.98	0.000	31.681	9.933	0.04231	-3.219
48	42.99	0.000	32.710	9.089	0.03246	0.825
49	53.01	1.687	34.148	13.634	0.07748	3.253
50	55.17	0.068	38.049	19.310	0.28098	-2.505
51	46.16	0.000	31.194	12.284	0.06682	2.483
52	42.63	0.000	33.804	13.875	0.24601	-5.187
53	50.93	0.000	32.531	17.624	0.10081	0.727
54	54.24	0.630	28.387	18.477	0.45106	6.616
55	50.46	0.242	32.993	17.326	0.58333	-0.255
56	56.39	1.167	38.447	21.732	0.32772	-5.160
57	41.99	0.000	27.938	13.117	0.13412	0.641
58	68.60	0.578	35.818	25.317	1.82288	6.552
59	48.67	0.063	33.952	16.375	0.64156	-2.564
60	58.12	0.474	34.651	21.329	0.76145	0.632
61	54.90	3.594	31.621	18.269	1.30829	0.430
62	56.29	2.379	33.316	22.969	1.09281	-3.480
63	49.13	0.431	34.456	15.386	0.07636	-2.210
64	54.54	0.385	32.305	18.105	0.28225	3.150
65	45.05	0.000	32.973	13.631	0.14105	-1.887
66	37.07	0.000	29.778	9.879	0.04279	-2.872
67	40.17	0.000	24.989	10.295	0.04371	4.599
68	58.08	0.467	35.663	22.187	1.31964	-0.462
69	36.31	0.000	27.086	10.739	0.04521	-1.869
70	42.67	1.023	31.921	13.067	0.12135	-3.834
71	48.88	0.000	35.452	10.307	0.04773	2.792
72	47.36	0.535	32.736	16.826	0.20076	-3.016
73	35.81	0.000	26.582	8.734	0.03768	0.270
74	49.81	0.745	29.597	15.076	0.14250	4.243

Detailed HELP Model Annual Water Balance Data for Configuration #1a (Year 290) – Continued:

Simulation	Precip-itation (in/yr)	Runoff (in/yr)	Evapotrans-piration (in/yr)	Lateral Drainage (in/yr)	Infiltration thru GCL (in/yr)	Change in Water Storage (in/yr)
75	56.43	3.856	34.388	17.642	0.09561	0.365
76	45.86	0.000	32.526	15.288	0.11158	-2.121
77	56.76	0.000	39.097	17.850	0.38550	-0.333
78	39.15	0.000	29.533	9.325	0.05160	0.229
79	48.87	0.000	30.941	12.997	0.42480	4.811
80	58.52	3.793	33.427	22.943	1.41438	-1.711
81	53.34	0.000	35.543	16.233	0.08419	0.849
82	55.18	0.000	35.773	17.903	0.32627	0.928
83	53.60	4.509	34.816	18.340	0.79840	-4.318
84	47.82	0.000	34.269	12.308	0.15485	0.728
85	44.69	0.000	30.826	9.810	0.03766	3.569
86	60.77	1.719	36.828	23.369	1.47079	-1.464
87	48.34	1.168	29.564	13.946	0.18718	2.963
88	36.18	1.202	26.159	14.907	0.77327	-6.540
89	58.29	2.755	35.467	15.610	0.45809	3.754
90	60.08	3.594	30.634	20.542	1.08636	4.804
91	55.49	0.000	35.928	20.273	0.97422	-1.451
92	44.51	0.219	32.151	14.149	0.14664	-2.722
93	35.83	0.000	29.630	10.092	0.05132	-4.661
94	45.02	0.000	32.831	10.210	0.03831	1.516
95	44.54	0.847	27.613	17.242	0.85699	-1.504
96	53.18	0.135	35.728	13.737	0.14323	3.353
97	48.03	0.382	31.463	16.482	0.21781	-0.694
98	62.58	1.139	41.443	16.174	0.16316	3.525
99	48.78	0.876	31.543	19.484	1.03971	-3.326
100	49.29	0.000	35.854	10.653	0.03974	2.262
Summary Statistics						
Count	100	100	100	100	100	100
Maximum	68.60	4.509	41.443	25.317	1.82288	6.616
Average	49.14	0.680	32.584	15.438	0.37093	0.095
Median	48.83	0.086	32.579	15.177	0.15878	0.250
Minimum	29.81	0.000	21.633	4.182	0.01340	-7.051
Std Dev	7.69	1.127	3.397	4.386	0.41897	2.964

Detailed HELP Model Annual Water Balance Data for Configuration #1a (Year 300):

Simulation	Precip-itation (in/yr)	Runoff (in/yr)	Evapotrans-piration (in/yr)	Lateral Drainage (in/yr)	Infiltration thru GCL (in/yr)	Change in Water Storage (in/yr)
1	40.07	0.000	31.643	4.099	0.06890	4.328
2	57.14	0.000	32.006	23.756	1.02620	1.373
3	52.64	0.000	31.112	20.480	0.76198	1.040
4	47.88	0.981	38.434	9.398	0.15971	-0.939
5	50.57	0.000	34.411	13.258	0.22826	2.893
6	42.28	0.000	27.896	12.932	0.27035	1.278
7	39.35	0.544	30.562	14.957	0.43328	-6.847
8	49.46	0.547	31.414	15.072	0.29156	2.244
9	48.59	0.000	33.552	13.697	0.23540	1.025
10	53.97	0.869	34.032	17.181	0.78962	1.604
11	57.63	4.338	32.415	18.779	1.05046	1.697
12	46.71	0.000	29.228	19.097	0.71754	-2.496
13	38.58	0.000	30.402	7.604	0.12860	-0.228
14	41.49	0.371	27.770	13.426	0.35926	-0.662
15	44.94	1.042	32.617	13.085	0.22523	-2.119
16	54.78	0.509	32.437	19.577	0.72848	1.939
17	29.81	0.000	21.649	9.726	0.17295	-1.879
18	49.55	0.000	34.832	11.296	0.19303	2.955
19	55.50	1.880	33.748	19.953	1.01043	-0.406
20	68.56	0.000	37.438	24.226	1.10517	6.347
21	51.14	1.125	33.780	19.051	0.88444	-3.697
22	51.22	0.000	36.721	14.811	0.25586	-1.322
23	47.94	0.000	36.592	14.921	0.54091	-4.080
24	59.17	1.838	31.599	20.184	0.93448	5.151
25	47.73	0.048	30.391	16.493	0.43694	0.197
26	50.56	0.219	31.894	16.502	0.63465	1.294
27	37.02	0.000	32.208	9.145	0.16931	-5.097
28	56.03	0.811	35.865	19.311	0.76925	-0.420
29	39.77	0.000	29.444	8.594	0.14609	1.306
30	46.55	0.328	33.840	12.238	0.20929	-0.408
31	39.45	0.084	28.826	13.783	0.32822	-3.632
32	45.35	0.404	29.775	12.624	0.23177	2.340
33	42.23	0.000	31.909	7.899	0.13312	2.121
34	37.81	0.000	27.299	12.000	0.22756	-1.815
35	48.19	0.315	34.059	14.069	0.24280	-0.457
36	62.28	3.544	34.031	18.989	0.62574	5.477

Detailed HELP Model Annual Water Balance Data for Configuration #1a (Year 300) – Continued:

Simulation	Precip- itation (in/yr)	Runoff (in/yr)	Evapotrans- piration (in/yr)	Lateral Drainage (in/yr)	Infiltration thru GCL (in/yr)	Change in Water Storage (in/yr)
37	55.96	0.000	40.400	16.580	0.30213	-1.163
38	40.26	0.000	28.220	13.127	0.23986	-1.434
39	60.02	4.111	35.106	19.258	0.90472	1.262
40	59.62	0.784	37.185	20.932	0.42094	0.126
41	47.60	0.000	31.581	15.488	0.43248	0.107
42	50.44	0.493	34.102	16.212	0.29214	-0.937
43	39.42	0.090	26.338	11.500	0.19758	1.038
44	48.61	0.000	34.007	13.970	0.27246	0.263
45	57.35	3.115	34.982	23.422	1.49229	-4.385
46	47.49	0.000	31.968	11.234	0.19427	3.391
47	38.98	0.000	31.654	9.835	0.16827	-3.166
48	42.99	0.000	32.709	8.975	0.15179	0.946
49	53.01	1.688	34.148	13.467	0.24952	3.332
50	55.17	0.067	38.032	19.085	0.50402	-2.278
51	46.16	0.000	31.179	12.160	0.21634	2.681
52	42.63	0.000	33.793	13.721	0.41471	-5.131
53	50.93	0.000	32.530	17.413	0.31128	0.623
54	54.24	0.633	28.375	18.258	0.60414	6.611
55	50.46	0.244	33.005	17.237	0.73125	-0.273
56	56.39	1.171	38.475	21.446	0.58096	-5.395
57	41.99	0.000	27.918	12.983	0.28775	0.504
58	68.60	0.811	35.844	25.080	1.75930	6.388
59	48.67	0.061	33.955	16.294	0.76380	-2.825
60	58.12	0.526	34.675	21.132	0.88330	0.697
61	54.90	3.658	31.691	18.183	1.24066	0.369
62	56.29	2.478	33.316	22.790	1.18183	-3.419
63	49.13	0.434	34.489	15.171	0.26260	-2.076
64	54.54	0.386	32.270	17.924	0.49264	3.437
65	45.05	0.000	32.977	13.464	0.31018	-1.861
66	37.07	0.000	29.777	9.752	0.16706	-2.960
67	40.17	0.000	24.976	10.180	0.17414	4.616
68	58.08	0.579	35.691	22.057	1.30281	-0.494
69	36.31	0.000	27.096	10.606	0.18132	-2.033
70	42.67	1.024	31.930	12.896	0.28228	-3.765
71	48.88	0.000	35.445	10.185	0.17536	2.891
72	47.36	0.538	32.729	16.615	0.40523	-2.883
73	35.81	0.000	26.588	8.626	0.14773	0.376
74	49.81	0.745	29.613	14.879	0.32343	4.290

Detailed HELP Model Annual Water Balance Data for Configuration #1a (Year 300) –
Continued:

Simulation	Precip- itation (in/yr)	Runoff (in/yr)	Evapotrans- piration (in/yr)	Lateral Drainage (in/yr)	Infiltration thru GCL (in/yr)	Change in Water Storage (in/yr)
75	56.43	3.859	34.418	17.401	0.30347	0.411
76	45.86	0.000	32.498	15.121	0.30172	-1.941
77	56.76	0.000	39.073	17.699	0.56046	-0.237
78	39.15	0.000	29.546	9.206	0.16860	0.065
79	48.87	0.000	30.960	12.887	0.51600	4.632
80	58.52	3.984	33.487	22.722	1.37606	-2.031
81	53.34	0.000	35.527	16.049	0.28014	0.728
82	55.18	0.000	35.777	17.721	0.50340	1.148
83	53.60	4.599	34.816	18.158	0.89548	-4.381
84	47.82	0.000	34.283	12.151	0.30004	0.544
85	44.69	0.000	30.792	9.713	0.16502	3.597
86	60.77	2.022	36.837	23.090	1.42349	-1.523
87	48.34	1.171	29.573	13.783	0.35056	2.964
88	36.18	1.249	26.140	14.844	0.81060	-6.587
89	58.29	2.756	35.516	15.408	0.59043	3.761
90	60.08	3.792	30.642	20.344	1.08221	4.728
91	55.49	0.000	35.907	20.115	1.05268	-1.324
92	44.51	0.220	32.158	14.075	0.32939	-2.817
93	35.83	0.000	29.631	9.961	0.17952	-4.578
94	45.02	0.000	32.871	10.037	0.17023	1.611
95	44.54	0.892	27.516	17.250	0.90549	-1.461
96	53.18	0.136	35.733	13.559	0.31335	3.329
97	48.03	0.383	31.458	16.293	0.40930	-0.589
98	62.58	1.143	41.433	15.984	0.35451	3.632
99	48.78	0.949	31.512	19.423	1.06354	-3.425
100	49.29	0.000	35.870	10.503	0.17809	2.081
Summary Statistics						
Count	100	100	100	100	100	100
Maximum	68.60	4.599	41.433	25.080	1.75930	6.611
Average	49.14	0.706	32.586	15.278	0.50333	0.099
Median	48.83	0.087	32.574	15.015	0.32881	0.162
Minimum	29.81	0.000	21.649	4.099	0.06890	-6.847
Std Dev	7.69	1.163	3.400	4.356	0.37255	2.965

Detailed HELP Model Annual Water Balance Data for Configuration #1a (Year 340):

Simulation	Precip-itation (in/yr)	Runoff (in/yr)	Evapotrans-piration (in/yr)	Lateral Drainage (in/yr)	Infiltration thru GCL (in/yr)	Change in Water Storage (in/yr)
1	40.07	0.000	31.641	3.983	0.13841	4.446
2	57.14	0.000	32.053	22.716	1.97132	2.366
3	52.64	0.000	31.076	19.782	1.48790	1.763
4	47.88	0.985	38.433	9.299	0.32707	-1.284
5	50.57	0.000	34.400	12.970	0.46196	2.486
6	42.28	0.000	27.879	12.734	0.55018	1.282
7	39.35	0.548	30.566	14.522	0.87093	-6.755
8	49.46	0.550	31.420	14.730	0.59841	1.914
9	48.59	0.000	33.543	13.450	0.47838	0.97
10	53.97	0.864	33.984	16.480	1.52724	1.962
11	57.63	4.185	32.403	17.989	2.03721	1.074
12	46.71	0.000	29.241	18.385	1.39412	-2.457
13	38.58	0.000	30.392	7.499	0.26232	-0.333
14	41.49	0.377	27.708	13.129	0.73798	-0.328
15	44.94	1.044	32.598	12.853	0.45773	-2.274
16	54.78	0.560	32.387	18.842	1.42281	2.495
17	29.81	0.000	21.658	9.598	0.36256	-2.423
18	49.55	0.000	34.803	11.070	0.39133	2.821
19	55.50	1.754	33.740	19.154	1.96140	-0.016
20	68.56	0.000	37.402	23.335	2.23543	6.729
21	51.14	0.908	33.798	18.249	1.67966	-4.575
22	51.22	0.000	36.728	14.510	0.51875	-1.161
23	47.94	0.000	36.626	14.404	1.08625	-3.809
24	59.17	1.798	31.588	19.291	1.84242	5.241
25	47.73	0.051	30.384	16.052	0.89287	-0.109
26	50.56	0.223	31.892	15.840	1.24061	1.293
27	37.02	0.000	32.230	9.031	0.35361	-5.235
28	56.03	0.813	35.873	18.529	1.50486	0.164
29	39.77	0.000	29.452	8.447	0.29704	0.748
30	46.55	0.331	33.919	11.946	0.42265	-0.403
31	39.45	0.088	28.826	13.437	0.68230	-3.22
32	45.35	0.408	29.771	12.361	0.47409	2.115
33	42.23	0.000	31.912	7.747	0.26997	2.093
34	37.81	0.000	27.320	11.761	0.46924	-1.739
35	48.19	0.319	34.096	13.760	0.49127	-0.399
36	62.28	3.547	34.040	18.322	1.24564	6.048

Detailed HELP Model Annual Water Balance Data for Configuration #1a (Year 340) – Continued:

Simulation	Precip- itation (in/yr)	Runoff (in/yr)	Evapotrans- piration (in/yr)	Lateral Drainage (in/yr)	Infiltration thru GCL (in/yr)	Change in Water Storage (in/yr)
37	55.96	0.000	40.417	16.267	0.63612	-1.55
38	40.26	0.000	28.232	12.867	0.49342	-1.676
39	60.02	4.017	35.118	18.485	1.74299	1.381
40	59.62	0.791	37.182	20.404	0.88645	0.171
41	47.60	0.000	31.575	15.080	0.89715	-0.065
42	50.44	0.489	34.083	15.935	0.60143	-0.954
43	39.42	0.094	26.323	11.332	0.40286	1.006
44	48.61	0.000	34.007	13.666	0.56295	0.382
45	57.35	2.893	34.951	22.281	2.87798	-4.229
46	47.49	0.000	31.963	10.998	0.39345	2.881
47	38.98	0.000	31.654	9.726	0.34438	-3.032
48	42.99	0.000	32.664	8.846	0.30947	0.878
49	53.01	1.692	34.183	13.162	0.50935	3.552
50	55.17	0.067	37.989	18.567	1.04719	-1.709
51	46.16	0.000	31.179	11.960	0.44112	2.323
52	42.63	0.000	33.810	13.290	0.84162	-5.189
53	50.93	0.000	32.511	17.048	0.64603	0.511
54	54.24	0.640	28.372	17.740	1.22664	7.008
55	50.46	0.248	33.017	16.480	1.39082	-0.786
56	56.39	1.178	38.546	20.738	1.22242	-5.093
57	41.99	0.000	27.934	12.681	0.57327	0.22
58	68.60	0.536	35.830	23.841	3.42360	7.256
59	48.67	0.057	33.952	15.508	1.43983	-4.119
60	58.12	0.516	34.679	20.285	1.69570	0.992
61	54.90	3.679	31.577	17.208	2.37294	0.206
62	56.29	2.406	33.323	21.750	2.21668	-3.346
63	49.13	0.441	34.427	14.968	0.53639	-2.007
64	54.54	0.390	32.271	17.391	0.99933	3.785
65	45.05	0.000	32.986	13.152	0.64382	-2.022
66	37.07	0.000	29.774	9.607	0.34050	-3.1
67	40.17	0.000	24.967	9.979	0.35310	4.611
68	58.08	0.490	35.679	20.945	2.49252	-0.148
69	36.31	0.000	27.103	10.440	0.36929	-2.438
70	42.67	1.028	31.912	12.620	0.58083	-3.535
71	48.88	0.000	35.458	10.001	0.35616	2.728
72	47.36	0.538	32.750	16.138	0.84977	-2.471
73	35.81	0.000	26.508	8.536	0.30234	0.152
74	49.81	0.745	29.598	14.526	0.65893	4.269

Detailed HELP Model Annual Water Balance Data for Configuration #1a (Year 340) – Continued:

Simulation	Precip-itation (in/yr)	Runoff (in/yr)	Evapotrans-piration (in/yr)	Lateral Drainage (in/yr)	Infiltration thru GCL (in/yr)	Change in Water Storage (in/yr)
75	56.43	3.866	34.404	17.118	0.61808	0.754
76	45.86	0.000	32.510	14.791	0.63229	-1.973
77	56.76	0.000	39.067	17.141	1.11501	-0.197
78	39.15	0.000	29.548	9.065	0.34972	-0.408
79	48.87	0.000	30.946	12.384	1.00169	4.848
80	58.52	3.756	33.408	21.708	2.67526	-2.247
81	53.34	0.000	35.513	15.741	0.58567	0.743
82	55.18	0.000	35.759	17.242	1.00700	1.422
83	53.60	4.598	34.829	17.338	1.76792	-4.705
84	47.82	0.000	34.293	11.810	0.60378	0.532
85	44.69	0.000	30.801	9.517	0.33493	3.512
86	60.77	1.677	36.811	22.069	2.80398	-1.143
87	48.34	1.178	29.557	13.439	0.71207	2.726
88	36.18	1.279	26.138	14.125	1.54259	-6.761
89	58.29	2.759	35.518	14.798	1.17519	4.05
90	60.08	3.625	30.605	19.535	2.12232	4.57
91	55.49	0.000	35.914	19.275	2.03570	-1.2
92	44.51	0.222	32.147	13.574	0.63205	-3.086
93	35.83	0.000	29.641	9.795	0.37299	-4.526
94	45.02	0.000	32.920	9.800	0.34374	1.595
95	44.54	0.916	27.595	16.376	1.69440	-0.945
96	53.18	0.140	35.745	13.216	0.64719	3.04
97	48.03	0.386	31.462	15.836	0.83417	-0.392
98	62.58	1.150	41.454	15.595	0.74345	3.608
99	48.78	0.901	31.558	18.421	2.02282	-3.693
100	49.29	0.000	35.881	10.335	0.36261	1.937
Summary Statistics						
Count	100	100	100	100	100	100
Maximum	68.60	4.598	41.454	23.841	3.42360	7.256
Average	49.14	0.687	32.583	14.807	0.99561	0.104
Median	48.83	0.091	32.555	14.628	0.67062	0.158
Minimum	29.81	0.000	21.658	3.983	0.13841	-6.761
Std Dev	7.69	1.134	3.402	4.093	0.71200	3.038

Detailed HELP Model Annual Water Balance Data for Configuration #1a (Year 380):

Simulation	Precip-itation (in/yr)	Runoff (in/yr)	Evapotrans-piration (in/yr)	Lateral Drainage (in/yr)	Infiltration thru GCL (in/yr)	Change in Water Storage (in/yr)
1	40.07	0.000	31.615	3.890	0.20504	4.564
2	57.14	0.000	31.992	21.770	2.93072	3.372
3	52.64	0.000	31.093	19.086	2.17186	1.831
4	47.88	0.988	38.418	9.205	0.49134	-2.096
5	50.57	0.000	34.339	12.726	0.68780	2.621
6	42.28	0.000	27.898	12.490	0.81861	1.434
7	39.35	0.552	30.578	14.110	1.30575	-7.023
8	49.46	0.553	31.424	14.389	0.90402	2.079
9	48.59	0.000	33.510	13.237	0.71467	0.962
10	53.97	0.917	33.983	15.787	2.16339	1.758
11	57.63	4.079	32.414	17.231	2.90802	0.967
12	46.71	0.000	29.209	17.773	2.00536	-2.325
13	38.58	0.000	30.399	7.388	0.39197	-0.377
14	41.49	0.377	27.728	12.775	1.10660	-0.136
15	44.94	1.047	32.597	12.609	0.68136	-2.343
16	54.78	0.623	32.365	18.150	2.03532	2.512
17	29.81	0.000	21.658	9.472	0.55581	-2.562
18	49.55	0.000	34.834	10.802	0.57927	2.849
19	55.50	1.659	33.737	18.411	2.80050	0.003
20	68.56	0.000	37.426	22.415	3.30805	7.420
21	51.14	0.769	33.782	17.538	2.36336	-5.350
22	51.22	0.000	36.730	14.230	0.77210	-0.982
23	47.94	0.000	36.601	13.964	1.62030	-3.960
24	59.17	1.786	31.569	18.444	2.67506	5.438
25	47.73	0.054	30.391	15.601	1.34624	-0.318
26	50.56	0.227	31.910	15.233	1.80970	1.322
27	37.02	0.000	32.206	8.925	0.53827	-5.233
28	56.03	0.816	35.880	17.820	2.17617	0.372
29	39.77	0.000	29.433	8.336	0.44459	0.505
30	46.55	0.335	33.956	11.667	0.62621	-0.227
31	39.45	0.091	28.842	13.099	1.04743	-3.137
32	45.35	0.411	29.789	12.086	0.71695	2.031
33	42.23	0.000	31.912	7.590	0.40113	2.023
34	37.81	0.000	27.302	11.565	0.71547	-1.542
35	48.19	0.322	34.222	13.367	0.72378	-0.446
36	62.28	3.550	34.036	17.708	1.82663	6.067

Detailed HELP Model Annual Water Balance Data for Configuration #1a (Year 380) – Continued:

Simulation	Precip-itation (in/yr)	Runoff (in/yr)	Evapotrans-piration (in/yr)	Lateral Drainage (in/yr)	Infiltration thru GCL (in/yr)	Change in Water Storage (in/yr)
37	55.96	0.000	40.398	15.979	0.97539	-1.658
38	40.26	0.000	28.245	12.619	0.74350	-1.699
39	60.02	3.961	35.093	17.782	2.50301	1.275
40	59.62	0.797	37.196	19.822	1.39309	0.479
41	47.60	0.000	31.547	14.698	1.35419	-0.363
42	50.44	0.485	34.082	15.636	0.92004	-0.816
43	39.42	0.097	26.338	11.142	0.60109	0.965
44	48.61	0.000	33.991	13.382	0.85372	0.470
45	57.35	2.745	34.945	21.205	4.09956	-4.470
46	47.49	0.000	31.961	10.753	0.59873	2.956
47	38.98	0.000	31.668	9.612	0.51655	-2.947
48	42.99	0.000	32.660	8.676	0.46036	0.784
49	53.01	1.696	34.165	12.898	0.76558	3.834
50	55.17	0.066	38.046	17.932	1.60266	-1.597
51	46.16	0.000	31.178	11.777	0.66196	2.005
52	42.63	0.000	33.789	12.919	1.25472	-5.271
53	50.93	0.000	32.507	16.651	0.99145	0.771
54	54.24	0.647	28.354	17.221	1.82911	7.247
55	50.46	0.252	32.975	15.879	1.97961	-1.353
56	56.39	1.183	38.460	20.134	1.90588	-4.848
57	41.99	0.000	27.932	12.409	0.86333	0.140
58	68.60	0.358	35.800	22.682	4.91517	7.924
59	48.67	0.054	33.950	14.826	2.02517	-5.077
60	58.12	0.517	34.650	19.540	2.41509	1.238
61	54.90	3.720	31.521	16.314	3.35715	0.010
62	56.29	2.361	33.312	20.829	3.11765	-3.244
63	49.13	0.449	34.490	14.663	0.79744	-1.870
64	54.54	0.394	32.288	16.852	1.48841	3.769
65	45.05	0.000	32.995	12.837	0.97768	-2.082
66	37.07	0.000	29.764	9.477	0.50964	-3.069
67	40.17	0.000	24.964	9.778	0.52473	4.642
68	58.08	0.445	35.614	19.993	3.53517	-0.272
69	36.31	0.000	27.115	10.277	0.55155	-2.433
70	42.67	1.032	31.925	12.329	0.87378	-3.351
71	48.88	0.000	35.471	9.814	0.53025	2.639
72	47.36	0.542	32.744	15.679	1.28382	-2.218
73	35.81	0.000	26.531	8.412	0.45204	-0.138
74	49.81	0.746	29.599	14.093	0.98329	4.490

Detailed HELP Model Annual Water Balance Data for Configuration #1a (Year 380) – Continued:

Simulation	Precip-itation (in/yr)	Runoff (in/yr)	Evapotrans-piration (in/yr)	Lateral Drainage (in/yr)	Infiltration thru GCL (in/yr)	Change in Water Storage (in/yr)
75	56.43	3.833	34.401	16.859	0.94639	0.826
76	45.86	0.000	32.497	14.500	0.96543	-2.179
77	56.76	0.000	39.094	16.577	1.63300	-0.213
78	39.15	0.000	29.554	8.921	0.53161	-0.521
79	48.87	0.000	30.946	11.928	1.43677	4.849
80	58.52	3.514	33.406	20.763	3.83496	-2.292
81	53.34	0.000	35.495	15.425	0.88598	0.978
82	55.18	0.003	35.790	16.730	1.50197	1.341
83	53.60	4.623	34.822	16.573	2.57200	-4.925
84	47.82	0.000	34.280	11.513	0.90004	0.671
85	44.69	0.000	30.836	9.290	0.49914	3.555
86	60.77	1.427	36.744	21.116	4.06917	-1.261
87	48.34	1.185	29.578	13.081	1.05554	2.935
88	36.18	1.314	26.138	13.503	2.17831	-7.082
89	58.29	2.763	35.540	14.190	1.72970	4.558
90	60.08	3.503	30.587	18.747	3.06255	4.259
91	55.49	0.000	35.887	18.525	2.91993	-1.016
92	44.51	0.225	32.143	13.151	0.90884	-3.347
93	35.83	0.000	29.625	9.645	0.56853	-4.452
94	45.02	0.000	32.843	9.691	0.51589	1.619
95	44.54	0.950	27.573	15.690	2.38987	-0.995
96	53.18	0.144	35.741	12.876	0.98776	3.104
97	48.03	0.388	31.460	15.396	1.24885	-0.293
98	62.58	1.157	41.417	15.229	1.15277	3.676
99	48.78	0.884	31.560	17.561	2.86843	-3.993
100	49.29	0.000	35.840	10.220	0.54416	2.029
Summary Statistics						
Count	100	100	100	100	100	100
Maximum	68.60	4.623	41.417	22.682	4.91517	7.924
Average	49.14	0.676	32.578	14.361	1.45688	0.108
Median	48.83	0.094	32.552	14.210	1.01944	0.007
Minimum	29.81	0.000	21.658	3.890	0.20504	-7.082
Std Dev	7.69	1.115	3.398	3.853	1.01005	3.156

Detailed HELP Model Annual Water Balance Data for Configuration #1a (Year 560):

Simulation	Precip-itation (in/yr)	Runoff (in/yr)	Evapotrans-piration (in/yr)	Lateral Drainage (in/yr)	Infiltration thru GCL (in/yr)	Change in Water Storage (in/yr)
1	40.07	0.000	31.620	3.335	0.52490	5.115
2	57.14	0.000	32.001	17.842	6.70690	6.123
3	52.64	0.173	31.119	16.526	4.51014	0.157
4	47.88	0.992	38.415	8.548	1.36749	-2.787
5	50.57	0.000	34.355	11.325	1.83254	3.565
6	42.28	0.000	27.889	11.220	2.25382	0.895
7	39.35	0.555	30.585	12.234	3.24378	-7.397
8	49.46	0.558	31.430	12.656	2.51319	2.622
9	48.59	0.000	33.439	12.051	1.95139	1.247
10	53.97	1.462	34.015	13.535	3.81441	0.953
11	57.63	4.854	32.428	14.560	4.85849	0.958
12	46.71	0.000	29.221	15.436	4.23975	-1.875
13	38.58	0.000	30.395	6.798	1.07859	-0.759
14	41.49	0.378	27.773	11.145	2.81033	-0.263
15	44.94	1.049	32.621	11.318	1.87466	-1.562
16	54.78	1.228	32.299	15.522	3.94365	2.309
17	29.81	0.000	21.632	8.656	1.68707	-3.315
18	49.55	0.000	34.947	9.536	1.52946	3.829
19	55.50	2.374	33.802	15.633	4.79972	-0.514
20	68.56	0.074	37.413	18.541	7.00987	8.337
21	51.14	1.286	33.741	15.085	4.45975	-6.319
22	51.22	0.000	36.737	12.804	2.08290	-0.507
23	47.94	0.000	36.722	12.019	3.68413	-4.882
24	59.17	2.226	31.606	15.310	5.14508	6.554
25	47.73	0.057	30.383	13.647	3.37544	-1.000
26	50.56	0.231	31.880	13.030	4.03430	1.408
27	37.02	0.000	32.220	8.054	1.56649	-5.605
28	56.03	0.819	35.854	15.142	4.72877	0.649
29	39.77	0.000	29.404	7.675	1.22456	0.312
30	46.55	0.338	33.969	10.508	1.68897	0.474
31	39.45	0.095	28.840	11.281	2.99354	-3.936
32	45.35	0.415	29.778	10.660	2.06707	2.741
33	42.23	0.000	31.921	6.848	1.08127	1.796
34	37.81	0.000	27.320	10.308	2.09623	-1.658
35	48.19	0.326	34.221	11.993	1.95588	0.141
36	62.28	3.554	34.042	15.331	4.17244	5.955

Detailed HELP Model Annual Water Balance Data for Configuration #1a (Year 560) – Continued:

Simulation	Precip-itation (in/yr)	Runoff (in/yr)	Evapotrans-piration (in/yr)	Lateral Drainage (in/yr)	Infiltration thru GCL (in/yr)	Change in Water Storage (in/yr)
37	55.96	0.000	40.372	14.085	2.91932	-2.194
38	40.26	0.000	28.254	11.249	2.14759	-1.707
39	60.02	4.571	35.087	15.005	4.59366	1.256
40	59.62	0.804	37.195	16.882	4.25665	1.696
41	47.60	0.000	31.585	12.774	3.32546	-1.557
42	50.44	0.482	34.085	13.771	2.76264	-0.450
43	39.42	0.101	26.330	10.222	1.65276	0.588
44	48.61	0.000	34.008	11.686	2.48936	0.523
45	57.35	3.612	34.952	17.470	6.93625	-4.794
46	47.49	0.000	31.979	9.479	1.71457	3.773
47	38.98	0.000	31.627	8.977	1.44592	-3.603
48	42.99	0.000	32.706	7.777	1.23337	1.215
49	53.01	1.699	34.174	11.417	2.16494	4.076
50	55.17	0.065	38.109	15.087	4.40283	-1.843
51	46.16	0.000	31.193	10.574	1.91838	1.545
52	42.63	0.000	33.819	11.120	3.04580	-5.363
53	50.93	0.000	32.483	14.543	2.92920	2.061
54	54.24	0.731	28.386	14.651	4.32884	7.644
55	50.46	0.254	33.009	13.622	4.19989	-2.817
56	56.39	1.189	38.488	16.675	5.39732	-4.907
57	41.99	0.000	27.902	10.963	2.33572	0.179
58	68.60	1.201	35.925	18.575	8.15622	7.945
59	48.67	0.050	33.986	12.614	4.20227	-5.529
60	58.12	0.812	34.655	16.690	4.84783	2.058
61	54.90	4.103	31.746	13.717	5.45228	-0.513
62	56.29	2.735	33.293	17.476	5.92823	-2.940
63	49.13	0.456	34.474	13.296	2.25333	-1.552
64	54.54	0.398	32.247	14.439	3.83507	3.463
65	45.05	0.000	33.008	11.259	2.67341	-2.236
66	37.07	0.000	29.751	8.709	1.40256	-3.202
67	40.17	0.000	24.964	8.775	1.41681	5.122
68	58.08	0.936	35.664	16.951	5.88617	-0.460
69	36.31	0.000	27.086	9.489	1.52563	-2.585
70	42.67	1.035	31.945	10.923	2.33771	-3.484
71	48.88	0.000	35.458	8.777	1.58620	2.985
72	47.36	0.549	32.744	13.380	3.49164	-2.205
73	35.81	0.000	26.525	7.750	1.24613	-0.581
74	49.81	0.747	29.591	12.238	2.56116	5.928

Detailed HELP Model Annual Water Balance Data for Configuration #1a (Year 560) – Continued:

Simulation	Precip- itation (in/yr)	Runoff (in/yr)	Evapotrans- piration (in/yr)	Lateral Drainage (in/yr)	Infiltration thru GCL (in/yr)	Change in Water Storage (in/yr)
75	56.43	3.840	34.399	14.999	2.87736	0.094
76	45.86	0.000	32.488	12.643	2.91936	-2.659
77	56.76	0.000	39.162	14.380	3.67676	-0.064
78	39.15	0.000	29.556	8.042	1.60636	-1.035
79	48.87	0.000	30.956	10.320	2.95767	4.903
80	58.52	4.383	33.483	17.168	6.32729	-2.064
81	53.34	0.000	35.517	13.683	2.57129	1.634
82	55.18	0.006	35.795	14.557	3.73943	0.807
83	53.60	4.836	34.919	13.852	5.08015	-5.295
84	47.82	0.000	34.258	10.137	2.29883	0.795
85	44.69	0.000	30.821	8.346	1.35390	4.090
86	60.77	2.454	36.875	17.282	6.69649	-1.709
87	48.34	1.192	29.566	11.561	2.70095	3.890
88	36.18	1.573	26.147	11.543	3.97801	-8.403
89	58.29	2.766	35.754	11.679	3.90867	6.596
90	60.08	4.300	30.621	15.728	5.17220	3.278
91	55.49	0.000	35.875	15.621	5.64945	-0.647
92	44.51	0.227	32.139	11.614	2.70785	-4.208
93	35.83	0.000	29.642	8.625	1.62957	-4.690
94	45.02	0.000	32.819	8.779	1.39877	2.367
95	44.54	1.306	27.503	13.625	4.25205	-1.865
96	53.18	0.147	35.716	11.160	2.72588	3.192
97	48.03	0.391	31.459	13.373	3.18160	-0.039
98	62.58	1.164	41.439	13.148	3.27342	3.912
99	48.78	1.223	31.523	15.091	4.88743	-4.203
100	49.29	0.000	35.872	9.363	1.49307	2.111
Summary Statistics						
Count	100	100	100	100	100	100
Maximum	68.60	4.854	41.439	18.575	8.15622	8.337
Average	49.14	0.794	32.591	12.455	3.22974	0.121
Median	48.83	0.124	32.555	12.426	2.91934	0.118
Minimum	29.81	0.000	21.632	3.335	0.52490	-8.403
Std Dev	7.69	1.274	3.410	3.034	1.61323	3.527

Detailed HELP Model Annual Water Balance Data for Configuration #1a (Year 1,000):

Simulation	Precip-itation (in/yr)	Runoff (in/yr)	Evapotrans-piration (in/yr)	Lateral Drainage (in/yr)	Infiltration thru GCL (in/yr)	Change in Water Storage (in/yr)
1	40.07	0.000	31.632	2.065	1.42524	6.372
2	57.14	0.215	33.812	10.988	11.01126	7.644
3	52.64	1.374	31.074	10.491	9.77980	-0.516
4	47.88	1.003	38.413	5.867	4.21810	-3.491
5	50.57	0.000	34.315	7.368	5.75111	5.023
6	42.28	0.000	27.885	7.019	6.23569	-0.077
7	39.35	0.566	30.563	8.326	7.40173	-7.815
8	49.46	0.573	31.416	8.205	6.85858	3.095
9	48.59	0.000	33.425	8.000	6.00889	1.207
10	53.97	2.456	34.409	8.575	7.45492	1.108
11	57.63	6.862	32.468	9.270	8.05018	0.619
12	46.71	0.244	29.215	10.316	9.02312	-1.422
13	38.58	0.000	30.401	4.727	3.29861	-1.274
14	41.49	0.380	28.038	7.303	6.42933	-0.671
15	44.94	1.056	32.594	7.494	5.70434	-1.262
16	54.78	2.114	32.581	9.742	8.52853	3.077
17	29.81	0.000	21.670	5.743	4.73140	-4.667
18	49.55	0.000	34.861	6.386	4.50976	5.317
19	55.50	4.036	33.719	9.978	8.88890	-1.125
20	68.56	2.759	37.470	11.271	11.15370	7.377
21	51.14	2.878	33.756	9.738	8.57974	-5.513
22	51.22	0.000	36.690	8.301	6.76102	0.884
23	47.94	0.933	36.549	7.938	7.00288	-6.570
24	59.17	3.563	31.724	9.497	8.76824	7.933
25	47.73	0.066	30.672	9.206	8.12028	-1.740
26	50.56	0.798	31.874	8.616	7.67948	1.825
27	37.02	0.000	32.229	5.591	4.46052	-6.881
28	56.03	0.921	36.384	9.672	9.29861	0.999
29	39.77	0.000	29.391	5.256	3.86490	0.191
30	46.55	0.349	33.888	7.073	5.08581	0.873
31	39.45	0.104	28.831	7.404	6.99460	-4.592
32	45.35	0.426	29.733	6.986	5.69272	3.166
33	42.23	0.000	31.951	4.648	3.22226	2.286
34	37.81	0.000	27.324	6.841	5.69122	-2.601
35	48.19	0.321	34.276	7.696	6.08097	0.668
36	62.28	3.564	34.297	9.831	8.92377	7.339

Detailed HELP Model Annual Water Balance Data for Configuration #1a (Year 1,000) –
Continued:

Simulation	Precip-itation (in/yr)	Runoff (in/yr)	Evapotrans-piration (in/yr)	Lateral Drainage (in/yr)	Infiltration thru GCL (in/yr)	Change in Water Storage (in/yr)
37	55.96	0.000	40.337	8.956	8.59651	-3.659
38	40.26	0.000	28.256	7.208	6.18378	-1.812
39	60.02	5.852	35.078	9.583	8.69042	1.654
40	59.62	0.824	37.215	10.420	10.05232	2.565
41	47.60	0.000	31.594	8.920	7.75947	-2.128
42	50.44	0.477	34.102	8.827	7.70095	-0.562
43	39.42	0.111	26.309	6.786	5.24158	-0.098
44	48.61	0.000	34.009	7.568	6.54059	0.796
45	57.35	5.663	36.108	10.692	10.30069	-4.828
46	47.49	0.000	32.029	6.174	5.07150	5.445
47	38.98	0.000	31.678	6.050	4.54483	-5.707
48	42.99	0.000	32.696	5.253	3.66070	1.996
49	53.01	1.710	34.168	7.579	5.91763	4.047
50	55.17	0.062	38.491	9.599	9.18582	-1.469
51	46.16	0.000	31.224	6.813	6.04955	0.615
52	42.63	0.000	33.793	7.620	6.60753	-5.270
53	50.93	0.000	32.467	9.368	7.87886	2.645
54	54.24	2.344	28.373	9.091	8.60137	6.741
55	50.46	0.794	33.049	9.058	7.84980	-1.422
56	56.39	1.181	39.668	10.417	10.44999	-5.706
57	41.99	0.000	27.857	7.278	6.29389	0.152
58	68.60	5.828	36.080	11.306	10.66880	6.645
59	48.67	0.677	34.342	8.244	7.61083	-4.618
60	58.12	1.530	34.629	10.538	10.01748	2.677
61	54.90	6.564	31.855	8.661	7.77593	-0.725
62	56.29	4.061	34.341	11.033	10.21725	-2.480
63	49.13	0.477	34.579	8.543	7.02569	-2.049
64	54.54	0.407	32.369	9.481	8.73729	4.374
65	45.05	0.000	33.003	7.580	6.30558	-3.009
66	37.07	0.000	29.761	5.864	4.39791	-3.823
67	40.17	0.000	24.958	5.831	4.24317	5.707
68	58.08	3.593	35.725	10.522	9.52958	0.262
69	36.31	0.000	27.074	6.338	4.74953	-2.999
70	42.67	1.046	31.932	7.065	6.27183	-4.213
71	48.88	0.000	35.438	5.747	4.64945	2.986
72	47.36	0.568	32.960	8.698	7.79815	-1.951
73	35.81	0.000	26.482	5.214	4.02157	-1.167
74	49.81	0.749	29.663	7.891	6.54767	7.331

Detailed HELP Model Annual Water Balance Data for Configuration #1a (Year 1,000) – Continued:

Simulation	Precip-itation (in/yr)	Runoff (in/yr)	Evapotrans-piration (in/yr)	Lateral Drainage (in/yr)	Infiltration thru GCL (in/yr)	Change in Water Storage (in/yr)
75	56.43	3.899	34.374	9.302	8.59267	-0.556
76	45.86	0.000	32.468	8.333	7.29723	-2.533
77	56.76	0.000	39.537	9.434	8.16016	0.029
78	39.15	0.000	29.527	5.459	4.48428	-1.976
79	48.87	0.000	30.988	6.952	6.22026	5.314
80	58.52	6.868	33.853	10.608	10.01420	-1.332
81	53.34	0.000	35.500	8.747	7.38449	2.239
82	55.18	0.030	35.864	9.417	8.80186	0.346
83	53.60	7.102	34.823	8.877	7.97333	-6.196
84	47.82	0.000	34.266	6.804	5.63873	0.722
85	44.69	0.000	30.807	5.578	4.14823	5.031
86	60.77	5.968	37.134	10.452	9.73232	-1.663
87	48.34	1.211	29.575	7.565	6.12872	4.027
88	36.18	2.782	26.166	7.850	7.03535	-9.558
89	58.29	2.798	36.271	7.062	6.82635	7.837
90	60.08	7.041	30.700	9.857	8.93212	2.602
91	55.49	1.676	35.896	10.064	9.23117	-0.456
92	44.51	0.233	32.142	7.867	7.05652	-4.356
93	35.83	0.000	29.654	5.716	4.60307	-5.028
94	45.02	0.000	32.830	5.929	4.15674	2.937
95	44.54	2.691	27.557	8.678	7.84374	-2.749
96	53.18	0.158	35.748	7.369	6.47526	3.366
97	48.03	0.398	31.458	8.794	7.65031	0.157
98	62.58	1.181	41.401	8.441	7.56849	4.475
99	48.78	3.205	31.551	9.863	8.43544	-4.126
100	49.29	0.000	35.818	6.497	4.56736	1.647
Summary Statistics						
Count	100	100	100	100	100	100
Maximum	68.60	7.102	41.401	11.306	11.15370	7.933
Average	49.14	1.293	32.691	8.068	7.01394	0.139
Median	48.83	0.365	32.645	8.224	7.03052	0.091
Minimum	29.81	0.000	21.670	2.065	1.42524	-9.558
Std Dev	7.69	1.964	3.471	1.782	2.02320	3.929

Detailed HELP Model Annual Water Balance Data for Configuration #1a (Year 1,800):

Simulation	Precip-itation (in/yr)	Runoff (in/yr)	Evapotrans-piration (in/yr)	Lateral Drainage (in/yr)	Infiltration thru GCL (in/yr)	Change in Water Storage (in/yr)
1	40.07	0.000	31.617	0.689	2.92003	7.764
2	57.14	2.578	35.038	4.415	12.36037	8.043
3	52.64	3.562	31.591	4.394	12.41347	0.680
4	47.88	1.021	38.372	2.821	9.51232	-5.445
5	50.57	0.000	34.364	2.617	9.88674	5.297
6	42.28	0.000	27.874	3.139	10.34040	0.442
7	39.35	0.873	31.061	3.797	11.26747	-8.183
8	49.46	0.601	31.509	3.457	11.49554	3.172
9	48.59	0.000	33.418	3.060	11.27052	0.893
10	53.97	3.203	34.812	3.356	11.10496	1.617
11	57.63	8.823	32.709	3.855	11.62245	0.077
12	46.71	0.812	29.738	4.423	12.44982	-0.094
13	38.58	0.000	30.381	1.939	7.63032	-2.085
14	41.49	0.532	28.709	2.940	9.72965	-1.468
15	44.94	1.066	32.580	2.792	10.46602	-1.237
16	54.78	2.618	32.718	3.926	12.23661	4.317
17	29.81	0.000	21.769	2.730	8.94171	-5.771
18	49.55	0.000	34.828	2.218	9.04005	5.373
19	55.50	5.091	33.966	4.341	12.41581	-0.083
20	68.56	7.676	38.401	4.788	12.44951	5.246
21	51.14	3.597	34.283	4.236	12.27674	-3.345
22	51.22	0.000	36.705	3.269	11.61141	-0.277
23	47.94	2.779	36.752	3.301	10.25907	-6.507
24	59.17	4.636	32.026	3.809	11.65692	8.402
25	47.73	2.320	31.061	3.921	12.06279	-1.952
26	50.56	1.554	31.875	3.713	11.41417	2.297
27	37.02	0.000	32.195	2.380	8.23922	-7.942
28	56.03	2.540	37.630	4.009	11.66284	2.033
29	39.77	0.000	29.371	1.997	7.67024	-0.510
30	46.55	0.367	33.900	2.419	9.87006	0.656
31	39.45	0.301	29.662	3.127	9.81805	-4.341
32	45.35	0.444	29.710	2.893	9.96628	3.048
33	42.23	0.000	31.918	1.560	6.52044	2.564
34	37.81	0.000	27.345	2.774	9.53139	-2.993
35	48.19	0.303	34.251	2.978	10.96184	0.958
36	62.28	4.209	34.597	4.051	12.24633	7.816

Detailed HELP Model Annual Water Balance Data for Configuration #1a (Year 1,800) – Continued:

Simulation	Precip-itation (in/yr)	Runoff (in/yr)	Evapotrans-piration (in/yr)	Lateral Drainage (in/yr)	Infiltration thru GCL (in/yr)	Change in Water Storage (in/yr)
37	55.96	0.910	42.078	4.170	11.76185	-3.574
38	40.26	0.000	28.267	3.226	10.57993	-2.359
39	60.02	6.851	35.709	4.043	12.00689	2.200
40	59.62	1.663	38.037	4.585	12.44982	3.256
41	47.60	3.084	31.654	3.889	11.92485	-3.174
42	50.44	0.495	34.299	3.833	12.31659	-0.365
43	39.42	0.119	26.288	2.722	9.65174	-0.923
44	48.61	0.000	34.009	3.229	10.83882	1.118
45	57.35	8.239	37.602	4.406	12.09124	-4.280
46	47.49	0.000	31.996	2.275	8.25569	5.297
47	38.98	0.000	31.678	2.641	9.04767	-6.361
48	42.99	0.000	32.711	1.740	7.36370	1.898
49	53.01	1.728	34.196	2.801	10.69219	4.245
50	55.17	1.257	38.844	3.986	11.98017	-0.426
51	46.16	0.000	31.655	3.141	10.07904	0.168
52	42.63	0.000	34.123	3.445	10.64663	-5.661
53	50.93	0.000	32.370	3.903	12.01256	3.986
54	54.24	4.903	28.679	4.057	12.15592	4.444
55	50.46	1.464	33.445	3.798	11.97734	-0.241
56	56.39	3.463	41.185	4.379	12.30251	-5.079
57	41.99	0.000	28.288	3.038	10.66625	-0.412
58	68.60	10.603	36.104	4.745	12.23968	5.474
59	48.67	2.499	34.541	3.483	10.46262	-3.730
60	58.12	2.123	36.048	4.561	12.44982	4.354
61	54.90	9.982	31.923	3.652	10.53308	-1.877
62	56.29	6.517	35.047	4.610	12.41581	-1.613
63	49.13	0.513	34.753	3.932	12.32467	-2.499
64	54.54	1.294	32.750	4.102	12.21120	4.285
65	45.05	0.295	32.808	3.549	11.51091	-3.602
66	37.07	0.000	29.740	2.168	8.02815	-4.418
67	40.17	0.000	25.031	2.055	8.02316	5.906
68	58.08	5.542	36.064	4.324	12.33146	1.016
69	36.31	0.000	27.031	2.657	9.62251	-3.843
70	42.67	1.064	32.220	2.961	9.90374	-3.985
71	48.88	0.000	35.424	2.243	8.22274	2.611
72	47.36	0.587	33.772	3.634	11.57637	-0.940
73	35.81	0.000	26.518	2.010	7.60896	-2.312
74	49.81	0.748	29.616	2.932	10.22010	8.739

Detailed HELP Model Annual Water Balance Data for Configuration #1a (Year 1,800) – Continued:

Simulation	Precip-itation (in/yr)	Runoff (in/yr)	Evapotrans-piration (in/yr)	Lateral Drainage (in/yr)	Infiltration thru GCL (in/yr)	Change in Water Storage (in/yr)
75	56.43	4.614	35.509	4.251	12.41581	-0.360
76	45.86	0.485	32.747	3.757	11.83602	-3.522
77	56.76	0.457	40.326	3.864	12.23124	0.438
78	39.15	0.000	29.520	2.254	7.92750	-2.846
79	48.87	0.061	31.298	3.059	9.47576	5.852
80	58.52	9.066	35.144	4.345	12.25038	-0.931
81	53.34	0.000	35.527	3.681	12.30302	1.888
82	55.18	2.517	36.167	3.883	12.17266	0.429
83	53.60	9.286	35.135	3.749	10.91194	-6.703
84	47.82	0.000	34.252	2.836	9.72266	1.187
85	44.69	0.000	30.786	1.857	7.62699	5.282
86	60.77	9.106	37.347	4.223	11.99861	-1.725
87	48.34	1.243	29.583	3.055	10.15844	4.305
88	36.18	5.071	26.758	3.278	9.88753	-10.512
89	58.29	4.056	36.504	2.759	8.15961	8.523
90	60.08	10.997	30.666	4.269	12.27683	1.872
91	55.49	3.027	36.027	4.533	12.40683	-0.504
92	44.51	0.242	32.121	3.697	11.20918	-3.351
93	35.83	0.000	29.694	2.438	8.73513	-5.429
94	45.02	0.000	32.821	1.939	8.29275	2.211
95	44.54	3.523	27.976	3.660	11.04999	-1.930
96	53.18	0.174	36.467	3.096	10.29668	2.874
97	48.03	0.415	31.944	3.696	12.16074	0.986
98	62.58	1.215	41.568	3.611	11.97673	4.173
99	48.78	4.627	31.660	4.293	12.41581	-4.077
100	49.29	0.004	35.804	2.263	9.37760	0.819
Summary Statistics						
Count	100	100	100	100	100	100
Maximum	68.60	10.997	42.078	4.788	12.44982	8.739
Average	49.14	2.076	32.986	3.354	10.65084	0.147
Median	48.83	0.675	32.749	3.470	11.07747	-0.003
Minimum	29.81	0.000	21.769	0.689	2.92003	-10.512
Std Dev	7.69	2.854	3.631	0.845	1.75062	4.084

Detailed HELP Model Annual Water Balance Data for Configuration #1a (Year 2,623):

Simulation	Precip-itation (in/yr)	Runoff (in/yr)	Evapotrans-piration (in/yr)	Lateral Drainage (in/yr)	Infiltration thru GCL (in/yr)	Change in Water Storage (in/yr)
1	40.07	0.000	31.634	0.194	3.78143	8.241
2	57.14	2.817	35.432	2.688	12.39841	8.238
3	52.64	4.626	31.891	2.777	12.41581	0.931
4	47.88	1.040	38.395	1.827	11.46492	-5.755
5	50.57	0.000	34.325	1.073	11.23743	4.842
6	42.28	0.000	27.928	1.758	11.99062	0.499
7	39.35	1.175	31.150	2.288	12.13086	-7.593
8	49.46	0.627	31.905	1.935	12.05772	3.241
9	48.59	0.000	33.520	1.662	12.41581	0.992
10	53.97	4.171	34.945	1.878	12.18205	0.782
11	57.63	9.335	32.898	2.281	12.35354	0.705
12	46.71	1.269	30.329	2.772	12.44982	-0.041
13	38.58	0.000	30.330	0.993	9.37878	-2.304
14	41.49	1.208	28.611	1.603	10.62567	-1.815
15	44.94	1.079	32.483	1.361	11.96268	-0.959
16	54.78	2.900	32.803	2.309	12.39654	4.824
17	29.81	0.215	22.410	1.676	10.04378	-6.374
18	49.55	0.000	34.754	0.816	10.71492	5.102
19	55.50	5.358	34.661	2.656	12.41581	0.412
20	68.56	9.966	38.490	3.100	12.44982	4.554
21	51.14	3.773	34.907	2.592	12.41581	-2.547
22	51.22	0.000	36.613	2.138	12.41581	0.053
23	47.94	4.231	36.824	1.959	11.30334	-7.417
24	59.17	4.974	32.060	2.293	11.82462	9.058
25	47.73	3.584	31.190	2.401	12.41581	-1.861
26	50.56	2.305	31.871	2.252	12.26855	1.859
27	37.02	0.000	32.036	1.413	9.80994	-8.096
28	56.03	3.105	38.082	2.386	12.06981	2.249
29	39.77	0.000	29.442	0.870	9.10912	-0.852
30	46.55	0.387	33.836	0.944	11.43581	0.598
31	39.45	0.538	29.847	1.741	10.58583	-4.264
32	45.35	0.430	29.705	1.563	11.26995	3.566
33	42.23	0.000	31.902	0.440	7.73873	1.952
34	37.81	0.000	27.418	1.524	10.65947	-2.736
35	48.19	0.283	34.240	1.532	12.24051	1.404
36	62.28	5.525	34.675	2.485	12.44982	7.145

Detailed HELP Model Annual Water Balance Data for Configuration #1a (Year 2,623) –
Continued:

Simulation	Precip-itation (in/yr)	Runoff (in/yr)	Evapotrans-piration (in/yr)	Lateral Drainage (in/yr)	Infiltration thru GCL (in/yr)	Change in Water Storage (in/yr)
37	55.96	1.978	42.089	2.560	12.35712	-3.097
38	40.26	0.000	28.432	1.898	11.97591	-2.259
39	60.02	7.103	35.767	2.470	12.41581	2.549
40	59.62	3.794	38.202	2.959	12.44982	2.215
41	47.60	3.396	31.708	2.349	12.41581	-2.269
42	50.44	0.517	34.557	2.584	12.41581	0.365
43	39.42	0.129	26.506	1.936	11.71783	-1.578
44	48.61	0.000	34.373	1.842	12.10824	0.680
45	57.35	9.112	37.768	2.698	12.41581	-4.330
46	47.49	0.000	31.991	0.993	9.46737	5.023
47	38.98	0.000	31.659	1.568	10.41059	-6.240
48	42.99	0.000	32.607	0.522	8.91232	1.620
49	53.01	1.748	34.151	1.249	12.24587	4.487
50	55.17	1.588	38.835	2.422	12.41581	-0.037
51	46.16	0.465	32.168	1.807	11.11002	-0.130
52	42.63	0.000	34.535	2.036	11.64013	-5.632
53	50.93	0.000	32.394	2.345	12.18456	4.796
54	54.24	6.205	29.833	2.622	12.41581	3.164
55	50.46	1.662	33.550	2.299	12.41581	0.533
56	56.39	4.939	41.245	2.813	12.44982	-5.057
57	41.99	0.000	28.741	1.585	12.37105	-0.751
58	68.60	12.134	36.077	2.998	12.40878	5.027
59	48.67	2.975	34.623	2.042	11.40184	-3.351
60	58.12	2.644	36.983	2.854	12.44982	4.169
61	54.90	10.680	31.970	2.137	11.67622	-1.704
62	56.29	7.168	35.006	2.920	12.41581	-1.080
63	49.13	0.507	36.193	2.537	12.41581	-2.523
64	54.54	2.510	32.839	2.506	12.44982	4.235
65	45.05	1.357	32.868	2.124	12.41581	-3.714
66	37.07	0.000	29.767	1.156	9.29780	-4.985
67	40.17	0.000	24.981	0.856	9.13394	5.891
68	58.08	6.149	36.093	2.705	12.44982	1.826
69	36.31	0.000	27.019	1.581	11.72174	-4.286
70	42.67	1.084	32.473	1.566	11.08400	-4.286
71	48.88	0.000	35.391	1.088	9.35494	2.607
72	47.36	0.796	34.233	2.070	12.11035	-0.386
73	35.81	0.000	26.521	1.038	8.85234	-2.882
74	49.81	0.740	29.738	1.551	10.72384	9.338

Detailed HELP Model Annual Water Balance Data for Configuration #1a (Year 2,623) – Continued:

Simulation	Precip-itation (in/yr)	Runoff (in/yr)	Evapotrans-piration (in/yr)	Lateral Drainage (in/yr)	Infiltration thru GCL (in/yr)	Change in Water Storage (in/yr)
75	56.43	5.739	36.139	2.689	12.41581	-0.552
76	45.86	1.447	32.856	2.274	12.44982	-3.167
77	56.76	1.198	40.388	2.314	12.41581	0.445
78	39.15	0.000	29.580	1.416	9.68895	-3.379
79	48.87	0.157	31.453	1.714	10.55745	5.706
80	58.52	9.554	35.422	2.701	12.44982	-0.479
81	53.34	0.000	36.405	2.325	12.41581	2.194
82	55.18	3.918	36.127	2.477	12.41581	0.243
83	53.60	10.623	35.238	2.278	11.78840	-6.994
84	47.82	0.000	34.212	1.527	11.18274	1.232
85	44.69	0.000	30.782	0.577	8.90625	4.698
86	60.77	9.749	37.383	2.554	12.41503	-1.273
87	48.34	1.266	29.581	1.829	11.40196	4.255
88	36.18	5.790	27.031	1.878	10.76264	-10.725
89	58.29	4.596	36.471	1.536	8.66518	8.471
90	60.08	12.332	31.033	2.649	12.41581	1.650
91	55.49	4.696	35.891	2.965	12.41581	-0.478
92	44.51	0.249	32.134	2.292	12.21529	-2.506
93	35.83	0.000	29.694	1.294	10.48303	-6.080
94	45.02	0.000	32.740	0.565	9.84076	1.947
95	44.54	3.488	28.485	2.096	11.81794	-1.304
96	53.18	0.193	36.711	1.669	11.51701	2.781
97	48.03	0.431	32.666	2.089	12.41581	1.187
98	62.58	1.252	42.186	2.297	12.41581	4.429
99	48.78	5.682	31.752	2.724	12.41581	-3.794
100	49.29	0.022	35.746	1.308	11.79714	-0.205
Summary Statistics						
Count	100	100	100	100	100	100
Maximum	68.60	12.332	42.186	3.100	12.44982	9.338
Average	49.14	2.487	33.155	1.955	11.47235	0.149
Median	48.83	1.130	32.848	2.056	12.10929	0.304
Minimum	29.81	0.000	22.410	0.194	3.78143	-10.725
Std Dev	7.69	3.202	3.633	0.665	1.39234	4.097

Detailed HELP Model Annual Water Balance Data for Configuration #1a (Year 3,200):

Simulation	Precip-itation (in/yr)	Runoff (in/yr)	Evapotrans-piration (in/yr)	Lateral Drainage (in/yr)	Infiltration thru GCL (in/yr)	Change in Water Storage (in/yr)
1	40.07	0.000	31.626	0.172	3.99192	8.271
2	57.14	2.678	35.389	2.677	12.40871	8.211
3	52.64	4.649	31.899	2.771	12.41581	0.905
4	47.88	1.053	38.376	1.817	11.61116	-5.810
5	50.57	0.000	34.315	0.983	11.35212	4.752
6	42.28	0.000	27.894	1.706	12.08741	0.508
7	39.35	1.000	31.144	2.287	12.23107	-7.416
8	49.46	0.635	31.807	1.914	12.09888	3.193
9	48.59	0.000	33.497	1.657	12.41581	1.020
10	53.97	4.191	34.943	1.854	12.31419	0.660
11	57.63	9.245	32.863	2.270	12.41285	0.842
12	46.71	1.240	30.348	2.765	12.44982	-0.090
13	38.58	0.000	30.328	0.964	9.53773	-2.397
14	41.49	1.082	28.601	1.576	10.73595	-1.767
15	44.94	1.088	32.409	1.305	12.09773	-0.893
16	54.78	2.827	32.788	2.291	12.40146	4.814
17	29.81	0.214	22.405	1.663	10.10705	-6.447
18	49.55	0.000	34.771	0.738	10.86171	5.048
19	55.50	5.192	34.701	2.647	12.41581	0.545
20	68.56	10.004	38.463	3.093	12.44982	4.550
21	51.14	3.774	34.915	2.584	12.41581	-2.548
22	51.22	0.000	36.740	2.105	12.41581	-0.041
23	47.94	4.149	36.784	1.943	11.43177	-7.345
24	59.17	4.953	31.995	2.282	11.83920	9.078
25	47.73	3.594	31.177	2.395	12.41581	-1.852
26	50.56	2.313	31.926	2.227	12.33302	1.758
27	37.02	0.000	31.922	1.392	9.89264	-8.078
28	56.03	3.055	38.034	2.376	12.10924	2.350
29	39.77	0.000	29.424	0.849	9.30616	-0.932
30	46.55	0.400	33.794	0.876	11.57213	0.564
31	39.45	0.379	29.855	1.713	10.64808	-4.242
32	45.35	0.418	29.639	1.520	11.44797	3.620
33	42.23	0.000	31.877	0.381	7.83118	1.836
34	37.81	0.000	27.490	1.474	10.64290	-2.793
35	48.19	0.270	34.206	1.474	12.25883	1.549
36	62.28	5.524	34.644	2.478	12.44982	7.184

Detailed HELP Model Annual Water Balance Data for Configuration #1a (Year 3,200) – Continued:

Simulation	Precip-itation (in/yr)	Runoff (in/yr)	Evapotrans-piration (in/yr)	Lateral Drainage (in/yr)	Infiltration thru GCL (in/yr)	Change in Water Storage (in/yr)
37	55.96	1.985	42.076	2.552	12.41226	-3.070
38	40.26	0.000	28.393	1.884	12.10670	-2.316
39	60.02	7.005	35.781	2.453	12.41581	2.563
40	59.62	3.809	38.179	2.951	12.44982	2.231
41	47.60	3.399	31.727	2.339	12.41581	-2.281
42	50.44	0.528	34.520	2.582	12.41581	0.394
43	39.42	0.135	26.492	1.931	11.88237	-1.617
44	48.61	0.000	34.279	1.815	12.22671	0.682
45	57.35	9.073	37.675	2.687	12.41581	-4.297
46	47.49	0.000	31.989	0.944	9.62691	4.914
47	38.98	0.000	31.648	1.530	10.43933	-6.246
48	42.99	0.000	32.636	0.468	9.01893	1.589
49	53.01	1.760	34.177	1.153	12.34454	4.460
50	55.17	1.427	38.838	2.399	12.41581	0.111
51	46.16	0.455	32.179	1.788	11.23072	-0.183
52	42.63	0.000	34.470	1.998	11.75228	-5.611
53	50.93	0.000	32.395	2.305	12.19512	4.746
54	54.24	5.954	29.999	2.609	12.41581	3.261
55	50.46	1.677	33.567	2.284	12.41581	0.516
56	56.39	4.936	41.208	2.806	12.44982	-5.009
57	41.99	0.000	28.760	1.588	12.41581	-0.774
58	68.60	12.135	36.048	2.983	12.41581	5.018
59	48.67	2.976	34.593	2.036	11.51746	-3.366
60	58.12	2.598	36.952	2.848	12.44982	4.184
61	54.90	10.685	31.970	2.119	11.82171	-1.785
62	56.29	7.057	34.996	2.912	12.41581	-1.000
63	49.13	0.482	36.192	2.535	12.41581	-2.494
64	54.54	2.658	32.715	2.507	12.44982	4.210
65	45.05	1.360	32.919	2.105	12.41581	-3.749
66	37.07	0.000	29.716	1.133	9.39335	-5.045
67	40.17	0.000	24.965	0.803	9.21723	5.835
68	58.08	6.089	36.092	2.694	12.44982	1.977
69	36.31	0.000	27.014	1.556	11.87818	-4.343
70	42.67	1.097	32.399	1.539	11.15940	-4.338
71	48.88	0.000	35.398	1.039	9.36065	2.598
72	47.36	0.713	34.210	2.056	12.14007	-0.255
73	35.81	0.000	26.514	1.020	8.92312	-2.972
74	49.81	0.732	29.709	1.540	10.73478	9.420

Detailed HELP Model Annual Water Balance Data for Configuration #1a (Year 3,200) – Continued:

Simulation	Precip-itation (in/yr)	Runoff (in/yr)	Evapotrans-piration (in/yr)	Lateral Drainage (in/yr)	Infiltration thru GCL (in/yr)	Change in Water Storage (in/yr)
75	56.43	5.801	36.111	2.677	12.41581	-0.575
76	45.86	1.437	32.830	2.272	12.44982	-3.129
77	56.76	1.226	40.378	2.311	12.41581	0.430
78	39.15	0.000	29.584	1.402	9.79704	-3.474
79	48.87	0.040	31.505	1.683	10.65599	5.669
80	58.52	9.473	35.338	2.705	12.44982	-0.286
81	53.34	0.000	36.444	2.336	12.41581	2.144
82	55.18	3.942	36.081	2.485	12.41581	0.257
83	53.60	10.673	35.255	2.259	11.87562	-7.047
84	47.82	0.000	34.242	1.472	11.24721	1.123
85	44.69	0.000	30.790	0.510	9.00359	4.661
86	60.77	9.590	37.227	2.566	12.41581	-0.984
87	48.34	1.152	29.607	1.846	11.58458	4.145
88	36.18	5.805	27.018	1.867	10.84968	-10.797
89	58.29	4.532	36.474	1.503	8.69155	8.533
90	60.08	12.358	31.017	2.643	12.41581	1.646
91	55.49	4.734	35.855	2.963	12.41581	-0.478
92	44.51	0.250	32.230	2.267	12.26783	-2.607
93	35.83	0.000	29.693	1.244	10.53893	-6.055
94	45.02	0.000	32.777	0.492	9.90859	1.861
95	44.54	3.339	28.481	2.077	11.91837	-1.119
96	53.18	0.186	36.592	1.650	11.66649	2.766
97	48.03	0.440	32.587	2.065	12.41581	1.179
98	62.58	1.272	42.143	2.297	12.41581	4.452
99	48.78	5.716	31.736	2.716	12.41581	-3.803
100	49.29	0.033	35.802	1.288	11.89609	-0.297
Summary Statistics						
Count	100	100	100	100	100	100
Maximum	68.60	12.358	42.143	3.093	12.44982	9.420
Average	49.14	2.467	33.142	1.933	11.52987	0.148
Median	48.83	1.085	32.809	2.046	12.16759	0.326
Minimum	29.81	0.000	22.405	0.172	3.99192	-10.797
Std Dev	7.69	3.193	3.625	0.680	1.36112	4.097

Detailed HELP Model Annual Water Balance Data for Configuration #1a (Year 5,600):

Simulation	Precip- itation (in/yr)	Runoff (in/yr)	Evapotrans- piration (in/yr)	Lateral Drainage (in/yr)	Infiltration thru GCL (in/yr)	Change in Water Storage (in/yr)
1	40.07	0.000	31.577	0.137	4.37716	8.354
2	57.14	2.508	35.324	2.647	12.41581	8.083
3	52.64	4.701	31.882	2.748	12.41581	0.893
4	47.88	1.111	38.346	1.746	11.84340	-5.873
5	50.57	0.000	34.231	0.841	11.59087	4.614
6	42.28	0.000	27.804	1.630	12.31108	0.496
7	39.35	0.884	31.224	2.204	12.32606	-7.335
8	49.46	0.616	31.633	1.857	12.16877	3.273
9	48.59	0.000	33.538	1.620	12.41581	1.016
10	53.97	4.189	34.829	1.832	12.41581	0.704
11	57.63	9.328	32.781	2.268	12.41581	0.837
12	46.71	1.260	30.250	2.747	12.44982	0.003
13	38.58	0.000	30.333	0.919	9.93707	-2.708
14	41.49	0.719	28.760	1.515	10.87559	-1.682
15	44.94	1.131	32.585	1.147	12.13645	-0.946
16	54.78	2.811	32.911	2.160	12.39281	4.791
17	29.81	0.046	22.344	1.622	10.19335	-6.347
18	49.55	0.000	34.766	0.584	11.19914	4.951
19	55.50	5.154	34.588	2.613	12.41581	0.728
20	68.56	10.109	38.393	3.054	12.44982	4.555
21	51.14	3.780	34.836	2.571	12.41581	-2.463
22	51.22	0.000	36.693	2.124	12.41581	-0.013
23	47.94	4.267	36.789	1.914	11.60778	-7.504
24	59.17	4.905	31.908	2.251	11.84577	9.126
25	47.73	3.655	31.083	2.381	12.41581	-1.805
26	50.56	2.363	31.765	2.236	12.41581	1.780
27	37.02	0.000	31.832	1.413	10.05933	-8.256
28	56.03	2.970	37.974	2.337	12.22256	2.499
29	39.77	0.000	29.400	0.800	9.67356	-1.103
30	46.55	0.355	33.689	0.756	11.88519	0.556
31	39.45	0.202	29.752	1.645	10.73390	-4.182
32	45.35	0.360	29.555	1.481	11.71095	3.797
33	42.23	0.000	31.862	0.278	8.00465	1.535
34	37.81	0.000	27.448	1.405	10.65138	-2.758
35	48.19	0.213	34.311	1.387	12.29342	1.655
36	62.28	5.519	34.622	2.442	12.44982	7.247

Detailed HELP Model Annual Water Balance Data for Configuration #1a (Year 5,600) – Continued:

Simulation	Precip- itation (in/yr)	Runoff (in/yr)	Evapotrans- piration (in/yr)	Lateral Drainage (in/yr)	Infiltration thru GCL (in/yr)	Change in Water Storage (in/yr)
37	55.96	2.026	42.063	2.510	12.41581	-3.054
38	40.26	0.000	28.287	1.880	12.33160	-2.295
39	60.02	6.907	35.759	2.420	12.41581	2.574
40	59.62	3.942	38.119	2.924	12.44982	2.185
41	47.60	3.411	31.752	2.306	12.41581	-2.284
42	50.44	0.586	34.480	2.563	12.41581	0.395
43	39.42	0.141	26.326	1.932	12.20079	-1.460
44	48.61	0.000	34.145	1.766	12.44721	0.531
45	57.35	8.857	37.676	2.643	12.41581	-4.241
46	47.49	0.000	31.984	0.862	9.86137	4.760
47	38.98	0.000	31.656	1.468	10.45028	-6.299
48	42.99	0.000	32.677	0.379	9.27328	1.592
49	53.01	1.818	34.151	1.013	12.41581	4.409
50	55.17	1.287	38.798	2.365	12.41581	0.304
51	46.16	0.461	32.117	1.755	11.43550	-0.227
52	42.63	0.000	34.375	1.941	12.00302	-5.552
53	50.93	0.000	32.440	2.215	12.20332	4.553
54	54.24	5.881	29.952	2.553	12.41581	3.438
55	50.46	1.736	33.477	2.281	12.41581	0.551
56	56.39	5.044	41.175	2.769	12.44982	-5.048
57	41.99	0.000	28.721	1.580	12.41581	-0.727
58	68.60	12.167	36.110	2.931	12.41581	4.976
59	48.67	3.047	34.616	1.974	11.59704	-3.445
60	58.12	2.572	36.901	2.817	12.44982	4.262
61	54.90	10.701	31.941	2.072	12.01771	-1.893
62	56.29	7.001	35.028	2.871	12.41581	-0.963
63	49.13	0.369	36.173	2.513	12.41581	-2.340
64	54.54	2.704	32.743	2.496	12.44982	4.147
65	45.05	1.385	32.858	2.083	12.41581	-3.691
66	37.07	0.000	29.714	1.107	9.51609	-5.274
67	40.17	0.000	24.943	0.701	9.35903	5.785
68	58.08	6.076	36.110	2.649	12.44982	2.185
69	36.31	0.000	26.991	1.495	12.17454	-4.450
70	42.67	1.154	31.991	1.482	11.44523	-4.182
71	48.88	0.000	35.481	0.939	9.47500	2.356
72	47.36	0.647	33.972	1.986	12.29701	-0.033
73	35.81	0.000	26.427	0.992	9.07226	-3.020
74	49.81	0.825	29.782	1.448	10.74475	9.350

Detailed HELP Model Annual Water Balance Data for Configuration #1a (Year 5,600) – Continued:

Simulation	Precip-itation (in/yr)	Runoff (in/yr)	Evapotrans-piration (in/yr)	Lateral Drainage (in/yr)	Infiltration thru GCL (in/yr)	Change in Water Storage (in/yr)
75	56.43	5.858	35.960	2.645	12.41581	-0.448
76	45.86	1.482	32.588	2.303	12.44982	-2.963
77	56.76	1.419	40.372	2.311	12.41581	0.242
78	39.15	0.000	29.579	1.368	10.02419	-3.610
79	48.87	0.000	31.166	1.588	11.09333	5.765
80	58.52	9.359	35.237	2.680	12.44982	-0.160
81	53.34	0.000	36.428	2.349	12.41581	2.147
82	55.18	4.060	36.220	2.404	12.41581	0.080
83	53.60	10.555	35.128	2.269	12.17725	-6.768
84	47.82	0.000	34.284	1.378	11.40203	0.732
85	44.69	0.000	30.825	0.398	9.08909	4.615
86	60.77	9.385	37.325	2.494	12.41581	-0.824
87	48.34	1.226	29.602	1.770	11.76041	3.978
88	36.18	5.587	26.966	1.831	10.97316	-10.623
89	58.29	4.477	36.373	1.443	8.85319	8.593
90	60.08	12.467	30.944	2.612	12.41581	1.641
91	55.49	4.805	35.817	2.929	12.41581	-0.477
92	44.51	0.261	32.282	2.223	12.39729	-2.685
93	35.83	0.000	29.674	1.165	10.66686	-5.994
94	45.02	0.000	32.633	0.404	10.17120	1.809
95	44.54	3.126	28.446	2.040	12.12681	-0.973
96	53.18	0.129	36.594	1.589	11.77700	2.643
97	48.03	0.487	32.404	2.024	12.41581	1.274
98	62.58	1.374	42.150	2.262	12.41581	4.379
99	48.78	5.749	31.733	2.686	12.41581	-3.805
100	49.29	0.086	35.659	1.305	12.11939	-0.227
Summary Statistics						
Count	100	100	100	100	100	100
Maximum	68.60	12.467	42.150	3.054	12.44982	9.350
Average	49.14	2.458	33.099	1.885	11.63212	0.147
Median	48.83	1.121	32.762	1.980	12.30404	0.273
Minimum	29.81	0.000	22.344	0.137	4.37716	-10.623
Std Dev	7.69	3.189	3.633	0.699	1.29806	4.085

Detailed HELP Model Annual Water Balance Data for Configuration #1a (Year 10,000):

Simulation	Precip-itation (in/yr)	Runoff (in/yr)	Evapotrans-piration (in/yr)	Lateral Drainage (in/yr)	Infiltration thru GCL (in/yr)	Change in Water Storage (in/yr)
1	40.07	0.000	31.579	0.114	4.52665	8.374
2	57.14	2.667	35.133	2.601	12.41581	8.014
3	52.64	4.913	31.729	2.713	12.41581	0.869
4	47.88	1.152	38.303	1.742	11.93695	-5.904
5	50.57	0.000	34.199	0.810	11.50687	4.703
6	42.28	0.000	27.657	1.656	12.41581	0.551
7	39.35	1.134	31.182	2.155	12.35988	-7.539
8	49.46	0.858	31.510	1.801	12.13932	3.211
9	48.59	0.000	33.483	1.548	12.41581	1.144
10	53.97	4.272	34.696	1.808	12.41581	0.778
11	57.63	9.589	32.888	2.118	12.41581	0.619
12	46.71	1.204	30.033	2.717	12.44982	0.306
13	38.58	0.000	30.373	0.927	10.16174	-2.951
14	41.49	0.693	28.694	1.469	10.89890	-1.637
15	44.94	1.208	32.421	1.121	12.28664	-0.781
16	54.78	2.863	32.894	2.110	12.39883	4.640
17	29.81	0.094	22.294	1.587	10.16003	-6.377
18	49.55	0.020	34.887	0.521	11.27135	4.901
19	55.50	5.245	34.492	2.573	12.41581	0.774
20	68.56	10.183	38.395	2.982	12.44982	4.550
21	51.14	3.792	34.749	2.534	12.41581	-2.350
22	51.22	0.049	36.690	2.115	12.41581	-0.050
23	47.94	4.361	36.731	1.887	11.71781	-7.511
24	59.17	5.165	31.654	2.212	11.82792	9.066
25	47.73	3.781	31.004	2.342	12.41581	-1.812
26	50.56	2.370	31.696	2.193	12.41581	1.885
27	37.02	0.000	32.076	1.337	9.86573	-8.416
28	56.03	3.179	37.816	2.301	12.25005	2.642
29	39.77	0.000	29.394	0.766	9.80424	-1.176
30	46.55	0.252	33.718	0.716	12.08162	0.516
31	39.45	0.308	29.542	1.584	10.71649	-4.135
32	45.35	0.288	29.499	1.479	11.80642	3.961
33	42.23	0.000	31.889	0.229	8.14115	1.302
34	37.81	0.000	27.223	1.386	10.66805	-2.522
35	48.19	0.199	34.215	1.452	12.33144	1.716
36	62.28	5.751	34.695	2.383	12.44982	7.001

Detailed HELP Model Annual Water Balance Data for Configuration #1a (Year 10,000) – Continued:

Simulation	Precip-itation (in/yr)	Runoff (in/yr)	Evapotrans-piration (in/yr)	Lateral Drainage (in/yr)	Infiltration thru GCL (in/yr)	Change in Water Storage (in/yr)
37	55.96	2.059	41.837	2.482	12.41581	-2.834
38	40.26	0.000	28.305	1.899	12.41567	-2.360
39	60.02	6.919	35.769	2.391	12.41581	2.525
40	59.62	4.163	38.056	2.871	12.44982	2.081
41	47.60	3.431	31.730	2.254	12.41581	-2.231
42	50.44	0.752	34.456	2.519	12.41581	0.297
43	39.42	0.060	26.395	1.869	12.19359	-1.402
44	48.61	0.000	34.086	1.757	12.44982	0.622
45	57.35	9.114	37.475	2.595	12.41581	-4.250
46	47.49	0.000	31.988	0.806	9.92257	4.740
47	38.98	0.000	31.664	1.445	10.55421	-6.329
48	42.99	0.000	32.672	0.332	9.40345	1.601
49	53.01	1.921	34.182	0.914	12.41581	4.240
50	55.17	1.295	38.564	2.355	12.41581	0.540
51	46.16	0.588	32.041	1.725	11.47594	-0.330
52	42.63	0.000	34.309	1.922	12.19758	-5.402
53	50.93	0.000	32.259	2.204	12.18703	4.542
54	54.24	6.159	29.868	2.517	12.41581	3.280
55	50.46	1.839	33.427	2.229	12.41581	0.550
56	56.39	5.157	41.054	2.708	12.44982	-4.979
57	41.99	0.000	28.704	1.553	12.41581	-0.683
58	68.60	12.535	35.919	2.864	12.41581	4.866
59	48.67	3.178	34.592	1.898	11.50684	-3.492
60	58.12	2.810	36.774	2.767	12.44982	4.305
61	54.90	10.735	31.912	1.999	12.07065	-1.874
62	56.29	7.159	35.124	2.796	12.41581	-1.146
63	49.13	0.260	36.049	2.469	12.41581	-2.064
64	54.54	2.994	32.532	2.460	12.44982	4.104
65	45.05	1.551	32.894	2.006	12.41581	-3.817
66	37.07	0.000	29.586	1.030	9.65530	-5.335
67	40.17	0.000	24.986	0.652	9.27465	5.877
68	58.08	6.198	35.889	2.641	12.44982	2.416
69	36.31	0.000	26.771	1.568	12.41565	-4.445
70	42.67	1.257	32.062	1.423	11.39086	-4.542
71	48.88	0.000	35.449	0.878	9.44645	2.470
72	47.36	0.792	33.899	1.961	12.35477	0.068
73	35.81	0.000	26.499	0.962	8.99181	-3.157
74	49.81	0.789	29.958	1.408	10.73139	9.438

Detailed HELP Model Annual Water Balance Data for Configuration #1a (Year 10,000) –
Continued:

Simulation	Precip-itation (in/yr)	Runoff (in/yr)	Evapotrans-piration (in/yr)	Lateral Drainage (in/yr)	Infiltration thru GCL (in/yr)	Change in Water Storage (in/yr)
75	56.43	6.096	35.693	2.604	12.41581	-0.379
76	45.86	1.577	32.668	2.258	12.44982	-3.092
77	56.76	1.295	40.303	2.285	12.41581	0.461
78	39.15	0.000	29.501	1.390	10.40285	-3.736
79	48.87	0.000	31.275	1.509	10.92852	5.561
80	58.52	9.383	35.096	2.641	12.44982	0.139
81	53.34	0.000	36.396	2.353	12.41581	2.175
82	55.18	4.250	36.175	2.356	12.41581	-0.016
83	53.60	10.555	35.126	2.214	12.27768	-6.708
84	47.82	0.000	34.041	1.371	11.76273	0.630
85	44.69	0.000	30.616	0.344	9.28389	4.575
86	60.77	9.411	37.245	2.445	12.41581	-0.724
87	48.34	1.374	29.607	1.727	11.92180	3.708
88	36.18	5.428	26.879	1.779	10.99995	-10.390
89	58.29	4.786	36.221	1.402	8.82675	8.540
90	60.08	12.458	31.028	2.545	12.41581	1.633
91	55.49	5.006	35.682	2.862	12.41581	-0.475
92	44.51	0.398	32.217	2.159	12.43193	-2.706
93	35.83	0.000	29.662	1.112	10.67820	-5.868
94	45.02	0.000	32.476	0.382	10.36816	1.874
95	44.54	3.108	28.370	1.994	12.24051	-1.051
96	53.18	0.023	36.340	1.621	12.15207	2.910
97	48.03	0.569	32.280	1.966	12.41581	0.987
98	62.58	1.508	42.120	2.207	12.41581	4.330
99	48.78	5.885	31.720	2.611	12.41581	-3.853
100	49.29	0.189	35.478	1.247	12.22508	-0.062
Summary Statistics						
Count	100	100	100	100	100	100
Maximum	68.60	12.535	42.120	2.982	12.44982	9.438
Average	49.14	2.526	33.034	1.845	11.67048	0.147
Median	48.83	1.178	32.780	1.942	12.37935	0.384
Minimum	29.81	0.000	22.294	0.114	4.52665	-10.390
Std Dev	7.69	3.233	3.612	0.695	1.27988	4.076

APPENDIX L.
DETAILED PROBABILITY BASED ROOT PENETRATION MODEL

This page intentionally left blank.

F-Area Tank Farm Closure Cap
Probability Model of Pine Tree Tap Root
Penetrations of the HDPE Geomembrane (U)

E.P. Shine

September 11, 2007

Computational and Statistical Sciences
Savannah River National Laboratory
Aiken, SC 29808

SRNL
SAVANNAH RIVER NATIONAL LABORATORY

DISCLAIMER

Reviews and Approvals

Author

E.P. Shine   9-11-2007

E.P. Shine, Statistical Consulting Section

Technical Reviewer

Thomas B Edwards   9-12-07

T.B. Edwards, Statistical Consulting Section

Approver

                   9-17-07

T.A. Nance, Manager, Statistical Consulting Section

This page left intentionally blank.

Table of Contents

List of Figures

List of Tables

List of Abbreviations

cm   centimeter

GCL   Geosynthetic clay liner

HDPE   High-density polyethylene – description of the geomembrane in the multi-
                    layered closure cap

sec   second

SRS   Savannah River Site

Executive Summary

The F-Area Tank Farm stores effluent waste streams at the Savannah River Site (SRS), near Aiken, SC. Once its mission is complete and the tanks are in their final configuration, the area will be covered with a multi-layer closure cap to minimize infiltration. The top of the cap will consist of six feet of soil. Below the soil is a high density polyethylene (HDPE) geomembrane over a geosynthetic clay liner (GCL). The GCL plugs holes in the overlying HDPE geomembrane. The HDPE geomembrane is a protective barrier that deflects roots before they can pierce the GCL. Cracks will materialize in the HDPE geomembrane over time, making it and the GCL locally vulnerable to root penetration. A moisture conduit is assumed to form in the GCL whenever a pine tree tap root encounters and penetrates a crack in the HDPE geomembrane, and then atrophies upon death, leaving a path for moisture.

This technical report documents a discrete event simulation that was used to compute a profile of the number of moisture conduits in the HDPE geomembrane over 10,000 years. Three modes of root penetration have been identified and built into the computational algorithm. These modes are as follows.

1. A pine tree tap root in its downward vertical growth phase strikes a crack on first contact with the HDPE geomembrane.
2. A new crack materializes under the growth tip of a tap root that is growing along the surface of the HDPE geomembrane.
3. A root in its horizontal growth phase enters a pre-existing crack while growing along the surface of the HDPE geomembrane.

Nearly all of the roots that penetrate cracks do so by the third mode. This occurs because the area lying in the pathway of tap roots growing on the surface of the HDPE geomembrane is much larger than the area of a crack.

The mean number of moisture conduits in the HDPE geomembrane and the GCL reaches 2,272 per acre after 10,000 years. The largest observed deviation from this mean was less than 5% in 33 simulation runs. The low 2,168 and high 2,339 numbers of dead roots in cracks per acre over the simulation runs represent a two-sided 90% confidence nonparametric tolerance interval covering 88.7% of the distribution.

The mean time between formation of moisture conduits in the GCL decreases over time with about 11.8, 4.4, and 2.4 years between formations after about 2,000, 5,000, and 10,000 years due to ever increasing numbers of cracks per acre. However, the percent of available cracks that are transformed into moisture conduits by tap root penetration stabilizes to approximately 0.45% per century.

The mean results for selected years are summarized in Table 5.1. Complete results at the time of every arrival event are provided in the Microsoft® Excel formatted file, Shine [2007].

This page left intentionally blank.

1 Introduction

The F-Area Tank Farm, located at the Savannah River Site (SRS) near Aiken, SC, receives effluent from various facilities at the site. The SRS Liquid Waste Organization (LWO) is tasked with waste stabilization and removal, and closure of the tanks. After the LWO completes its mission in the F-Area Tank Farm, and the tanks are in their final configuration, the area will be covered with a closure cap that inhibits infiltration.

The closure cap will be constructed from a multi-layer design that includes six feet of soil on top of a high density polyethylene (HDPE) geomembrane which, in turn, is placed over a geosynthetic clay liner (GCL). The HDPE geomembrane limits infiltration, and when cracks begin to develop, the GCL plugs holes in the geomembrane.

The closure cap is expected to be actively managed for the first one hundred years of its existence. Thereafter, the site is susceptible to pine tree inhabitation. Once a pine tap root penetrates a crack in the geomembrane, it also penetrates the GCL below the crack. The root will begin to atrophy upon death of the tree, leaving a moisture conduit through the HDPE geomembrane and the GCL.

This report documents an investigation to determine the number of pine tap roots per acre that are expected to penetrate cracks in the HDPE geomembrane over a 10,000 year period following cessation of active maintenance of the clay cap. An overarching model, Phifer, et. al. [2007], will fuse inputs from this report and other information in order to study the performance of the closure cap.

The objective of this study is the determination of the number of moisture channels opened through the HDPE geomembrane and the GCL over time. One moisture channel is recorded for each crack penetrated by a tap root upon the death of the tree (root).

2 Probability model assumptions

The probability model is based on a number of assumptions. The assumptions are organized according to the growth characteristics of a pine tree, the pine tree inhabitation process, the characteristics of the HDPE geomembrane and the GCL, and tap root interaction with the HDPE geomembrane and the GCL. All assumptions regarding pine trees, tap roots, the inhabitation process, and the tap root interaction with the HDPE geomembrane and the GCL were provided by Nelson, E.A. [2007].

2.1 Growth characteristics of a pine tree

Pine trees live approximately 100 years, attaining maturity after 40 years. Pine trees have five tap roots. One tap root has potential to extend downward about 12 feet, and the other four tap roots have potential to extend downward about 6 feet. The growth stages of a pine tap root are illustrated in Figure 2.1. A tap root will grow vertically downward, not drawn by moisture or nutrients, until it hits an obstruction. After thirty years it reaches a depth of six feet and atrophies over approximately a thirty-year period following the death of the tree. This is much longer than the atrophic process for surface roots due to lower microbial activity at depth.
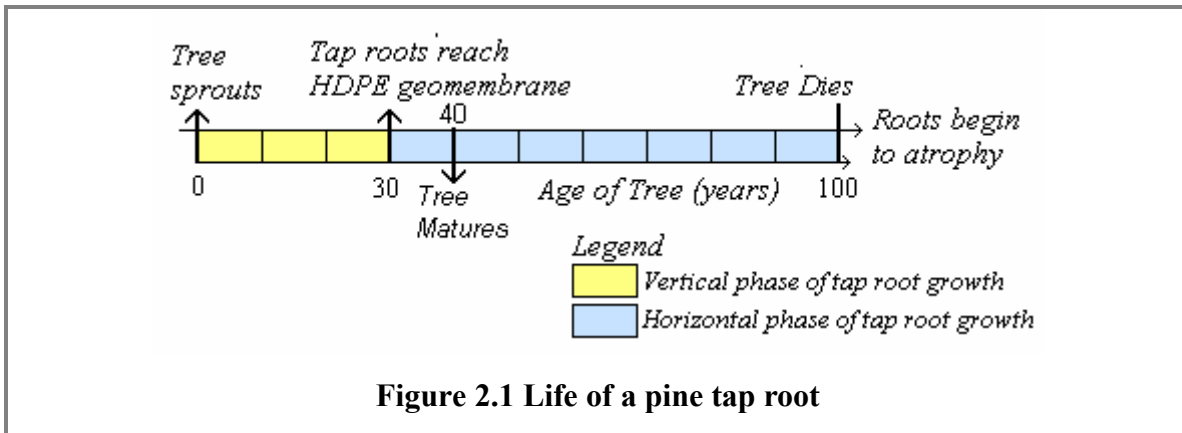

Figure 2.1 Life of a pine tap root

2.2 Pine tree inhabitation process

No pine trees will establish themselves on the closure cap during the period of active maintenance. Once forestation of the closure cap has begun, pine tap roots are assumed to be randomly distributed over its surface. Inhabitation of the closure cap will result in about 400 mature pine trees per acre per century. The times when pine tap roots reach the HDPE geomembrane are discussed in Section 4: Simulation inputs.

2.3 Characteristics of the HDPE geomembrane and the GCL

The surface of the HDPE geomembrane slopes downward at a 2% grade from its highest point and is covered by six feet of soil. The HDPE geomembrane is impregnated with an anti-oxidant

to forestall embrittlement and subsequent crack formation. Cracks appearing over time in the HDPE geomembrane are assumed to be randomly distributed over its surface. Cracks persist, so the total number of cracks is assumed to increase over time. However, the model does not assume that existing cracks expand in size over time. The GCL is assumed to plug all holes in the HDPE geomembrane unless it has been punctured by a tap root. The times at which cracks develop in the HDPE geomembrane are discussed in Section 4: Simulation inputs. This probability model assumes that the area of a crack is 3.1 cm^2.

2.4 Tap root interaction with the HDPE geomembrane and the GCL

Whenever a pine tap root encounters a crack in the HDPE geomembrane, it is assumed to penetrate the HDPE geomembrane and puncture the GCL below the crack. A tap root is assumed to plug a crack preventing water intrusion as long as the tree lives. A second root will not penetrate a crack that has already been plugged by a root. However, the probability model makes the conservative assumption that a conduit for moisture opens immediately upon the death of the tree even though a pine tap root atrophies slowly following the death of the tree.

If a pine tap root encounters a non-cracked region of the HDPE geomembrane during its vertical descent, it will begin to grow along the HDPE surface in the direction of steepest downward slope. As shown in Figure 2.1, this horizontal phase of growth begins when the pine tree is thirty years old. After a 12-foot tap root hits a non-cracked area of the HDPE, it is assumed to grow at a constant rate along the HDPE surface for 6 feet over the next 70-years, i.e., over the remainder of the tree's 100-year life, or until it encounters a crack. After a 6-foot tap root hits a non-cracked area of the HDPE, it is assumed to grow at a constant rate along the HDPE surface for 6 inches over the next 70 years, i.e., over the remainder of the tree's 100-year life, or until it encounters a crack. A crack is assumed sufficiently large to permit at most one tap root to enter.

3 Probability models for penetration of cracks in the HDPE geomembrane

The number of moisture channels per acre through cracks in the HDPE geomembrane is determined by a discrete event simulation algorithm. Each use of the algorithm is called a run. A run provides one possible alternative 10,000 year history for the closure cap site, and will, in general, differ from all other runs based on chance alignments of tap roots with cracks in the HDPE geomembrane. The simulation exercise generated 33 runs.

A single run is based on a series of discrete events. A discrete event can be the arrival of one or more roots at the HDPE geomembrane during their downward vertical growth phase or the materialization of a new crack in the HDPE geomembrane. In either case a probability rule randomly determines whether or not a root has encountered a crack. If so, a penetration of the HDPE geomembrane and the GCL has occurred, and will be recorded as a moisture conduit upon the death of the tree at age 100 years.

Live roots that have not penetrated a crack upon contact with the HDPE geomembrane halt their vertical descent and begin to grow along the HDPE surface. This horizontal growth phase occurs between the discrete arrival events, so the number of roots that grow into pre-existing cracks in the geomembrane must be determined for the time interval between arrival events.

It is assumed that penetration of the HDPE geomembrane results in a puncture of the GCL. In reality, once the tree dies and the tap root atrophies, the puncture becomes an open channel for moisture, although this model conservatively records that a moisture channel is formed immediately upon the death of a tree. Figure 3.1 illustrates a potential sequence of events. The horizontal axis is an event calendar. Two types of events are recognized: (1) a new crack forms in the HDPE geomembrane or (2) new roots encounter the HDPE geomembrane on their vertical descent. In either case, the crack or roots are added to the inventory of total cracks and live roots, respectively.

Figure 3.1 A sequence of arrival events
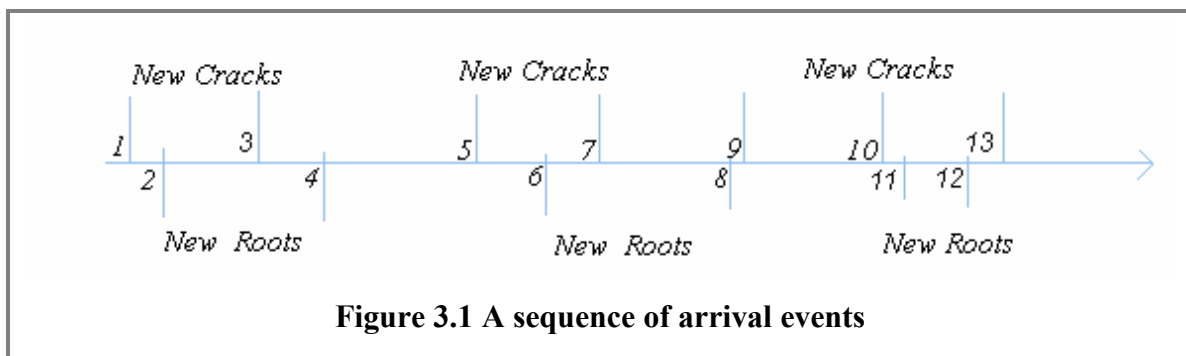
There are several distinct modes in which a pine tap root can penetrate the HDPE geomembrane. They are as follows.

1   A tap root growing vertically downward encounters a crack when it first touches the HDPE geomembrane.
2   A new crack forms directly under an existing root tip on the surface of the HDPE geomembrane.
3   A root penetrates a pre-existing crack by growing horizontally on the surface of the HDPE geomembrane.

In the sequence in Figure 3.1, the first event is the development of a new crack, and the second event is the arrival of a group of roots at the HDPE geomembrane while they are in a vertical descent phase of growth. The HDPE geomembrane is penetrated in the first mode if one or more roots are aligned directly above existing cracks; otherwise, the roots' vertical growth is initially obstructed by the geomembrane. The third event is the materialization of a new crack at a random location in the HDPE geomembrane. If the crack develops directly below the growth tip of a pine tap root, then the root penetrates the crack via the second mode.

Roots grow on the HDPE surface between arrival events. The third mode of root penetration occurs when a root, after missing all existing cracks while growing vertically downward, encounters a pre-existing crack while growing horizontally on the HDPE surface. Since this mode of root penetration describes an existing root entering a pre-existing crack; no arrival of a new root or crack has taken place.

At the onset of an event, the algorithm moves through a series of queries in order to update the status of the numbers of roots and cracks. These numerical summaries are saved in an Event History file. Each row of the file corresponds to the state of the HDPE geomembrane after an arrival event. Table 3.1 contains the Event History column descriptions. Entries S1, Event time, and S2, Event type, describe the time of an arrival event and whether the type of event was the arrival of roots or a crack, respectively.

Table 3.1 Event history file column descriptions

S1 – Event time.
S2 – Event type.

R1 – The total number of roots that have reached the HDPE geomembrane.
R2 – The number of live long (12 foot) tap roots that have not encountered a crack.
R3 – The number of live short (6 foot) tap roots that have not encountered a crack.
R4 – The number of live roots that have penetrated a crack.
R5 – The number of roots that have penetrated a crack and then died.
R6 – The number of dead roots that have not encountered a crack.

C1 – The number of cracks that have not been penetrated by a root.
C2 – The total number of cracks that have formed in the HDPE geomembrane.

The remaining columns are counters that form a profile of the inventory of roots and cracks per acre over time. The first six of these counters numerically partition all of the roots that have reached the HDPE geomembrane up to and including the time of the current event. Column R1 is the total number of pine tap roots that have encountered the HDPE geomembrane. Columns R2 through R4 apply only to roots that are still living at the time of the event. Columns R2 and R3 total the number of 12 foot (long) and 6 foot (short) living roots per acre, respectively, that are not in cracks after the current event, while the number of living roots that have penetrated a crack are recorded in column R4. The sum of the entries R2 and R3 are the number of available roots per acre that have potential to grow horizontally on the HDPE surface into a pre-existing crack.

Eventually, all pine tap roots die. Columns R5 and R6 account for dead tap roots. Column R5 totals all roots that have previously penetrated cracks and subsequently died, and column R6 sums all roots that have died without ever having encountered a crack. The number of roots in column R5 is of primary interest, because the number of dead roots in cracks is the number of moisture conduits through the HDPE geomembrane and the GLC at the time of the current event. In any row of the Event History file, the number of roots in R2 equals the sum of all entries in columns R3 through R6.

Column C1, the number of available cracks, counts those cracks that have not been entered by a root, and column C2 defines the entire number of cracks that have formed in the HDPE geomembrane by the current event time. The total number of cracks to date that have been penetrated by a root is the difference between counters C2 and C1. Since a root cannot penetrate more than one crack, this difference equals the sum of columns R4 and R5 in each row of the Event History file.

The algorithm contains an event loop that is executed once for each arrival event. Each of these iterations presents a series of queries that determines the values of the counters in the Event History file after an event has occurred. These are presented in Figure 3.2 in the form of a flow chart. When a new crack or root arrives at the HDPE surface, Query 1 addresses whether any roots growing horizontally on the HDPE surface have encountered pre-existing cracks since the last event. Then Query 2 updates the ages of all living pine tap roots, and determines the number of roots that have died (reached 100 years of age) since the last event. Once the event history up to the current arrival event is updated, Query 3 determines whether the current event is the arrival of a crack or roots. If the current event is the arrival of a new crack, then Query 4A ascertains whether the crack materialized under an existing root. If the current event is the arrival of a group of roots, then query 4B asks whether one or more roots encountered cracks when they contacted the HDPE surface in their vertical descent.

The following sections describe the probability models used to implement the queries in Figure 3.2.
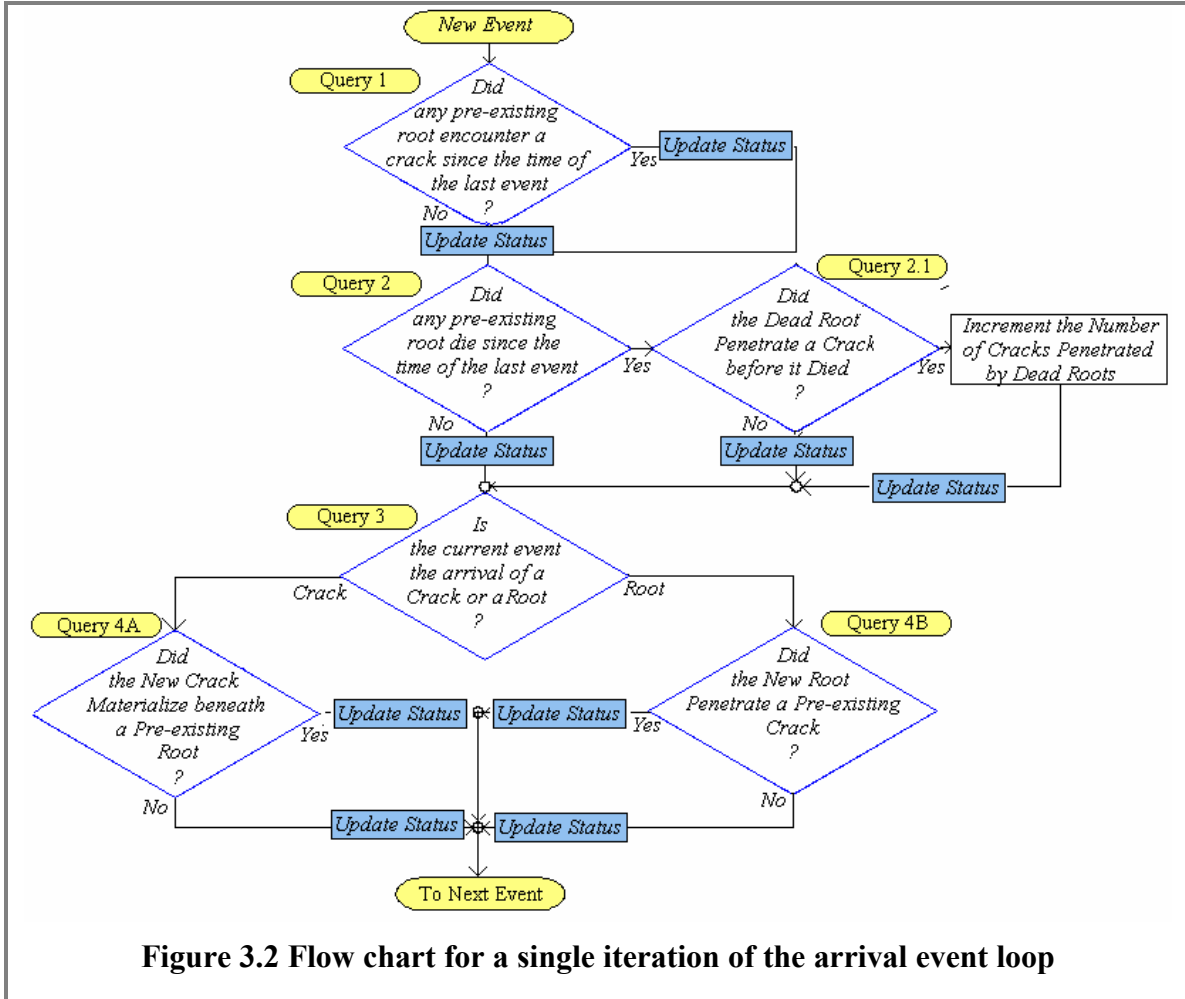
Figure 3.2 Flow chart for a single iteration of the arrival event loop

3.1 A pre-existing crack is penetrated by a root in its vertical growth phase

This section describes a probability model for the case of a new root contacting the area of a circular crack with diameter *d* centimeters at the end of its vertical phase of growth. This is first mode of root penetration presented earlier in Section 3. The probability model is simply the ratio of the area of the circular crack A_C to the area of an acre A_{acre}, both determined in the same units of measure. Given that a single crack exists in the HDPE geomembrane,

$$P\{R_V = 1 | N_C = 1\} = \frac{A_C}{A_{acre}} = \frac{\mathrm{p}\left(\frac{d\ cm}{2}\right)^2}{1\ acre} \cdot F\frac{acres}{cm^2} = 1.9407595 \cdot 10^{-8}\, d^2 \, , \tag{3.1}$$

where R_V is 1 if the root hit the crack, N_C is the number of cracks in the geomembrane that had not been previously penetrated by another root, and the conversion factor for acres to square

centimeters is F = $2.47105383 \cdot 10^{-8}$ acres per sq cm, Weast and Astle [1980]. If the root missed the crack on its downward descent, then R_V is 0 and $P\{R_V = 0 | N_C = 1\} = 1 - P\{R_V = 1 | N_C = 1\}$.

The model is easily extended to the case where there is more than one crack in the geomembrane. If there are $N_C \geq 1$ non-overlapping cracks that have not yet been penetrated by a root, then the probability that a single new root encounters one of these cracks at the end of its vertical phase of growth is

$$P\{R_V = 1 | N_C \geq 1\} = \frac{N_C A_C}{A_{acre}} = \frac{N_C A_C}{1\ acre} \cdot F \frac{acres}{cm^2} = \frac{N_C p \left(\frac{d\ cm}{2}\right)^2}{1\ acre} \cdot F \frac{acres}{cm^2} = 1.9407595 \cdot 10^{-8} N_C d^2 .$$

(3.2)

If the root missed the crack on its downward descent, then R_V is 0 and $P\{R_V = 0 | N_C \geq 1\} = 1 - P\{R_V = 1 | N_C \geq 1\}$. When more than one new root first reaches the geomembrane since the last crack formed, the probability of r_V roots encountering cracks is approximately

$$\Pr\{R_V = r_V | N_C \geq N_R \geq 1\} \approx \binom{N_R}{r_V} \left(\frac{N_C A_C}{A_{acre}}\right)^{r_V} \left(1 - \frac{N_C A_C}{A_{acre}}\right)^{N_R - r_V}$$

$$= \binom{N_R}{r_V} \left(\frac{N_C A_C F}{1 acre}\right)^{r_V} \left(1 - \frac{N_C A_C F}{1 acre}\right)^{N_R - r_V}$$

$$= \binom{N_R}{r_V} \left(1.9407595 \cdot 10^{-8} N_C d^2\right)^{r_V} \left(1 - 1.9407595 \cdot 10^{-8} N_C d^2\right)^{N_R - r_V}, r_V = 0, 1, \ldots, N_R \qquad (3.3)$$

Equation 3.3 is used to resolve Query 4B in the Figure 3.2 flow chart.

3.2 A new crack materializes directly under the tip of a root

This section describes a probability model for the case that a new crack materializes directly under an existing root. This is second mode of root penetration presented earlier in Section 3. Probability model 3.4 describes that probability that a single new crack develops under an existing root. When more than one root is in its horizontal growth phase, then the probability that a new crack materializes under any one of the $N_R \geq 1$ roots is

$$P\{R_H = 1 | N_R \geq 1\} = \frac{N_R A_C}{A_{acre}} = \frac{N_R A_C}{1\ acre} \cdot F \frac{acres}{cm^2}$$

$$= \frac{N_R p \left(\frac{d\ cm}{2}\right)^2}{1\ acre} \cdot F \frac{acres}{cm^2} = 1.9407595 \cdot 10^{-8} N_R d^2 ,$$

(3.4)

where R_H is 1 if the crack develops under any of the roots, and N_R is the number of roots in contact with the geomembrane at the time that the new crack appears. If the crack did not materialize under a pine tap root, then R_H is 0 and $P\{R_H=0|N_C\geq1\}=1-P\{R_H=1|N_C\geq1\}$. It is possible that the new crack materializes under more than one root if the roots are nearby. However, only one of the roots is assumed to be able to penetrate the crack. It is important to identify the root that penetrated the crack because its age and whether it is a long or short root affects the probability of crack penetration. The assignment of a specific root is made with probability $1/N_R$ whenever $R_H=1$ occurs. Equation 3.4 and this assignment rule are used to resolve Query 4A in the Figure 3.2 flow chart.

3.3 A pre-existing crack is penetrated by a root in its horizontal growth phase

This section determines the probability that one or more existing roots growing on the HDPE surface encounter pre-existing cracks between arrival events. The result that a root entered a crack in this manner is assessed at the onset of a new arrival event. The time of growth is either the time between the current and previous arrival events, if the root lived during the entire time period, or the time from the previous event until the root died.

The locations in Figure 3.3 represent the set of possible center points of a circular crack. Previously, a pine tap root in its vertical descent contacted the HDPE surface in an area that did not contain a crack. The center of the black circle in this figure represents the point of contact of the tap root with the HDPE surface. No center of a circular crack was in this black region; otherwise, the pine tap root would have penetrated the crack on its vertical descent, and the tap root would no longer be available to grow along the HDPE surface. The same argument holds for a root that was already in its horizontal growth phase in the previous time interval. In this latter case, the center of the black circle is the location of the root at the time of the previous event, and no center of a circular crack could have been located within the black region without the root having entered the crack.
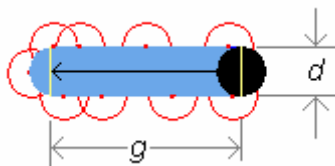
Figure 3.3 The pathway of a pine tap root growing

horizontally on the HDPE surface.

The steepest angle of descent lies to the left of the point of impact, so the blue area represents the pathway of the root in its horizontal growth phase since the previous arrival event. The travel distance for the growing tip of the tap root along the pathway is $g=s\Delta t$, where s is the rate of growth in cm and the period of time, Δt in cm per sec, is the time that the root was growing since

the previous event. Since more than one pine tap root is in its horizontal growth phase between events, the rate of growth may differ among the available tap roots because some roots may be short and others long, and the time of growth may differ among tap roots because some roots may live throughout the assessment period, while others may die during the period.

The width of the pine tap root growth path is the diameter of a circular crack. If a tap root to the top or the bottom were within one half of a diameter then its center would fall on the growth pathway and the tap root would enter the crack. The red circles in the Figure 3.3 are at a distance of one-half of a diameter from the center of the root growth pathway. Since the centers of these circles lie of the growth pathway, a tap root would penetrate a crack centered on any of the red circles. Therefore, the width of the pathway that would allow the pine tap root to enter a crack is double this or one full diameter. Thus, the area of the horizontal growth pathway for a single root is $A_r = d\,g_r = d\,s_r\Delta t_r$, where d is the diameter of a circular crack in cm, and the subscript r is placed on the other terms to associated them with tap root $r, r = 1, 2, \ldots, N_R$.

Assume that the growth pathways of different pine tap roots do not to overlap. The consequences of this assumption are that the total area of pathways of different tap roots is the sum of the individual areas and two or more tap roots cannot enter the same circular crack. The total area of the horizontal growth pathways of all existing pine tap roots is

$$A_P = \sum_{r=1}^{N_R} A_r = \sum_{r=1}^{N_R} g_r\, d\,\Delta t_r\,, \tag{3.5}$$

and the probability that the centers of r_C cracks coincide with tap root growth pathways is approximately

$$P\{R_C = r_C \,|\, N_C \geq 1\} = \binom{N_C}{r_C}\left(\frac{A_P}{A_{acre}}\right)^{r_C}\left(1 - \frac{A_P}{A_{acre}}\right)^{N_C - r_C}$$

$$= \binom{N_C}{r_C}\left(\frac{\sum_{r=1}^{N_R} g_r\, d\,\Delta t_r\, F\,\frac{acres}{cm^2}}{acre}\right)^{r_C}\left(1 - \frac{\sum_{r=1}^{N_R} g_r\, d\,\Delta t_r\, F\,\frac{acres}{cm^2}}{acre}\right)^{N_C - r_C}, \tag{3.6}$$

where the value of F is $2.47105383 \cdot 10^{-8}$ cm^2/acre.

It is possible, but highly unlikely, for the number of cracks on the pathways of horizontally growing roots to exceed the number of roots available. It is assumed that only one root can enter a single crack. In this scenario all available roots, N_R, would penetrate N_R cracks, and the number of available cracks remaining would be $N_C - N_R$.

It is important to identify which roots entered cracks if at least one center of a circular crack was determined to lie on a root pathway. The probability that a particular pine tap root r entered a

crack is g_r/g, where $r=1,2,\ldots,N_R$. The pine tap root that entered a crack is identified by first computing "cumulative" probabilities G_r for the N_R roots, where $G_0=0$, and $G_r=\sum_{j=1}^{r}g_r/g, r=1,2,\ldots,N_r$. A uniform random number U is generated on [0,1], and the decision is made by comparing its value to the set of cumulative probabilities. If U lies in the interval $(g_{r-1},g_r]$, then identify root r as having entered a crack. In the unlikely event that more than one tap root entered cracks in the same period, two independent random numbers on [0,1] are generated and compared to the set of cumulative probabilities. If the two random numbers fall into separate intervals, then two distinct tap roots are identified. If the two random numbers fall into the same interval, discard the results and repeated the process until two distinct roots have been chosen.

4 Simulation inputs

There are two basic inputs to this discrete event simulation: roots and cracks. The inputs are given on a per acre basis. The first is a schedule for the arrival of cracks in the HDPE geomembrane. This schedule was developed by Phifer, et.al. [2007]. Due to its length, the crack arrival schedule is saved separately on the Microsoft® Excel formatted file, Shine [2007].

The other input is the root arrival schedule. Each pine tree has five tap roots. One long tap root has potential to grow about 12 feet, and the four short tap roots have potential to grow about 6 feet. Every pine tree that sprouts eventually has five tap roots that will grow vertically downward until they strike the HDPE geomembrane. At thirty years old pine tap roots contact the HDPE geomembrane. At 100 years old, the pines are assumed to die. The entries for years 590 and 600 are repeated for every 20-year period from year 610 through year 10,050.The tap roots are about 30 years old when they contact the geomembrane.

A mature pine tree is between 40 and 100 years old. There are about 400 mature pine trees, yielding 400 long tap roots and 1,600 short tap roots per century once forestation of the closure cap has stabilized. Table 4.1 is the schedule for pine tree inhabitation of the closure cap. As an example, there are 5 sets of 80 pine trees identified by the blue entries in the table that reach maturity between years 460 and 550.

Prior to year 250 no pine trees are established on the closure cap. Beginning in year 250, the number of sprouts per decade is given in the table. Every ten years the number of pine trees in age cohorts is shown by column. As an example, the red entries in the table correspond to the same set of pine trees every ten years. With each advance of ten years, the pine trees are shown to be ten years older.

Table 4.1 Number of pine trees by age cohort up to year 600.

year	sprouts	10-yr olds	20-yr olds	30-yr olds	40-yr olds	50-yr olds	60-yr olds	70-yr olds	80-yr olds	90-yr olds	100-yr-olds (dead trees)	Current total of all living trees
250												0
260	133											133
270		133										133
280	67		133									200
290		67		133								200
300	67		67		133							267
310		67		67		133						267
320	67		67		67		133					334
330		67		67		67		133				334
340	66		67		67		67		133			400
350		66		67		67		67		133		400
360	80		66		67		67		67		133	347
370		80		66		67		67		67		347
380	80		80		66		67		67		67	360
390		80		80		66		67		67		360
400	80		80		80		66		67		67	373
410		80		80		80		66		67		373
420	80		80		80		80		66		67	386
430		80		80		80		80		66		386
440	80		80		80		80		80		66	400
450		80		80		80		80		80		400
460	80		80		80		80		80		80	400
470		80		80		80		80		80		400
480	80		80		80		80		80		80	400
490		80		80		80		80		80		400
500	80		80		80		80		80		80	400
510		80		80		80		80		80		400
520	80		80		80		80		80		80	400
530		80		80		80		80		80		400
540	80		80		80		80		80		80	400
550		80		80		80		80		80		400
560	80		80		80		80		80		80	400
570		80		80		80		80		80		400
580	80		80		80		80		80		80	400
590		80		80		80		80		80		400
600	80		80		80		80		80		80	400

5 Simulation results

The simulation consisted of 33 independent runs using a different random number seed for each run. The area of the closure cap is normalized to one acre, so that all results are given on a per acre basis. A single run provides one realization of the 10,000 year time period that begins with cessation of active maintenance. The mean results for selected years appear in Table 5.1. The total roots that reached the HDPE surface agree on a case by case basis with the input file[1]. Since there are 5 tap roots per pine tree, and the increase in the total roots per century after year 400 is 2,000 tap roots per century, the simulation results indicate that there are 400 pine trees per century per acre after year 400. This agrees with the assumption of 400 pine trees per acre. Similarly, the total crack given in the right column of the table agrees with the input file for cracks.

The number of moisture conduits through the HDPE geomembrane and the GCL is given by the column headed "Dead Roots in Cracks" in Table 5.1. The number of these root penetrations is increasing with time. The number of dead roots that never encountered cracks in the HDPE

Table 5.1 The mean results by year

Year	Total Roots	Live Long Roots	Live Short Roots	Live Roots in Cracks	Dead Roots in Cracks	Dead Roots Not in Cracks	Cracks Without Roots	Total Cracks
100	0	0	0	0	0	0	26	26
200	0	0	0	0	0	0	41	41
300	665	133	532	0	0	0	63	63
400	2,400	280	1,120	0	0	1,000	180	181
500	4,400	319	1,280	1	1	2,799	297	299
600	6,400	319	1,280	1	3	4,797	412	416
700	8,400	319	1,280	1	5	6,795	527	533
800	10,400	319	1,280	1	8	8,792	642	651
900	12,400	319	1,280	2	11	10,789	755	768
1,000	14,400	319	1,279	2	15	12,785	870	886
1,250	19,200	238	960	2	26	17,974	1,151	1,179
1,500	24,400	318	1,279	3	41	22,759	1,428	1,472
1,750	29,200	237	959	3	60	27,940	1,702	1,765
2,000	34,400	317	1,279	4	81	32,719	1,974	2,059
2,500	44,400	316	1,278	5	136	42,664	2,504	2,646
3,000	54,400	315	1,278	7	204	52,596	3,022	3,233
3,500	64,400	314	1,278	9	281	62,519	3,531	3,820
4,000	74,400	313	1,277	9	370	72,430	4,026	4,406
4,500	84,400	313	1,277	10	474	82,326	4,510	4,993
5,000	94,400	313	1,277	11	588	92,212	4,981	5,580
5,500	104,400	311	1,277	13	710	102,090	5,444	6,167
6,000	114,400	310	1,276	14	845	111,955	5,895	6,754
7,000	134,400	309	1,276	14	1,144	131,656	6,769	7,927
8,000	154,400	309	1,275	16	1,488	151,312	7,597	9,101
9,000	174,400	307	1,275	18	1,862	170,938	8,394	10,274
10,000	194,400	306	1,274	20	2,272	190,528	9,157	11,449

---

[1] The input file is not reproduced in this report due to its length.

geomembrane is considerably larger than those that had penetrated cracks. The number of live roots in cracks remains small relative to the total roots, and the percentage of cracks that were penetrated by a root remained less than 10% for the first 4,500 years. The numbers of long and short roots available dips by about 80 and 320 in years 1250 and 1750, respectively. This is an artifact caused by adding 80 pine trees to the closure cap every twenty years. These are the only two years in the table in which there were no additions to the pine tree inventory.

Figure 5.1 plots the number of moisture conduits, that is, the number of dead roots in cracks by year, for each of the 33 simulation runs. The thick black curve represents the mean number of dead roots in cracks by year. The run to run deviations about the average appear to be reasonably tight.
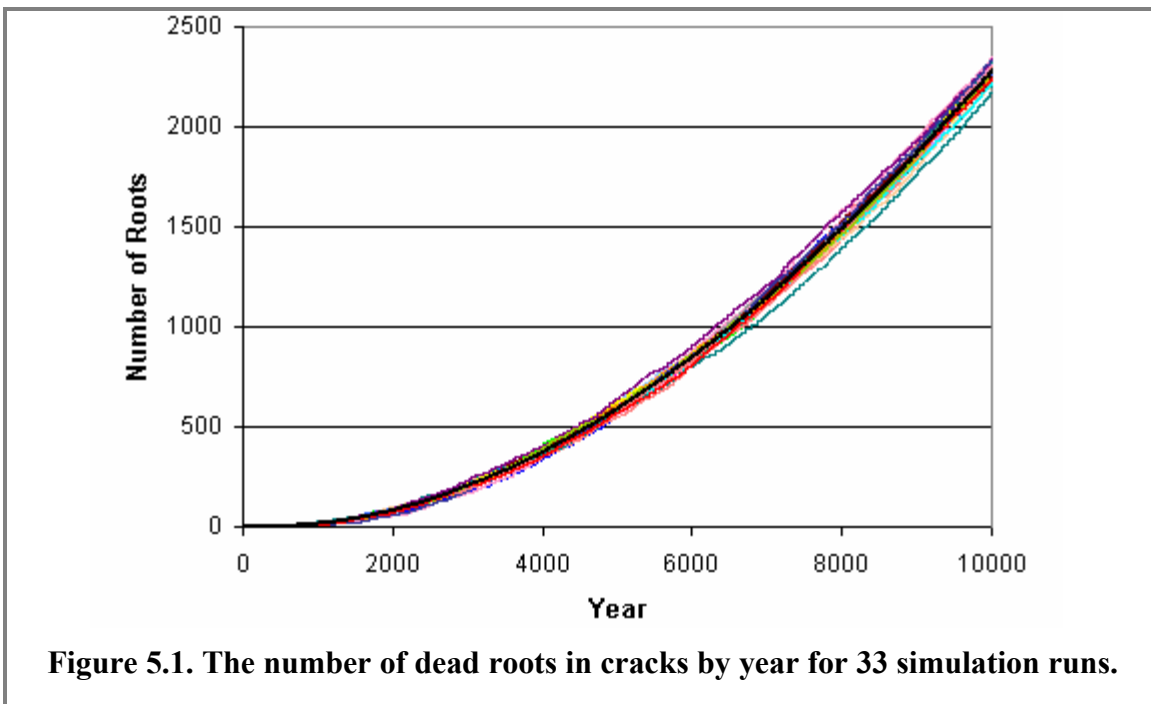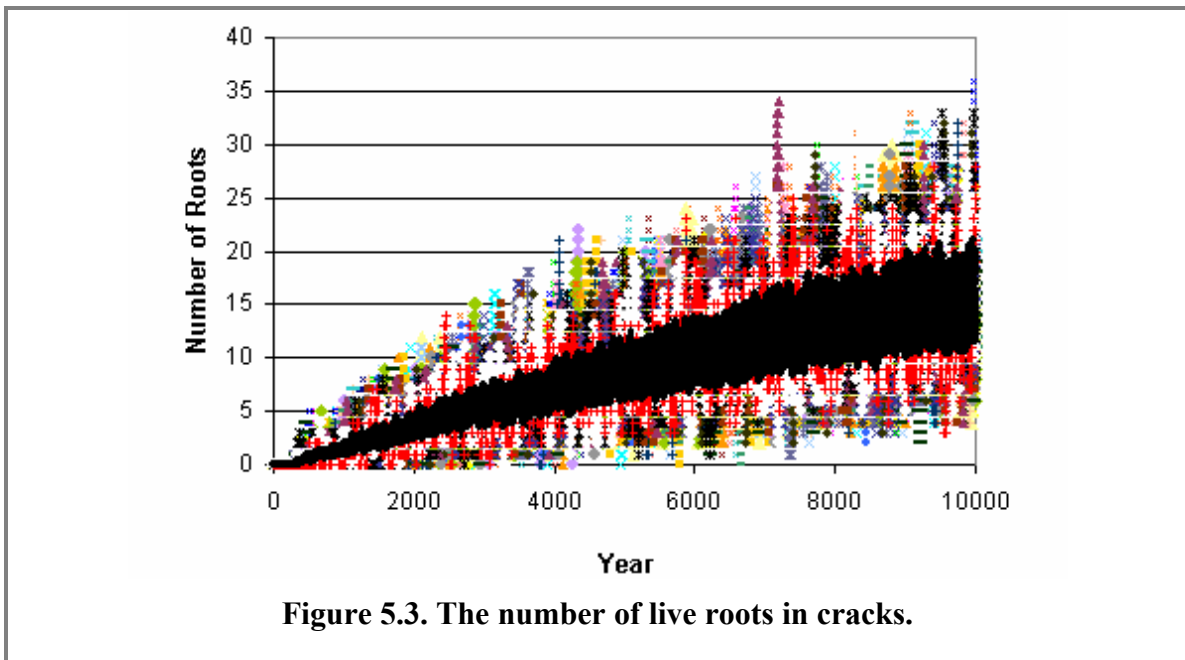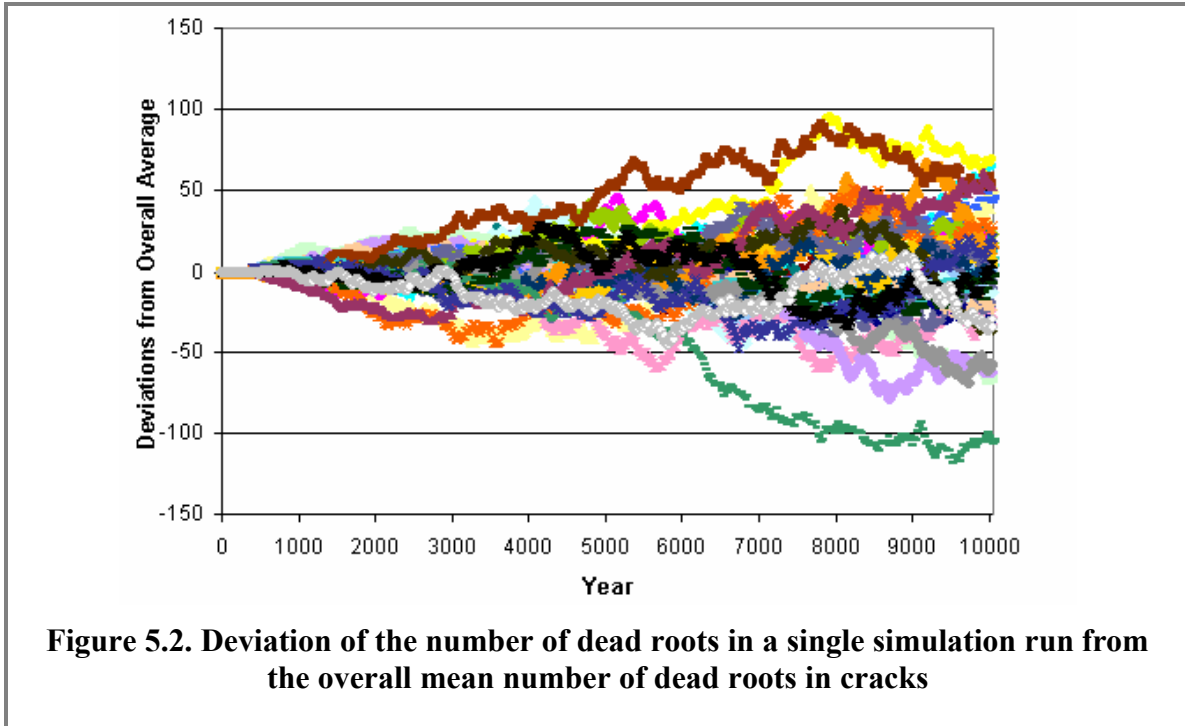

Figure 5.1. The number of dead roots in cracks by year for 33 simulation runs.

Figure 5.2 provides a different perspective on the deviations of individual runs from the overall average number of dead roots in cracks. The largest deviation on the high side in any simulation run is no more than 100 roots greater than the mean for the number of dead roots in cracks.

Figure 5.3 plots the number of live roots that have penetrated cracks over time. The number of such roots adds to the number of moisture conduits when the roots die. The average is represented by the black area, while individual runs are plotted in colors. The number of such live roots is small but varies considerably since roots are constantly dying off and being replaced by newly added root penetrations of cracks.

The results for year 10,000 are summarized in Table 5.2. Counts of roots and cracks were summarized by the minimum, mean, and maximum counts over the 33 runs. About 20% of the cracks had been penetrated by a root, while only about 1.2% of the dead roots had penetrated one of the cracks. The number of dead roots in cracks, representing the number of moisture conduits

formed in the HDPE geomembrane and the GLC, ranged from 2,192 to 2,367 with a mean of 2,298 roots over the 33 simulation runs. The low 2,192 and high 2,367 number of dead roots in cracks represent a two-sided 90% confidence nonparametric tolerance interval covering 88.7% of the distribution, Conover [1971].

Figure 5.2. Deviation of the number of dead roots in a single simulation run from the overall mean number of dead roots in cracks

Figure 5.3. The number of live roots in cracks.

The mean time between crack penetrations decreases over time as would be expected since the number of cracks not yet penetrated by a root increases by century. Around the year 2,000, there is a mean of about 10 years between crack penetrations. By the year 5,000, the number of years between crack penetrations has decreased to about 4.5 years, and, by the year 10,000 to about 2.4 years. The percent of available cracks that are transformed into moisture conduits stabilizes to approximately 0.45% per century.

Figure 5.4 is a run by run plot of the mean number of dead roots in cracks in the simulation order. This quality control check indicates that the runs do not have a trend over time. The overall mean of the 33 runs is depicted by the thick black horizontal line. The overall variability is within plus or minus 5% of the mean.

**Table 5.2 The low, mean, and high results
over the 33 simulation runs after 10,000 years**

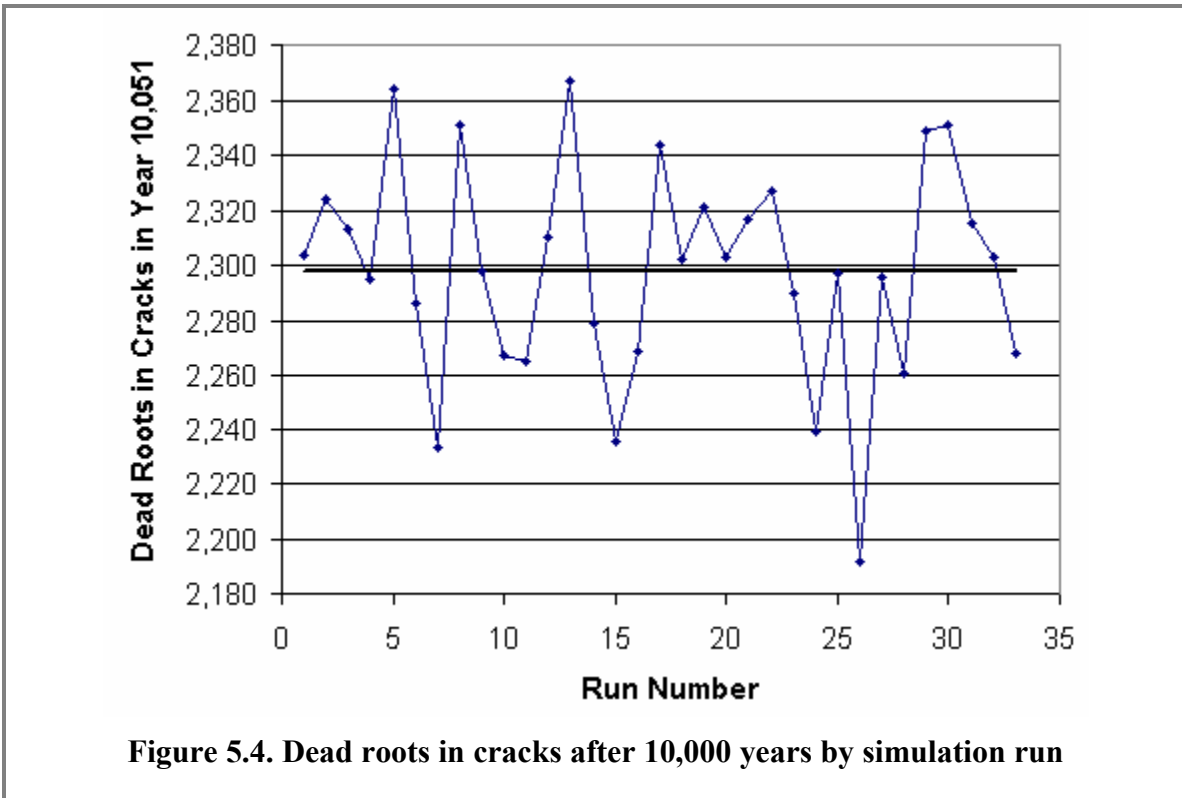|	Total Roots	Live Long Roots	Live Short Roots	Live Roots in Cracks	Dead Roots in Cracks	Dead Roots Not in Cracks	Cracks Without Roots	Total Cracks
Low	194,400	302	1,267	11	2,168	190,461	9,090	11,449
Average	194,400	306	1,274	20	2,272.2	190,528	9,157	11,449
High	194,400	312	1,279	30	2,339	190,632	9,262	11,449

Figure 5.4. Dead roots in cracks after 10,000 years by simulation run

6 Conclusions

A discrete event simulation model has been developed in order to determine a 10,000 year profile for the number of moisture conduits per acre created by root penetrations of the HDPE geomembrane and the GCL. The number of cracks in the HDPE geomembrane, as well as the number of cracks that have been penetrated by tap roots, increases with time. However, the percent of available cracks that are transformed into moisture conduits stabilizes to approximately 0.45% per century. This is the immediate consequence of assuming that the number of mature pine trees remains constant at about 400 trees per century.

The mean number of moisture conduits in the HDPE geomembrane and GCL reaches 2,272 per acre after 10,000 years. The largest observed deviation over 33 simulation runs was less than 5% over the mean. The low 2,168 and high 2,339 numbers of dead roots in cracks per acre represent a two-sided 90% confidence nonparametric tolerance interval covering 88.7% of the distribution.

The time between root penetrations of cracks decreases with time with about 10, 4.5, and 2.4 years between crack penetrations after about 2,000, 5,000, and 10,000 years.

The mechanism of horizontal root growth on the HDPE surface appears to be the dominant mode of root penetration. This is consistent with the much larger "search" area for cracks associated with horizontal root growth than the area associated with a direct strike of a crack by a root growing in the downward vertical growth phase or the area associated with a crack that may materialize directly below the growth tip of a tap root.

The mean results per acre for selected years are summarized in Table 5.1. Complete results at the time of every root or crack arrival event are provided on the Microsoft® Excel formatted file, Shine [2007].

7 References

[1971] Conover, W.J. **Practical Nonparametric Statistics**, John Wiley & Sons, Inc.

[1975] Bishop, Fienberg, and Holland. **Discrete Multivariate Analysis: Theory and Practice**, The MIT Press, Cambridge, MA.

[2007] Phifer, M. A.; Jones, W.E.; Nelson, E.A.; Denham, M.E.; Lewis, M.R.; Shine, E.P., WSRC-STI-2007-00184, Revision 2 (September).

[2007] Nelson, E.A. Personal communication. SRNL, Environmental Analysis and Biotechnology.

[2007] Shine, E.P. "Tables of pine tree tap root inputs and simulation results for the F-area Tank Farm Closure Cap inhabitation model," SRNL-SCS-2007-00046, Microsoft® Excel format.

[1980] Weast, R.C. and Astle, M.J. **CRC Handbook of Chemistry and Physics, 61st edition**, Boca Raton, FL: CRC Press.

[2003] Wolfram Research, Inc. **Mathematica Book, 5th edition**, Wolfram Media, Champaign, IL.

Distribution:

T. C. Robinson, Jr., 766-H
K. H. Rosenberger, 766-H
J. L. Newman, 766-H
M. H. Layton, 766-H
T. W. Coffield, 766-H
J. C. Griffin, 773-A
H. H. Burns, 999-W
B. T. Butcher, 773-43A
E. L. Wilhite, 773-43A
G. A. Taylor, 773-43A
D. I. Kaplan, 773-43A
R. S. Aylward, 773-42A
M. A. Phifer, 773-42A
M. R. Millings, 773-42A
G. P. Flach, 773-42A
T. Whiteside, 773-64A
W. E. Jones, 773-42A
J. M. Jordan, 773-42A
WPT file (2 copies), 773-43A, Rm. 213